SYNTHESIS OF USEFUL ORGANIC MOLECULES BY C-C BOND FORMATION AND C-H ACTIVATION REACTIONS

THESIS SUBMITTED FOR THE DEGREE OF
DOCTOR OF PHILOSOPHY (SCIENCE)
OF
JADAVPUR UNIVERSITY
2024

BY
DEBABRATA PATRA

INDEX NO. : 86/19/CHEM./26
ORGANIC CHEMISTRY SECTION
DEPARTMENT OF CHEMISTRY
JADAVPUR UNIVERSITY
KOLKATA-700032
INDIA

Dedicated

To

My Family Members

যা দ ব পু র বি শ্ব বি দ্যা ল য়
ক ল কা তা – ৭০০ ০৩২, ভারত

JADAVPUR UNIVERSITY
KOLKATA-700 032, INDIA

FACULTY OF SCIENCE : DEPARTMENT OF CHEMISTRY : ORGANIC CHEMISTRY SECTION

Dr. Amit Saha (Assistant Professor)

Organic Chemistry Section
Department of Chemistry
Jadavpur University
Telephones: 033-24572981, 91-9433950204
E-mail: amit.saha@jadavpuruniversity.in
amitsahaiacs@yahoo.co.in

Residence:

44/B1 Urban Sabujayan, P.O.
Mukundapur, Kolkata 700099

TO WHOM IT MAY CONCERN

This is to certify that the thesis entitled **"Synthesis of useful organic molecules by C-C bond formation and C-H activation reactions"**, submitted by **Mr. Debabrata Patra** who got his name registered on 16.08.2019 for the award of Ph.D. (Science) degree, Jadavpur University, is absolutely based upon his own research work under my supervision and that neither this thesis nor any part of it has been submitted for either any degree or diploma or other academic award anywhere else before.

Place: Jadavpur, Kolkata

Date: 25.07.2024

A. Saha 25.07.2024

Dr. Amit Saha
Assistant Professor
Department of Chemistry
Jadavpur University
Kolkata-700032, India

Signature of the Supervisor with official seal

Preface

Investigation embodied in this desertion entitled "**Synthesis of useful organic molecules by C-C bond formation and C-H activation reactions**" was initiated in July 2018 under the supervision of **Dr. Amit Saha**, Assistant Professor, Organic Chemistry Section, Department of Chemistry, Jadavpur University, Kolkata 700032.

The prime focus of this research work is to explore C-C bond forming reactions and C-H activations for the synthesis useful organic molecules using heterogeneous catalyst, homogeneous catalyst and under metal free condition.

✓ **C-C bond formation reactions**	**Heterogeneous metal catalysis**
	Homogeneous metal catalysis
	Metal free protocol
✓ **C-H activation reactions**	**Heterogeneous metal catalysis**

This thesis has been categorized into four chapters. **Chapter-1** consists of two sections, **Section-1** includes a short review on current progress in C-C cross-coupling reactions using heterogeneous catalyst and **Section-2** describes the heterogeneous magnetic Pd(II) catalyzed C-C cross coupling reactions of organosilanes with terminal alkenes and allylic acetates. **Chapter-II** has been divided into two sections. **Section-1** demonstrates a short review on the various synthetic routes of thioamide and its derivatives *via* metal mediated cross coupling reactions. Synthesis of thioamide compounds *via* Pd(II)-catalyzed decarboxylative-decarbonylative C-C bond formation reactions has been discussed in **Section-2.** In **Chapter-III** synthesis of thioamide and related compounds have been discussed and the chapter is divided into two sections. **Sections-1** describes a general review synthesis of substituted thioamide and their relative derivative compounds via C-C cross coupling reactions using transition metal free protocol. **Section-2** describes the diverse role of dithiocarbamate as precursor in synthesis of substituted thioamide compounds. **Chapter-IV** consists of two sections which describe C-H activation reactions. **Sections-1** includes a short review of C-H activation reactions using heterogeneous metal catalysis. Synthesis of fused-isoindolinones compounds using magnetic heterogeneous Pd-catalyst in aqueous medium has been discussed in **Sections-2.**

Acknowledgement

It is great pleasure for me to express my sincere gratitude and respect to Dr. Amit Saha, Assistant Professor, Organic Chemistry Section, Department of Chemistry, Jadavpur University, Jadavpur, Kolkata 700032, for introducing me to the fascinating field of "Synthetic Organic Chemistry". I proclaim my indebtedness to him for his constant encouragement along with useful suggestions and constructive criticism during the entire tenure of this work. Being embowered always by his graceful behaviour, I feel proud that I have enjoyed the full freedom while carrying out my research work with him.

I am grateful to Dr. Mijanur Rahaman Molla (Department of Chemistry, Calcutta University) and Professor Rina Ghosh (Department of Chemistry, JU) for their advice in different occasions.

I proffer my heartiest appreciation to Mr. Koushik Mondal for his tremendous help during my research period. I also express my thanks to Dr. T. K. Mondal and his scholars for helping me in HRMS analysis, Mr. Raju Biswas (Microanalyst, Dept. of Chemistry), Mr. Sumanta Jana, Mr. Subhashis Mondal for their help in getting NMR spectra, Mr. Krishna mohan Das for recording IR spectra and also Mr. Susanta Dinda for recording XRD data.

I am grateful to Prof. Kajol Krishna Rajak (HOD, Department of Chemistry, JU), Mr. D. Chakraborty, Mr. M. Mukherjee and Mr. S. A. Rahaman for their cooperation in various official works during these years.

I am very much thankful to Dr. M. A. Mondal, Dr. A. Thakur, Dr. T. Bhoumik, Dr. S. Guha, Dr. U.C. Halder, Dr. G. Maity, Dr. S. Bhar, Dr. U. Jana, Dr. T. Ghosh, for their kind help during my research work. Special thanks are also offered to my teachers Dr. C. Santra, Dr. A. Barik and Mr. A. Manna.

I am really proud to have some lab-mates like Mr. Soumya Dutta, Mr. Manas Mondal, Mr. Sourav Mondal, Mr. Anirban Bera, Mr. Debasish Ghosh, Mr. Avrajit Manna, Ms. Ipsita Chakraborty, Mr. Samim, Mr. Pintu Das, Mr. Subir Panja, Mr. Tubai Ghosh, Mr. Arunavo Misra, Ms. Sudipta Mondal for their wholehearted co-operation during my research work.

It is high time to acknowledge my gratitude to my fellow colleagues Dr. D. Halder, Dr. S. Mondal, Mr. S. Saha, Mr. S. Nandi, Mr. K. Mondal for their helpful co-operation during my stay here.

At the moment of submitting my thesis, I express my deep respect and love to all of my family members, and relatives for their blessing as well as inspiration for my Ph. D. work.

Finally, I must sincerely acknowledge CSIR for awarding me fellowship, which has enabled me to carry out my research work successfully.

Debabrata Patra

Organic Chemistry Section
Department of Chemistry
Jadavpur University
Jadavpur, Kolkata-700032,
India

Table of Contents

Chapter-I

Section-I

C-C Cross Coupling Reactions Using Heterogeneous metal catalyst

1/a Introduction

In the recent times, heterogeneous catalysts have received significant attention in the area of synthetic organic chemistry. The C-C bond formation reactions are important tool for synthesizing complex organic framework. C−C Cross-coupling reactions[1] like Sonogashira,[2] Suzuki− Miyaura, [3] Hiyama,[4] Heck,[5] have been used to synthesize natural products, heterocycles, molecular electronics, dendrimers, and conjugated polymers etc. Among these, Suzuki−Miyaura coupling reactions offer an effective process for the preparation of pharmaceuticals[6] because of compatibility of functional groups and accessibility of organoboron compounds under mild reaction conditions.[7] Homogeneous catalysts based on transition metals often involve a monotonous catalyst separation step. Magnetic nanoparticles (MNPs) show important properties such as high recyclability, easy preparation, large surface area, functionalization, facile catalyst separation by an external magnet, and high loading capacity. Recently, MNPs have been extensively used for the heterogenization of homogeneous catalysts.[8] The surface coating of MNPs may increase the chemical stability, avoiding aggregation in solutions and providing functional groups on the surface.[9] Recently, multicomponent reactions (MCRs), which are effective in the synthesis of heterocycle compounds in organic chemistry,[10] are mostly reported because of their high sustainability and great ecofriendly conditions.[11] Pd-catalyzed C−C coupling reactions are one of the most important advancements in synthetic organic chemistry due to high production yields, fast reaction rates, high turnover frequency and selectivity.[12] Biomedical sciences extensively use nanoparticles for different purposes like drug delivery, tumor targeting, magnetic resonance imaging etc. Carbon nanomaterials have been utilized as efficient catalyst supports for numerous organic transformations.[13] In recent years, graphene oxide (GO) and reduced graphene oxide (rGO) nano materials have emerged as valuable supports for various metal complexes and nanoparticles among carbon-based materials. Carbon, oxygen, and hydrogen are combined in different proportions to form graphene oxide and rGO, which are commonly produced by subjecting graphite to powerful oxidizing agents. GO and rGO have garnered significant attention in the field of heterogeneous catalysis due to their remarkable chemical and physical properties, simple functionalization, dispersion in various solvents and high effective surface area. As a result, nanomaterials based on GO or rGO have been extensively investigated as catalyst supports.[14] It is important to highlight that both GO and rGO nanomaterials have the potential to enhance the dispersion and immobilization of nanoparticles (NPs). Additionally, the two-dimensional monolayer of graphene provides ample availability of reactants to active cores, as stated in reference.[14] Hence, the modified GO-/rGO-metal nanocomposites exhibit great potential as catalysts due to their cost-effectiveness in production, large surface area, exceptional purity, and straightforward preparation techniques.[15] Surface modification of GO and rGO involves the use of both covalent and noncovalent modifications with different species. Covalent bonding takes place between organic molecules and the basal planes or edges of graphene sheets, utilizing functional groups like carboxyl, hydroxyl, and epoxy groups. Various chemical reactions such as nucleophilic and electrophilic substitution, as well as condensation reactions, are employed

for covalent bonding. Covalent and noncovalent alterations are employed to modify the surface of GO and rGO with different species. Organic molecules form covalent bonds with specific functional groups like carboxyl, hydroxyl, and epoxy groups on the basal planes or edges of graphene sheets. Covalent bonds are formed through a range of chemical reactions, including nucleophilic and electrophilic substitution, as well as condensation reactions. Several interactions, such as π–π interactions, hydrogen bonding, ionic and cationic interactions, hydrophobic interactions, and van der Waals bonding,[16] can lead to noncovalent functionalization. The surface modification of GO and rGO is significant as it prevents their agglomeration and promotes the development of a stable dispersion. However, synthesis of optically active molecules, which are precursors to important pharmaceutical compounds, is achieved through the employment of asymmetric catalysts. The application of numerous chiral catalysts with high selectivity, developed in the past three decades, is hindered by their exorbitant costs and the challenges involved in removing minute amounts of toxic metals from the organic products in industrial processes. To overcome these problems, scientists have approached many different ways to generate heterogenized asymmetric catalysts. Therefore, it is crucial to establish innovative and novel approaches in the development of recoverable and reusable asymmetric catalysts.

1/b Review

Aryl–aryl (Ar–Ar) bond formation and the heteroaryl analogues (Ar-Het and Het–Het) are undoubtedly one of the most important transformations in organic chemistry, and compounds containing the Ar–Ar, Ar-Het and Het–Het moieties are ubiquitous in the pharmaceutical industries. Classical methods for the creation of these bonds include well-known transformations such as the Suzuki–Miyaura, Stille, Negishi and other named reactions. Asymmetric catalysis provides a powerful method for the synthesis of optically active molecules that serve as precursors to pharmaceutically important compounds. Although numerous highly selective chiral catalysts have been developed in the past three decades, their practical applications in industrial processes are hindered by their high costs as well as difficulties in removing trace amounts of toxic metals from the organic products. To overcome these problems, many different approaches have been used to generate heterogenized asymmetric catalysts. The heterogenized catalysts are, however, typically less effective than their homogeneous counterparts. Thus, there exists a need to develop new and innovative approaches toward the design of recoverable and reusable heterogeneous catalysts.

I. Kumada-Corriu catalytic reaction of Grignard agents with halide compounds in presence of nickel/rGO-40 composite for the synthesis of substituted biaryl compounds:

De *et.al* [17] reported the catalytic efficiency of nickel nanoparticles (NPs) supported on reduced graphene oxide (Ni/rGO-40) with a nickel content of approximately 40 wt.% as a catalyst for the Kumada coupling reaction (Scheme 1.1). The results obtained indicated that

different haloarenes underwent reactions with Grignard reagents in the presence of a catalytic amount of Ni/rGO-40, resulting in the formation of corresponding products with yields ranging from 72% to 91%. The Ni/rGO-40 composite successfully achieved a substantial Ni loading of 40 wt.% without any visible agglomeration. This was made possible by the planar structure and large effective surface area of reduced GO, which effectively hindered the aggregation of Ni NPs into larger particles. The catalyst demonstrated considerable technological significance and exhibited notable reusability in the reaction between 4-iodoanisole and phenyl magnesium chloride. Through X-ray diffraction (XRD) and Raman spectroscopy analysis, it was determined that there were no alterations in the crystalline phase and structure of the restored composite. The rGO surface was found to contain a significant number of free electrons, effectively maintaining the nickel NPs in a metallic state. Additionally, there were no observable modifications in the oxidation state of nickel within the recovered composite.

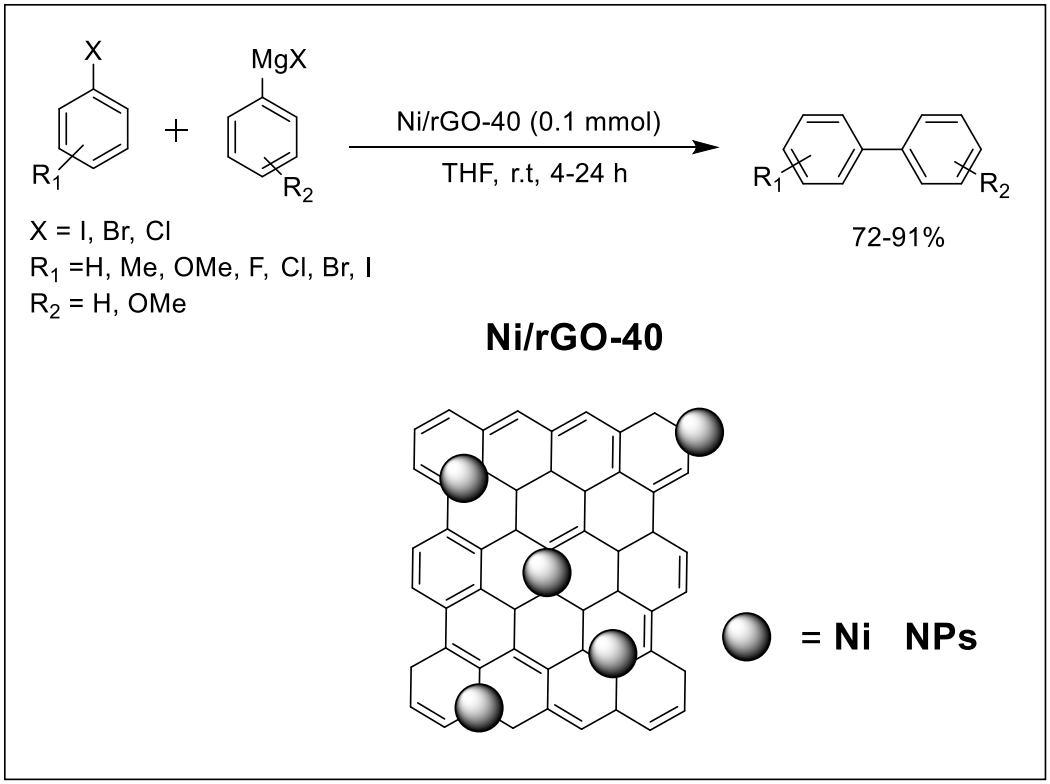

Scheme-1.1

II. Mizoroki-Heck cross-coupling reaction catalyzed by ErGO-Pd:

Nagarkar [18] developed the efficiency of the electrochemically co-deposited rGO and palladium nanoparticles (ErGO-Pd) in catalyzing the Mizoroki Heck cross-coupling (Scheme 1.2). An investigation was carried out to assess the catalytic activity of electrochemically co-deposited reduced graphene oxide and palladium (ERGO-Pd) in Heck coupling reactions. Its catalytic activity and stability proved to be highly effective in facilitating the Heck coupling reaction. Utilizing cyclic voltammetry, the electrochemical preparation of Pd-reduced GO (ERGO-Pd) was carried out. This involved scanning from 0 to -1.4 V for 10 cycles in a GO

dispersion, with the electrolyte being a 1 M KCl solution containing 5 mM $PdCl_2$. Subsequently, the GO was diminished using the identical method, but without addition of $PdCl_2$. The catalytic performance of the ERGO-Pd nanocomposite in the Mizoroki-Heck coupling was exceptional, and it exhibited the ability to be reused for five consecutive runs without any significant decrease in its performance.

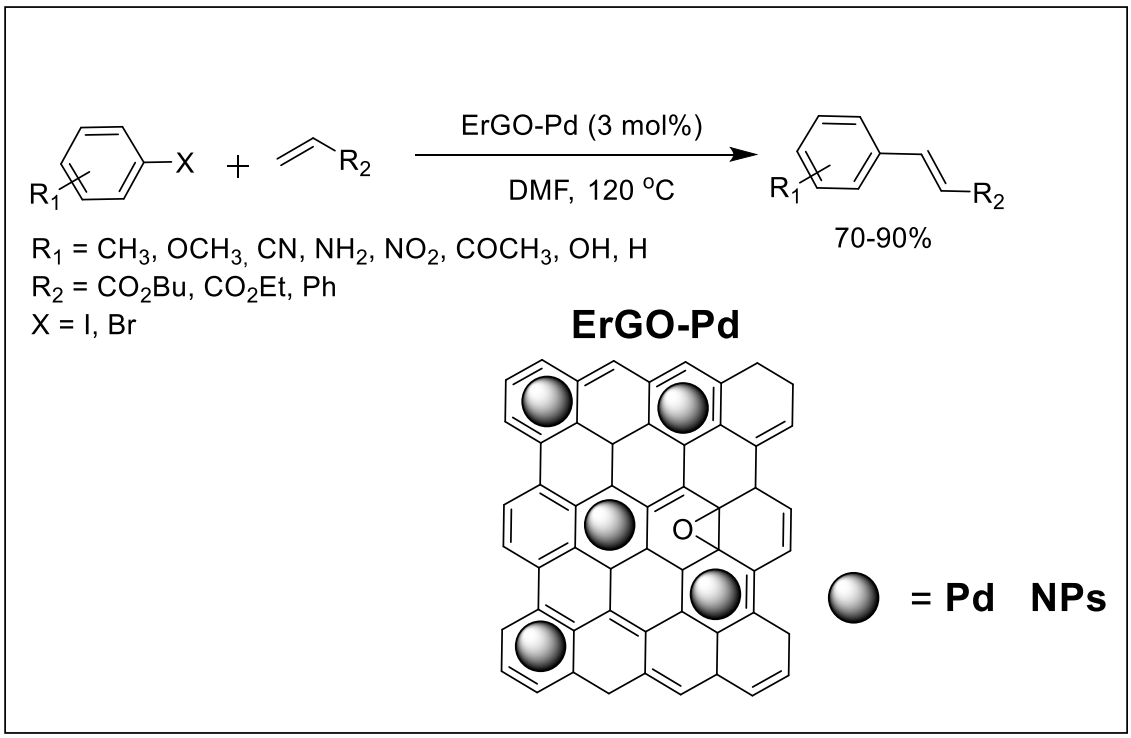

Scheme-1.2

III. Synthesis of various stilbene molecules using the GL-Pd NPS catalyst:

Premi and colleagues [19] developed a nanocomposite consisting of palladium supported on reduced graphene oxide (rGO) (Scheme 1.3). The graphene oxide (GO) was modified using a bi-dentate compound that contained nitrogen and sulfur elements, resulting in GL-Pd. The GL-Pd catalyst was developed by preparing thiol-functionalized graphene (GSH) *via* thiolation of GO. Subsequent insertion of pyridine into GSH led to the formation of the GS-Py complex. Ultimately GL-Pd material was produced by introducing palladium acetate to the GS-Py complex. The GL-Pd hybrid catalyst, incorporating N- and S-functionalized GO-Pd NPs, was subjected to testing in the Mizoroki-Heck coupling reaction. A wide range of functionalized substrates were employed to investigate the catalyst's performance. The GL-Pd catalyst was thoroughly examined for its ability to catalyze the coupling reaction between various iodo- or bromo-aryl compounds and different styrene molecules, leading to the production of a variety of stilbenes. After 24 hours, the desired coupling product produced with excellent yields. The GL-Pd material demonstrated exceptional catalytic performance, even at a low palladium loading of 0.02 mol%. Notably, there was no loss of catalytic activity observed even after three successive runs. The catalytic performance of the GL-Pd material was found to be exceptional, even with a low palladium loading of 0.02 mol%. Furthermore,

there was no observed decline in catalytic activity even after three consecutive runs. The catalyst exhibited enhanced activity due to the coordination of N and S atoms with Pd, resulting in a higher dispersion and loading of palladium nanoparticles on the functionalized rGO material.

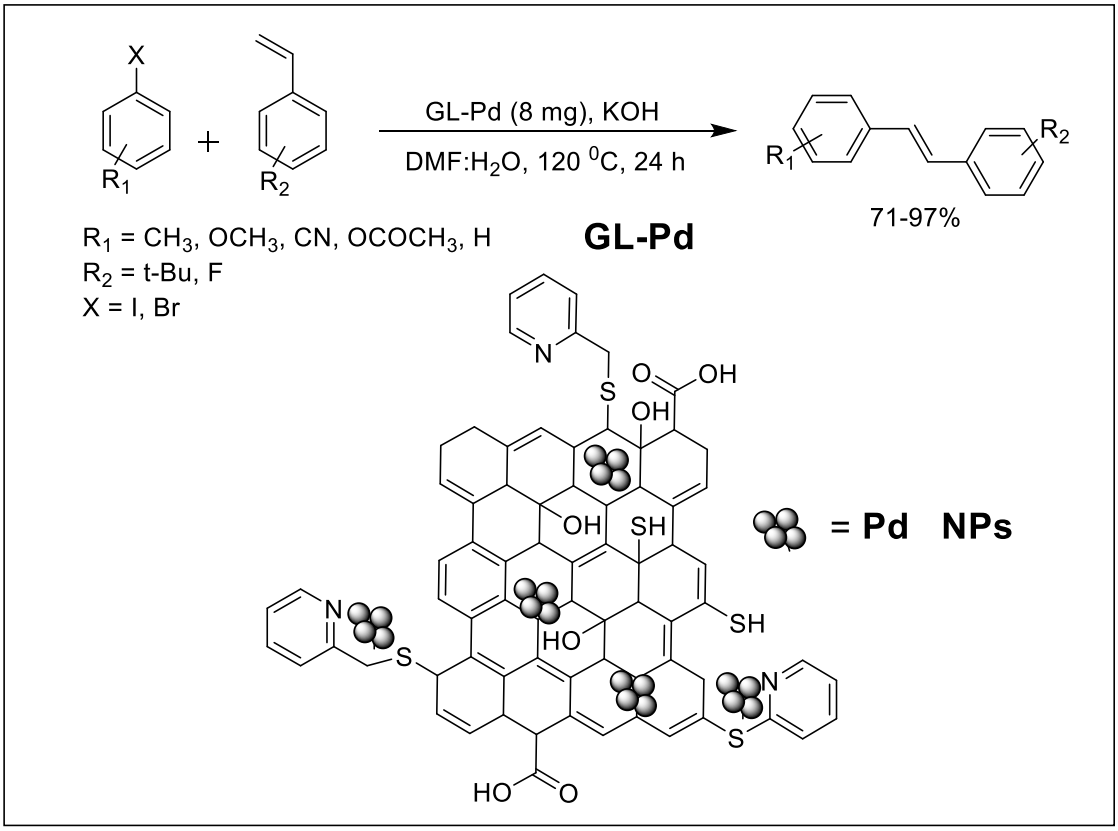

Scheme-1.3

IV. Mizoroki-Heck reaction-catalyzed by Pd@GOF:

Azadi and his group[20] have developed a catalyst that involves a Pd nanoparticle (NP) embedded within a framework of graphene oxide (Pd@GOF) (Scheme1.4). This framework exhibits well-organized macro- and mesoporous structures. The first step involved the selection of 5,50-diamino-2,20-bipyridine as the cross-linking agent for the covalent modification of GO nanosheets. This selection led to the formation of a three-dimensional (3D) framework that contained interlayer spaces. Within this framework, well-dispersed and ultra-small Pd NPs were able to grow and become embedded. The 3D Pd@GOF nanopores, which have been synthesized, serve as nanoreactors facilitating complete contact between the reaction substrates and the surface of Pd NPs. As a result, they demonstrate remarkable activity in the Heck reaction, a phenomenon that has rarely been reported in relation to Pd NPs supported on one-side functionalized graphene. The catalytic activity of the Pd@GOF catalyst remains stable even after being used 10 times, indicating its long-term stability without any significant decrease in performance. As a result, the covalently assembled GOF has been proposed as a universal framework for accommodating noble metal NPs, enabling

the construction of metal@GOF nanocatalysts with enhanced activity and stability. These nanocatalysts have the potential to be utilized across various practical applications.

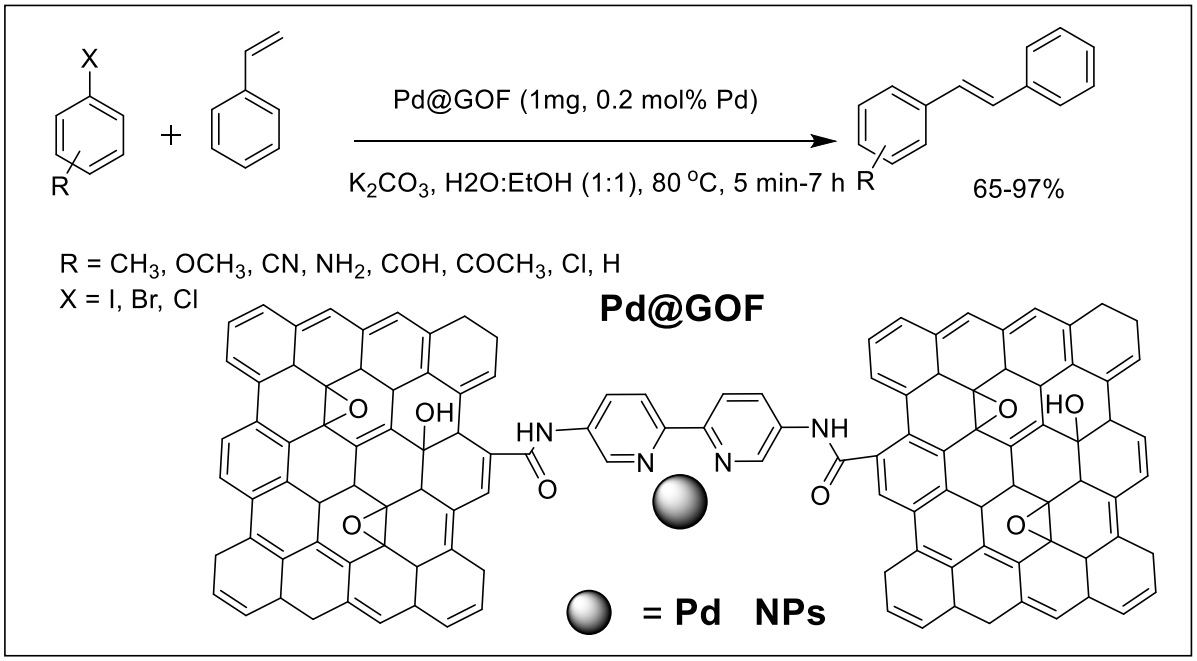

Scheme-1.4

V. Mizoroki–Heck coupling reaction using Pd NPs/rGONH_2 catalyst:

Boukherroub and his group[21] illustrated that the Pd NPs/rGONH_2 catalyst, consisting of Pd nanoparticles on rGO functionalized with diethylenetriamine, exhibited high activity in the Mizoroki-Heck reaction of various halide compounds and alkenes. The use of Et_3N as a base resulted in the formation of corresponding coupling products with yields ranging from 59% to 100% after 4 hours (Scheme 1.5). The synthesis of rGO-NH_2 involved subjecting a combination of diethylenetriamine and an ethanolic suspension of GO to sonication. Subsequently, the sonication of rGO-NH_2 with H_2PdCl_4 solution in an ultrasonic cleaning unit at room temperature led to the synthesis of Pd NPs/rGONH_2. In the XRD pattern of the Pd NPs/rGONH_2 catalyst, peaks at 2θ = 40.01°, 46.54°, and 67.93° were assigned to the (111), (200), and (220) crystalline planes of Pd, respectively, with a broad peak at 2θ = 26° attributed to rGO. The X-ray photoelectron spectroscopy (XPS) data obtained from the catalyst indicated a significant presence of Pd in the +2 oxidation state, along with some Pd (0) in a Pd (II)/Pd(0) ratio of 3.02. Over the course of 6 consecutive cycles, the performance of the Pd NPs/rGONH_2 catalyst showed no significant deterioration, indicating its potential for sustained usage.

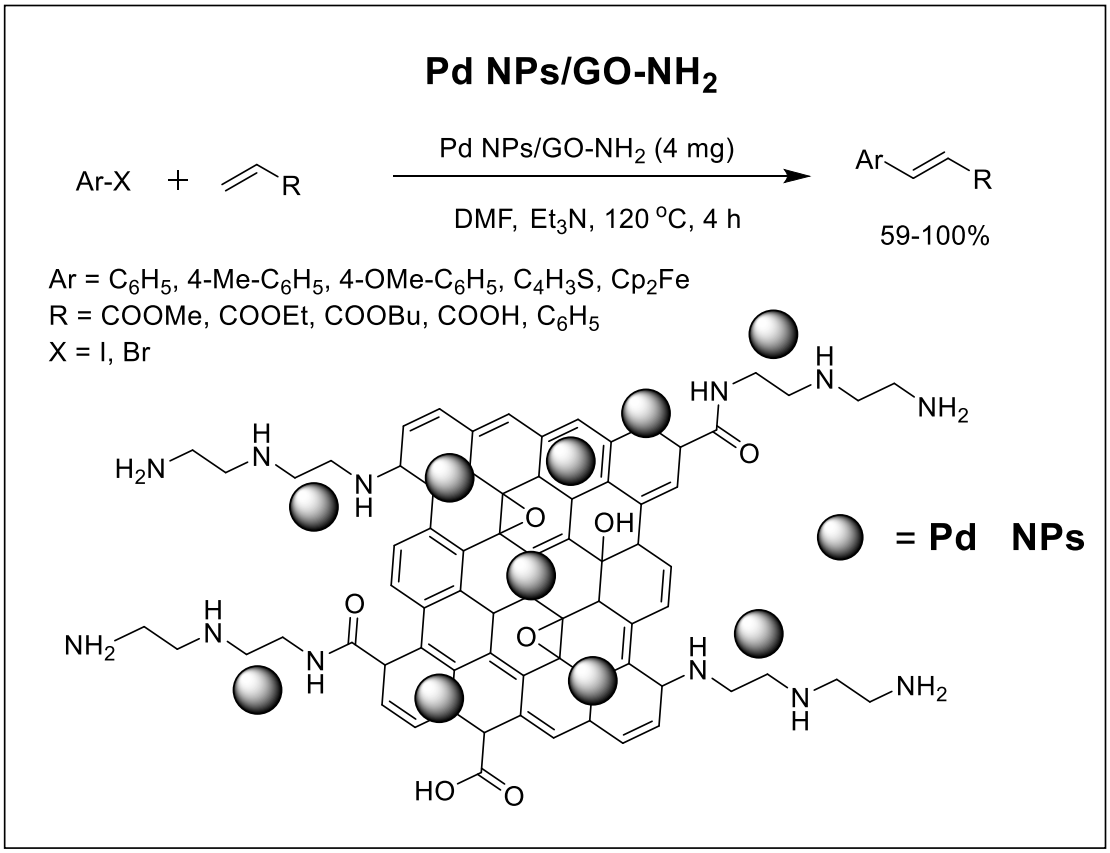

Scheme-1.5

VI. Sonogashira coupling reaction using PdCo NPs-3DG catalyst and CuI co-catalyst:

Zhai and his group[22] reported Pd phosphine complexes and CuI are widely recognized for their excellent selectivity and activity in this reaction. The Sonogashira reaction in H_2O media was investigated using CuI, PPh_3, and K_2CO_3 with PdCo bimetallic NPs supported on three-dimensional graphene (3DG). A hydrothermal reaction involving GO and ethylenediamine as a crosslinking substance was employed to synthesize the 3DG. PdCo nanoparticles were immobilized onto 3DG through the reduction of $PdCl_2$ and $CoCl_2$ with the use of ethylene glycol. The outcome indicated that the PdCo NPs–3DG composite was effective, with only a 14% decrease observed after seven runs. The product was obtained with an 80% yield after seven runs (Scheme 1.6).

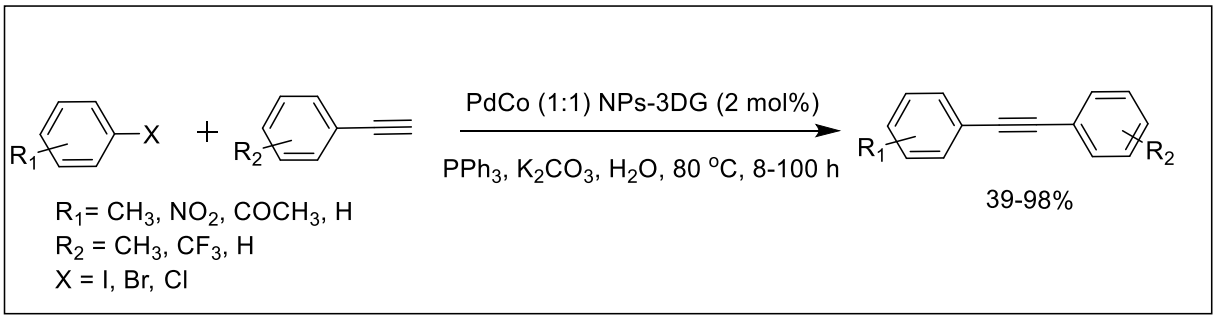

Scheme-1.6

VII. Sonogashira coupling reaction using PdCo ANP-PPI-g-graphene:

Mahyari and coworkers[23] reported that the application of PdCo alloy nanoparticles loaded onto polypropylenimine dendrimers, cultivated on a graphene support (PdCo ANP-PPI-g-graphene) in Sonogashira cross-coupling reactions. Initially, graphene functionalized with malononitrile was produced by combining GO and malononitrile, followed by reduction with $NaBH_4$ in the presence of Co(II) ions. The product obtained was incrementally introduced to acrylonitrile and MeOH, then stirred at ambient temperature in a nitrogen atmosphere for a duration of 5 days. The excess reactant and solvent were subsequently eliminated using a vacuum. MeOH and acetone were used to wash the obtained product. Subsequently, the product underwent reduction using $NaBH_4$ in the presence of Co(II) ions. This process resulted in the synthesis of first, second, and third generation PPI dendrimers on the amino functionalized graphene. Following this, a Pd(II) and PPI-g-graphene aqueous solution was sonicated with an ultrasonic bath. Subsequently, a Co(II) aqueous solution was introduced and sonicated for a duration of 20 minutes. The reaction mixture was stirred for 24 hours after the addition of a $NaBH_4$ solution, resulting in the formation of PdCo ANP-PPI-g-graphene composite. The Sonogashira coupling reaction was successfully conducted under copper and solvent-free conditions at ambient temperature, resulting in a high yield of the desired product. The catalyst exhibited the ability to be recovered and reused up to 6 times without any significant decrease in its activity. (Scheme 1.7)

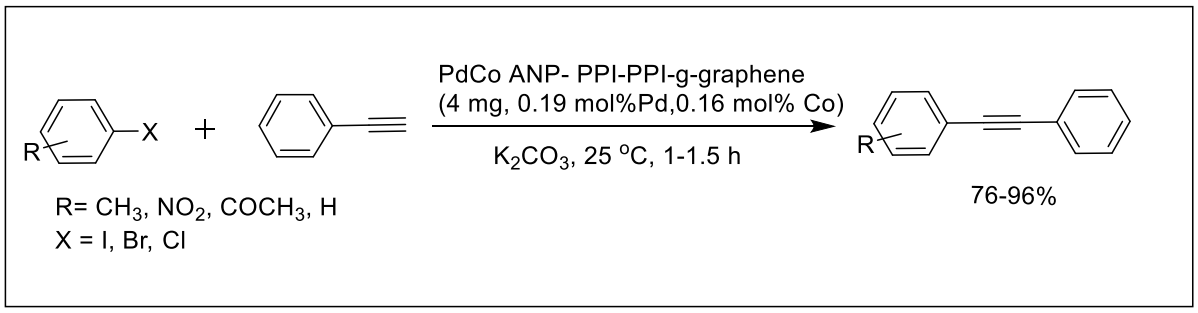

Scheme-1.7

VIII. rGO@$Cu_{48}Pd_{52}$ catalyzed the Sonogashira reaction:

Metin et. al[24] explored the use of CuPd alloy nanoparticles with a controlled ratio in the Sonogashira reaction (Scheme 1.8). Synthesis of diverse copper-palladium alloy nanoparticles and their subsequent loading onto reduced graphene oxide (rGO@CuPd) were achieved using the self-assembly process under sonication. These mixtures were utilized in the coupling reaction of several halide substances with phenylacetylene. Based on the results, it can be concluded that the rGO@$Cu_{48}Pd_{52}$ composite offers high yields in a shorter reaction time of 1-5 hours. Findings from the reusability analysis, indicated that the rGO@$Cu_{48}Pd_{52}$ composite exhibited the ability to be reused for a consecutive series of 5 cycles.

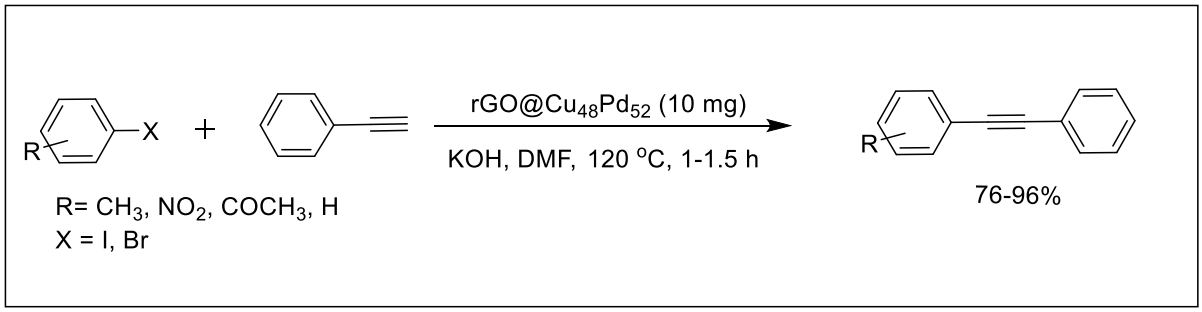

Scheme-1.8

IX. Pd/Cu@GO composite catalyzed the Sonogashira reaction:

The Sonogashira reaction, which was documented by Sultana et al. in 2020, involves the use of palladium-copper bimetallic nanoparticles loaded on GO as a catalyst.[25] Synthesis of the bimetallic composite involved the reduction of $CuSO_4.5H_2O$ and $Pd(NO_3)_2$ in water, facilitated by the addition of an extract of tulsi leaves, and subsequently treated with GO. The Sonogashira reaction between alkynes and halide compounds was facilitated by a Pd/Cu@GO catalyst, resulting in the production of internal alkynes with yields ranging from 57% to 99% (Scheme 1.9). The performance of the Pd/Cu@GO composite remained consistently high over 9 consecutive runs, without any significant decrease. The coupling process was found to proceed heterogeneously through the application of a hot-filtration experiment.

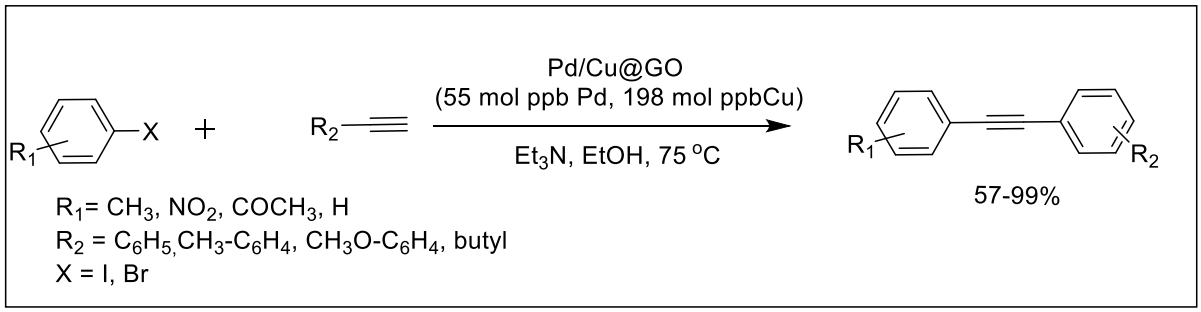

Scheme-1.9

X. Cu_2O/rGO catalyzed the Sonogashira cross-coupling reaction:

Guo and his group[26] achieved Cu_2O nanoparticles supported on reduced graphene oxide through a liquid-phase reduction method. High activity and selectivity are observed in the catalyst during the reaction between aryl halides and phenylacetylene without the presence of palladium or ligands. These nanoparticles proved to be an efficient heterogeneous catalyst for the Sonogashira cross-coupling reaction, showcasing their potential in catalytic applications. Cu_2O NPs loaded rGO (Cu_2O/rGO) was synthesized via a liquid-phase reduction technique and applied in the Sonogashira coupling of halide compounds and phenyl acetylene without the need for Pd and ligands. The Cu_2O/rGO composite proved to be efficient in the coupling reaction and maintained high stability. Despite this, a minor decline in performance was observed after five cycles (Scheme 1.10).

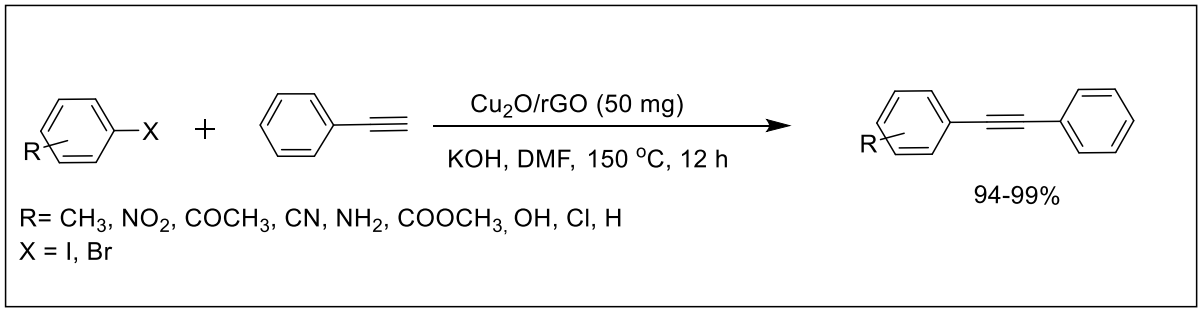

Scheme-1.10

XI. Synthesis of biaryl compounds using the heterogeneous GO-Pd nanocomposite:

Bhat[27] and his group have developed biaryl products which were synthesized using the GO-Pd nanocomposite in the Suzuki-Miyaura coupling process. The catalyst was prepared by introducing $PdCl_2$ into a graphene oxide solution in ethylene glycol, followed by sonication for 1 hour to produce a stable suspension. An autoclave lined was used to heat mixture at 180 °C for 24 h. Deionized H_2O was used to immerse the black monolith for the purpose of removing ethylene glycol. Following the freeze-drying process, the composite was dried at 80°C for the entire night. X-ray diffraction (XRD) analysis verified the presence of Pd(0) nanoparticles, measuring between 15 and 22 nm, in the GO-Pd nanocomposite. In the presence of the GO-Pd nanocomposite, boronic acid and halide compounds were successfully coupled in dioxane as the solvent and NaOMe as the base (Scheme 1.11). The significance of the catalyst's heterogeneity cannot be overlooked in the recovery of the composite. The GO-Pd material demonstrated consistent performance over 5 consecutive runs without any notable decrease. Analysis using scanning electron microscopy (SEM) and transmission electron microscopy (TEM) revealed that the particle size and shape of the catalyst remained unchanged after 5 cycles, with no agglomeration observed.

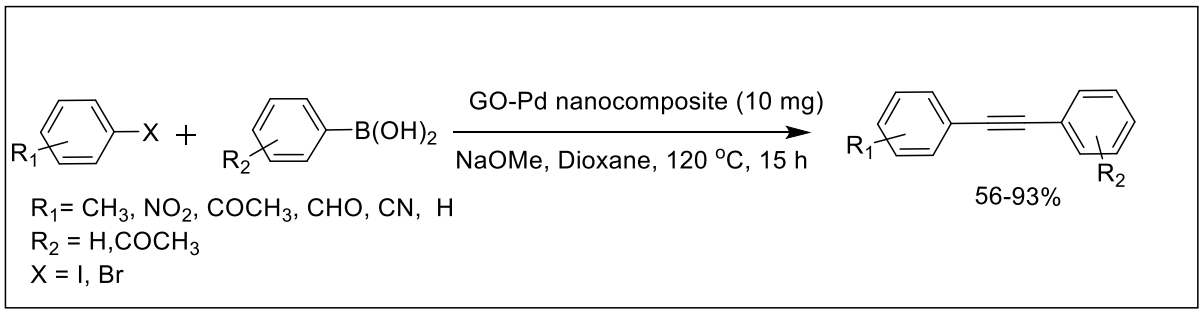

Scheme-1.11

XII. Synthesis of biaryl compounds using CDG-Pd catalyst:

Metin and his group[28] reported that the Suzuki-Miyaura cross coupling of phenylboronic acid with various aryl halides under mild conditions was carried out using monodisperse Pd NPs supported on chemically derived graphene (CDG) catalyst (CDG-Pd) (Scheme-1.12). The preparation of 5 nm Pd nanoparticles involved the reduction of Pd(II) acetylacetonate with morpholine borane complex in oleylamine, followed by their attachment onto CDG via a

liquid phase self-assembly process. Based on the TEM image and particle size histogram, it can be concluded that the Pd NPs exhibit a uniform size distribution. The average diameter of these nanoparticles is approximately 5 nm, with a standard deviation in diameter of less than 10%. This level of monodispersity is indicative of their consistent size. The X-ray diffraction pattern of the Pd nanoparticles exhibited the characteristic features of a face-centered cubic crystal structure of Pd. The CDG-Pd catalyst demonstrated the ability to be reused for up to 15 catalytic cycles, with the results showing that the catalyst retained 82% of its original catalytic activity without leaching of Pd.

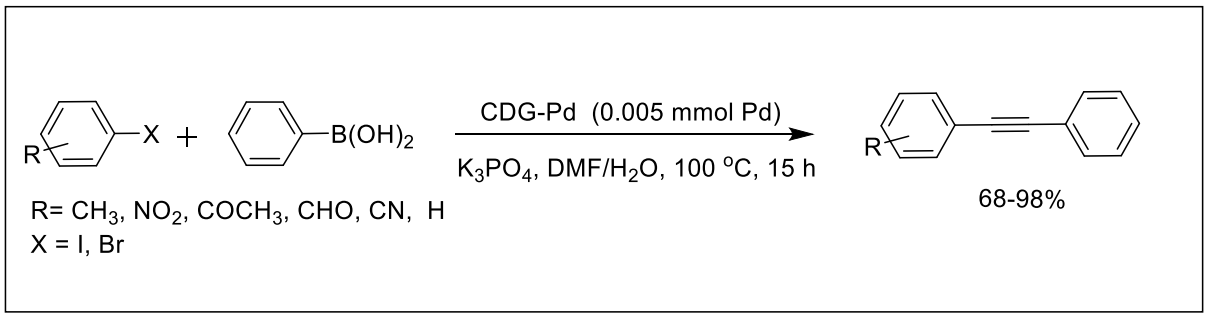

Scheme-1.12

XIII. Synthesis of diaryl ethers:

Karvembu and his group[29] have developed the use of CuO nanocatalyst enabled the C–O/C–S cross coupling reaction between aryl halides and phenol or thiophenol to take place at room temperature without the requirement of ligands. Various aryl halides and substituted phenols were successfully incorporated into the reaction scope under optimized conditions. A novel catalytic system comprising of efficient, selective, and reusable heterogeneous nano CuO has been successfully developed for facilitating room temperature C–O and C–S Ullmann type cross coupling reactions with good yields (scheme 1.13).

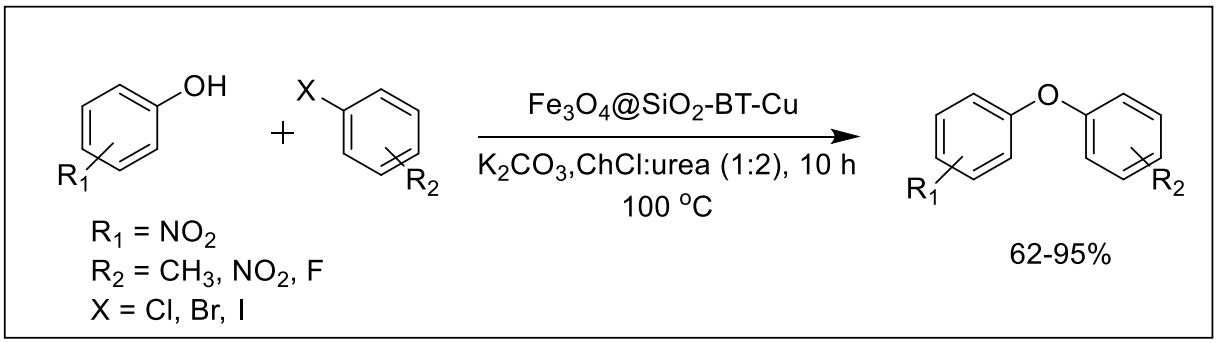

Scheme-1.13

XIV. An apparent transition metal-free direct arylation of arenes:

An interesting transition-metal-free system was reported by Jiang and co-workers[30]. Care must be taken when describing such reactions as transition metal-free. It has been shown that trace (ppb level) available in the inorganic bases used can turnover cross-coupling reactions. Jiang described an aluminium-based MOF (Al(OH)(BPYDC)) used in the DA of arenes with aryl iodides and bromides (scheme 1.14). The p,p-stacking and ion–p interactions between

the metal–organic framework, the potassium ion and the arenes apparently allow the direct arylation in absence of transition metals.

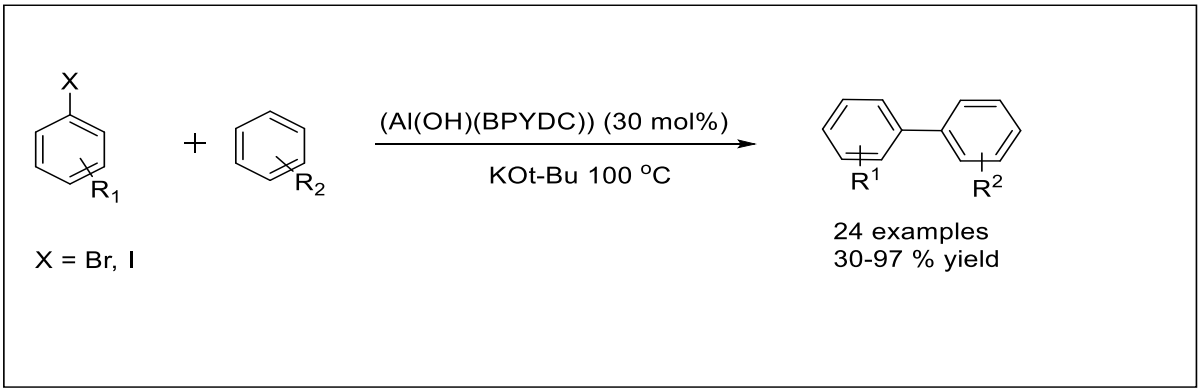

Scheme-1.14

XV. Synthesis of polyfluorobiaryls via heterogeneous copper(I)-catalyzed decarboxylative cross-coupling of potassium polyfluorobenzoates with aryl halides:

Cai and his group[31] developed the heterogeneous catalyst which using the decarboxylative cross-coupling reaction of potassium polyfluorobenzoates with aryl iodides and bromides was achieved in diglyme or DMAc at 130 °C or 160 °C in the presence of 10–20 mol% of a 1,10-phenanthroline-functionalized MCM-41-immobilized copper(I) complex, [MCM-41-PhenCuI], yielding a variety of polyfluorobiaryls in good to excellent yields (Scheme 1.15). This heterogeneous copper(I) complex could easily be prepared via a simple procedure from commercially readily available and inexpensive reagents, exhibited the same catalytic activity as the homogeneous CuI/Phen system, and was recovered by filtration of the reaction solution and recycled at least 8 times without significant loss of catalytic activity.

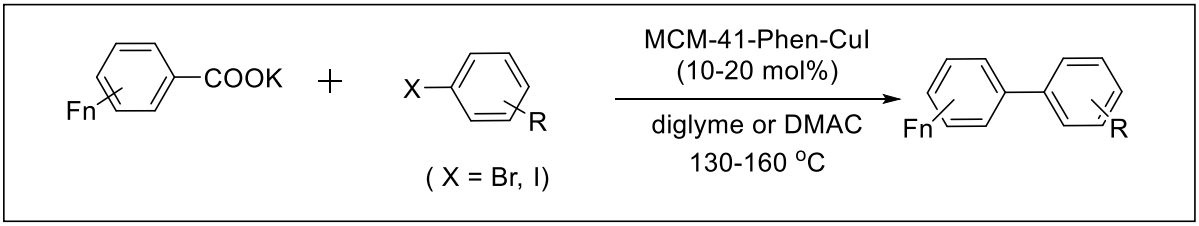

Scheme-1.15

XVI. The newly formed C–C bonds are coloured red in the products:

Owing to the shortcomings of Pd-based homogeneous catalysis, Chen and co-workers[32] performed a comparative study that incorporates the utilization of Pd atoms affixed/ anchored on exfoliated graphitic carbon nitride, *viz*., Pd–ECN and conventional homogeneous catalysts $Pd(PPh_3)_4$. These studies suggested that Pd–ECN surpasses $Pd(PPh_3)_4$ in terms of the high chemoselectivity, functional group tolerance (Scheme 1.16), and its most fascinating feature

of averting metallic lixiviation, which agrees well with the applicability and adaptability of the heterogeneous Pd catalysts, rather than state-of-the-art homogeneous catalyst for SMCR.

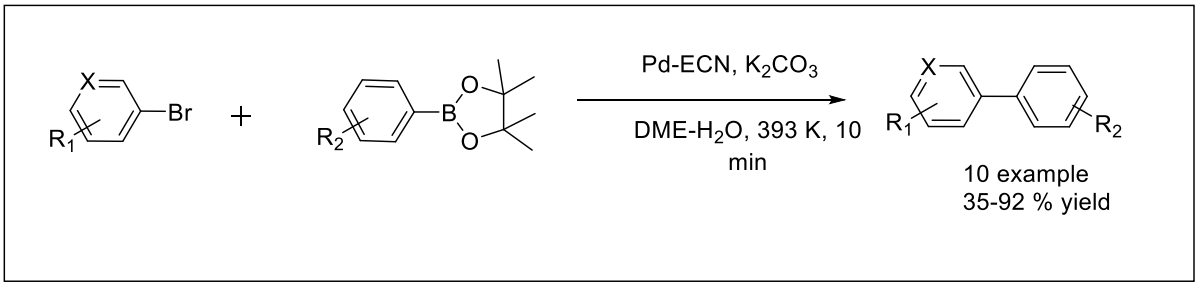

Scheme-1.16

XVII. Synthesis of the biphenyl precursor for the sartan series of drugs by using Pd/Fe_3O_4@PDA nanoparticles:

Dubey and his co-workers[33] reported Pd nanoparticles immobilized on polydopamine-coated nano-Fe3O4 catalyzed SMCR of 4-methylphenylboronic acid and 2-bromobenzonitrile, which gave 4′-methyl-[1,1′-biphenyl]-2- carbonitrile.74 This can be used as a substrate for the synthesis of potential drugs of the sartan family, like losartan, valsartan, irbesartan, olmesartan, telmisartan and candesartan (Scheme 1.17). The protocol demonstrated its suitability for the coupling of phenylboronic acid with aryl iodides with both electron-donating and electronwithdrawing groups, such as 4-methoxy, 3-methyl, 4-methyl, 4-nitro, 4-cyano, 2-pyridyl, 3-pyridyl 2-acetyl and 4-formyl (71– 91% yield). The synthetic strategy is also efficiently used for the synthesis of compounds with diverse functionalities, which may be used for the construction of prospective drug molecules. Besides, the Pd/Fe_3O_4@PDA catalyst is magnetically recoverable and the longevity studies performed on the coupling reaction of phenylboronic acid and 4-methoxy iodobenzene established its usage up to five cycles (96% yield at 5th cycle), which implies the potentiality of the catalyst.

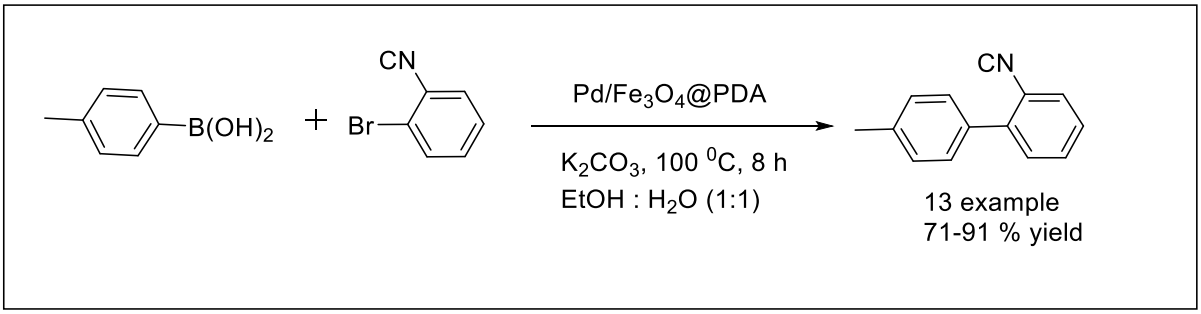

Scheme-1.17

XVIII. Pd@NH_2-MPRN catalyzed SMCR of aryl bromide and phenyl boronic acid:

Wang and co-workers[34] designed a synthetic strategy for the stabilization of Pd-nanoparticles that incorporates the usage of a primary amine-functionalized mesoporous phenolic resin to give Pd@NH_2-MPRNs, which possessed high surface area and properly dispersed Pd NPs owing to the efficient complexation with primary amine. The aryl bromides with

functionalities, such as hydroxyl, methoxy, methyl, chloro, and acetyl exhibited 73–99% yields, whereas functional groups like o-nitro, p-cyano, p-phenyl showed lower yields, viz., 24–56%. It is noteworthy that terphenyl bromide demonstrated 4.1% yield, which highlights the fact that the size of the substrate plays a crucial role in entering the pores of the catalyst. The reusability studies revealed that Pd@NH_2- MPRNs may be used up to 7 cycles without compromising the selectivity and no significant reduction in the yields (>95% yields) (scheme-1.18).

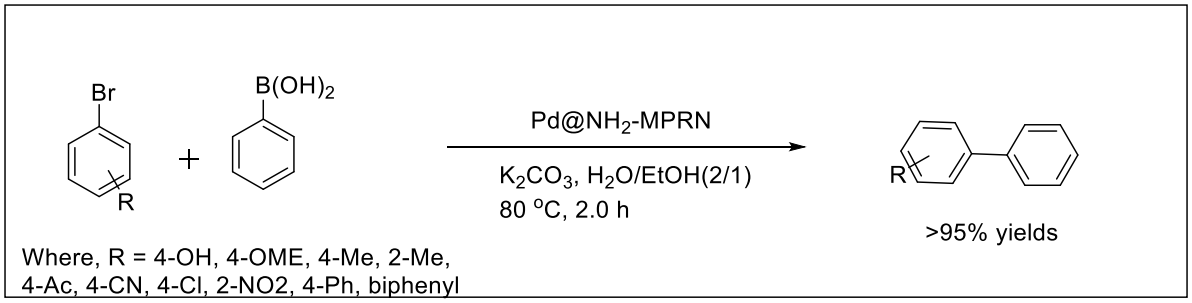

Scheme-1.18

XIX. Pd-complex catalyzed Heck reaction of aryl halides with olefins:

Yusff *et. al.*[35] prepared the heterogeneous Pd-complex was first used in Heck coupling reaction. The coupling of iodobenzene with butyl acrylate in the presence of Na_2CO_3 in aqueous DMA with 1.5 mol% of Pd complex was initially studied as a model reaction which delivered 100% conversion of the product. The Heck reaction was also efficiently promoted of aryl bromides with isopropyl acrylamide and styrene to give the corresponding coupling products in up to 92% yield (Scheme1.19). Interestingly, aryl chlorides were also promoted this coupling reaction under the similar reaction conditions with relatively poor yields.

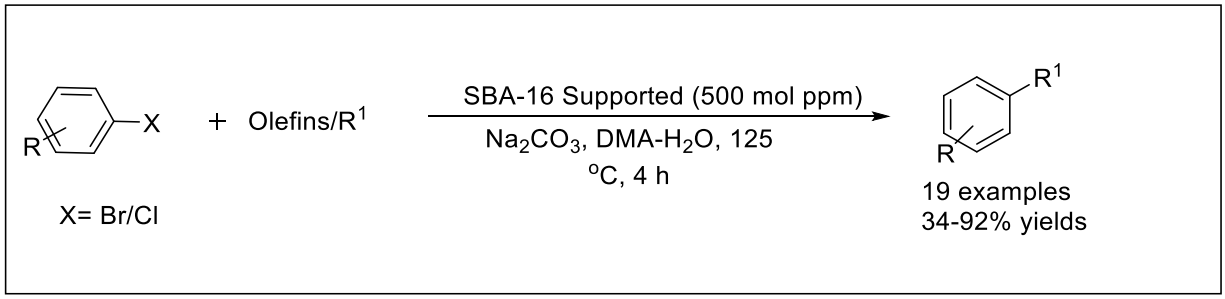

Scheme-1.19

XX. Sonogashira cross-coupling of various aryl halides in the presence of the catalyst:

The same group[33] prepared Silica-immobilized N-heterocyclic carbine Pd complex which has recently been reported as a catalyst for Suzuki cross-coupling reaction. By observing the high catalytic activity of SBA-16 supported Pd-complex in the Heck reaction hence, we turned our attention to further testify our Pd-complex for the Suzuki- Miyaura cross coupling reaction. With the heterogeneous Pd-complex (0.01 mol%, 100 mol ppm) in hand, we then tested

Suzuki-Miyaura cross coupling reaction of 4-iodoanisole with phenylboronic acid in aqueous ethanol at 90 ºC for 6 h provided the corresponding biaryl product in 92% yield. High catalytic activity was observed in the coupling of deactivated aryl iodides such as 4-iodotoluene, 4-iodophenol and 4-iodoaniline as well as activated 4-iodoacetophenone. In order to investigate the scope of aryl halides in the coupling with phenylboronic acid, various aryl bromides were used in the coupling reaction. The coupling of activated or deactivated aryl bromides proceeded cleanly with 0.01 mol% of Pd-complex to give the corresponding coupling products in up to 93% yield. It should be noted that activated 4-chloroacetophenone and deactivated 4-chloroanisole and 4-chlorotoluene were also efficiently promoted the cross-coupling reaction to provide the corresponding coupling products in up to 73% yields (Scheme 1.20).

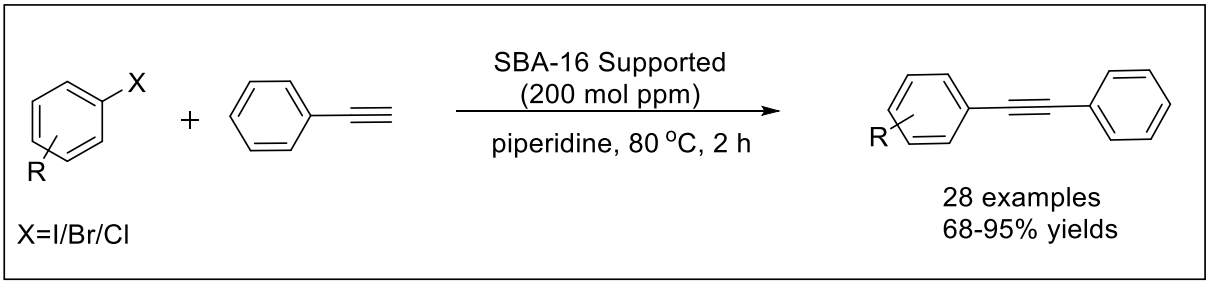

Scheme-1.20

XXI. Mizoroki–Heck cross coupling reaction:

Khorsandi and his group[36] examined the generality and versatility of this supported, cobalt-catalyzed, Mizoroki–Heck cross-coupling of aryl halides with olefins. Under the optimized conditions, a diversity of aryl iodides, bromides, and chlorides containing electron-donating and electron-withdrawing substituents efficiently reacted with methyl acrylate and styrene in air under mild conditions at 80 °C to afford the desired cross coupling products in high yields (Scheme 1.21). The experimental results showed that the electronic properties of the substituents on the aromatic rings of the starting materials had no significant effect on the reaction; however, aryl iodides were found to be more reactive than aryl bromides. Among aryl halides, aryl chlorides were found to be the ideal substrates for coupling reactions because they are inexpensive and widely available as compared to their bromide or iodide counterparts.

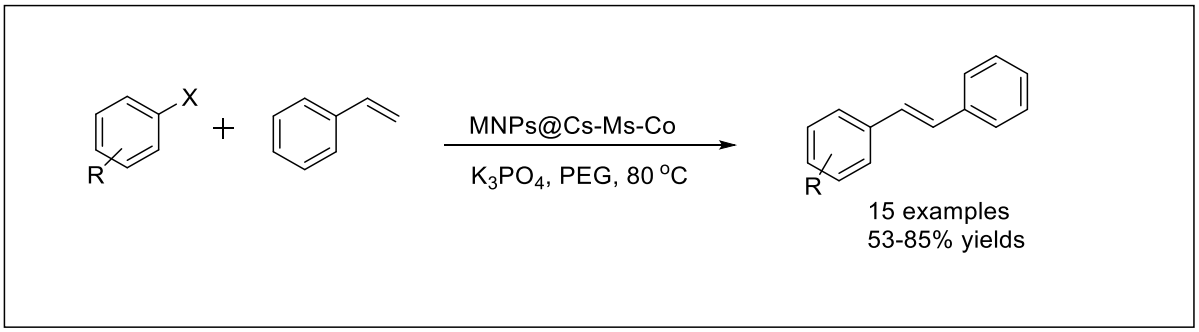

Scheme-1.21

XXII. SBA-16 supported Pd-complex catalyzed Sonogashira reaction of aryl halides:

Encouraged by the results obtained in the Heck cross-coupling, Yusoff and his co-workers[37] investigated the potential of Co-MS@MNPs/CS catalyst in the Sonogashira reaction (Scheme 1.22). To obtain the optimum experimental conditions, the reaction of phenyl acetylene with iodobenzene was considered as a model reaction in the presence of this catalyst. The effects of the reaction conditions, such as the type of base and solvent, temperature, and catalyst amount, were tested, and a summary of the optimization experiments is provided in Table 4. As can be seen, the best result was obtained using iodobenzene (1 mmol), phenyl acetylene (1.1 mmol), KOH (1.5 mmol), and 10 mg of Co-MS@MNPs/CS (1.1 mol% Co) in DMSO at 140 °C. Using the optimized reaction conditions, a variety of structurally divergent aryl iodides, bromides, and chlorides were used in the reaction with phenyl acetylene to generate the desired coupling products. The corresponding alkyne products were obtained in moderate to good yields.

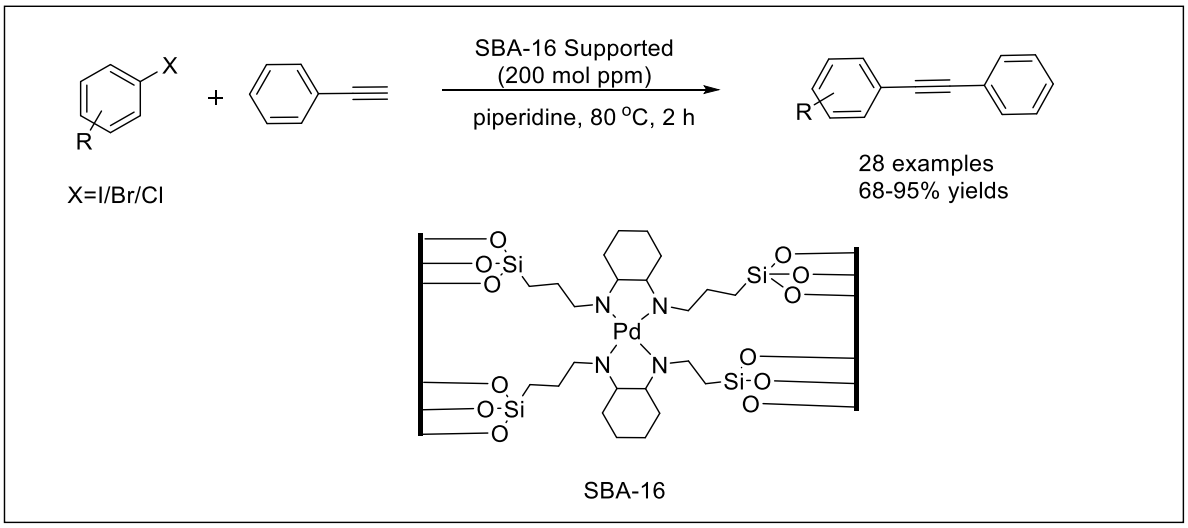

Scheme-1.22

XXIII. Reaction of aryl carbamates or sulfamates, phenylboronic acid and arylboronic acid:

Inaloo and co-works[38] synthesized a nickel-based heterogeneous magnetically separable nanocomposite known as Fe_3O_4@SiO_2–EDTA–Ni(II) MNPs. They investigated its catalytic performance in the Suzuki coupling of aryl carbamates and sulfamates with aryl boronic acid (Scheme 1.23) to produce biphenyls (>80% yield) with various functionalities using $NaOC_2H_4OH$ and ethylene glycol at 100 °C for 6 hours. The substrate scope of arylboronic acid encompassed a diverse range of aryl functionalities, including *o-, m-, p*-tolyl, naphthyl, 4-methoxyphenyl, 4-cyanophenyl, 4-nitrophenyl, 4-formylphenyl, 4-trifluoromethylphenyl, and thiophen-2-yl. Notably, both types of coupling partners, namely aryl carbamates and sulfamates with yields 80-93%. However, the substrates concerning aryl carbamates and sulfamates included the functionalities mentioned above, such as *p*-fluorophenyl, pyridin-2-

yl, pyridin-2-yl, and purimidin-4-yl groups with 79–93% yields. The diversity of functional groups in both coupling partners demonstrates their capacity to produce industrially significant compounds.

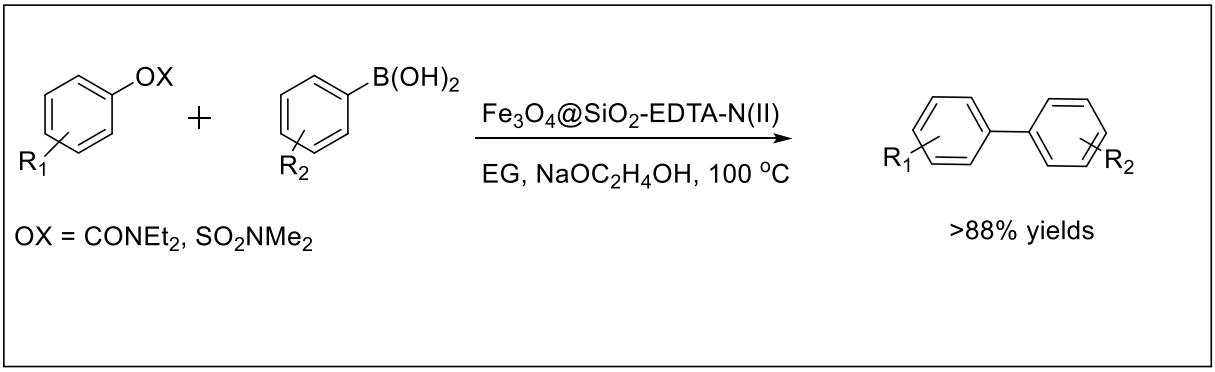

Scheme-1.23

1/c Conclusion

The C–C coupling reaction is a topic of great interest to the researchers in the field of catalysis and organic synthesis due to its significance in preparing synthetic intermediates, drugs, and organic dyes. The Suzuki-Miyaura cross-coupling reaction (SMCR) has been extensively studied using arylboronic acid/esters and aryl halide as the substrates. However, recent advancement reveals that substrates with diverse functionalities, including 1,4-naphthoquinones, alkynes, pyrido[2,3-d] pyrimidines, substituted thiophenes, aldehydes, 1,2,7-triene, and N-acyl-glutarimide amides, also can be utilized effectively in the Pd-based catalytic reactions. The utilization of Pd has been widely recognized in the selective mono-carbonylation reaction of diverse substrates. Nonetheless, challenges such as contamination of the product by Pd, leaching of metallic elements, expensive synthetic techniques, and the necessity for product purification are the limitations of Pd-based reaction protocols. Given this, a number of researchers have delved into alternative transition metals to Pd, aiming to enable the synthesis of C–C coupled products in a cost-effective and environmentally sustainable manner. Nickel has become prominent among the transition metals due to its unique features, including its smaller size, oxidation states of Ni (0)/Ni (II), as well as Ni(I)/Ni(III), and its higher nucleophilic character. On the other hand, Pd exists in a redox state of Pd (0)/Pd (II) despite its potential role as Pd (III) and Pd (IV). The recycling of the catalyst is an important issue in heterogeneous catalysis system. Transition metal catalyzed C-C cross coupling is an indispensable tool in modern synthetic chemistry. The organosilicon compounds are very attractive as the coupling partner in the C-C cross coupling reactions, mainly because of low toxicity and high natural abundance of silicon. Most of the existing methods of organosilicon compound mediated C-C cross coupling reactions involve the use of homogeneous or semi-heterogeneous catalyst which cannot be recycled. In this work, we have demonstrated the use of heterogeneous magnetic palladium catalyst in oxidative Heck coupling and Tsuji-Trost allylic coupling reactions involving organosilanes as the aryl donors. Transition metal catalyzed C-C cross coupling is an indispensable tool in modern synthetic

chemistry. The organosilicon compounds are very attractive as the coupling partner in the C-C cross coupling reactions, mainly because of low toxicity and high natural abundance of silicon. Most of the existing methods of organosilicon compound mediated C-C cross coupling reactions involve the use of homogeneous or semi-heterogeneous catalyst which cannot be recycled. In this work, we have demonstrated the use of heterogeneous magnetic palladium catalyst in oxidative Heck coupling and Tsuji-Trost allylic coupling reactions involving organosilanes as the aryl donors. Starch coated magnetic nanoparticles were used as the heterogeneous support to immobilize the Pd(II) on the surface of it. The biopolymer coated magnetic nanoparticles are well explored in the area of biomedical applications. However, this nano-material is first time used in this study to design the heterogeneous catalyst for C-C cross coupling reactions. In both the cases, the reactions were carried out under the open aerial condition in presence of magnetic catalyst. Thus, necessity of inert moisture and air free reaction set-up is avoided. The catalyst was easily recovered from the reaction mixture by an external magnet and it was recycled up to 4 times without much loss of reactivity. The oxidative Heck coupling and Tsuji-Trost allylic coupling were tested for a wide range of substrates. Efficient catalyst recyclability, benign reaction condition and good yields of the products make the protocols economically sustainable.

Section-II

Present Work:

Heterogeneous magnetic Pd (II) catalyst in C-C cross coupling reactions of organosilanes with terminal alkenes and allylic acetates

2/a Introduction

The pioneering route for constructing C-C bonds involves the cross-coupling reactions using various organometallic and organometalloid reagents. Heck coupling and Tsuji-Trost coupling are two important tools for C-C bond formations leading to total synthesis of many natural products and biologically active organic compounds.[39] The oxidative Heck reaction has recently gained more attention mainly because of air and moisture insensitive reaction conditions using organoboron,[40] organotin [41] and organosilicon [42] reagents as the coupling partners. Among common organometallic reagents organosilicon compounds are attractive due to their stability, low toxicity, low-cost and high natural abundance of silicon.[43] Although, organosilicon compounds have been employed in oxidative Heck coupling reaction for a number of times, but the use of expensive non-recyclable homogeneous catalysts makes them economically less potent. In this report, we demonstrate the use of magnetic heterogeneous catalyst to carry out the oxidative Heck coupling reactions of organosilane compounds with terminal alkenes in aerial condition. Organosilanes have also been used in this study to perform Tsuji-Trost allylation reactions with allylic acetates in presence of magnetic nano-catalyst.

Heterogeneous magnetic catalysts[44] have become popular due to easy magnetic separation of the catalyst from the reaction mixture. Additionally, the heterogeneous catalysts with good recyclability offer economic sustainability. Here, we have used the starch coated magnetic ferrite nanoparticles as the heterogeneous support of Pd (II) catalyst. The starch coated Fe_3O_4 nanoparticles have extensively been used in biomedical sciences for different purposes like drug delivery, tumor targeting, magnetic resonance imaging etc. Here We have explored the starch coated magnetic Fe_3O_4 nanoparticles to immobilize the Pd (II) catalyst on the surface of the nanoparticles. The synthesized magnetic palladium nano-catalyst has been tested to catalyze the C–C cross coupling reactions of organosilanes with alkenes and allylic acetates. Various terminal alkenes underwent smooth C (sp2)–H arylation by aryltrimethoxysilanes in presence of magnetic-Pd (II) catalyst, tetrabutylammonium fluoride (TBAF) and pbenzoquinone (BQ) as the oxidizing agent in open air condition (Scheme 1). C–C cross-coupling of allylic acetates were also performed with organosilanes using magnetic-Pd (II) catalyst and TBAF in aerial atmosphere (Scheme 1.24).

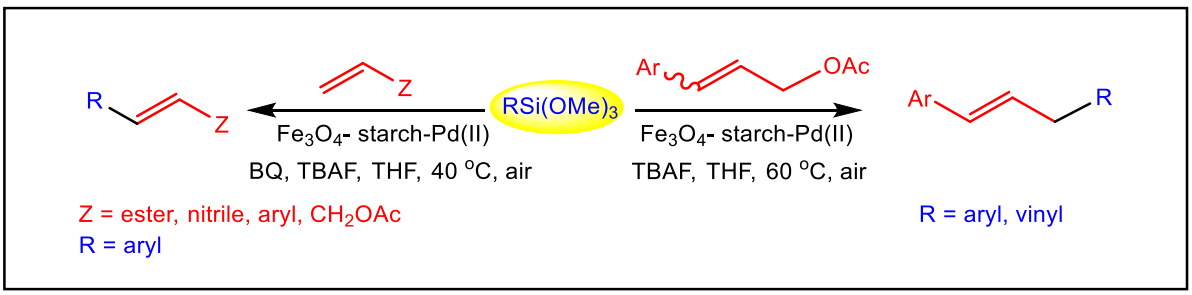

Scheme-1.24

2/b Results and Discussion

The starch coated magnetic ferrite nanoparticles were prepared following the similar methods reported earlier.[45] The Fe^{3+} and Fe^{2+} salts were dissolved in an aqueous solution of starch by heating at 60 ^{o}C. Black colored starch coated Fe_3O_4 nanoparticles were started to appear upon addition of aqueous ammonia solution. The black nanoparticles were centrifuged, washed with acetone and dried under vacuum. The Pd (II) was immobilized on the surface of starch coated Fe_3O_4 nanoparticles by stirring the methanolic suspension of the nanoparticles with $PdCl_2$ at room temperature for 15 h. The sizes of the Pd (II) immobilized starch coated magnetic nanoparticles were checked by TEM (transmission electron microscopy) experiment and it was found be 7 - 19 nm (Fig. 1.1). The surface morphology and the amount of palladium in the supported catalyst were determined by SEM (scanning electron microscope) (Fig. 1.2) along with the EDX (Energy Dispersive X-ray) (Fig. 1.3) experiments.

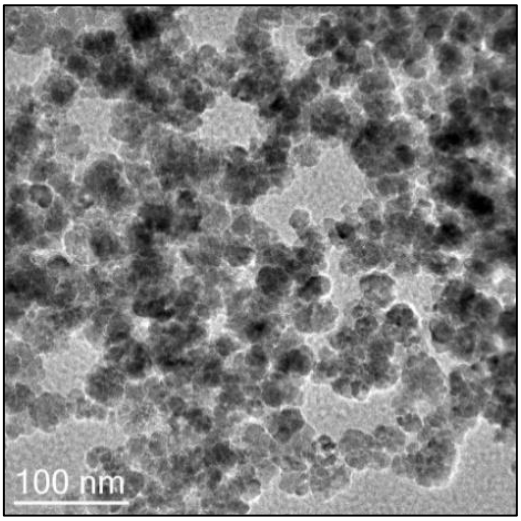

Figure 1.1 TEM image of the Pd(II) nano-catalyst.

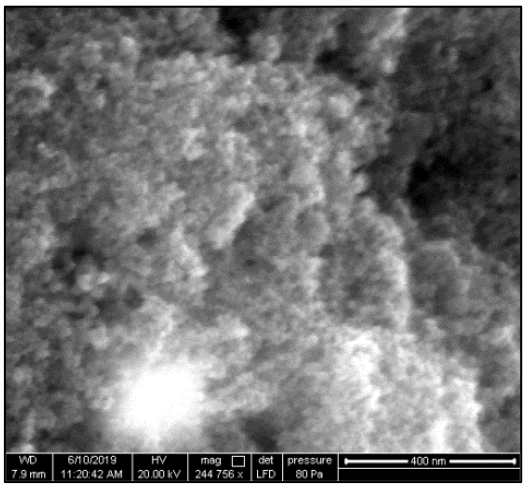

Figure 1.2 SEM image of the Pd(II) nano-catalyst.

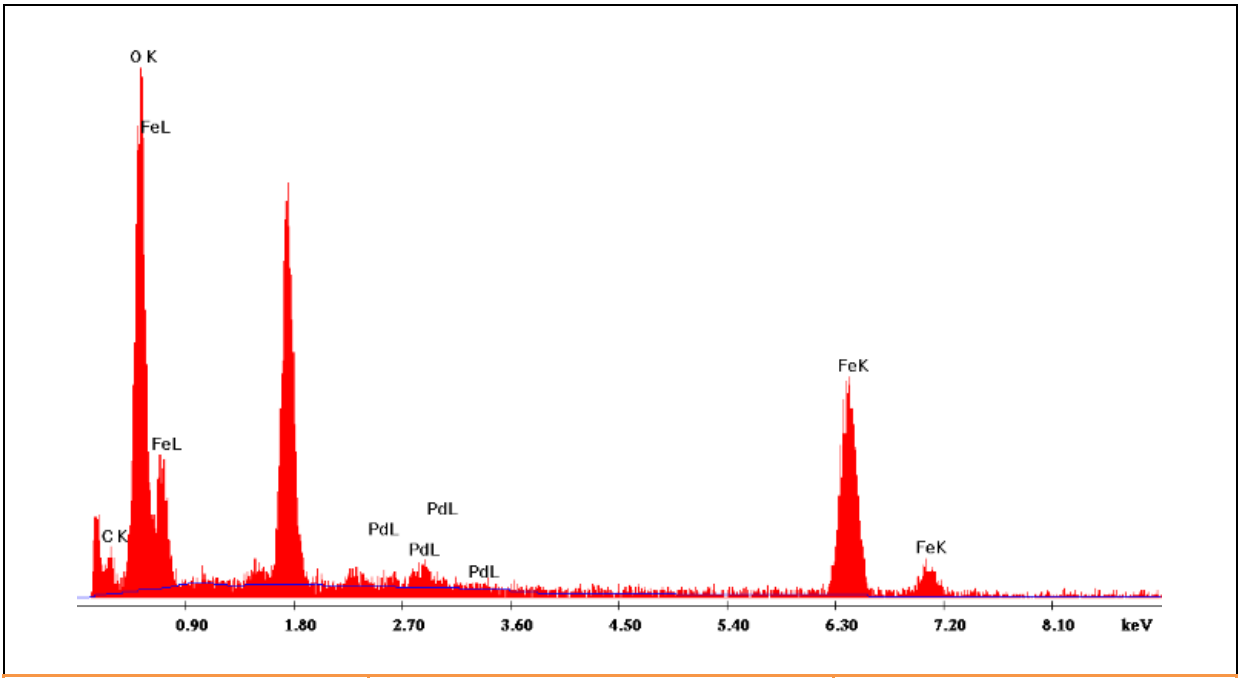

Element	Weight %	Atomic %
C K	15.06	28.42
O K	38.09	53.46
Pd L	4.92	1.05
Fe K	41.93	17.07

Figure 1.3 Energy Dispersive X-ray spectrum (EDX) and the elemental analysis table of the Pd (II) nano-catalyst [Fe_3O_4-starch-Pd (II)].

The weight percentage of palladium in the supported magnetic catalyst is found to be 4.92 as per the EDX elemental compositional analysis (Fig. 1.3, elemental analysis table).The oxidative Heck coupling reaction was performed by simple experimental procedure. The solution of terminal alkene and organosilane (1.5 equiv.) in THF solvent was stirred at 40 ^{o}C in presence of p-benzoquinone (BQ), tetrabutylammonium fluoride (TBAF) and Pd (II) magnetic catalyst under aerial atmosphere for a certain time period. Upon completion of reaction (monitored by TLC), the catalyst was separated magnetically and the desired product was obtained by usual work-up followed by column chromatographic purification.

The reaction condition was optimized by performing a set of reactions between butyl acrylate and phenyltrimethoxysilane with variation of different reaction parameters (Table 1.1). The coupling between butyl acrylate and phenyltrimethoxysilane was first tried using Pd (II)-magnetic nanocatalyst in presence of *p*-benzoquinone (BQ) and TBAF in DMF solvent (entry 1, Table 1.1). However, the yield was not satisfactory (48%). Other common solvents like DMSO, water, acetonitrile (entries 2 - 4, Table 1.1) were also not suitable for the coupling reaction.

Table 1.1 Optimization of the reaction condition for oxidative Heck coupling reaction.[a]

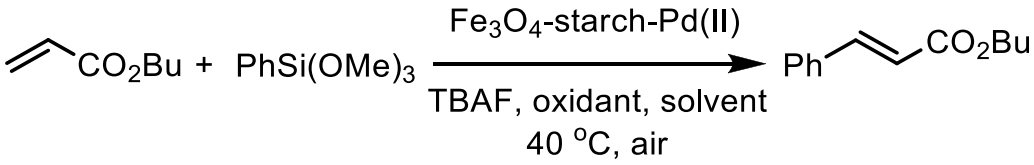

Entry	Amount of $PhSi(OMe)_3$, (equiv.)	Solvent	Oxidant	Time (h)	Yield (%)
1	1.5	DMF	BQ	12	48
2	1.5	DMSO	BQ	12	39
3	1.5	H_2O	BQ	12	28
4	1.5	CH_3CN	BQ	12	16
5	**1.5**	**THF**	**BQ**	**12**	**80**
6	1.2	THF	BQ	12	60
7	1.5	THF	BQ	10	73
8	1.5	THF	DDQ	12	-
9	1.5	THF	-	12	26

[a] Reaction condition: Butyl acrylate (51 mg , 0.4 mmol), phenyl trimethoxysilane (120 mg, 0.6 mmol), Pd-catalyst (7 mg), BQ (64 mg, 0.6 mmol), TBAF (1 M Solution in THF, 0.6mL, 0.6 mmol) in THF (2 mL), at 40 ^oC for 12h.

The reaction was found to proceed efficiently in presence of magnetic-Pd (II)catalyst, p-benzoquinone oxidant and TBAF in THF medium under aerial condition at 40 ^oC to produce the desired product with 80% of yield in 12 h of reaction time period (entry 5, Table 1.1). The reaction remained incomplete within 10 h of tim period (entry 7, Table 1.1). However, the yield of the reaction did not improve prolonging the reaction time period beyond 12 h. In presence of DDQ as the oxidizing agent, a complex reaction mixture was obtained with the formation of several unidentified side-products (entry 8, Table 1.1). The crucial role of *p*-benzoquinone oxidant in the coupling reaction of butyl acrylate and phenyltrimethoxysilane was established by the control experiment (entry 9, Table 1.1) which produces the desired product only in 26% of yield in absence of *p*-benzoquinone. The reaction did not initiate at all without the Pd-catalyst.

Table 1.2 Oxidative Heck coupling using aryltrimethoxysilanes.[a]

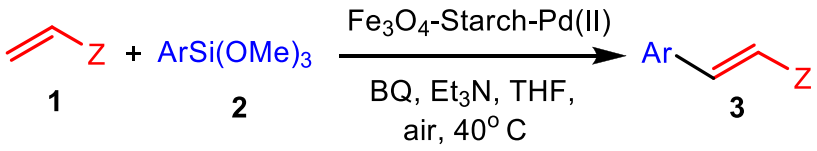

1 2 3

Entry	Z	Ar	Time (h)	Product	Yield[b] (%)
1	CO_2Bu	Ph	12	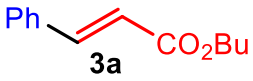 3a	80
2	CO_2Et	Ph	12	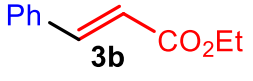 3b	77
3	CO_2Me	Ph	12	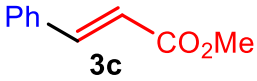 3c	76
4	Ph	Ph	13	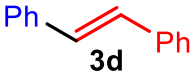 3d	74
5	CN	Ph	12	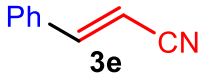 3e	78
6	*p*-F-C_6H_4	Ph	12	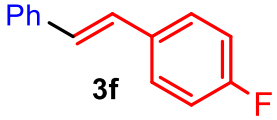 3f	76
7	*m*-CH_3-C_6H_4	Ph	14	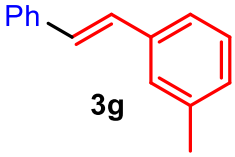 3g	72
8	*p*-CH_3-C_6H_4	Ph	15	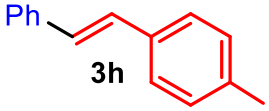 3h	68
9[c]	CH_2OAc	Ph	14	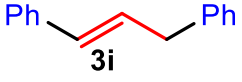 3i	69
10	CO_2Bu	*p*-CH_3-C_6H_4	14	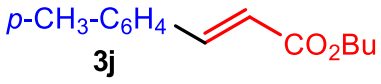 3j	70
11	Ph	*p*-OCH_3-C_6H_4	14	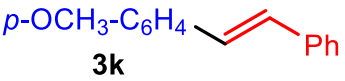 3k	68

[a] Reaction condition: alkene (0.4 mmol), aryl trimethoxysilane (0.6 mmol), Pd-catalyst (7 mg, 0.8 mol%), BQ (64 mg, 0.6 mmol), TBAF (1 M Solution in THF, 0.6mL, 0.6 mmol) in THF (2 mL), at 40 °C for certain time period. [b] Yields are isolated yields. [c] The reaction was performed using 1.2 mmol (3 equiv.) of phenyltrimethoxysilane.

The optimized reaction protocol (entry 5, Table 1.1) was explored to perform a series of oxidative coupling reactions (Table 1.2). Various electron deficient alkenes such as methyl acrylate, ethyl acrylate, butyl acrylate and acrylonitrile underwent oxidative C-H arylation reactions with the organosilicon compounds to produce the desired coupling products in good yields (**3a** - **3c**, **3e**, **3j**, Table 1.2). Styrene, 4-fluorostyrene, 3-methylstyrene and 4-methylstyrene were also employed in the oxidative cross coupling reactions resulting the products **3d**, **3f** - **3h**, **3k** (Table 1.2) satisfactorily. Under the similar reaction condition, allyl acetate produces 1,3-diphenyl propene (43%) along with trace amount of cinnamyl acetate in presence of 1.5 equivalent of phenyltrimethoxysilane in 14 h of time period (reaction 1, Scheme 1.25). However, the same reaction produces cinnamyl acetate (30%) and trace amount 1,3-diphenyl propene within 3 h of time period (reaction 2,). With time, the amount of 1,3-diphenyl propene gradually increases in the reaction mixture and the concentration of cinnamyl acetate decreases. Thus, allyl acetate participates in cascade oxidative coupling followed by Tsuji-Trost allylation reaction. In presence of large excess of phenyltrimethoxysilane (3 equivalent), exclusive formation of 1,3-diphenyl propene was obtained in good amount (69%) within 14 h of time period (entry 9, Table 1.2) *via* the cascade oxidative coupling and allyl-aryl cross coupling reactions.

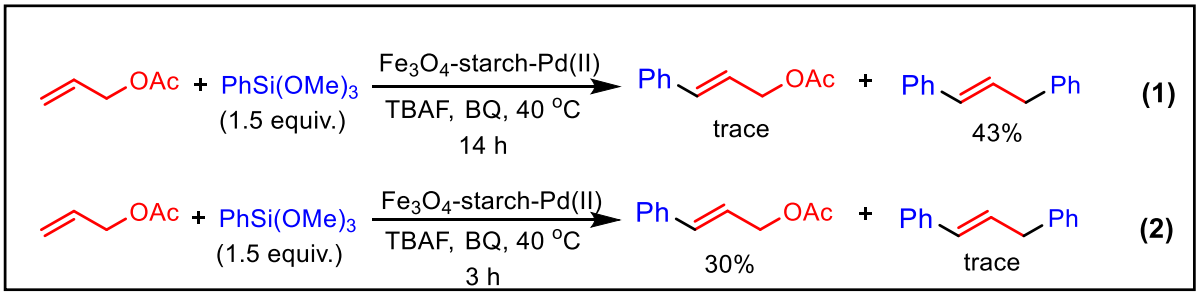

Scheme-1.25 Reactions of allyl acetate with phenyltrimethoxysilane.

This result motivated us to explore the Pd-magnetic catalyst in Tsuji-Trost allylation reaction of cinnamyl acetate. It was found that cinnamyl acetate undergoes Tsuji-Trost cross-coupling reaction with phenyltrimethoxysilane efficiently to provide the desired coupling product, 1,3-diphenyl propene in good yield (84%) (entry 1, Table 1.3) in presence of Fe_3O_4-starch-Pd (II) catalyst and TBAF in THF solvent at 60 ^oC under open aerial condition. Tsuji-Trost allylic couplings were performed with a series of cinnamyl acetate derivatives using various organosilane compounds (Table 1.3).

Table 1.3 Tsuji-Trost allylic couplings using organosilane compounds.[a]

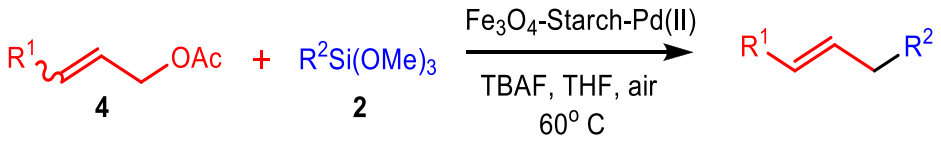

Entry	allylic acetate	R^2	time(h)	Product	Yield[b] (%)
1	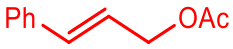	Ph	4	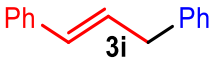 **3i**	84
2		Ph	4	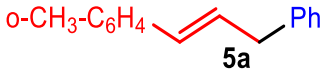 **5a**	70
3		Ph	4.5	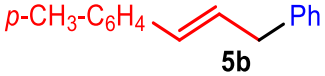 **5b**	76
4		p-CH3-C6H4	6	 **5c**	60
5		Ph	5	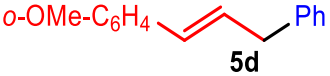 **5d**	68
6		Ph	4.5	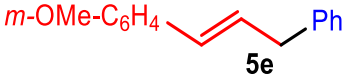 **5e**	78
7	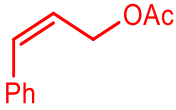	Ph	4	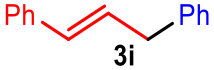 **3i**	82
8		Ph	4	 **5g**	89
9		p-CH3-C6H4	4.5	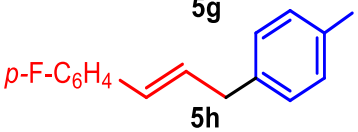 **5h**	74
10		Ph	4.5	 **5i**	86
11	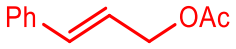	C2H3	4.5	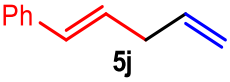 **5j**	74

[a] Reaction condition: allylic acetate (0.4 mmol), organosilicon compound (0.6 mmol), Pd-catalyst (7 mg, 0.8 mol%), TBAF (1 M Solution in THF, 0.6mL, 0.6 mmol) in THF (2 mL), at 60 °C for certain time period. [b] Yields are isolated yields.

The substituents like *o*-Me, *p*-Me, *o*-OMe, *m*-OMe, *p*-F, *p*-Cl (entries 2 - 6, 8 - 10, Table 1.3) present in the aromatic ring of cinnamyl acetates remain unaltered under the present reaction condition. In case of *p*-chlorocinnamyl acetate, the C^{sp2}-Cl functionality did not involve in C-C cross coupling with phenyltrimethoxysilane and selective allyl-aryl cross coupling occurred to provide the desired 1,3-diaryl propene (**5i**) product in good yield (86%) (entry 10, Table 1.3) under the present reaction condition. The vinyltrimethoxysilane was also found reactive

to transfer the vinyl group resulting the formation of 1,4-diene product (**5j**) in 74% yield (entry 11, Table 1.3). Interestingly, the *cis*-cinnamyl acetate undergoes Tsuji-Trost coupling with phenyltrimethoxysilane (entry 7, Table 1.31) to provide *trans*-1,3-diphenylpropene (**3i**) exclusively. This result suggests the formation of -allyl complex of palladium (**A**) as the key intermediate (Scheme 1.26) which equilibrates with its *trans*-geometry (**C**), *via* the well-known η1-σ-alkyl complex (**B**)[46] and reductive elimination from the more stable *trans*-intermediate (**C**) produces *trans*-1,3-diphenylpropene (**3i**) as the sole product.1

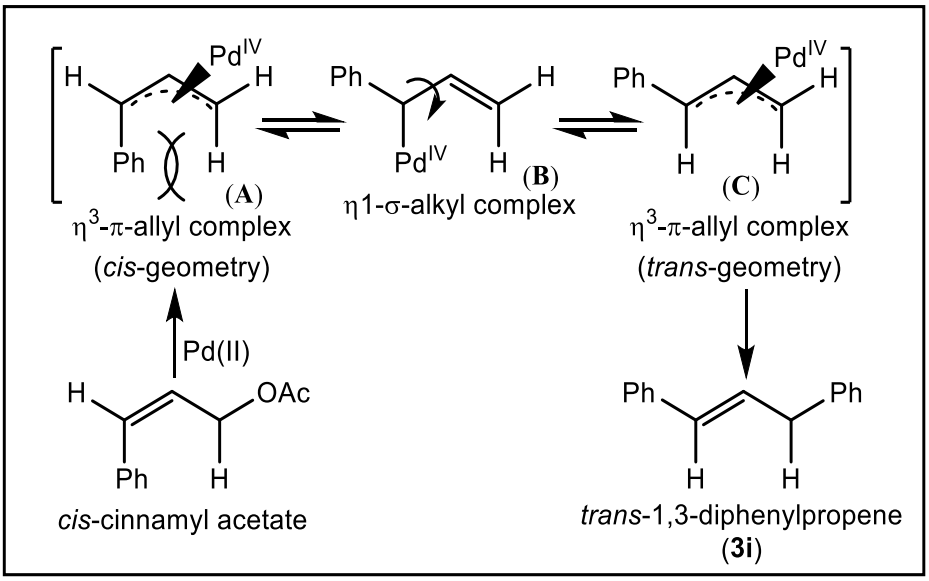

Scheme-1. 26 Formation of *trans*-1,3-diphenylpropene from *cis*-cinnamyl acetate *via* -allyl complex.

Upon completion of the reaction, the magnetic palladium catalyst can be recovered easily from the reaction mixture with the aid of an external magnet (Fig 1.4). After washing the catalyst with acetone and drying under vacuum, the catalyst was used in the next batch of reaction efficiently. It has been found that the catalyst can be recycled for 4 times without much loss of catalytic activity.

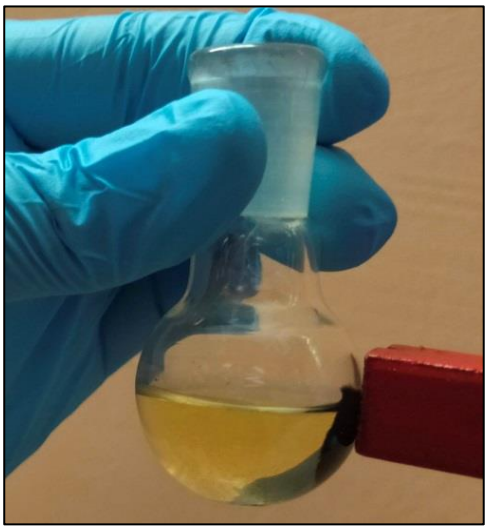

Figure-1.4 Magnetic separation of Fe_3O_4-starch-Pd(II) catalyst by an external magnet.

2/c Conclusion

In conclusion, efficient protocols for C-C cross coupling reactions such as oxidative Heck coupling and Tsuji-Trost allylation have been developed using organosilicon compounds as aryl donors and heterogeneous magnetic palladium catalyst. The biopolymer (starch) coated magnetic nanoparticles were used as the heterogeneous support for palladium catalyst which is easy to recover and shows good recyclability. The catalyst allows the reactions to proceed under open aerial condition and thus avoids the necessity of moisture and oxygen free inert atmosphere. Catalyst reusability, air compatibility and good yields of the products make the protocols economically sustainable.

2/d Experimental Section

All the commercial starting materials and reagents were used without further purification. Silica gel (silica gel, f24) TLC plates were purchased from Merck. In column chromatographic purification process, silica gel 60-120 mesh has been used. ^{1}H NMR spectra were recorded using Brucker Spectrometer at 400 MHz and 500 MHz. ^{13}C NMR spectra were recorded at 100 MHz and 125 MHz. In all NMR, $CDCl_3$ and TMS have been used as solvent and internal standard respectively. The chemical shifts are reported in ppm scale considering standard signal of TMS at 0.00 ppm. The coupling constants (*J* values) are measured in Hz. The ICP-AES elemental analysis was performed in Model Spectrometer ARCOS 130 MV (Spectro Analytical Instruments GmbH, Kleve, Germany).

General experimental procedure for cross-coupling reactions:

Representative experimental procedure for oxidative-Heck coupling reaction of n-butyl acrylate with phenyl trimethoxysilane

A mixture of n- butyl acrylate (0.051 g, 0.4 mmol), phenyl trimethoxysilane (0.120 g, 0.6 mmol), Pd-catalyst (7 mg, 0.8 mol%), TBAF (1M solution in THF, 0.6 mL, 0.6 mmol), and BQ (0.064 g, 0.6mmol), in THF (2 ml), was stirred at 40 ^{o}C for 12h under aerial atmosphere. The progress of the reaction was monitored by TLC. After completion of the reaction the Pd-catalyst was separated by an external magnet and the crude product was obtained by usual work- up using EtOAc. The crude product was purified by column chromatography over silica gel using petroleum ether-ethyl acetate (97:3) solvent mixture. The desired product, n-butyl cinnamate (3a) was obtained as colorless oil (65 mg, 80%).

Representative experimental procedure for Tsuji-Trost coupling of cinnamyl acetate with phenyl trimethoxysilane

A mixture of cinnamyl acetate (0.070 g, 0.4 mmol), phenyl trimethoxysilane (0.120 g, 0.6 mmol), Pd-catalyst (7 mg, 0.8 mol%) and TBAF (1 M solution in THF, 0.6 mL, 0.6 mmol) in THF (2 mL) was stirred at 60 ^{o}C for 4h under air atmosphere. The reaction was monitored by TLC. After catalyst separation by external magnet, the reaction mixture worked-up by usual procedure using ethyl acetate. The crude product was purified by column chromatography over silica gel using petroleum ether-ethyl acetate (99:1) solvent mixture to get the desired product, 1,3-diphenyl propene (3i) as a colorless oil (65.4 mg, 84%).

Characterization data of all products

(E)-n- Butyl cinnamate (3a, Table 2): Colorless oil; ^{1}H NMR ($CDCl_3$, 400 MHz) δ 7.68 (d, *J*=16.0 Hz, 1H) 7.54-7.51 (m, 2H), 7.39-7.37 (m, 3H), 6.44 (d, *J*=16 Hz, 1H), 4.21 (t, *J*=6.8 Hz, 2H), 1.73-1. 65(m, 2H), 1.48-1.39 (m, 2H), 0.96(t, *J*=7.2 Hz, 3H), ^{13}C NMR ($CDCl_3$) δ 167.21, 144.62, 134.65, 130.31, 128.99, 128.17, 118.47, 64.56, 30.94, 19.34, 13.87.

(E)-Ethyl cinnamate (3b, Table 2): colorless oil; ^{1}H NMR ($CDCl_3$, 400 MHz) δ 7.68 (d, *J*=16 Hz, 1H); 7.53-7.51 (m, 2H), 7.38-7.37 (m, 3H), 6.43 (d, *J*=16 Hz, 1H), 4.26 (q, *J*=7.2 Hz, 2H), 1.34 (t, *J*=7.2 Hz, 3H). ^{13}C NMR ($CDCl_3$) δ 167.00, 144.58, 134.51, 130.20, 128.87, 128.04, 118.32, 60.50, 14.32.

(E) –Methyl cinnamate (3c, Table 2): colorless oil; ^{1}H NMR ($CDCl_3$, 400 MHz) δ 7.69 (d, *J*=16 Hz 1H), 7.52-7.51 (m, 2H), 7.39-7.37 (m, 3H), 6.44 (d, *J*=16 Hz, 1H), 3.80 (s, 3H), ^{13}C NMR ($CDCl_3$) δ 167.54, 144.99,134.54, 130.41, 129.01, 128.19, 117.96, 51.81.

trans-Stilbene (3d, Table 2): white solid; ^{1}H NMR (CDCl3,400 MHz) δ 7.53 (d, *J*=7.2 Hz, 4H), 7.37 (t, *J*=7.6 Hz, 4H), 7.28-7.25 (m, 2H), 7.12(s, 2H), ^{13}C NMR (CDCl3) δ 137.50, 128.87, 128.82, 127.76, 126.66.

(E)-Cinnamonitrile (3e, Table 2): colorless oil; ^{1}H NMR (CDCl3, 400 MHz) δ 7.45-7.25 (m, 6H), 5.87 (d, *J*= 16.4 Hz, 1H), ^{13}C NMR ($CDCl_3$) δ 150.58, 133.56, 131.21, 129.12, 127.35, 118.10, 96.39.

(E)-4-Fluorostilbene (3f, Table 2): white solid; ^{1}H NMR (CDCl3, 400 MHz) δ 7.51-7.46 (m, 4H), 7.38-7.35 (m, 2H), 7.28-725 (m, 1H), 7.09-7.00 (m, 4H), ^{13}C NMR (CDCl3,) δ 164.02, 137.22, 133.56, 128.71, 128.54, 128.02, 127.67, 127.52, 126.45, 115.61.

(E) -3-Methylstilbene (3g, Table 2): white solid; ^{1}H NMR ($CDCl_3$, 400 MHz) δ 7.52 (d, *J*=7.6 Hz, 2H), 7.38-7.32 (m, 4H), 7.27-7.24 (m, 2H), 7.10-7.08 (m, 3H), 2.39 (s, 3H), ^{13}C NMR ($CDCl_3$) δ 138.35, 137.60, 137.44, 128.98, 128.80, 128.71, 128.65, 128.59, 127.67, 127.35, 126.62, 123.85, 21.57.

(E)-4-Methylstilbene (3h, Table 2): white solid;^{1}H NMR ($CDCl_3$, 400 MHz) δ 7.52 (d, *J*=7.6 Hz, 2H), 7.43 (d, *J*=8 Hz, 2H), 7.36 (t, *J*=7.6 Hz, 2H),7.27-7.26 (m, 1H), 7.18 (d, *J*=7.6 Hz, 2H), 7.1-7.09 (m , 2H), 2.37 (s, 1H), ^{13}C NMR (CDCl3) δ 137.69, 137.66 , 134.73, 129.54, 128.79, 127.87, 127.54, 126.58, 126.54, 21.38.

(E)-1,3-Diphenylpropene (3i, Table 2): colorless oil; ^{1}H NMR ($CDCl_3$, 400 MHz) δ 7.41-7.22 (m, 10H), 6.50 (d, *J*=15.6 Hz, 1H), 6.43-6.36 (m, 1H), 3.59, (d, *J*=6.4 Hz, 2H), ^{13}C NMR ($CDCl_3$) δ 140.18, 137.51, 131.09, 129.24, 129.01, 128.67, 128.50, 127.11, 126.18, 126.14, 39.36.

(E)-n-Butyl 3-p-tolylacrylate (3j, Table 2): colorless oil; ^{1}H NMR ($CDCl_3$, 400 MHz) δ 7.65 (d, *J*=16Hz, 1H 7.42 (d, *J*=8Hz, 2H) 7.18 (d, *J*=7.6Hz, 2H),, 6.39(d, *J*=16Hz, 1H), 4.20 (t, *J*=6.4Hz, 2H), 2.37(s, 3H), 1.72-1.65 (m, 2H), 1.46-1.41 (m, 2H), 0.96 (t, *J*= 7.2 Hz, 3H), ^{13}C NMR ($CDCl_3$) δ 167.28, 144.53, 140.58, 131.79, 129.59, 128.03, 117.24, 64.33, 30.81, 21..43, 19.20, 13.73.

(E)-4-Methoxystilbene (3k, Table 2): white solid; ^{1}H NMR ($CDCl_3$, 400 MHz) δ 7.50-7.44 (m, 4H), 7.34 (t, *J*=7.2 Hz, 2H), 7.25-7.23(m, 1H), 7.07 (d, *J*=16 Hz, 1H), 6.93 (d, *J*=16 Hz, 1H), 6.90(d, *J*=8.4Hz, 2H), 3.83(s, 3H), ^{13}C NMR ($CDCl_3$) δ 159.49, 137.83, 130.34, 128.79, 128.39, 127.87, 127.36, 126.81, 126.41, 114.31, 55.48.

(E)-1-(2-Methylphenyl)-3-phenylpropene(5a, Table 3): colorless oil ; ^{1}H NMR ($CDCl_3$, 400 MHz) δ 7.44-7.42 (m, 1H), 7.34-7.21(m, 5H), 7.16-7.14(m,3H), 6.68(d, *J*=15.6 Hz, 1H), 6.28-6.20(m, 1H), 3.59(d, J=6.8 Hz, 2H), 2.35(s,3H), ^{13}C NMR ($CDCl_3$) δ 140.49, 136.76, 135.22, 130.65, 130.31, , 129.18, 128.75, 128.61,127.17, 126.27, 126.15, 125.74, 39.78, 19.95.

(E)-1-(4-Methylpphenyl)-3-phenylpropene(5b, Table 3):colorless oil;^{1}H NMR ($CDCl_3$, 400 MHz) δ 7.35-7.22 (m, 7H), 7.13 (d, *J*=8 Hz, 2H), 6.46(d, *J*=16 Hz, 1H), 6.37-6.31(m, 1H), 3.56(d, J=6.8 Hz, 2H), 2.35(s, 3H), ^{13}C NMR: ($CDCl_3$) δ 140.41, 136.87, 134.78, 131.00, 129.25, 128.72, 128.52, 128.23, 126.18, 126.09, 39.40, 21.20.

(E)-1,3-Ditolylpropene (5c, Table 3):white solid:^{1}H NMR ($CDCl_3$, 400 MHz) δ 7.26(d, *J*=8 Hz, 2H), 7.16-7.10(m, 6H), 6.43(d, *J*=15.6 Hz, 1H), 6.34-6.28(m, 1H), 3.51(d, *J*=6.8 Hz, 2H), 2.34(s, 3H), 2.33(s, 3H), ^{13}CNMR ($CDCl_3$) δ 137.27, 136.77,135.62,134.81, 130.72, 129.18,128.56, 128.50, 126.03, 38.93,21.14, 21.02.

(E)-1-(2-Methoxyphenyl)-3-phenylpropene(5d, Table 3): colorless oil;^{1}H NMR ($CDCl_3$, 400 MHz) δ 7.42 (d, *J*=7.6 Hz, 1H), 7.32-7.17(m, 6H), 6.92-6.80 (m, 3H), 6.39-6.33 (m, 1H), 3.85 (s, 3H), 3.58(d, *J*=7.2 Hz, 2H), ^{13}C NMR ($CDCl_3$) δ 156.48,140.57,129.81, 128.65, 128.44, 128.12, 126.64, 126.58, 126.06, 125.80, 120.64, 110.86, 55.48, 39.87.

(E)-1-(3-Methoxyphenyl)-3-phenylpropene (5e, Table 3): colorless oil;^{1}H NMR (CDCl3, 400 MHz) δ 7.34-7.19 (m, 6H), 6.96 (d, *J*=7.6 Hz, 1H), 6.90 (s, 1H), 6.78-6.76 (m, 1H),6.42-6.38(m, 2H) 3.8 (s, 3H), 3.55(d, *J*=6.4 Hz, 2H), ^{13}C NMR ($CDCl_3$) δ 159.83, 140.11, 138.98, 131.00, 129.59, 129.46, 128.69, 128.50, 126.20, 118.85, 112.88, 1111.4, 55.20, 39.31.

(E)-1(4-Florophenyl)-3-phenylpropene (5f, Table 3): colorless oil ^{1}H NMR ($CDCl_3$, 400 MHz) δ 7.38-7.34 (m, 4H),7.30-7.26 (m, 3H), 7.03 (t, J=8.5 Hz, 2H), 6.46 (d, *J*=16 Hz, 1H), 6.35-6.29(m, 1H), 3.59 (d, *J*=6.5 Hz, 2H), ^{13}C NMR ($CDCl_3$) δ 162.07, 140.08, 133.68, 129 .88, 129.05, 128.67, 128.54, 127.63, 127.52, 126.25, 115.37, 39.30.

(E)-1(4-Florophenyl)-3-(4-methylphenyl)propene (5g, Table 3): colorless oil : ^{1}H NMR($CDCl_3$, 500 MHz) δ 7.34-7.32 (m, 2H), 7.16(s, 4H), 7.02-6.98 (m, 2H), 6.43 (d, *J*=15.5 Hz, 1H), 6.31-6.25 (m, 1H), 3.52(d, *J*=6.5 Hz, 2H), 2.36 (s, 3H), ^{13}C NMR ($CDCl_3$) δ 162.0, 136.99, 135.75, 133.78, 129.67, 129.23, 129.2, 128.55, 127.5, 115.3, 38.88, 21.01.

(E)-1(4-Chlorophenyl)-3-phenylpropene (5h, Table 3): colorless oil: ^{1}H NMR ($CDCl_3$, 400 MHz) δ 7.39-7.214(m, 9H), 6.45-6.33 (m, 2H), 3.57(d, *J*=6.4, 2H), ^{13}C NMR ($CDCl_3$) δ 140.00, 136.13, 132.80, 130.16, 129.99, 128.79, 128.76, 128.67, 127.46, 126.41, 39.44.

(E)-1-Phenyl-1,4-pentadiene (5i, Table 3): colorless oil: ^{1}H NMR ($CDCl_3$, 500 MHz); 7.37-7.19 (m, 5H), 6.42 (d, *J*=16 Hz, 1H), 6.25-6.21 (m,1H), 5.96-5.88 (m, 1H), 5.15-5.06 (m, 2H), 2.99-2.96 (m, 2H), ^{13}NMR ($CDCl_3$) δ 137.64, 136.48, 130.86, 128.490, 128.2, 127.02, 126.04, 115.66, 37.00.

2/e

^{1}H and ^{13}C NMR spectra of all synthesized products described in Section -2

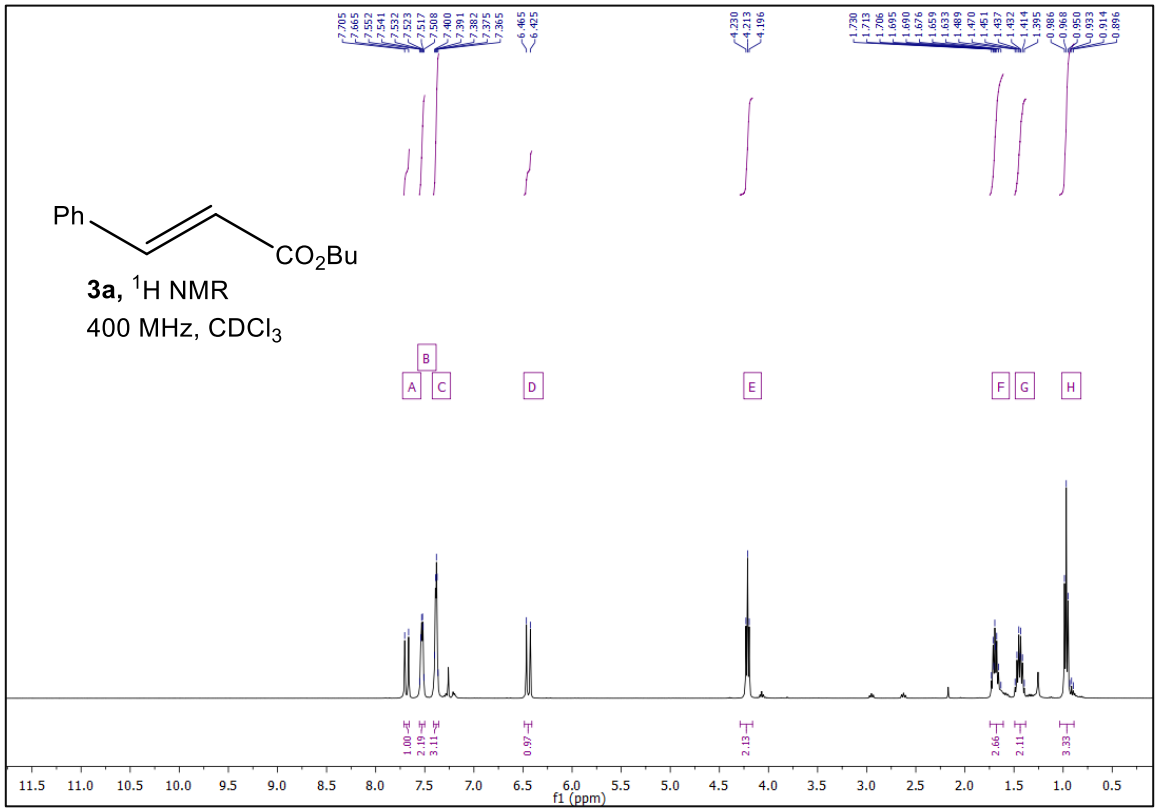
Ph
CO2Bu
3a, 1H NMR
400 MHz, CDCl3
f1 (ppm)

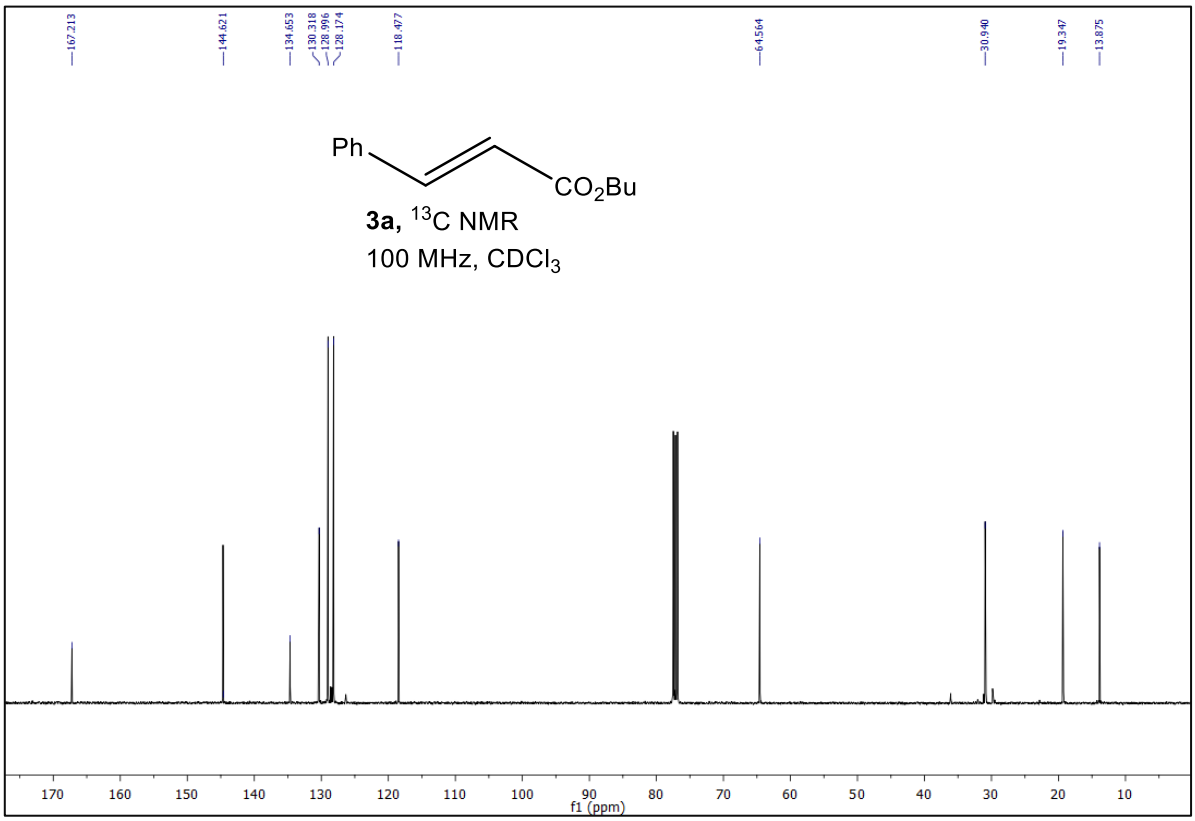
Ph
CO2Bu
3a, 13C NMR
100 MHz, CDCl3
f1 (ppm)

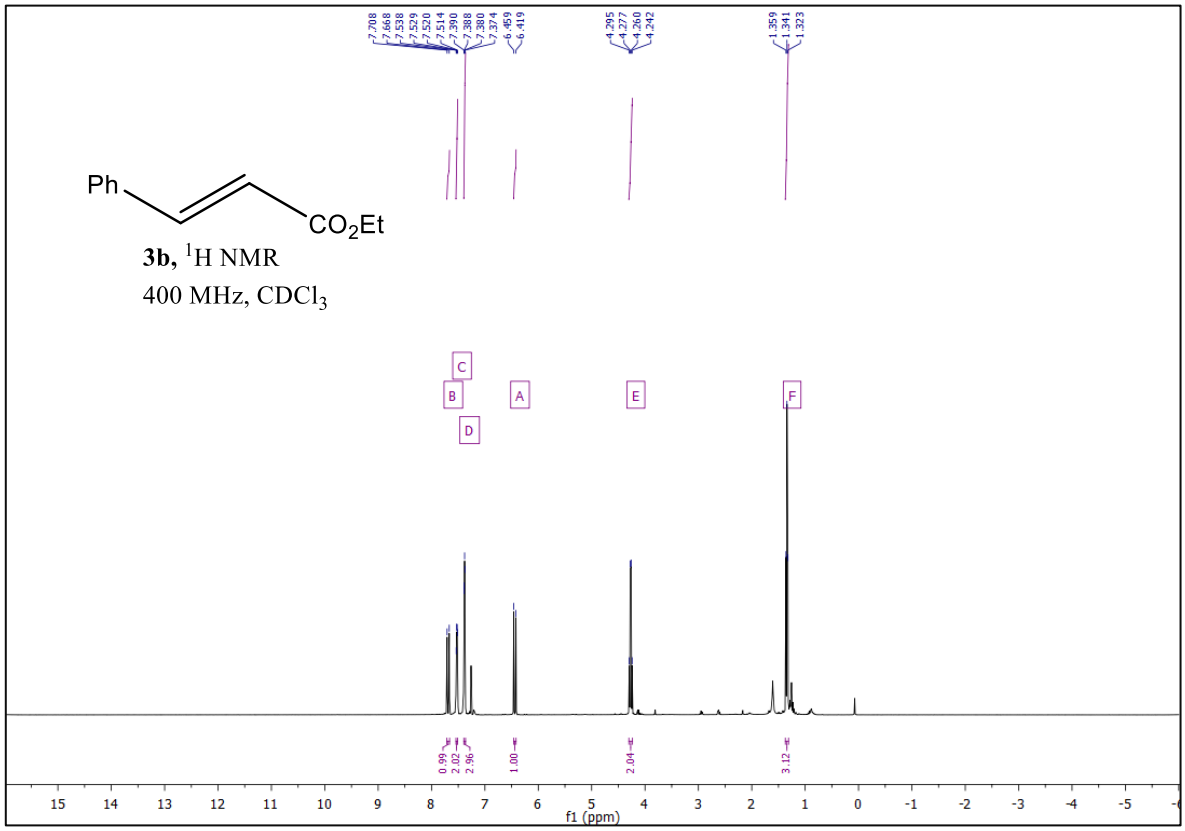
Ph
CO2Et
3b, 1H NMR
400 MHz, CDCl3
f1 (ppm)

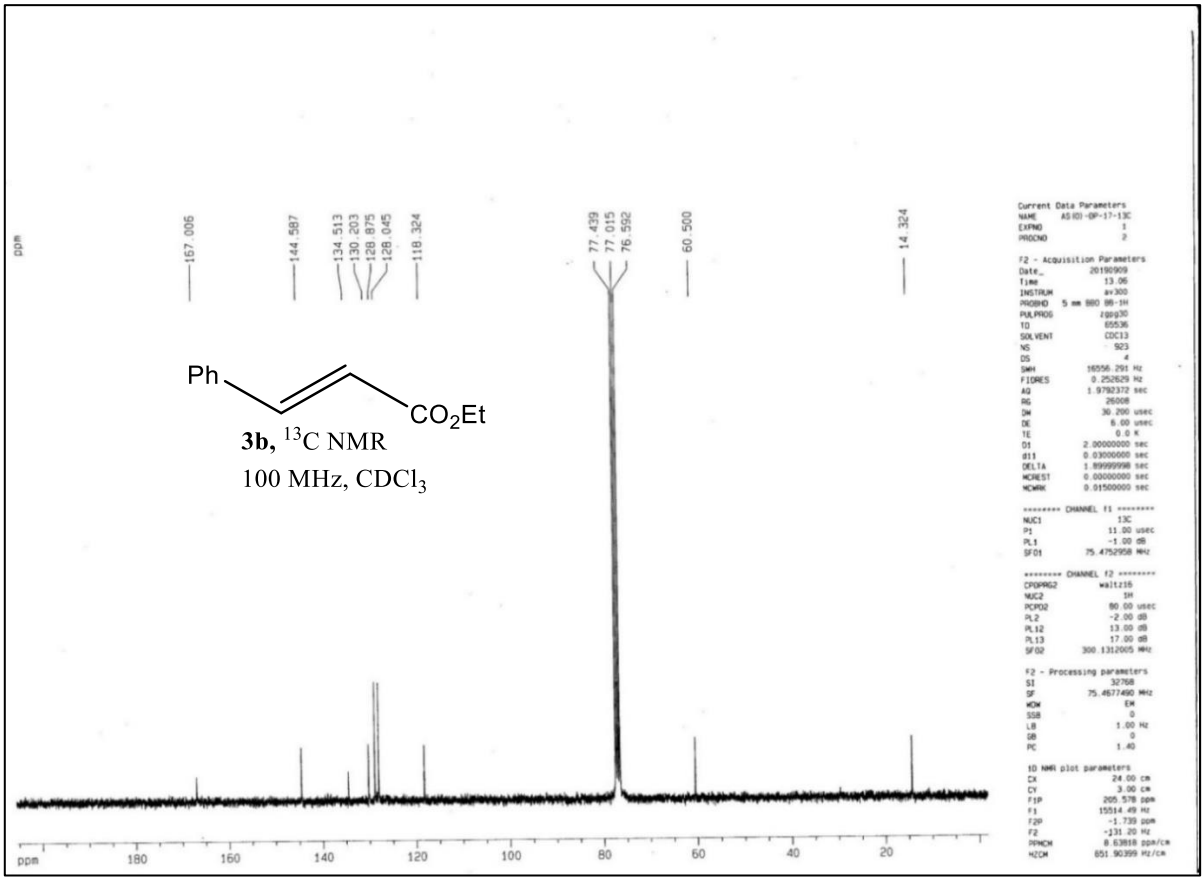
Ph
CO2Et
3b, 13C NMR
100 MHz, CDCl3
ppm

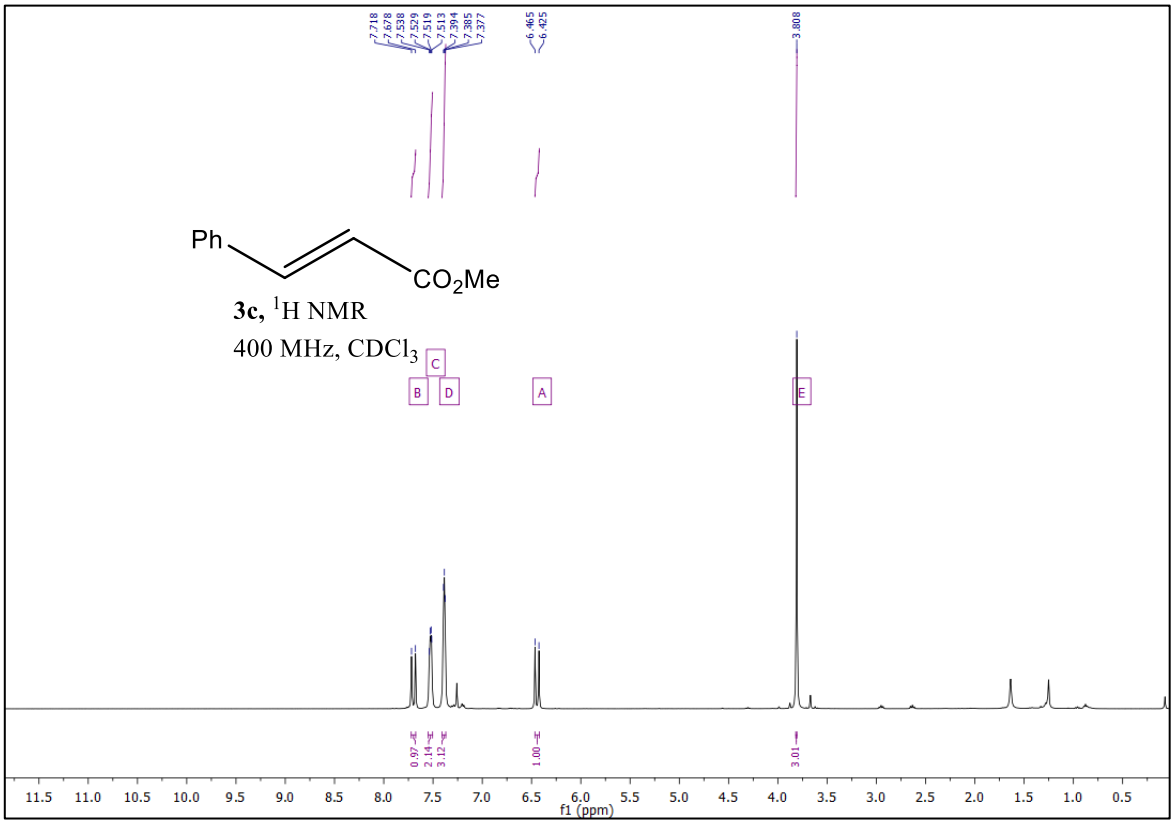
7.718
7.678
7.538
7.529
7.519
7.513
7.394
7.385
7.377
6.465
6.425
3.808
Ph
CO2Me
3c, 1H NMR
400 MHz, CDCl3
C
B
D
A
E
0.97
2.14
3.12
1.00
3.01
11.5 11.0 10.5 10.0 9.5 9.0 8.5 8.0 7.5 7.0 6.5 6.0 5.5 5.0 4.5 4.0 3.5 3.0 2.5 2.0 1.5 1.0 0.5
f1 (ppm)

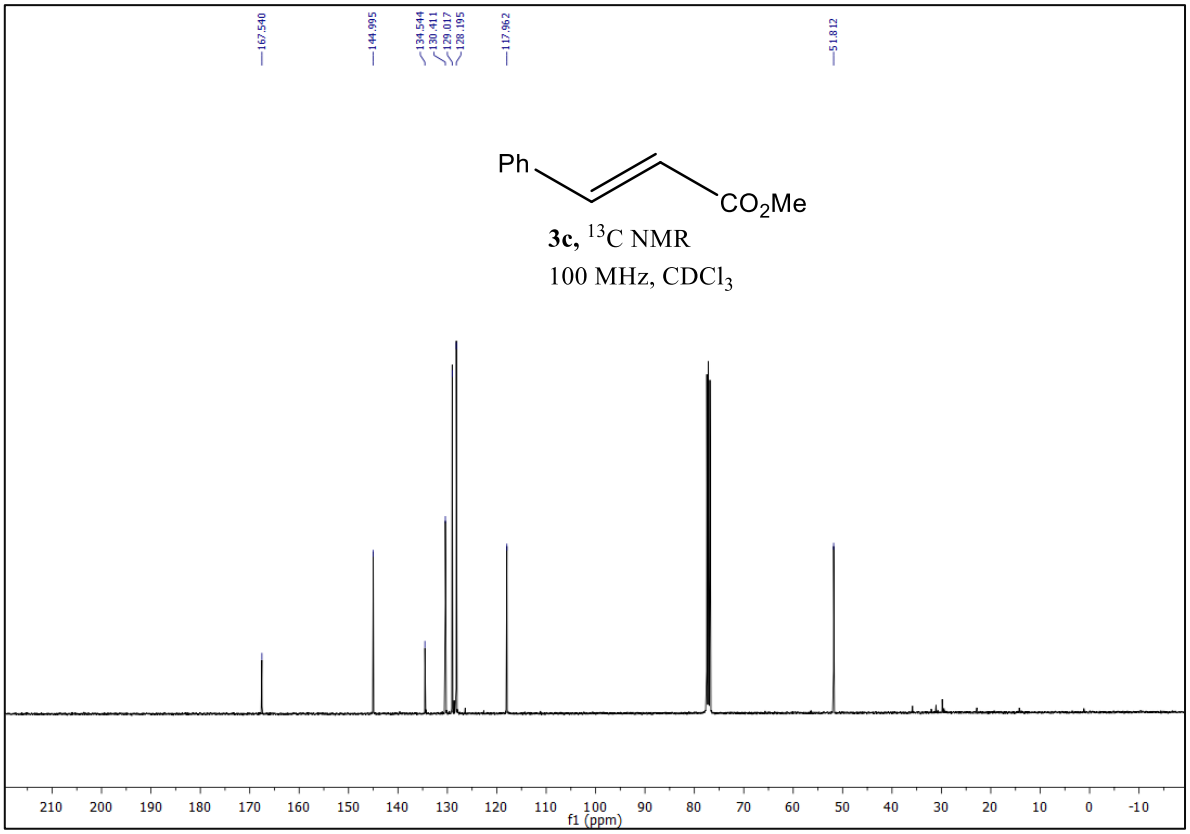
167.540
144.995
134.544
130.411
129.017
128.195
117.962
51.812
Ph
CO2Me
3c, 13C NMR
100 MHz, CDCl3
210 200 190 180 170 160 150 140 130 120 110 100 90 80 70 60 50 40 30 20 10 0 -10
f1 (ppm)

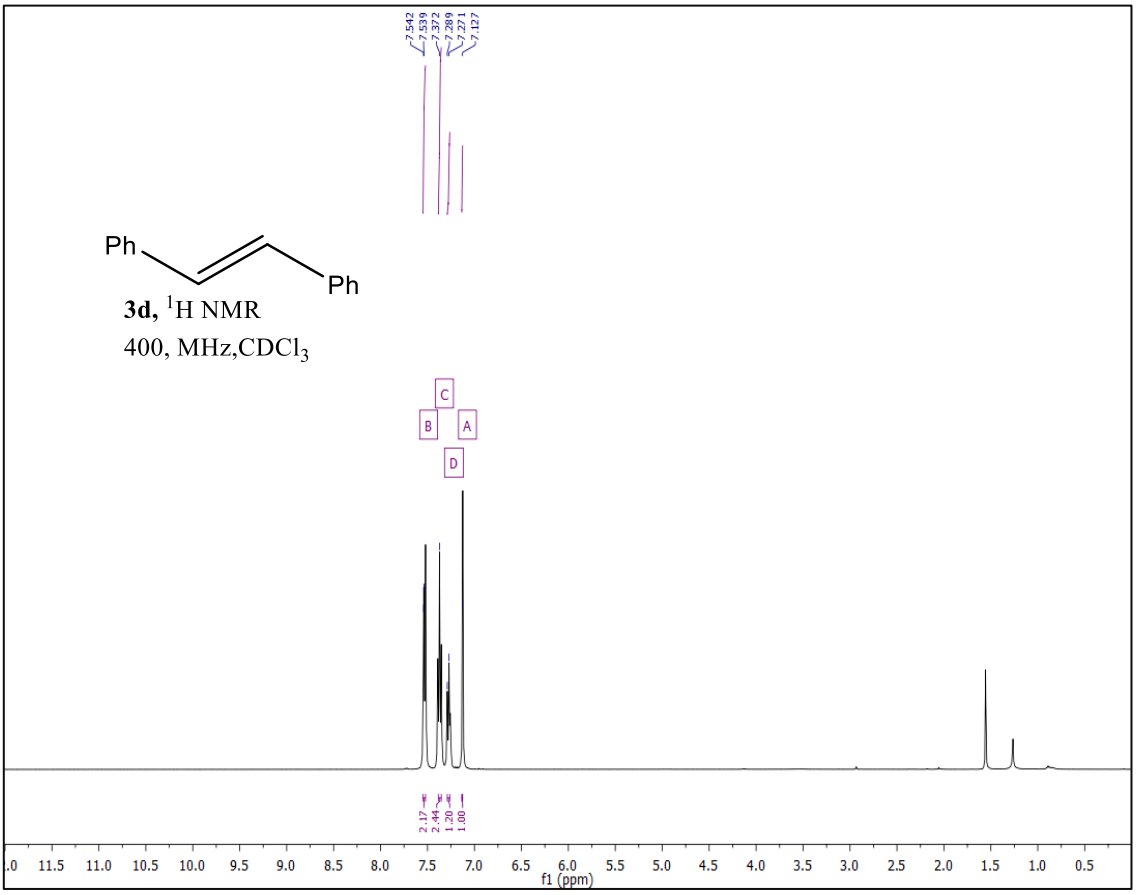

3d, ^{1}H NMR
400, MHz,$CDCl_3$

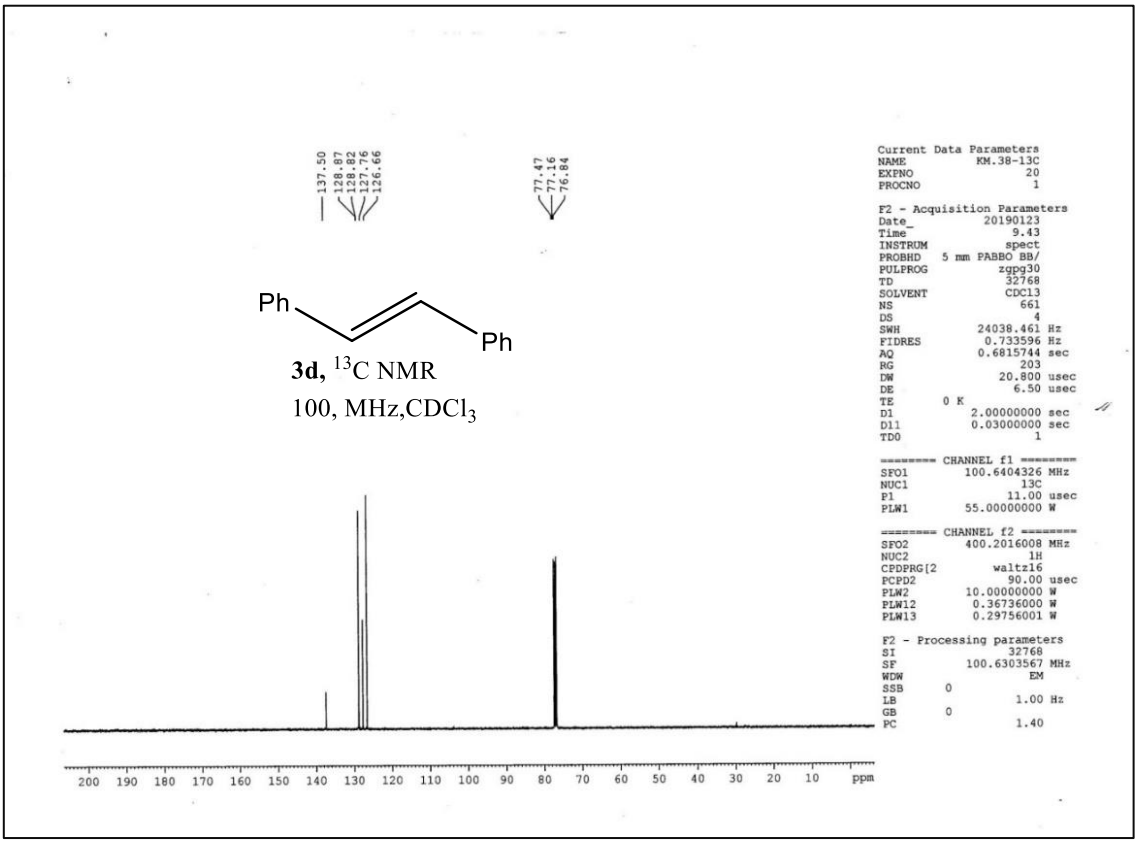

3d, ^{13}C NMR
100, MHz,$CDCl_3$

3e, ^{1}H NMR
400 MHz, $CDCl_3$

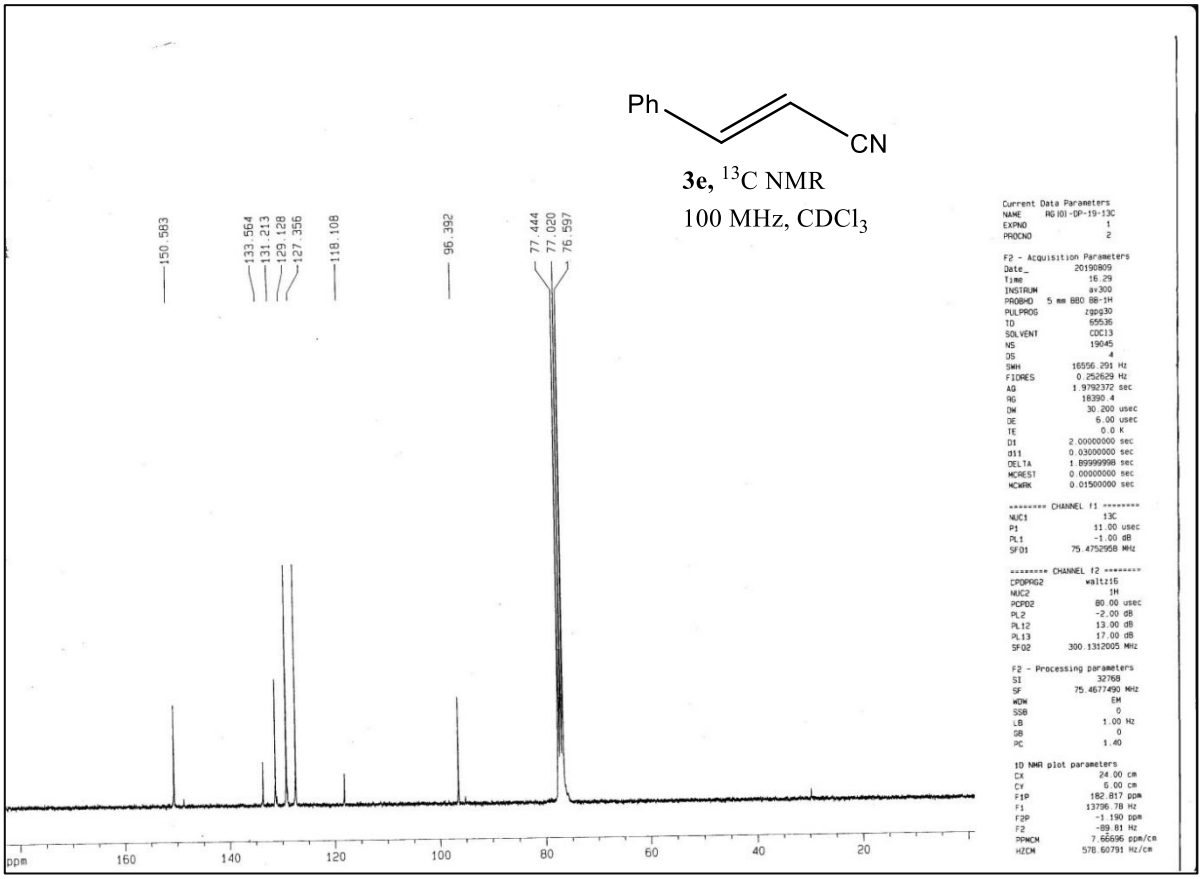

3e, ^{13}C NMR
100 MHz, $CDCl_3$

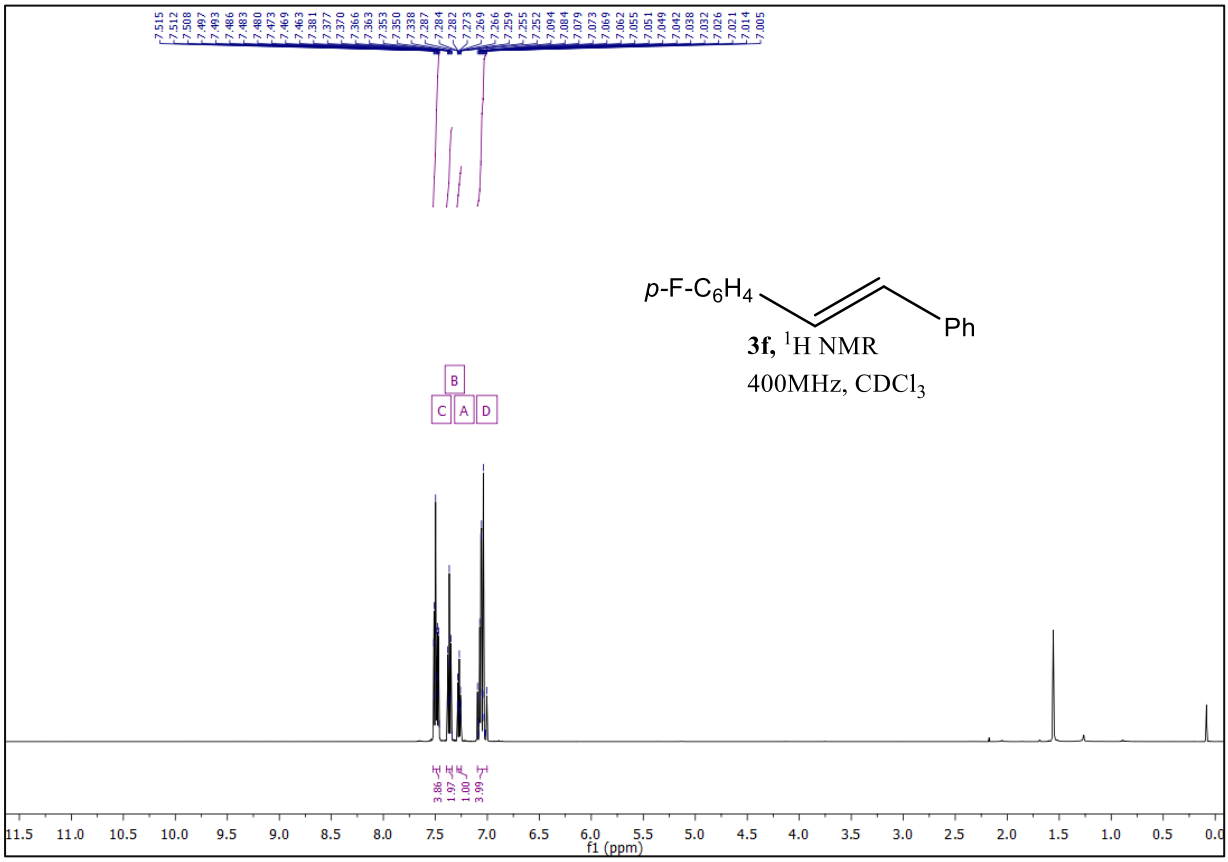
p-F-C6H4
Ph
3f, 1H NMR
400MHz, CDCl3
f1 (ppm)

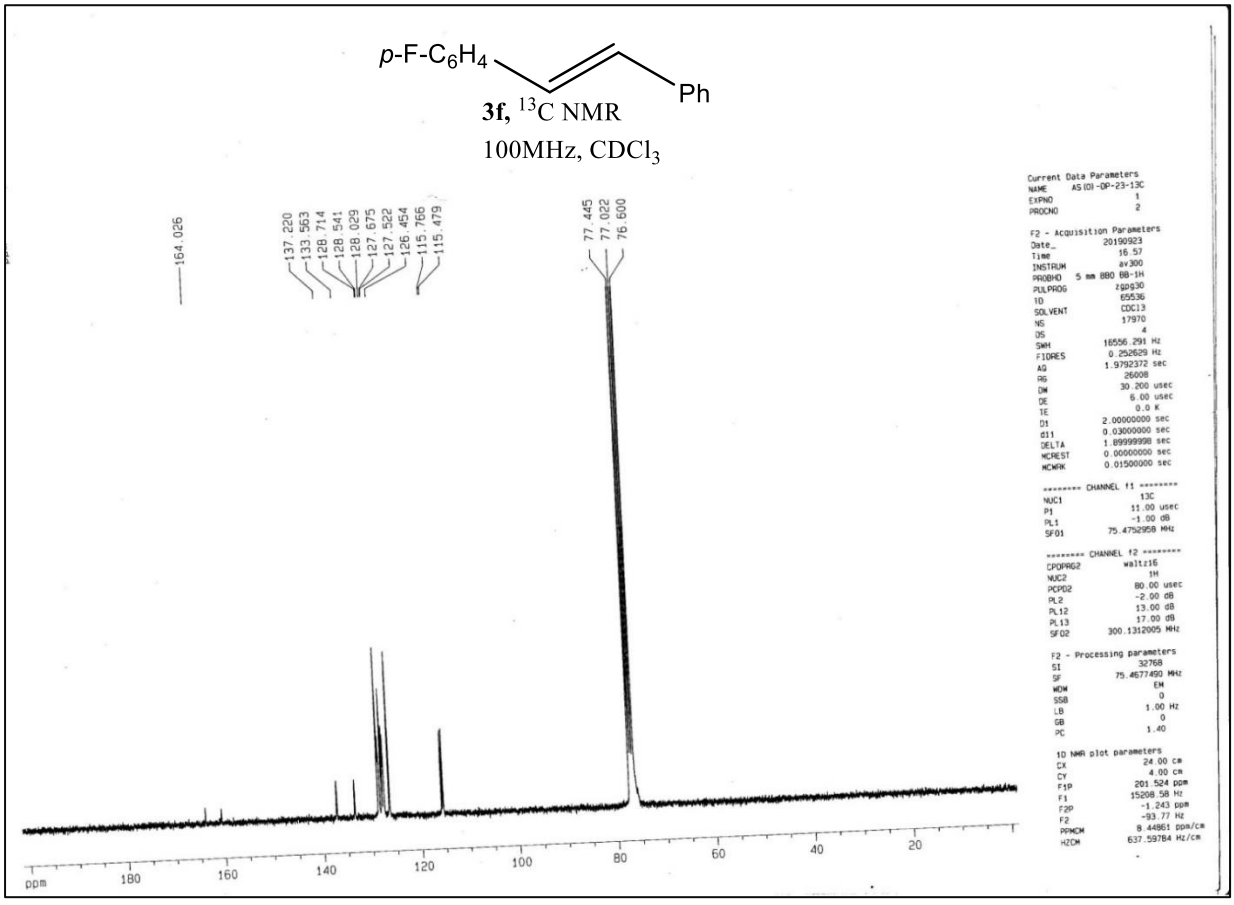
p-F-C6H4
Ph
3f, 13C NMR
100MHz, CDCl3
ppm

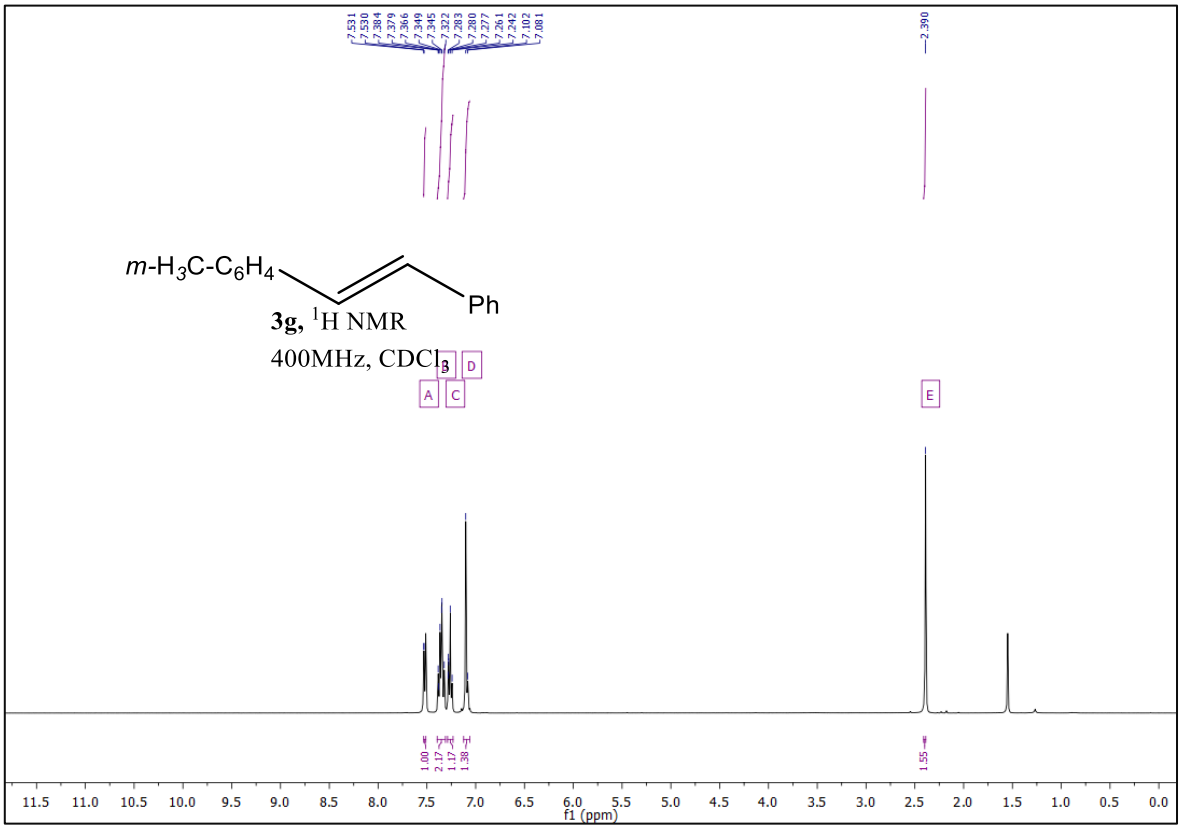
m-H3C-C6H4
Ph
3g, 1H NMR
400MHz, CDCl3
A
B
C
D
E
f1 (ppm)

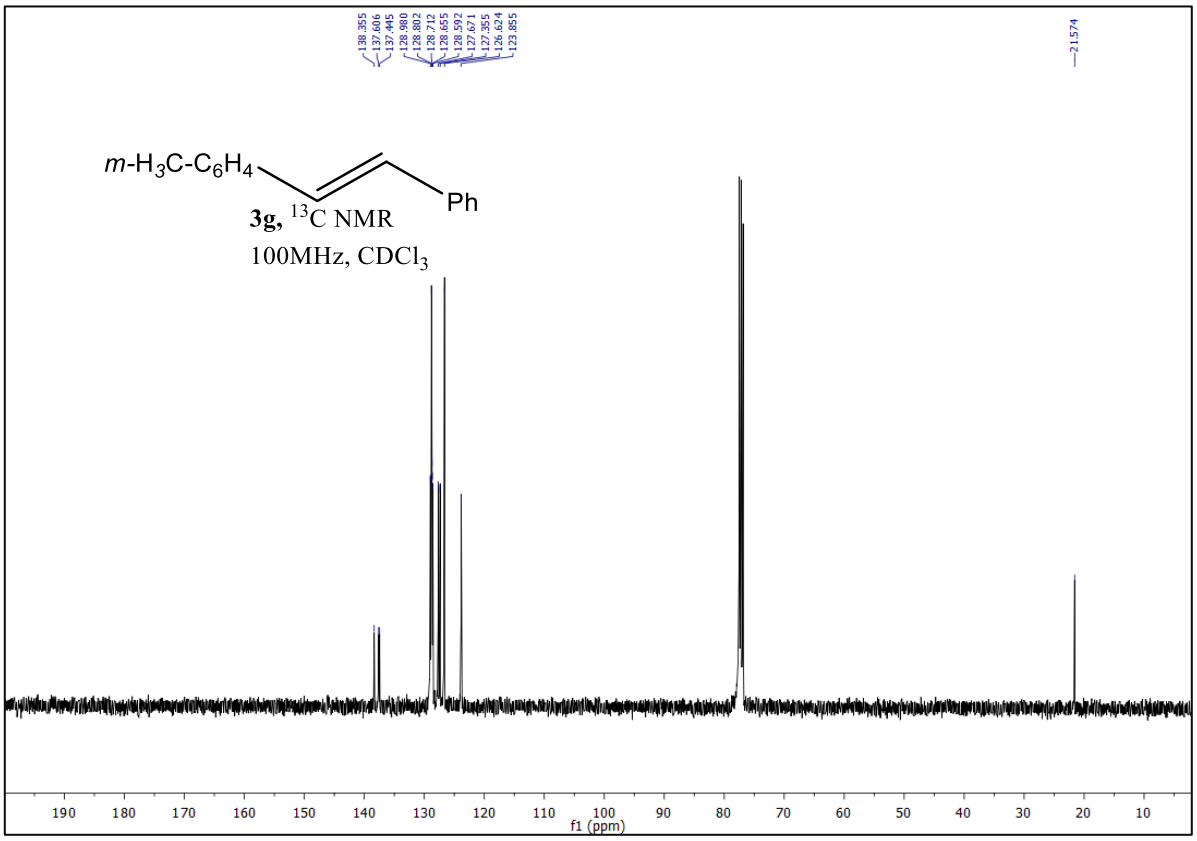
m-H3C-C6H4
Ph
3g, 13C NMR
100MHz, CDCl3
f1 (ppm)

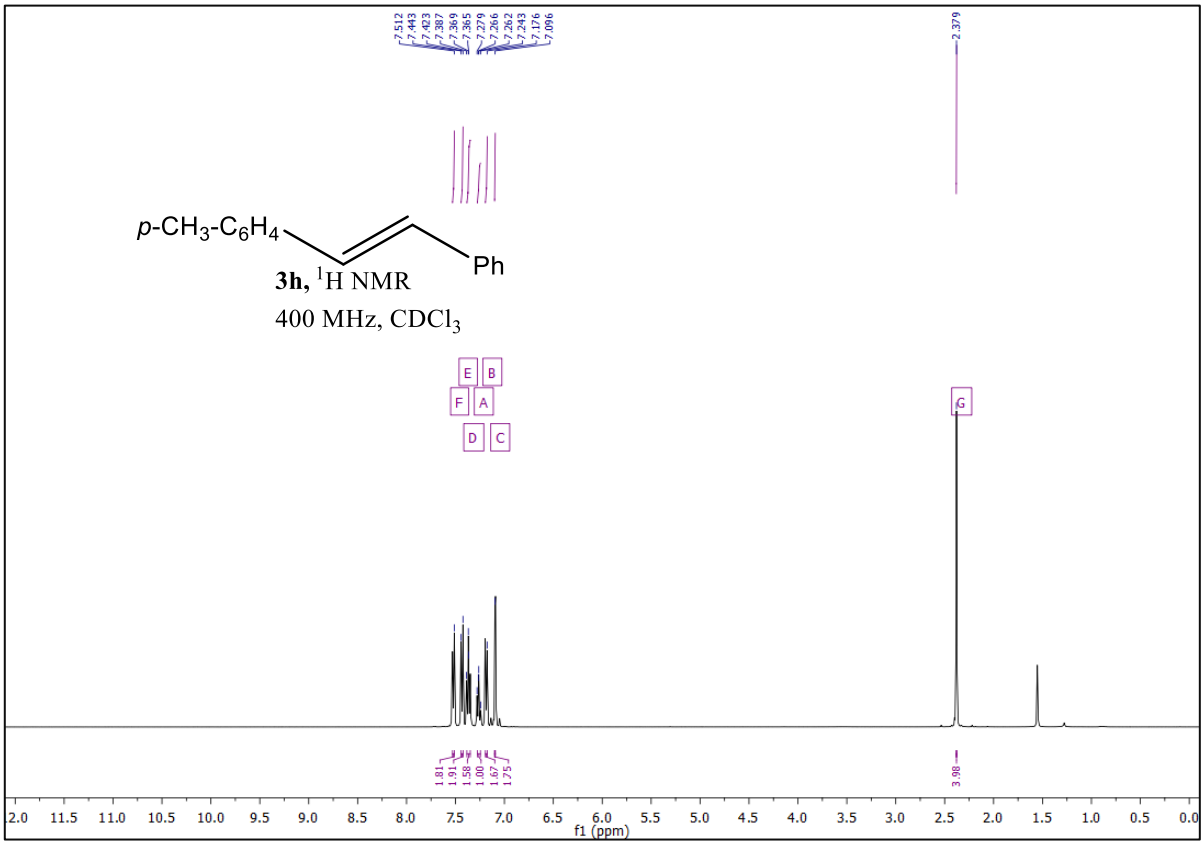
p-CH3-C6H4
Ph
3h, 1H NMR
400 MHz, CDCl3
f1 (ppm)

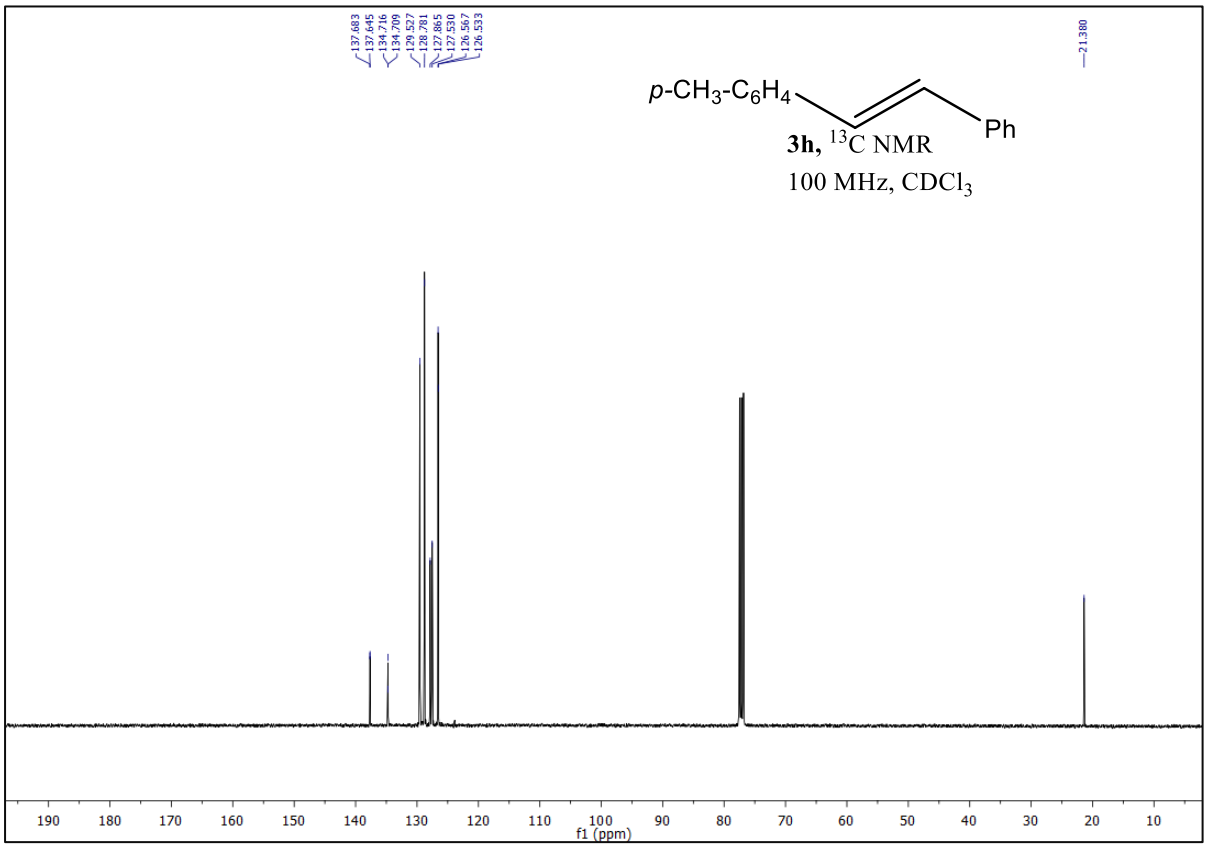
p-CH3-C6H4
Ph
3h, 13C NMR
100 MHz, CDCl3
f1 (ppm)

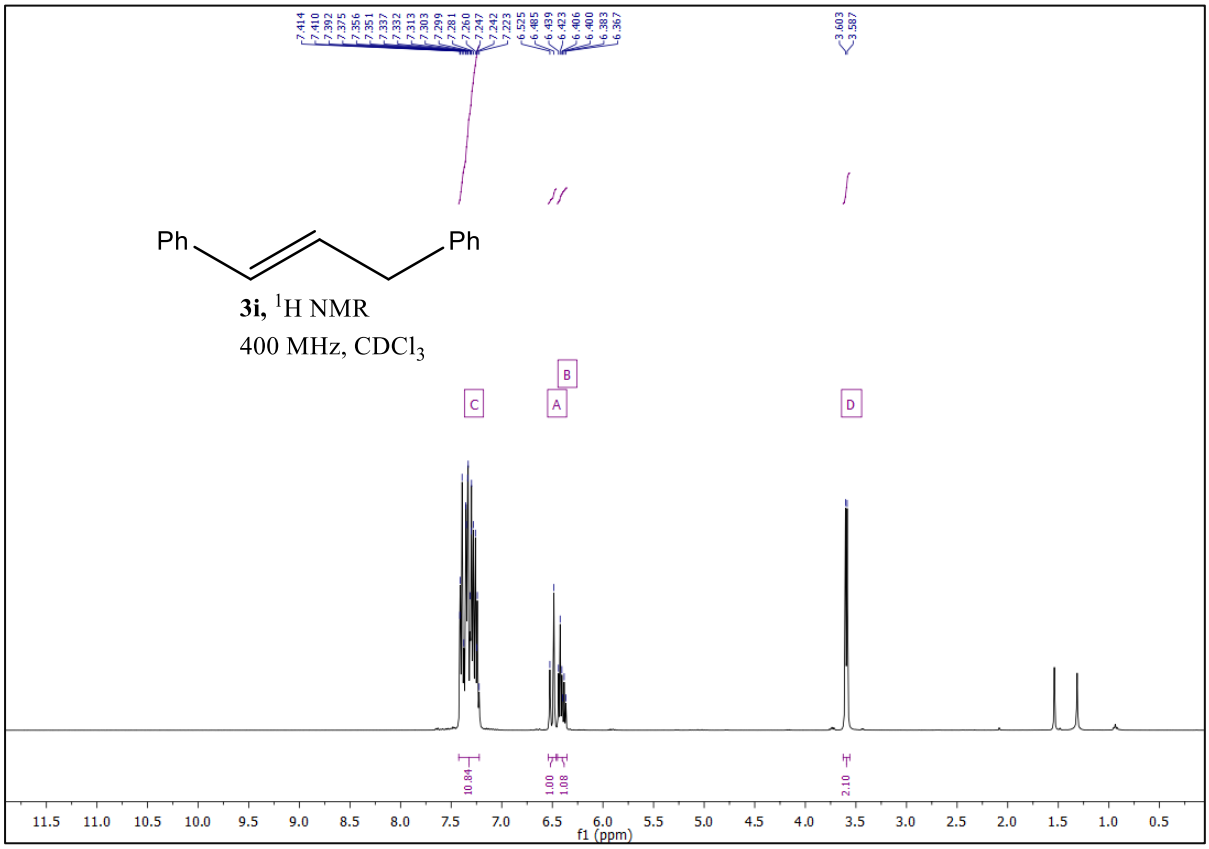
Ph
Ph
3i, 1H NMR
400 MHz, CDCl3
f1 (ppm)

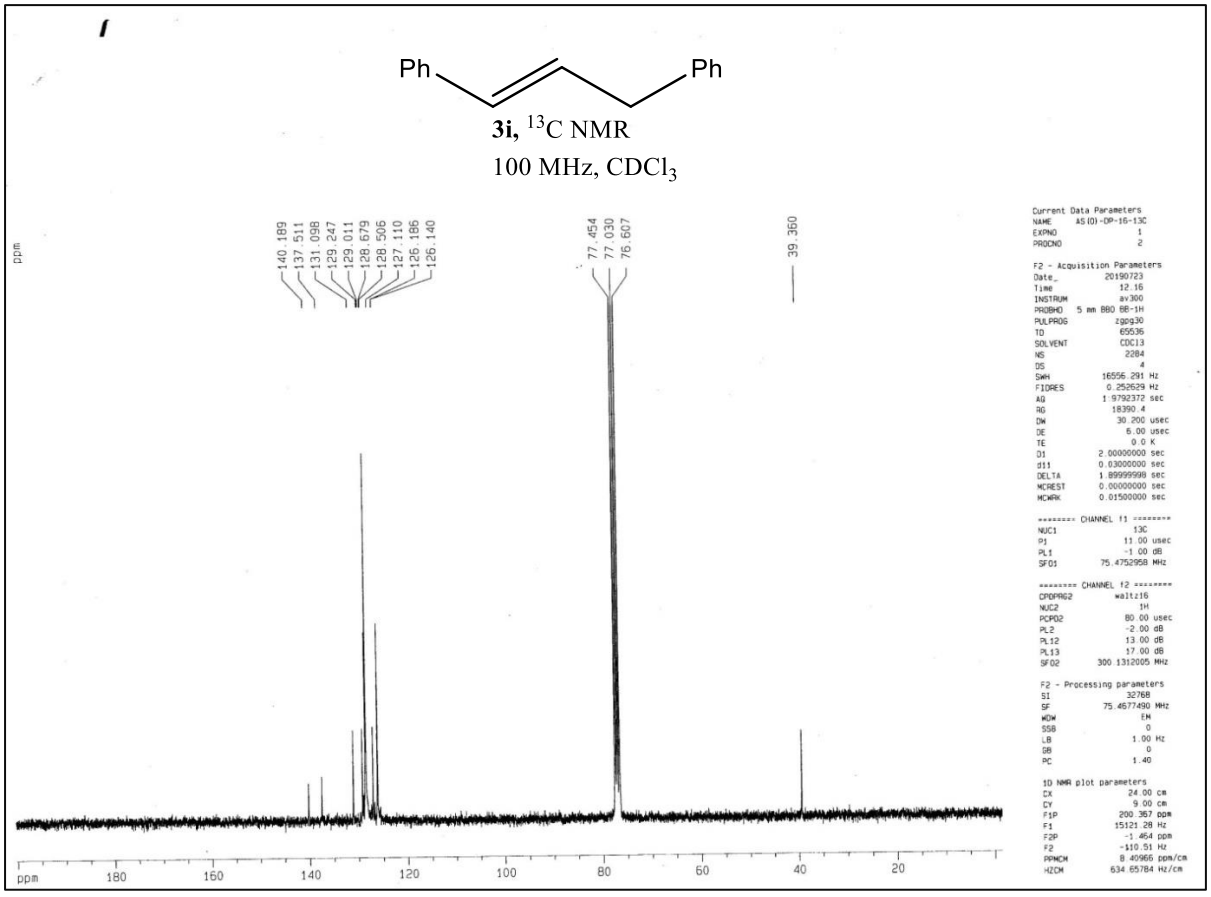
Ph
Ph
3i, 13C NMR
100 MHz, CDCl3
ppm

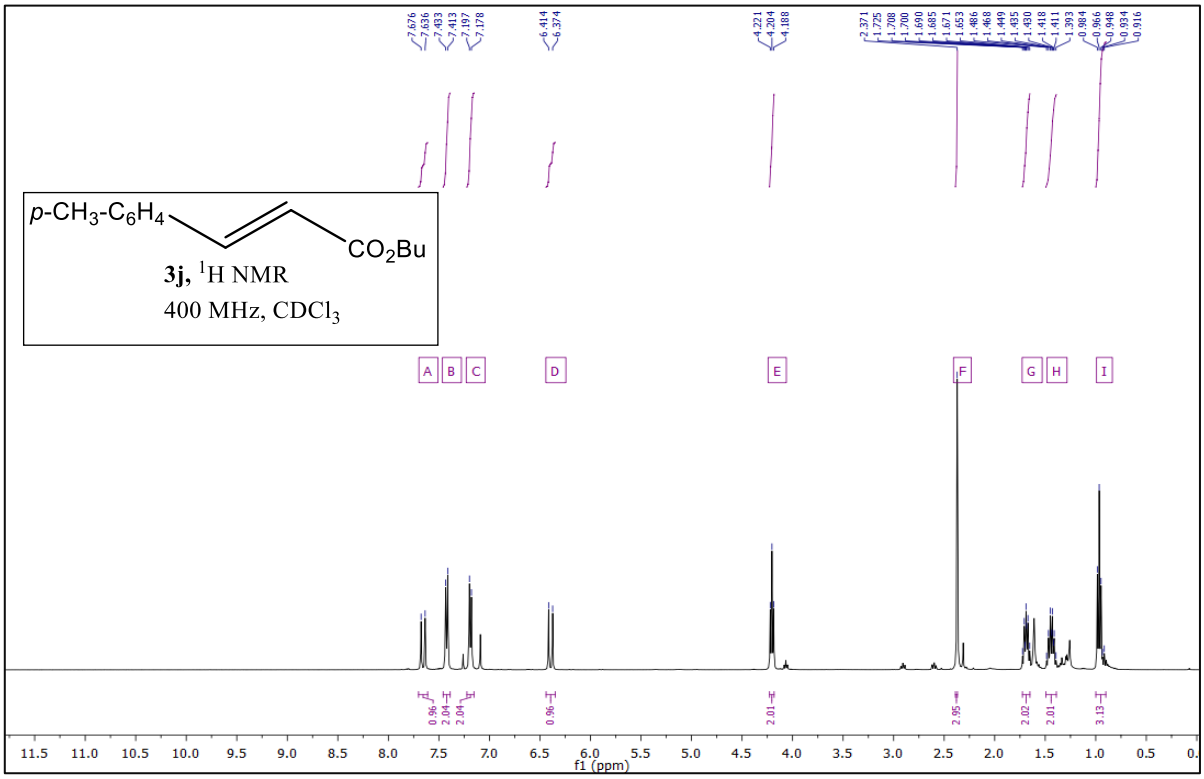
p-CH3-C6H4
CO2Bu
3j, 1H NMR
400 MHz, CDCl3
f1 (ppm)

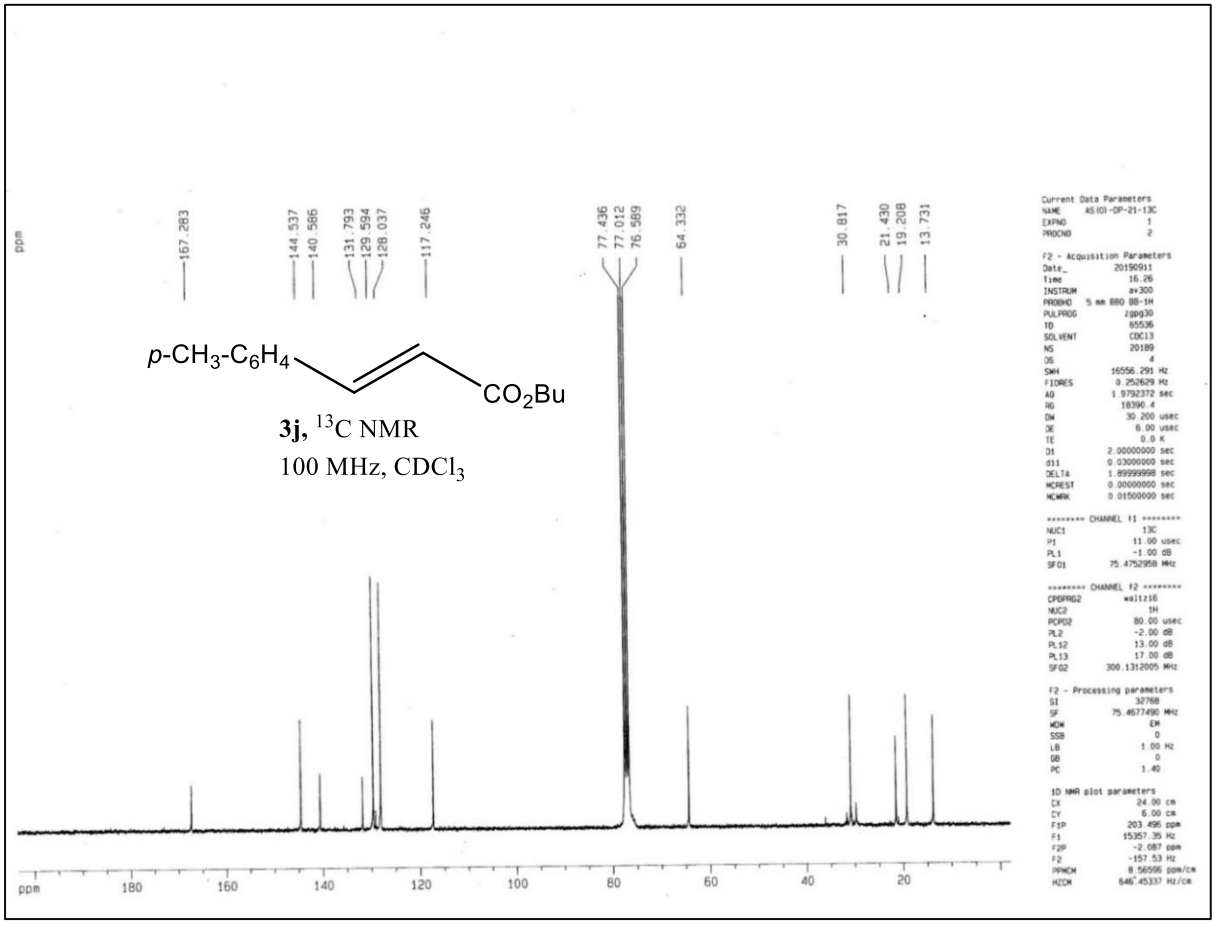
p-CH3-C6H4
CO2Bu
3j, 13C NMR
100 MHz, CDCl3
ppm

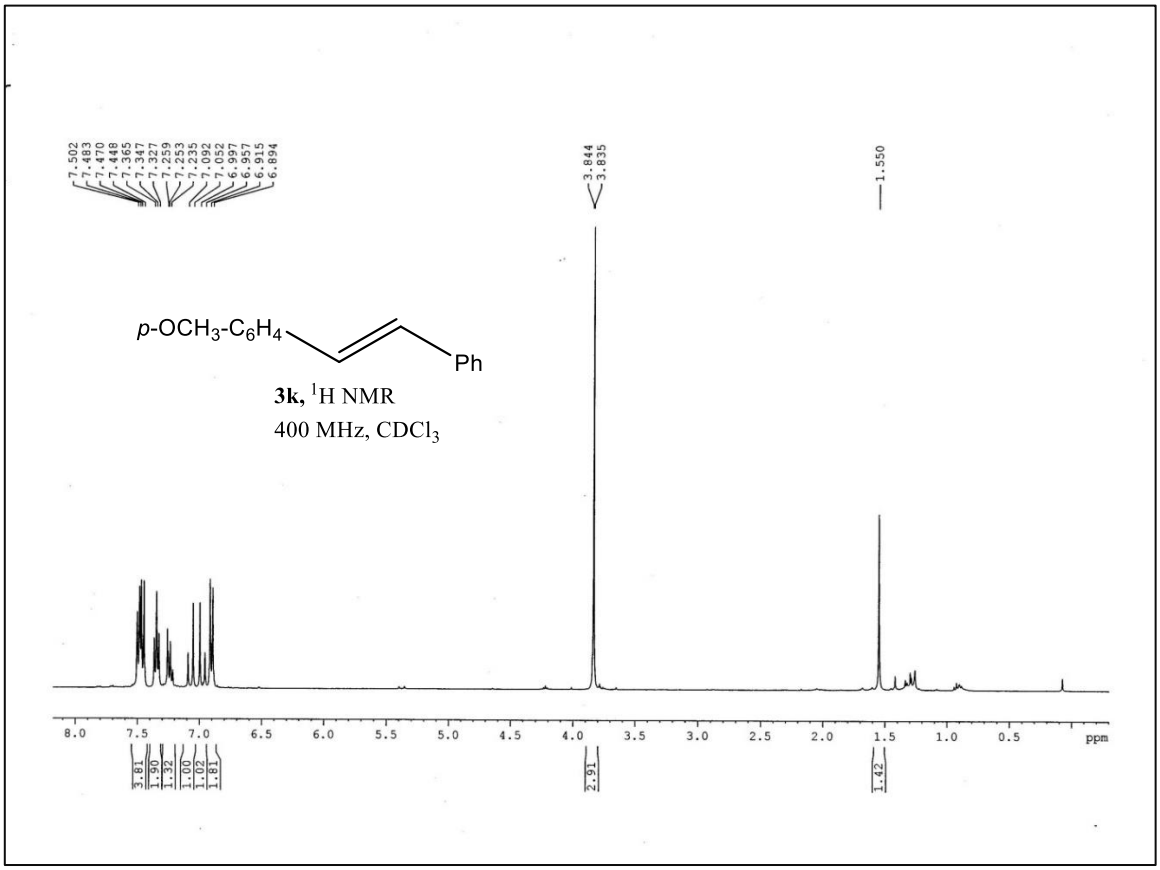
7.502
7.483
7.470
7.448
7.365
7.347
7.327
7.259
7.253
7.235
7.092
7.052
6.997
6.957
6.915
6.894
3.844
3.835
1.550
p-OCH3-C6H4
Ph
3k, 1H NMR
400 MHz, CDCl3
8.0 7.5 7.0 6.5 6.0 5.5 5.0 4.5 4.0 3.5 3.0 2.5 2.0 1.5 1.0 0.5 ppm
3.81
1.90
1.32
1.00
1.02
1.81
2.91
1.42

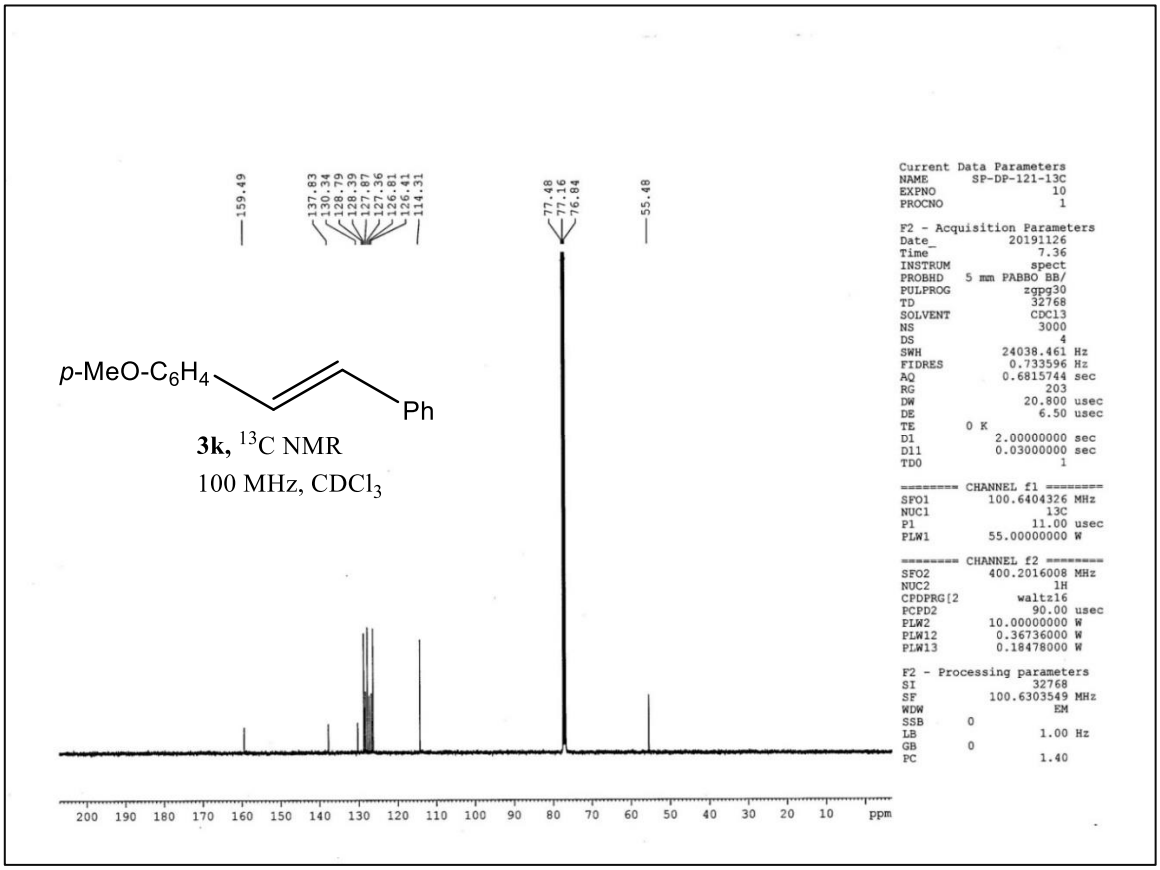
159.49
137.83
130.34
128.79
128.39
127.87
127.36
126.81
126.41
114.31
77.48
77.16
76.84
55.48
p-MeO-C6H4
Ph
3k, 13C NMR
100 MHz, CDCl3
200 190 180 170 160 150 140 130 120 110 100 90 80 70 60 50 40 30 20 10 ppm
Current Data Parameters
NAME SP-DP-121-13C
EXPNO 10
PROCNO 1
F2 - Acquisition Parameters
Date_ 20191126
Time 7.36
INSTRUM spect
PROBHD 5 mm PABBO BB/
PULPROG zgpg30
TD 32768
SOLVENT CDCl3
NS 3000
DS 4
SWH 24038.461 Hz
FIDRES 0.733596 Hz
AQ 0.6815744 sec
RG 203
DW 20.800 usec
DE 6.50 usec
TE 0 K
D1 2.00000000 sec
D11 0.03000000 sec
TD0 1
======== CHANNEL f1 ========
SFO1 100.6404326 MHz
NUC1 13C
P1 11.00 usec
PLW1 55.00000000 W
======== CHANNEL f2 ========
SFO2 400.2016008 MHz
NUC2 1H
CPDPRG[2 waltz16
PCPD2 90.00 usec
PLW2 10.00000000 W
PLW12 0.36736000 W
PLW13 0.18478000 W
F2 - Processing parameters
SI 32768
SF 100.6303549 MHz
WDW EM
SSB 0
LB 1.00 Hz
GB 0
PC 1.40

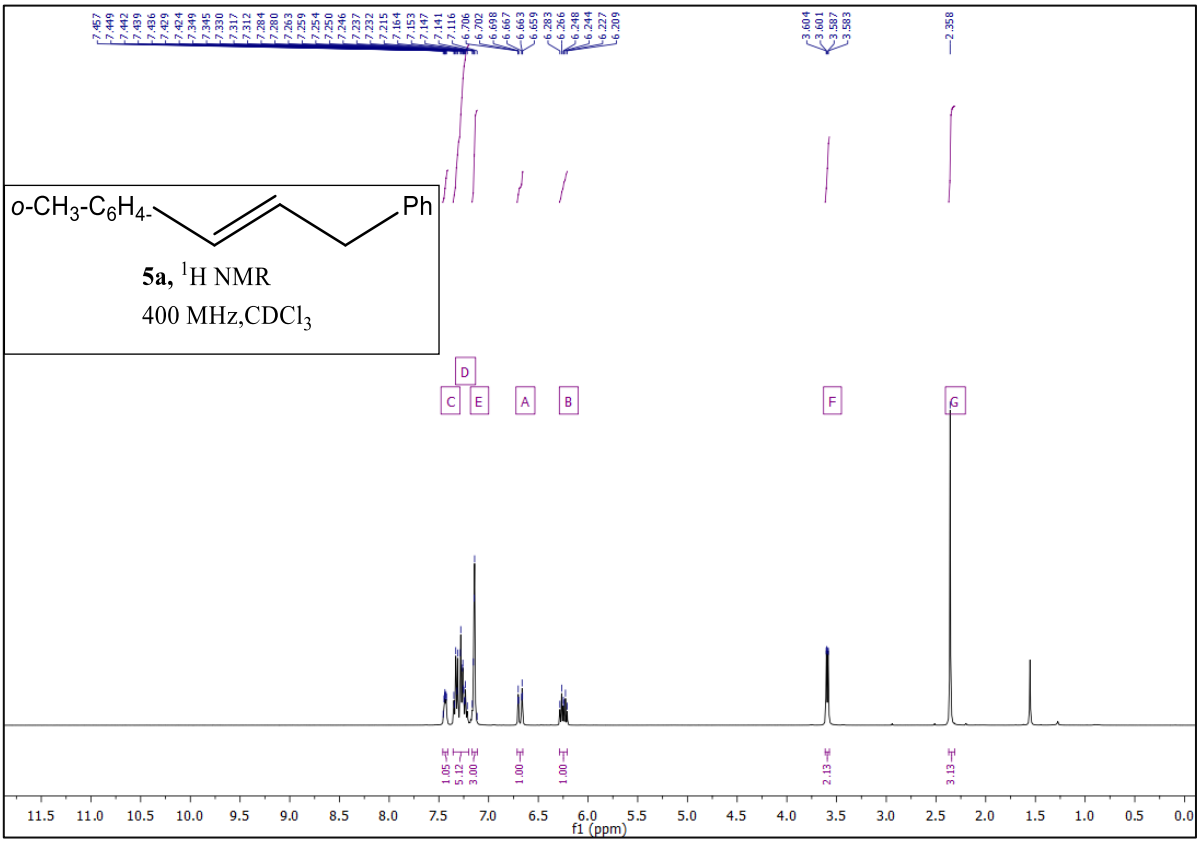
o-CH3-C6H4-
Ph
5a, 1H NMR
400 MHz,CDCl3
f1 (ppm)

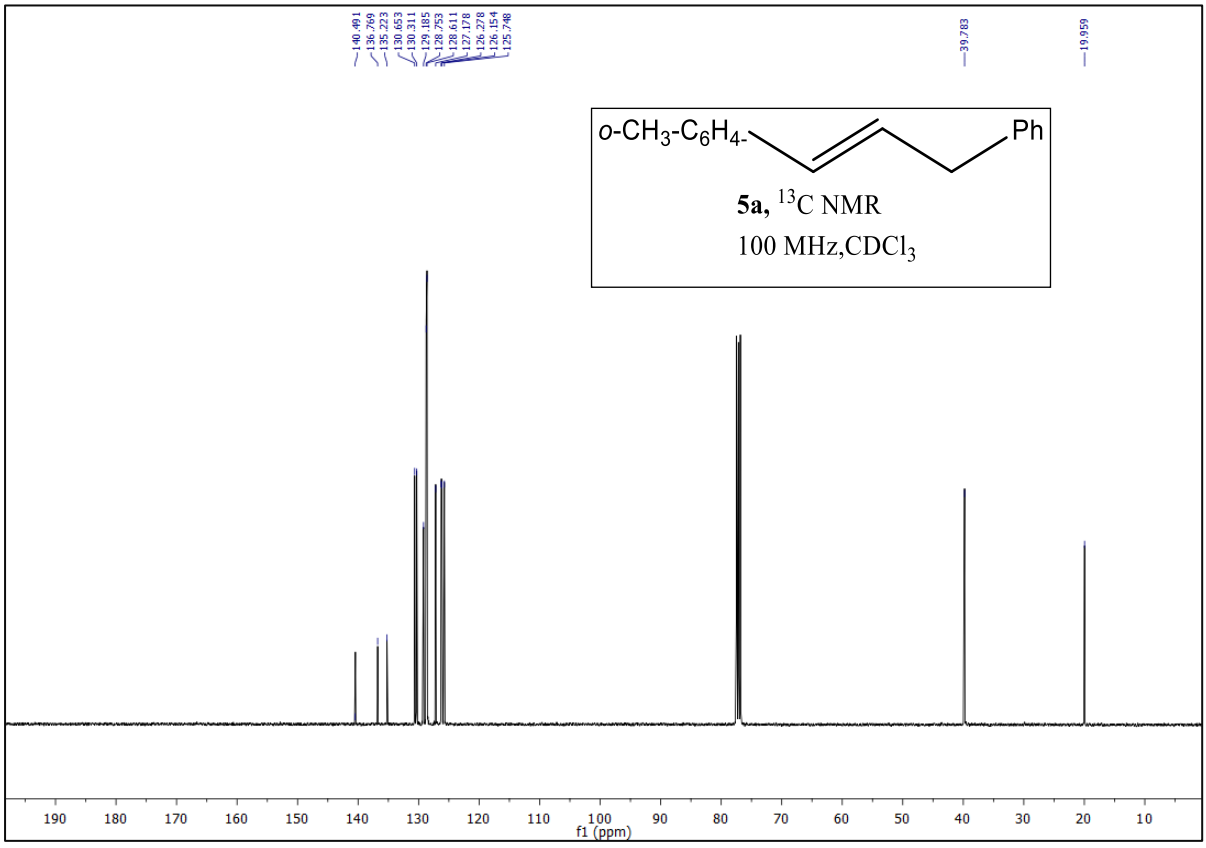
o-CH3-C6H4-
Ph
5a, 13C NMR
100 MHz,CDCl3
f1 (ppm)

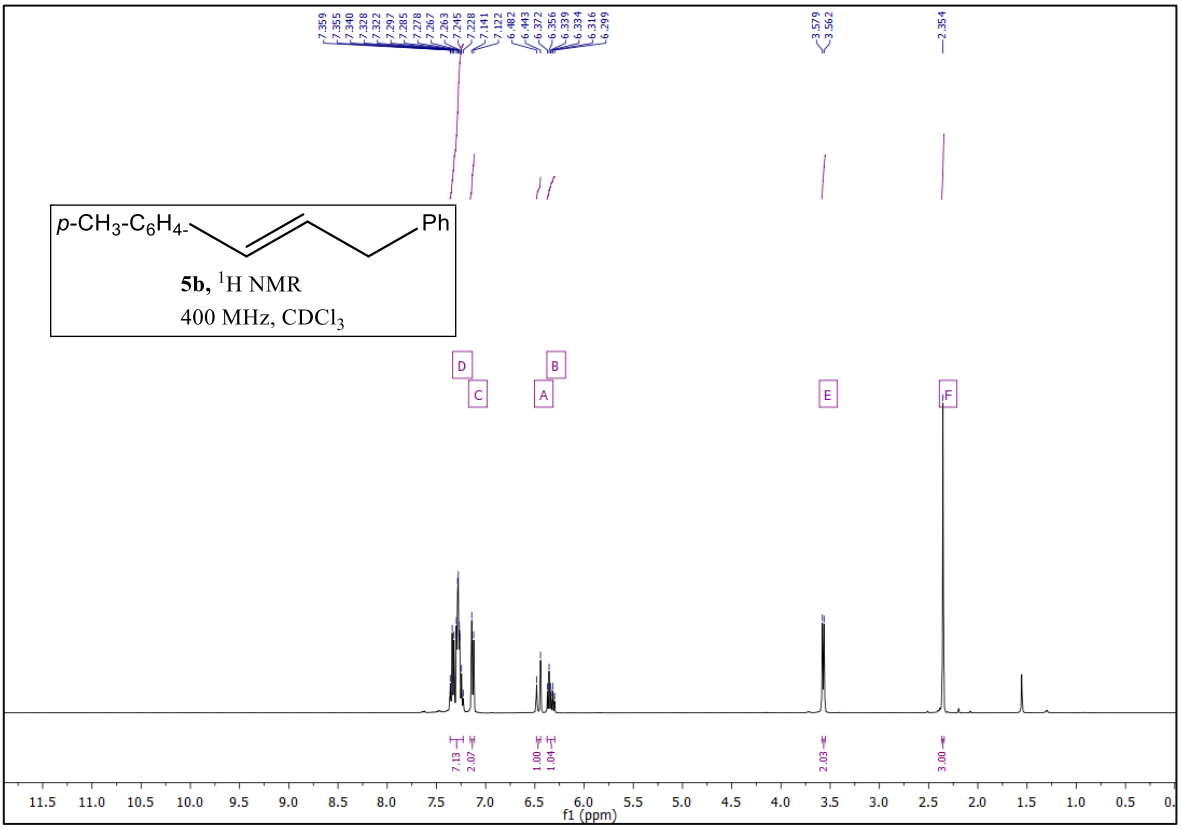
p-CH3-C6H4-
Ph
5b, 1H NMR
400 MHz, CDCl3
f1 (ppm)

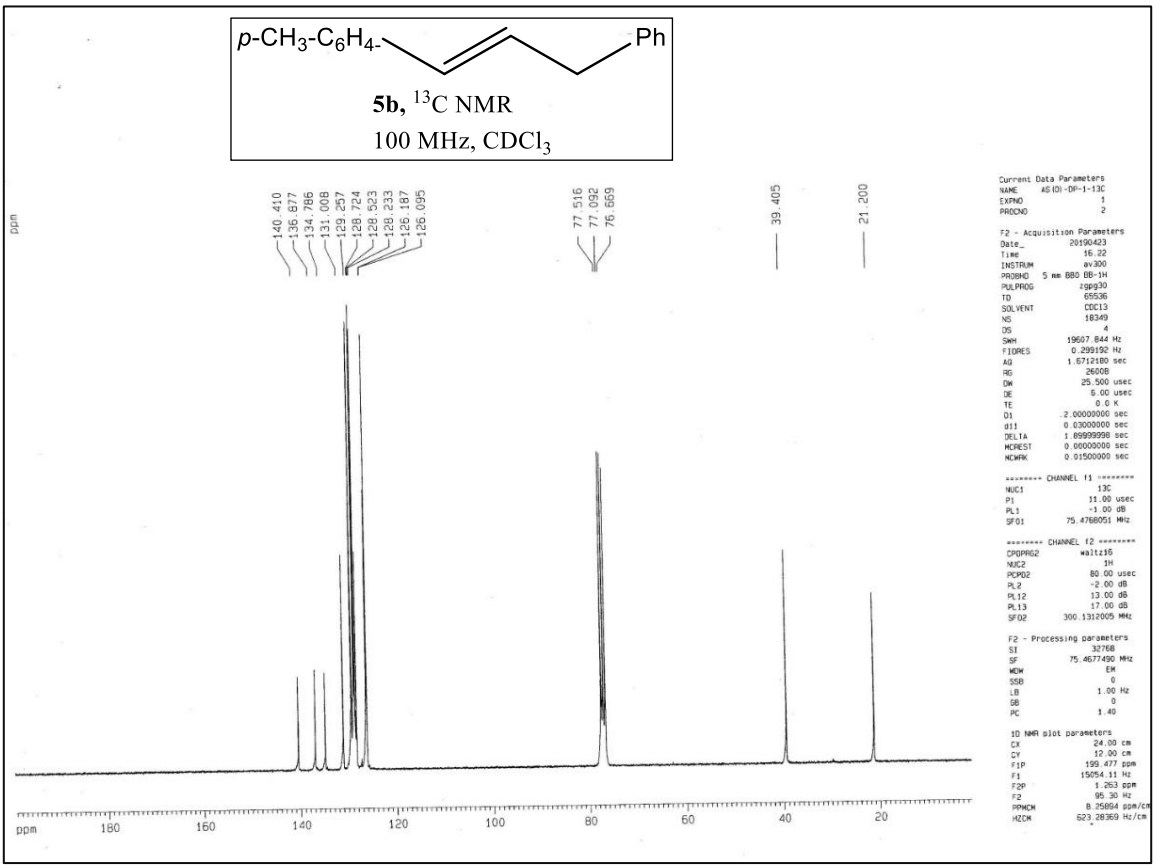
p-CH3-C6H4-
Ph
5b, 13C NMR
100 MHz, CDCl3
ppm

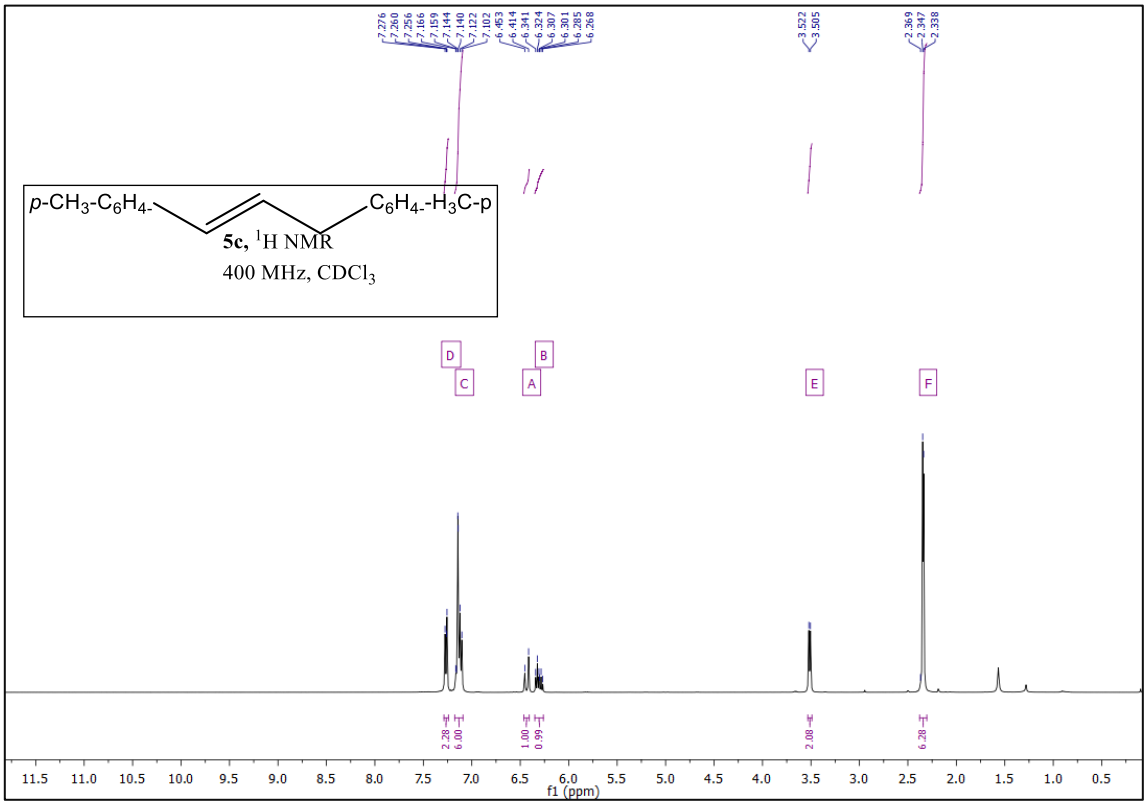
p-CH3-C6H4-
C6H4-H3C-p
5c, 1H NMR
400 MHz, CDCl3
f1 (ppm)

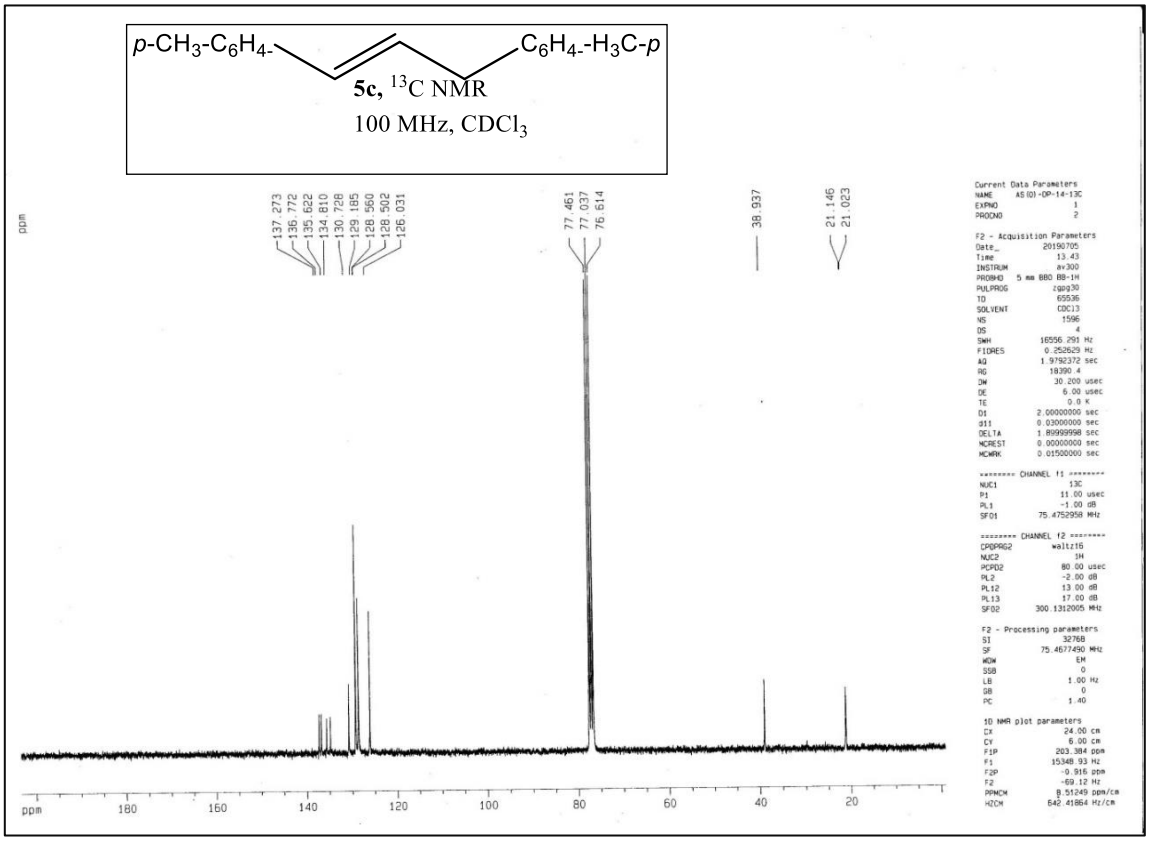
p-CH3-C6H4-
C6H4-H3C-p
5c, 13C NMR
100 MHz, CDCl3
ppm

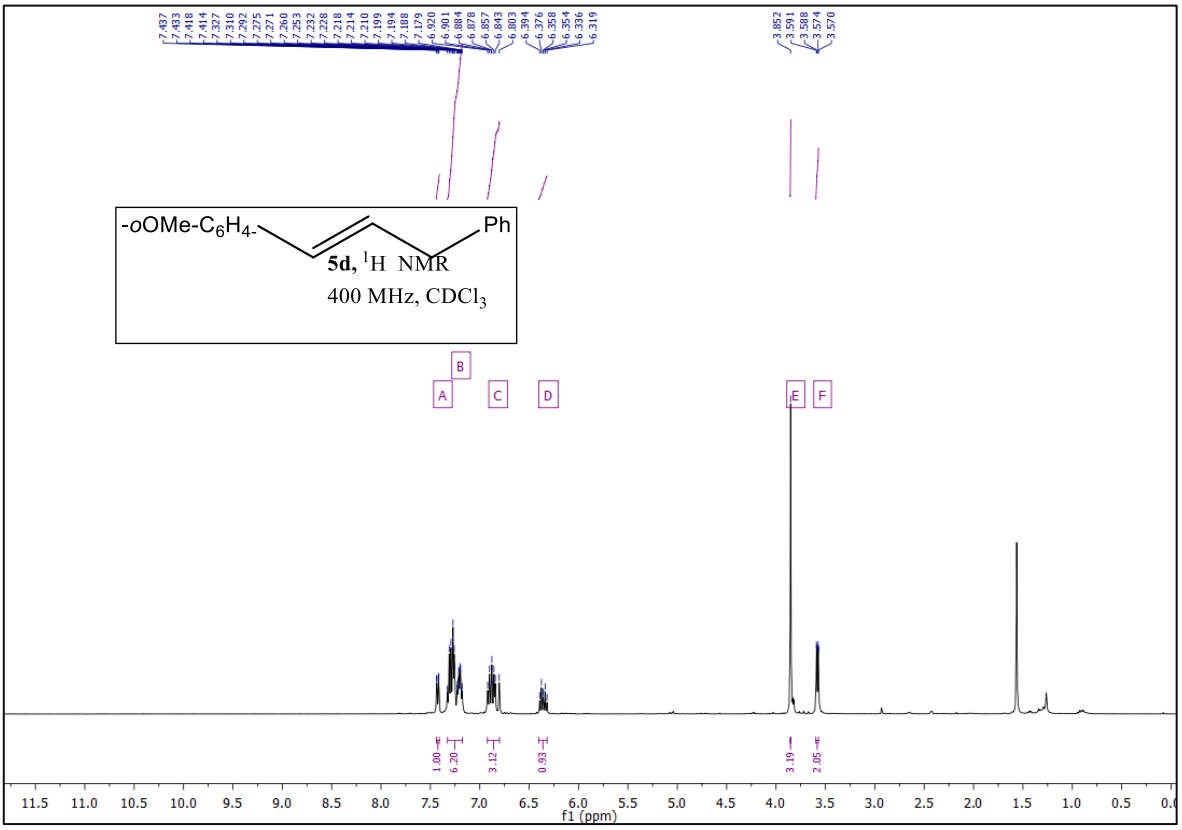
-oOMe-C6H4-
Ph
5d, 1H NMR
400 MHz, CDCl3
A
B
C
D
E
F
f1 (ppm)

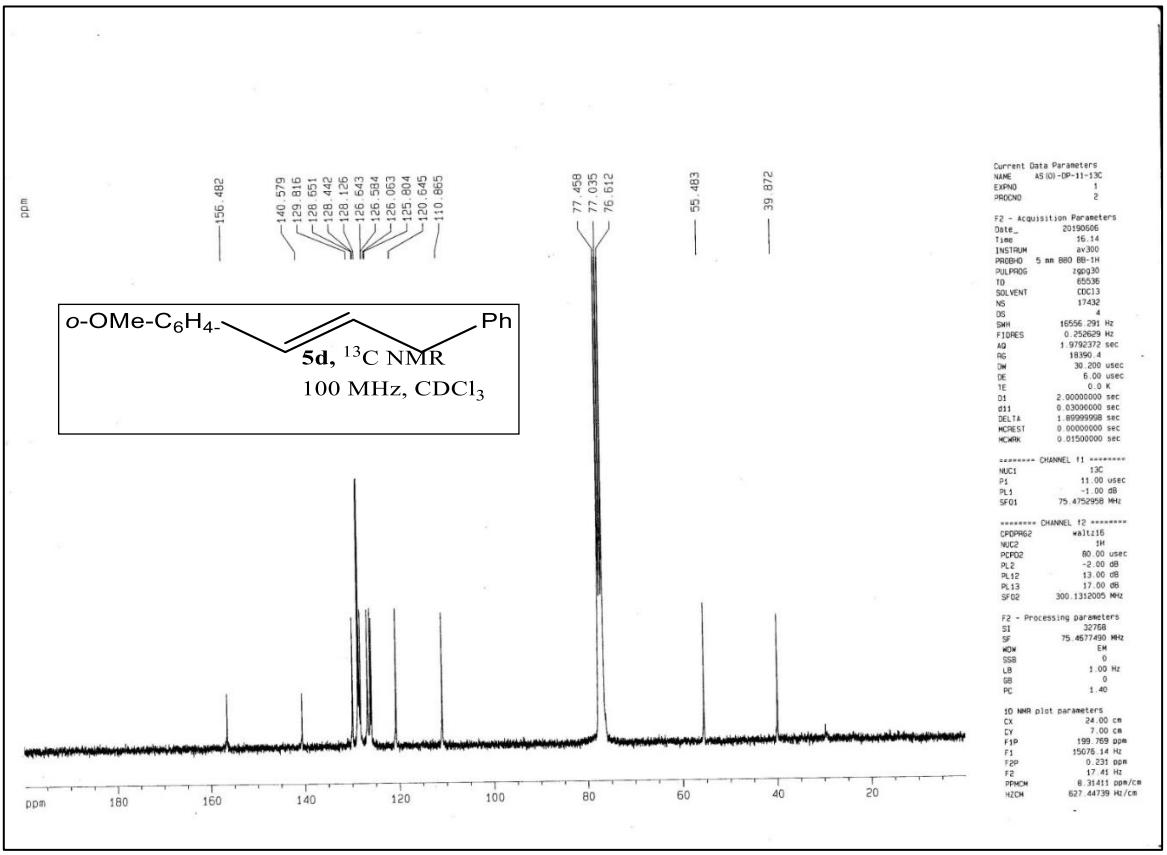
o-OMe-C6H4-
Ph
5d, 13C NMR
100 MHz, CDCl3
ppm

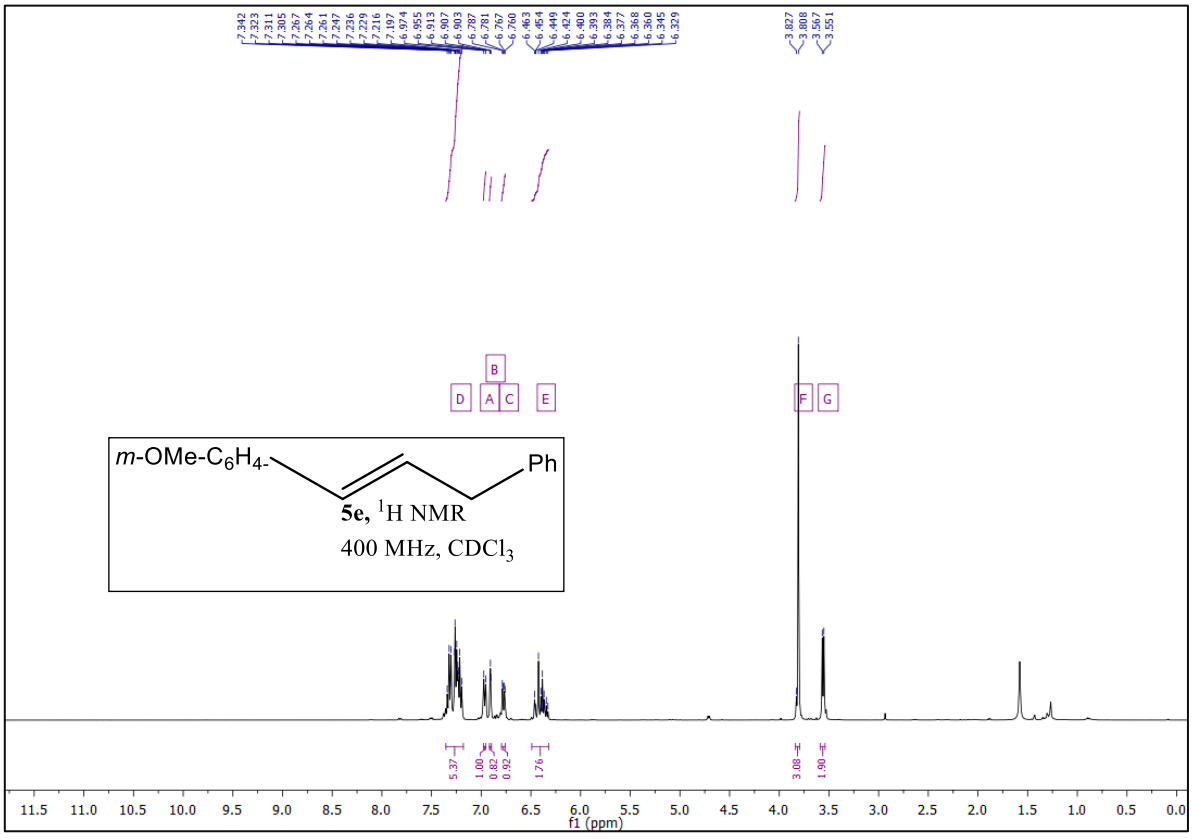
m-OMe-C6H4-
Ph
5e, 1H NMR
400 MHz, CDCl3
f1 (ppm)

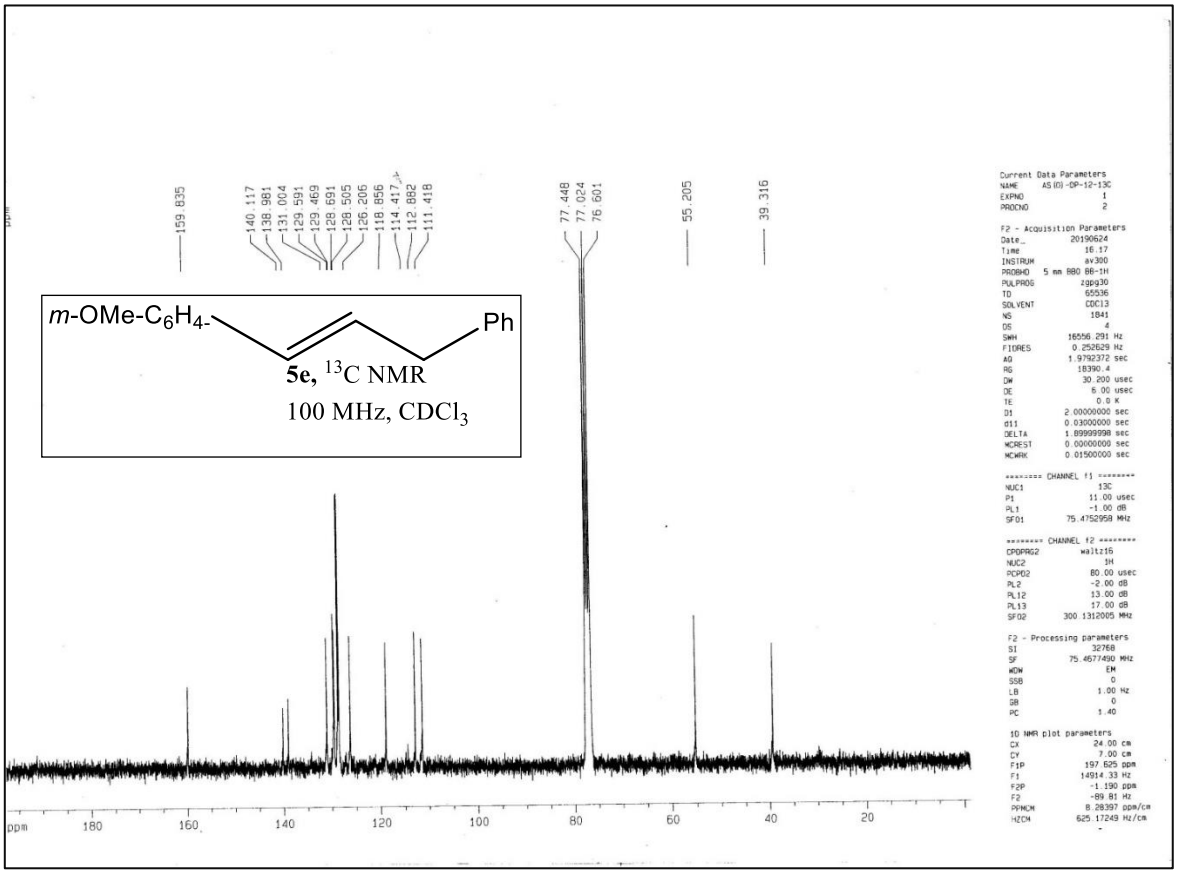
m-OMe-C6H4-
Ph
5e, 13C NMR
100 MHz, CDCl3
ppm

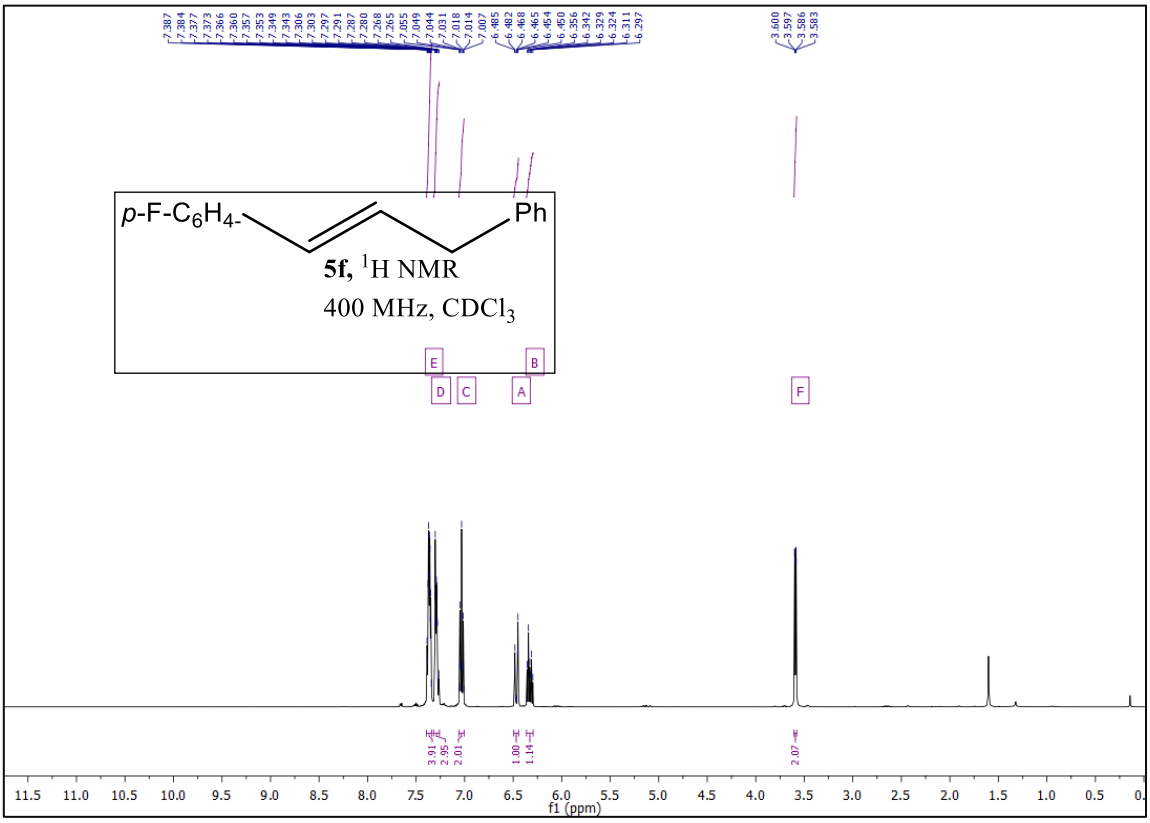
p-F-C6H4-
Ph
5f, 1H NMR
400 MHz, CDCl3
E
B
D
C
A
F
f1 (ppm)

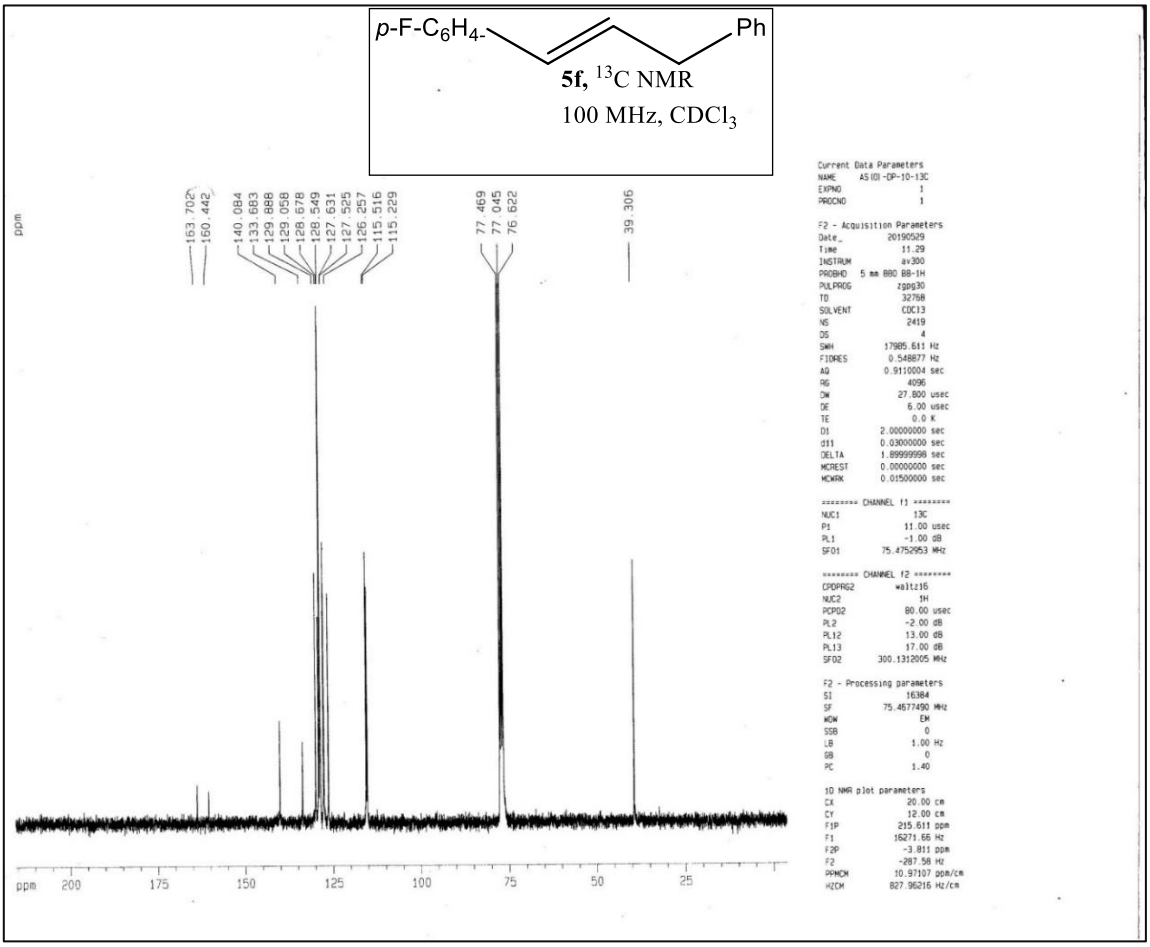
p-F-C6H4-
Ph
5f, 13C NMR
100 MHz, CDCl3
ppm

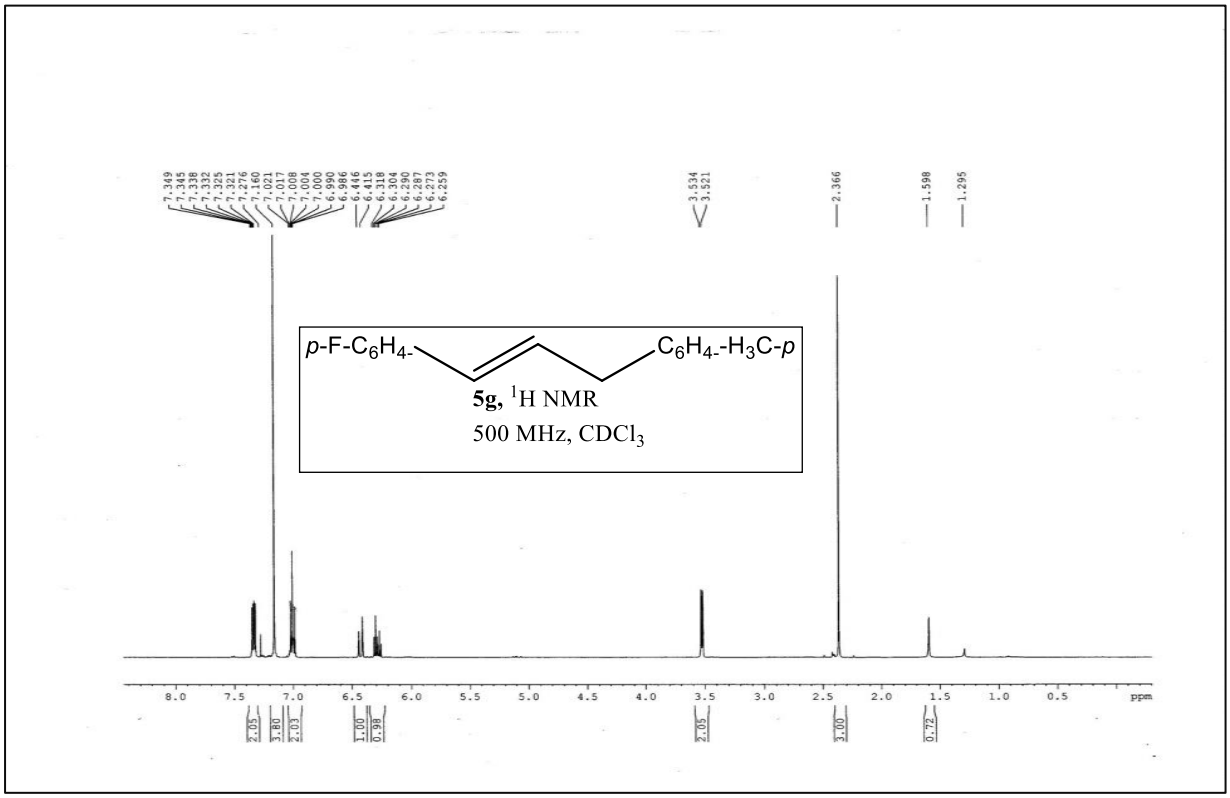
p-F-C6H4-
C6H4-H3C-p
5g, 1H NMR
500 MHz, CDCl3
7.349
7.345
7.338
7.332
7.325
7.321
7.316
7.160
7.021
7.017
7.008
7.004
7.000
6.990
6.986
6.446
6.415
6.318
6.304
6.290
6.287
6.273
6.259
3.534
3.521
2.366
1.598
1.295
8.0
7.5
7.0
6.5
6.0
5.5
5.0
4.5
4.0
3.5
3.0
2.5
2.0
1.5
1.0
0.5
ppm
2.05
3.80
2.03
1.00
0.98
2.05
3.00
0.72

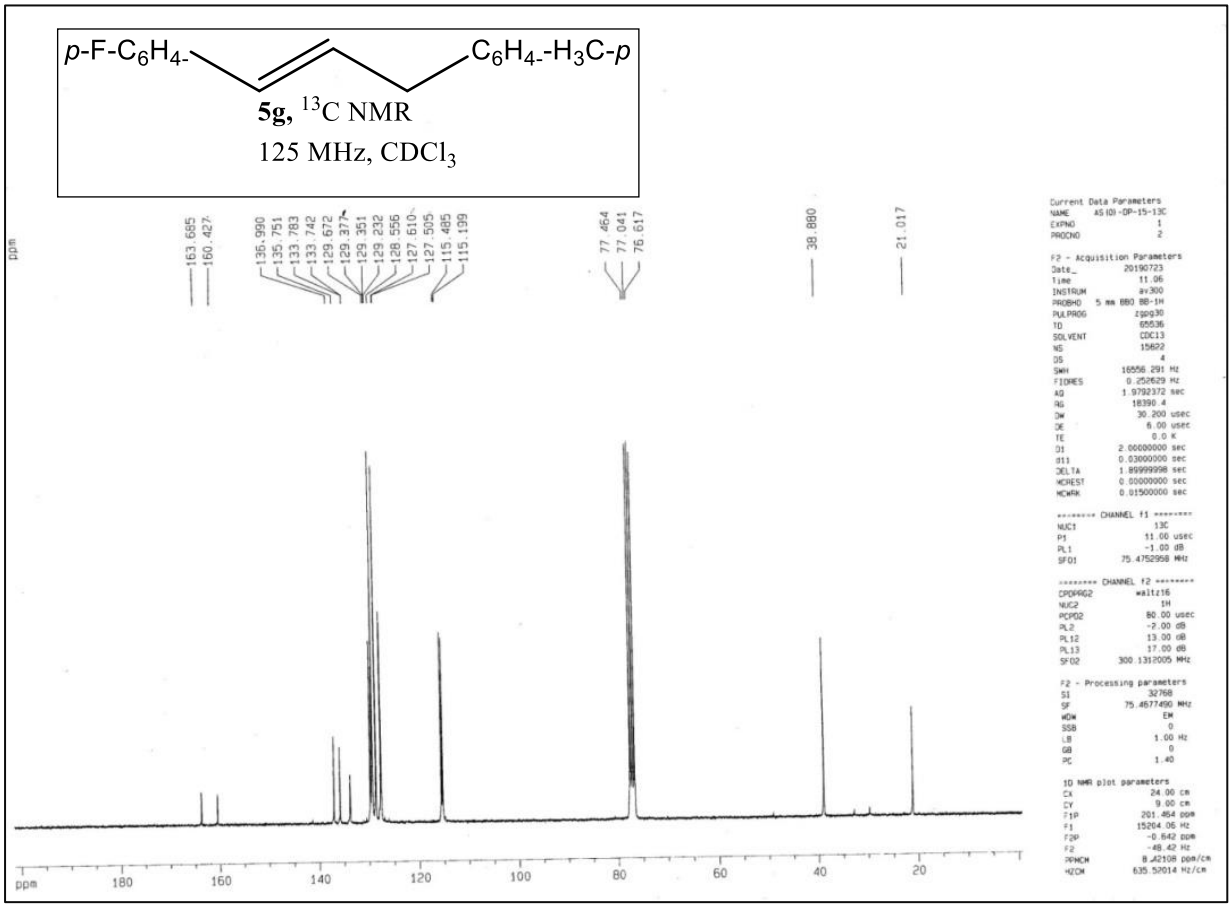
p-F-C6H4-
C6H4-H3C-p
5g, 13C NMR
125 MHz, CDCl3
ppm
163.685
160.427
136.990
135.751
133.783
133.742
129.672
129.374
129.351
129.232
128.556
127.610
127.505
115.485
115.199
77.464
77.041
76.617
38.880
21.017
Current Data Parameters
NAME AS 101-DP-15-13C
EXPNO 1
PROCNO 2
F2 - Acquisition Parameters
Date_ 20190723
Time 11.06
INSTRUM av300
PROBHD 5 mm BBO BB-1H
PULPROG zgpg30
TD 65536
SOLVENT CDCl3
NS 15622
DS 4
SWH 16556.291 Hz
FIDRES 0.252629 Hz
AQ 1.9792372 sec
RG 18390.4
DW 30.200 usec
DE 6.00 usec
TE 0.0 K
D1 2.00000000 sec
D11 0.03000000 sec
DELTA 1.89999998 sec
MCREST 0.00000000 sec
MCWRK 0.01500000 sec
CHANNEL f1
NUC1 13C
P1 11.00 usec
PL1 -1.00 dB
SFO1 75.4752958 MHz
CHANNEL f2
CPDPRG2 waltz16
NUC2 1H
PCPD2 80.00 usec
PL2 -2.00 dB
PL12 13.00 dB
PL13 17.00 dB
SFO2 300.1312005 MHz
F2 - Processing parameters
SI 32768
SF 75.4677490 MHz
WDW EM
SSB 0
LB 1.00 Hz
GB 0
PC 1.40
1D NMR plot parameters
CX 24.00 cm
CY 9.00 cm
F1P 201.464 ppm
F1 15204.06 Hz
F2P -0.642 ppm
F2 -48.42 Hz
PPMCM 8.42108 ppm/cm
HZCM 635.52014 Hz/cm
180
160
140
120
100
80
60
40
20

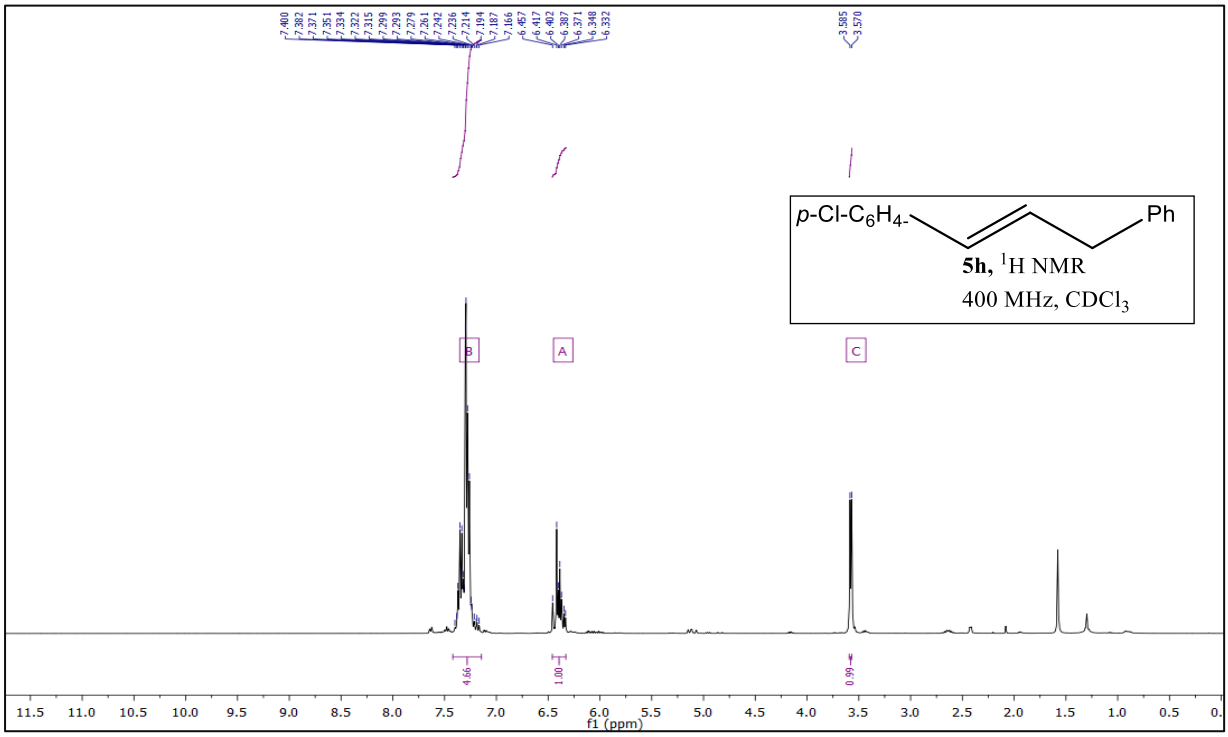
p-Cl-C6H4-
Ph
5h, 1H NMR
400 MHz, CDCl3
f1 (ppm)

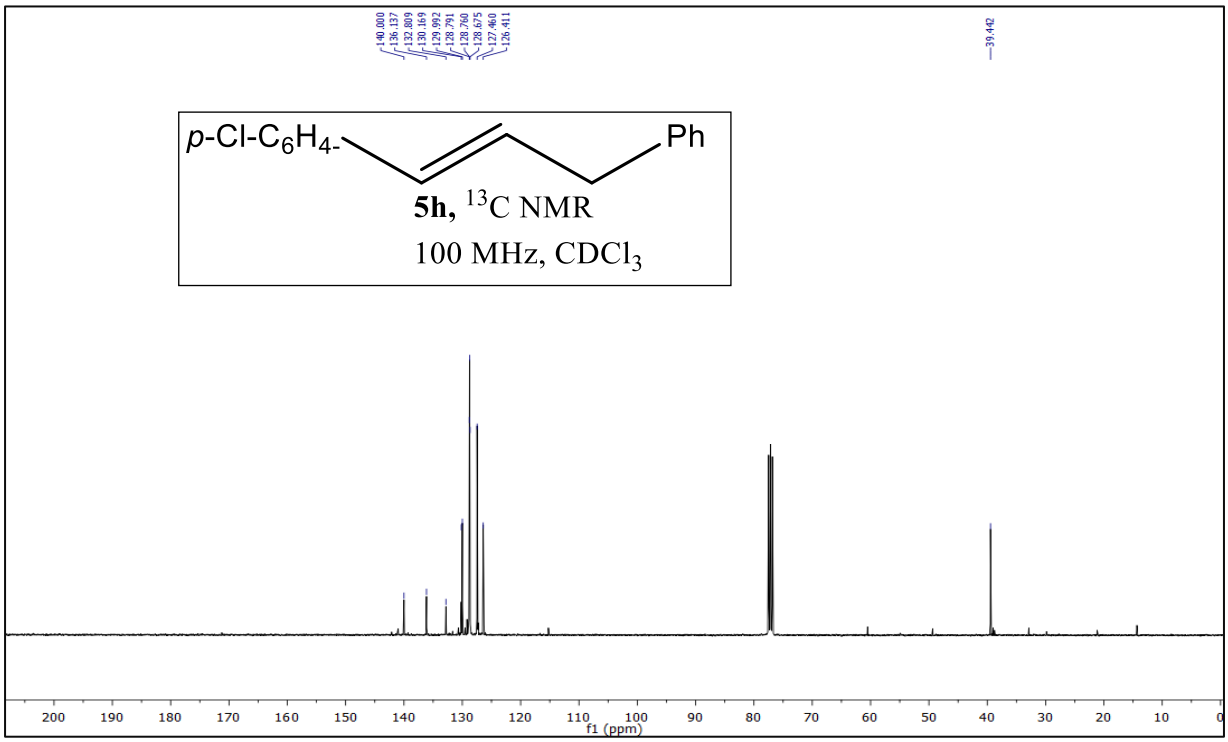
p-Cl-C6H4-
Ph
5h, 13C NMR
100 MHz, CDCl3
f1 (ppm)

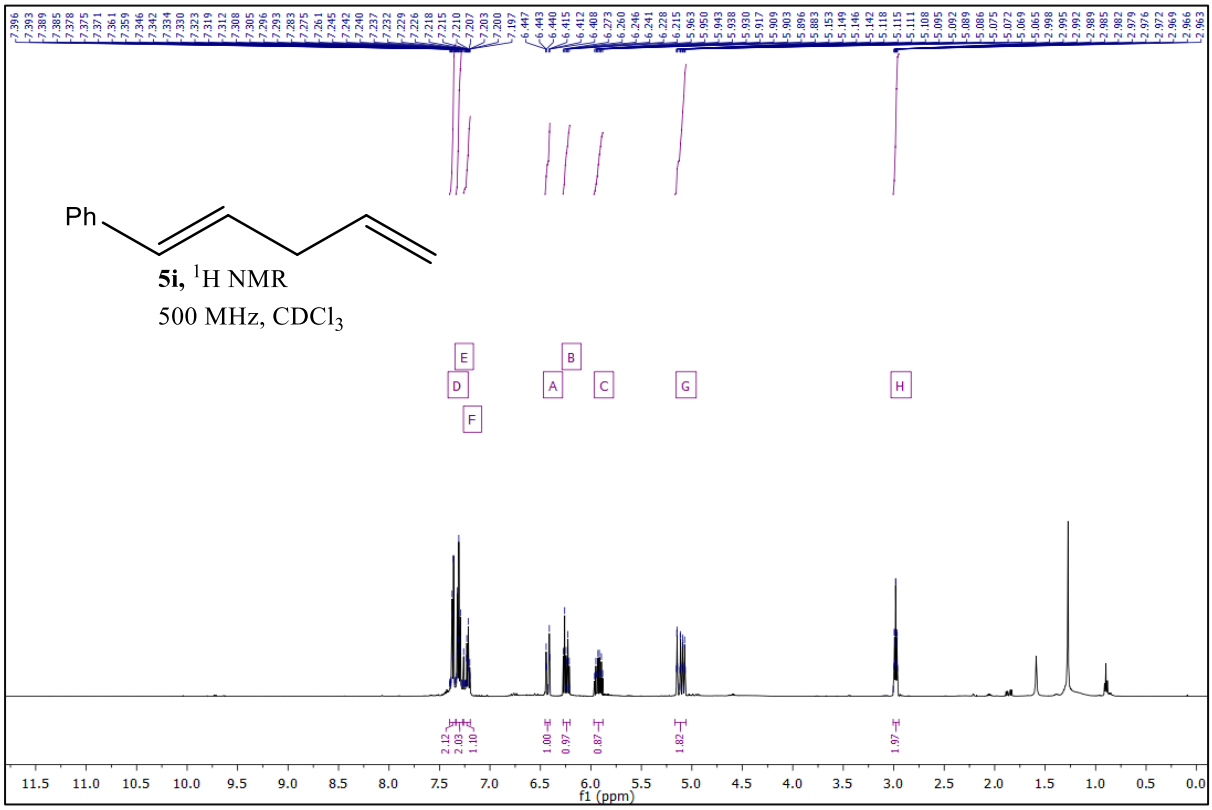
Ph
5i, 1H NMR
500 MHz, CDCl3
E
B
D
A
C
G
H
F
2.12
2.03
1.10
1.00
0.97
0.87
1.82
1.97
f1 (ppm)

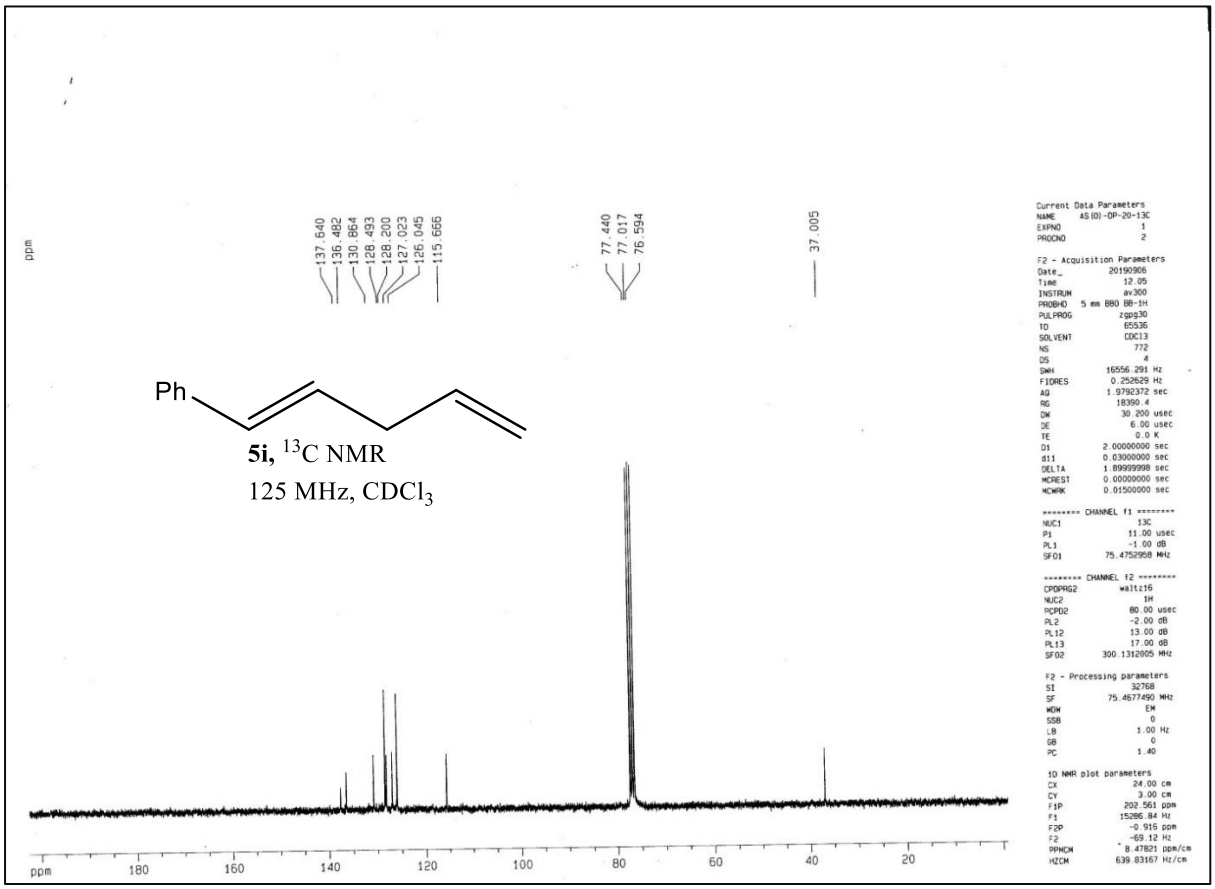
137.640
136.482
130.864
128.493
128.200
127.023
126.045
115.666
77.440
77.017
76.594
37.005
Ph
5i, 13C NMR
125 MHz, CDCl3
ppm

2/f References

1. M. Nasrollahzadeh, Z. Issaabadi, R. S. Varma, *ACS Omega*, **2019**, *4*, 14234−1424.
2. (a) F. Mohajer, M. M. Heravi, V. Zadsirjan and N Poormohammad, *RSC Adv.*, **2021,** *11*, 6885–6925. (b) K. Sonogashira, *J. Organomet. Chem.* **2002** *46*, 653.
3. P. Lei, G. Meng, Y. Ling, M. Szostak, *Org. Lett.* **2017**, *19*, 6510–6513.
4. (a) Francisco Foubelo, Carmen Najera and Miguel Yus *Chem. Rec*. **2016**, *16*, 2521–2533. (b) V. W. Bhoyare, E. D. Sosa, C. C. Chintawar, V. Gandon, N. T. Patil, *J. Am. Chem. Soc.* **2023**, *145*, 16, 8810–8816.
5. (a) I. Favier, D. Madec, E. Teuma, M. Gomez, *Curr. Org. Chem*. **2011**, *15*, 3127–3174, (b) A.V. Subrahmanyam, S. Thayumanavan, G.W. Huber, *ChemSusChem* **2010,** *3*, 1158–1161. (C) A. Fihri, M. Bouhrara, B. ekoueishahraki, J.-M. Basset, V. Polshettiwar, *Chem. Soc. Rev.,* **2007**, *40,* 5181–5203, (d) J. Hassan, M. Sevignon, C. Gozzi, E. Schulz, M. Lemaire, *Chem. Rev.* **2002,** *102* 1359–1470.
6. (a) N. M, Z. Issaabadi, R.S. Varma, *ACS Omega.* **2019**, *22*, 14234-14241. (b) P. R-C. Stephen, L. Buchwald. *Chem. Rev.* **2016**, *116*, 12564–12649.
7. Naghipour, A. Fakhri, *Catalysis Communications* **2016**, *73*, 39–45.
8. M. Bilal, H. M.N. Iqbal, S. F. Adil, M. R. Shaik, A. Abdelgawad, M. R. Hatshan, M. Khan, *Journal of Advanced Research* ***2022***,*38*, 157–177.
9. R. Javahershenas, S. Nikzat *RSC Adv.,* **2023**, *13*, 16619–16629.
10. R. d. S. Corrêaa, U. R. d. Oliveiraa, M. M. Abdallaa, *Vicente Aprigliano Fernandes Cleaner Waste Systems* **2022**. 100003.
11. (a) N. Blommaerts. N. Hoeven, D. A. Esteban, R Campos, M. Mertens, R. B. Antonella, G. K. D. Wael, S. Bals. S, L Sammy, W. V. P. Col, *Chemical Engineering Journal* **2021,** *410* 128234. (b) S. Anantharaj, P. E. Karthik, S. Noda, *Angew. Chem. Int. Ed.* **2021**, *60*, 23051 – 23067. (C) S. Kozuch, J. M. L. Martin, *ACS Catal.* **2012,** *2*, 2787−2794.
12. (a)N Baig, I. Kammakakam, W. Falath, *Mater. Adv.,* **2021**, *2*, 1821–1871. (b) R. Dubey, D. Dutta, A. Sarkar and P. Chattopadhya, *Nanoscale Adv.*, **2021**, *3*, 5722–5744.
13. C.Q. Wang, R.J. Zhao, H. Gui, J.F. Jin, F.F. Xia, Y.Z. Zhang, Coord. Xia, *Chem. Rev.* 2016, *326*, 86–110,
14. Shaabani, M. Mahyari, J. Mater. *Chem. A1* **2013**, 9303–9311, doi:10.1039/c3ta11706e.
15. S. Diyarbakir, H. Can, Ö. Metin, *ACS Appl*. *Mater. Interfaces* 2015,7, 3199–3206, doi:10.1021/am507764u.
16. (a)M. Raji, N. Zari, A. Qaiss, R. Bouhfid, **2019**, *1-20*, doi:10.1016/ b978-0-12-814548-7.00001-5.; (b) X. Wang, W. Xing, P. Zhang, L. Song, H. Yang, Y. Hu, *Compos. Sci. Technol.* 2012, 72, 737–743.
17. (a) Wang, W. Yu, Z. Huang, F. Zhou, J. Song, Y. Song, L. Long, M.P. Cifuentes, M.G. Humphrey, L. Zhang, J. Shao, C. Zhang, *Sci. Rep*. **2016**, *6*, 23325, (b) W. Yang, S. Akhtar, K. Leifer, H. Grennberg, *Int. Sch. Res. Notices* **2013**, 656185, (c) V.

Georgakilas, J.N. Tiwari, K.C. Kemp, J.A. Perman, A.B. Bourlinos, K.S. Kim, R. Zboril, *Chem. Rev.* 2016, 116, 5464–5519.
18. K. Bhowmik, D. Sengupta, B. Basu, G. De, *RSC Adv.* **2014,** 4,35442–35448.
19. S.S. Shendage, J.M. Nagarkar, *Sci. Commun.* **2014,** *1* 47–49.
20. C. Premi, N. Jain, *RSC Adv.* **2016,** *6,* 74961–74967.
21. Shekarizadeh, R. Azadi, *Appl. Organomet. Chem.* **2020,** *34,* e5775.
22. M. Mirza-Aghayan, M. Mohammadi, A. Addad, R. Boukherroub, *Appl. Organometal. Chem*. **2020**, *34*, e5524.
23. Z. Tong, P. Gao, H. Deng, L. Zhang, Peng-Fei X, H. Zhai *Synlett* **2008**, *20*, 3239-3241.
24. A. Shaabani, M. Mahyari, *J. Mater. Chem. A1*. **2013**, 9303–9311.
25. S. Diyarbakir, H. C. Ö. Metin, *ACS Appl. Mater. Interfaces* **2015**, *7*,3199–3206.
26. S. D. ltana, F.L. Mech, P. Hussain, G. Pahari, P. Borah, K. Gogoi, *RSC. Adv*. **2020**,*10,* 23108–23120.
27. B. Wang, Y. Wang, X. Guo, Z. Jiaoa, G. Jin, X. Guo, *Catal. Commun.* **2017**, *101,* 36–39.
28. S. J. Kumara, G.N. Krishnamurthy, U. Jinendra, S. Bhat, *Proc*. **2021**, *46*, 2874– 2879.
29. F. Durap, Ö. Metin, Turk. *J. Chem*. **2015,** *39.* 1247–1256.
30. S. G. Babu, R. Karvembu, *Tetrahedron Letters*, **2013**, *54*,1677–1680.
31. H. Liu, B. Yin, Z. Gao, Y. Li and H. Jiang, *Chem. Commun.,* **2012**, *48*, 2033.
32. (a) R. Xiao, H. Zhao and M. Cai, *Tetrahedron,* **2013**, *69*, 5444– 5545. (b) H. Zhao, W. He, R. Yao and M. Cai, *Adv. Synth. Catal.,* **2014**, 356, 3092–3098. (c) M. Cai, R. Yao, L. Chen and H. Zhao, *J. Mol. Catal. A: Chem.,* **2014**, *395*, 349–354; (d) H. Zhao, Y. Jiang, Q. Chen and M. Cai, *New J. Chem.,* **2015**, *39*, 2106–2111; (e) H. Zhao, W. He, L. Wei and M. Cai, Catal. Sci. Technol., **2016**, *6*, 1488–1495.
33. Z. Chen, E. Vorobyeva, S. Mitchell, E. Fako, M. Ortuño, N. López, S. Collins, P. Midgley, S. Richard, G. Vilé and J. Pérez-Ramírez, *Nat. Nanotechnol.,* **2018**, *13*, 702–707.
34. M. Lamblin, L. Nassar-Hardy, J-C. Hierso, E. Fouquet, and F-X Felpin, *Adv. Synth. Catal.* **2010**, *352*, 33 – 79.
35. K. Wang, J. Liu, F. Zhang, Q. Zhang, H. Jiang, M. Tong, Y. Xiao, N. Phan and F. Zhang, *ACS Appl. Mater. Interfaces,* **2019**, *11*, 41238–41244.
36. S. M. Sarkar, Md. L. Rahman, M. M. Yusoff, *N. J. Chem.* DOI: 10.1039/x0xx00000x.
37. A. R. Hajipour, F. Rezaeia and Z. Khorsandi, *Green Chem.,* **2017**, *19*, 1353–1361.
38. S. M. Sarkar, Md. L. Rahman, M. M. Yusoff, *N. J. Chem.* DOI: 10.1039/x0xx00000x.
39. I. Inaloo, S. Majnooni, H. Eslahi and M. Esmaeilpour, *ACS Omega*, **2020**, *13*, 7406–7417.
40. (a) A. B.Dounay, L. E. Overman, *Chem. Rev.* **2003**, *103*, 2945 – 2964; (b) A. Bianco, C. Cavarischia, M. Guiso, *Natural Product Research*, **2006**, *20*, 93–97; (c) A. Madin, C. J. O'Donnell, T. Oh, D. W. Old, L. E. Overman, M. J. Sharp, *J. Am. Chem. Soc.* **2005**, *127*, 18054 - 18065; (d) B. M. Trost, M. L. Crawley, *Chem. Rev.* **2003**, 103,

2921 – 2944; (e) B. M. Trost, *Tetrahedron* **2015**, *71*, 5708–5733; (f) Y. Zhang, H. -C. Shen, Y. -Y. Li, Y. –S. Huang, Z. –Y. Han, X. Wu, *Chem. Commun*. **2019**, *55*, 3769 – 3772.

41. (a) Y. Li, Z. Qi, H. Wang, X. Fu, C. Duan, *J. Org. Chem.* **2012**, *77*, 2053−2057; (b) A. -L. Lee, *Org. Biomol. Chem.* **2016**, *14*, 5357 – 5366.
42. J. P. Parrish, Y. C. Jung, S. Il Shin, K. W. Jung, *J. Org. Chem.* **2002**, *67*, 7127 – 7130.
43. (a) T. Koike, X. Du, T. Sanada, Y. Danda, A. Mori, *Angew. Chem. Int. Ed.* **2003**, *42*, 89 – 92; (b) K. Hirabayashi, J. –i. Ando, J. Kawashima, Y. Nishihara, A. Mori, T. Hiyama, *Bull. Chem. Soc. Jpn.* **2000**, *73*, 1409 – 1417; (c) A. Mori, Y. Danda, T. Fujii, K. Hirabayashi, K. Osakada, *J. Am. Chem. Soc.* **2001**, *123*, 10774 - 10775; (d) Z. Ye, F. Chen, F. Luo, W. Wang, B. Lin, X. Jia, J. Cheng, *Synlett* **2009**, *13*, 2198–2200; (e) T. Mino, M. Shibuya, S. Suzuki, K. Hirai, M. Sakamoto, T. Fujita, *Tetrahedron* **2012**, *68*, 429 – 432; (f) K. Hirabayashi, Y. Nishihara, A. Mori, T. Hiyama, *Tetrahedron Lett.* **1998**, *39*, 7893-7896.
44. Y. Nakao, T. Hiyama, *Chem. Soc. Rev.* **2011**, *40*, 4893–4901.
45. (a) A. Saha, J. Leazer, R. S. Varma, *Green Chem.* **2012**, *14*, 67 – 71; (b) B. R. Vaddula, A. Saha, J. Leazer, R. S. Varma, *Green Chem.* **2012**, *14*, 2133 - 2136; (c) Q. Zhang, X. Yang, J. Guan, *ACS Appl. Nano Mater.* **2019**, *2*, 4681-4697; (e) M. -N. Chen, L. -P. Mo, Z. -S. Cui, Z. -H. Zhang, *Current Opinion in Green and Sustainable Chemistry*, **2019**, *15*, 27–37; (f) R. B. N. Baig, R. S. Varma, *Chem. Commun.* **2013**, *49*, 752 – 770; (g) Z. B. Shifrina, L. M. Bronstein, Front. Chem. **2018**, *6*, 298; h) V. Polshettiwar, R. Luque, A. Fihri, H. Zhu, M. Bouhrara, J. –M. Basset, *Chem. Rev.* **2011**, *111*, 3036 – 3075.
46. (a) N. H. Abdullah, K. Shameli, E. C. Abdullah, L. C. Abdullah, *Chinese Chemical Letters*, **2017**, *28*, 1590 – 1596; (b) J. –S. Jiang, Z. –F. Gan, Y. Yang, B. Du, M. Qian, P. Zhang, *J. Nanopart. Res.* **2009**, *11*, 1321 – 1330; (c) M. Zheng, J. Lu, D. Zhao, *Science of the Total Environment* **2018**, *622 – 623*, 930 – 941; (d) A. J. Cole, A. E. David, J. Wang, C. J. Galbán, H. L. Hill, V. C. Yang, *Biomaterials* **2011**, *32*, 2183 – 2193. (e) D. K. Kim, M. Mikhaylova, F. H. Wang, J. Kehr, B. Bjelke, Y. Zhang, T. Tsakalakos, M. Muhammed, *Chem. Mater.* **2003**, *15*, 4343-4351; (f) T. T. Dung, T. M. Danh, L. T. M. Hoa, D. M. Chien, N. H. Duc, *Journal of Experimental Nanoscience* **2009**, *4*, 259 – 267; (g) C. Jin, Z. Haiyan, L. Liping, Z. Li, *Digest Journal of Nanomaterials and Biostructures* **2014**, *9*, 143 – 149; (h) C. Saikia, A. Hussain, A. Ramteke, H. K. Sharma, T. K. Maji, *Starch/Stärke* **2014**, *66*, 760 – 771.
47. (a) A. Saha, B. C. Ranu, *Org. Biomol. Chem.* **2011**, *9*, 1763 – 1767; (b) A. Ariafard, Z. Lin, *Organometallics* **2005**, *24*, 3800 - 3806; (c) B. Wucher, M. Moser, S. A. Schumacher, F. Rominger, D. Kunz, *Angew. Chem. Int. Ed.* **2009**, *48*, 4417 – 4421.

Chapter-II

Section-I

Synthesis of thioamides via decarboxylative C-C bond formation reactions using elemental sulfur and homogeneous catalyst

2/a Introduction

Chemistry of thioamides have received considerable attention to the organic chemists due to their immense importance in the area of peptide chemistry, medicinal chemistry and organic synthesis. Thioamides are naturally existing isosteres of amide bonds in which chalcogen atom of the carbonyl oxygen changed to sulfur. Thioamide [CSNH] bond length and bond angle is 0.01A and 0.5^{o} compared with in natural amide bond. Thioamide scaffolds possess a plethora of biological properties like herbisidial, pesticidal, antifungal, antituberculous, antithyroid, anthelmintic, antihypertensive, hypnotic or anesthetic, hypotensive, anticancer, analgesic, antiepileptic, antioxidants, and antimicrobial, [fig. 2.1].[1-11] Recently a new class of thioamide derivatives have been identified which act as potent inhibitors of β-glucronidase, the B_1 domain of protein G (GB1) α-amylase, α-glucosidase, cholinesterase, glucose-6-phosphate, histone deacetylase and phenoloxidase enzyme.[12] Antithyroid drug contening thioamides (propylthiouracil, thiamazole and carbimazole) have been synthesized of T_4 by preventing iodination of tyrosine residues and propylthiouracil conversion of T_4 to T_3.[13] Thioamide can also be used in thyroid function tests.[14] They can also block the active sites by absorbing into metal surface. Carbimazole is rapidly converted to active metabolite thiaimazole.[15] In addition, thioamide derivatives also show plant growth regulating, insect repellant, anion sensing and transport properties.[16]Thioamide compounds are also used in commercial purposes like in dyes, photographic films, textile and polymer industries.[17]They are extensively used as organocatalyst,[18] chemosensors,[19] ligands,[20] textile treating agents,[21] metallic electrodes, [22] vulcanization accelerator,[23] active component of polymers, [24] biomimetic models,[25] and synthetic building blocks.[26] Presence of conjugating sulfur it act as a donor sites in thioamide compounds make it more facile to coordinated with metal ion to form chelate complex which is further used as homogeneous catalysis, redox sensing and magnetic materials.[27] Higher stability of such metal complex due to better donor properties of sulfur atom in thioamide compounds.[28] Possibility of mode of binding like neutral, monovalent, or polyvalent ions makes it extremely flexible as ligands.[29] Moreover, metal complex of thioamide are organic parts of complex shows advantageous properties of both elements.[30] Endothioamide containing thioamide may reveals critical information on the importance of particular amide bond.[31] A brief review on various synthetic strategies of decarboxylative thioamidation derivatives and their application in synthetic fields has been presented below.

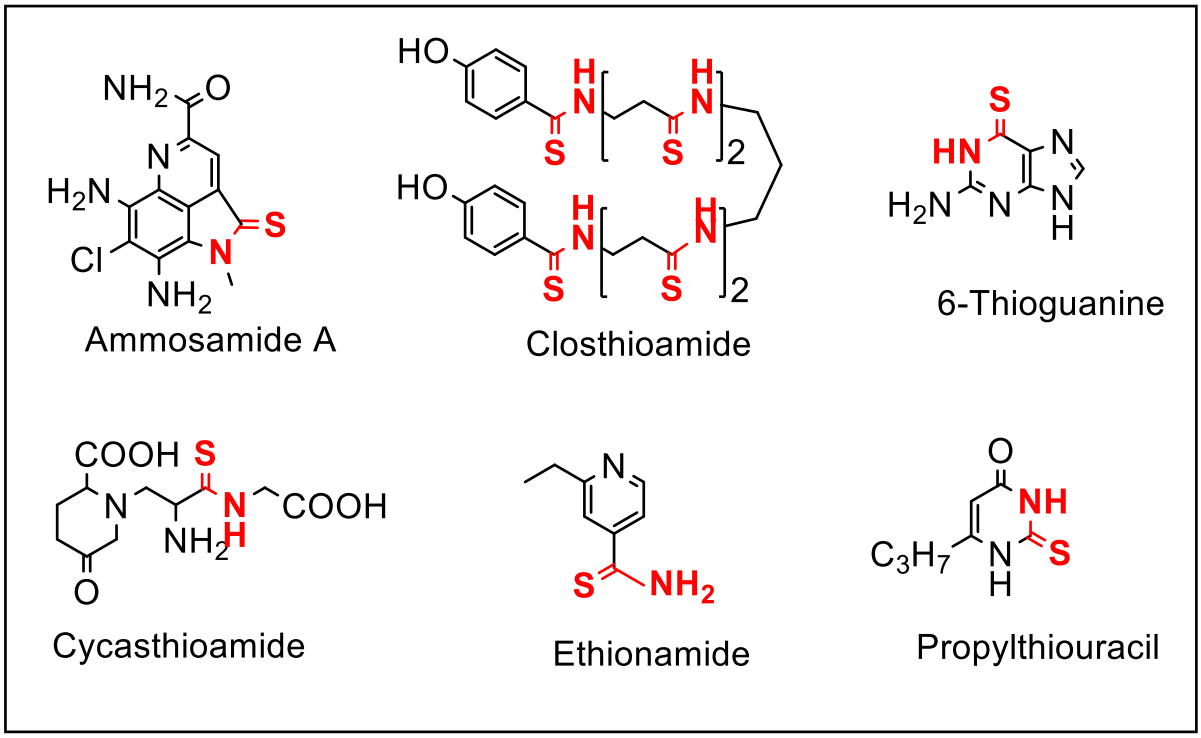

Figure 2.1 Few biologically active thioamide molecules.

1/b Review

Due to the immense importance of thioamide derivatives in pharmaceuticals as well as in synthetic organic chemistry, chemists have put great attention to the synthesis and application of thioamides. As a result of that, a large number of synthetic strategies were developed to synthesize thioamide derivatives either using conventional methods or using some modern techniques. This short review demonstrates various synthetic approaches of thioamide compounds.

I. Decarboxylation of *α* -imino acids:

Grigg and his co-worker[31] developed a general synthetic procedure of thioamide derivatives *via* decarboxylation of *α*-keto acid. *α*-Imino acids prepared from *α*-keto acid rection between primary amines and the combined regent elemental sulphur in benzene or methylene chloride solvent at 80 ^{o} C within 20 min. (Scheme-2.1). Decarboxylation proceeds *via* a 1,2-ylide which can be trapped by sulphur to give the corresponding secondary thioamides in good yield (up to 95%).

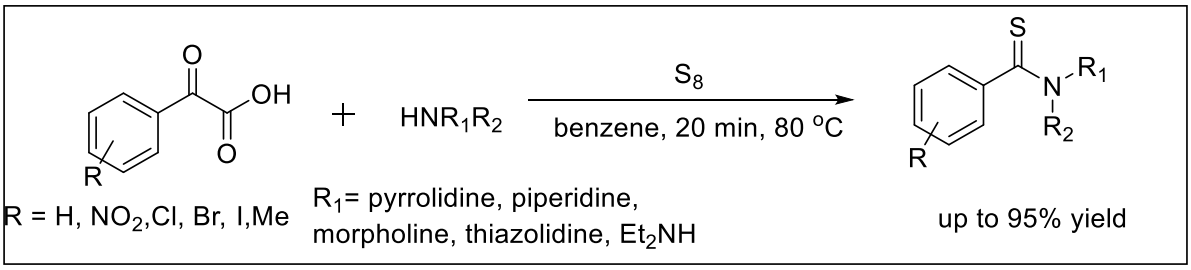

Scheme-2.1

II. Mild and chemoselective thioacylation of amines enabled by the nucleophilic activation of elemental sulfur:

Takemoto and his co-worker[32] developed a mild and chemoselective method for the synthesis of thioacylation of amines using *α*-keto acid and elemental sulfur. One of the convenient synthetic route to produce thioamide derivative is the reaction between *α*-keto acid within amine and elemental sulfur in THF solvent at a very short duration (Scheme 2.2). The key to success of this transformation is the nucleophilic activation of elemental sulfur by 1-dodecanethiols and a variety of unprotected functional groups such as hydroxyl, carboxyl. amide, sulfide and tertiary amine moieties, are tolerated under identical reaction condition with good yield.

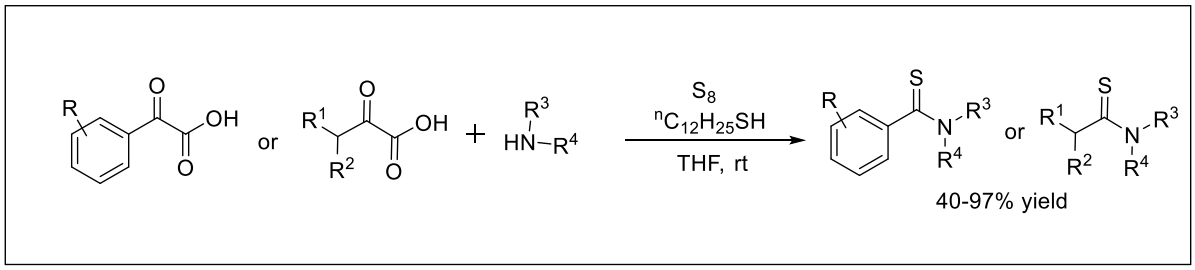

Scheme-2.2

III. Decarboxylative thioamidation of arylacetic acids:

A new decarboxylative route for thioamide synthesis from cinnamic acid derivatives was reported by Singh et al[33] where it was synthesized by the reaction between arylacetic acid, amines and elemental sulfur powder without the need of a transition metal and an external oxidant, forming imene intermediated which further reacted with sulfurbased nucleophile at 80 ^{o} C for 6 h afford the desired product in yield (Scheme 2.3). Synthesis of thioamides are efficient one-pot metal-free decarboxylation reaction.

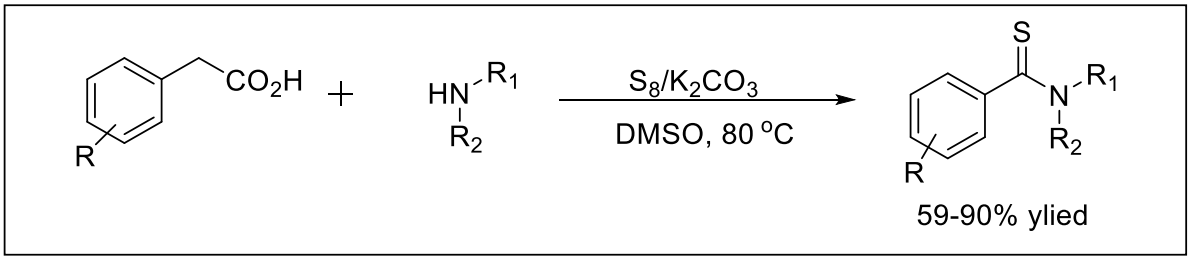

Scheme-2.3

IV. Decarboxylative thioamidation of cinnamic acids:

Krishna and his group[34] developed a general synthetic procedure of substituted thioamide by the reaction between cinnamic acids, amines and the combined reagent of elemental sulfur in DMSO solvent within 8 h at 100 ^{o} C (Scheme 2.4). At the end of the reaction substituted thioamides were also formed with desired product.

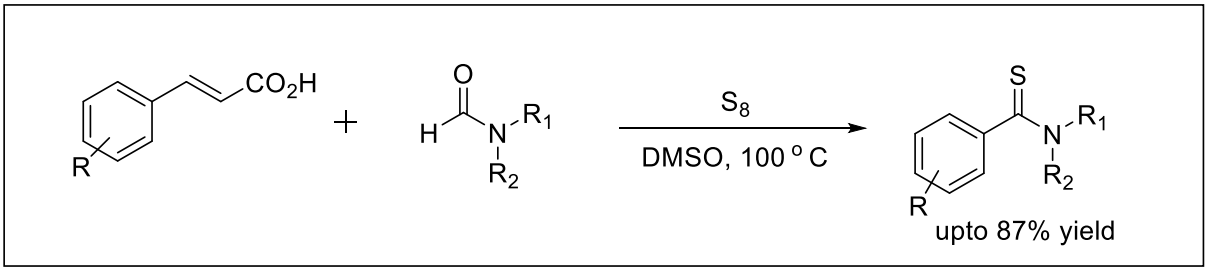

Scheme-2.4

V. New direct synthesis of thioamides from carboxylic acids:

Goswami and his co-workers[35] demonstrated O, O-diethyl dithiophoric acid (DDTPA) promoted synthesis of substituted thioamide starting from arylglyoxalic acid. The synthetic root of thioamides is a novel one-pot reaction between arylglyoxalic acid and amines in the presence of O, O-dithiophocid (DDTPA)in toluene solvent under reflux condition resulting the formation of substituted thioamide derivatives in good yield (Scheme 2.5). Such method involves catalyst free, high atom economy, easy work-up and production of pure, hindered thioamide substrate.

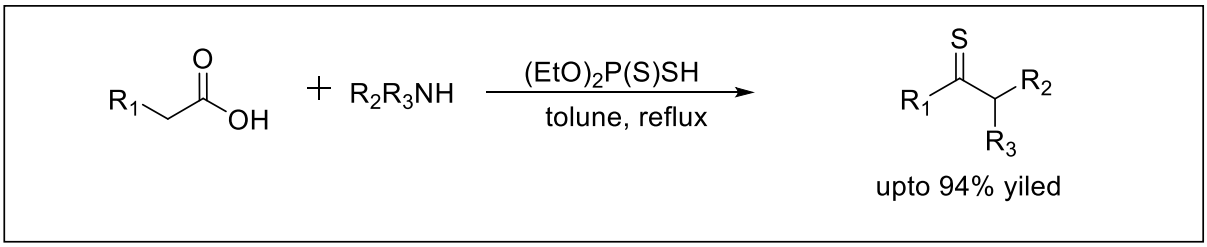

Scheme-2.5

VI. Thiol as a Synthon for preparing thiocarbonyl: aerobic oxidation of thiols for the synthesis of thioamides:

Another environment friendly, atom-economical and step-economical approach was reported by Jang and his co-workers[36] for the preparation of thioamide where the reaction between thiols, amine, Cu (II) catalyst oxidant TBD and O_2 without using any solvent resulted reasonable yields (Scheme 2.6). This is the first successful conversion of thiols to

thiocarbonyls using molecular oxygen as an oxidant, conversion of thiols to thioamide under aerobic oxidation conditions without the use of exogenous sulfur reagents.

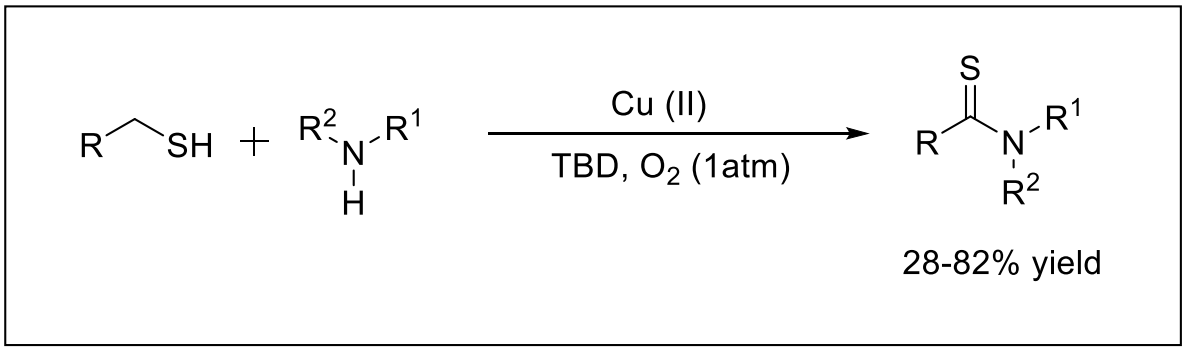

Scheme-2.6

VIII. Carbon nitride creates thioamides by the photocatalytic Kindler reaction:

Savateev et al[37] developed a new convent method for synthesis of thioamides using amines and elemental sulfur as a bulding blocks under visible light irradiation. Potassium poly(heptazine imide) and carbon nitride used as photo-catalyst. The chance of the developed methodology was confirmed using different kinds of several amines such as primary, secondary, substituted benzylamines and hetero-cyclic and aliphatic methylamines which were converted into thioamides in 68-92% yield (Scheme 2.7).

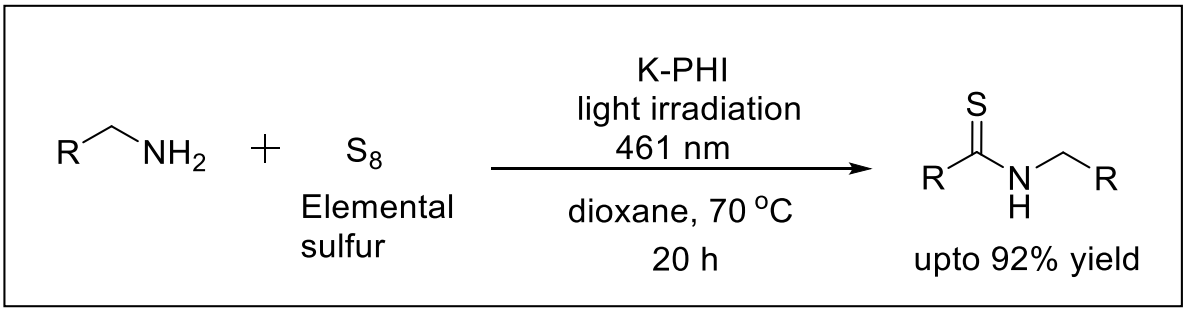

Scheme-2.7

VIII. Copper(II)-Catalyzed Reactions of Dimethylformamide with Phenylacetonitrile and Sulfur to Form N,N-Dimethylthioamides

Zhou and his coworkers[38] developed a novel method for selective synthesis N, N-dimethylthiobenzamide and N, N-dimethyl-2-phenylethanethioamide by copper–catalyzed three component reaction of phenylacetonitrile, sulfur and DMF (dimethyformamide) in yields up to 96% (Scheme 2.8). The synthesis of 3-phenylthiophene derivatives was anticipated to involve the reaction between phenylacetonitrile, elemental sulfur, and an aldehyde such as n-valeraldehyde. The significance of these observations lies in their ability to provide alternative methods for synthesizing N,N-disubstituted thiobenzamides and their derivatives.

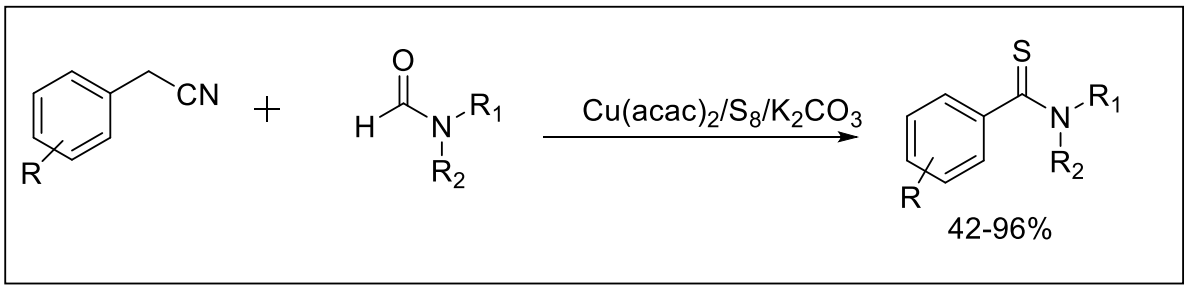

Scheme-2.8

1/c Conclusion

Several decarboxylative synthetic approaches of thioamides have been described in this short review. It reveals that such protocols are still in demand due to their operational simplicity, cheap starting materials, wide substrate scope, functional group tolerance and ease of isolation of desired product. However, in most of the cases huge excess of elemental sulfur has been used. Also it has been found that electron donating group containing arylglyoxylic acid does not respond in previously reported thioamidation reactions. Keeping this in mind, we are going to discuss a new and convenient method to prepare thioamide compounds by decarboxylative-decarbonylative thioamidation of aryglyoxylic acids.

Section-II

Present Work:

Pd (II)-Catalyzed decarboxylative-decarbonylative C-C Bond Formation reactions: Synthesis of thioamide compounds

2/a Introduction

Arylglyoxylic acids have been employed in a novel decarboxylative-decarbonylative thioamidation reaction with the dithiocarbamate intermediates prepared *in situ* by the prompt reaction of amines and carbon disulfide. Although, α-keto acids are very common to undergo decarboxylative mechanistic pathways,[39] the decarboxylative-decarbonylative techniques[40] are comparatively less explored. A series of thioamide compounds were synthesized involving different arylglyoxylic acids and various secondary amines, primary amine, aniline, amino acid derivative. The reaction is proposed to proceed *via* acyl radical intermediate in presence of persulfate oxidant and Pd (II) catalyst (Scheme 2.9).

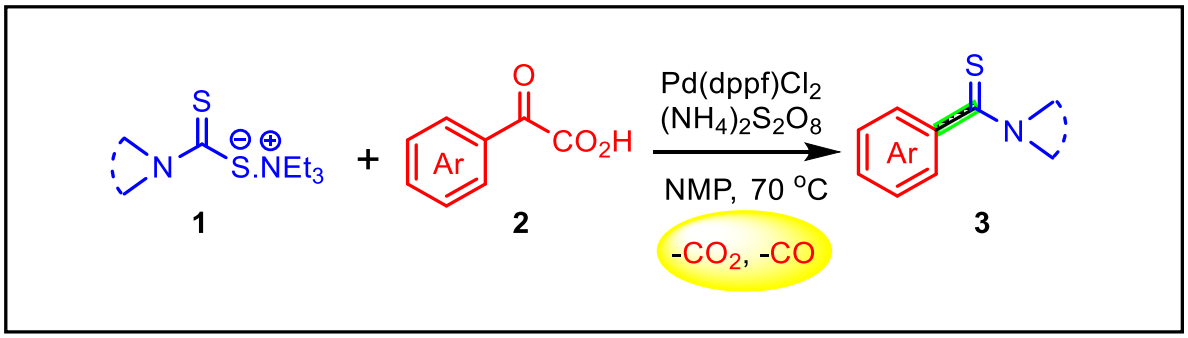

Scheme-2.9

2/b Results and discussion

The experimental procedure is very simple. An NMP solution of dithiocarbamate salt, freshly prepared by the reaction of amine and CS_2 in presence of trimethylamine, was stirred with arylglyoxylic acid, Pd-catalyst and $(NH_4)_2S_2O_8$ at 70 ^oC for 8 h. After completion of the reaction (checked by TLC), the crude product, obtained by usual aqueous work-up, was purified by column chromatography. Inorder to standardize the reaction condition, piperidine-dithiocarbamate salt (1a) and phenylglyoxylic acid (2a) were chosen as the model substrates and a series of reactions were performed with variable reaction parameters (Table 2.1). Initially we tried the reaction in THF medium in presence of $PdCl_2$ catalyst and $(NH_4)_2S_2O_8$ oxidant (entry 1, Table 2.1). However, the desired thioamide product (3a) was formed only with 16% of yield. Other solvent media, like 1,4-dioxane, acetonitrile, DCE, DMF were also not found to be suitable for the reaction (entries 2 - 5, Table 2.1). However, the yield of the desired product increased significantly (64%) in NMP solvent medium (entry 6, Table 2.1). To improve the yield of reaction, we employed other Pd-catalysts, such as $Pd(OAc)_2$ and $(dppf)PdCl_2$. The reaction was found to proceed smoothly providing an excellent yield of the reaction (96%) in presence of $(dppf)PdCl_2$ within 8 h at 70 ^oC (entry 8, Table 2.1). Other oxidant, like $K_2S_2O_8$ was found to be comparatively less effective for the reaction (entry 9, Table 2.1). Use of K_2CO_3 instead of trimethylamine was not at all competent for the reaction (entry 15, Table 2.1). Elevation of the reaction temperature beyond 70 ^oC shows an adverse effect on the reaction providing decreased yield of the

desired product (entry 12, Table 2.1). The reaction remains incomplete lowering either the reaction time period or the temperature (entries 13, 14, Table 2.1). The reaction does not proceed at all either in absence of the catalyst-(dppf) $PdCl_2$ or the oxidant-$(NH_4)_2S_2O_8$ (entries 10, 11, Table 2.1). Thus, the catalyst and the oxidant have crucial roles in the present organic transformation.

Table 2.1 Standardization of the reaction condition

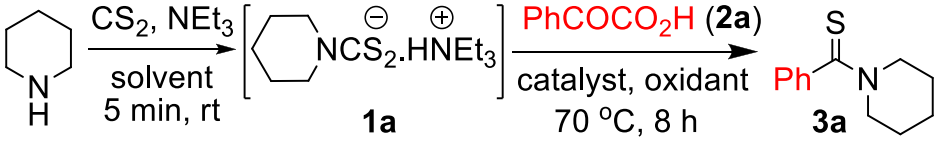

Entry	Catalyst	Oxidant	Solvent	Yield [%]
1	$PdCl_2$	$(NH_4)_2S_2O_8$	THF	16
2	$PdCl_2$	$(NH_4)_2S_2O_8$	dioxane	20
3	$PdCl_2$	$(NH_4)_2S_2O_8$	CH_3CN	–
4	$PdCl_2$	$(NH_4)_2S_2O_8$	DCE	12
5	$PdCl_2$	$(NH_4)_2S_2O_8$	DMF	43
6	$PdCl_2$	$(NH_4)_2S_2O_8$	NMP	64
7	$Pd(OAC)_2$	$(NH_4)_2S_2O_8$	NMP	53
8	$(dppf)PdCl_2$	$(NH_4)_2S_2O_8$	NMP	96
9	$(dppf)PdCl_2$	$K_2S_2O_8$	NMP	67
10	$(dppf)PdCl_2$	–	NMP	–
11	–	$(NH_4)_2S_2O_8$	NMP	–
12[a]	$(dppf)PdCl_2$	$(NH_4)_2S_2O_8$	NMP	92
13[b]	$(dppf)PdCl_2$	$(NH_4)_2S_2O_8$	NMP	75
14[c]	$(dppf)PdCl_2$	$(NH_4)_2S_2O_8$	NMP	82
15[d]	$(dppf)PdCl_2$	$(NH_4)_2S_2O_8$	NMP	23

Reaction condition: A mixture of piperidine (1 mmol), CS_2 (1.5 mmol), Et_3N (2 mmol) was stirred in 2 ml of solvent for 5 min at room temperature. ***2a*** *(0.8 mmol), Pd-catalyst (10 mol%), oxidant (1 mmol) were added to the reaction mixture and stirred for 8 h at 70 °C. Yields reported are the isolated yields. [a]The reaction mixture was stirred at 100 °C. [b]The reaction time period was 4 h. [c]The reaction mixture was stirred at 50 °C. [d]K_2CO_3 (2 mmol) has been used instead of triethylamine.*

The optimized reaction condition was followed to prepare several thioamide compounds (**3**) (Table 2.2) with different functional groups and structural variations. Arylglyoxylic acids (**2**) containing both electron donating groups (Me, OMe) and electron withdrawing groups (Cl, Br, NO_2) underwent the decarboxylative-decarbonylative thioamidation reaction efficiently producing good yields of the corresponding thioamides (**3e - 3t**). In the previously reported protocols[41] it was not

Table 2.2 Synthesis of thioamides from arylglyoxylic acids

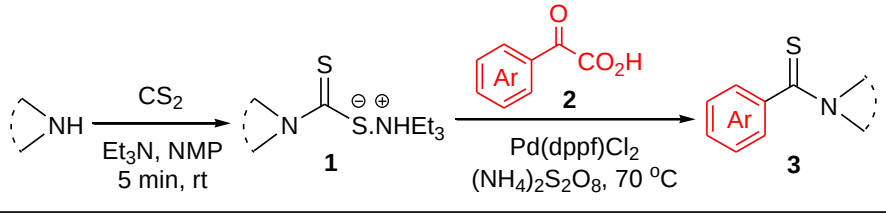

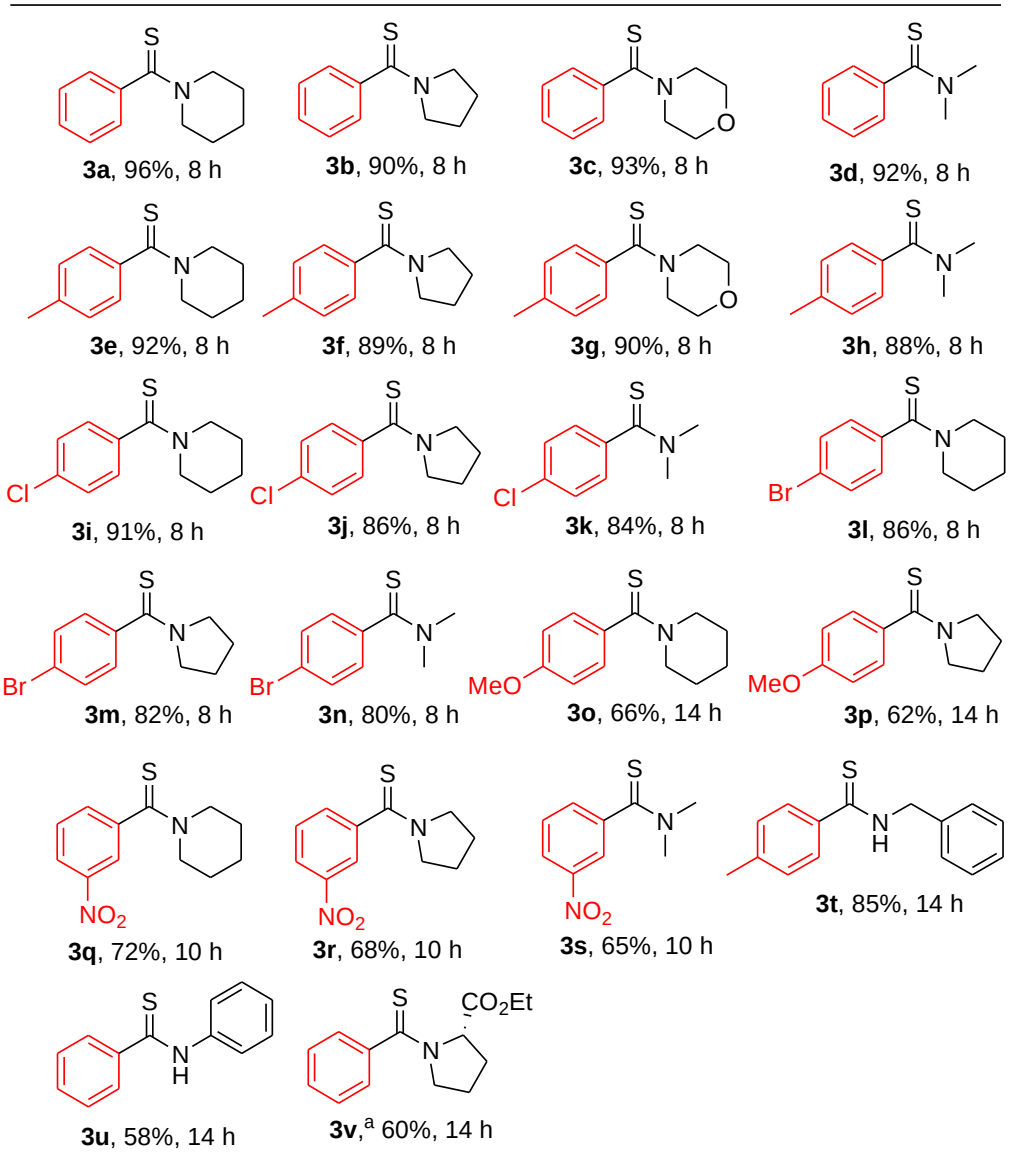

*Reaction condition: A mixture of amine (1 mmol), CS_2 (1.5 mmol), Et_3N (2 mmol) was stirred in 2 ml of NMP for 5 min at room temperature. Arylglyoxylic acid (**2**) (0.8 mmol), $(dppf)PdCl_2$ (10 mol%), $(NH_4)_2S_2O_8$ (1 mmol) were added to the reaction mixture and stirred at 70 °C for the certain time period. Yields reported are the isolated yields. [a]Instead of Et_3N, $^iPr_2NEt$ has been used.*

possible to employ arylglyoxylic acids containing electron donating groups in the synthesis of aryl thioamides (such as **3e - 3h**, **3o**, **3p**). A variety of secondary amines, like piperidine, pyrrolidine, morpholine, dimethylamine participated to the reaction successfully producing desired products in good yields. Primary amine, like benzylamine was also found to be reactive enough to produce the desired product (**3t**). However, aniline shows moderate activity in the current protocol providing the thioamide, **3u** in 58% yield. Interestingly, amino acid derivative, L-proline ethyl ester has successfully been used in the thioamidation reaction to obtain the corresponding amino acidbased thioamide (**3v**) which exists as the mixture of two rotamers. To understand the mechanism, we have performed a set of control experiments. Initially we considered elemental sulfur which might be generated by decomposition of dithiocarbamate in the presence of oxidizing agent,[42] as the key sulfurizing agent in the thioamidation reaction and the reaction proceeds through Takemoto's type mechanism[43] (Scheme 2.10a) *via* imine formation between secondary amine and phenylglyoxylic acid followed by nucleophilic attack by the elemental sulfur-based nucleophile. However, the reaction between piperidine and phenylglyoxylic acid in presence of 4 equivalent of elemental sulfur produced the desired thioamide product (3a) only in trace amount along with formation of benzil under the identical reaction condition (Scheme 2.11a). Even arylglyoxylic acids containing electron donating groups were not used by Takemoto's group probably because of the lower electrophilicity of the resulting imine-intermediate. However, electron donating group (*p*-Me, *p*-OMe) containing arylglyoxylic acids responded well under our reaction condition to provide the desired thioamides in good yields (Table 2.2).

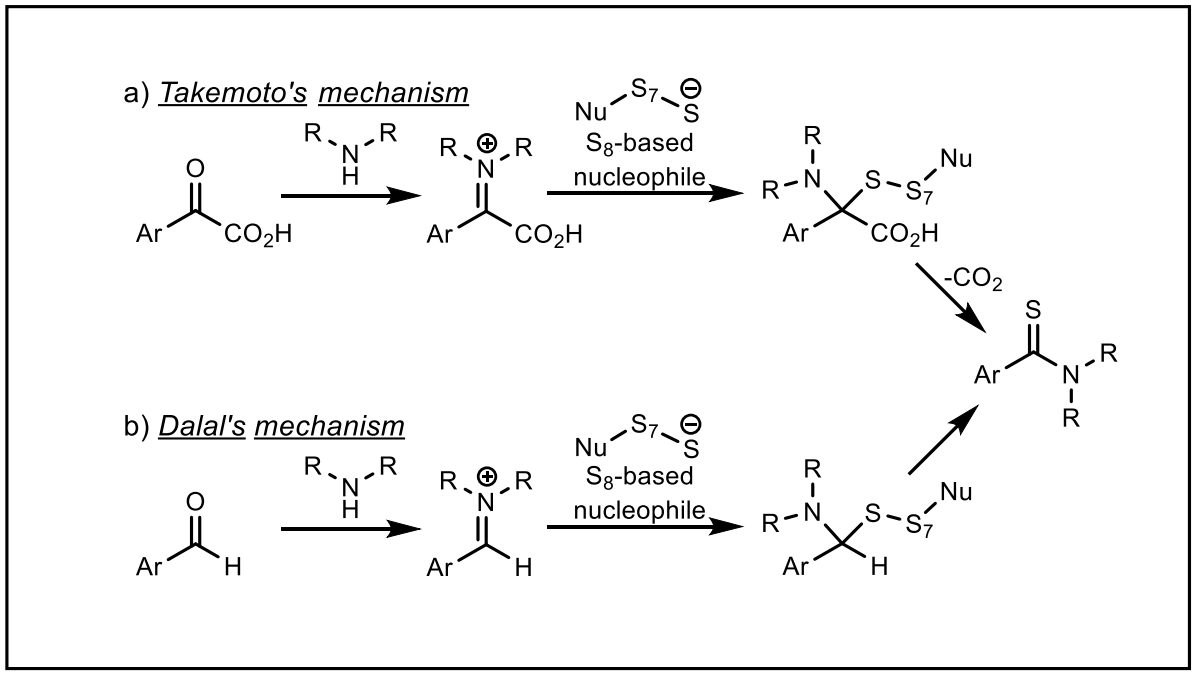

Scheme-2. 10 Reported mechanistic pathways.

Thus, the present thioamidation protocol does not follow Takemoto's type mechanism. Phenylglyoxylic acid is also known to produce benzaldehyde intermediate in presence of persulfate *via* decarboxylation.[44] Dalal *et. al.* reported thioamidation of the aromatic aldehyde by secondary amine and elemental sulfur[45] following a similar mechanism involving imine intermediate and nucleophilic attack of elemental sulfur-based nucleophiles (Scheme 2.10b). However, weakly nucleophilic secondary amine like ethyl L-prolinate remains absolutely unresponsive in the thioamidation reaction with benzaldehyde under the reaction condition as reported by Dalal's group
(Scheme 2.11b). Although, ethyl L-prolinate shows good reactivity under our optimized protocol (3v, Table 2.2). Thus, formation of benzaldehyde intermediate in our reaction condition via decarboxylation of phenylglyoxylic acid was ruled out. We checked the reaction between 1a and 2a in presence of a radical quencher TEMPO (2,2,6,6-tetramethylpiperidine-N-oxide) under the identical reaction condition (Scheme 2.11c). The thioamidation reaction was found to be fully arrested without any formation of the desired thioamide (3a) product. The benzoyl radical (PhCO•) formed in the reaction medium has found to be trapped as O-benzoylated-TEMPO (4). Thus, the reaction is considered to follow a radical mechanistic pathway via the formation of benzoyl radical intermediate. The structure of O-benzoylated-TEMPO (4) was confirmed by ^{1}H and ^{13}C NMR spectroscopy (spectra included in the Supplementary Information). The dithiocarbamate salt (1a) prepared by the reaction of piperidine and CS_2 in presence of triethylamine has been found to react with (dppf)$PdCl_2$ in NMP solvent at room temperature to produce dithiocarbamate-Pd cationic complex (5) (Scheme 2.11d) which was isolated as PF_6-salt and characterized by ^{1}H and ^{13}C NMR spectroscopy (spectra included in the Supplementary Information).

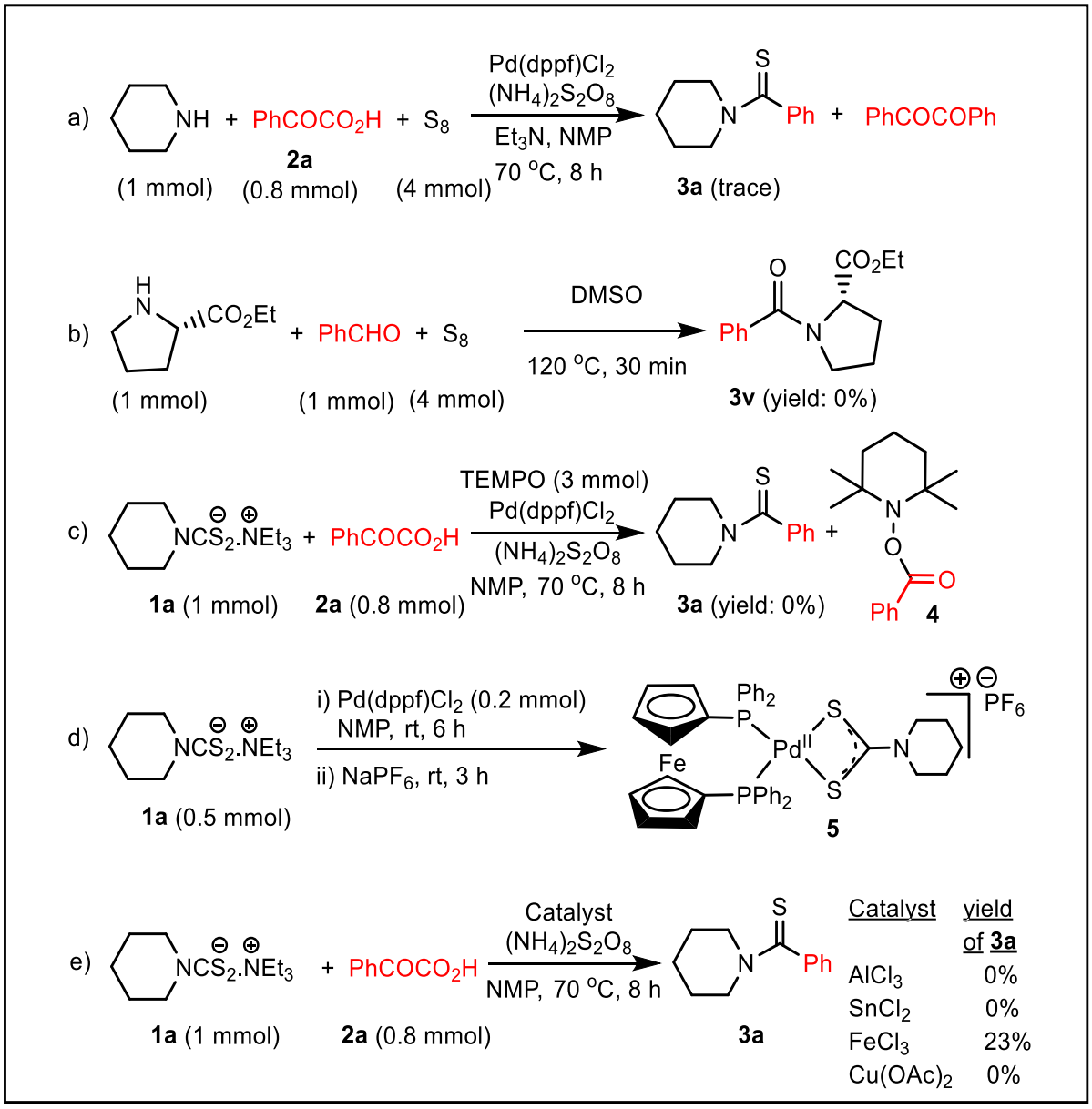

Scheme-2.11 Control experiments

Thus, we believe the involvement of similar dithiocarbamate-Pd complex in our current thioamidation protocol. In the present reaction, Pd(II)-phosphine complex shows crucial role as Lewis acid catalyst to activate the thiocarbonyl group of dithiocarbamate moiety. A few other metal based common Lewis acid catalysts, such as $AlCl_3$, $SnCl_2$, $FeCl_3$, $Cu(OAc)_2$ were tested in the reaction. None of them shows any catalytic activity, except $FeCl_3$ which has been found to be somewhat active producing the desired product only with a poor yield (23%) (Scheme 2.11e).

Based on our experimental observation and the reported literatures we propose a palladium catalytic cycle involving benzoyl radical intermediate as shown in Scheme 2.12. Pd(II) is believed to act as Lewis acid catalyst and forms a Pd-dithiocarbamate complex (**5'**)[46] which reacts with phenyl radical (Ph$^{\bullet}$) to produce the desired thioamide (**3**) product with simultaneous desulfurization to generate the elemental sulfur.[48]

During the course of reaction we observed the formation of pale yellow elemental sulfur which was isolated by filtering the reaction mixture (Fig. 2.2). In the desulfurization step, Pd(I)[49] is formed which is oxidized by $(NH_4)_2S_2O_8$ to regenerate the Pd(II) catalyst. Phenylglyoxylic acid undergoes decarboxylation in presence of persulfate[50] to produce the $PhCO^{\bullet}$ which is known to undergo decarbonylation[51] to produce $Ph^{\bullet}$ radical intermediate. The acyl radical ($PhCO^{\bullet}$) undergoes similar decarbonylation in our reaction condition to produce the $Ph^{\bullet}$ radical which attacks the thiocarbonyl carbon of dithiocarbamate coordinated with Pd (II).

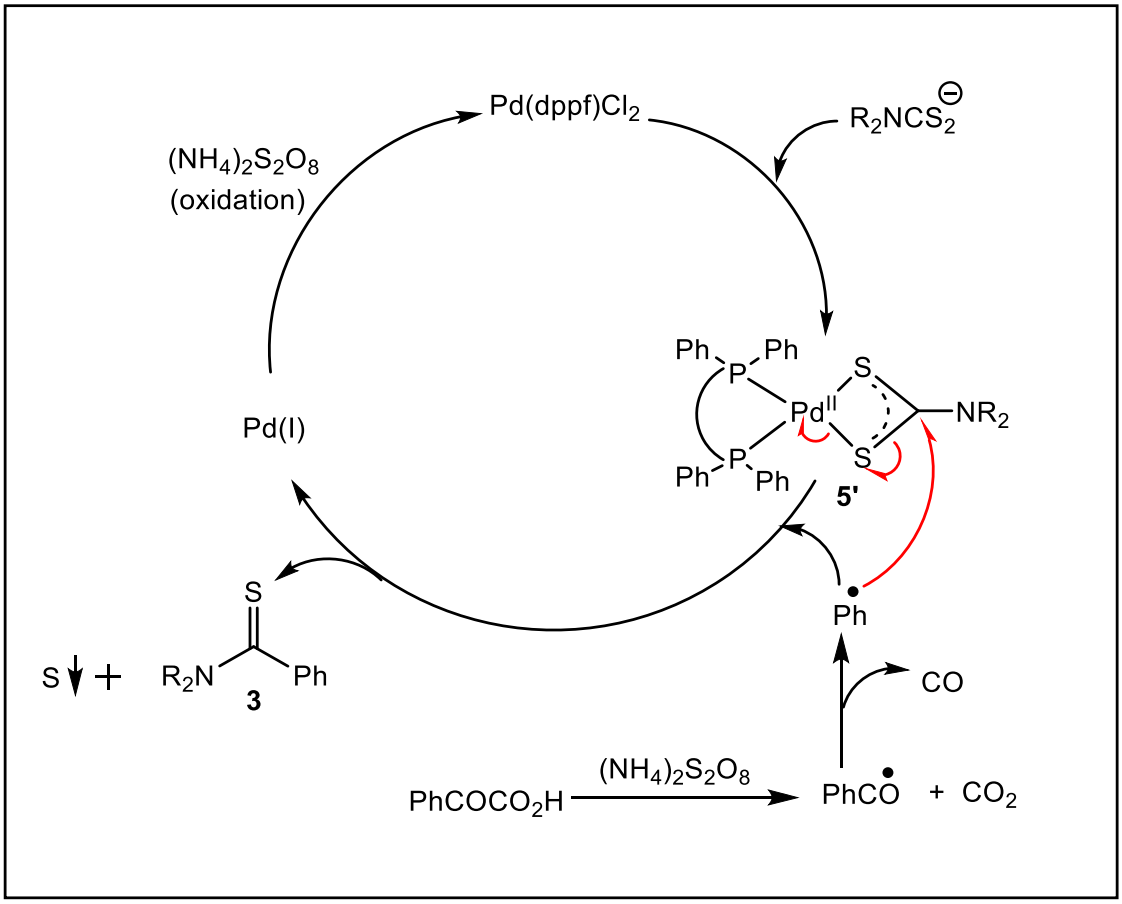

Scheme-2.12 Proposed mechanistic pathway.

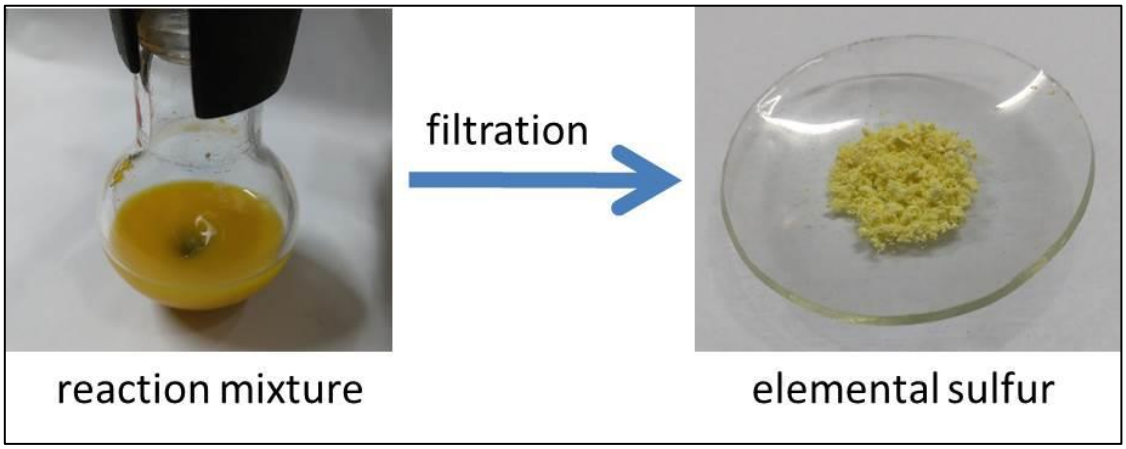

Figure 2.2 Formation of elemental sulfur.

2/c Conclusions

In conclusion, we have demonstrated a convenient and general method to prepare thioamide compounds by decarboxylative-decarbonylative thioamidation of arylglyoxylic acids involving the dithiocarbamate intermediates which are easily prepared *in situ* by the reactions of amines and CS_2. To the best of our knowledge, this is the first report of dithicarbamate mediated decarboxylative-decarbonylative thioamide synthesis. Operational simplicity, wide substrate scope, effective usage of sulfur source and good yield of products have made the protocol synthetically useful.

2/d Experimental Section

^{1}H NMR spectra were recorded using Brucker Spectrometer at 300 MHz, 400 MHz. ^{13}C NMR spectra were recorded at 75 MHz, 100 MHz. In all NMR, $CDCl_3$ and TMS have been used as solvent and internal standard respectively. The chemical shifts are reported in ppm scale considering standard signal of TMS at 0.00 ppm. The coupling constants (*J* values) are measured in Hz and splitting patterns of the proton are described as s (singlet), d (doublet), t (triplet), and m (multiplet). In NMR data, the rotamers are mentioned as #1 and #2.

General Experimental Procedure for the Preparation of Thioamides (3)

CS_2 (0.1 mL, 1.5 mmol) was added drop wise to a solution of secondary amine (1 mmol) and Et_3N (0.28 mL, 2 mmol) in NMP (2 ml) at 5 ^oC. The resulting solution was stirred at room temperature for 5 min. Arylglyoxylic acid (**2**) (0.8 mmol), (dppf)$PdCl_2$ (10 mol %), and $(NH_4)_2S_2O_8$ (1 mmol, 228 mg), were added to the solution of dithiocarbamate anion (**1**) containing Et_3N. The reaction mixture was allowed to stir at 70 ^oC for a certain time period under Ar atmosphere. The progress of the reaction was monitored by TLC. After completion of the reaction, the crude product was obtained by usual work-up using EtOAc. The crude product was purified by column chromatography over silica gel using petroleum ether-ethyl acetate solvent mixture.

Characterization data of all synthesized products

Phenyl(piperidin-1-yl)methanethione (3a, Table 2): Yellow solid; Yield**:** 96% (157 mg); ^{1}H NMR (300 MHz, $CDCl_3$): δ 7.34-7.24 (5H, m), 4.37-4.33 (2H, m), 3.52-3.48 (2H, m), 1.83-1.70 (4H, m), 1.59-1.51 (2H, m). ^{13}C NMR (75 MHz, $CDCl_3$): δ 199.54, 143.41, 128.42, 128.37, 125.43, 53.20, 50.63, 26.91, 25.52, 24.71.

Phenyl(pyrrolidin-1-yl)methanethione (3b, Table 2): Yellow liquid; Yield**:** 90% (137 mg); ^{1}H NMR (300 MHz, $CDCl_3$): δ 7.37-7.32 (5H, m), 3.98 (2H, t, *J*=6Hz), 3.47 (2H, t, *J*=6 Hz), 2.11-2.04 (2H, m), 2.01-1.95 (2H, m). ^{13}C NMR (75 MHz, $CDCl_3$): δ 197.33, 144.01, 128.75, 128.34, 125.67, 53.82, 53.44, 26.51, 24.70.

Morpholino(phenyl)methanethione (3c, Table 2): Yellow solid; Yield**:** 93% (154 mg); ^{1}H NMR (400 MHz, $CDCl_3$): δ 7.35-7.31 (3H, m), 7.28-7.24 (2H, m), 4.44-4.40 (2H, m), 3.88-

3.85 (2H, m), 3.62-3.57 (4H, m). ^{13}C NMR (100 MHz, $CDCl_3$): δ 200.99, 142.48, 128.89, 128.56, 125.90, 66.75, 66.53, 52.53, 49.56.

N,N-dimethylbenzothioamide (3d, Table 2): Yellow solid; Yield**:** 92% (121 mg); ^{1}H NMR (400 MHz, $CDCl_3$): δ 7.37-7.27 (5H, m), 3.59 (3H, s), 3.15 (3H, s). ^{13}C NMR (100 MHz, $CDCl_3$): δ 201.28, 143.40, 128.59, 128.35, 125.75, 44.19, 43.26.

Piperidin-1-yl(p-tolyl)methanethione (3e, Table 2): Pale yellow solid; Yield**:** 92% (161 mg); ^{1}H NMR (400 MHz, $CDCl_3$): δ 7.17-7.11 (4H, m), 4.34-4.32 (2H, m), 3.54-3.51 (2H, m), 2.33 (3H, s), 1.80-1.73 (4H, m), 1.72-1.53 (2H, m). ^{13}C NMR (100 MHz, $CDCl_3$): δ 199.99, 140.65, 138.44, 128.97, 125.58, 53.21, 50.75, 26.91, 25.52, 24.20, 21.25.

Pyrrolidin-1-yl(p-tolyl)methanethione (3f, Table 2): White solid; Yield**:** 89% (145 mg); ^{1}H NMR (400 MHz, $CDCl_3$): δ 7.24 (2H, d, J=12 Hz), 7.12 (2H, d, *J*=8 Hz), 3.93 (2H, t, *J*=8 Hz), 3.46 (2H, t, *J*=8 Hz), 2.32 (3H, s), 2.07-2.00 (2H, m), 1.97-1.89 (2H, m). ^{13}C NMR (100 MHz, $CDCl_3$): δ 197.42, 141.23, 138.79, 128.83, 125.78, 53.87, 53.52, 26.50, 24.69, 21.29.

Mopholino(*p*-tolyl)methanethione (3g, Table 2): Yellow solid; Yield**:** 90% (159 mg); ^{1}H NMR (400 MHz, $CDCl_3$): δ 7.18-7.12 (4H, m), 4.41-4.38 (2H, m), 3.85-3.83 (2H, m), 3.60 (4H, m), 2.32 (3H, s). ^{13}C NMR (100 MHz, $CDCl_3$): δ 201.30, 139.69, 139.07, 129.11, 126.07, 66.76, 66.53, 52.60, 49.70, 21.32.

N,N,4-trimethylbenzothioamide (3h, Table 2): Pale yellow solid; Yield**:** 88% (126 mg); ^{1}H NMR (400 MHz, $CDCl_3$): δ 7.22-7.13 (4H, m), 3.59 (3H,s), 3.18 (3H,s), 2.34 (3H, s). ^{13}C NMR (100 MHz, $CDCl_3$): δ 201.66, 140.60, 138.71, 128.90, 125.91, 44.20, 43.35, 21.26.

(4-chlorophenyl)(piperidin-1-yl)methanethione (3i, Table 2): Yellow liquid; Yield**:** 91% (175 mg); ^{1}H NMR (400 MHz, $CDCl_3$): δ 7.31-7.28 (2H, m), 7.21-7.19 (2H, m), 4.32-4.30 (2H, m), 3.51-3.48 (2H, m), 1.81-1.71 (4H, m), 1.70-1.52 (2H, m). ^{13}C NMR (100 MHz, $CDCl_3$): δ 198.10, 141.71, 134.32, 128.63, 126.99, 53.27, 50.70, 26.90, 25.47, 24.10.

(4-chlorophenyl)(pyrrolidin-1-yl)methanethione (3j, Table 2): Yellow solid; Yield**:** 86% (156 mg); ^{1}H NMR (400 MHz, $CDCl_3$): δ 7.33-7.28 (4H, m), 3.95-3.92 (2H, m), 3,47-3.43(2H, m), 2.11-2.04 (2H, m), 2.03-1.93 (2H, m). ^{13}C NMR (100 MHz, $CDCl_3$): δ 195.85, 142.26, 134.71, 128.52, 127.22, 53.85, 53.55, 26.53, 24.64.

4-chloro-N,N-dimethylbenzothioamide (3k, Table 2): Pale yellow solid; Yield**:** 84% (134 mg); ^{1}H NMR (300 MHz, $CDCl_3$): δ 7.32-7.29 (2H, m), 7.24-7.21 (2H, m), 3.56 (3H, s), 3.14 (3H, s). ^{13}C NMR (75 MHz, $CDCl_3$): δ 199.78, 141.68, 134.54, 128.57, 127.31, 44.21, 43.33.

(4-bromophenyl)(piperidin-1-yl)methanethione (3l, Table 2): White solid; Yield**:** 86% (195 mg); ^{1}H NMR (300 MHz, $CDCl_3$): δ 7.47 (2H, d, *J*= 9 Hz), 7.15 (2H, d, *J*= 6 Hz), 4.33 (2H, t, *J*=6 Hz), 3.51 (2H, t, *J*=6 Hz), 1.81-1.75 (4H, m), 1.61-1.56 (2H, m). ^{13}C NMR (75 MHz, $CDCl_3$): δ 198.16, 142.16, 131.61, 127.20, 122.50, 53.26, 50.68, 26.90, 25.46, 24.12.

(4-bromophenyl)(pyrrolidin-1-yl)methanethione (3m, Table 2): Light brown solid; Yield**:** 82% (177 mg); ^{1}H NMR (300 MHz, $CDCl_3$): δ 7.48 (2H, d, *J*= 9 Hz), 7.24 (2H, d, *J*=9 Hz), 3.95 (2H, t, *J*= 6 Hz), 3.46 (2H, t, J= 6 Hz), 2.11-2.04 (2H, m), 2.02-1.96 (2H, m). ^{13}C NMR (75 MHz, $CDCl_3$): δ 195.90, 142.71, 131.56, 131.50, 127.43, 122.94, 53.83, 53.52, 26.53, 24.64.

4-bromo-N,N-dimethylbenzothioamide (3n, Table 2): Yellow liquid; Yield**:** 80% (156 mg); ^{1}H NMR (400 MHz, $CDCl_3$): δ 7.50-7.47 (2H, m), 7.20-7,18 (2H, m), 3.59, (3H, s), 3.17 (3H, s). ^{13}C NMR (100 MHz, $CDCl_3$): δ 199.95, 142.15, 131.54, 127.52, 122.76, 44.15, 43.29.

(4-methoxyphenyl)(piperidin-1-yl)methanethione (3o, Table 2); White solid; Yield**:** 66% (124 mg); ^{1}H NMR (300 MHz, $CDCl_3$): δ 7.27-7.24 (2H, m), 6.86-6.84 (2H, m), 4.33 (2H, t, *J*=6 Hz), 3.81 (3H, s), 3.57 (2H, t, *J*=6 Hz), 1.81-1.74 (4H, m), 1.60-1.55 (2H, m). ^{13}C NMR (75 MHz, $CDCl_3$): δ 199.87, 159.92, 135.95, 127.58, 113.63, 55.40, 53.36, 51.09, 26.95, 25.51, 24.23.

(4-methoxyphenyl)(pyrrolidin-1-yl)methanethione (3p, Table 2): White solid; Yield**:** 62% (109 mg); ^{1}H NMR (400 MHz, $CDCl_3$): δ 7.35 (2H, d, *J*= 8 Hz), 6.84 (2H, d, *J*= 8 Hz), 3.95 (2H, t, *J*= 8 Hz), 3.80 (3H, s), 3.52 (2H, t, *J*= 4Hz), 2.08-2.04 (2H, m), 1.96-1.93 (2H, m). ^{13}C NMR (100 MHz, $CDCl_3$): δ 197.14, 160.10, 136.52, 127.76, 113.44, 55.40, 54.02, 53.75, 26.57, 24.72.

(3-nitrophenyl)(piperidin-1-yl)methanethione(3q, Table 2): Yellow solid; Yield**:** 72% (144 mg); ^{1}H NMR (400 MHz, $CDCl_3$): δ 8.09-8.03 (2H, m), 7.54-7.45 (2H, m), 4.28-4.25 (2H, m), 3.47-3.43 (2H, m), 1.78-1.69 (4H, m), 1.54-1.50 (2H, m). ^{13}C NMR (100 MHz, $CDCl_3$): δ 195.57, 147.92, 144.50, 131.35, 129.72, 122.99, 120.60, 53.46, 50.65, 26.88, 25.42, 23.93.

(3-nitrophenyl)(pyrrolidin-1-yl)methanethione (3r, Table 2): Yellow solid; Yield**:** 68% (128 mg); ^{1}H NMR (400 MHz, $CDCl_3$): δ 8.11-8.06 (2H, m), 7.61(1H, d, *J*=8 Hz), 7.49-7.45 (1H, m), 3.86 (2H, t, *J*=8 Hz), 3.40 (2H, t, *J*=8Hz), 2.06-1.99 (2H, m), 1.96-1.89 (2H, m). ^{13}C NMR (100 MHz, $CDCl_3$): δ 193.37, 147.76, 144.99, 131.70, 129.64, 123.30, 120.82, 53.97, 53.86, 26.56, 24.56.

N,N-dimethyl-3-nitrobenzothioamide (3s, Table 2): Yellow solid; Yield**:** 65% (109 mg); ^{1}H NMR (400 MHz, $CDCl_3$): δ 8.19-8.15 (2H, m), 7.65-7.63 (1H, m), 7.56-7.52 (1H, m), 3.61 (3H, s), 3.19 (3H, s). ^{13}C NMR (100 MHz, $CDCl_3$): δ 197.62, 147.92, 144.53, 131.74, 129.65, 123.26, 120.85, 44.26, 43.31.

N-benzyl-4-methylbenzothioamide (3t, Table 2): Yellow solid; Yield**:** 85% (164 mg); ^{1}H NMR (400 MHz, $CDCl_3$): δ 7.68 (2H, d, J= 8 Hz), 7.41-7.38 (5H, m), 7.18 (2H, d, *J*= 8 Hz), 5.00 (2H, d, *J*= 8 Hz), 2.37 (3H, s). ^{13}C NMR (100 MHz, $CDCl_3$): δ 198.94, 141.81, 138.82, 136.34, 129.18, 129.06, 128.41, 128.24, 126.71, 51.09, 21.35.

N-phenylbenzothioamide (3u, Table 2): Yellow solid; Yield**:** 58% (99 mg); ^{1}H NMR (400 MHz, $CDCl_3$): δ 9.09 (1H, br. S), 7.84-7.73 (4H, m), 7.50-7.42 (5H, m), 7.41-7.29 (1H, m), ^{13}C NMR (100 MHz, $CDCl_3$): δ 198.59, 143.15, 139.05, 131.32, 129.08, 128.66, 127.03, 126.77, 123.81.

ethyl (phenylcarbonothioyl)-L-prolinate (3v, Table 2): Pale yellow solid; Yield**:** 60% (126 mg); ^{1}H NMR (400 MHz, $CDCl_3$): δ 7.39-7.29 (5H, m, #1), 7.23-7.22 (1.12H, m, #2), 7.22-7.21 (0.67, m, #2), 5.12-5.09 (1H, m, #1), 4.28-4.23 (0.29H, m, #2), 4.10 (2H, q, *J*=8 Hz, #1), 4.03-4.00 (0.52H, q, *J*=7.4 Hz, #2), 3.67-3.62 (0.67H, m, #2), 3.57-3.54 (1H, m, #1), 3.53-3.51 (1H, m, #1), 2.46-2.43 (1H, m, #1), 2.42-2.40 (0.22H, m, #2), 2.16-2.10 (2.92H, m, #1, #2), 2.09-1.92 (1H, m, #1), 1.32 (3H, t, *J*=8Hz, #1), 1.14 (0.89H, t, *J*=7.2 Hz, #2). ^{13}C NMR

(100 MHz, $CDCl_3$): δ 199.79 (C=S, #2), 199.47 (C=S, #1), 170.65 (CO_2Et, #2), 170.4 (CO_2Et, #1), 143.85 (C, #2), 143.58 (C, #1), 128.96 (CH, #1), 128.63 (CH, #2), 128.35 (CH, #2), 128.32 (CH, #1), 125.67 (CH, #1), 125.40 (CH, #2), 64.87 (2-CH, #1), 64.67 (2-CH, #2), 61.65(OCH_2CH_3, #2),61.45 (OCH_2CH_3, #1), 54.10 (5-CH_2, #1), 53.46 (5-CH_2, #2), 31.52 (3-CH_2, #2), 29.73 (3-CH_2, #1), 25.20 (4-CH_2, #1), 22.84 (4-CH_2, #2), 14.21 (OCH_2CH_3, #1), 14.03 (OCH_2CH_3, #2).

2,2,6,6-tetramethylpiperidin-1-yl benzoate (4): White solid; ^1H NMR (400 MHz, $CDCl_3$): δ 8.08-8.06 (2H, m), 7.60-7.56 (1H, m), 7.55-7.44 (2H, m), 1.82-1.48 (6H, m), 1.28 (6H, s), 1.12 (6H, s). ^{13}C NMR (100 MHz, $CDCl_3$): δ 166.44, 132.87, 129.74, 129.59, 128.47, 60.44, 39.08, 32.00, 31.95, 20.89, 20.85, 17.02.

^{1}H and ^{13}C NMR spectra of all synthesized products described in Section-2

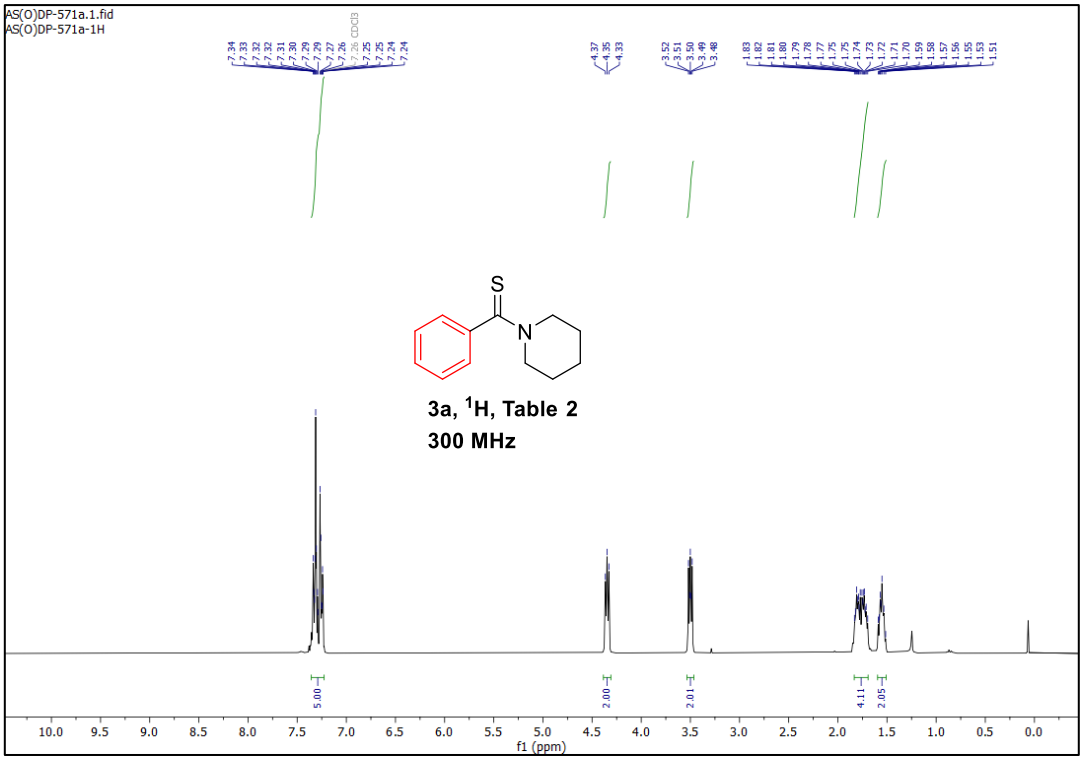
AS(O)DP-571a.1.fid
AS(O)DP-571a-1H
S
N
3a, 1H, Table 2
300 MHz
f1 (ppm)

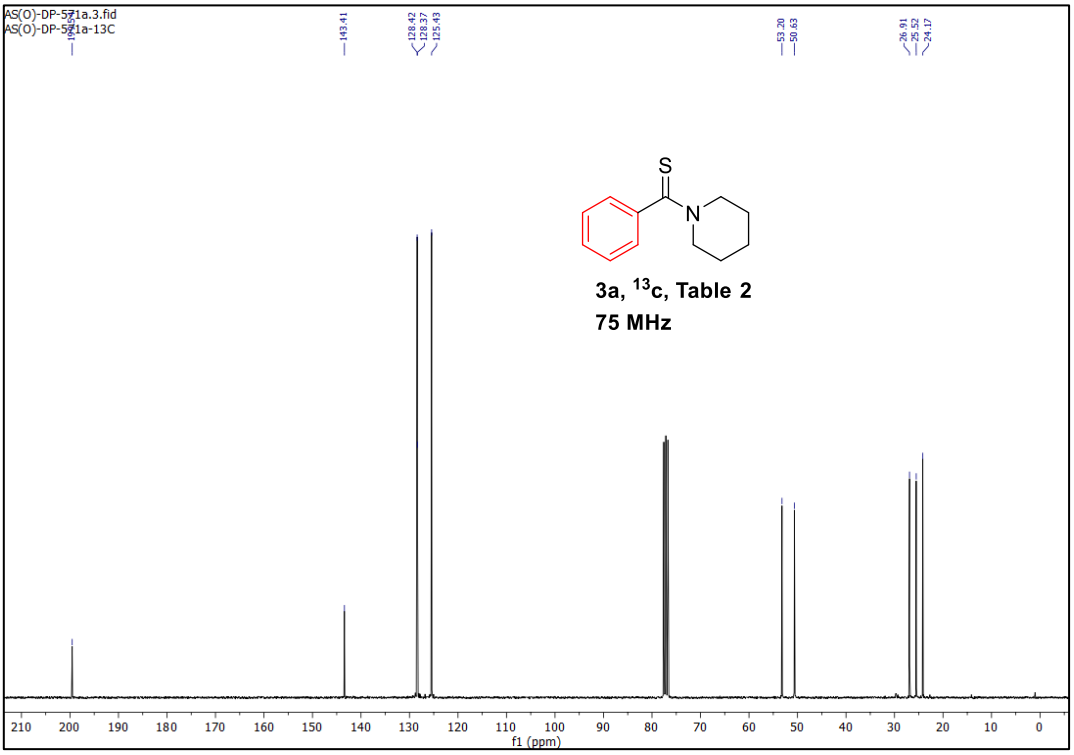
AS(O)-DP-571a.3.fid
AS(O)-DP-571a-13C
S
N
3a, 13c, Table 2
75 MHz
f1 (ppm)

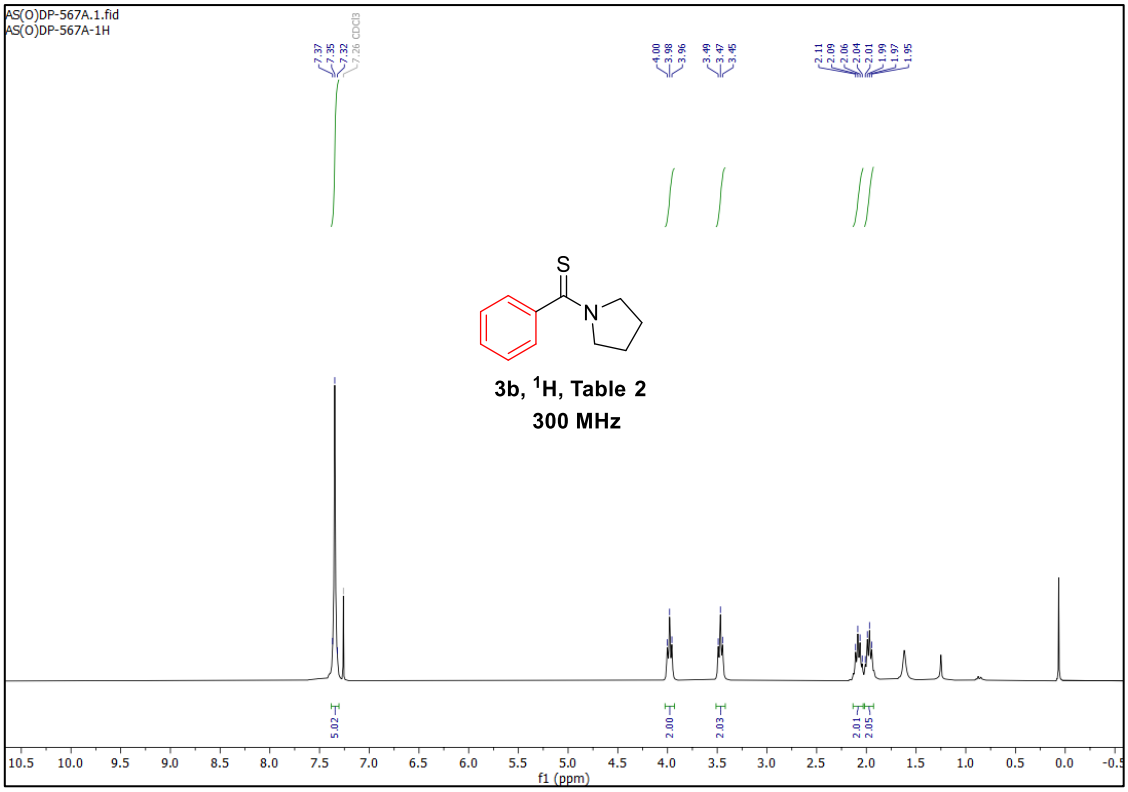
AS(O)DP-567A.1.fid
AS(O)DP-567A-1H
S
N
3b, 1H, Table 2
300 MHz
f1 (ppm)

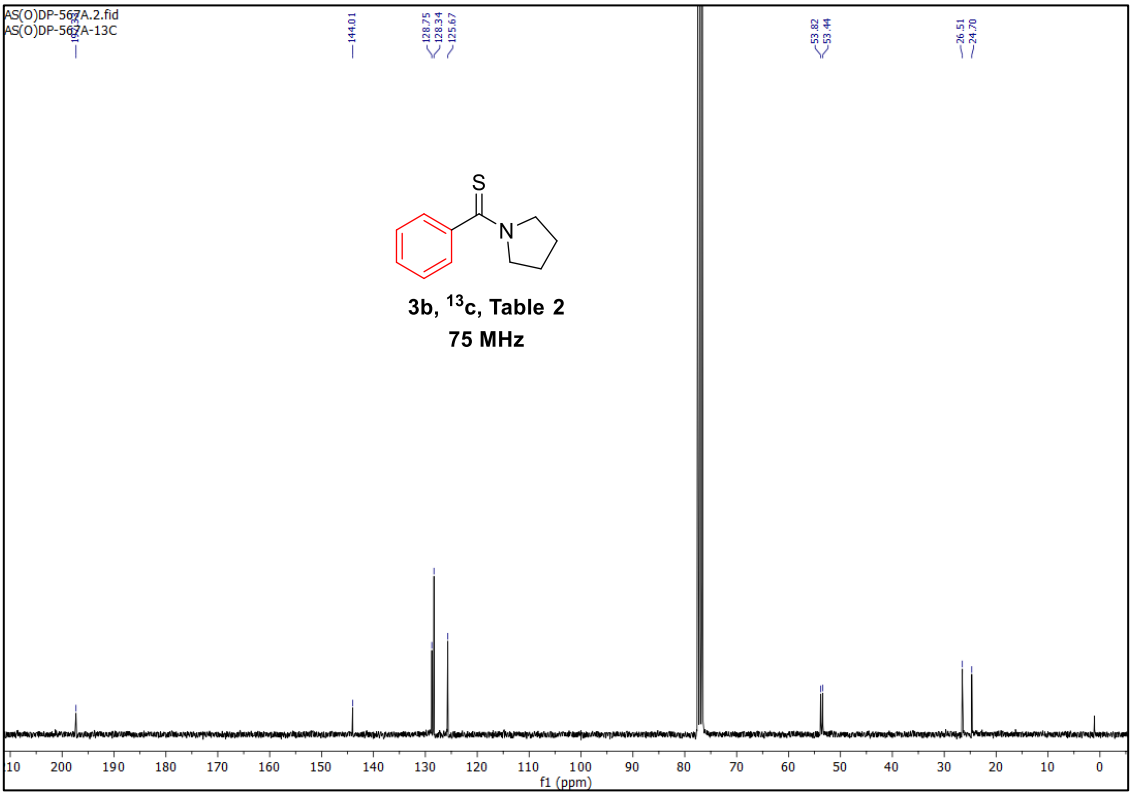
AS(O)DP-567A.2.fid
AS(O)DP-567A-13C
S
N
3b, 13c, Table 2
75 MHz
f1 (ppm)

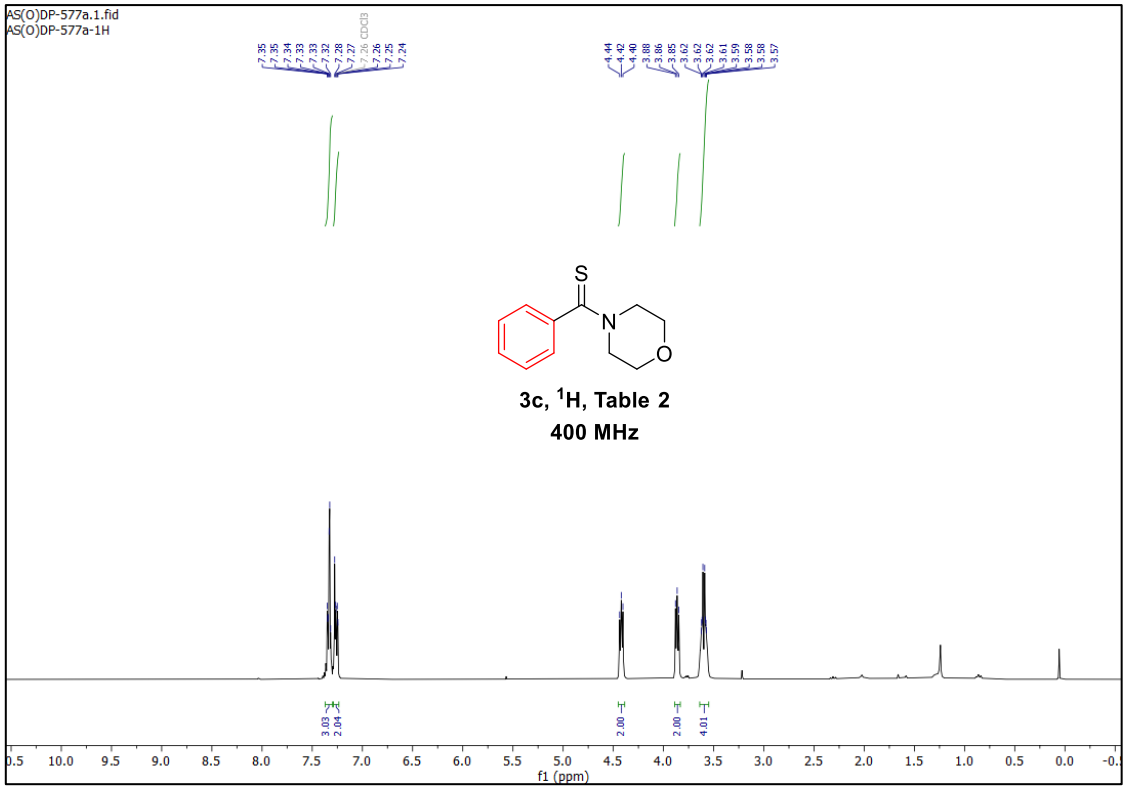
AS(O)DP-577a.1.fid
AS(O)DP-577a-1H
S
N
O
3c, 1H, Table 2
400 MHz
f1 (ppm)

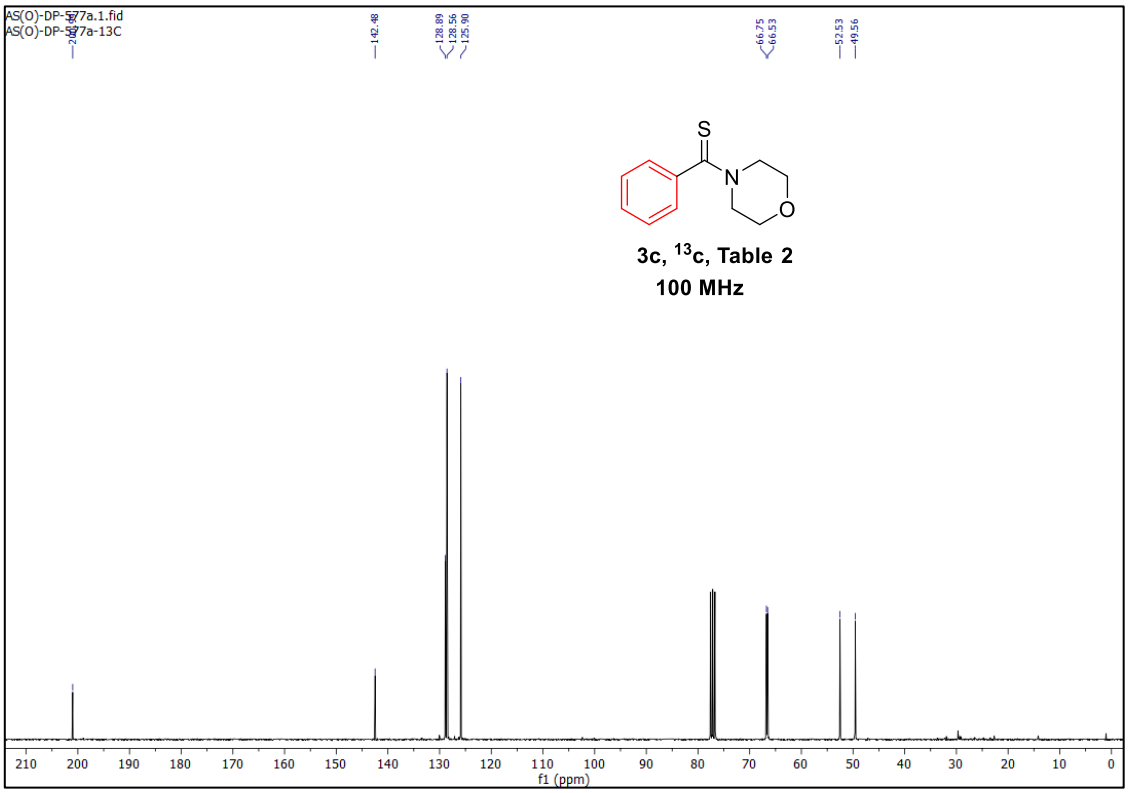
AS(O)-DP-577a.1.fid
AS(O)-DP-577a-13C
S
N
O
3c, 13c, Table 2
100 MHz
f1 (ppm)

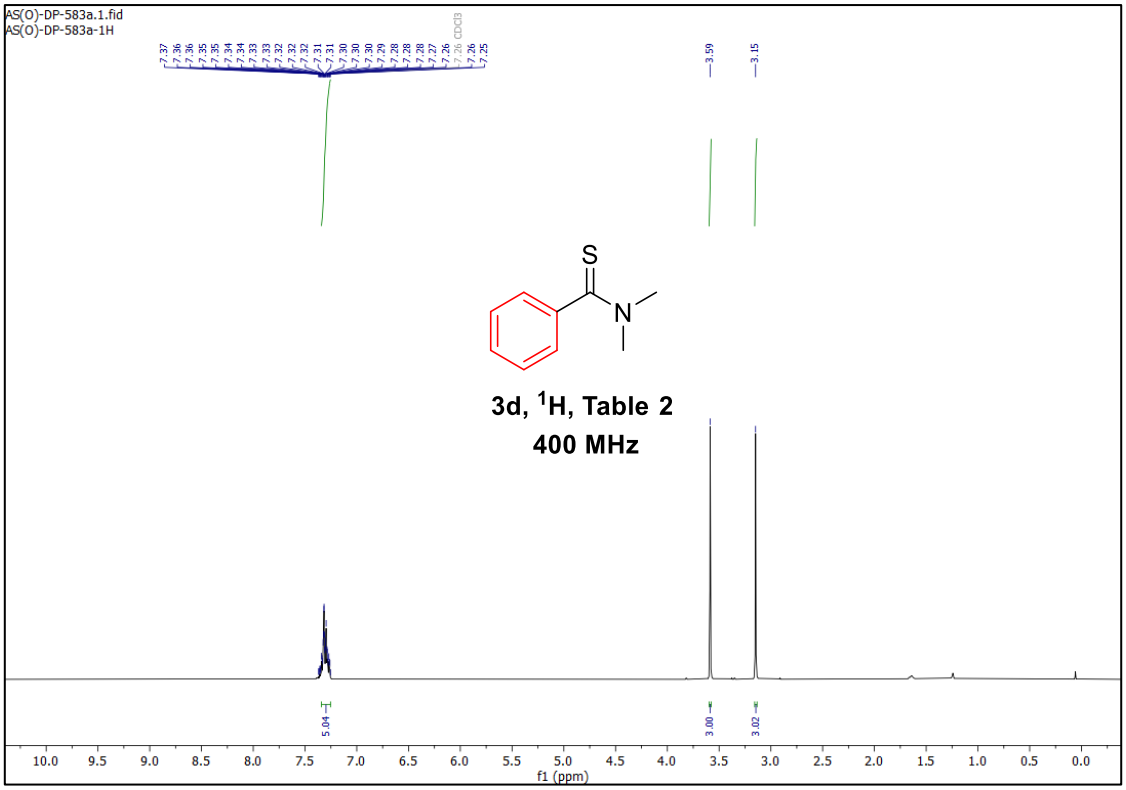
AS(O)-DP-583a.1.fid
AS(O)-DP-583a-1H
3.59
3.15
S
N
3d, 1H, Table 2
400 MHz
5.04
3.00
3.02
f1 (ppm)

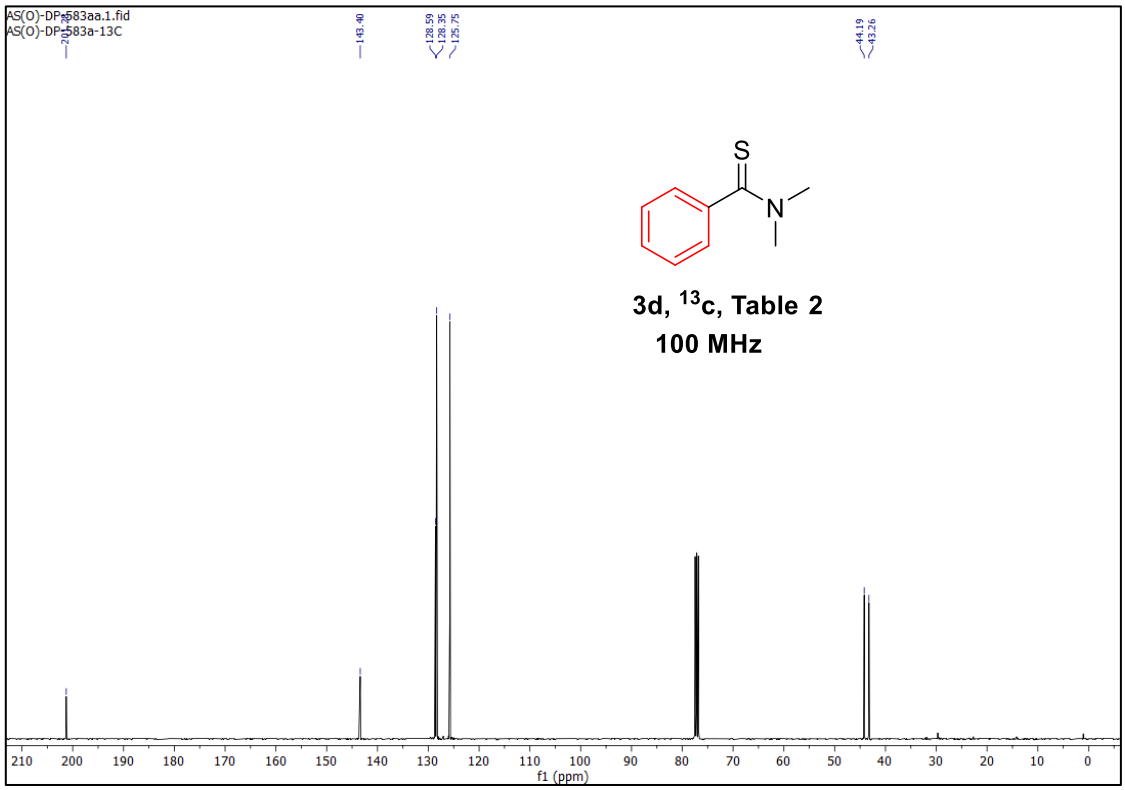
AS(O)-DP-583aa.1.fid
AS(O)-DP-583a-13C
143.40
128.59
128.35
125.75
44.19
43.26
S
N
3d, 13c, Table 2
100 MHz
f1 (ppm)

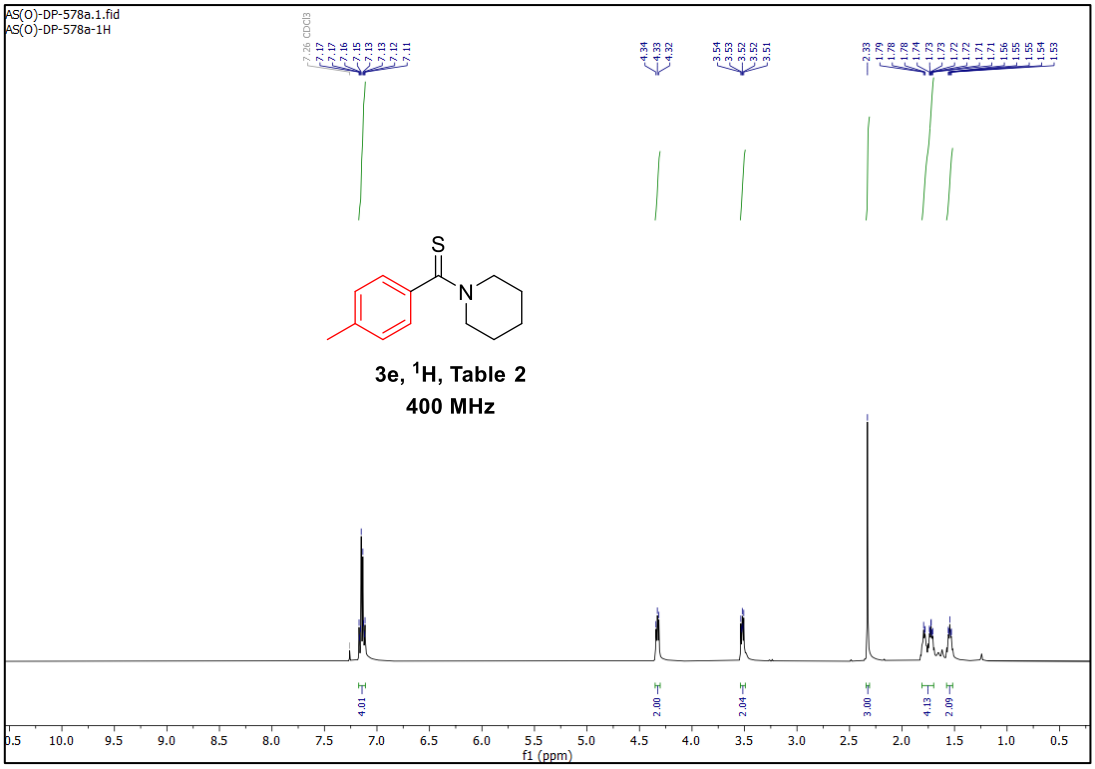
AS(O)-DP-578a.1.fid
AS(O)-DP-578a-1H
S
N
3e, 1H, Table 2
400 MHz
f1 (ppm)

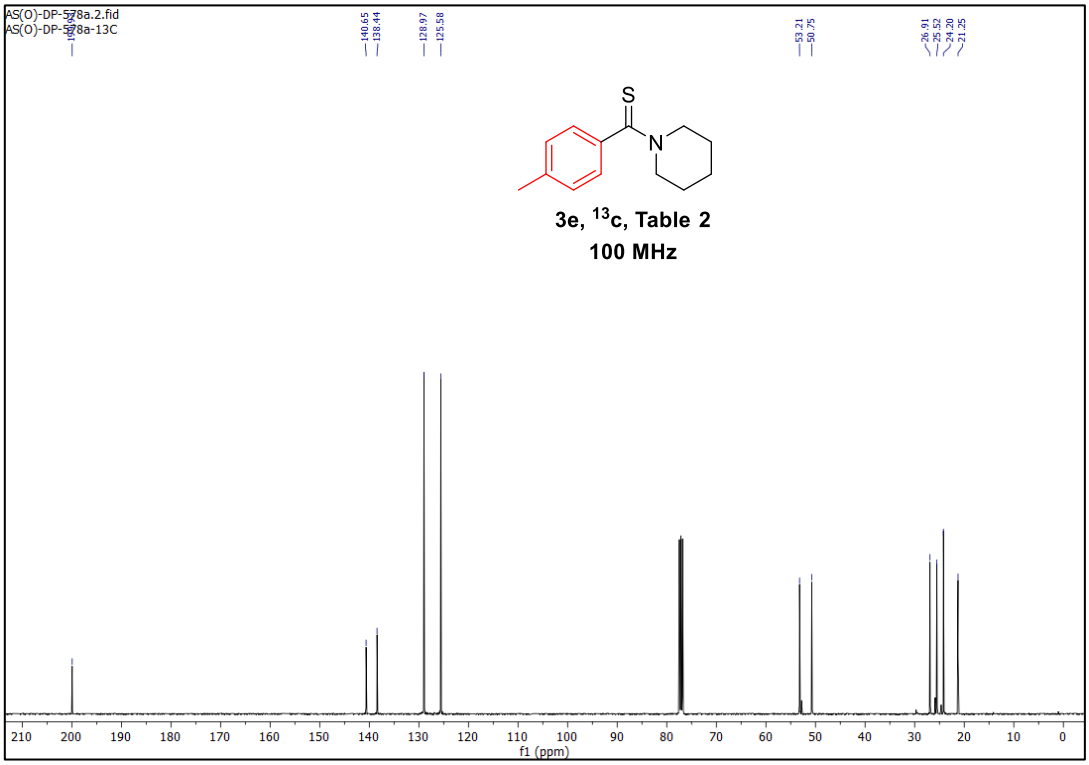
AS(O)-DP-578a.2.fid
AS(O)-DP-578a-13C
S
N
3e, 13c, Table 2
100 MHz
f1 (ppm)

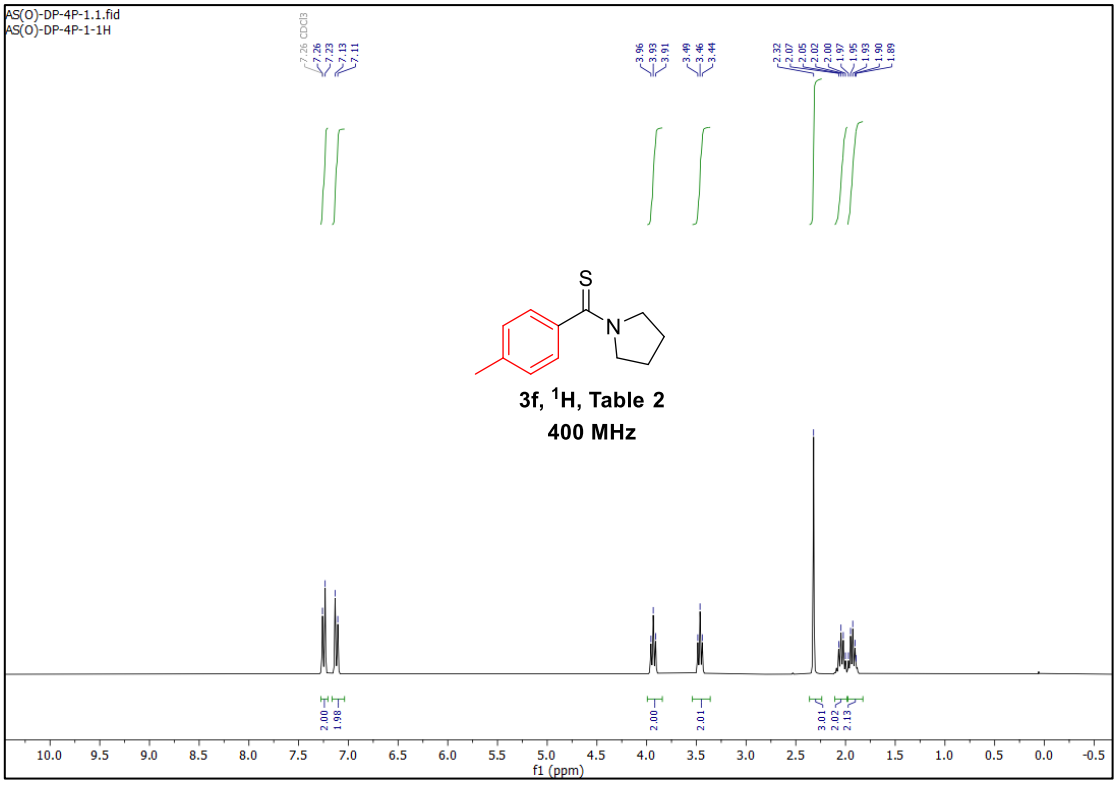
AS(O)-DP-4P-1.1.fid
AS(O)-DP-4P-1-1H
S
N
3f, 1H, Table 2
400 MHz
f1 (ppm)

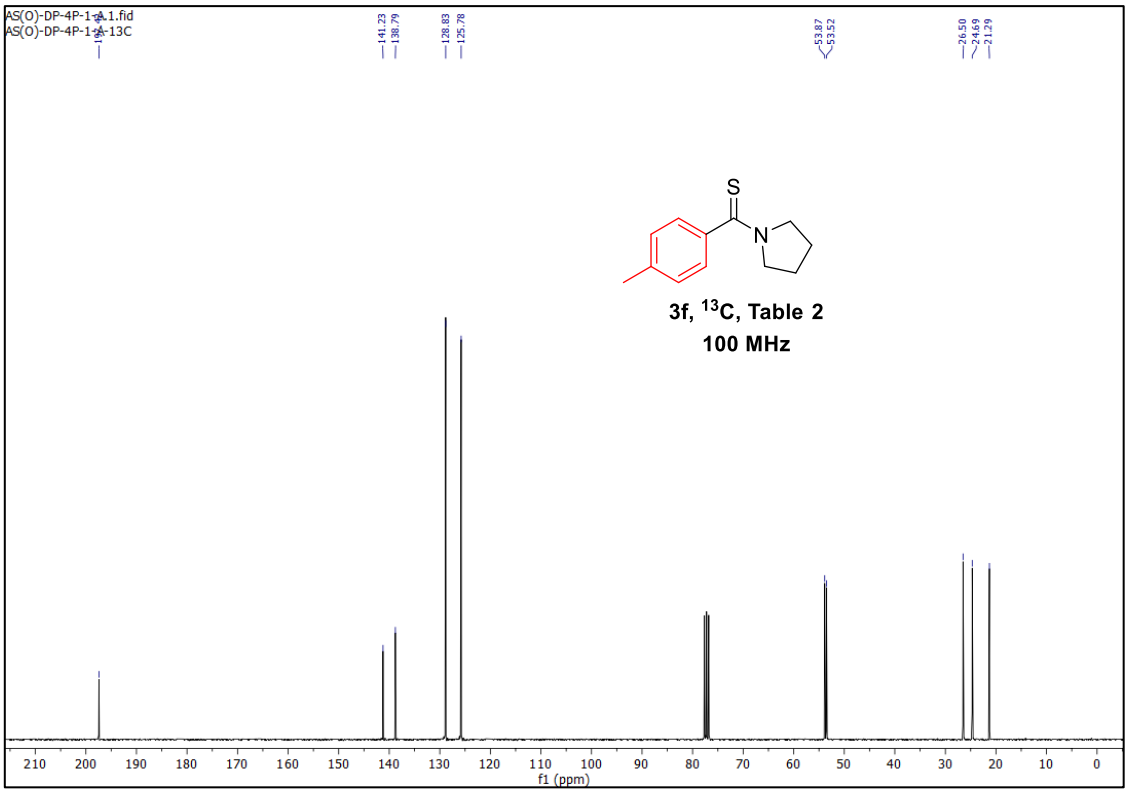
AS(O)-DP-4P-1-A1.fid
AS(O)-DP-4P-1-A-13C
S
N
3f, 13C, Table 2
100 MHz
f1 (ppm)

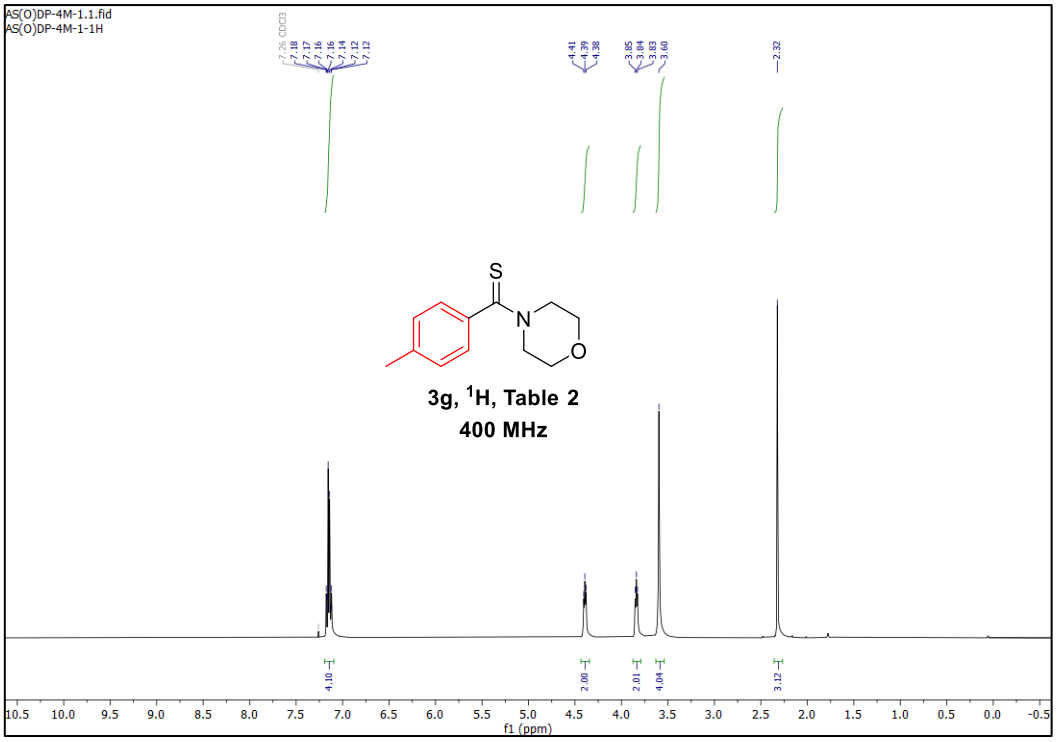
AS(O)DP-4M-1.1.fid
AS(O)DP-4M-1-1H
S
N
O
3g, 1H, Table 2
400 MHz
f1 (ppm)

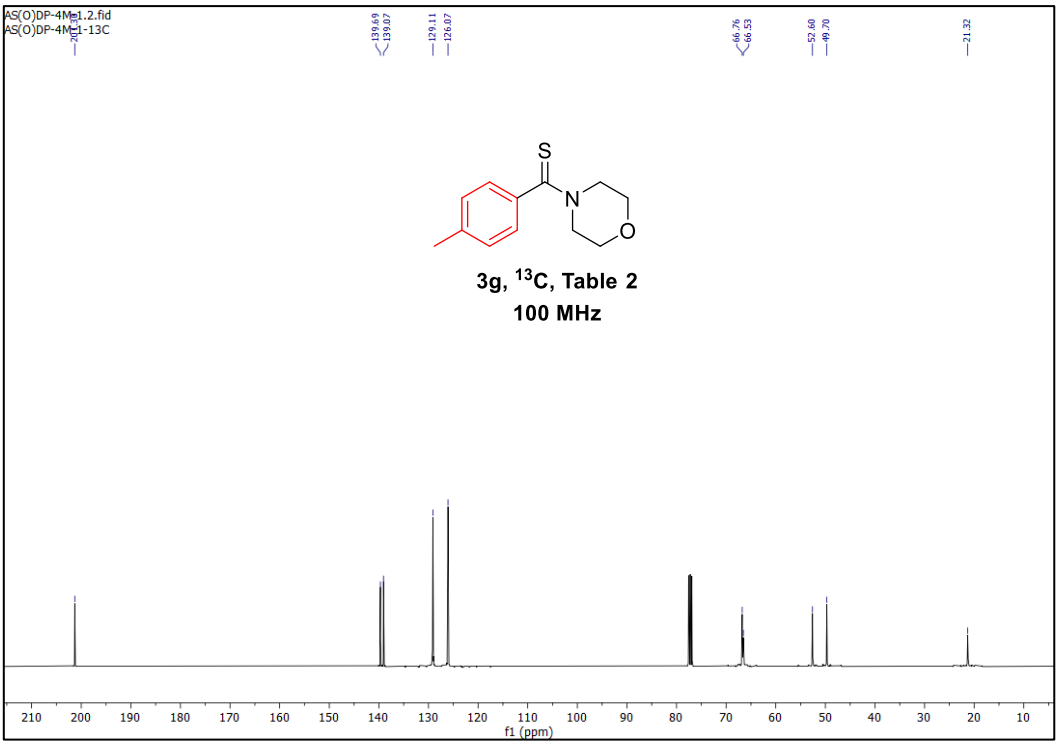
AS(O)DP-4M-1.2.fid
AS(O)DP-4M-1-13C
S
N
O
3g, 13C, Table 2
100 MHz
f1 (ppm)

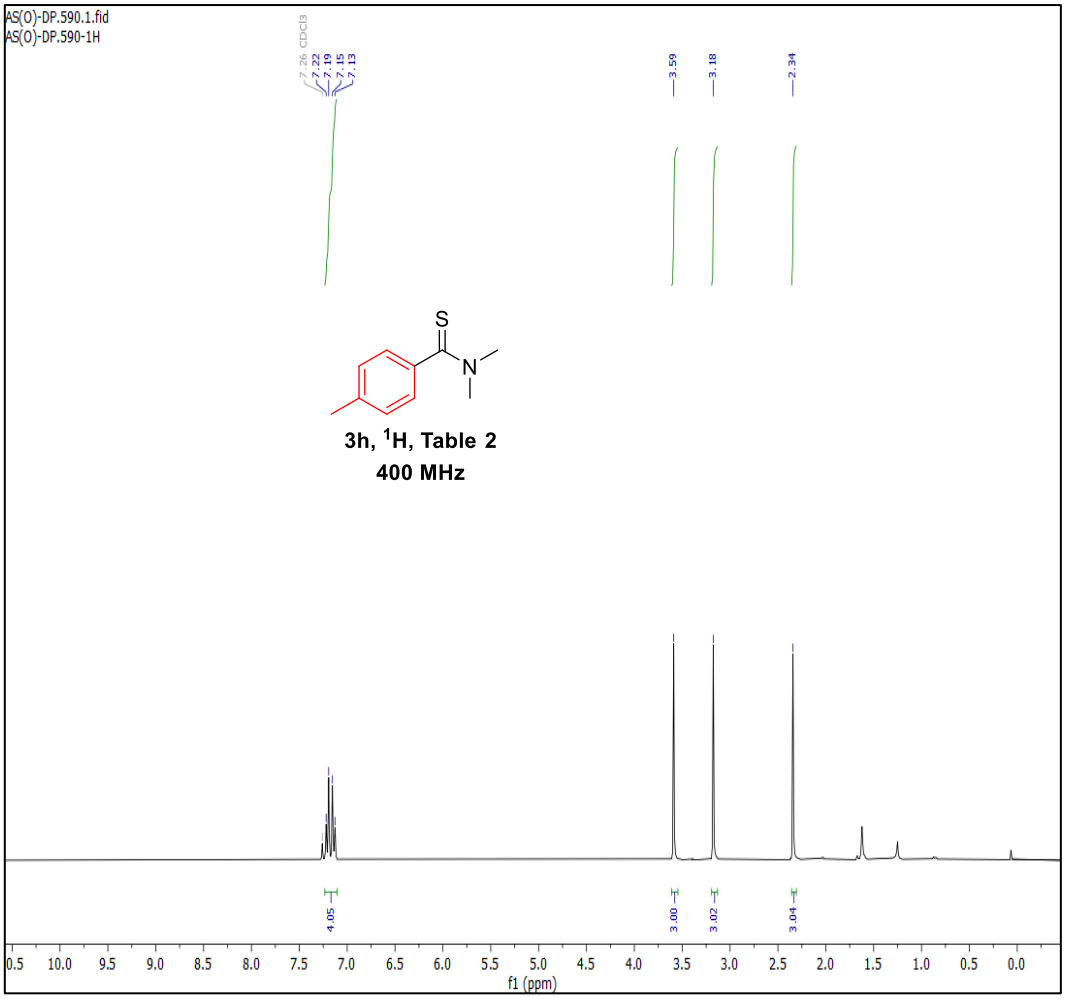
AS(O)-DP.590.1.fid
AS(O)-DP.590-1H
7.26 CDCl3
7.22
7.19
7.15
7.13
3.59
3.18
2.34
S
N
3h, 1H, Table 2
400 MHz
4.05
3.00
3.02
3.04
f1 (ppm)

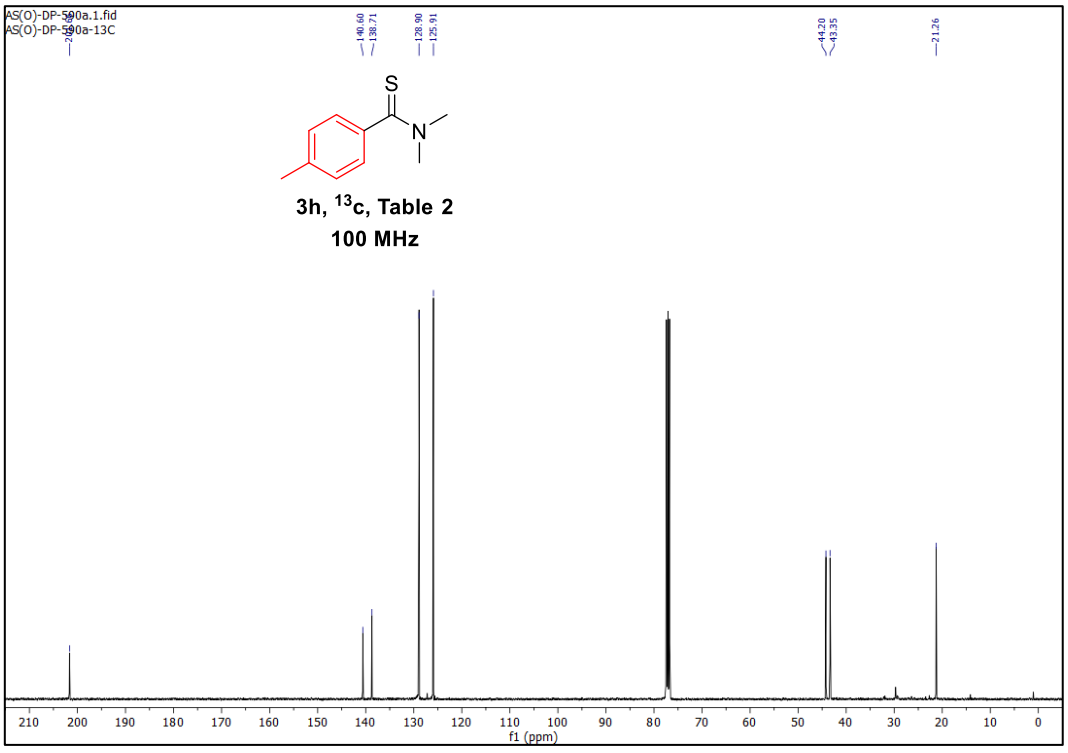
AS(O)-DP-590a.1.fid
AS(O)-DP-590a-13C
140.60
138.71
128.90
125.91
44.20
43.35
21.26
S
N
3h, 13c, Table 2
100 MHz
f1 (ppm)

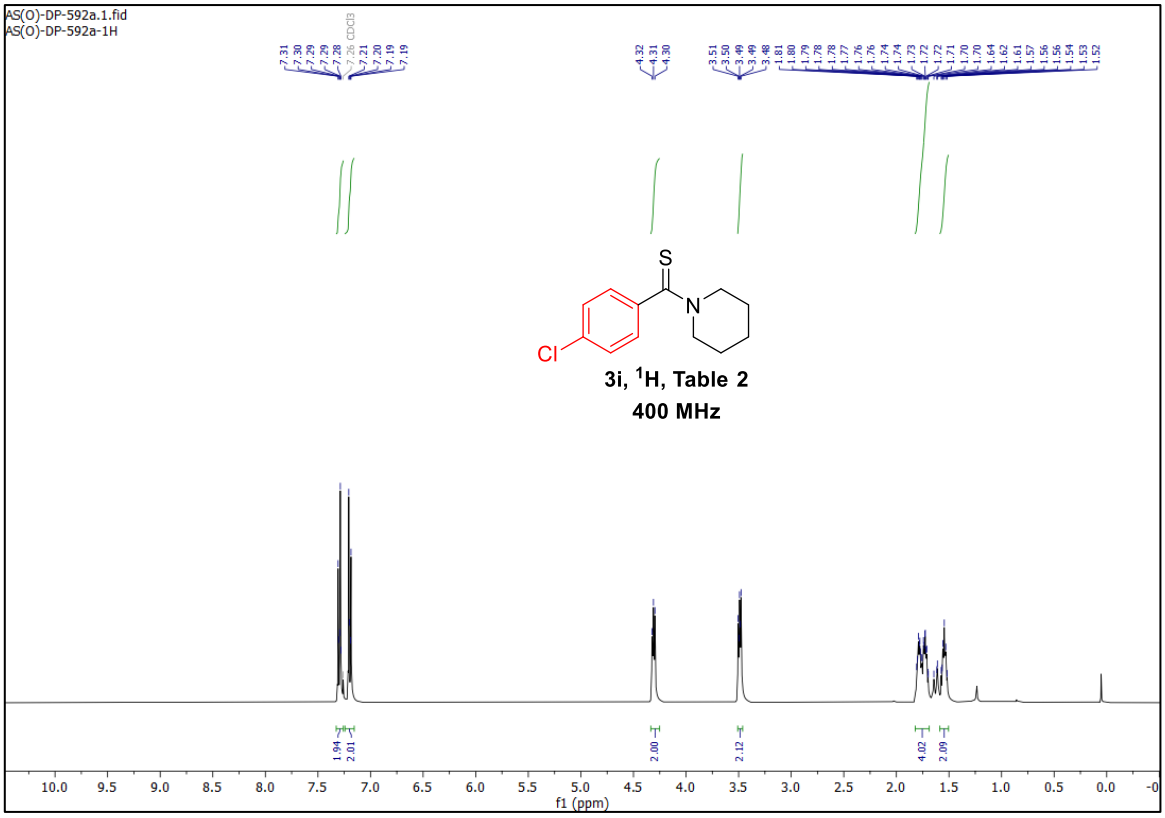
AS(O)-DP-592a.1.fid
AS(O)-DP-592a-1H
S
N
Cl
3i, 1H, Table 2
400 MHz
f1 (ppm)

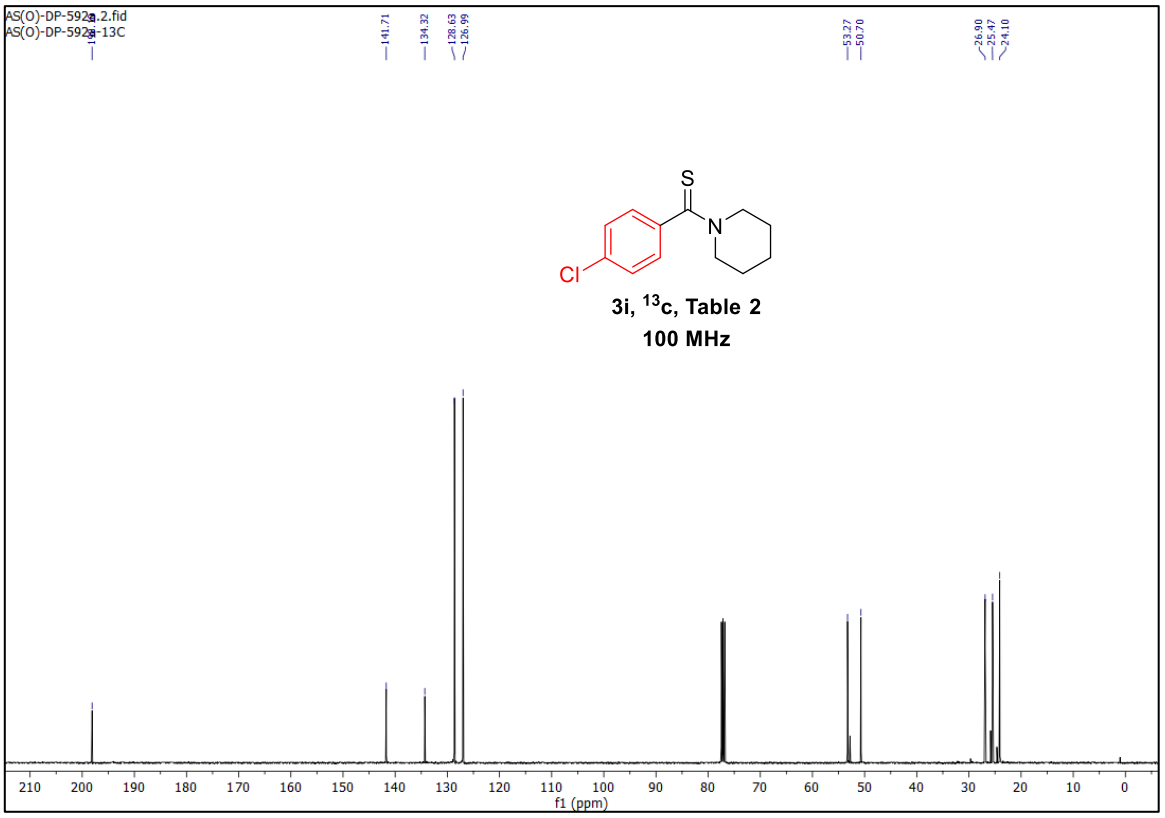
AS(O)-DP-592a.2.fid
AS(O)-DP-592a-13C
S
N
Cl
3i, 13c, Table 2
100 MHz
f1 (ppm)

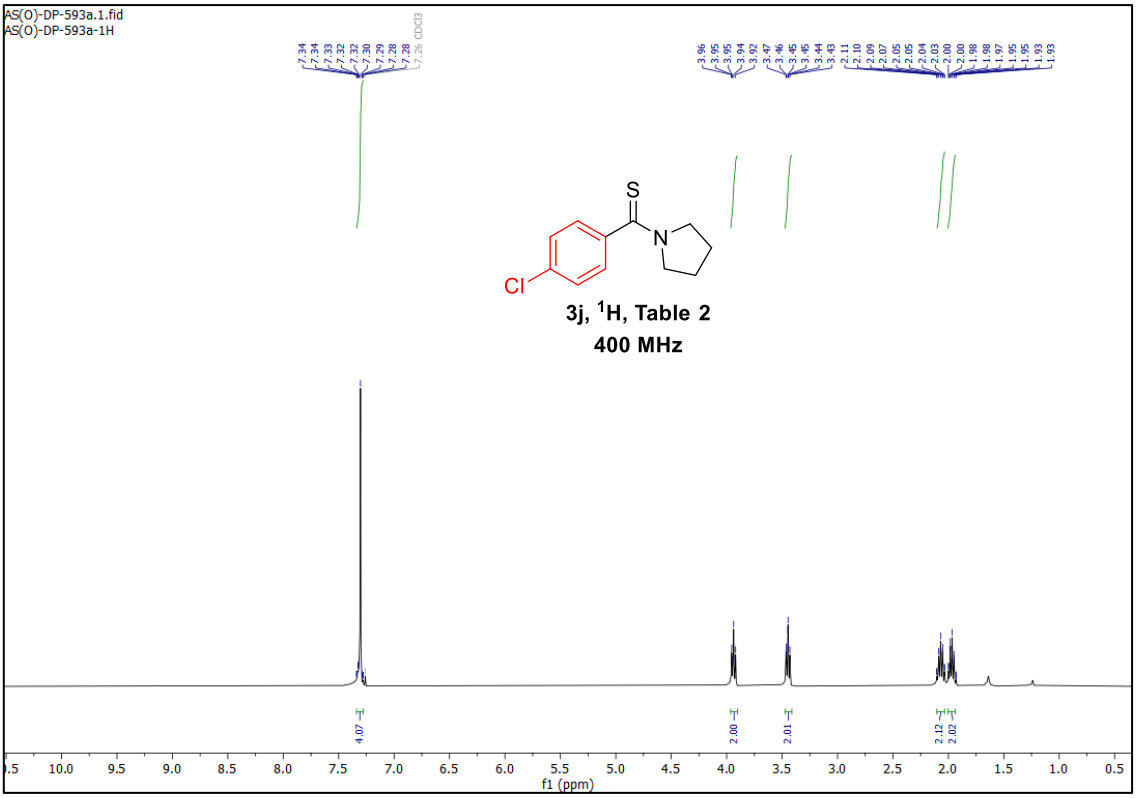
AS(O)-DP-593a.1.fid
AS(O)-DP-593a-1H
S
N
Cl
3j, 1H, Table 2
400 MHz
f1 (ppm)

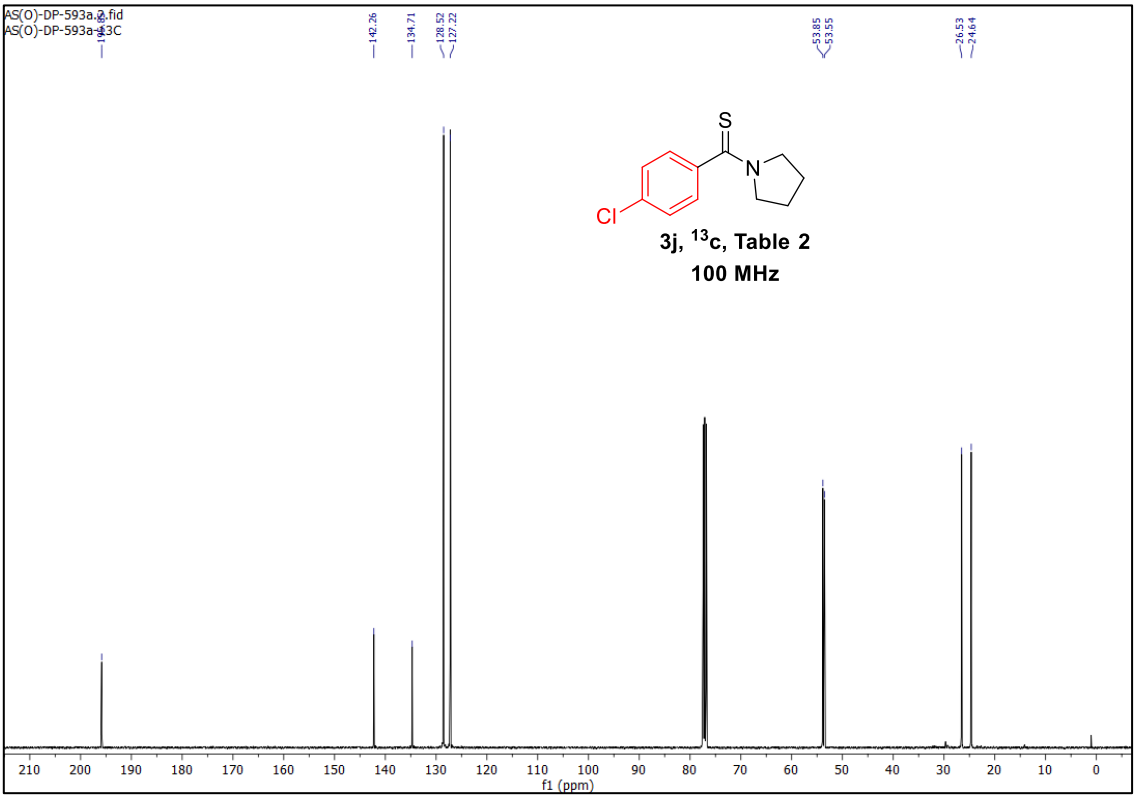
AS(O)-DP-593a.2.fid
AS(O)-DP-593a-13C
S
N
Cl
3j, 13c, Table 2
100 MHz
f1 (ppm)

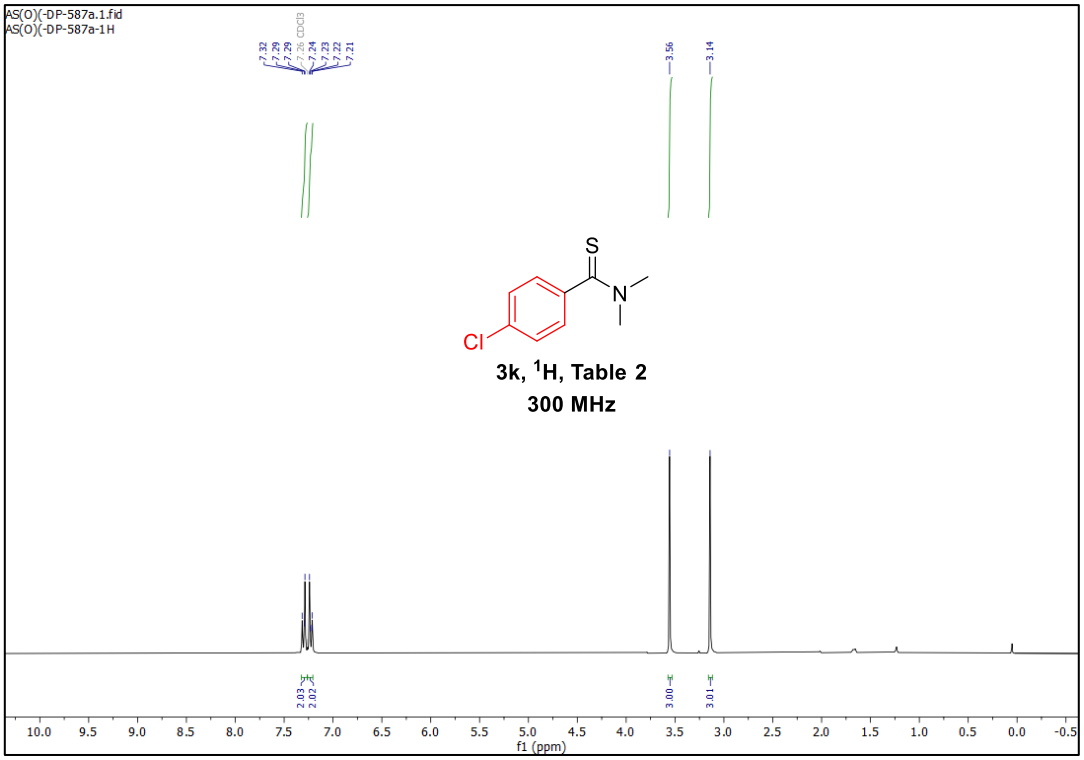
AS(O)(-DP-587a.1.fid
AS(O)(-DP-587a-1H
7.32
7.29
7.29
7.26 CDCl3
7.24
7.23
7.22
7.21
3.56
3.14
S
N
Cl
3k, 1H, Table 2
300 MHz
2.03
2.02
3.00
3.01
10.0 9.5 9.0 8.5 8.0 7.5 7.0 6.5 6.0 5.5 5.0 4.5 4.0 3.5 3.0 2.5 2.0 1.5 1.0 0.5 0.0 -0.5
f1 (ppm)

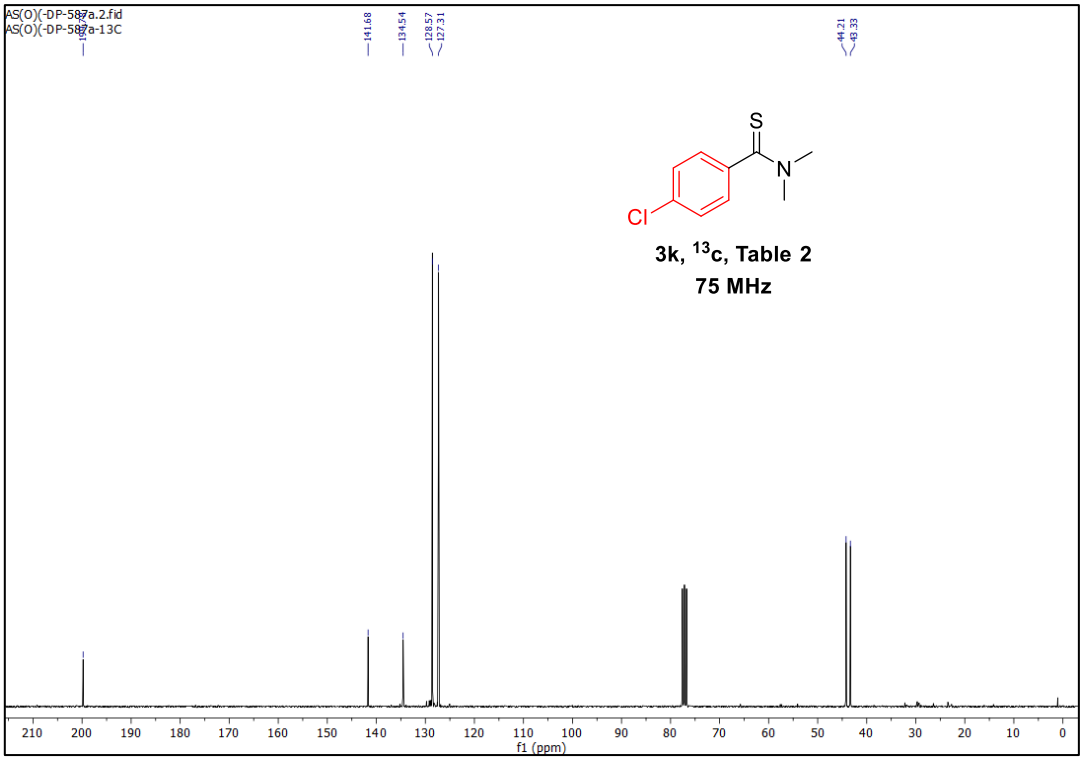
AS(O)(-DP-587a.2.fid
AS(O)(-DP-587a-13C
141.68
134.54
128.57
127.31
44.21
43.33
S
N
Cl
3k, 13c, Table 2
75 MHz
210 200 190 180 170 160 150 140 130 120 110 100 90 80 70 60 50 40 30 20 10 0
f1 (ppm)

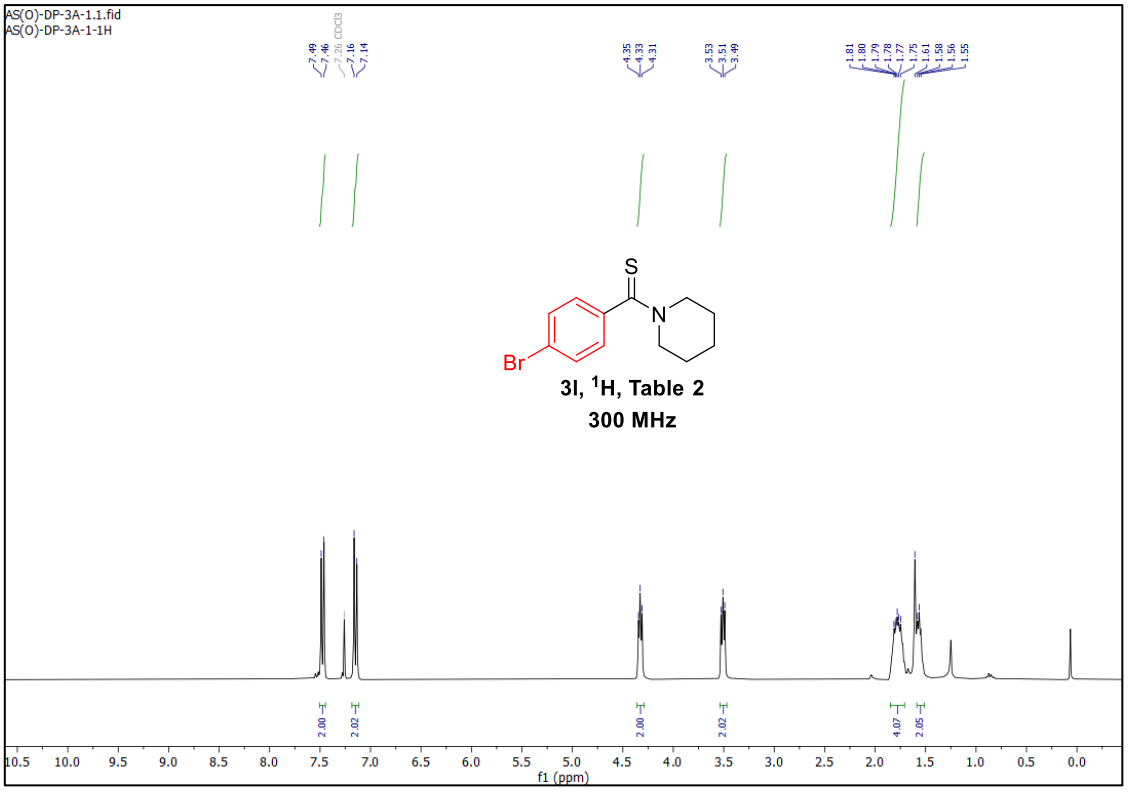
AS(O)-DP-3A-1.1.fid
AS(O)-DP-3A-1-1H
7.49
7.46
7.26 CDCl3
7.16
7.14
4.35
4.33
4.31
3.53
3.51
3.49
1.81
1.80
1.79
1.78
1.77
1.75
1.61
1.58
1.56
1.55
S
N
Br
3l, 1H, Table 2
300 MHz
2.00
2.02
2.00
2.02
4.07
2.05
f1 (ppm)

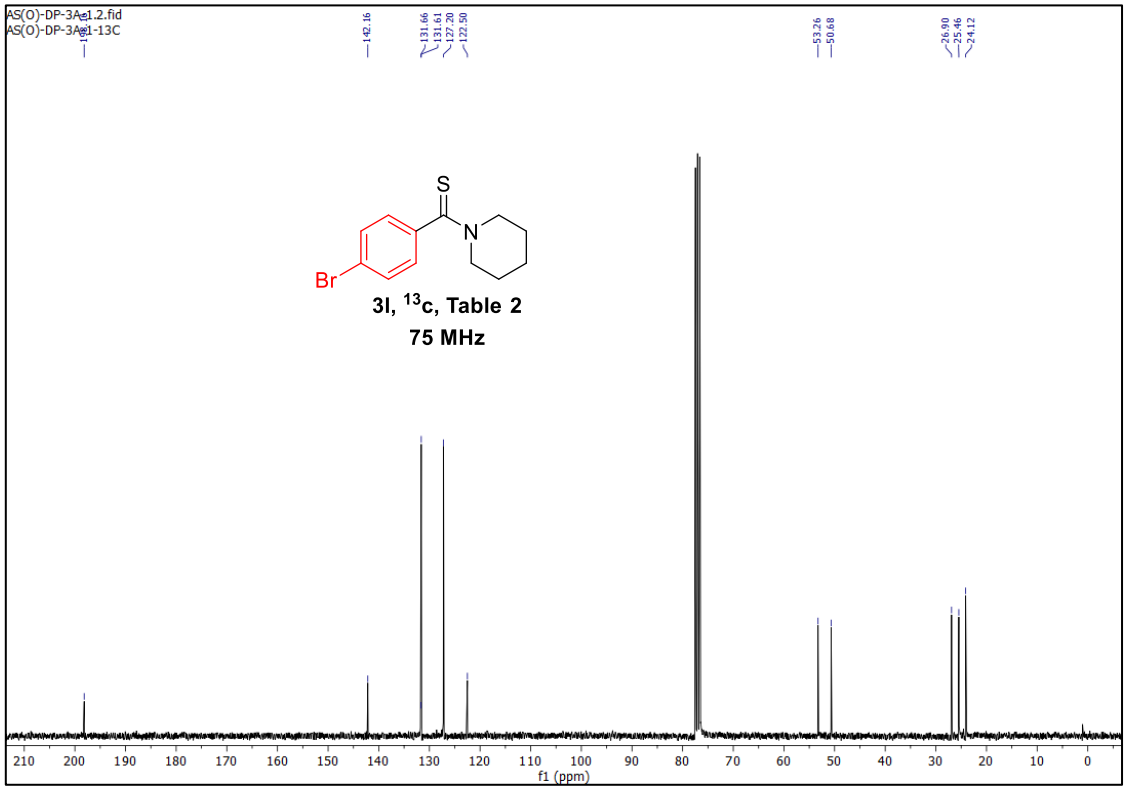
AS(O)-DP-3A-1.2.fid
AS(O)-DP-3A-1-13C
142.16
131.66
131.61
127.20
122.50
53.26
50.68
26.90
25.46
24.12
S
N
Br
3l, 13c, Table 2
75 MHz
f1 (ppm)

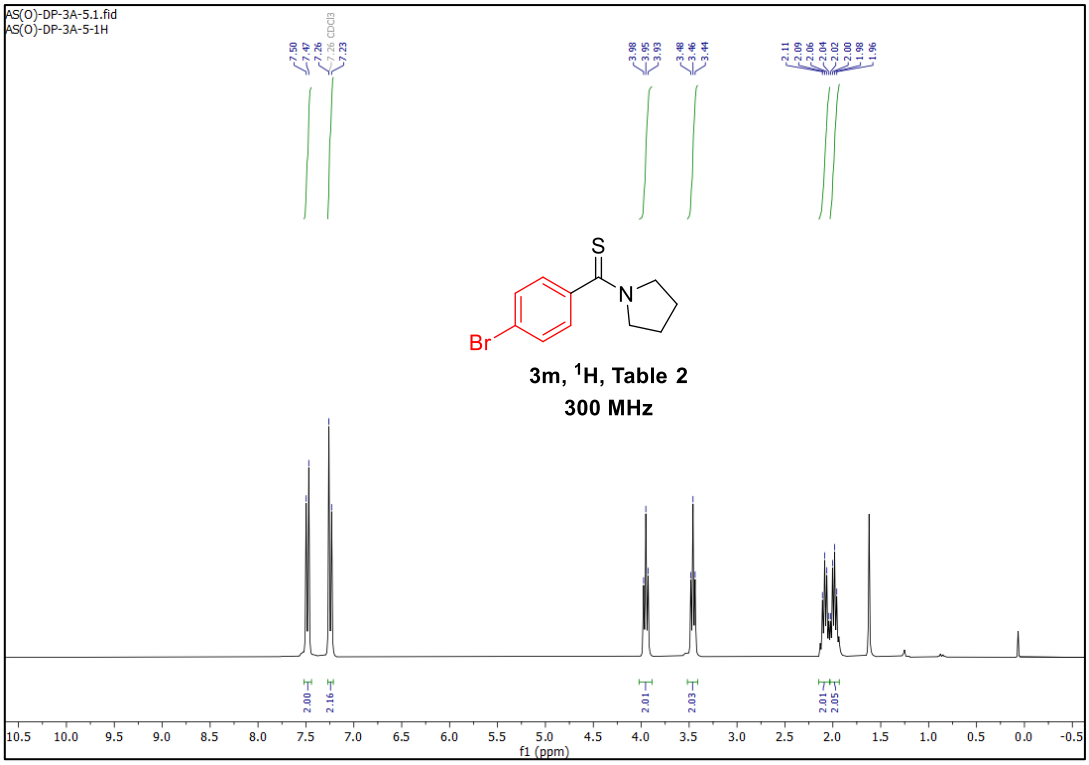
AS(O)-DP-3A-5.1.fid
AS(O)-DP-3A-5-1H
7.50
7.47
7.26
7.26 CDCl3
7.23
3.98
3.95
3.93
3.48
3.46
3.44
2.11
2.09
2.06
2.04
2.02
2.00
1.98
1.96
S
N
Br
3m, 1H, Table 2
300 MHz
2.00
2.16
2.01
2.03
2.01
2.05
f1 (ppm)

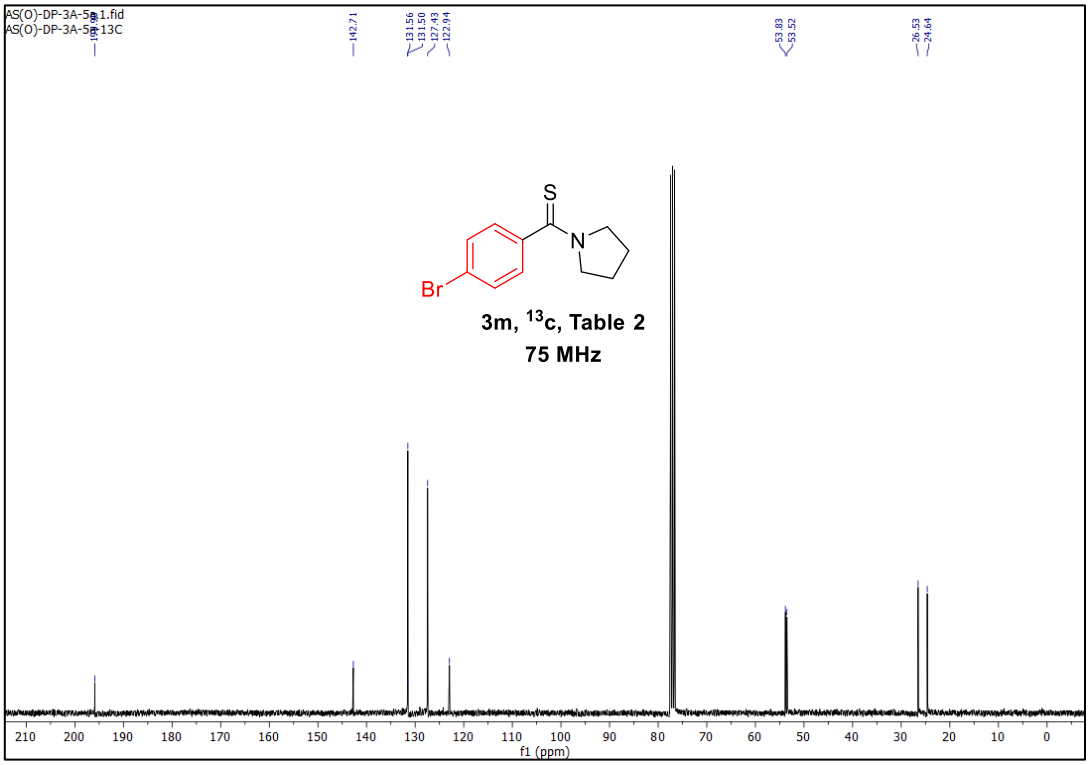
AS(O)-DP-3A-5a.1.fid
AS(O)-DP-3A-5a-13C
142.71
131.56
131.50
127.48
122.94
53.83
53.52
26.53
24.64
S
N
Br
3m, 13c, Table 2
75 MHz
f1 (ppm)

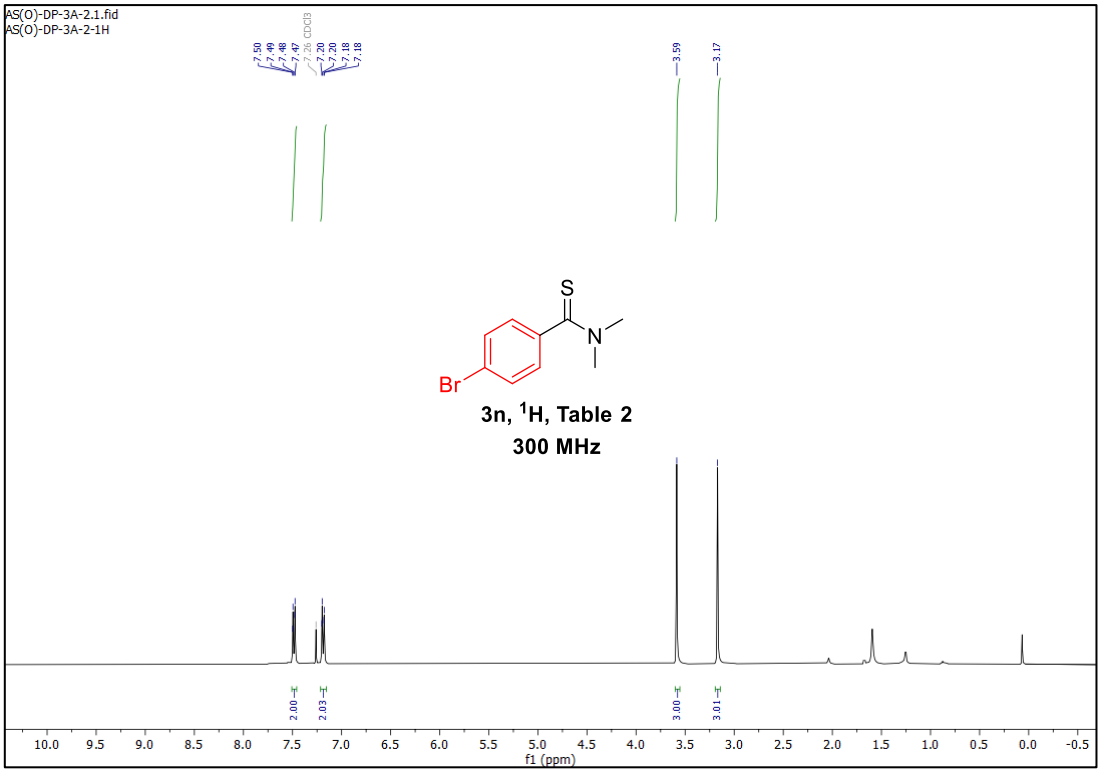
AS(O)-DP-3A-2.1.fid
AS(O)-DP-3A-2-1H
7.50
7.49
7.48
7.47
7.26 CDCl3
7.20
7.20
7.18
7.18
3.59
3.17
S
N
Br
3n, 1H, Table 2
300 MHz
2.00
2.03
3.00
3.01
10.0 9.5 9.0 8.5 8.0 7.5 7.0 6.5 6.0 5.5 5.0 4.5 4.0 3.5 3.0 2.5 2.0 1.5 1.0 0.5 0.0 -0.5
f1 (ppm)

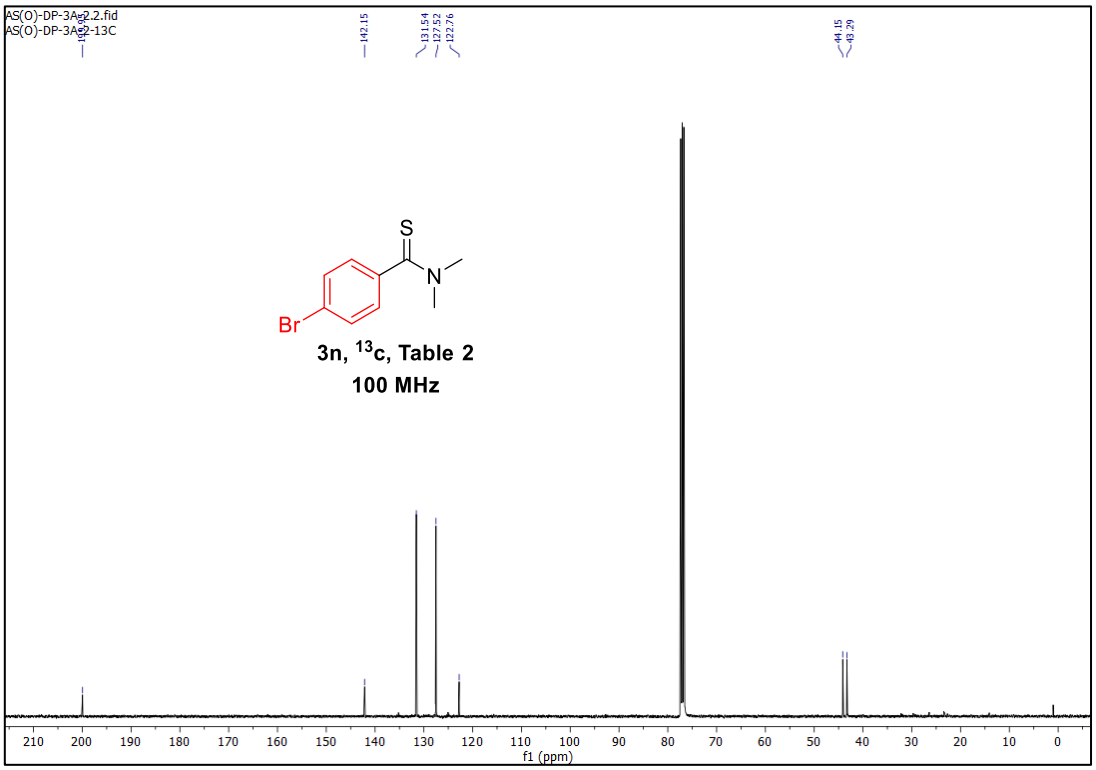
AS(O)-DP-3A-2.2.fid
AS(O)-DP-3A-2-13C
142.15
131.54
127.52
122.76
44.15
43.29
S
N
Br
3n, 13c, Table 2
100 MHz
210 200 190 180 170 160 150 140 130 120 110 100 90 80 70 60 50 40 30 20 10 0
f1 (ppm)

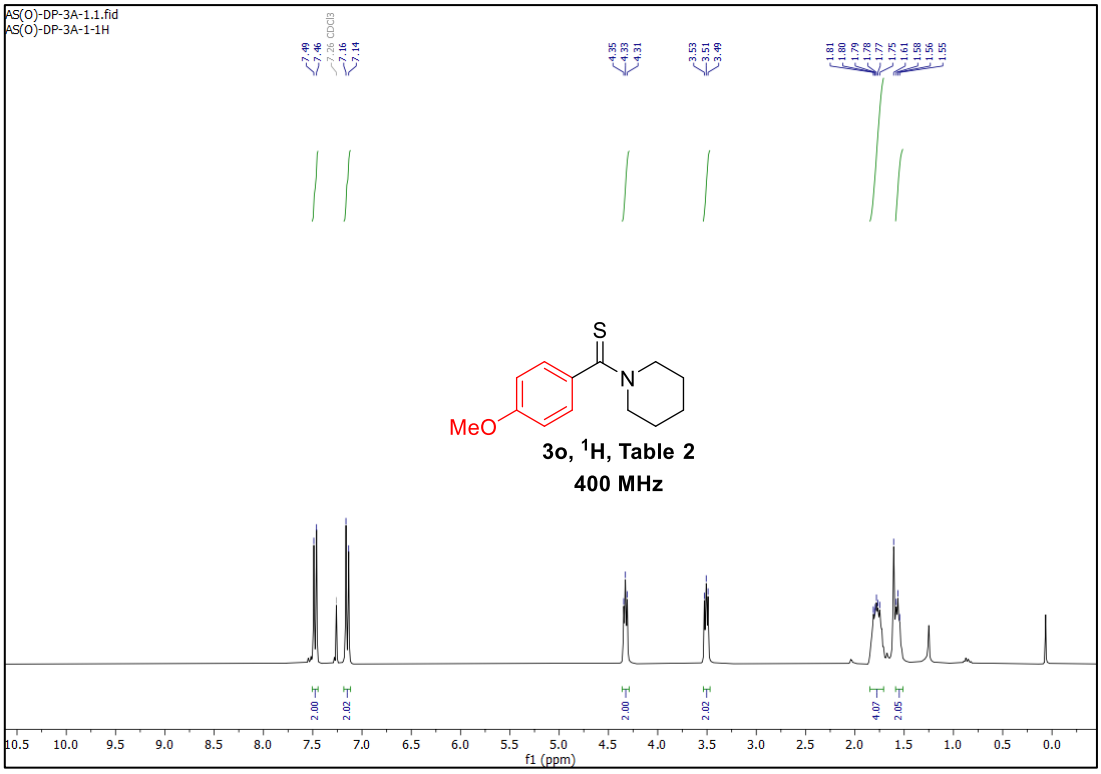

3o, ^{1}H, Table 2
400 MHz

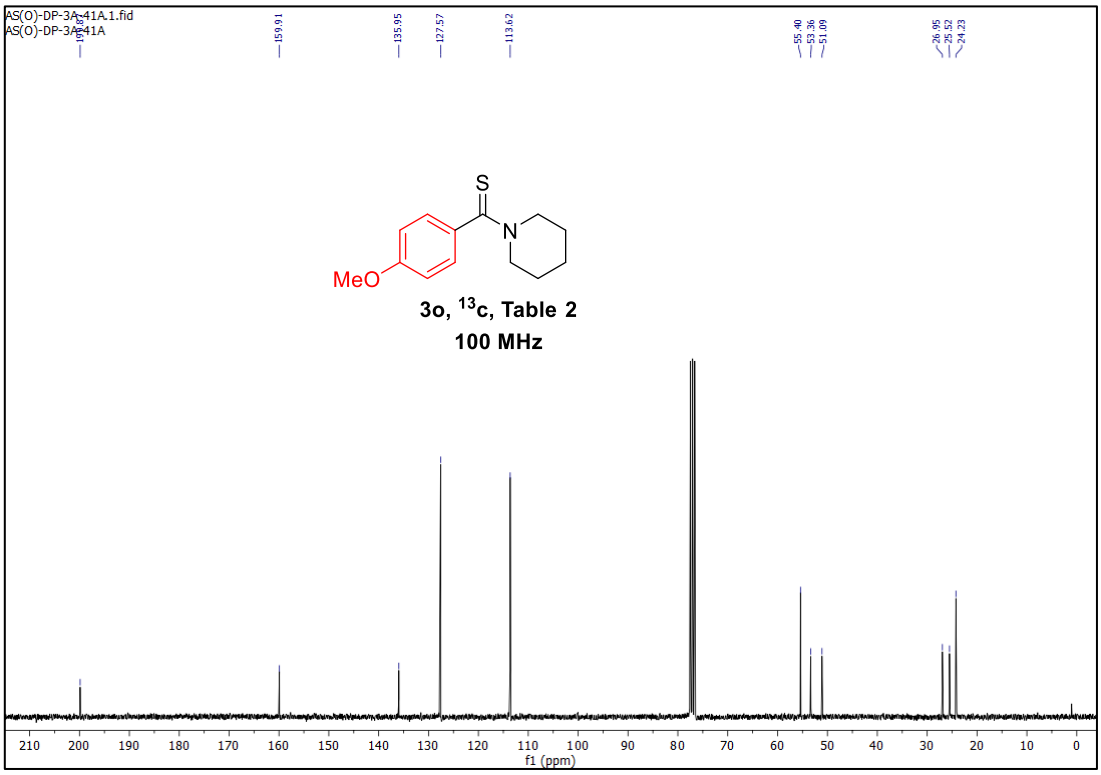

3o, ^{13}c, Table 2
100 MHz

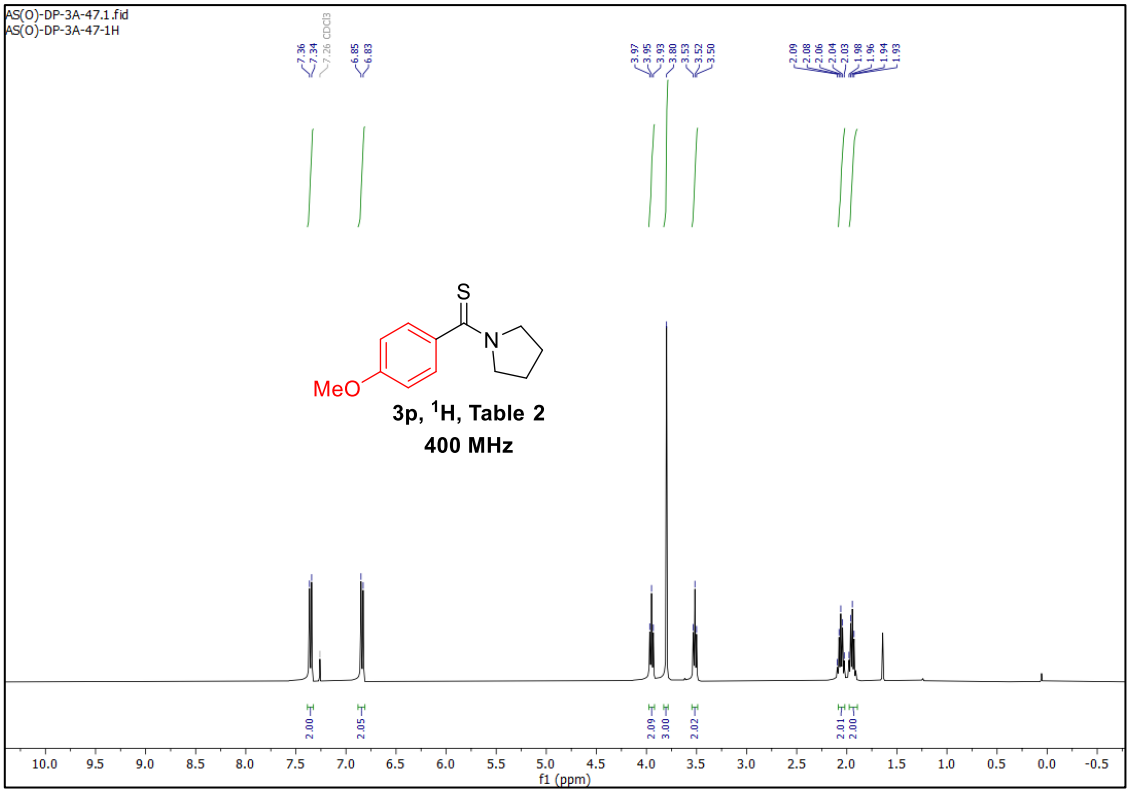
AS(O)-DP-3A-47.1.fid
AS(O)-DP-3A-47-1H
S
N
MeO
3p, 1H, Table 2
400 MHz
f1 (ppm)

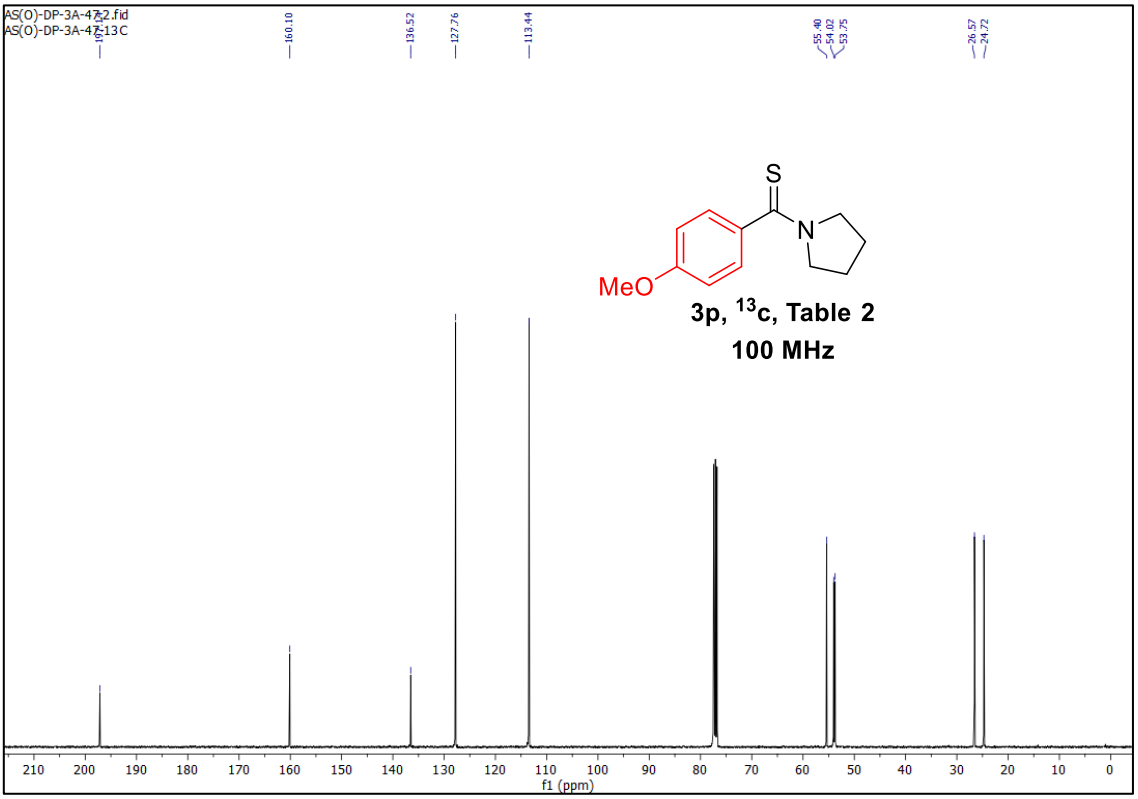
AS(O)-DP-3A-47-2.fid
AS(O)-DP-3A-47-13C
S
N
MeO
3p, 13c, Table 2
100 MHz
f1 (ppm)

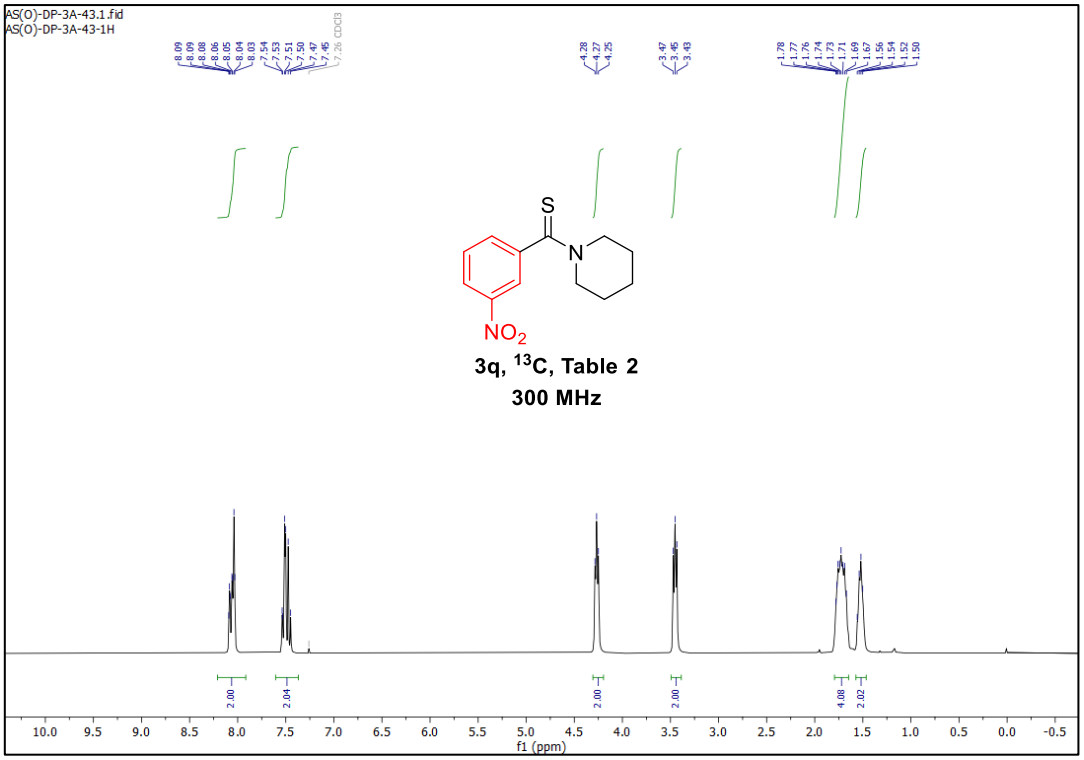
AS(O)-DP-3A-43.1.fid
AS(O)-DP-3A-43-1H
S
N
NO2
3q, 13C, Table 2
300 MHz
f1 (ppm)

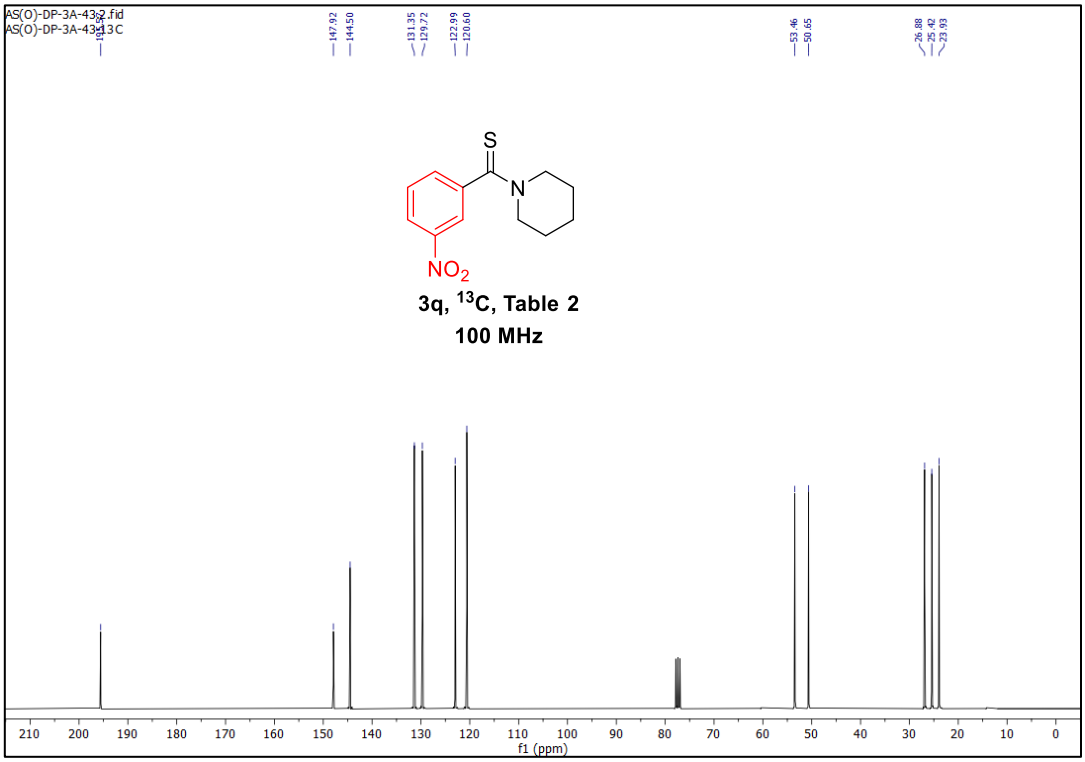
AS(O)-DP-3A-43-2.fid
AS(O)-DP-3A-43-13C
S
N
NO2
3q, 13C, Table 2
100 MHz
f1 (ppm)

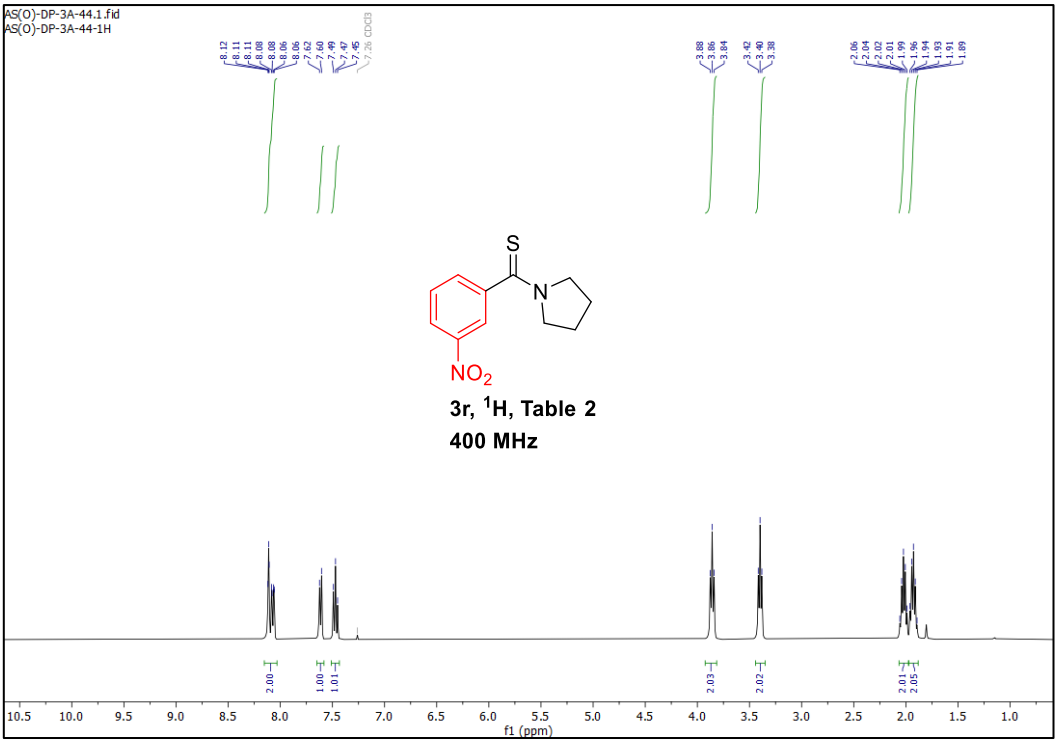

3r, ^{1}H, Table 2
400 MHz

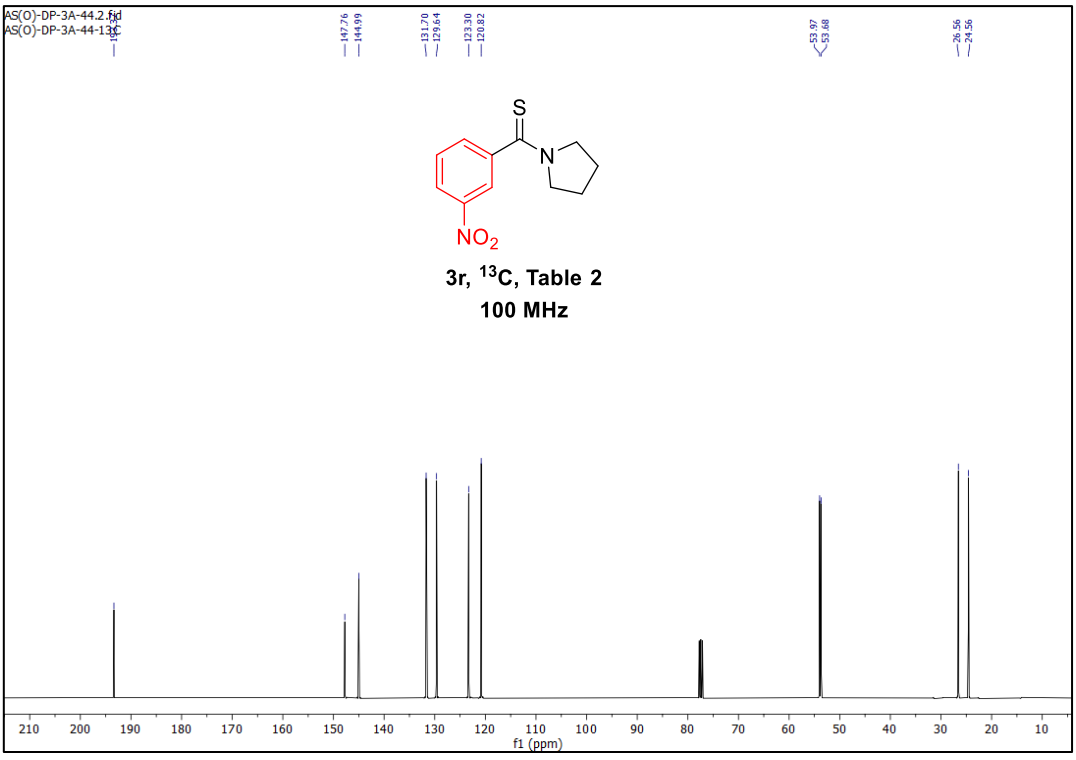

3r, ^{13}C, Table 2
100 MHz

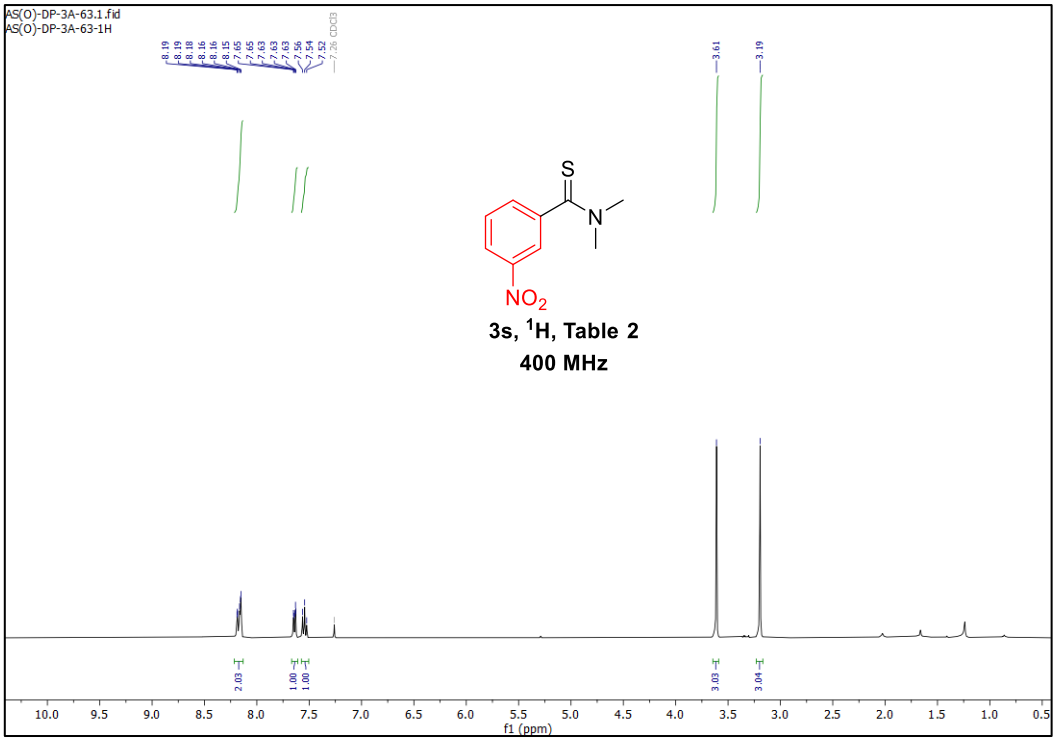
AS(O)-DP-3A-63.1.fid
AS(O)-DP-3A-63-1H
S
N
NO2
3s, 1H, Table 2
400 MHz
f1 (ppm)

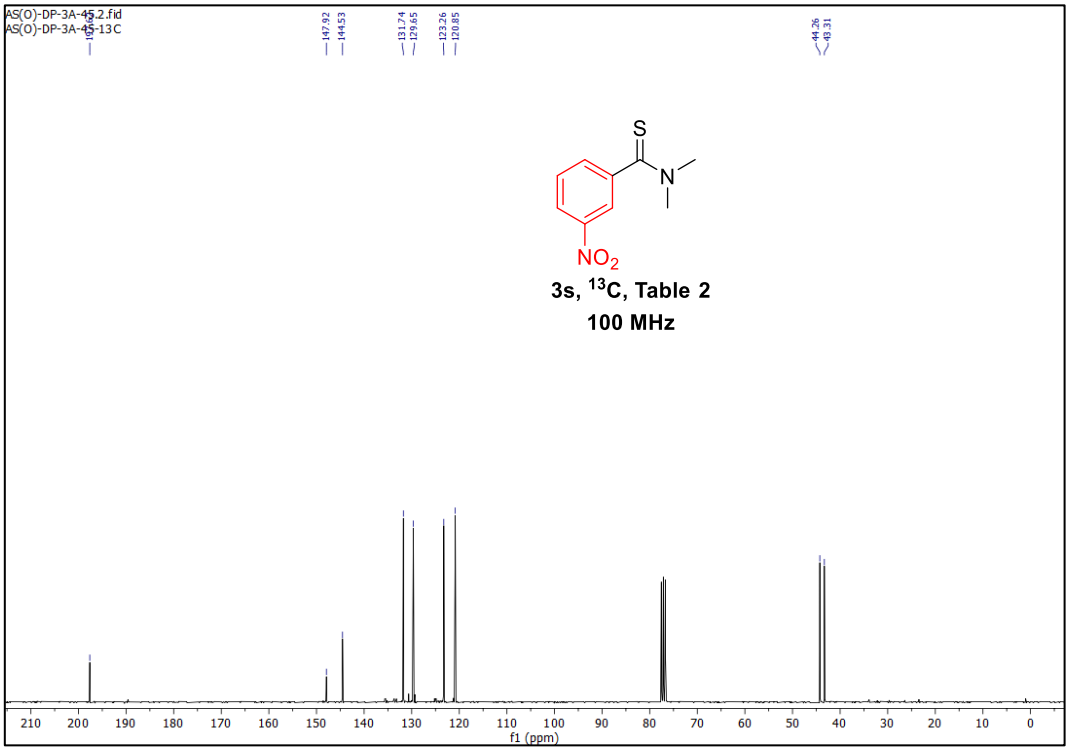
AS(O)-DP-3A-45.2.fid
AS(O)-DP-3A-45-13C
S
N
NO2
3s, 13C, Table 2
100 MHz
f1 (ppm)

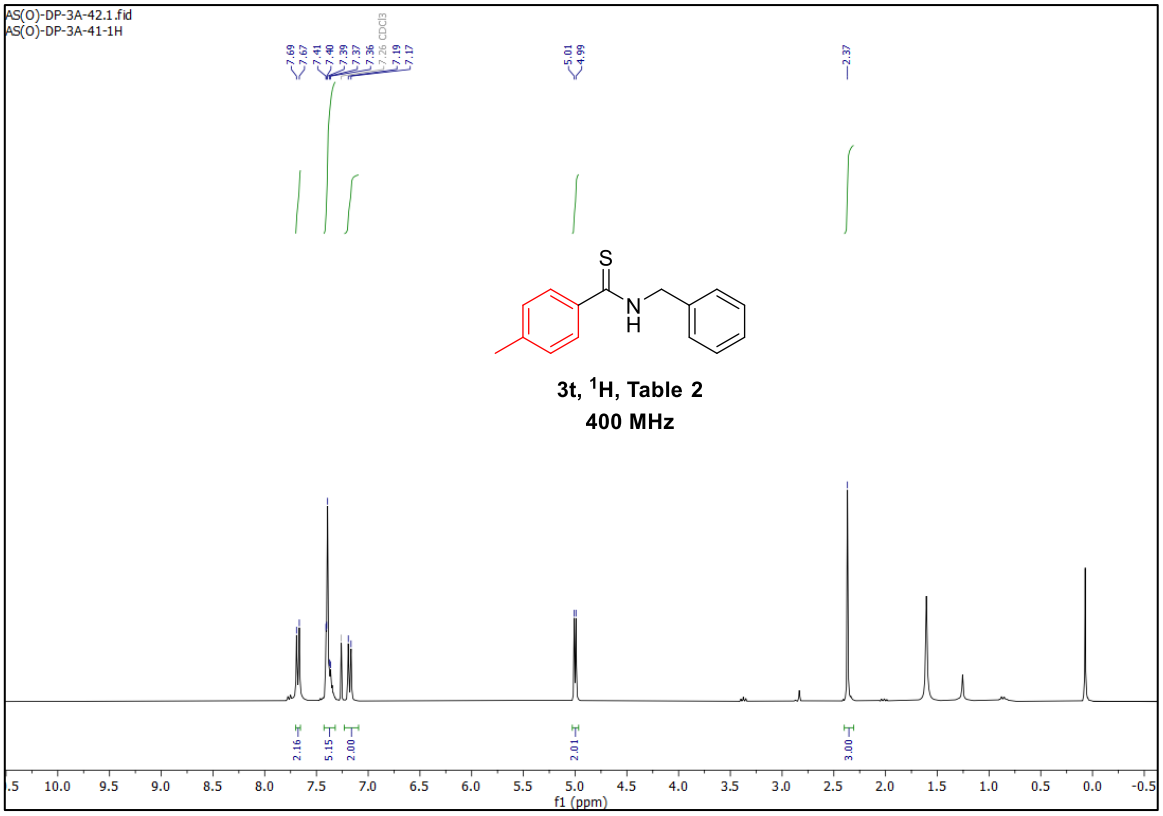

3t, ^{1}H, Table 2
400 MHz

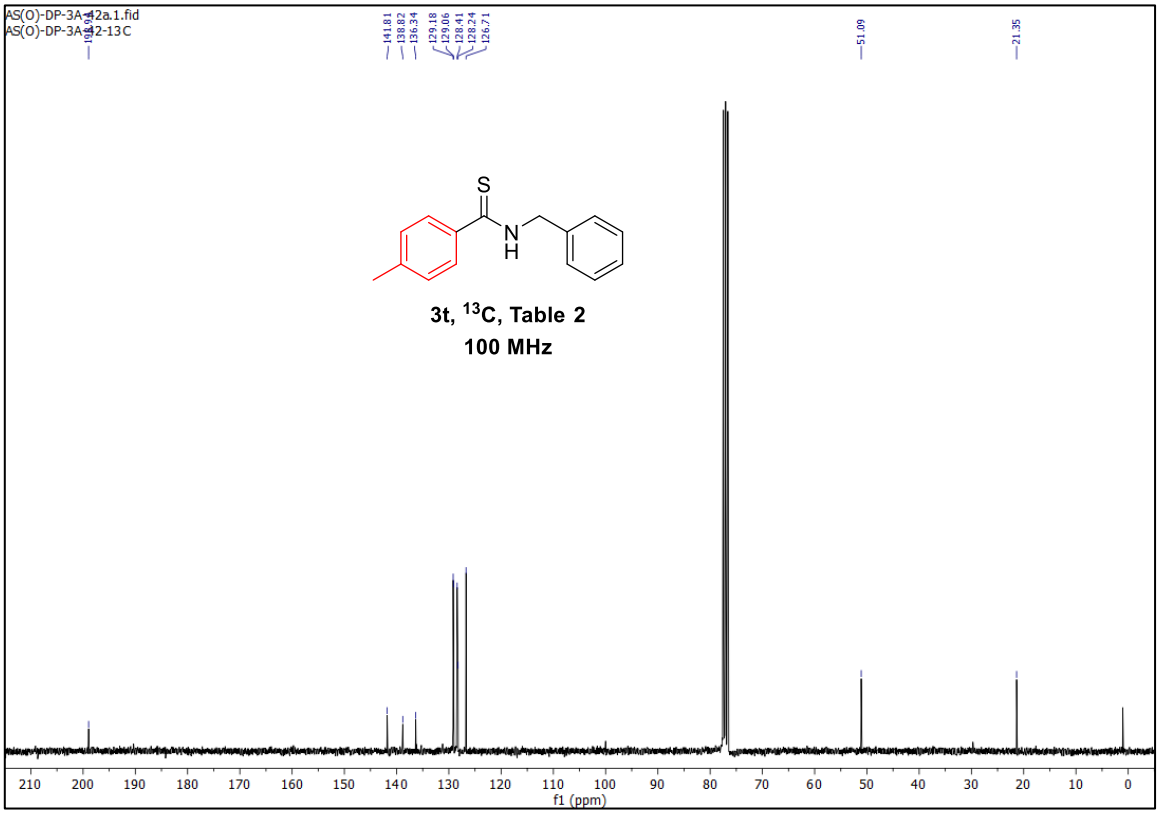

3t, ^{13}C, Table 2
100 MHz

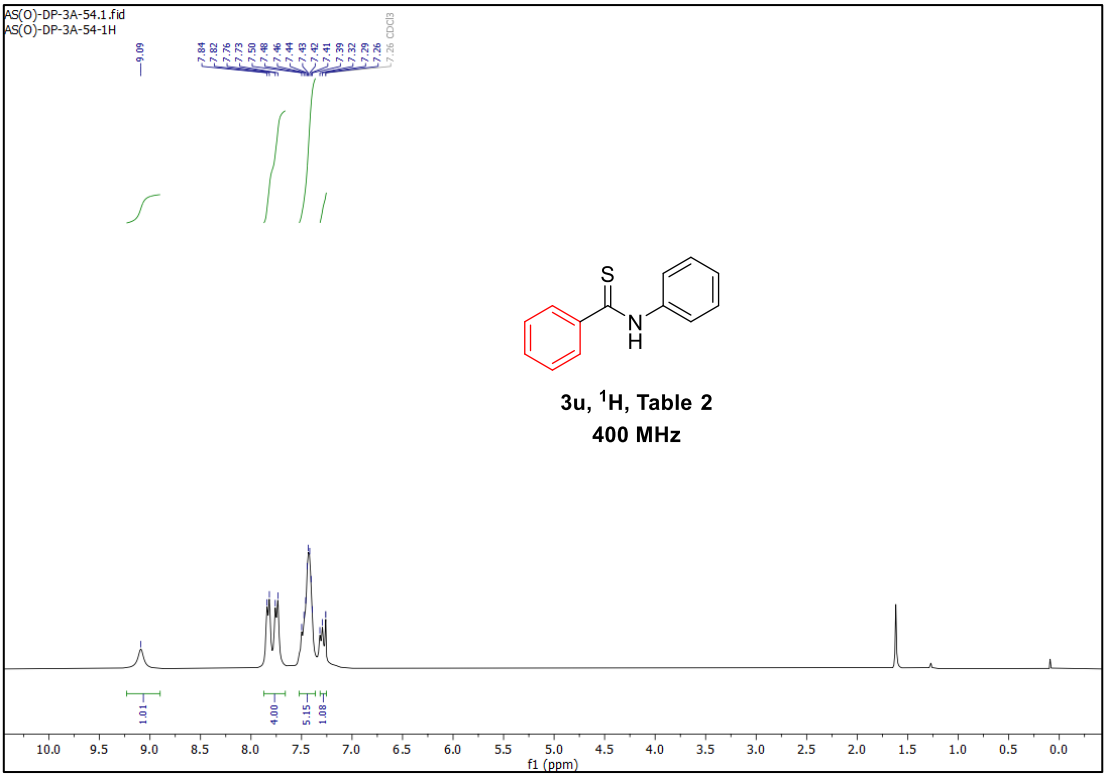

3u, ^{1}H, Table 2
400 MHz

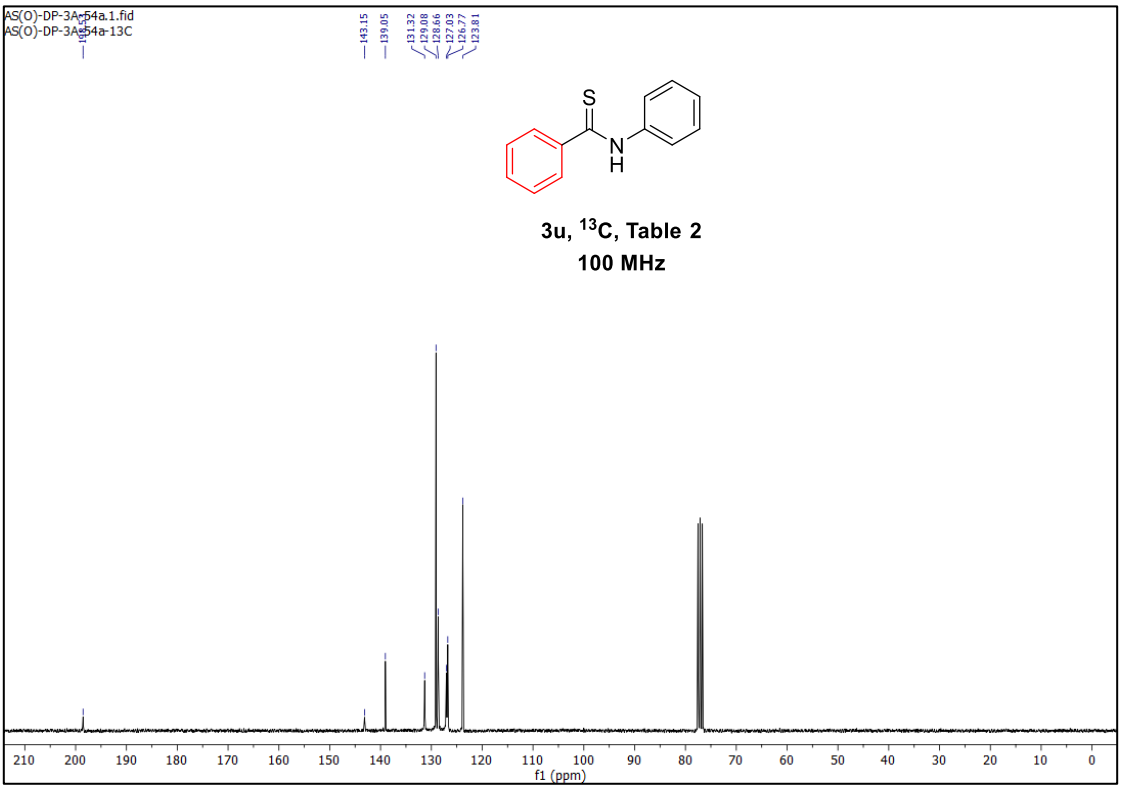

3u, ^{13}C, Table 2
100 MHz

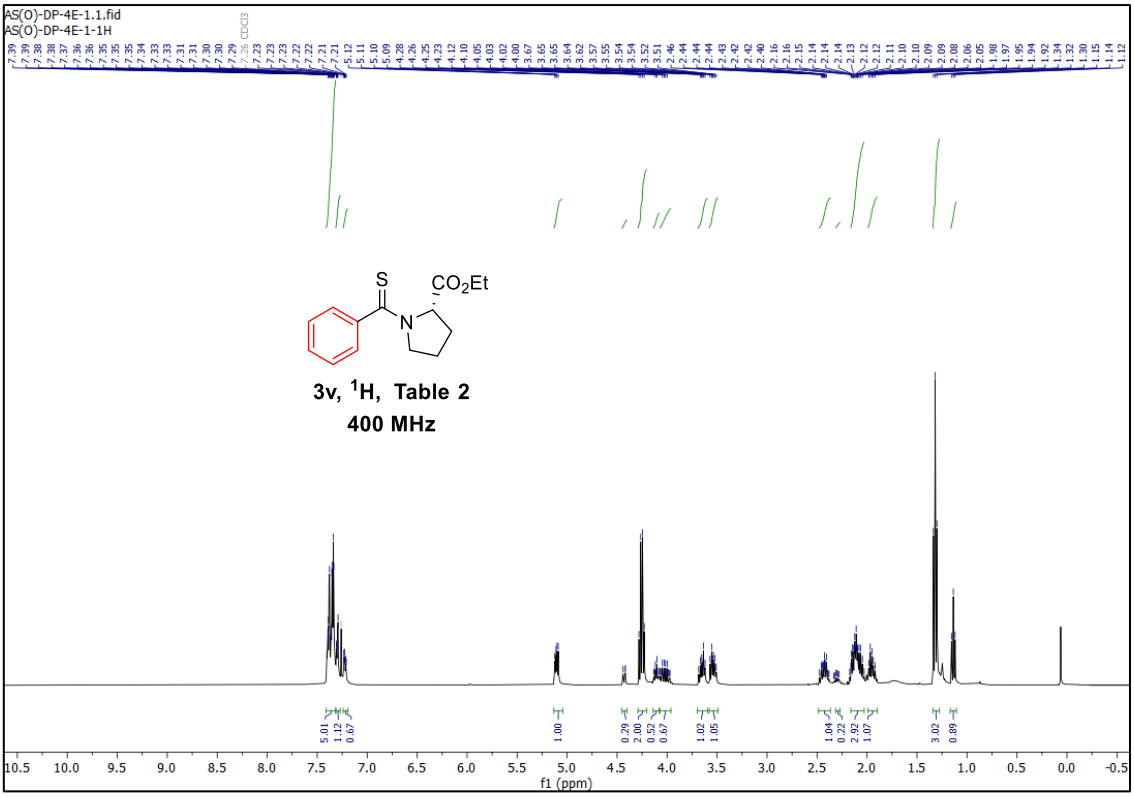
AS(O)-DP-4E-1.1.fid
AS(O)-DP-4E-1-1H
S
CO2Et
N
3v, 1H, Table 2
400 MHz
f1 (ppm)

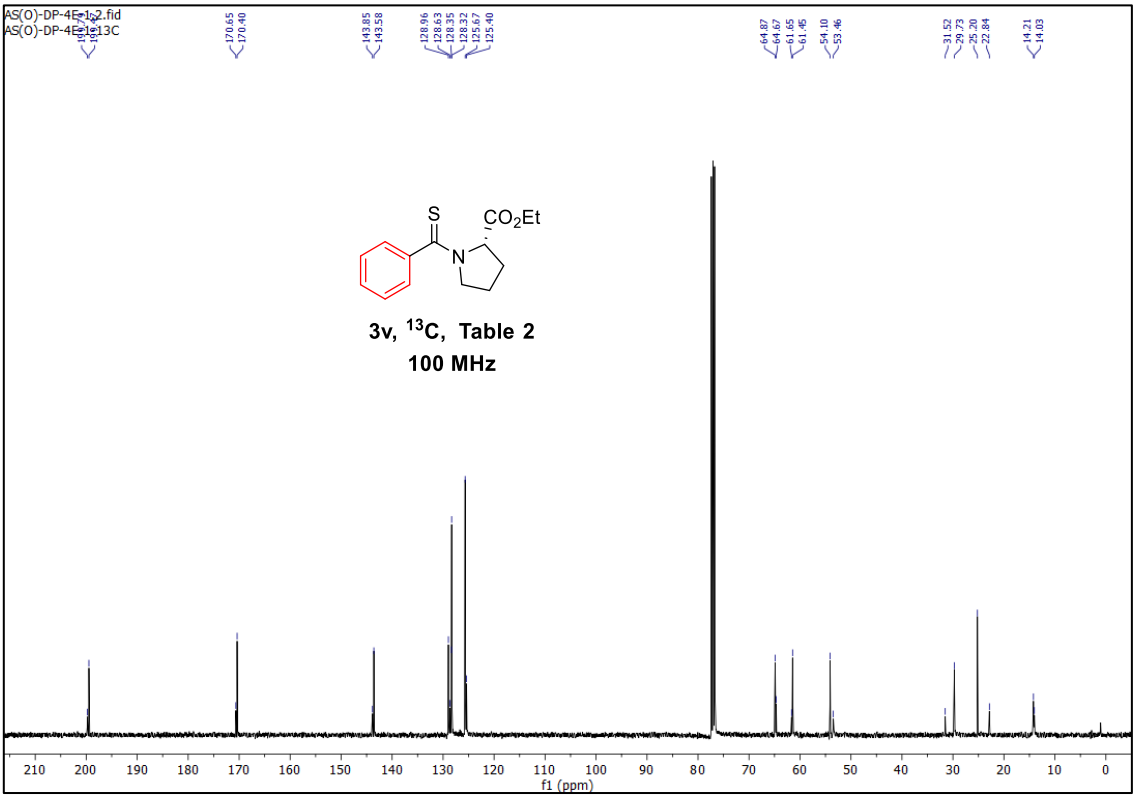
AS(O)-DP-4E-1c2.fid
AS(O)-DP-4E-1c13C
S
CO2Et
N
3v, 13C, Table 2
100 MHz
f1 (ppm)

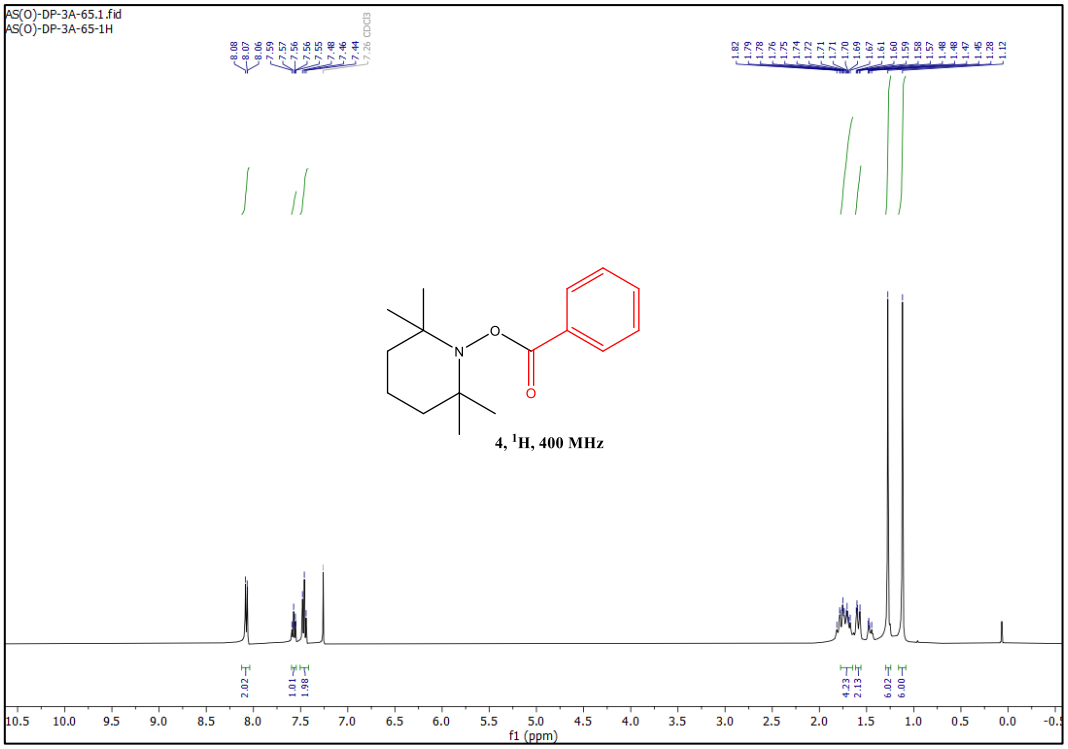

4, ^{1}H, 400 MHz

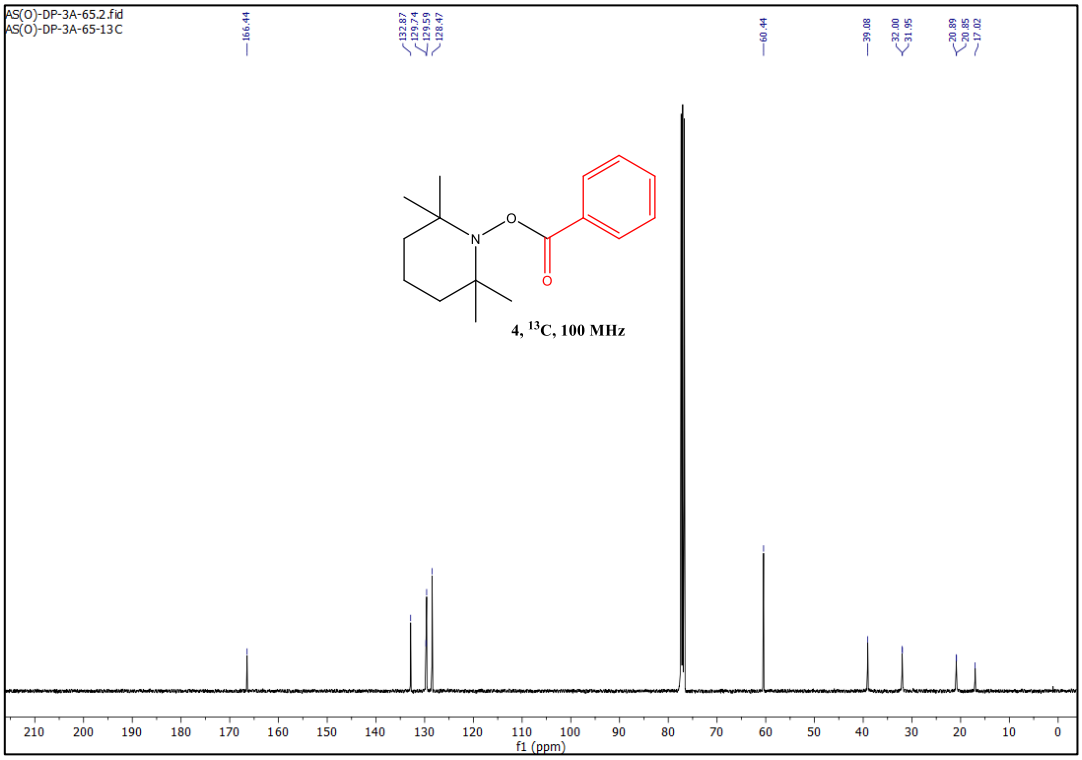

4, ^{13}C, 100 MHz

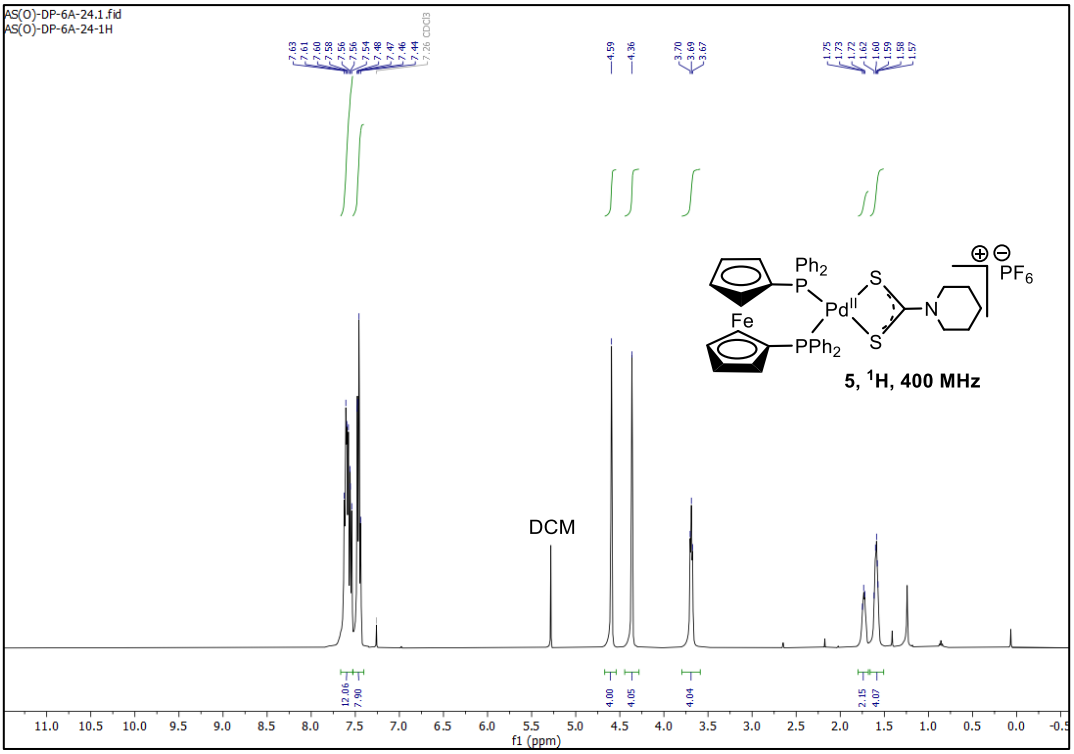
AS(O)-DP-6A-24.1.fid
AS(O)-DP-6A-24-1H
DCM
5, ^{1}H, 400 MHz
f1 (ppm)

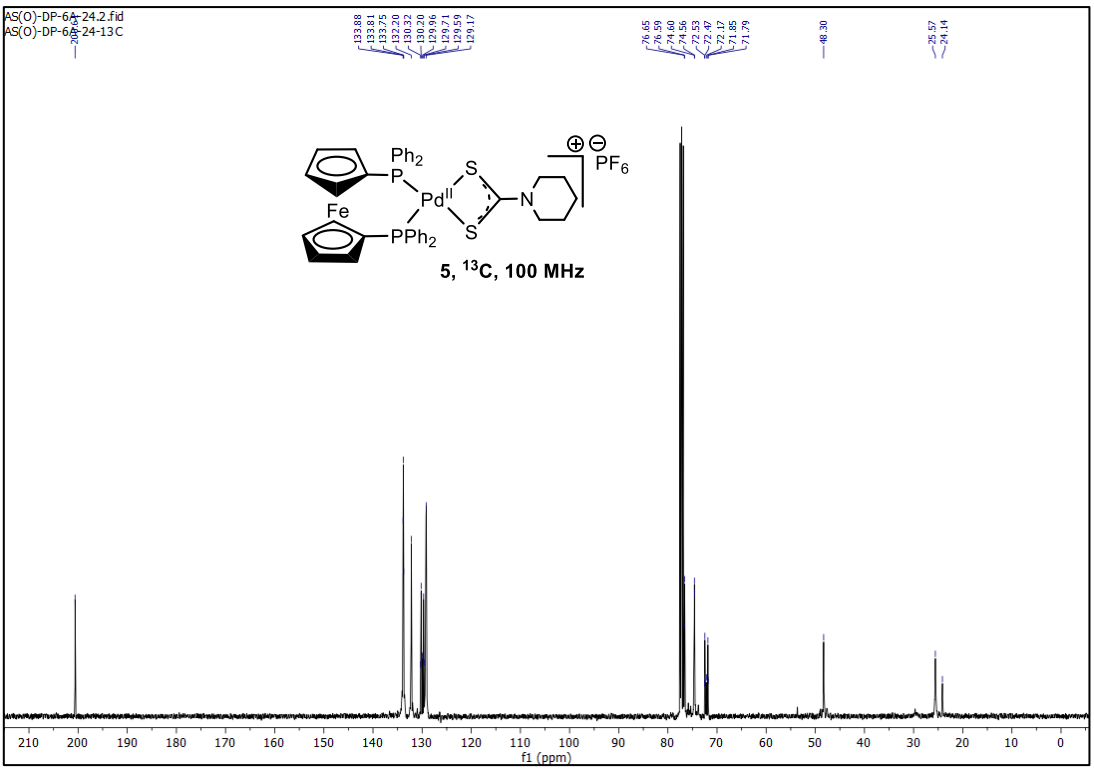
AS(O)-DP-6A-24.2.fid
AS(O)-DP-6A-24-13C
5, ^{13}C, 100 MHz
f1 (ppm)

2/f References

1. (a) N. Mahanta, D. Miklos Szantai-Kis, E. James Petersson and D. A Mitchell, *ACS Chem. Biol.,* **2019,** *14*, 142–163. (b) X. Chen, E.G. Mietlicki-Baase, T. M. Barrett, L. E. McGrath, K. Koch-Laskowski, J. J. Ferrie, M. R. Hayes, E. J. Petersson, *J. Am. Chem. Soc.*, **2017**, *139*, 16688–16695. (c) H. T. Phan, S. G. Giannakoulias, T. M. Barrett, C. Liu and E. J. Petersson, *Chem. Sci.* **2021**, *12*, 10825–10835. (d) Y. J. Wang, D. M. Szantai-Kis and E. J. Petersson, *Org. Biomol. Chem.*, **2015**, *13*, 5074-5081.
2. (a) H. Watanabe and M. Kamigaito, *J. Am. Chem. Soc*. **2023,** *145*, 10948–10953. (b) F. Pourhassan and H. Eshghi, *Catalysis Letters*, **2020**, *150*, 1287–1300. (c) W. Czepa, S. Witomska, P. Samorì and A. Ciesielski, *Small Sci*., **2023**, *3*, 2300013.
3. C. Walpole, S. Y. KO, M. Brown, D. Beattie, E. Campbell, F. Dickenson, S. Ewan, G. A. Hughes, M. Lemaria, J. Lerpiniers, S. Patel and L. Urban, *J. Med. Chem*., **1998**, *41*, 3159.
4. (a) A. Kaluszyner, R. Mechoulam and M. Breuer, Bull. Res. Council Israel, 1958, 7A, 135; (b) D. Duerr and V. Dittrich, ciba; Patent US 3395233, NL 6604132, **1966**; Chem. Abstr., **1967**, *66*, 55249; (c) R. Spaum, P. Brenneisen, A. Rochat, J. Gallay and S. A. Agripat, Patent CH 542828, **1973;** Patent DE 2143838, US3781290, **1972**; Chem. Abstr., **1972**, *77*, 97750; (d) D. Duerr and M. V. Orelli, Ciba, Patent US 3927087, 1975. (e) D. Derr and M. V. Orelli, Ciba, Patent US 3927087, 1975.
5. (a) J. Bernstein, H. L. Yale, K. Losee, M. Holsing, J. Martins and W. A. Lott, *J. Am. Chem. Soc*., **1951**, *73*, 906; (b) B. Love, P. E. Bender, H. Bowman, A. Helt, R. McLeean and T. Jen, *J. Med. Chem*., **1972**, 20-24; (c) G. Vasilev and Z. Tomaleav, Arich. *Phytopathal pflanzenshuts,* **1973**, *9***,** 309; (d) G. Krause, R. Franke and G. N. Vasilev, *Biochem. Physiol. Pflanz.,* **1979**, *174*, 128; (e) C.S. Madabhushi, K. K. R. Mallu, V. S. Vangipuram, S. Kurva, Y. Poornachandra and C. G. Kumar, *Bioorg Med Chem Lett*., **2014**, *24,* 4822.
6. (a) A. Mahajan, S. Yeh, M. Nell, C. E. J.-V. Rensburg and K. Chibale, Biorg. Med. Chem. Lett., **2007**, *17*, 5683; (b) M. B. Krajacic, M. Peric, G. Landek, J. Padovan, D, Jelic, A. Ager, W. K. Milhous, W. Ellis, R. Spaventic and C. Ohrt, J. Med. Chem., **2011**, *43*, 381.
7. (a) J. D. Bloom, M. J. DiGrandi, R. G. Dushin, K. J.Curan, A. A. Ross, E. B. Norton, E. Terefenko, T. R. Jones, B. Feld and S. A. Lang, Bioorg. Med. Chem. Lett., **2003**, *13*, 2929; (b) E. Tatar, S. G. Kucukguzel, S. Rollas and E. De Clercq, Eur. J. Med. Chem., **2008**, ***43***, 381.
8. A. Ranise, A. Spallarossa, O. Burno, S. Schenone, P. Fossa, G. Menozzi, F. Bondavalli, L. Mosti, A. Capuano, F. Mazzeo, G. Falcone and W. Filippeli, Farmaco, **2003**, *58*, 765.
9. (a) A. M. M. E. Omar, A. M. Farghaly, A. A. B. Hazari, N. H. Eshba, F. M. Sharabi, T. T. Daabees, J. pharm. Sci., **1981**, *70*, 1075; (b) A. Ulrich and J. Schlessinger, Cell, **1990**, *61*, 203; (c) Y. .Dai, Y. Frey, R. R. Gauo, Z. Ji, M L. Curtin, A. A. Ahmed, D. H. Albert, L. Armold, S. S. Arries, T. Barlozzari, J. L. Bauch, J. J. Bouska; P. F. Bousquet, G. A. Cunha, K. B. Glaser, J. Guo, J. Li, P. A. Marcotte, K. C. Marsh, M.

D. Moskey, L.J. Pease, K. D. Stewart, V.S. Stoll, P. Tapang, N. Wishart, S. K. Davidsen and M. R. Michaelides, J. Med. Chem., **2006**, *49*, 2357; (e) S. K. Sharma, Y. Wu and Stienbergs, J. Med. Chem., **2010**, *53*, 5197.

10. J. Lee, M. Kang, M. Shim, J. M. Kim, S.U, Kang, J. O. Lim, H. K. Choi, Y. G. Suh, H. G. Park, U. Oh, H. D. Kim, Y. H Park, H. J. Ha, Y. H. Kim, A. Toth, Y. Wang, R. Tran, L. V. Parce, D. J. Lundberg, and P. M, Blumberg, J. Med. Chem., **2003,** 46, 3116.
11. (a) A. K. Mallams, J. B, Morton and P. Reichert, *J. Chem. Soc.,* Perkin Trans., **1981**, *1***,** 2186; (b) S. Cunha, F. C. Macedo, G. A. N. Costa, M. T. Recordings, R. B. V. Verde, L. C. de Souza Neta, I. Vencato, C. Lariucci and F. P. Sa, Monatsh. Chem., **2007**, *138,* 511.
12. (a) A. G. Makhsumov, A. S. Safaev and S. V. Abidova, Katal Pererab. Uglevodordn. Syrya, **1968**, *101*; *Chem. Abstr.,* **1969**, *71*, 101668v; (b) K. Sivapriya, P. Suguna, A. Banerjee, V. Saravana, D. N. Raob and S. Chandraasekarana, Bioorg. Med. Chem. Lett., **2007**, 17**,** 6387; (c) M. Taha, N. H. Ismail, W. Jamil, K. M. Khan, U. Salar, S. M. Kashif, F. Rahim and Y. Latif, Med. Chem. Res., **2015**, 24**,** 3166; (d) D. H. Al-Amily and M. H. Mohammed, Sci.Pharm., **2019**, *87*, 28; (e) S. Naz, M. Zahoor, M. N. Umar, S. Alghamdi, M.U. K. Sahibzada and W. UlBari, Open Chemistry, **2020**, *18***,** 764**.**
13. J, Chen , W, Yu, W, Zhang, C, Sun , W, Zhang, *J Clin Med.,* **2014**. *13*, 1397-406.
14. (a) D. L. Geffner, M. Azukizawa, J. M. Hershman, *J Clin Invest*., **1975**, *55,* 224-231. (b) Schimmel M, U. RD. *Ann Intern Med*., **1977**, *87*, 760-768.
15. (a) D. Forrest, J. Nunez, *Encycl. of Neuroscience*, **2009**, 993-1000.(b) D. Braun, U. Schweizer, *Tetrahedron Lett.*, **2018**, *106*, 19-44.
16. (a) E. B. Veale, G. M. Tocci, F. M. Pfeffer, P. E. Kruger and T. Gunnlaugsson, *Org. Biomol. Chem*., **2009**, *7*, 3447; (b) C. Caltagirone and P. A. Gale, *Chem. Soc. Rev*., **2009**, *7*, 3447; (c) Y. Tang, L. Deng, Y. Zhang, G. Dong, J. Chen and Z. Yang, *Org. Lett*., **2005**, *7*, 1657; (d) J. Li, L.-L. Shi, J. Chen, J.Gong and Z. Yang, Synthesis, **2014**, *46*, 2007.
17. B. Mertschenk, F. beck and W. Bauer, Thiourea and Thiourea Derivatives, in Ullman 's Encyclopedia of Industrial Chemistry, **2002**, Wiley-VCH Verlag GmbH & Co. KGaA.
18. J. Zao and G. Cui, *International Journal of Electrochemical Science*, **2011**, *6*, 4048.
19. P. K. Mohanta, S. Dhar, S. K. Samal, H. I1a and H. Junjappa, *Tetrahedron*, **2000**, *56*, 629.
20. (a) B. G. Ateya, B. E. El-Anadouli and F. M. El-Nizamy, *Corros. Sci*., **1984**, *24*, 497; (b) N. C Subramanyam, B. S. Sheshadri, S. M Mayanna, *Corros. Sci*., **1993**, *34*, 563; (c) M. A. Quraishi, F. A. Ansari and D. Jamal, Mater. *Chem. Phys*., **2003**, *77*, 687. (d) M. Ozcan, I. Dehri and N.S Abd-Elshafi, Electrochim, Acta, **2006**, *51*, 3296; (f) V. V. Torres, V. A. Rayol, M. Magalhaes, G. M. Viana, L. C. S. Aguiar, S. P. Machado, V. W. Faria, G. F. de Andrade, E. D' Elia, M. F. Carbal, B. A. Cotrim, G. O. Resende and F. C. deSouza, *Phosphours, Sulfer, and Silicon and the Related Elements*, **2015**, *8*, 1366.

21. F. A. A. Ngh, E. I. Zakariah, N. I. Hassan, B. Yamim, S. Sapari,and S. A. Hasbullah, *Malaysian Journal of Analytical Sciences*, **2017**, *21*, 1226.
22 (a) J. Smith, J. L. Liras, S. E. Scheider and E. V. Anslyn, *J. Org. Chem*., **1996**, *61*, 8811; (b) Y. Tobe, S. Sasaki, K. Hirose and K. Naemura, *Tetrahedron Lett*., **1997**, *38*, 4791.
23. (a) T.S. Griffin, T. S. Woods and D. L. Klayman, Thioureas in the synthesis of hetrocycles, in Advances in Heterocyclic Chemistry, ed. A. R. Katritzky and A. J. Boulton, **1975**, *18*, 99; (b) D. G. Patil and M. R. Chedekel, *J. Org. Chem*., **1984**, *49*, 997; (c) S. Kasmi, J. Haelin and H. Benhaoua, *Tetrahedron Lett*., **1998**, *63*, 196; (e) C. Boga, L. Forlain, C. Silvestroni, A. B. Corradi and P. Sgarabotto, *J. Chem. Soc.,* **1999**, *1363*; (f) M. Kidwai, R. Venkataramana and B. Dave, *Green Chem.,* **2001**, ***3,*** 278; (g) S. Paul, M. Gupta, R. Venkataramanan and B. Dave, *Green Chem*., **2001**, *3*, 278; (g) S. Paul, M. Gupta, R. Gupta and A. Loupy, *Synthesis*, **2002**, *1*, 75; (h) W. Du and D. P. Curran , *Org. Lett*., **2003**, *5*, 1765; (i) U. Heinelt, D. Schultheis, S. Jager, M. Lindenmarie, A. Pollex and H. S. G. Beckmann, *Tetrahedron*, **2004**, *60*, 9883; (j) S. Huang, Y. Pan, Y . Zhu and A. Wu, *org. Lett*., **2005**, *7*, 3797.
24. A. Singh, M. K. Bharty, P. Bharati, S. Singh and N. K. Singh, *Polyhedron*, **2015**, *85*, 918.
25. F. A. Saad, *International Journal of Electrochemical Science*, **2014**, *9*, 4761.
26. H. Arsalan, N. Duran, G. Borekci, O. Koray and C. Akbay, *Molecules*, **2009**, *14*, 519.
27. A. Saeed, N. Abbas. Z. Ashraf and M. Bolte, *South African Journalof chemistry*, **2013**, *66*, 273.
28. R. G. Kumari, V. Ramkrishnan, M. L. Carlolin, J. kumar, A. Sarua and M. L. Carolin, J. Kumar, A. Sarua and M. Kuball, *Spectrochimica Acta Part A*, **2009**, *73*, 263.
29. F. Duus; in Comprehensive Organic Chemistry, ed. N. J. Jones; Pergamon Press, Oxford, **1979**, *3*, 465.
30. K. Ramadas, *Tetrahdron Letters*. **1996**, *37*, 5161.
31. (a) S.M. Losanitsch, *Chem. Ber*., **1996**, *37*, 5161. (b) A. Hugershoff, *Chem. Ber.,***1899**, *32*, 224; (c)E. A. Werner, *J. Chem. Soc*., **1920**, *117***,** 1046. (c) N. S. Drozdov, *J. Gen. Chem.,* 1936, 6, 1368.
32. (a) S. M. Losasitsch, *Chem. Ber*., **1891**, *24*, 3021; (b) F. B. Danis, R. Q. Brewster and C.P Olander, *Univ. Kansas Sci. Bull*., **1922,** *13*, 1-14; *Chem. Abstracts*, **1923**, *17*, 543.
31. F. Alu and R. Gruoo, *Tetrahedron*, **1988,** *44*. 7271 – 7282.
32. M. Saito, S. Murakami, T. Nanjo, Y. Kobayashi, and Y. Takemoto, *J. Am. Chem. Soc.* **2020**, *142,* 8130−8135.
33. Y. Qu, Z. Li, H. Xiang, and X. Zhou, *Adv. Synth. Catal*. **2013**, *355*, 3141 – 3146.
34. Y. Qu, Z. Li, H. Xiang, and X. Zhou, *Adv. Synth. Catal*. **2013**, *355*, 3141 – 3146.
35. N. Borthakur and A. Goswami, *Tetrahedron Lett.,* **1995**, *36*, 6745-6746.
36. X. Wang, M. Ji, S. Lim, H. Y. Jang, *J. Org. Chem*. **2014**, *79*, 7256−7260.
37. B. Kurpil, B. Kumru, T. Heil, M. Antonietti, A. Savateev, *Green Chem*., **2018**, *20*, 838–842.
38. Y. Qu, Z. Li, H. Xiang, and X. Zhou, *Adv. Synth. Catal.* **2013**, *355*, 3141 – 3146.
39. (a) R. W. Hanson, Decarboxylation of α-keto acids, *J. Chem. Educ.,* **1987**, *64,* 591-595; (b) K. Yan, D. Yang, _ W. W. Jing Zhao, Y. Shuai, L. Tian and H.

Wang, *Org. Biomol. Chem.,* **2015**, *13*, 7323-7330; (c) H. Wang, Li−Na. Guo, S. Wang and X.H. Duan, *Org. Lett.*, **2015**, *17*, 3054–3057; (d) S. Panja, P. Maity and B. C. Ranu, *J. Org. Chem.,* **2018**, *83*, 12609–12618; (e) H. B. Wang and J. M. Huang, *Adv. Synth. Catal.*,**2016**, *358*, 1975–1981; (f) Y. Xiang, G. Zeng, X. Sang, X. Li, Q. Ding and Y. Peng, *Tetrahedron,* **2021**, *91*, 132193; (g) T. Patra and D. Maiti, *Chem. Eur. J.*, **2017**, *23*, 7382–7401; (h) K. Yan, D. Yang, W. Wei, F. Wang, Y. Shuai. Q. Li and H. Wang, *J. Org. Chem.,* **2015**, *80*, 1550−1556; (i) C. Wang, S. Yang, Z. Huang and Y. Zhao, *Molecules*., **2022**, *27*, 1980; (j) X.-L. Xu, W.-T. Xu, J.-W. Wu, J.-B. He and H.-J. Xu, *Org. Biomol. Chem.,* **2016**, *14*, 9970-9973; (k) J. S. Tucker and M. E. Morgan, *Appl. Microbiol.*, **1967**, *15*, 694–700; (l) S. M. Hutson, Branched chain alpha-keto acid oxidative decarboxylation in skeletal muscle mitochondria. Effect of isolation procedure and mitochondrial delta pH, *J. Biol. Chem.*, **1986**, *261*, 4420-4425; (m) D. Patra and A. Saha, *Eur. J. Org. Chem*., **2022**, e202201042, https://doi.org/10.1002/ejoc.202201042; (n) R. S. K. Lalji, P. Kumar, M. Gupta, V. S. Parmar and B. K. Singh, *Adv. Synth. Catal.*, **2020**, *362*, 552-560.

40. (a) L. K. D. L. Cruz, X. Yang, A. Menshikh, M. Brewer, W. Lu, M. Wang, S. Wang, X. Ji, A. Cachuela, H. Yang, D. Gallo, C. Tan, L. Otterbein, M. d. Caestecker and B. Wang, *Chem. Sci*., **2021**, *12***,** 10649–10654; (b) T. Kitagawa, H. Kuroda, K. Iida, M. Ito and M. Nakamura, *Chem. Pharm. Bull*., **1989**, *37*, 3225-3228; (c) F. Zhou, L. Li, K. Lin, F. Zhang, G.-J. Deng and H. Gong, *Chem. Eur. J*., **2020**, 26**,** 4246 – 4250.
41. (a) M. Saito,S. Murakami. T. Nanjo, Y. Kobayashi and Y. Takemoto, Mechanism and applications to thioamide synthesis, *Tetrahedron*, **1988**, *44*, 7271-7282.
42. (a) N. B. Kuotsu, L. Jamir, T. Phucho and U. B. Sinha, *Acta Chim. Slov.*, **2017**, *64*, 832–841; (b) S. Kanchi, P. Singh, K. Bisetty, *Arab. J. Chem.*, **2014**, *7*, 11–25.
43. (a) M. Saito, S. Murakami. T. Nanjo, Y. Kobayashi and Y. Takemoto, *J. Am. Chem. Soc.*, **2020**, *142*, 8130−8135;
44. (a) G.-H. Niu, P.-R. Huang and G. J. Chuang, *Asian J. Org. Chem.*, **2016,** *5*, 57 – 61; (b) S. Jaspal, V. N. Shinde, N. Meena, D. S. Nipate, K. Rangan and A. Kumar, *Org. Biomol. Chem.*, **2020**, *18*, 9072-9080; (c) T. A. To, Y. H. Vo, H. T.T. Nguyen, P. T. M. Ha, S. H. Doan, T. L. H. Doan, S. Li, H. V. Le, T. N. Tu, N. T. S. Phan, J. Catal., **2019**, *370*, 11–20; (d) T. Cohen and I. H. Song, *J. Am. Chem. Soc.*, **1965**, *87*, 3780-3781; (e) T. Vencel, K. Gáplovská, A. Gáplovský, Š. Toma, F. Šeršen,. *A: Chem.*, **2004**, *162*, 53–62.
45. (a) A. D. Kale, Y. A. Tayade, S. D. Mahale, R. D. Patil, and D. S. Dalal, Tetrahedron, **2019**, *75*, 130575.
46. (a) D. Ferraris, B. Young, T. Dudding and T. Lectka, *J. Am. Chem. Soc.*, **1998**, *120*, 4548-4549; (b) N. Asao, T. Nogami, K. Takahashi and Y. Yamamoto, *J. Am. Chem. Soc.*, **2002**, *124*, 764–765; (c) K. Mikami, M. Hatano, K. Akiyama, *Top. Organomet. Chem.*, **2005**, *14*, 279–321.
47. (a) F. P. Andrew and P. A. Ajibade, *Journal of Molecular Structure*, **2018**, *1155*, 843-855; (b) A. M. Paca, P. A. Ajibade, F. P. Andrew, *Arabian Journal of Chemistry***, 2021**, *14*, 103326; (c) V. Uivarosi, M. Badea, V. Aldea, L. Chirigiu

and R. Olar, *J. Therm. Anal. Calorim.*, **2013**, *111*, 1177–1182; (d) A. Trevisan, C. Marzano, P. Cristofori, M. B. Venturini, L. Giovagnini and D. Fregona, *Arch. Toxicol.*, 2002, **76**, 262–268; (e) S. D. Xu and X. H. Wu, *J. Chem. Res.*, **2019**, *43*, 437–442.

48. (a) H. Ghosh, R. Yella, J. Nath and B. K. Patel, *Eur. J. Org. Chem.*, **2008**, 6189–6196; (b) J. Nath, B. K. Patel, L. Jamir, U. B. Sinha and K. V. V. V. Satyanarayana, *Green Chem.*, **2009**, *11*, 1503–1506.
49. (a) X.-Y. Chen, M. Pu, H.-G. Cheng, T. Sperger and F. Schoenebeck, *Angew. Chem. Int. Ed.*, **2019**, ***58***, 11395 –11399; (b) C. C. C. J. Seechurn, T. Sperger, T. G. Scrase, F. Schoenebeck and T. J. Colacot, *J. Am. Chem. Soc.*, **2017**, *139*, 5194−5200; (c) Q. Simpson, M. J. G. Sinclair, D. W. Lupton, A. B. Chaplin, *Org. Lett.*, **2018**, *20*, 5537−5540; (d) G. N. Tran, B. S. Bouley and L. M. Mirica, *J. Am. Chem. Soc.*, **2022**, *144*, 20008−20015.
50. (a) J. Lee, U. v. Gunten and J.-H. Kim, *Environ. Sci. Technol.*, **2020**, *54*, 3064−3081; (b) X. Zhou, P. Wang, L. Zhang, P. Chen, M. Ma, N. Song, S. Ren and M. Li, *J. Org. Chem.*, **2018**, *83*, 588−603; (c) I. M. Ogbu, G. Kurtay, F. Robert and Y. Landais, *Chem. Commun.*, **2022**, *58*, 7593–7607.
51. A. Moazzam, M. Khodadadi, F. Jafarpour and M. Ghandi, *J. Org. Chem.*, **2022**, *87*, 3630.

Chapter-III

Section-I

C-C Cross coupling reactions under metal free condition

1/a Introduction

Over the past few decades, dithiocarbamates which are stable and easily available organic scaffold, have unique chemical reactivity and immense significance in different branches of chemistry ranging from medicinal to material. Dithocarbamates are used as ligands which have the ability to form stable complexes with transition metals. This chelating ability has been utilized in numerous applications. Compounds containing dithiocarbamate organic scaffolds have been used in enzyme inhibition, treatment of HIV and emphasized specially for remarkable pharmacological effects as antifungal,[1] antioxdition,[2] antiparasitic,[3] antiviral,[4] antibacterial,[5] antitubercolesis,[6] antibiofilm,[7] antibioflim,[8] fungicidal,[8] insecticidal,[9] pesticidal,[10] herbicidal,[11] algicidal,[12] antiliprocy,[13] antitubercular,[14] antimicrobial,[3] antiprotozoal,[3] anthelmintic,[15] antihistaminic,[16] antifouling,[17] anticancer,[18] anti-alzheimar,[19] growth depressant[20] activities. They also act as cell apoptosis monoacylglycerollipase and indoleamine 2,3-dioxygenase inhibitors[21] (Fig. 3.1). Probably, the presence of HS-groups of physiologically important enzymes in dithiocarbamates helps in antibacterial activities by transferring the alkyl groups of DTCs to the HS-function of the enzymes. For various indications of different fatal diseases like HIV, chronic alcoholism, arteriosclerosis and fungi- and bacteria-related diseases,[22] several DTCs are under clinical trials. As dithiocarbamates are four electron donor,[23] they have a strong tendency to undergo complexation as monodentate and bidentate ligands or podands with a wide variety of metals in all accessible oxidation states. DTCs can also be used in proliferation of influenza A (H1N1) virus, scavenging superoxide anions and as potential auxiliaries in oncological chemotherapy.[24] They have also various applications in photochemistry,[26] RAFT polymerization as a radical chain transfer agents,[27] detection and analysis of nitric oxide (NO) produced endogenously from NO synthases,[28] catalysis in the vulcanization of rubber,[29] determination of heavy metals and waste water treatment.[30] DTCs also act as synthons for the synthesis of trifluoromethylamines, isothiocyanates, alkoxyamines, thioureas, ionic liquids and various heterocyclic compounds,[31] linkers in solid phase organic synthesis,[32] protecting groups in peptide chemistry[33] and in the molecular electronic devices.[34] In materials and separation sciences, they have also a broad range of applications. DTCs can be used in synthesis of useful thioamide compounds. Thioamide is an important synthetic tool and its functionalization has been found interest in the area of peptide modification[35], medicinal chemistry[36] and polymer science.[37] Thioamides moieties are present in many natural products,[38] pharmaceutical drug[39] and take important role in regulating the metabolic pathways[40] in synthesis of useful organic molecules,[41] they act as valuable synthetic building blocks. Thioamide compounds are synthesized from benzaldehyde,[42] benzyl alcohol,[43] benzyl chloride,[44] benzyl mercaptan,[45] benzyl disulfide,[46] benzylamine,[47] phenylacetylene,[48] styrene[49] and styryl derivatives[50] but the classical route involves thionation with phosphorous petasulfide/Lawesson reagent and Willgerodt-Kindler reaction.[51]

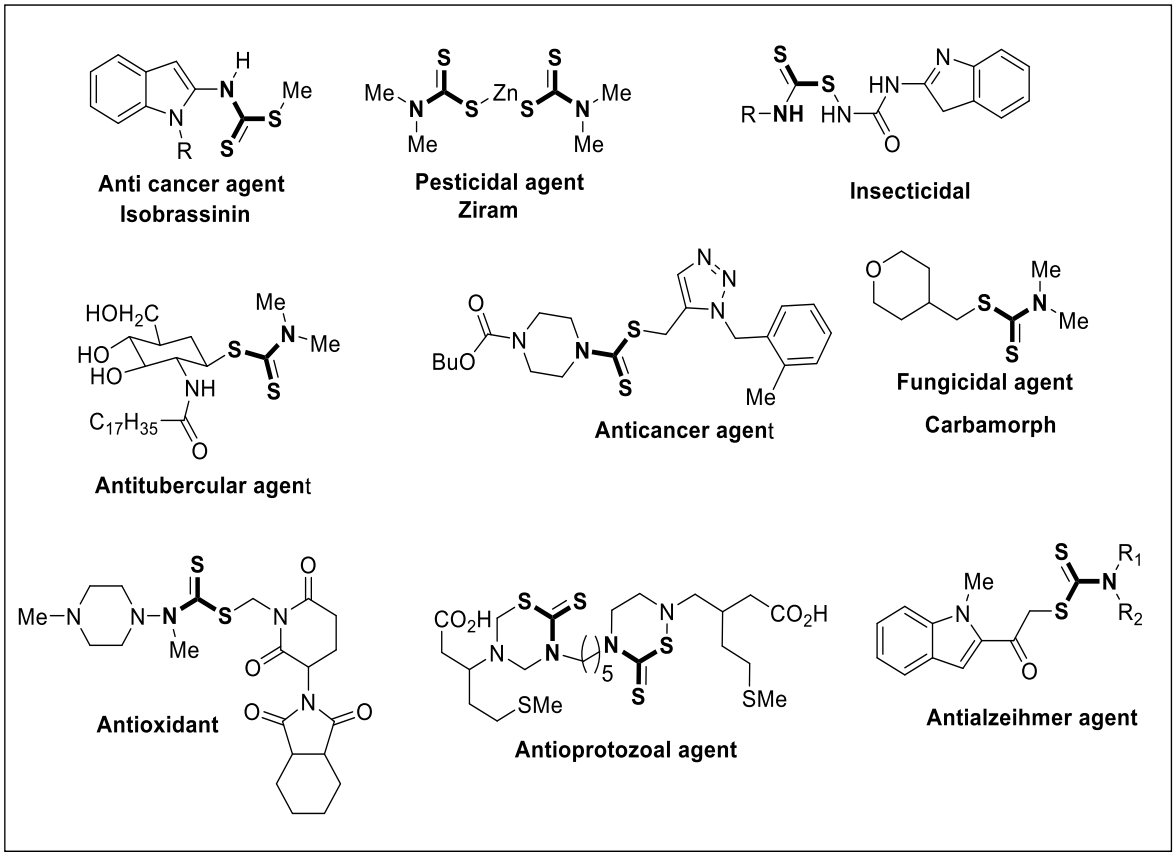

Figure 3.1 Biologically active molecules contain dithiocarbamate moiety.

1/b Review

In this short review, all the synthetic strategies of thioamide compounds that were developed by several groups have been demonstrated.

I. An efficient catalyst for synthesis of thioamides via Kindler reaction:

D. S. Dalal, *et al*[52] developed general method for the synthesis of thioamide derivatives in DMSO at room temperature and 120 ^{o}C *via* a one-pot, three component reaction between substituted aromatic aldehydes, elemental sulfur powder and cyclic secondary amines. By optimization of reaction parameters such as sulfur powder, amines and aromatic aldehydes, which have successfully carried out Willgerodt-Kindler reaction at room temperature and 120 ^{o}C. This thioamidation reaction performs in catalyst free condition with lower reaction time at room temp. On gram-scale, the reaction is successful to produce the desired thioamide product with good yields (Scheme 3.1).

Scheme-3.1

II. Catalyst- and Solvent-Free Thioamidation of Aromatic Aldehydes:

Zhou and his group[53] developed a simple one-pot procedure for the synthesis of thioamides using three component reactions such as amines, aldehydes, and elemental sulfur or hydrogen sulfide in water medium at 100 °C in the absence of a catalyst. The reaction protocol has good advantage in compared to other methods: water is used in the reaction medium as a "green'' solvent instead of commonly used organic solvents and catalyst is not necessary during the reaction which avoid possible metal pollution caused by use of metal catalysts. This reaction protocol is efficient and environmentally friendly for the synthesis of series of thioamide compounds with good to excellent yields up to 88% (Scheme 3.2).

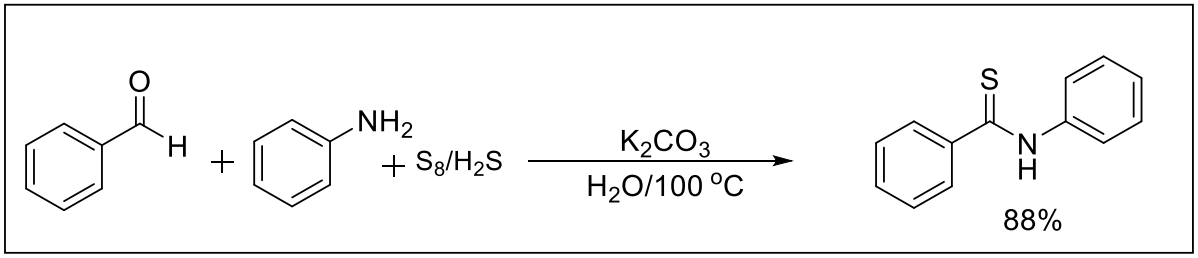

Scheme-3.2

III. Synthesis of 2-naphthylthioacetamides:

Zali-Boinee and co-workers[54] have developed a convenient method for synthesis and application of the thioamide product obtained from Willgerodt-Kindler reaction using acetophenone, sulfur and morpholine and application in the reaction synthesis of S- or N-containing heterocycles. Thioamide undergo a Claisen rearrangement in the presence of propargyl bromide to form tetrasubstituted thiophenes. (Scheme 3.3).

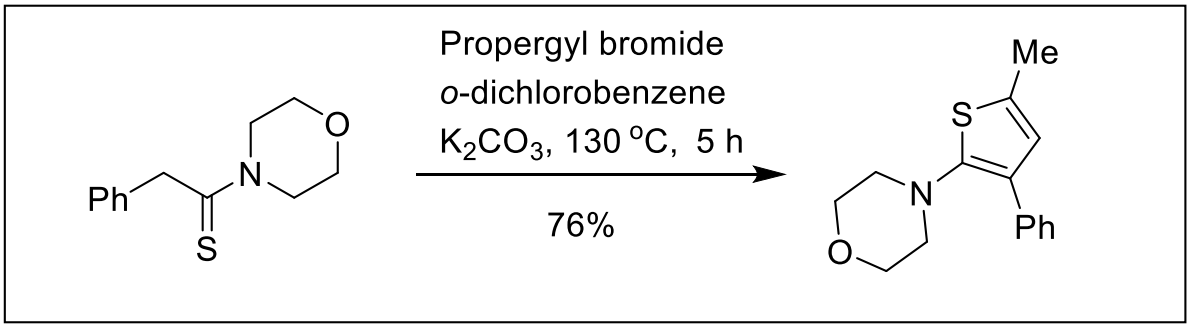

Scheme-3.3

IV. Protected carbonyl compounds as efficient substrates for this reaction:

Darabi and his group[55] reported that nitrogen derivatives of carbonyl compounds such as oximes, hydrazones and semicarbazones were found to be excellent candidates for Willgerodt-Kindler reactions in solvent free condition under microwave conditions. They have developed a simple and environmentally friendly for synthesis of thioamides using nitrogen derivatives of carbonyl compound, amine and elemental sulfur powder under microwave heating condition. Therefore, nitrogen derivative of a carbonyl compounds could be readily converted to thioamides with good yields (Scheme 3.4).

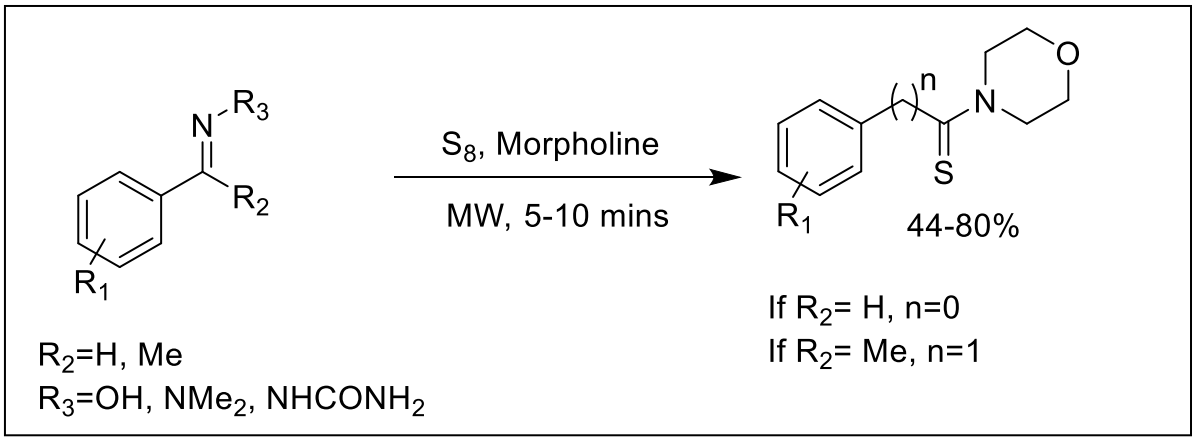

Scheme-3.4

V. The microwave-assisted Willgerodt–Kindler reaction of nitriles:

Ketone and aldehyde[56] are used as model substrates for Willgerodt-Kindler reaction. Moghaddam and co-workers developed a new convent method, the high yielding transformation of nitriles into thioamides using amines and elemental sulfur under microwave conditions. This methodology was used different kinds of several amines such as primary, secondary, hetero-cyclic and aliphatic amines which were converted into thioamides with good yield up to 90% (Scheme-3.5).

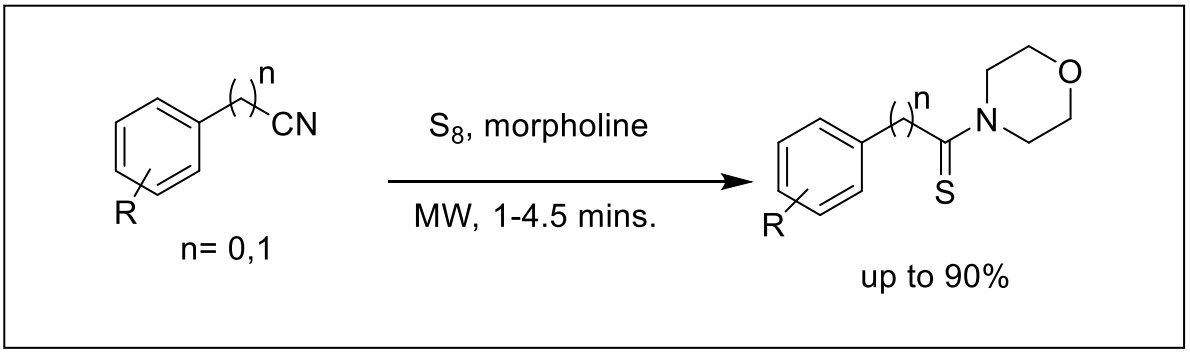

Scheme-3. 5

VI. The Willgerodt–Kindler reaction with various benzylic substrates:

Darabi and co-workers[57] described their investigation of solvent-free willgerodt-Kindler reaction on benzylic substrates. Thiobenzmorpholide were isolated in exceptional yield from benzyl amine and benzyl thiol. As a result of this reactions, N-benzylmorpholine was the major product isolated from the benzyl halides followed by thio-morpholinamide. A trace amount of thioamide product was produced when the reaction was carried out in benzyl alcohol or toluene (Scheme 3.6).

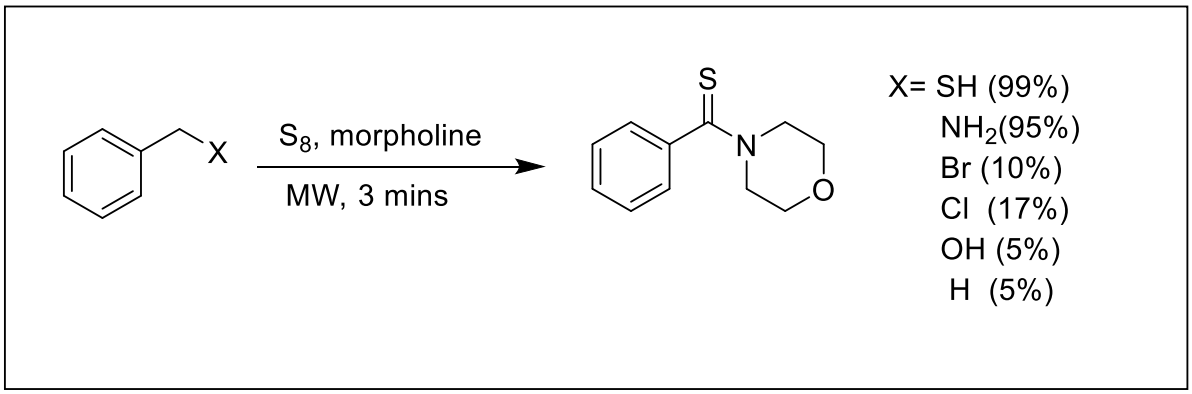

Scheme-3.6

VII. The reactivity of *β*-ketoesters and b-diketones in the Willgerodt– Kindler reaction:

Darabi and his group[58] prepared acyloxythioamides by using the Willgerodt–Kindler reaction. Various 1,3-ketoesters and their corresponding enamines were treated by the Willgerodt–Kindler reaction to yield their corresponding 1,n-acyloxy thioamides 81% (Scheme 3.7). Under the standard condition, b-ketoesters performed well in this process. Inorder to further investigate this reaction, the morpholine enaminoester was prepared and reacted with morpholine and sulfur at elevated temperatures in order to obtain the acyloxythioamide. Using this methodology, it was confirmed that an enamine intermediate was formed from the ketone in the Willgerodt–Kindler reaction.

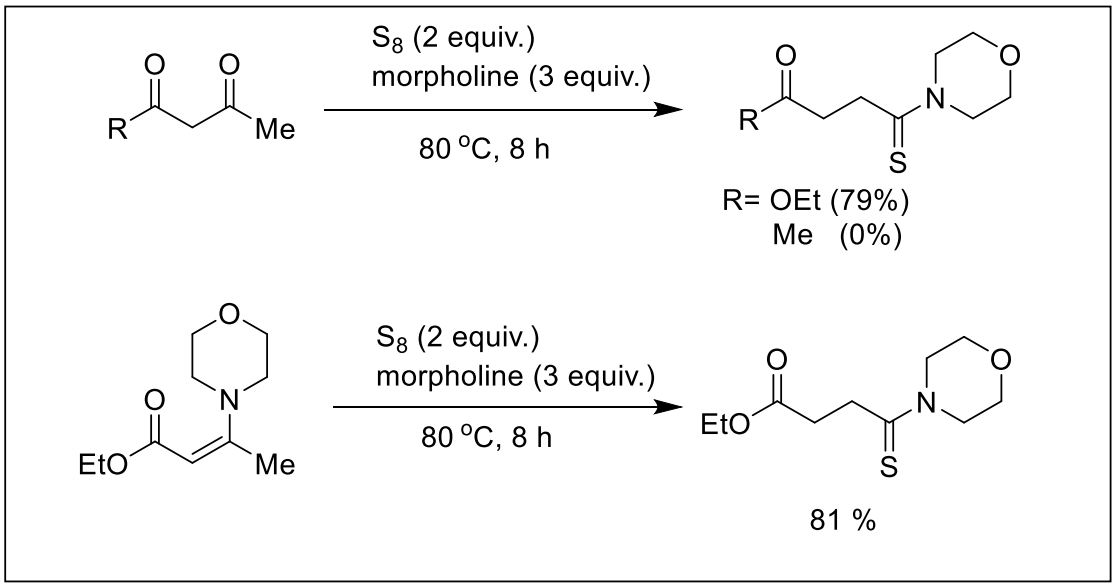

Scheme-3.7

VIII. The Willgerodt–Kindler reaction of various phenethyl substituted substrates:

Darabi and co-workers[59] reported the reactivity of phenethyl-type substrates. The phenylthiol acetomorpholide adduct was formed under standard Willgerodt–Kindler conditions in only four minutes under microwave-assisted heating (Scheme 3.8). Under solvent free condition, this group performed both classical (reflux, room temperature), and nonclassical reactions. A benzyl halides' poor performance can be attributed to its amine type, unlike benzylamine or benzylmarcaptan. Based on the experimental result the proposed reaction pathway involves oxidation coupling of benzylic substrates followed by thiolation and amine attack on the thiolated product.

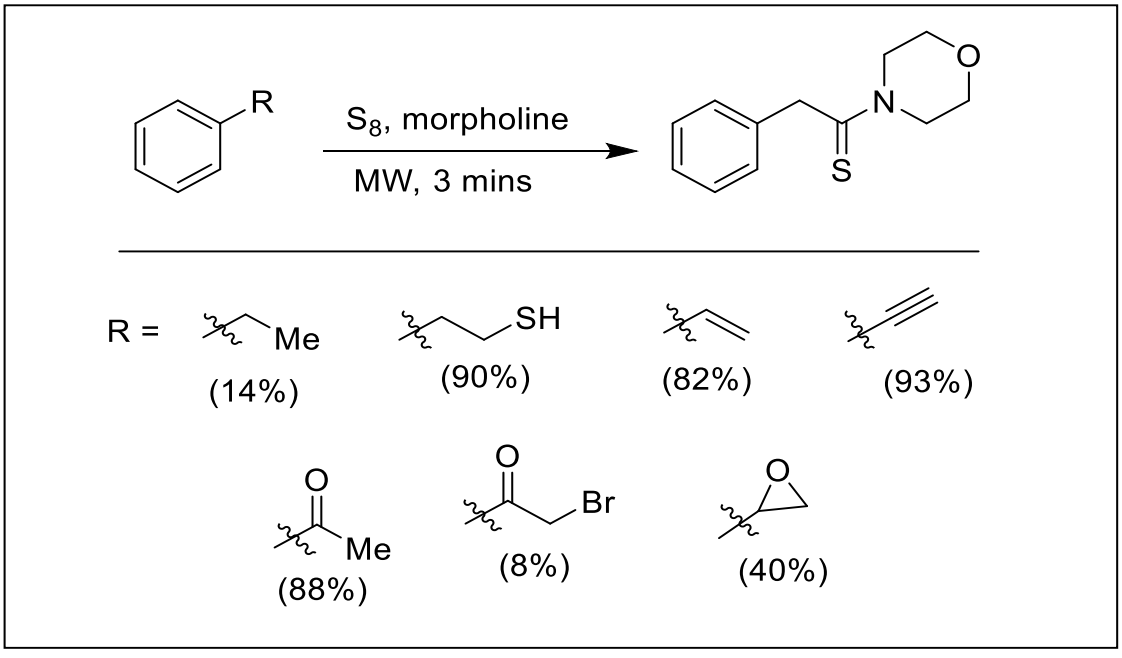

Scheme-3.8

IX. The sodium sulfide catalysed Willgerodt–Kindler reaction:

A new convent method was developed by Kanbara and co-workers[60] in which catalytic amounts of sodium sulfide nonahydrate, aldehyde and elemental sulfur powder were used for synthesis of thiobenzanilides at 115 ^{o} C in a DMF solvent. The reaction between anilines and benzaldehydes, known as the Willgerodt-Kindler reaction, can easily occur in the presence of a small amount of $Na_2S{\cdot}9H_2O$ catalyst, resulting in the formation of thiobenzanilides with moderate to good yields (Scheme 3.9). The primary thiobenzamide could also be prepared using the base catalyst. The primary thiobenzamide can also be prepared using the synthetic protocol.

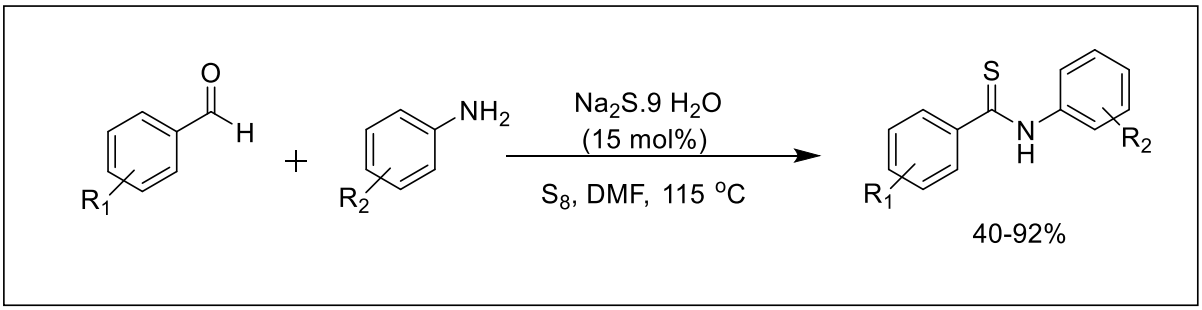

Scheme-3.9

X. The sodium sulfide catalysed Willgerodt–Kindler reaction:

The Willgerodt reaction, initially reported by Conrad Willgerodt,[61] entails the oxidation and rearrangement of a ketone to produce a terminal amide or the ammonium salt of the corresponding carboxylic acid (Scheme 3.10). In 1923, Karl Kindler discovered a modified method for the synthetic transformation that replaced ammonium polysulfide with elemental sulfur (S_8) and a secondary amine like morpholine. This reaction was carried out under thermal conditions to produce the thioamide derivative.

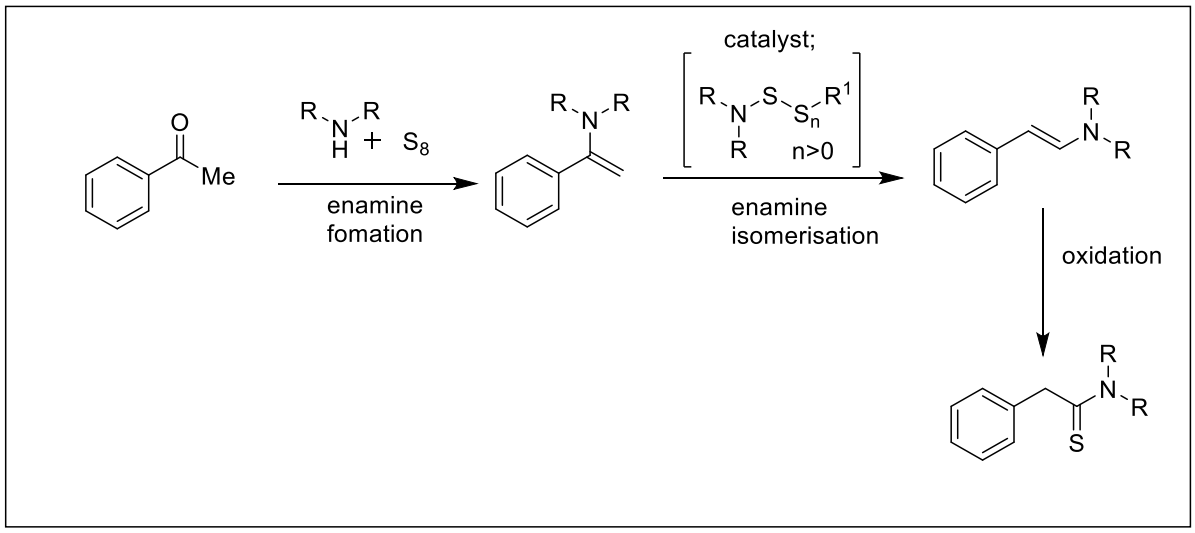

Scheme-3.10

XI. The one-pot synthesis of phenylacetic acids from acetophenones:

Penieres-Carrillo and co-workers[62] reported the initial use of infrared irradiation in the Willgerodt-Kindler reaction. Synthesis of thioamides and α-ketothioamides is carried out under solvent-free and noncatalyst conditions, with IR energy serving as the source of activation. In most cases, the use of IR energy in these reactions has been demonstrated to result in a mixture of thioamide and *α*-ketothioamide as the primary products, with the latter being more dominant. The yields of α-ketothioamides from these reactions are generally higher compared to previous reports (Scheme 3.11).

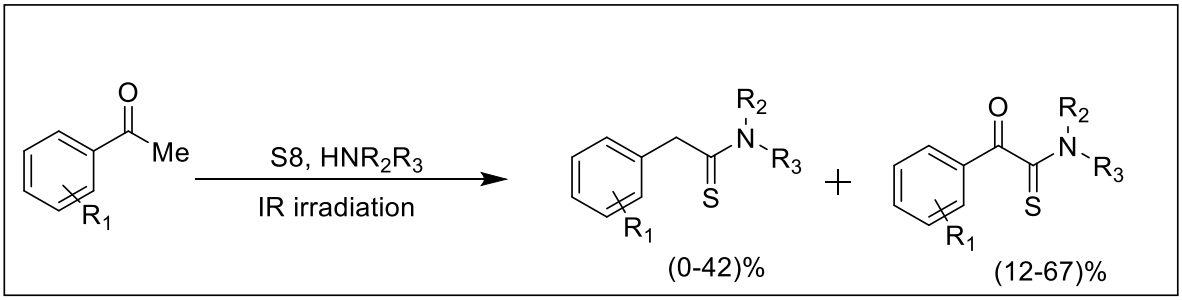

Scheme-3.11

XII. The Willgerodt–Kindler reaction with piperazines:

Obushchak and his co-works[63] developed a general methodology for synthesis of a set of (hetero)arylpiperazine thioamide derivatives with pharmaceutical significance using aldehydes and the Willgerodt-Kindler reaction conditions (Scheme 3.12). While the Willgerodt-Kindler reaction is commonly studied using morpholine, various primary and secondary amine derivatives have also been utilized in this process. The Wilgerodt-Kindler reaction involving 5-arylfurfurals or arylaldehydes, secondary amines (such as monosubstituted piperazines, morpholine, and piperidine), and sulfur resulted in the formation of N-substituted thioamides with moderate to good yields.

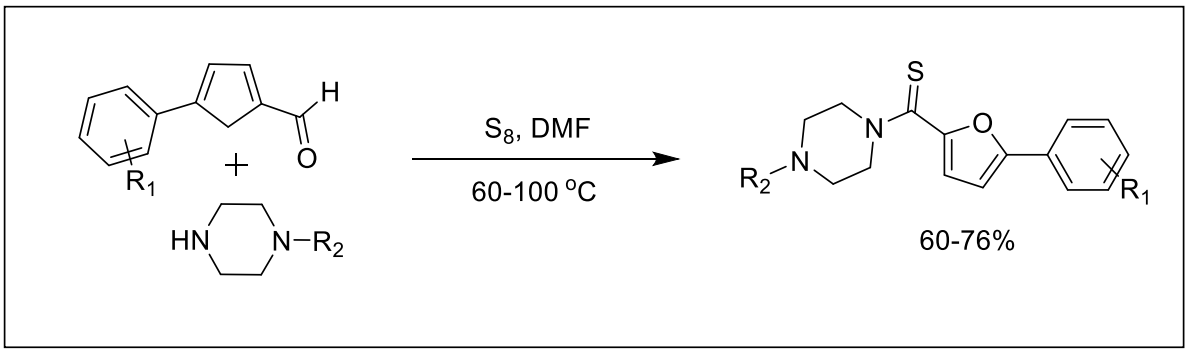

Scheme-3.12

XIII. The one-pot synthesis of phenylacetic acids from acetophenones:

Kul'ganek and his co-works[64] demonstrated that the addition of a catalytic amount of *p*-toluenesulfonic acid to the reaction mixture could greatly decrease the amount of morpholine

needed for the Willgerodt–Kindler reaction with aldehydes (Scheme 3.13). This reaction protocol was also used to demonstrate that the Willgerodt–Kindler reaction was applicable to dialdehydes such as *o*-, *m*-, and *p*-phthalaldehyde.

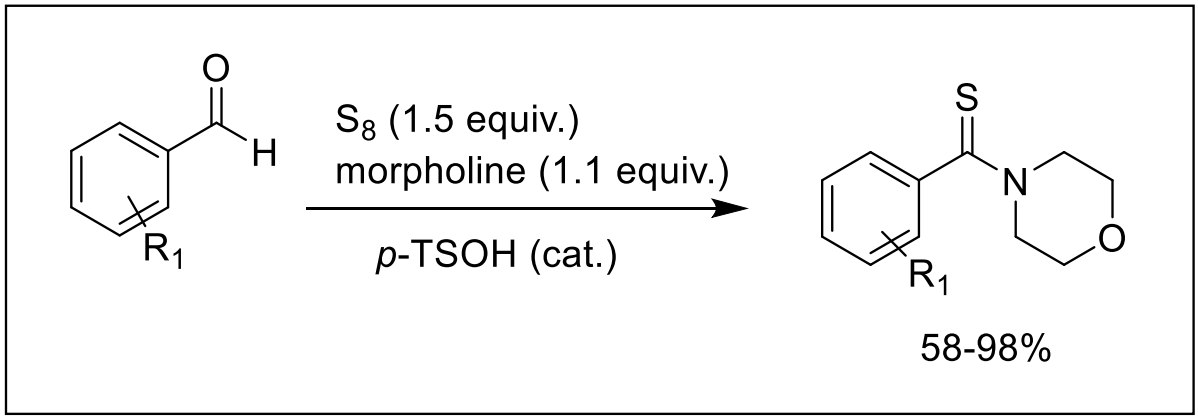

Scheme-3.13

XIV. Base-Controlled Three Component Reactions:

Huayue and his group[65] have studied three component reaction by using olefins amines, and sulfur which selectively afforded two kinds of thioamides through the choice of base. In presence of two different bases 2-phenylethanethioamides and benzothioamides were obtained selectively from styrene. The synthetic methodology was carried out under catalyst - free condition. This following protocol provides a simple and efficient method for the synthesis of thioamides with good yield (Scheme 3.14).

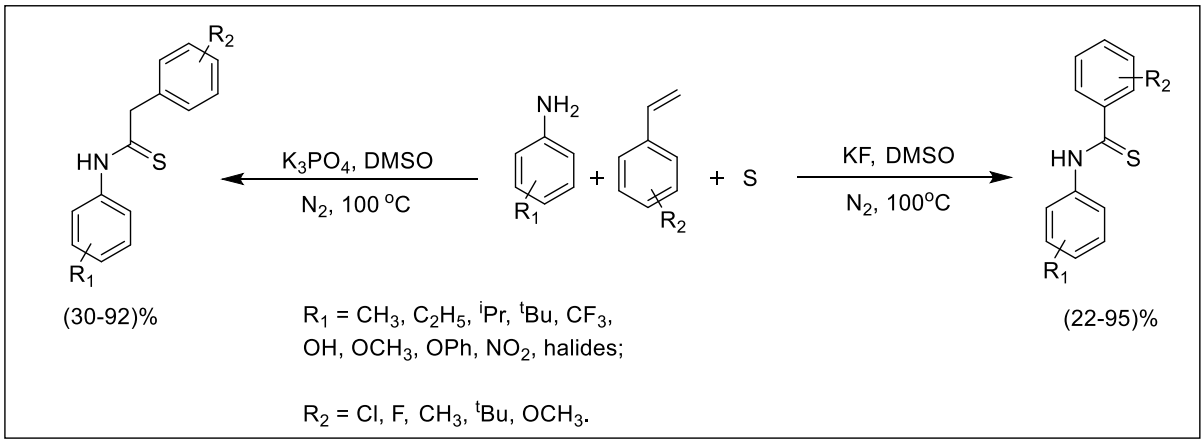

Scheme-3.14

XV. Transition-metal-free cleavage of C–C double bonds:

Wu and his group[66] have developed a new and convenient method for cleavage of unstrained C–C double bonds without transition metal catalyst. This protocol involves a three-component reaction using aromatic alkenes, S_8, and amides to selectively produce a series of aryl thioamides with yields of up to 94% (Scheme 3.15). The reaction protocol can be applied to internal aromatic alkenes and/or inactive acetamides.

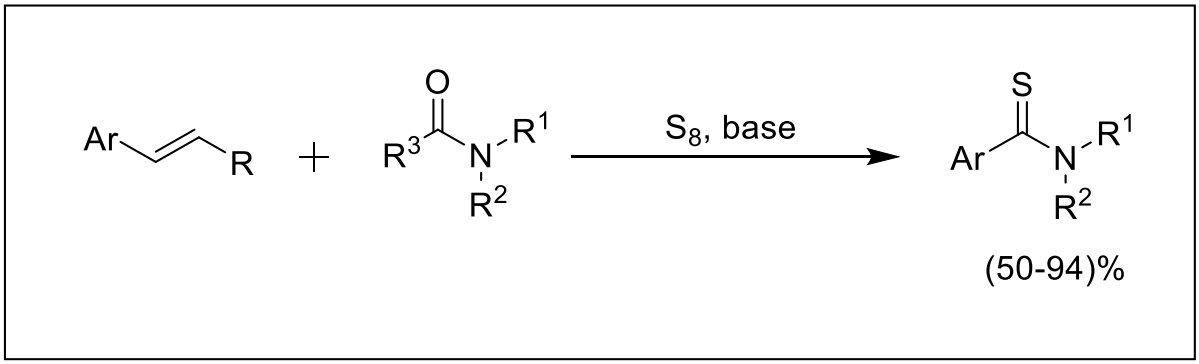

Scheme-3.15

XVI. Transition-metal-free cleavage of C-C triple bonds in aromatic alkynes:

Lanta and his group[67] have developed a novel, new and convenient method for cleavage reaction of C−C triple bonds in aromatic alkynes with S_8 and amides without transition metal catalyst furnishes arylthioamides in moderate to excellent yields (Scheme 3.16). The reaction protocol can be applied to internal aromatic alkenes and/or inactive acetamides.

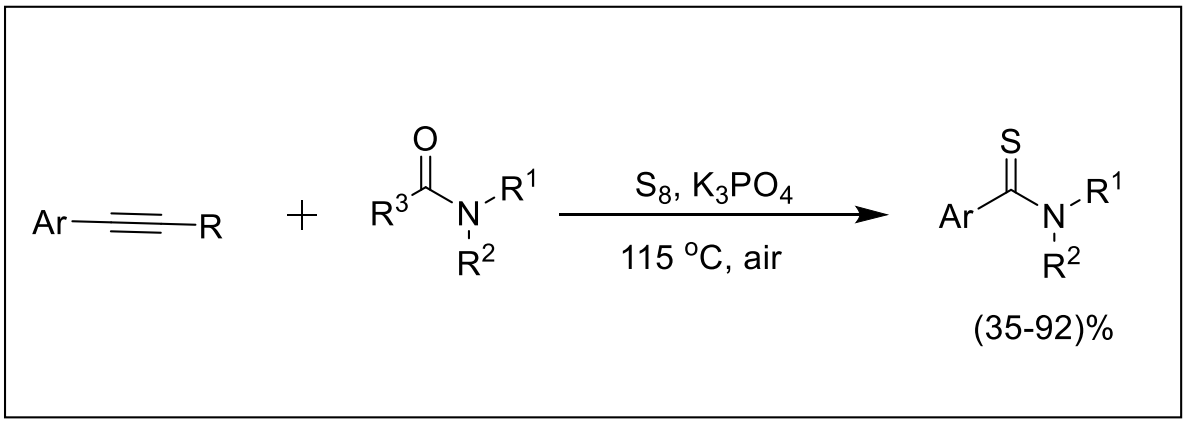

Scheme-3.16

XVII. A thiophene by-product formed during an attempted thioamide synthesis:

Pifferi and his group[68] developed the synthesis of alkoxythiobenzamides using the Willgerodt–Kindler reaction (Scheme 3.17). After the formation of thioamide, the cyclization occurs at the benzylic position of the phenylalkane chain. Thionation of the corresponding amides or the Willgerodt-Kindler reaction was used to prepare some thiomorpholides of alkoxyphenylalkanoic acids. The synthesis of new antisecretory and antiulcer alkoxythiobenzamides, specifically 3,4,5-trimethoxythiobenzamides, which are similar to trithiozine, was achieved by reacting primary amines, acyclic secondary amines, and different amino acids with either methyl 3,4,5-trimethoxydithiobenzoate or (3,4,5-trimethoxythiobenzoylthio) acetic acid.

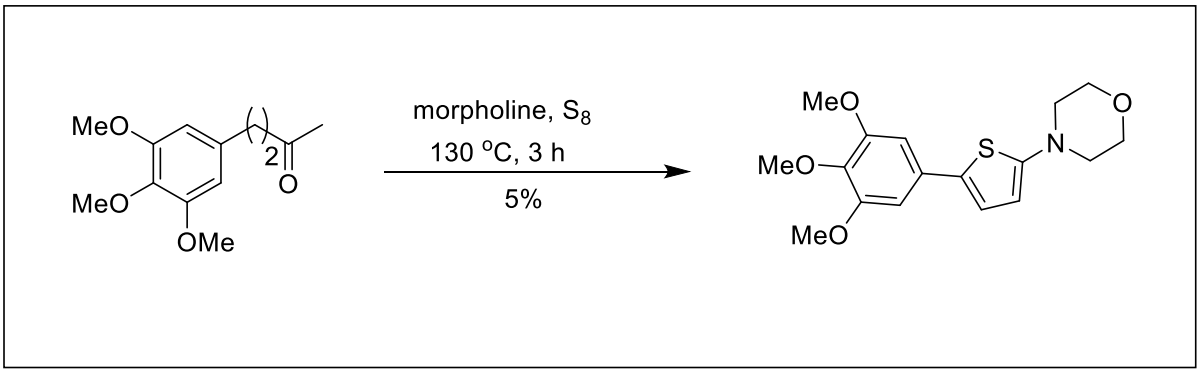

Scheme-3.17

XVIII. The preparation of various S-heterocycles under Willgerodt–Kindler conditions:

Dyker and his co-workers[69] reported a sophisticated domino redox annulation process that takes place under Willgerodt-Kindler conditions. Under Willgerodt-Kindler conditions, the efficient introduction of butanone side chains at arenes and hetarenes through a Heck-type reaction results in the transformation of these chains into annulated thieno[3,2-b] thiophenes in a domino redox process (Scheme 3.18). However, the reaction protocol mainly resulted in the formation of various sulfur-containing heterocyclic adducts, which greatly depended on the aromatic substitution pattern of the starting substrate. After the formation of thioamide, then cyclization occurs produce desired product with low to moderate yield (22-59) %.

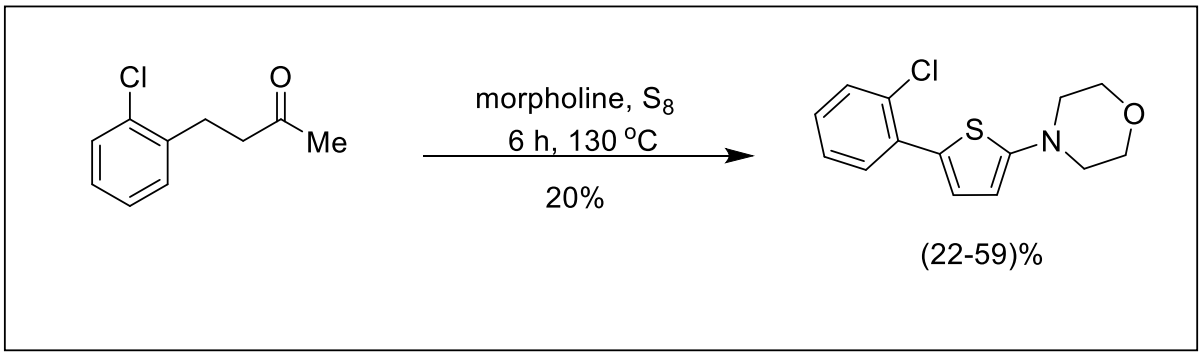

Scheme-3.18

XIX. A heterocyclic naphthyl derivative prepared under Willgerodt–Kindler conditions:

Using Willgerodt–Kindler reaction conditions, Nomura and co-workers[70] developed a simple general method synthesis of diverse sulfur-containing heterocycles. It has also been reported that several additional novel heterocycles can be formed under identical condition. According to Nomura and co-workers[71], synthesis of 1,3-thiazines from polycyclic aromatic amines and benzaldehyde by incorporating two equivalents of the aldehyde (Scheme 3.19).

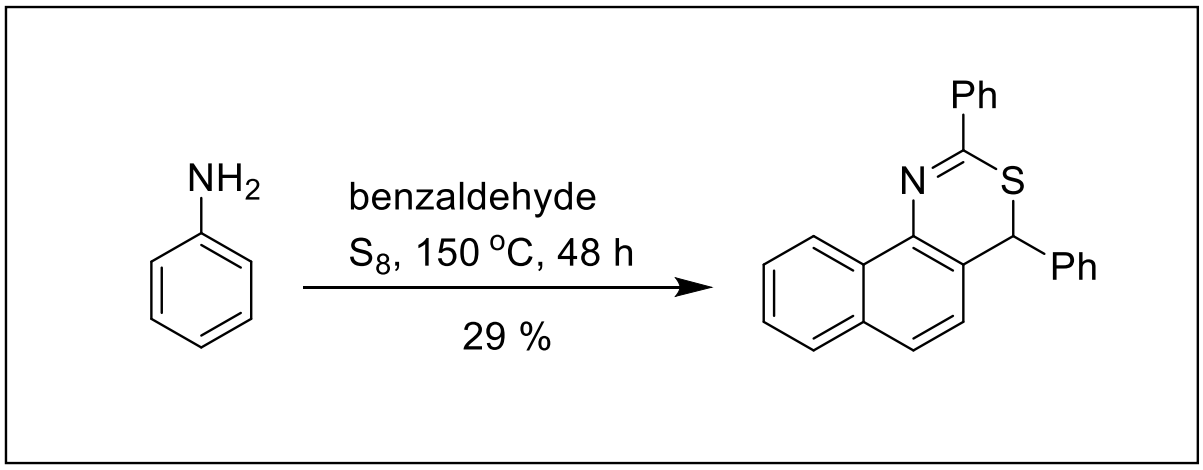

Scheme-3.19

XX. The synthesis of a benzothiophene under Willgerodt–Kindler reaction conditions:

Neckers and his group[71] reported a convenient one-pot synthesis of amino substituted benzo[b]thiophenes and Androsov and co-workers revised the original structure, thought to be the 2-amino substituted heterocycles, to be the 3-amino benzo[b]thiophenes following X-ray crystallography. By using secondary amines, 3-amino substituted benzo[b]thiophenes were formed in moderate yield, such as allylamine derivatives. Whereas the use of ammonium chloride, in the presence of a large excess of base, gave the 3-methyl-5-nitrobenzo[d]isothiazole as the major product (Scheme 3.20).

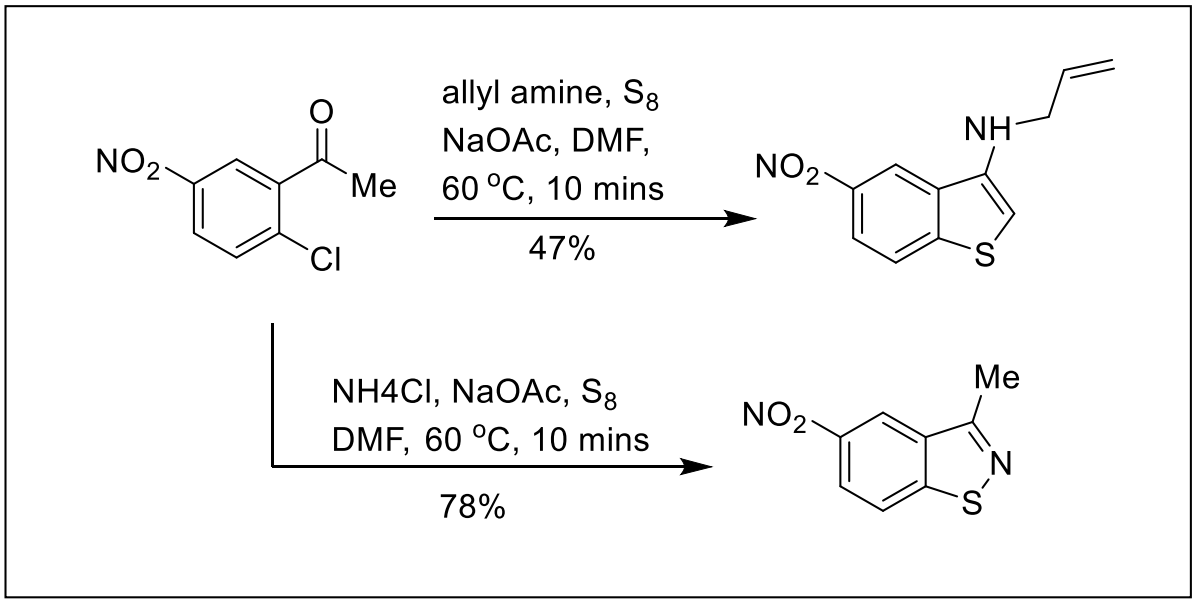

Scheme-3.20

1/c Conclusion

In conclusion, the Willgerodt–Kindler reaction is an efficient method for the synthesis of thioamides. The synthetic routes described in this short review reveal that such protocols are still in demand due to their operational simplicity, cheap reacting materials, wide substrate scope, functional group tolerance and ease of isolation of desired product and allows the terminal functionalisation of arylalkyl ketones. Keeping this in mind, we are going to discuss a simple, general and efficient protocol for C-C thioamidation of styrenes using freshly prepared dithiocarbamate salts and ammonium persulfate under aerial condition. One of the common methods of styrene functionalization involves C=C double bond functionalization. However, $C(sp^2)$-$C(sp^2)$ bond activation of styrene remains comparatively less studied. To the best of our knowledge, this is the first report of thioamidation of styrene *via* $C(sp^2)$-$C(sp^2)$ single bond cleavage. The present protocol is further extended on decarbonylative thioamidation of benzaldehyde and toluene derivatives and also on the decarboxylative thioamidation of aromatic carboxylic acids. Thus, dithiocarbamate appears as an active thioamide surrogate for styrene as well as for benzaldehyde, toluene and benzoic acid in presence of persulfate oxidant.

Section-II

Present Work:

Dithiocarbamate mediated thioamidation via C-C single bond cleavage of styrene and decarbonylative and decarboxylative thioamidations

2/a Introduction

As a continuation of our work, we are reporting here a dealkenylative approach for the synthesis of thioamides from styrene using the freshly prepared dithiocarbamate salts. Styrene functionalization is a popular technique to achieve complex organic frameworks. One of the popular approaches of styrene functionalization involves the C=C double bond functionalization.[72] However, the C(Ar)-C(alkenyl) single bond functionalization is more challenging due to its high bond strength[73] and remains comparatively less studied.[74] Styrene has been employed here in a C-C single bond thioamidation reaction with the dithiocarbamate salt in presence of ammonium persulfate and molecular oxygen from air without using any transition-metal-catalyst (Scheme 3.21b). Only a few research groups have studied the thioamidation reactions on styrene and its derivative compound. The reported protocols for thioamidation of styrene involve elemental sulfur mediated cleavage of C=C bond (Scheme 3.21c).[75] *β*-Nitrostyrene has also been used to prepare thioamide compounds by a similar approach of C=C bond cleavage (Scheme 3.21d).[76] However, the protocols suffer from use of huge excess of elemental sulfur, involvement of fluoride source or strong base like potassium *tert*-butoxide and high reaction temperature. To the best of our knowledge, this is the first report of dithiocarbamate mediated styrene thioamidation which proceeds through C(sp^2)-C(sp^2) bond cleavage of styrene (Scheme 3.21e) in presence of persulfate and air.

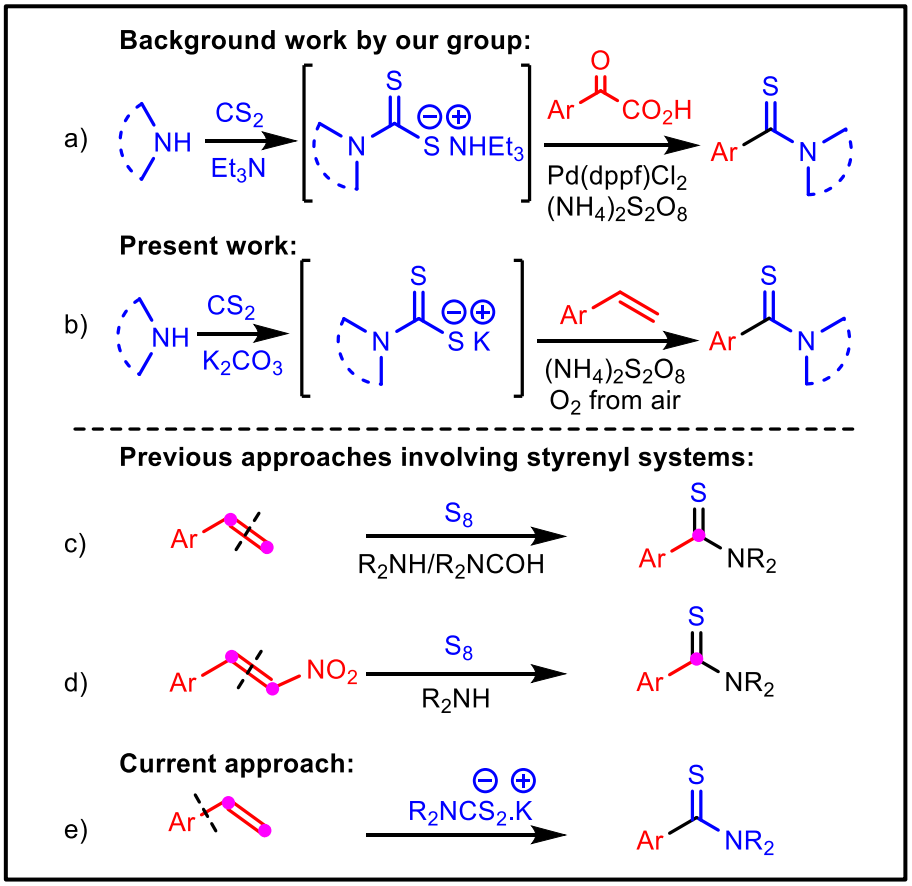

Scheme-3.21 Thioamidation reactions: Current protocol and other reported work

2/b Results and discussion

The experimental procedure is very simple. Freshly prepared dithiocarbamate salt was stirred with styrene and ammonium persulfate in DMSO medium at 80 ^{o}C under aerial condition (or using zero air balloon). After completion of reaction (checked by TLC) the crude product was isolated by usual work-up and was purified by column chromatography. In order to standardize the reaction condition, a series of experiments were performed with the potassium salt of piperidine-dithiocarbamate and styrene as the model substrates (Table 3.1).

Table 3.1 Standardization of the Reaction Condition

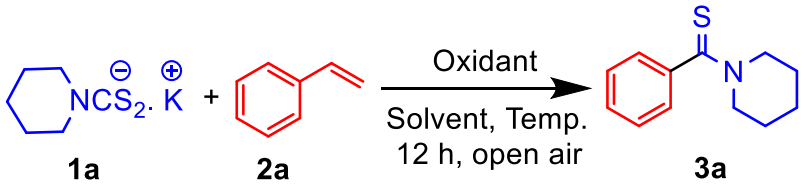

1a **2a** **3a**

Entry	Oxidant	Solvent	Temp. (^{o}C)	Yield [%][a]
1	$(NH_4)_2S_2O_8$	THF	70	18
2	$(NH_4)_2S_2O_8$	Dioxane	70	46
3	$(NH_4)_2S_2O_8$	Dioxane	80	51
4	$(NH_4)_2S_2O_8$	Dioxane	90	50
5	$(NH_4)_2S_2O_8$	DMF	80	trace
6	$(NH_4)_2S_2O_8$	NMP	80	trace
7	$(NH_4)_2S_2O_8$	DCE	80	22
8	$(NH_4)_2S_2O_8$	H_2O	80	–
9	$(NH_4)_2S_2O_8$	DMSO	80	88
10	$(NH_4)_2S_2O_8$	DMSO	85	85
11	$(NH_4)_2S_2O_8$	DMSO	60	82
12	$K_2S_2O_8$	DMSO	80	73
13	–	DMSO	80	–
14[b]	$(NH_4)_2S_2O_8$	DMSO	80	22
15[c]	$(NH_4)_2S_2O_8$	DMSO	80	65
16[d]	$(NH_4)_2S_2O_8$	DMSO	80	88

Reaction condition: ***1a*** *was prepared freshly by stirring the mixture of piperidine (1 mmol), CS_2 (1.5 mmol) and K_2CO_3 (2 mmol) in 2 ml of solvent for 5 min at room temperature.* ***2a*** *(0.8 mmol) and oxidant (1.2 mmol) were added to the reaction mixture and was stirred at 80 ^{o}C for 12 h under air. [a] Yields reported are the isolated yields. [b]0.5 mmol of oxidant was used. [c]The reaction time period was 5 h. [d]The reaction was performed using zero air balloon instead of open air.*

In our first attempt, piperidine-dithiocarbamate salt ($C_5H_{10}NCS_2.K$, **1a**) which was freshly prepared by the prompt reaction of piperidine and CS_2 in presence of K_2CO_3, was allowed to react with styrene (**2a**) in THF medium in presence of $(NH_4)_2S_2O_8$ as the oxidizing agent. However, the reaction produced the desired thioamide product (**3a**) only in 18% yield (entry 1, Table 3.1). Changing the reaction solvent to dioxane, DMF, NMP, DCE did not improve the yield of the product satisfactorily (entries 2-7, Table 3.1). Aqueous medium was also not suitable for the reaction (entry 8, Table 3.1). However, in presence of DMSO solvent the reaction proceeded well and produced the desired thioamide (**3a**) in 88% yield (entry 9, Table 3.1).

Table 3.2 Substrate scope for thioamidation of styrene

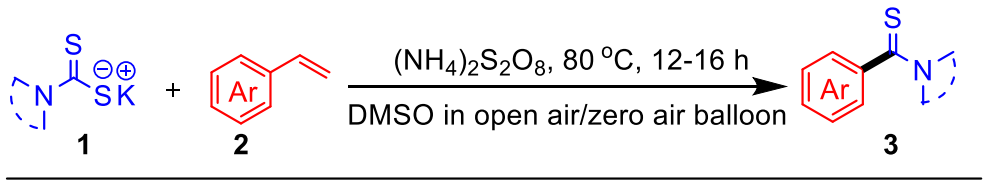

R = H, **3a**, 88%, 12 h
(gram scale yield[a]: 83%)
R = F, **3d**, 82%, 12 h
R = Me, **3g**, 78%, 12 h
R = Cl, **3k**, 82%, 12 h
R = Br, **3p**, 70%, 12 h
R = OMe, **3s**, 57%, 16 h
R = NO_2, **3v**, 68%, 14 h

R = H, **3b**, 85%, 12 h
R = F, **3e**, 88%, 12 h
R = Me, **3h**, 80%, 12 h
R = Cl, **3l**, 78%, 12 h
R = Br, **3q**, 75%, 12 h
R = OMe, **3t**, 51%, 18 h

R = H, **3c**, 87%, 12 h
R = F, **3f**, 86%, 12 h
R = Me, **3i**, 77%, 12 h
R = Cl, **3m**, 84%, 12 h
R = OMe, **3u**, 62%, 16 h

3n, 86%, 12 h

3x[b], 65%, 14 h

R = Me, **3j**, 72%, 12 h
R = Cl, **3o**, 80%, 12 h
R = Br, **3r**, 70%, 12 h
R = NO_2, **3w**, 68%, 15 h

3z, 78%, 14 h

3y, 56%, 15 h

*Reaction condition: Dithiocarbamate salt (**1**) was freshly prepared by stirring the mixture of amine (1 mmol), CS_2 (1.5 mmol) and K_2CO_3 (2 mmol) in 2 ml of solvent for 5 min at room temperature. Styrene (**2**) (0.8 mmol) and ammonium persulfate (1.2 mmol) were added to the reaction mixture and was stirred at 80 °C under open air atmosphere. Yields reported are the isolated yields. [a]Yield in gram scale reaction: **2a** (1 gm, 9.6 mmol), **1a** (12 mmol), persulfate (14.5 mmol), DMSO (10 ml), 80 °C, 14 h, open air. [b]Instead of K_2CO_3, N,N-Diisopropylethylamine (4 mmol) has been used to prepare the dithiocarbamate salt.*

Upon increasing the temperature, the yield of the desired product decreases with the formation of some unidentified side products. The reaction remains incomplete at 60 ^{o}C (entry 11, Table 3.1). Potassium persulfate was found to be less effective for the reaction compared to the ammonium persulfate (entry 12, Table 3.1). In absence of oxidant the reaction does not initiate at all. Thus, use of oxidant appears to be crucial for the present thioamidation reaction (entry 13, Table 1). The reaction was found to be incomplete upon decreasing either the amount of oxidant (entry 14, Table 3.1) or the reaction time period (entry 15, Table 1). Upon using zero air balloon (instead of open-air condition), the reaction produces similar result (entry 16, Table 3.1). We have developed a simple, general and efficient protocol for C-C thioamidation of styrenes using freshly prepared dithiocarbamate salts in presence of ammonium persulfate under aerial condition.

One of the common methods of styrene functionalization involves C=C double bond functionalization. However, C(sp^2)-C(sp^2) bond activation of styrene remains comparatively less studied. To the best of our knowledge, this is the first report of thioamidation of styrene *via* C(sp^2)-C(sp^2) single bond cleavage The optimized reaction condition has been explored to establish the substrate scope (Table 3.2). Styrene molecules containing different substituents (-Me, -OMe, -F, -Cl, -Br, -NO_2) participated to the thioamidation reaction to produce desired thioamide compounds (**3d**-**3w**, **3y**, **3z**) with good to excellent yields (Table 3.2). Dithiocarbamate-salts (**1**), obtained from cyclic secondary amines, such as piperidine, pyrrolidine, morpholine and acyclic secondary amines, such as dimethylamine, diethylamine, were used to prepare the corresponding thioamides (**3a**-**3w**) efficiently. L-proline based thioamide (**3x**) was prepared from dithiocarbamate salt of methyl L-prolinate. Aromatic amine, such as aniline and primary amine, such as benzylamine were also found to be reactive to produce the desired thioamide compounds, **3y** and **3z** respectively. The thioamidation reaction was scaled-up to check the industrial importance of the current protocol. Styrene (**2a**) shows good efficiency even in 1 gram scale reaction with the piperidine-dithiocarbamate salt (**1a**) to produce the desired thioamide-**3a** in 83% yield (Table 3.2).

In search of the mechanistic pathway of thioamidation reaction, we have considered the possibility of prior C=C double bond cleavage of styrene to generate the benzaldehyde intermediate[77] by the action of ammonium persulfate oxidant. To prove the intermediacy of benzaldehyde, we performed the thioamidation reaction with benzaldehyde as the starting material under the identical reaction condition. We were delighted to find the efficient conversion of benzaldehydes (**2'**) to the desired thioamides (**3**) in presence of dithiocarbamate salts (**1**) and ammonium persulfate as the oxidant (Scheme 3.22a). In continuation, we tried toluene as the substrate for dithiocarbamate mediated thioamidation reaction. Surprisingly, toluene and its substituted derivatives (**2''**) were also found to be active for the identical thioamidation reactions under the similar reaction condition (Scheme 3.2b). Further, we were interested to check the protocol on decarboxylative thioamidation reaction using aromatic carboxylic acid, $ArCO_2H$ (**2'''**) as the reaction substrate. Aromatic carboxylic acids were smoothly converted to the corresponding thioamide compounds by the reactions with

triethylamine-dithiocarbamate salts, $R_2NCS_2.NHEt_3$ (**1'**) in presence of ammonium persulfate oxidant (Scheme 3.22c).

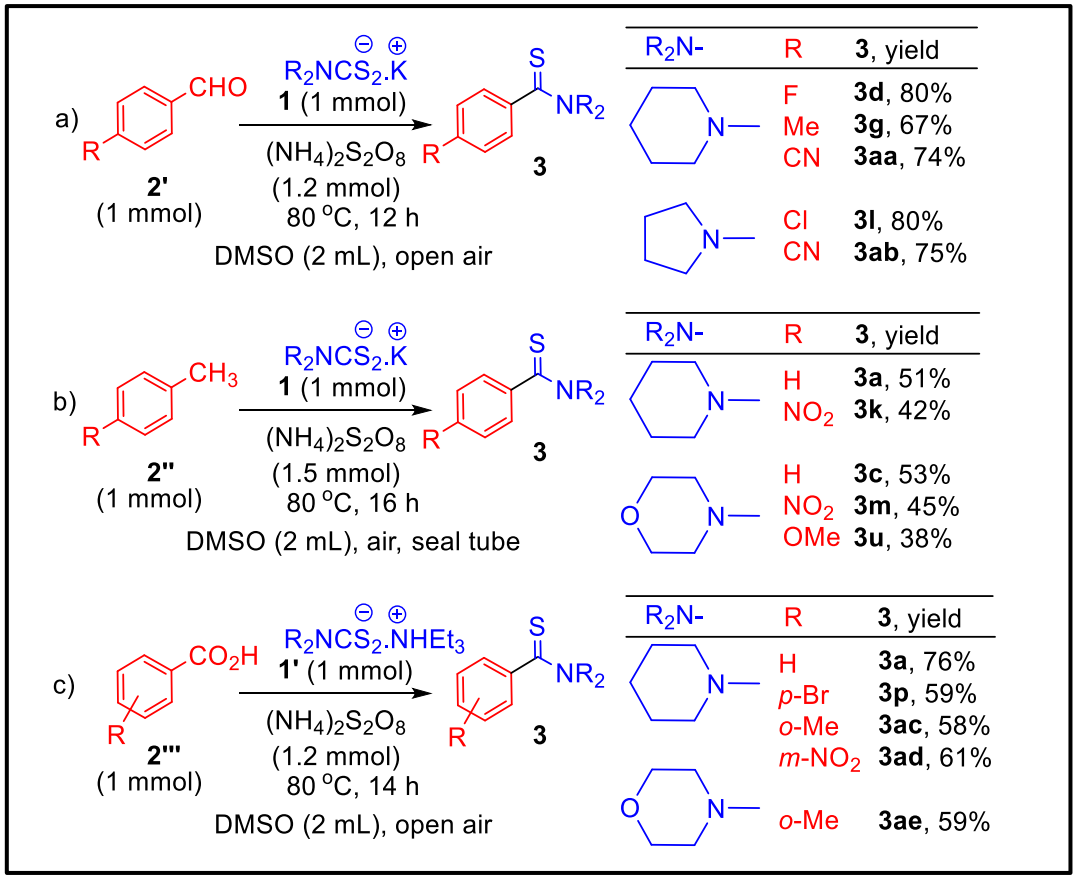

Scheme-3.22 Thioamidation of benzaldehyde, toluene and benzoic acid systems

We believe that benzaldehyde is a possible reaction intermediate in the thioamidation reactions of styrene (2) as well as toluene (2''). We carried out a series of control experiments (Scheme 3.23) to explain the mechanistic pathway of the thioamidation reactions. To check the possibilities of radical pathway, we conducted the thioamidation of styrene (2a) with piperidine-dithiocarbamate salt (1a) in presence of 3 equivalent of TEMPO, a radical quencher (Scheme 3.23a). The reaction was found to be completely arrested in presence of TEMPO which trapped the acyl radical intermediate (PhCO•) as the form of O-benzoylated-TEMPO (characterized by ^{1}H and ^{13}C NMR, spectra included in ESI). Thus, generation of PhCO• radical intermediate has been proposed in the thioamidation of styrenes. The reaction of benzaldehyde (2a') with dithiocarbamate salt (1a) does not proceed at all in absence of ammonium persulfate (Scheme 3.23b), which is supposed to be responsible to generate the PhCO• from benzaldehyde intermediate. The dithiocarbamate-salt (1a) has been found to be transformed into the corresponding thiuram disulfide (Scheme 3.23c) by the action of ammonium persulfate under the similar reaction condition. However, thiuram disulfide was not found to be effective in the thioamidation of styrene in presence of persulfate oxidant (Scheme 3.23d). In absence of styrene, the potassium-dithiocarbamate salt of aniline ($PhNHCS_2.K$) has been observed to be converted to phenyl isothiocyanate (Ph-N=C=S) under the identical reaction condition (Scheme 3.23e). Phenyl isothiocyanate was isolated from the reaction mixture and was characterized by ^{1}H, ^{13}C NMR spectroscopy

(spectra included in ESI). We allowed phenyl isothiocyanate to react separately with styrene in presence of ammonium persulfate (Scheme 3.23f) and found the formation of desired thioamide compound (3y') under the identical reaction condition. Thus, we believe the formation of isothiocyanate moiety as the possible reaction intermediate in case of aniline based dithiocarbamate salt. To understand the role of aerial oxygen in our protocol we conducted a series of control experiments (Scheme3.23g – 3.23o) with styrene, benzaldehyde, toluene and benzoic acid. We performed the thioamidation of styrene with pyrrolidine-dithiocarbamate salt in presence of persulfate oxidant under argon atmosphere (Scheme 3.23g). However after 12 h of reaction no desired thioamide product was formed. The crude reaction mixture contains unreacted styrene and the dimer of dithiocarbamate, thiuram disulfide (^{1}H NMR of crude reaction mixture is included in ESI). Thus oxygen plays a crucial role in thioamidation of styrene. However, benzaldehyde has been observed to undergo smooth thioamidation with dithiocarbamate salt in presence of persulfate oxidant under the argon atmosphere (Scheme 3.23h). It proves oxygen does not play any role in thioamidation of benzaldehyde. Thus, molecular oxygen (from air/zero air) probably assists the oxidative cleavage of styrene to produce benzaldehyde intermediate. To understand the involvement of oxygen we treated styrene with persulfate oxidant under oxygen atmosphere (O_2 balloon) (Scheme 3.23i) and after 5 h of reaction the crude reaction mixture was analyzed by ^{1}H NMR spectroscopy which reveals efficient formation of benzaldehyde intermediate with no unreacted styrene left (^{1}H NMR of crude reaction mixture is included in ESI). However, similar reaction of styrene under argon atmosphere does not produce benzaldehyde at all (Scheme 3.23j). When styrene was treated with persulfate oxidant for 12 h of time period in presence of TEMPO under oxygen atmosphere (O_2 balloon), we found the formation of benzoyl radical intermediate which was trapped as O-benzoylated-TEMPO (characterized by ^{1}H NMR) (Scheme 3.23k). Thus, it is clear that molecular oxygen is essential for the formation of benzaldehyde from styrene. To check the role of molecular oxygen in thioamidation of toluene we conducted the thioamidation of toluene with dithiocarbamate salt in presence of persulfate oxidant under argon atmosphere (Scheme 3.3l). After 16 h of reaction no desired product was formed. When toluene was treated with $(NH_4)_2S_2O_8$ under O_2 atmosphere (Scheme 3.23m) we found the formation of benzaldehyde intermediate within 5 h of time period. The ^{1}H NMR of crude reaction mixture shows the presence of benzaldehyde as the major component along with some unreacted toluene. Thus, toluene undergoes thioamidation via formation of benzaldehyde intermediate in presence of molecular oxygen and persulfate oxidant. The formation of benzoyl radical intermediate in the reaction of toluene with persulfate under O_2 atmosphere was proved by PhCO• undergoes decarbonylation78 to generate the Ph• radical intermediate. Whereas, benzoic acid follows decarboxylative pathway to generate Ph• radical in the trapping of PhCO• by TEMPO (Scheme 3.23n). O-Benzoylated-TEMPO was characterized by ^{1}H NMR. The thioamidation reaction of benzoic acid with piperidine-dithiocarbamate salt was found to proceed under argon atmosphere in presence of ammonium persulfate (Scheme 3.23o). Thus, molecular oxygen does not have any role in decarboxylative thioamidation of benzoic acid.

Based on above experimental observations and reported literatures, we propose the probable reaction pathway as shown in Scheme 3.24. Styrene undergoes oxidative cleavage by the action of persulfate and molecular oxygen to produce benzaldehyde intermediate.[79] Toluene also produces benzaldehyde intermediate in presence of persulfate oxidant and

molecular oxygen.[80] Formation of benzaldehyde intermediate from styrene and toluene has been proved by ^{1}H NMR analysis of the crude reaction mixtures obtained from the control experiments shown in Scheme 3i and 3m respectively. Benzaldehyde intermediate produces PhCO$^\bullet$ radical species by the action of persulfate. Formation of PhCO$^\bullet$ radical intermediate has been proved by trapping it with TEMPO (Scheme 3.23a, 3.23k, 3.23n). presence of persulfate[81] *via* the formation of carboxyphenyl radical intermediate (PhCOO$^\bullet$) The formation of aryl radical in decarbonylative and decarboxylative functionalization of benzaldehyde and benzoic acid derivatives are well known in the literature.[82] Persulfate oxidant converts the dithiocarbamate anion (**1** or **1'**) to the corresponding dithiocarbamate radical (**4**) which undergoes decomposition to produce radical intermediate-**5** and elemental sulfur (Scheme 24a). In the absence of styrene, dithiocarbamate radical (**4**) undergoes dimerization to produce the thiuram disulfide (Scheme 3.23c). The generation of radical intermediate-**5** was confirmed by GC-MS analysis of the crude reaction mixture obtained after quenching the reaction between piperidine-dithiocarbamate salt and styrene for an intermediate time period of 2 h stirring under the optimized reaction condition. The radical intermediate-**5** reacts with Ph$^\bullet$ to produce the desired thioamide product (**3**). In case of aniline-dithiocarbamate salt (PhNHCS$_2$.K), $SO_4^{\bullet-}$ radical anion may abstract the H$^\bullet$ from the corresponding radical intermediate-**5'** to produce the PhNCS intermediate (Scheme 3.24b) which reacts with Ph$^\bullet$ to produce the desired thioamide **3y'** in presence of HSO_4^- anion. Benzylamine-dithiocarbamate is also expected to follow the similar mechanism as that of aniline-dithiocarbamate. Under the aerial condition, elemental sulfur generated probably gets oxidized to SO_3 (detected by GC-MS analysis) in presence of ammonium persulfate.

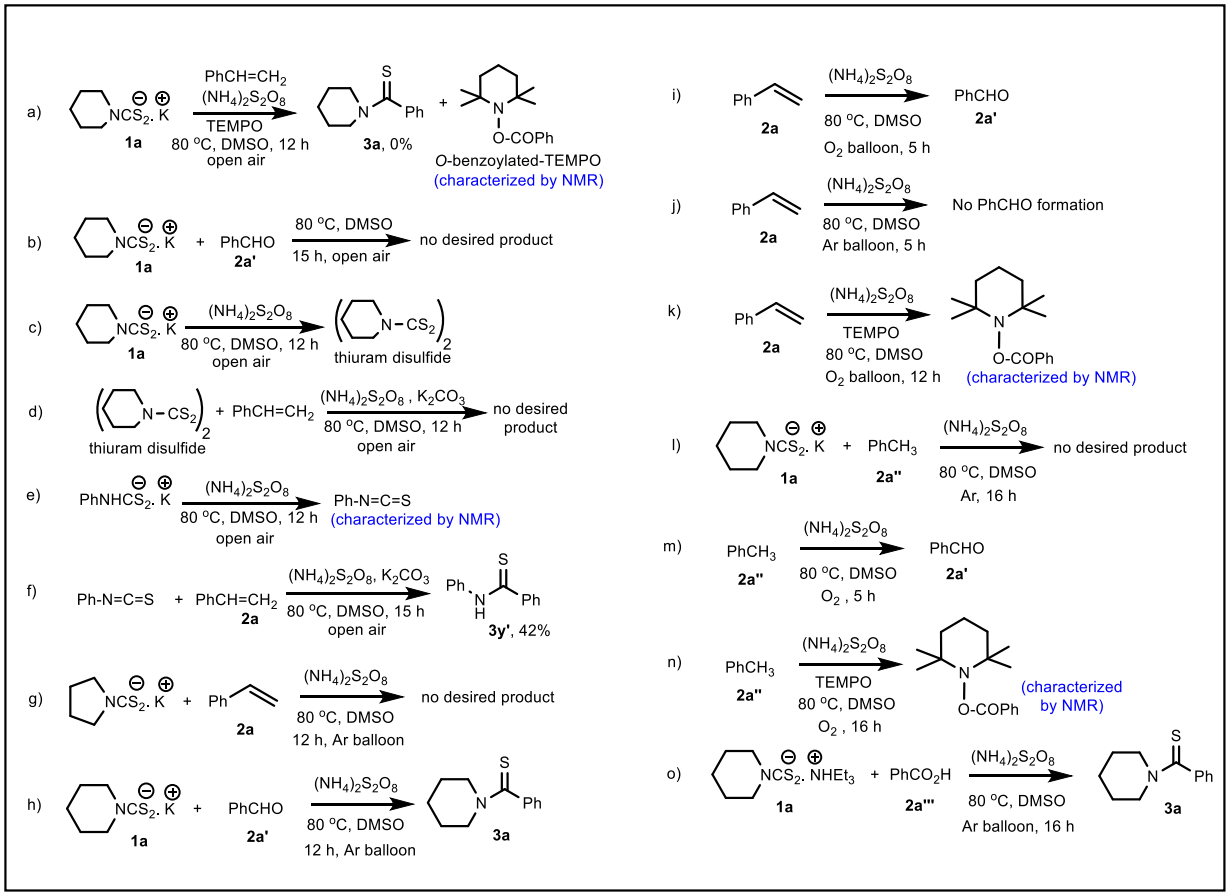

Scheme-3.23 Control Experiments

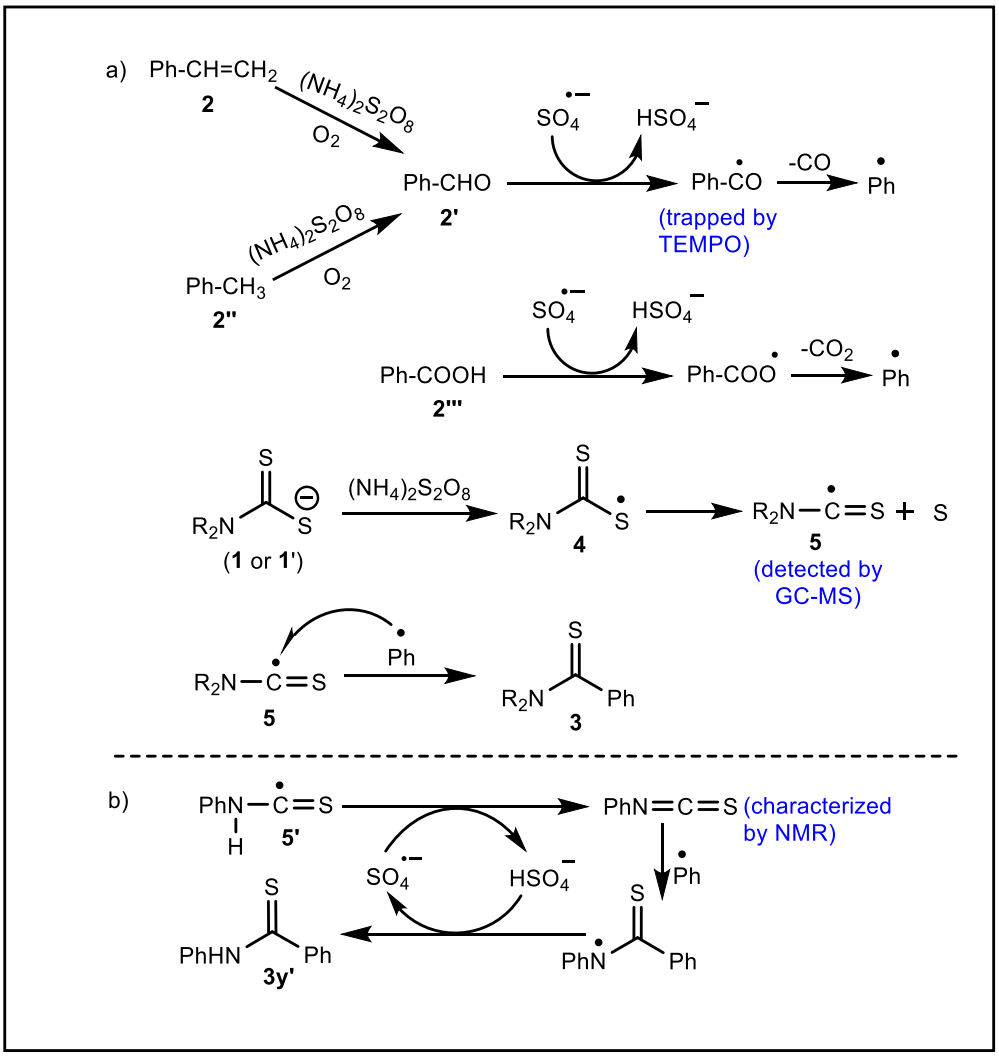

Scheme-3.24 Probable Reaction Pathway

In order to explore the applicative potential of the synthesized thioamide compounds, 3a was subjected to successful C-C cross coupling reaction with iodobenzene in presence of $PdCl_2$-PPh_3 catalytic system and copper (II) acetate monohydrate to produce benzophenone as the product (54% yield) (Scheme 3.25).

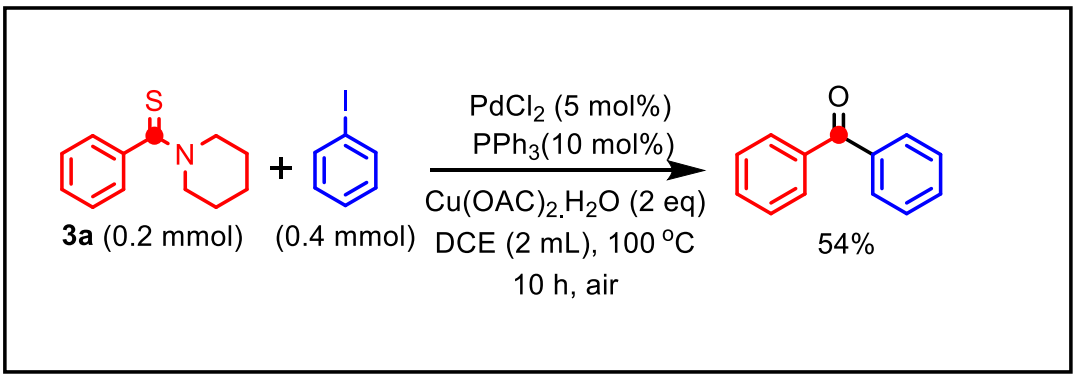

Scheme-3.25. Post-synthetic modification of thioamide-3a to produce diaryl ketone

2/c Conclusion

In conclusion, we have developed a novel protocol for C-C thioamidation of styrene *via* a dealkenylative approach using freshly prepared dithiocarbamate salts as the thioamide surrogate. The protocol was generalized with benzaldehyde, toluene and benzoic acid derivatives to prepare the thioamide compounds efficiently. The reaction mechanism has been explained with the help of a series of control experiments, isolation of reaction intermediate and GC-MS analysis of crude reaction mixture. Cheap and easily available starting materials/reagent, operational simplicity, wide substrate scope, scalability of the method, moisture and air insensitive reaction condition make the protocol economically and industrially attractive.

2/d Experimental Section

All the commercial starting materials and reagents were used without further purification. Silica gel (silica gel, f24), TLC plates were purchased from Merck. In column chromatographic purification process, silica gel 60-120 mesh has been used. ^{1}H NMR spectra were recorded using Brucker Spectrometer at 300 MHz, 400 MHz. The ^{19}F spectra of synthesized fluorinated product was recorded in $CDCl_3$ on Brucker Spectrometer, 300 MHz. ^{13}C NMR spectra were recorded at 75 MHz, 100 MHz. In all NMR, $CDCl_3$ and TMS have been used as solvent and internal standard respectively. The chemical shifts are reported in ppm scale considering standard signal of TMS at 0.00 ppm. The coupling constants (J values) are measured in Hz and splitting patterns of the proton are described as s (singlet), d (doublet), t (triplet), and m (multiplet). In NMR data, the rotamers are mentioned as #1 and #2. HRMS were measured in methanol solvent on a waters Micromass Q-tofMicromass spectrometer. GC-MS data were collected from PerkinElmer Clarus SQ 8 C Mass spectrometer.

General Experimental Procedure for the Preparation of Thioamides (3)

CS_2 (0.1 mL, 1.5 mmol) was added drop wise to a solution of secondary amine (1 mmol) and K_2CO_3 (276 mg, 2 mmol) in DMSO (2 ml) at 5 ^{o}C. The resulting solution was stirred at room temperature for 5 min. Styrene (**2**) (0.8 mmol), and $(NH_4)_2S_2O_8$ (1.2 mmol, 273 mg), were added to the solution of dithiocarbamate anion (**1**) containing K_2CO_3. The reaction mixture was allowed to stir at 80 ^{o}C for a certain time period under open air/zero air-balloon. The progress of the reaction was monitored by TLC. After completion of the reaction, the crude product was obtained by usual work-up using EtOAc. The crude product was purified by column chromatography over silica gel using petroleum ether-ethyl acetate solvent mixture.

Similar procedure was followed for the synthesis of thioamide compounds from benzaldehyde derivatives (**2'**). In this case, all the reactions were carried out in DMSO solvent under open air atmosphere (Scheme 3.22a). [For operational simplicity, all the reactions with benzaldehyde derivatives were performed under open air, although molecular oxygen does not have any role in the thioamidation of benzaldehyde.]

In case of toluene derivative (**2''**), similar experimental procedure was followed. Here, all the reactions were performed in seal tube (Scheme 3.22b).

Thioamides have been synthesized from benzoic acid derivatives (**2'''**) following similar experimental procedure using Et_3N base (instead of K_2CO_3) and DMSO solvent under open air atmosphere (Scheme 3.22c). [For operational simplicity, the reactions with benzoic acid derivatives were performed under open air, although molecular oxygen does not have any role in the thioamidation of benzoic acid.

Characterization data of all synthesized products

phenyl(piperidin-1-yl)methanethione (3a, Table 1): White solid; Yield: 88% (145 mg); ^{1}H NMR (300 MHz, $CDCl_3$): δ 7.36-7.22 (5H, m), 4.35-4.32 (2H, m), 3.51-3.47 (2H, m), 1.81-1.70 (4H, m), 1.56-1.53 (2H, m). ^{13}C NMR (75 MHz, $CDCl_3$): δ 199.49, 143.44, 128.37, 128.33, 125.43, 53.17, 50.60, 26.89, 25.50, 24.13.

phenyl(pyrrolidin-1-yl)methanethione methanethione (3b, Table 1): White solid; Yield: 85% (129 mg); ^{1}H NMR (300 MHz, $CDCl_3$): δ 7.31-7.30 (5H, m), 3.93 (2H, t, *J*=6.2 Hz), 3.42 (2H, t, *J*=6 Hz), 2.05-2.00 (2H, m), 1.95-1.89 (2H, m). ^{13}C NMR (75 MHz, CDCl3): δ 197.21, 144.04, 128.66, 128.26, 125.63, 53.77, 53.40, 26.47, 24.63.

morpholino(phenyl)methanethione (3c, Table 1): White solid; Yield: 87% (144 mg); ^{1}H NMR (400 MHz, $CDCl_3$): δ 7.31-7.29 (3H, m), 7.24-7.22 (2H,m), 4.38 (2H, t, *J*=5Hz), 3.82 (2H, t, *J*=5Hz), 3.59-3.52 (4H, m). ^{13}C NMR (100 MHz, $CDCl_3$): δ 200.96, 142.53, 128.84, 128.52, 125.90, 66.72, 66.49, 52.52, 49.56.

(4-fluorophenyl)(piperidin-1-yl)methanethione (3d, Table 1): Pale yellow solid; Yield: 82% (146 mg); ^{1}H NMR (300 MHz, $CDCl_3$): δ 7.31-7.26 (2H, m), 7.07-7.01 (2H, m), 4.37-4.33 (2H, m), 3.55-3.51 (2H, m), 1.84-1.74 (4H, m), 1.63-1.56 (2H, m). ^{13}C NMR (75 MHz, CDCl3): δ 198.55, 164.21, 160.92, 139.49, 139.44, 127.70, 127.59, 115.56, 115.27, 53.31, 50.88, 26.92, 25.49, 24.13. ^{19}F NMR (75 MHz, $CDCl_3$): -112.65.

(4-fluorophenyl)(pyrrolidin-1-yl)methanethione (3e, Table 1): White solid; Yield: 88% (146 mg); ^{1}H NMR (300 MHz, $CDCl_3$): δ 7.34-7.30 (2H, m), 6.99-6.94 (2H, m), 3.89 (2H, t, *J*=5.4Hz), 3.42 (2H, t, *J*=5.4Hz), 2.04-1.99 (2H, m), 1.95-1.90 (2H, m). ^{13}C NMR (75 MHz, $CDCl_3$): δ 196.01, 163.92, 161.45, 140.14, 140.10, 127.94, 127.86, 115.28, 115.07, 53.89, 53.62, 26.51, 24.62. ^{19}F NMR (75 MHz, $CDCl_3$): -112.23

(4-fluorophenyl)(morpholino)methanethione (3f, Table 1): White solid; Yield: 86% (155 mg); ^{1}H NMR (400 MHz, $CDCl_3$): δ 7.28-7.24 (2H, m), 7.04-6.99 (2H, m), 4.38 (2H, t, *J*=5.2Hz)), 3.84 (2H, t, *J*=5Hz), 3.62-3.52 (4H, m). ^{13}C NMR (100 MHz, $CDCl_3$): δ 199.89, 164.04, 161.56, 138.62, 138.59, 128.21, 128.13, 115.64, 115.42, 66.65, 66.46, 52.64, 49.77. ^{19}F NMR (100 MHz, $CDCl_3$): -111.64.

piperidin-1-yl(p-tolyl)methanethione (3g, Table 1): White solid; Yield: 78% (102 mg); ^{1}H NMR (400 MHz, $CDCl_3$): δ 7.13-7.07 (4H, m), 4.29-4.27 (2H, m), 3.49-3.46 (2H, m), 2.28 (3H, s), 1.75-1.69 (4H, m), 1.67-1.48 (2H, m). ^{13}C NMR (100 MHz, $CDCl_3$): δ 199.82, 140.70, 138.32, 128.91, 125.57, 53.17, 50. 69, 26.90, 25.50, 24.15, 21.23.

pyrrolidin-1-yl(p-tolyl)methanethione (3h, Table 1): White solid; Yield: 80% (130 mg); ^{1}H NMR (400 MHz, $CDCl_3$): δ 7.22 (2H, d, J= 8 Hz), 7.10 (2H, d, *J*=8 Hz), 3.91 (2H, t, *J*=5.4 Hz), 3.43 (2H, t, *J*=5Hz), 2.30 (3H, s), 2.03-1.98 (2H, m), 1.93-1.88 (2H, m). ^{13}C NMR (100 MHz, $CDCl_3$): δ 197.44, 141.29, 138.71, 128.79, 125.76, 53.80, 53.47, 26.48, 24.65, 21.25.

morpholino(p-tolyl)methanethione (3i, Table 1): White solid; Yield: 77% (136 mg); ^{1}H NMR (400 MHz, $CDCl_3$): δ 7.18-7.13 (4H, m), 4.42-4.39 (2H, m), 3.83 (2H, t, *J*=4.8Hz), 3.6o-3.61 (4H, m), 2.33 (3H, s). ^{13}C NMR (100 MHz, $CDCl_3$): δ 201.41, 139.75, 139.06, 129.09, 129.06, 66.75, 66.52, 52.59, 49.70, 21.25.

N,N,4-trimethylbenzothioamide (3j, Table 1): Pale yellow liquid; Yield: 72% (103 mg); ^{1}H NMR (400 MHz, $CDCl_3$): δ 7.40-7.29 (4H, m), 3.72 (3H, s), 3.31(3H, s), 2.48 (3H, s). ^{13}C NMR (100 MHz, $CDCl_3$): δ 201.66, 140.60, 138.71, 128.90, 125.91, 44.20, 43.35, 21.26.

(4-chlorophenyl)(piperidin-1-yl)methanethione (3k, Table 1): White solid; Yield: 82% (157 mg); ^{1}H NMR (400 MHz, $CDCl_3$): δ 7.27 (2H, d, *J*=7.8 Hz), 7.18 (2H, d, *J*=8 Hz), 4.29-4.26 (2H, m), 3.48-3.45 (2H, m), 1.77-1.68 (4H, m), 1.53-1.50 (2H, m). ^{13}C NMR (100 MHz, $CDCl_3$): δ 197.96, 141.76, 134.20, 128.57, 127.01, 53.25, 50.66, 26.88, 25.45, 24.06.

(4-chlorophenyl)(pyrrolidin-1-yl)methanethione (3l, Table 1): White solid; Yield: 78% (141 mg); ^{1}H NMR (300 MHz, $CDCl_3$): δ 7.28-7.28 (4H, m), 3.90 (2H, t, *J*=5.8Hz), 3.42 (2H, t, *J*=5.6Hz), 2.06-2.00 (2H, m), 1.97-1.92 (2H, m). ^{13}C NMR (75 MHz, $CDCl_3$): δ 195.67, 142.32, 134.56, 128.44, 127.24, 53.82, 53.53, 26.51, 24.60.

(4-chlorophenyl)(morpholino)methanethione (3m, Table 1): White solid; Yield: 84% (161 mg); ^{1}H NMR (400 MHz, $CDCl_3$): δ 7.32-7.29 (2H, m), 7.22-7.19 (2H, m), 4.39-4.36 (2H, m), 3.85-3.82 (2H, m), 3.61-3.55 (4H,m). ^{13}C NMR (100 MHz, $CDCl_3$): δ 199.50, 140.81, 134.86, 128.75, 127.46, 66.65, 66.46, 52.60, 49.62.

4-chloro-N,N-diethylbenzothioamide (3n, Table 1): Yellow liquid; Yield: 86% (155 mg); ^{1}H NMR (300 MHz, $CDCl_3$): δ 78.32-7.30 (2H, m), 7.19-7.18 (2H, m), 4.10 (2H, q, *J*=3.6Hz), 3.45 (2H, q, *J*=3.4) 1.37 (3H, t, *J*=3 Hz), 1.14 (3H, t, *J*=3 Hz). ^{13}C NMR (75 MHz, $CDCl_3$): δ 198.95, 142.25, 133.97, 128.60, 126.54, 47.87, 46.21, 13.86, 11.26.

4-chloro-N,N-dimethylbenzothioamide (3o, Table 1):Pale yellow liquid; Yield: 80% (127 mg); ^{1}H NMR (300 MHz, $CDCl_3$): δ 7.36-7.26 (4H, m), 3.60 (3H, s), 3.19 (3H, m). ^{13}C NMR (75 MHz, $CDCl_3$): δ 199.78, 141.68, 134.54, 128.57, 127.31, 44.21, 43.33.

(4-bromophenyl)(piperidin-1-yl)methanethione (3p, Table 1): White solid; Yield: 70% (158 mg); ^{1}H NMR (400 MHz, $CDCl_3$): δ 7.38-7.36 (2H, m), 7.08-7.06 (2H, m), 4.23-4.20 (2H, m), 3.42-3.39 (2H, m), 1.73-1.60 (4H, m), 1.48-1.42 (2H, m). ^{13}C NMR (100 MHz, $CDCl_3$): δ 197.72, 142.20, 131.48, 127.27, 122.32, 53.25, 50.61, 26.90, 25.46, 24.05.

(4-bromophenyl)(pyrrolidin-1-yl)methanethione (3q, Table 1): White solid; Yield: 75% (172 mg); ^{1}H NMR (400 MHz, $CDCl_3$): δ 7.45-7.43 (2H, m), 7.22-7.20 (2H, m), 3.90 (2H, t, *J*=4.8Hz), 3.42 (2H, t, *J*=4.8 Hz), 2.06-2.01 (2H, m), 1.97-1.92 (2H, m). ^{13}C NMR (100 MHz, $CDCl_3$): δ 195.57, 142.74, 131.42, 127.45, 122.82, 53.83, 53.52, 26.52, 24.61.

4-bromo-N,N-dimethylbenzothioamide (3r, Table 1): Pale yellow liquid; Yield: 70% (136 mg); ^{1}H NMR (400 MHz, $CDCl_3$): δ 7.50-7.47 (2H, m), 7.20-7.17 (2H, m), 3.58 (3H, s), 3.17

(3H, s). ^{13}C NMR (100 MHz, $CDCl_3$): δ 199.95, 142.15, 131.54, 127.52, 122.76, 44.15, 43.29.

(4-methoxyphenyl)(piperidin-1-yl)methanethione (3s, Table 1): White solid; Yield: 57% (106 mg); ^{1}H NMR (400 MHz, $CDCl_3$): δ 7.19-7.16 (2H, m), 6.78-6.76 (2H, m), 4.24-4.23 (2H, m), 3.72 (3H, s), 3.50-3.48 (2H, m), 1.73-1.66 (4H, m), 1.49-1.46 (2H, m). ^{13}C NMR (100 MHz, $CDCl_3$): δ 199.65, 159.86, 135.93, 127.52, 113.57, 55.40, 53.32, 51.00, 26.91, 25.48, 24.15.

(4-methoxyphenyl)(pyrrolidin-1-yl)methanethione (3t, Table 1): White solid; Yield: 51% (89 mg); ^{1}H NMR (400 MHz, $CDCl_3$): δ 7.36-7.34 (2H, m), 6.85-6.83 (2H, m), 3.95 (2H, t, *J*=5.6Hz), 3.80 (3H, s), 3.51(2H, t, *J*=5.2Hz), 2.09-2.02 (2H, m), 1.98-1.91 (2H, m), ^{13}C NMR (100 MHz, $CDCl_3$): δ 197.20, 160.11, 136.58, 127.74, 113.45, 53.39, 53.96, 53.71, 26.55, 24.70.

(4-methoxyphenyl)(morpholino)methanethione (3u, Table 1): White solid; Yield: 62% (116 mg); ^{1}H NMR (400 MHz, $CDCl_3$): δ 7.24-7.22 (2H, m), 6.83-6.81 (2H, m), 4.36 (2H, m), 3.81 (2H, t, *J*=4Hz), 3.76 (3H, s), 3.60 (4H, m). ^{13}C NMR (100 MHz, $CDCl_3$): δ 201.14, 160.29, 134.95, 128.09, 113.73, 66.69, 66.53, 55.44, 52.80, 50.02.

(4-nitrophenyl)(piperidin-1-yl)methanethione (3v, Table 1): White solid; Yield: 68% (136 mg); ^{1}H NMR (400 MHz, $CDCl_3$): δ 8.22-8.19 (2H, m), 7.42-7.38 (2H, m), 4.34-4.32 (2H, m), 3.48-3.45 (2H, m), 1.84-1.75 (4H, m), 1.61-1.56 (2H, m). ^{13}C NMR (100 MHz, $CDCl_3$): δ 196.13, 148.93, 147.26, 126.25, 124.00, 53.28, 50.31, 26.87, 25.41, 24.01.

N,N-dimethyl-4-nitrobenzothioamide (3w, Table 1): Yellow liquid; Yield: 68% (114 mg); ^{1}H NMR (400 MHz, $CDCl_3$): δ 8.19-8.16 (2H, m), 7.43-7.41 (2H, m), 3.57 (3H, s), 3.14, (3H, s). ^{13}C NMR (100 MHz, $CDCl_3$): δ 197.92, 148.95, 147.34, 126.61, 123.92, 44.04, 42.98.

methyl (phenylcarbonothioyl)-L-prolinate (3x, Table 1): White crystalline solid; Yield: 65% (129 mg); ^{1}H NMR (400 MHz, $CDCl_3$): δ 7.46-7.37 (5H, m, #1), 7.35-7.27 (0.87H, m, #2), 7.26-7.24 (0.52, m, #2), 5.17-5.13 (1H, m, #1), 4.52-4.48 (0.28H, m, #2), 4.16-4.14 (0.54H, m, #2), 3.84 (3H, s, #1), 3.72-3.64 (2H, m, #1),3.61-3.59 (0.74, m, #2), 2.52-2.48 (1H, m, #1), 2.47-2.45 (0.34H, m, #2), 2.23-2.08 (3H, m, #1), 2.07-1.96 (0.89H, m, #2). ^{13}C NMR (100 MHz, $CDCl_3$): δ 199.75 (C=S, #2), 199.41 (C=S, #1), 171.10 (CO_2Me, #2), 170.93 (CO_2Me, #1), 143.82(C, #2), 143.46 (C, #1), 129.00 (CH, #1), 128.65 (CH, #2), 128.35 (CH, #2), 128.30 (CH, #1), 125.69 (CH, #1), 125.28 (CH, #2), 64.81 (2-CH, #1), 64.51(2-CH, #2), 54.14 (5-CH_2, #1), 53.46 (5-CH_2, #2), 52.51 (OCH_3, #2), 52.46 (OCH_3, #1), 31.51 (3-CH_2, #2), 29.73 (3-CH_2, #1), 25.22 (4-CH_2, #1), 22.89 (4-CH_2, #2). HRMS (ESI) m/z calcd for $C_{13}H_{15}NO_2S$ $[M + H]^+$ 250.082, found 250.146.

4-methyl-N-phenylbenzothioamide (3y, Table 1): Yellow solid; Yield: 56% (95 mg); ^{1}H NMR (400 MHz, $CDCl_3$): δ 9.14 (1H, brs), 7.75-7.71 (4H, m), 7.42-7.39 (2H, m), 7.29-7.19 (3H, m), 2.39 (3H, s). ^{13}C NMR (100 MHz, $CDCl_3$): δ 198.31, 141.85, 139.21, 129.29, 129.19, 129.03, 128.99, 126.84, 123.90, 21.40.

N-benzyl-4-methylbenzothioamide (3z, Table 1): White solid; Yield: 74% (149 mg); ^{1}H NMR (400 MHz, $CDCl_3$): δ 7.97 (1H, brs), 7.66-7.63 (2H, m), 7.37-7.35 (5H, m), 7.14-7.12

(2H, m), 4.96-4.95 (2H, m), 2.36 (3H, s). ^{13}C NMR (100 MHz, $CDCl_3$): δ 198.90, 141.75, 138.72, 136.47, 129.13, 1278.97, 128.30, 128.08, 126.87, 50.75, 21.41.

4-(piperidine-1-carbonothioyl)benzonitrile (3aa): Yellow solid; Yield: 74% (170 mg); ^{1}H NMR (400 MHz, $CDCl_3$): δ 7.59 (2H, d, *J*=8Hz), 7.31 (2H, d, *J*=8Hz), 4.29-4.26 (2H, m), 3.43-3.40 (2H, m), 1.80-1.68 (4H, m), 1.54-1.49 (2H, m). ^{13}C NMR (100 MHz, $CDCl_3$): δ 196.39, 147.21, 132.41, 126.09, 118.31, 118.81, 53.27, 50.34, 26.85, 25.40, 23.97.

4-(pyrrolidine-1-carbonothioyl)benzonitrile (3ab): Pale yellow solid; Yield: 75% (161 mg); ^{1}H NMR (400 MHz, $CDCl_3$): δ 7.59 (2H, d, *J*=8.2Hz), 7.38 (2H, d, *J*=8Hz), 3.88 (2H, t, *J*=4.8Hz), 3.35 (2H, t, *J*=4.8Hz), 2.05-2.00 (2H, m), 1.97-1.92 (2H, m). ^{13}C NMR (100 MHz, $CDCl_3$): δ 192.51, 145.80, 130.45, 124.48, 116.41, 110.31, 51.82, 51.49, 24.60, 22.61.

piperidin-1-yl(o-tolyl)methanethione (3ac): Yellow liquid; Yield: 58% (126 mg); ^{1}H NMR (400 MHz, $CDCl_3$): δ 7.17-7.11 (3H, m), 7.07-7.04 (1H, m), 4.63-4.57 (1H, m), 4.12-4.08 (1H, m), 3.41-3.36 (1H, m), 3.32-3.29 (1H, m), 2.24 (3H, s), 1.79-1.68 (4H,m), 1.51-1.48 (2H, m). ^{13}C NMR (100 MHz, $CDCl_3$): δ 198.83, 143.02, 131.46, 130.40, 127.82, 126.10, 124.95, 52.15, 49.51, 26.67, 25.51, 24.11, 18.93.

(3-nitrophenyl)(piperidin-1-yl)methanethione (3ad): Yellow solid; Yield: 61% (152 mg); ^{1}H NMR (400 MHz, $CDCl_3$): δ 7.91-7.90 (2H, m), 7.41-7.32 (2H, m), 4.16-4.13 (2H, m), 3.35-3.31(2H, m), 1.66-1.55 (4H, m), 1.41-1.38 (2H, m). ^{13}C NMR (100 MHz, $CDCl_3$): δ 195.57, 147.92, 144.50, 131.35, 129.71, 122.99, 120.60, 53.46, 50.65, 26.88, 25.42, 23.93.

morpholino(o-tolyl)methanethione (3ae): Pale yellow solid; Yield: 59% (130 mg); ^{1}H NMR (400 MHz, $CDCl_3$): δ 7.20-7.14 (3H, m), 7.08-7.05 (1H, m), 4.58-4.53 (1H, m), 4.33-4.27 (1H, m), 3.86-3.83 (2H, m), 3.60-3.56 (2H, m), 3.42-3.37, (2H, m), 2.25 (3H, m). ^{13}C NMR (100 MHz, $CDCl_3$): δ 200.30, 142.21, 131.61, 130.54, 128.25, 126.30, 125.29, 66.60, 66.51, 51.38, 48.45, 18.98. HRMS (ESI) m/z calcd for $C_{12}H_{15}NOS$ $[M + H]^+$ 222.087, found 222.096.

2,2,6,6-tetramethylpiperidin-1-yl benzoate : Crystalline solid; Yield; ^{1}H NMR (400 MHz, $CDCl_3$): δ 8.09-8.06 (2H, m), 7.57-7.55 (1H, m), 7.48-7.43 (2H, m), 1.79-1.60 (4H, m), 1.61-1.55 (2H, m), 1.27 (6H, s), 1.12 (6H, s). ^{13}C NMR (100 MHz, $CDCl_3$): δ 166.46, 132.89, 129.71, 129.59, 128.48, 60.44, 39.06, 31.97, 20.88, 17.02.

Isothiocyanatobenzene : Colorless oil; ^{1}H NMR (400 MHz, $CDCl_3$): δ 7.37-7.31 (2H, m), 7.30-7.26 (1H, m), 7.24-7.19 (2H, m). ^{13}C NMR (100 MHz, $CDCl_3$): δ 135.29, 131.25, 129.59, 127.36, 125.79.

Benzophenon : White solid; ^{1}H NMR (400 MHz, $CDCl_3$): δ 7.83-7.79 (4H, m), 7.61-7.56 (2H, m), 7.51-7.45 (4H, m).^{13}C NMR (100 MHz, $CDCl_3$): δ 196.76, 137.63, 132.44, 130.07, 128.30.

2/e

^{1}H and ^{13}C NMR spectra of all synthesized products described in Section -2

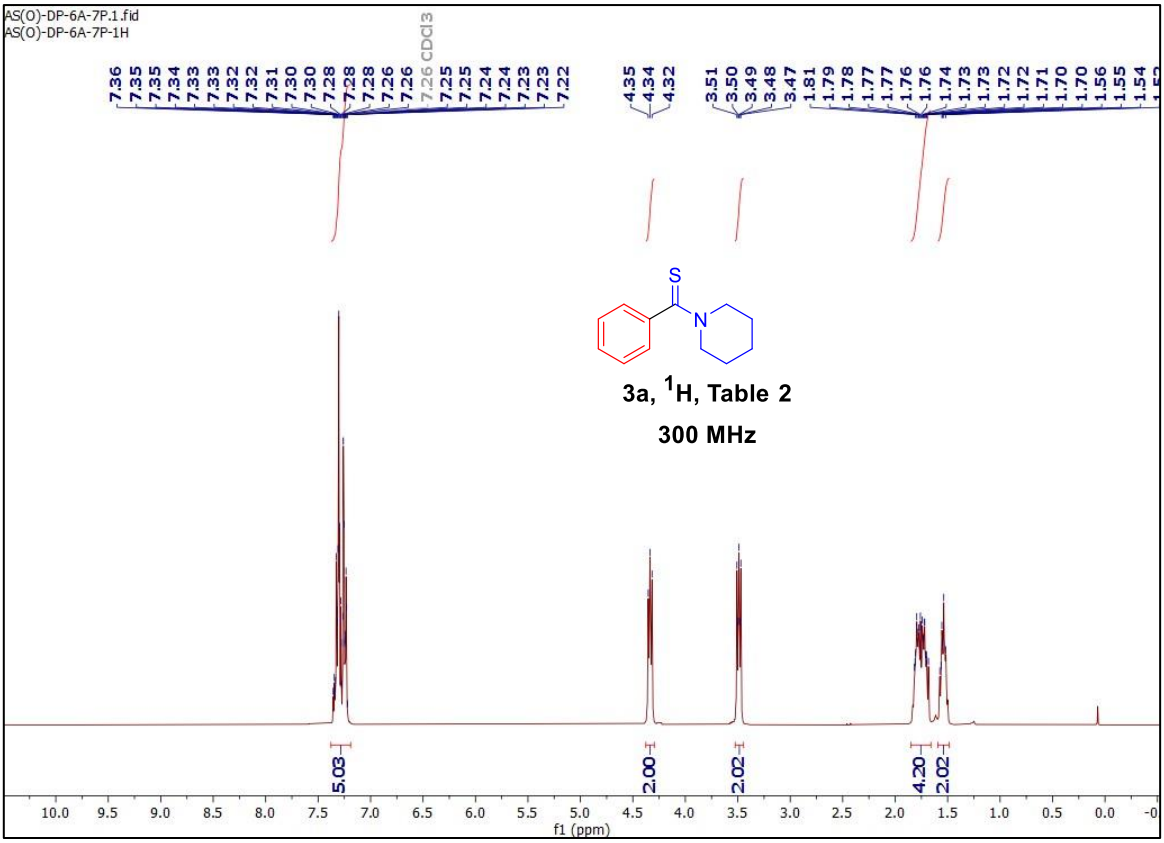
AS(O)-DP-6A-7P.1.fid
AS(O)-DP-6A-7P-1H
7.26 CDCl3
S
N
3a, 1H, Table 2
300 MHz
5.03
2.00
2.02
4.20
2.02
f1 (ppm)

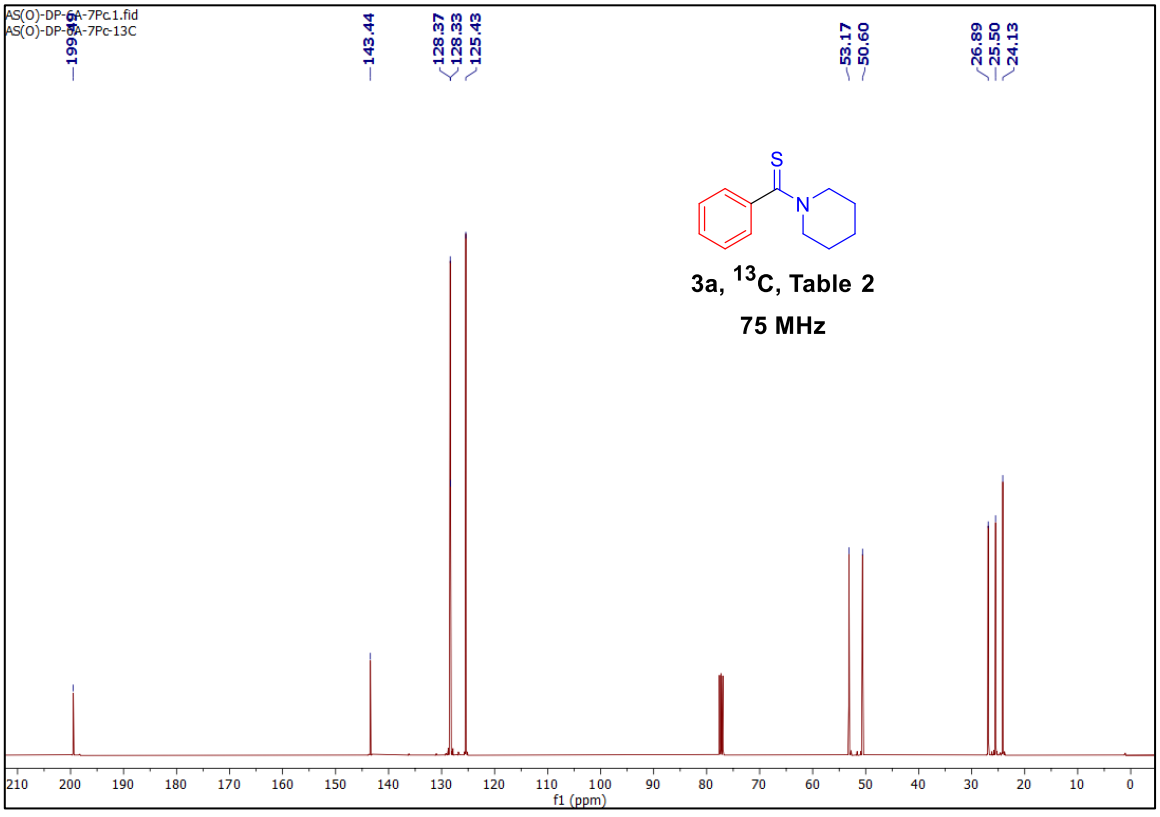
AS(O)-DP-6A-7Pc.1.fid
AS(O)-DP-6A-7Pc-13C
143.44
128.37
128.33
125.43
53.17
50.60
26.89
25.50
24.13
S
N
3a, 13C, Table 2
75 MHz
f1 (ppm)

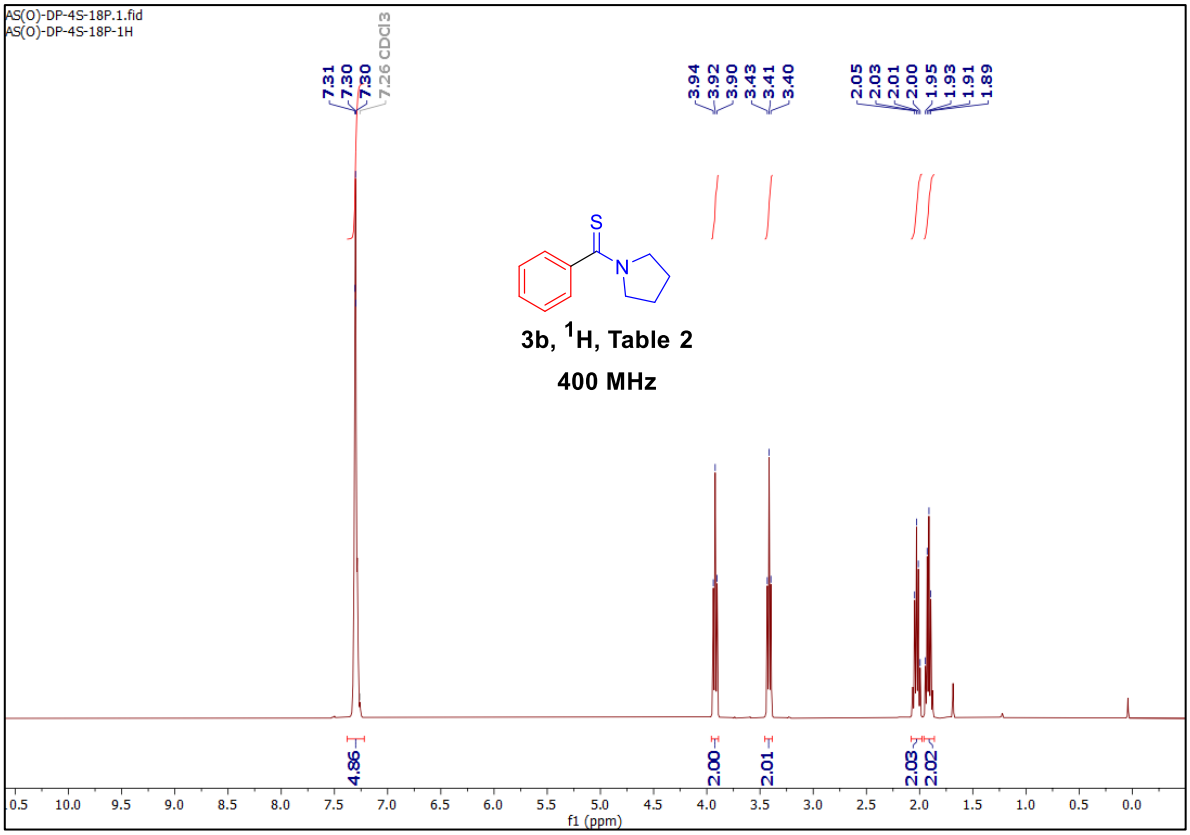
AS(O)-DP-4S-18P.1.fid
AS(O)-DP-4S-18P-1H
7.31
7.30
7.30
7.26 CDCl3
3.94
3.92
3.90
3.43
3.41
3.40
2.05
2.03
2.01
2.00
1.95
1.93
1.91
1.89
S
N
3b, 1H, Table 2
400 MHz
4.86
2.00
2.01
2.03
2.02
f1 (ppm)

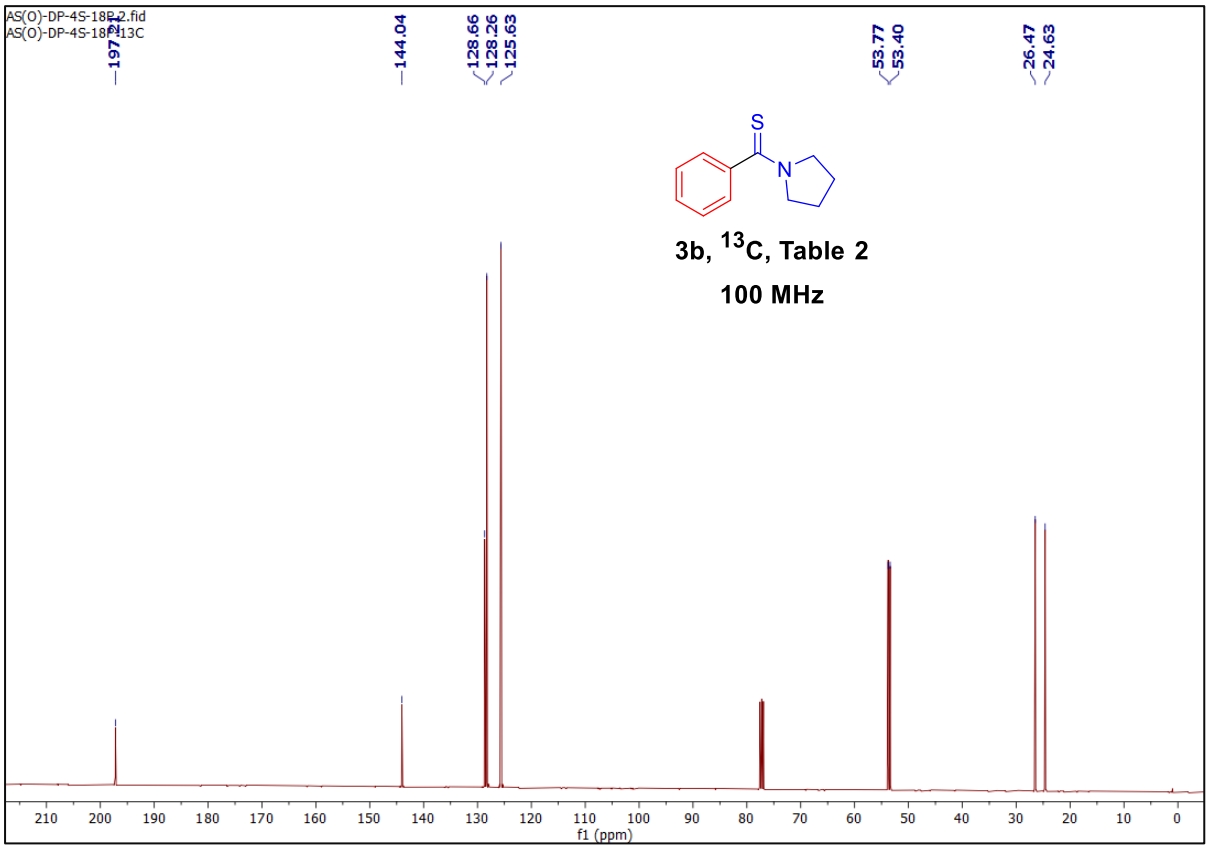
AS(O)-DP-4S-18P-2.fid
AS(O)-DP-4S-18P-13C
197.21
144.04
128.66
128.26
125.63
53.77
53.40
26.47
24.63
S
N
3b, 13C, Table 2
100 MHz
f1 (ppm)

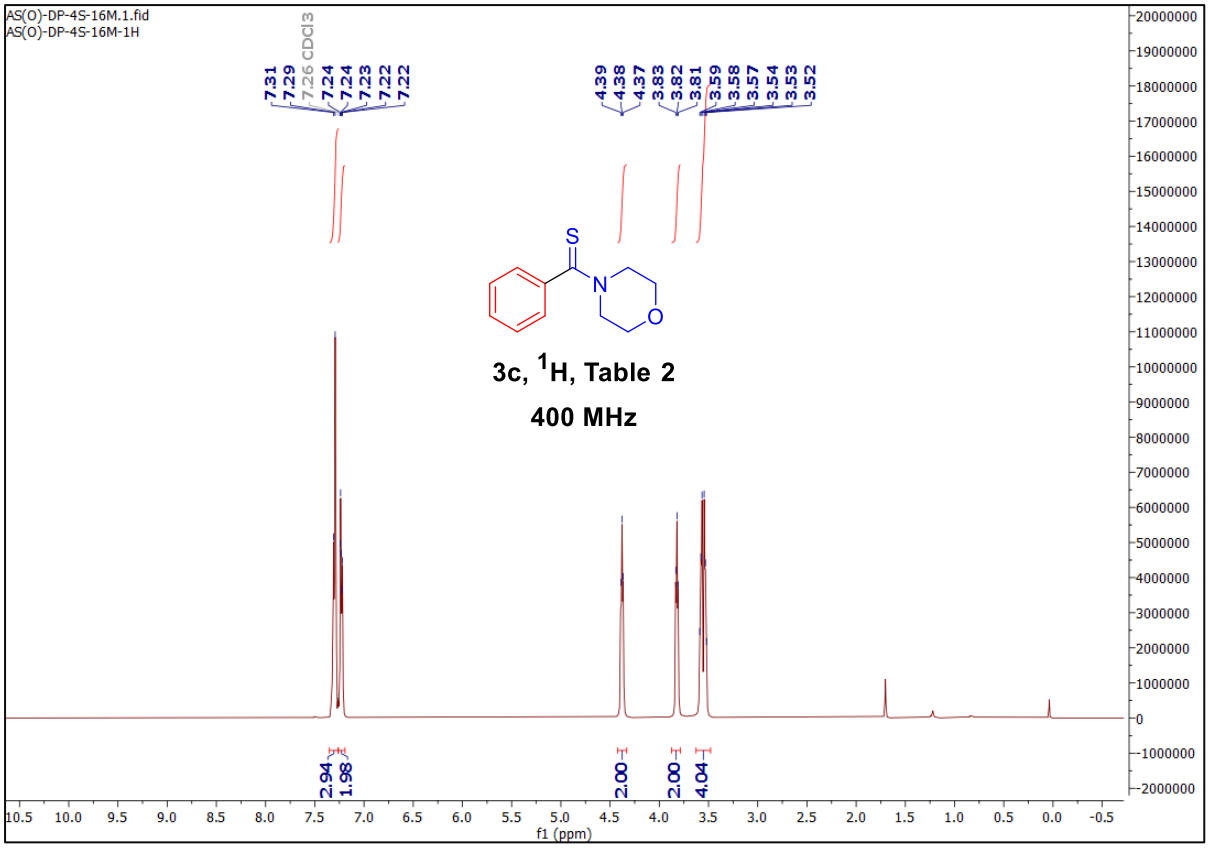
AS(O)-DP-4S-16M.1.fid
AS(O)-DP-4S-16M-1H
7.31
7.29
7.26 CDCl3
7.24
7.24
7.23
7.22
7.22
4.39
4.38
4.37
3.83
3.82
3.81
3.59
3.58
3.57
3.54
3.53
3.52
S
N
O
3c, 1H, Table 2
400 MHz
2.94
1.98
2.00
2.00
4.04
f1 (ppm)

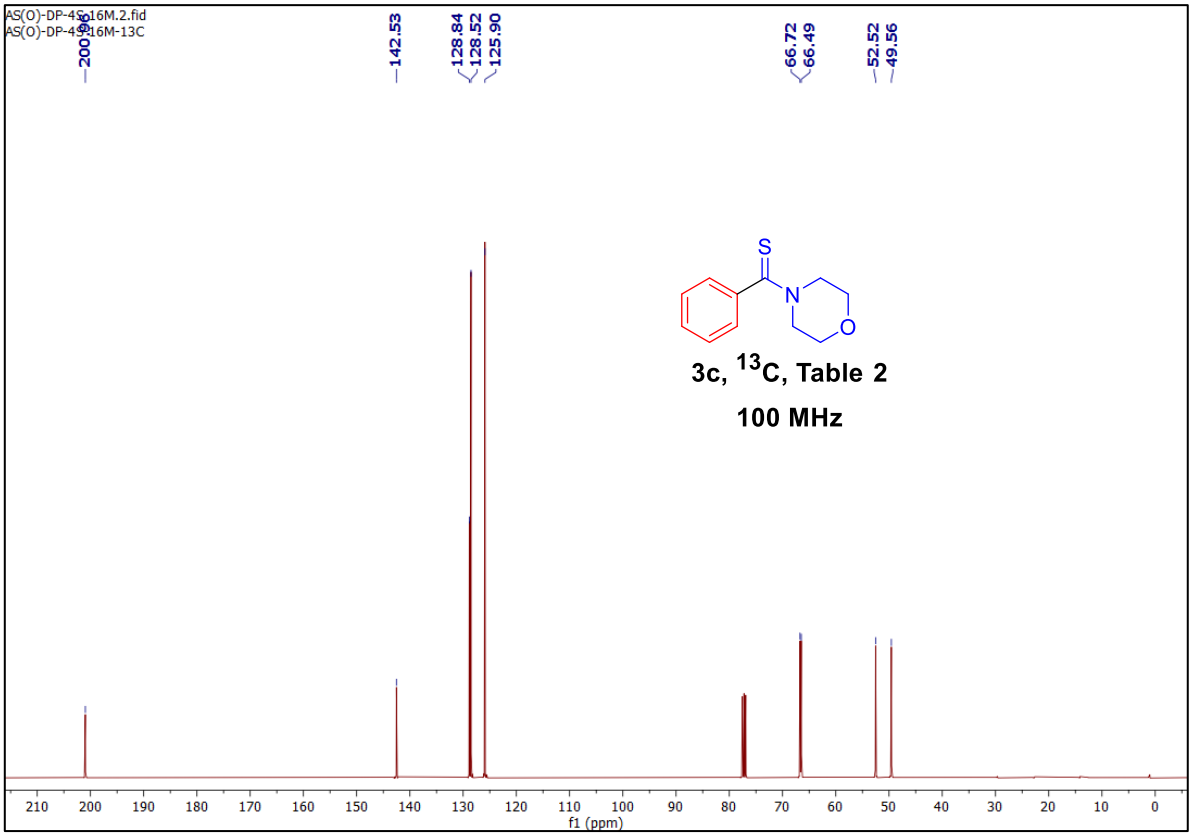
AS(O)-DP-4S-16M.2.fid
AS(O)-DP-4S-16M-13C
200.90
142.53
128.84
128.52
125.90
66.72
66.49
52.52
49.56
S
N
O
3c, 13C, Table 2
100 MHz
f1 (ppm)

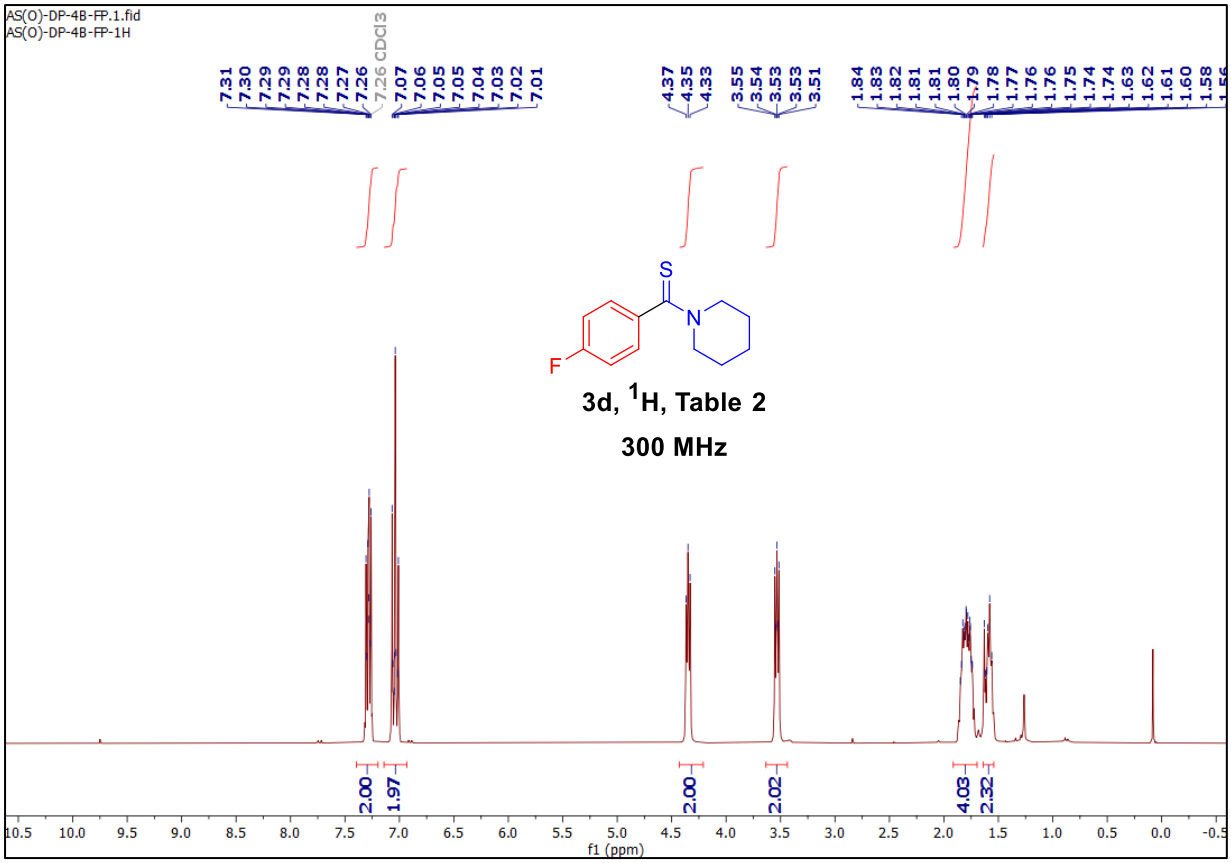
AS(O)-DP-4B-FP.1.fid
AS(O)-DP-4B-FP-1H
7.26 CDCl3
S
N
F
3d, 1H, Table 2
300 MHz
f1 (ppm)

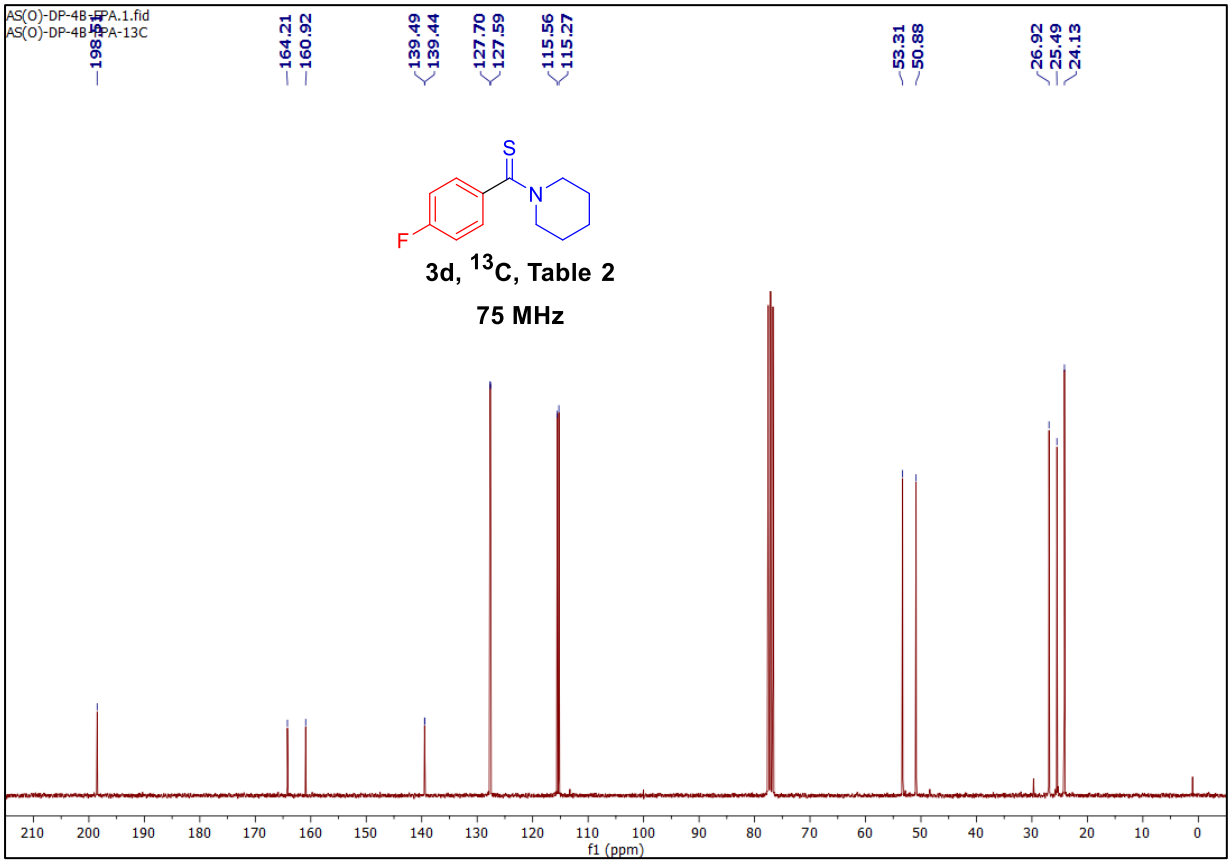
AS(O)-DP-4B-FPA.1.fid
AS(O)-DP-4B-FPA-13C
S
N
F
3d, 13C, Table 2
75 MHz
f1 (ppm)

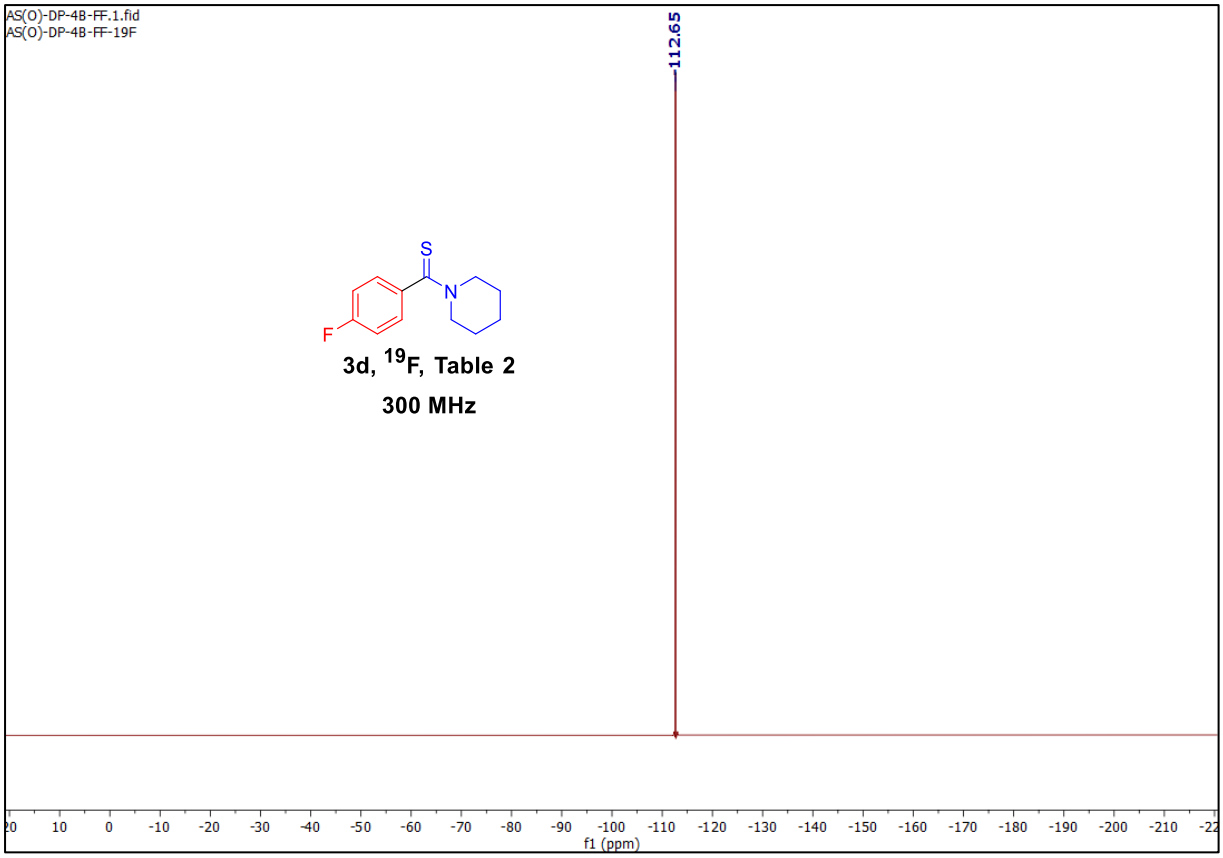
AS(O)-DP-4B-FF.1.fid
AS(O)-DP-4B-FF-19F
112.65
S
N
F
3d, 19F, Table 2
300 MHz
f1 (ppm)

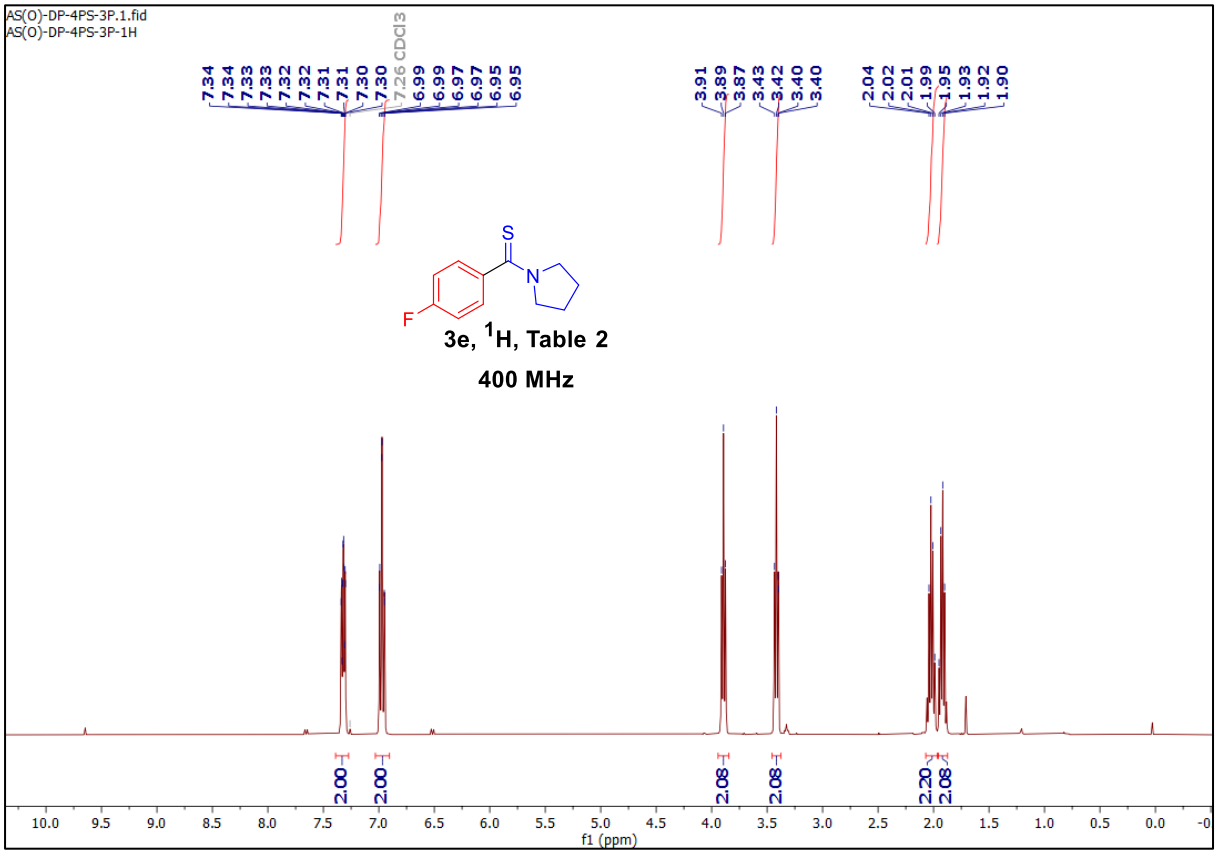
AS(O)-DP-4PS-3P.1.fid
AS(O)-DP-4PS-3P-1H
7.34 7.34 7.33 7.33 7.32 7.32 7.31 7.31 7.30 7.30 7.26 CDCl3 6.99 6.99 6.97 6.97 6.95 6.95
3.91 3.89 3.87 3.43 3.42 3.40 3.40
2.04 2.02 2.01 1.99 1.95 1.93 1.92 1.90
S
N
F
3e, 1H, Table 2
400 MHz
2.00 2.00 2.08 2.08 2.20 2.08
f1 (ppm)

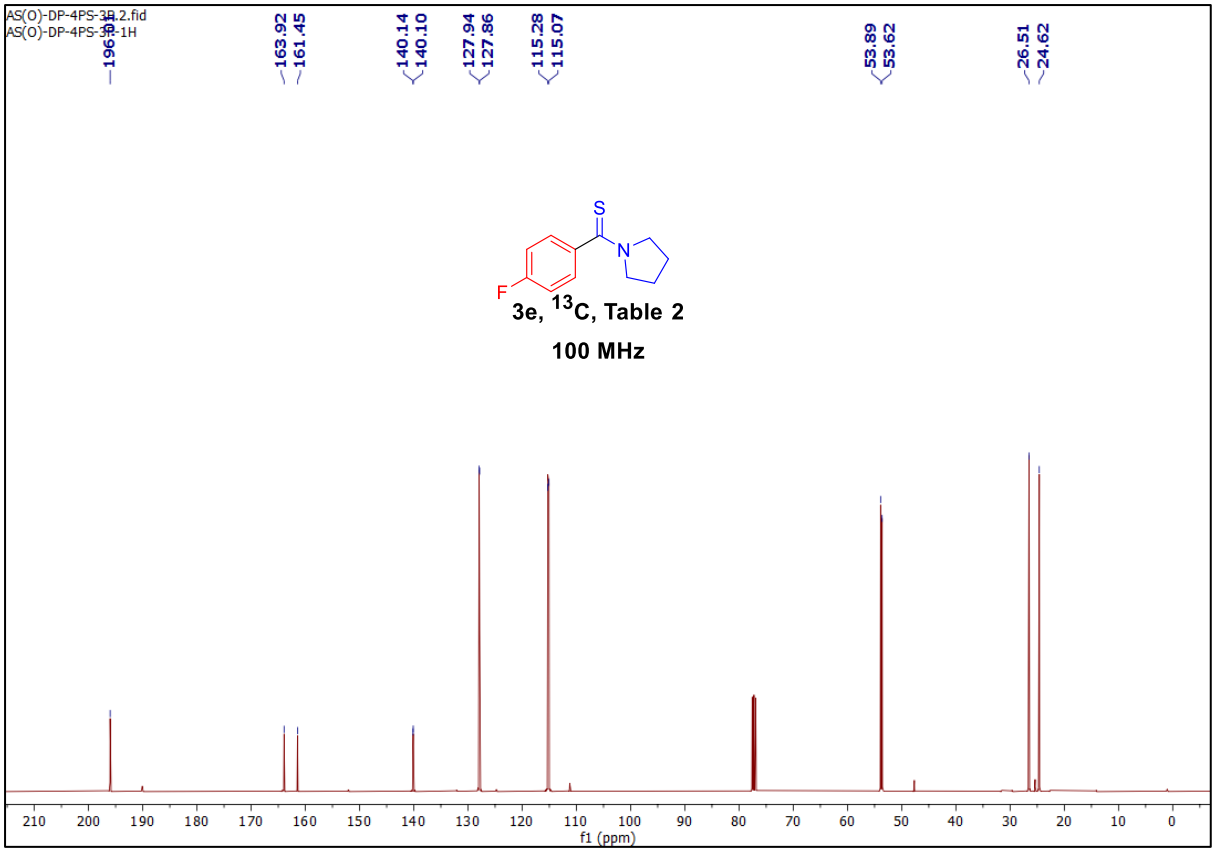
AS(O)-DP-4PS-3P.2.fid
AS(O)-DP-4PS-3P-1H
196.31
163.92
161.45
140.14
140.10
127.94
127.86
115.28
115.07
53.89
53.62
26.51
24.62
S
N
F
3e, 13C, Table 2
100 MHz
f1 (ppm)

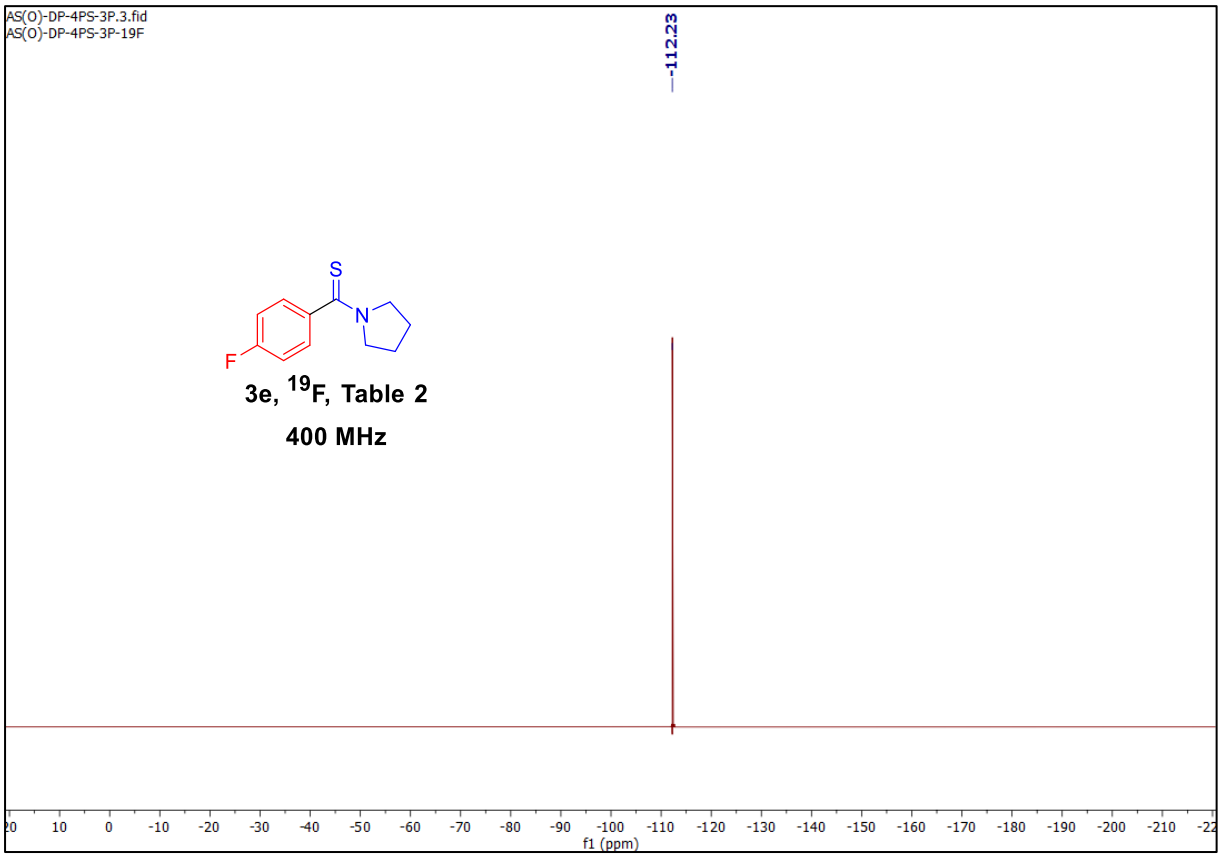
AS(O)-DP-4PS-3P.3.fid
AS(O)-DP-4PS-3P-19F
-112.23
S
N
F
3e, 19F, Table 2
400 MHz
f1 (ppm)

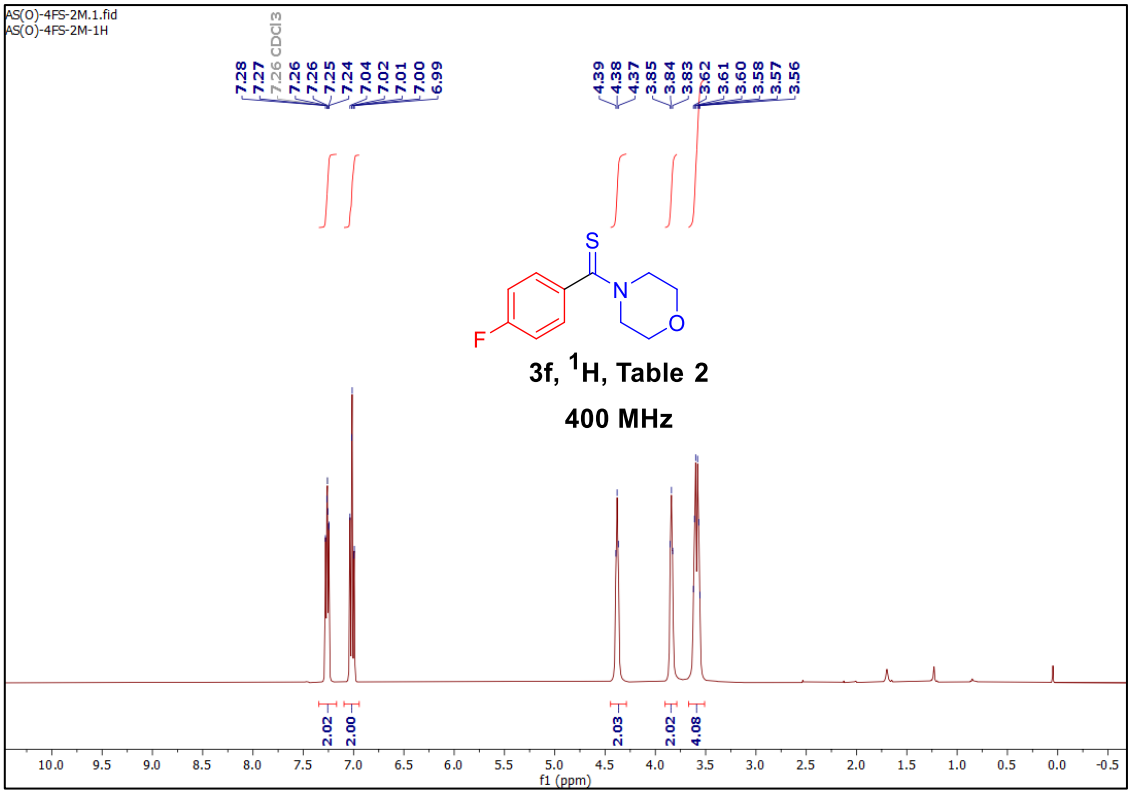
AS(O)-4FS-2M.1.fid
AS(O)-4FS-2M-1H
7.28
7.27
7.26 CDCl3
7.26
7.26
7.25
7.24
7.04
7.02
7.01
7.00
6.99
4.39
4.38
4.37
3.85
3.84
3.83
3.62
3.61
3.60
3.58
3.57
3.56
S
N
O
F
3f, 1H, Table 2
400 MHz
2.02
2.00
2.03
2.02
4.08
f1 (ppm)

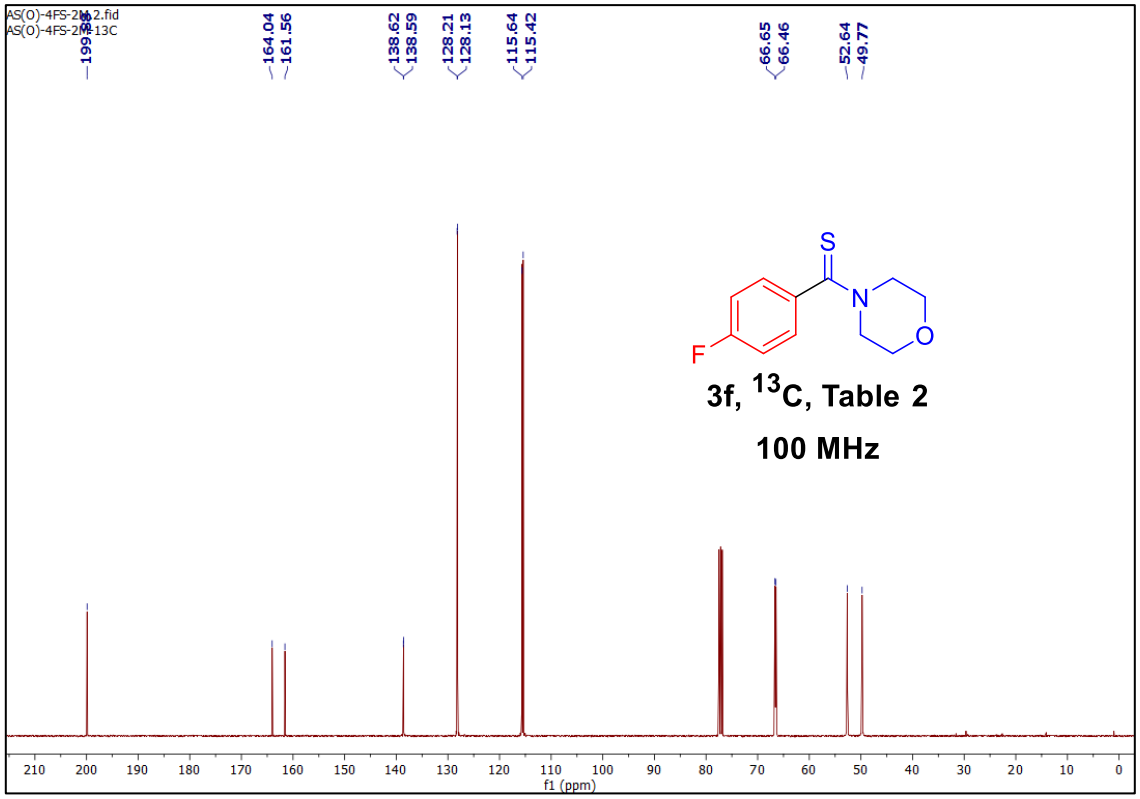
AS(O)-4FS-2M2.fid
AS(O)-4FS-2M-13C
199.72
164.04
161.56
138.62
138.59
128.21
128.13
115.64
115.42
66.65
66.46
52.64
49.77
S
N
O
F
3f, 13C, Table 2
100 MHz
f1 (ppm)

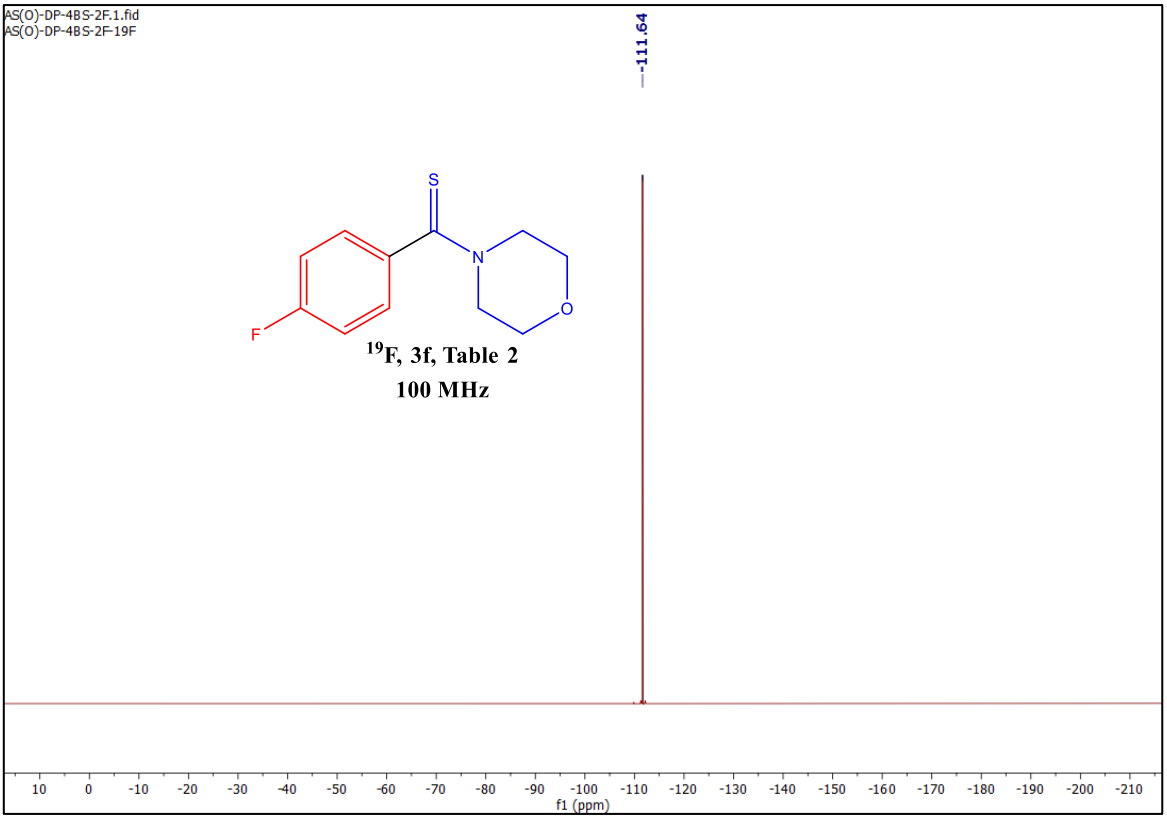

^{19}F, 3f, Table 2

100 MHz

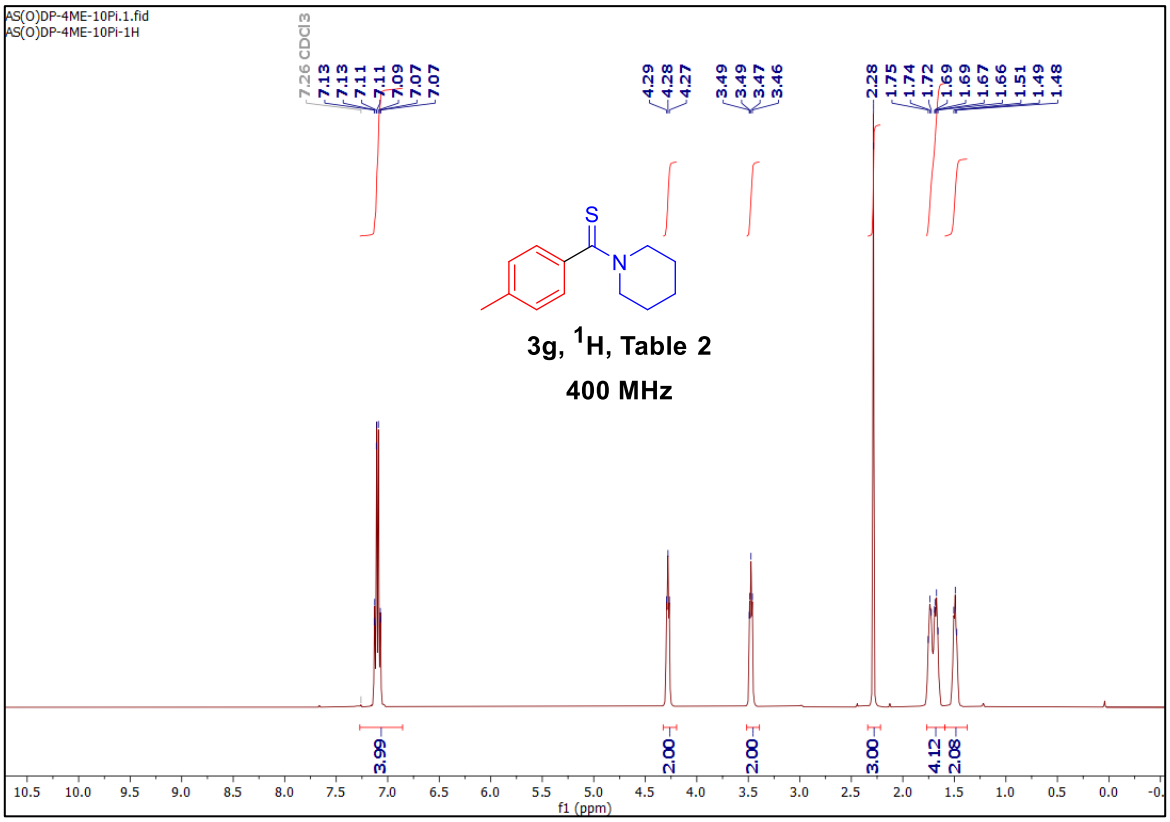

3g, ^{1}H, Table 2

400 MHz

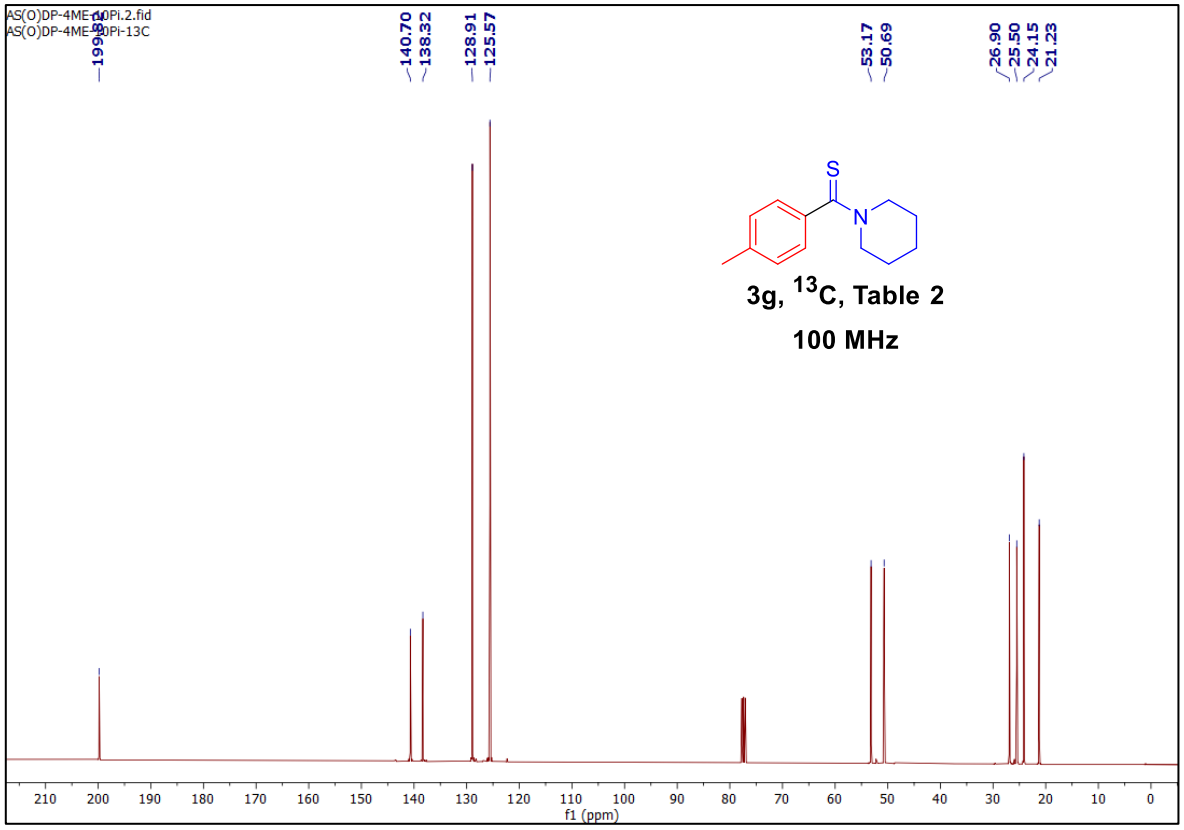
AS(O)DP-4ME-14Pi.2.fid
AS(O)DP-4ME-14Pi-13C
199.88
140.70
138.32
128.91
125.57
53.17
50.69
26.90
25.50
24.15
21.23
S
N
3g, 13C, Table 2
100 MHz
f1 (ppm)

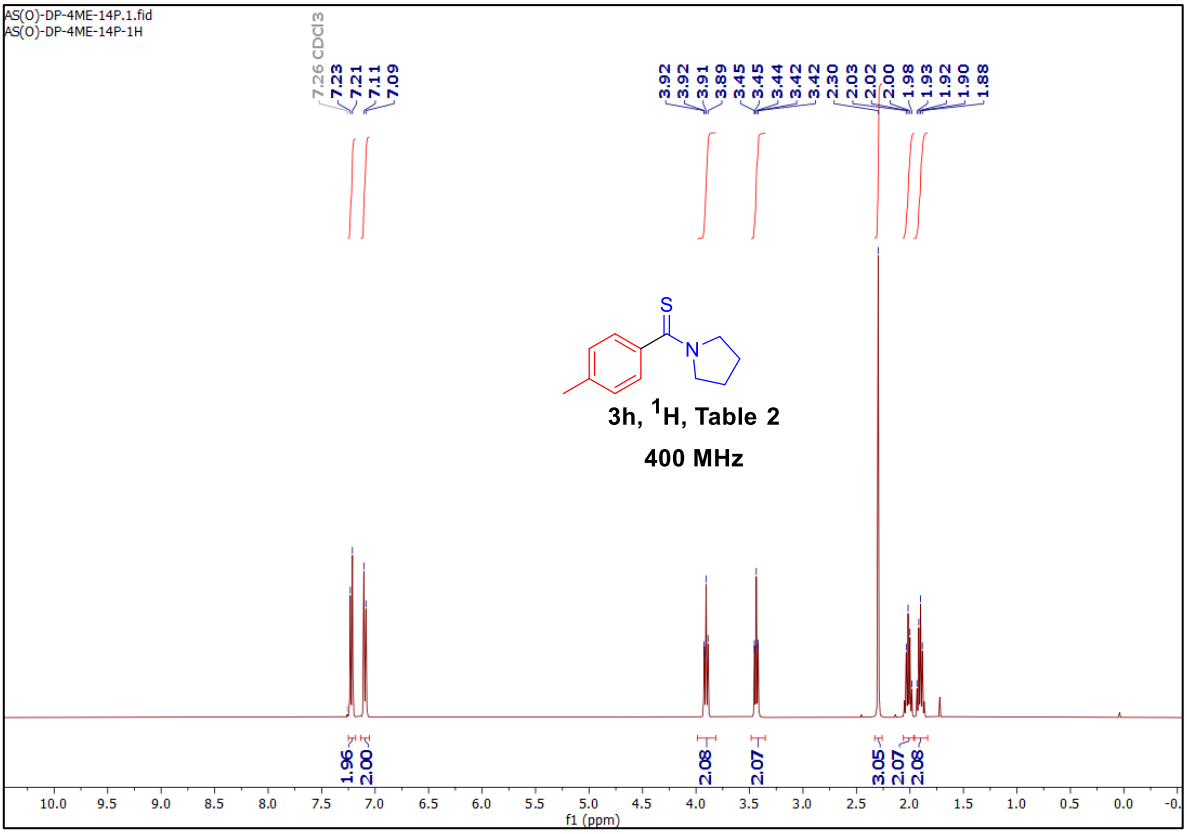
AS(O)-DP-4ME-14P.1.fid
AS(O)-DP-4ME-14P-1H
7.26 CDCl3
7.23
7.21
7.11
7.09
3.92
3.92
3.91
3.89
3.45
3.44
3.42
3.42
2.30
2.03
2.02
2.00
1.98
1.93
1.92
1.90
1.88
S
N
3h, 1H, Table 2
400 MHz
1.96
2.00
2.08
2.07
3.05
2.07
2.08
f1 (ppm)

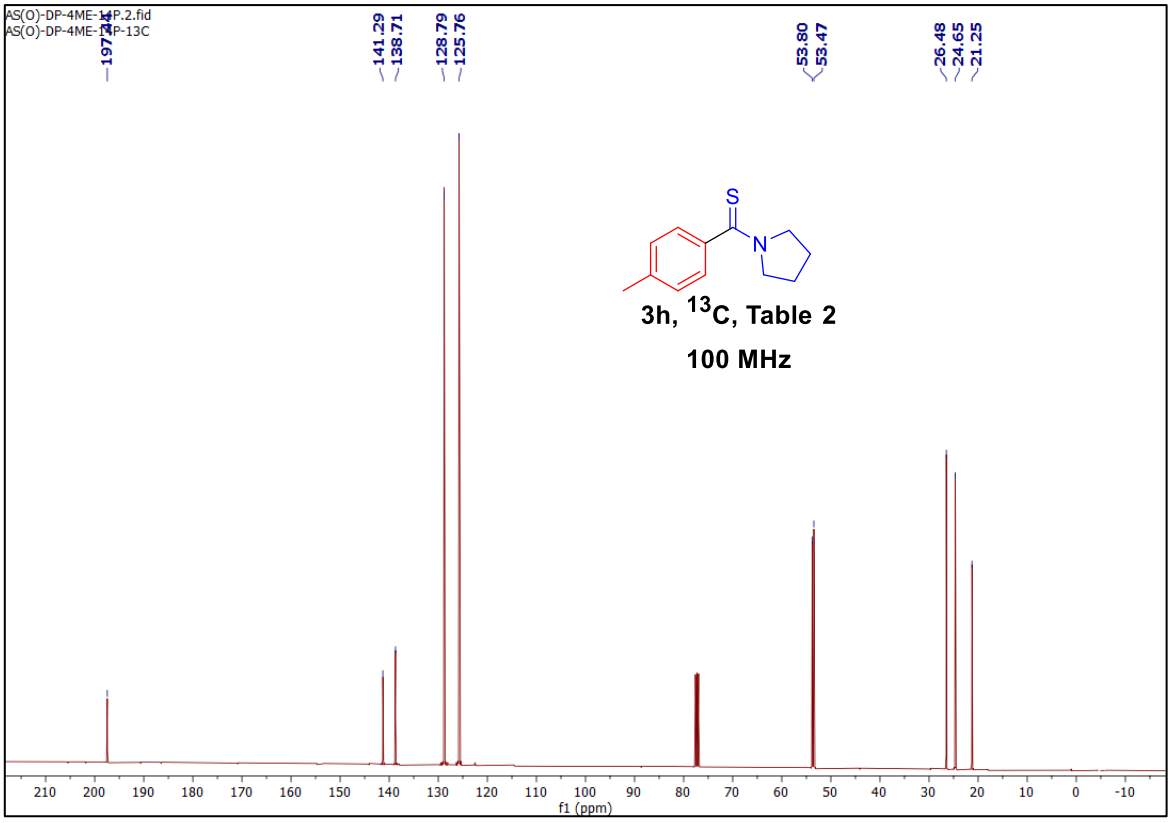
AS(O)-DP-4ME-1HP.2.fid
AS(O)-DP-4ME-13P-13C
197.24
141.29
138.71
128.79
125.76
53.80
53.47
26.48
24.65
21.25
S
N
3h, 13C, Table 2
100 MHz
f1 (ppm)

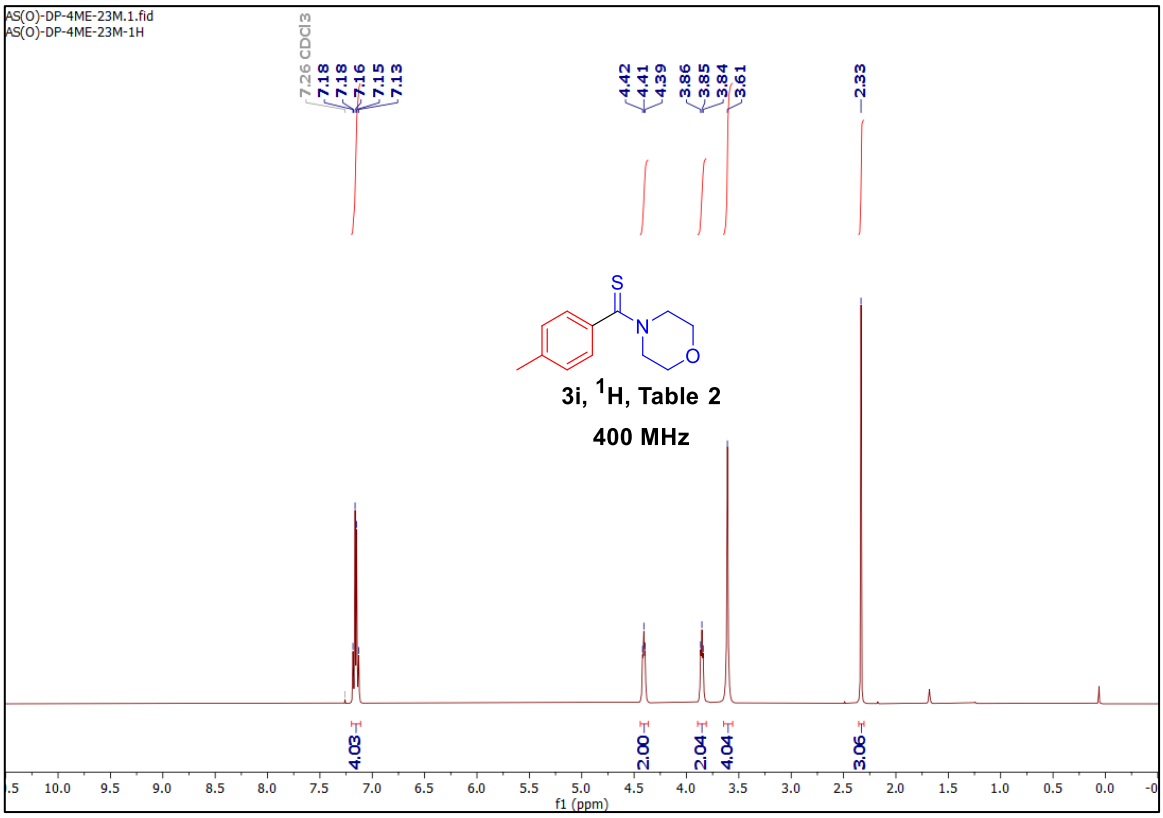
AS(O)-DP-4ME-23M.1.fid
AS(O)-DP-4ME-23M-1H
7.26 CDCl3
7.18
7.18
7.16
7.15
7.13
4.42
4.41
4.39
3.86
3.85
3.84
3.61
2.33
S
N
O
3i, 1H, Table 2
400 MHz
4.03
2.00
2.04
4.04
3.06
f1 (ppm)

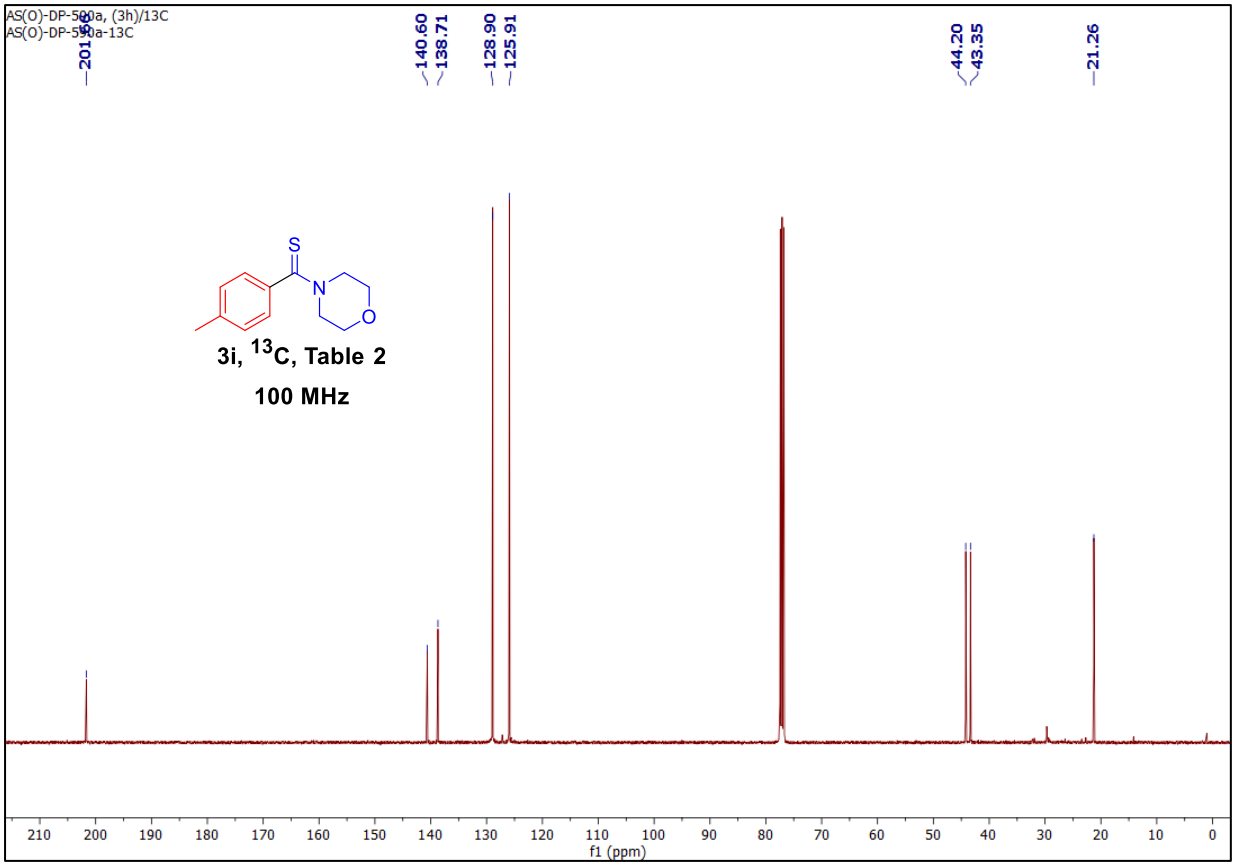
AS(O)-DP-590a, (3h)/13C
AS(O)-DP-590a-13C
201.86
140.60
138.71
128.90
125.91
44.20
43.35
21.26
S
N
O
3i, 13C, Table 2
100 MHz
f1 (ppm)

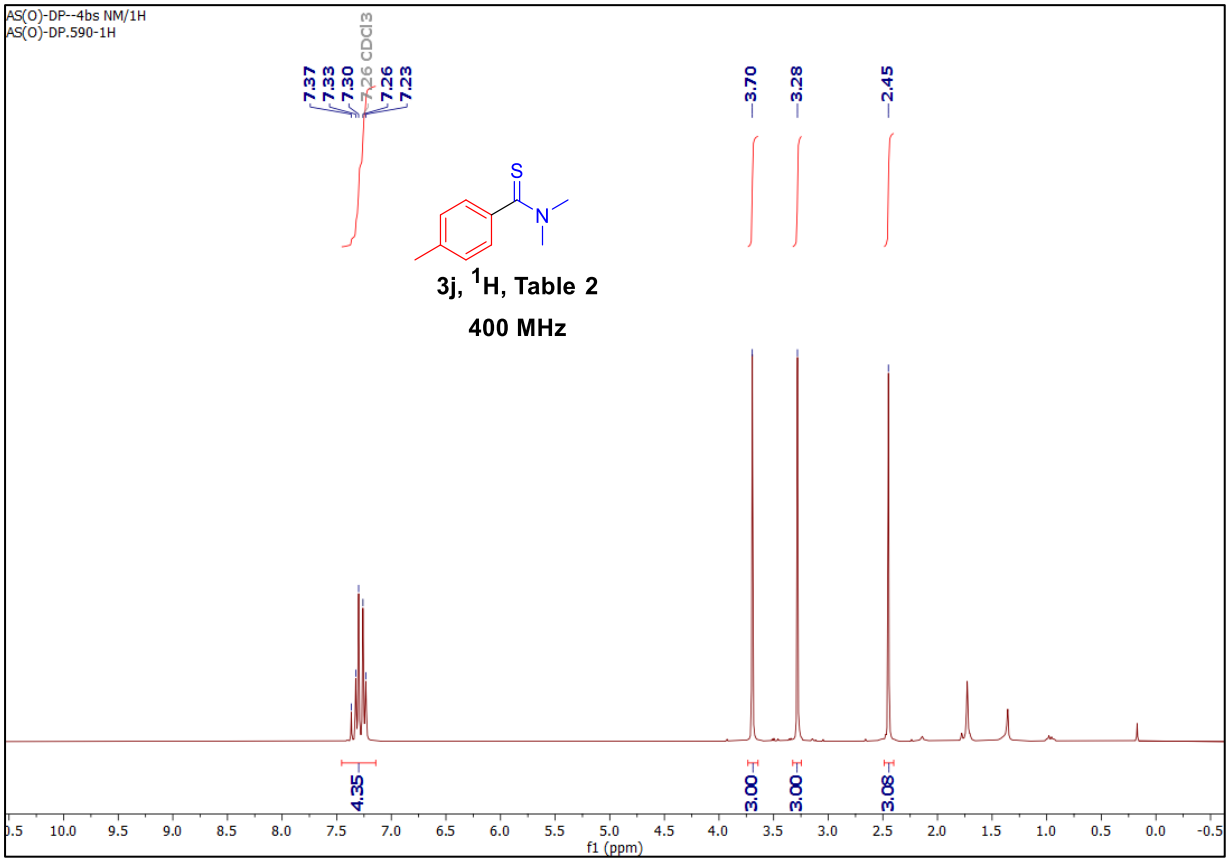
AS(O)-DP--4bs NM/1H
AS(O)-DP.590-1H
7.37
7.33
7.30
7.26 CDCl3
7.26
7.23
3.70
3.28
2.45
S
N
3j, 1H, Table 2
400 MHz
4.35
3.00
3.00
3.08
f1 (ppm)

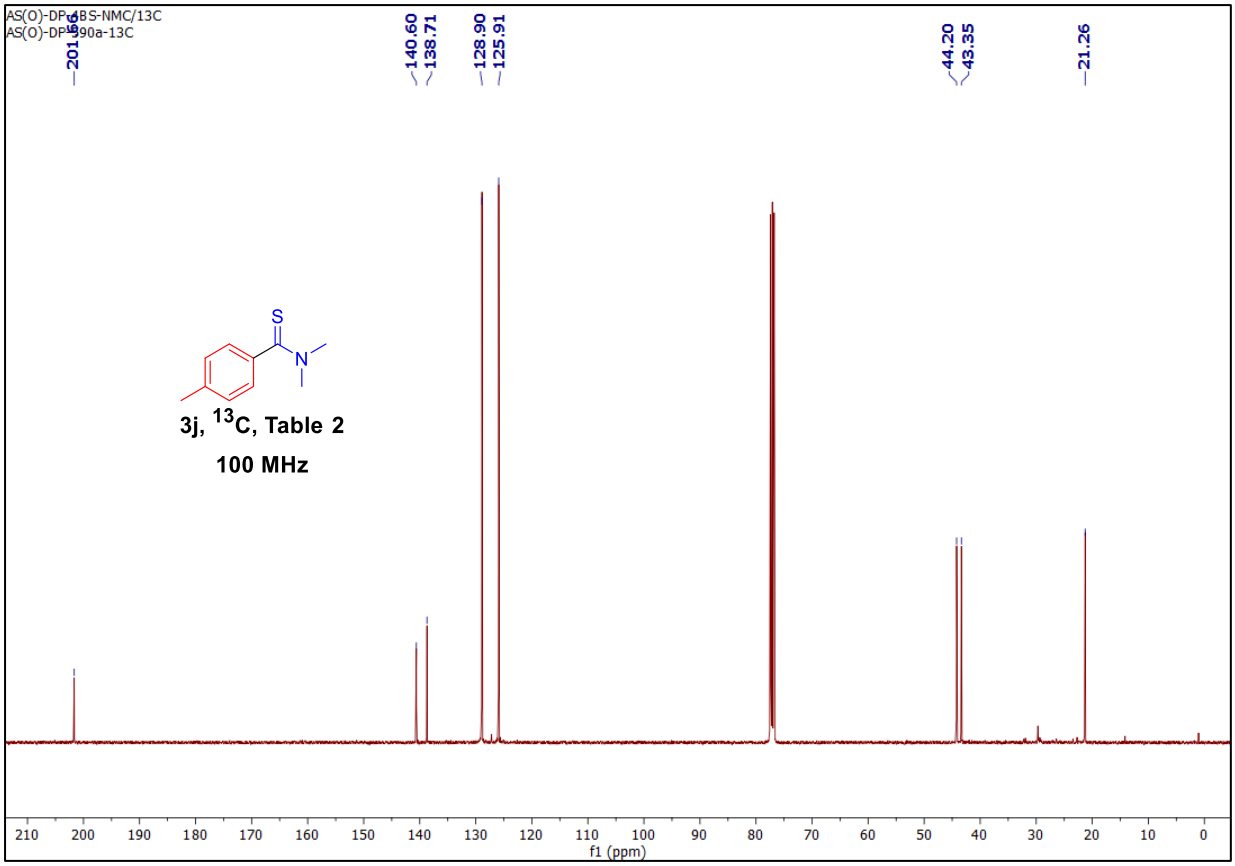
AS(O)-DP-4BS-NMC/13C
AS(O)-DP-390a-13C
201.16
140.60
138.71
128.90
125.91
44.20
43.35
21.26
S
N
3j, 13C, Table 2
100 MHz
f1 (ppm)

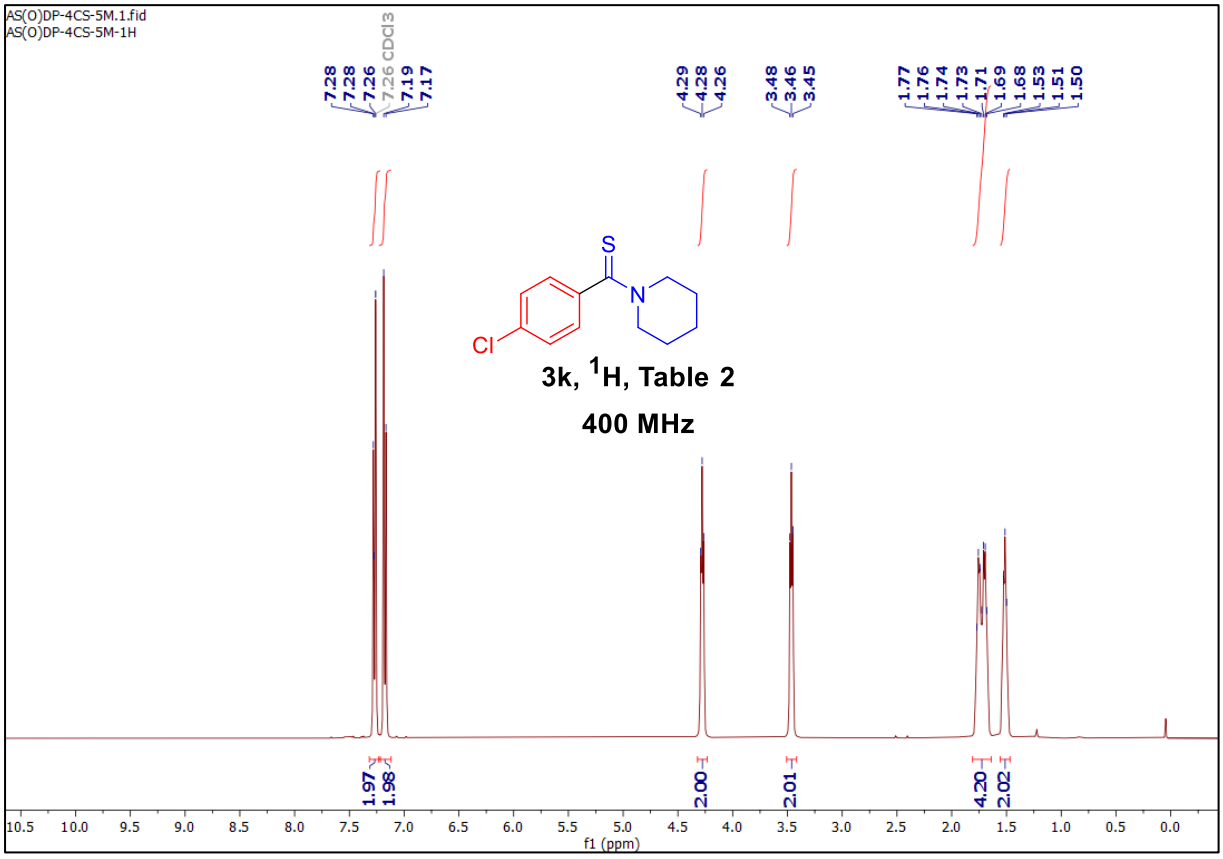
AS(O)DP-4CS-5M.1.fid
AS(O)DP-4CS-5M-1H
7.28
7.28
7.26
7.26 CDCl3
7.19
7.17
4.29
4.28
4.26
3.48
3.46
3.45
1.77
1.76
1.74
1.73
1.71
1.69
1.68
1.53
1.51
1.50
S
N
Cl
3k, 1H, Table 2
400 MHz
1.97
1.98
2.00
2.01
4.20
2.02
f1 (ppm)

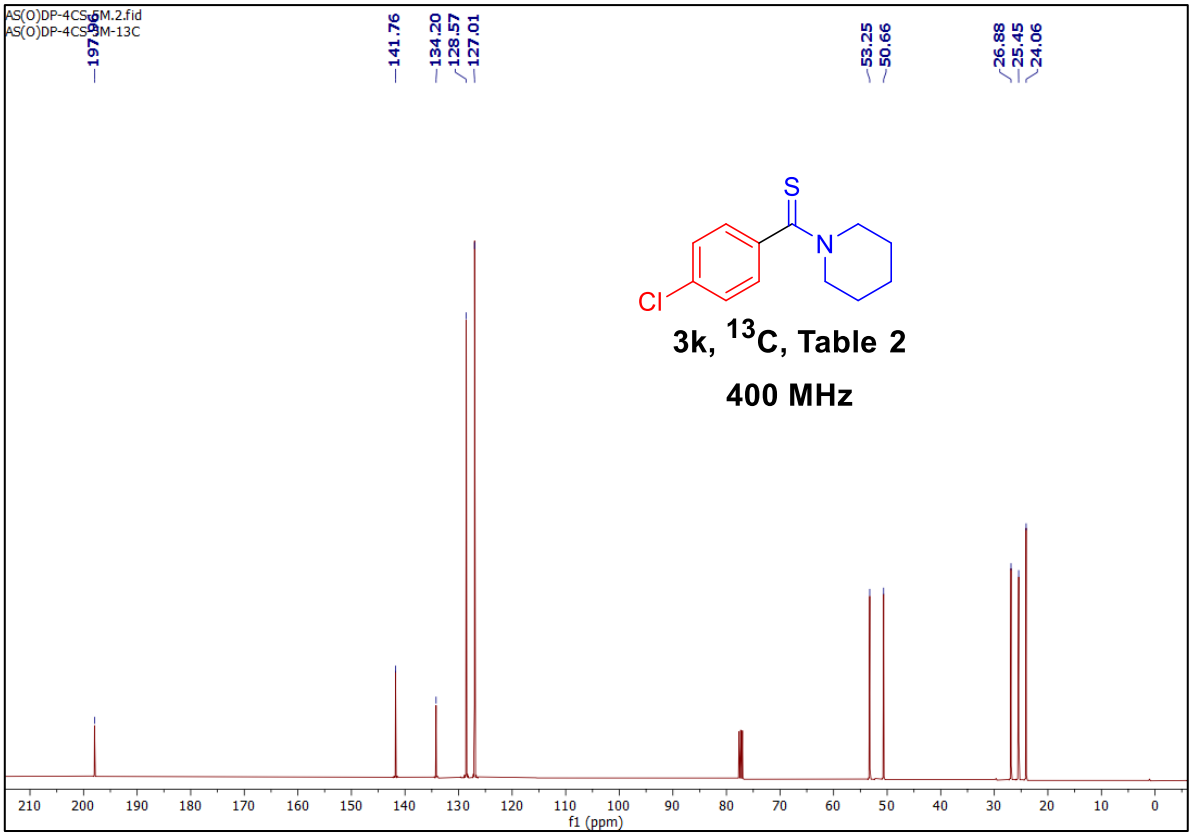
AS(O)DP-4CS-6M.2.fid
AS(O)DP-4CS-6M-13C
197.96
141.76
134.20
128.57
127.01
53.25
50.66
26.88
25.45
24.06
S
N
Cl
3k, 13C, Table 2
400 MHz
f1 (ppm)

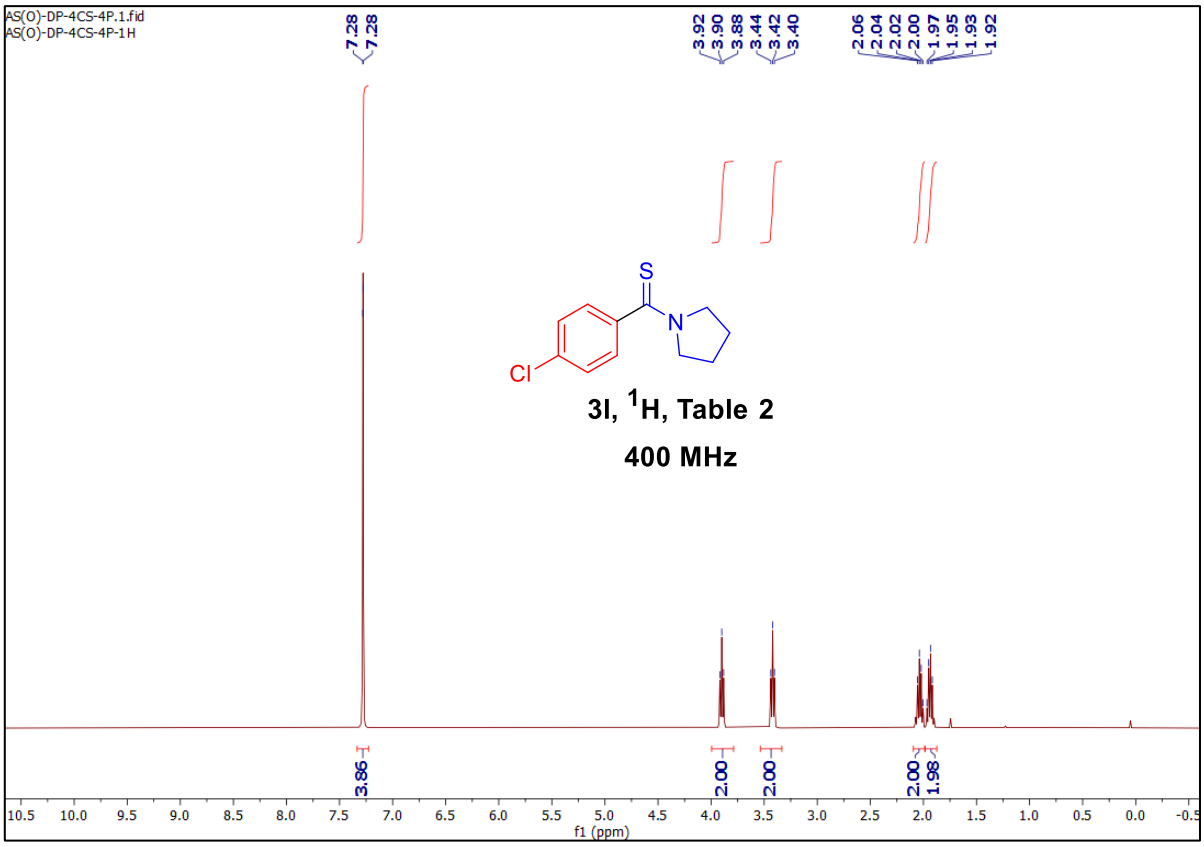
AS(O)-DP-4CS-4P.1.fid
AS(O)-DP-4CS-4P-1H
7.28
7.28
3.92
3.90
3.88
3.44
3.42
3.40
2.06
2.04
2.02
2.00
1.97
1.95
1.93
1.92
S
N
Cl
3l, 1H, Table 2
400 MHz
3.86
2.00
2.00
2.00
1.98
f1 (ppm)

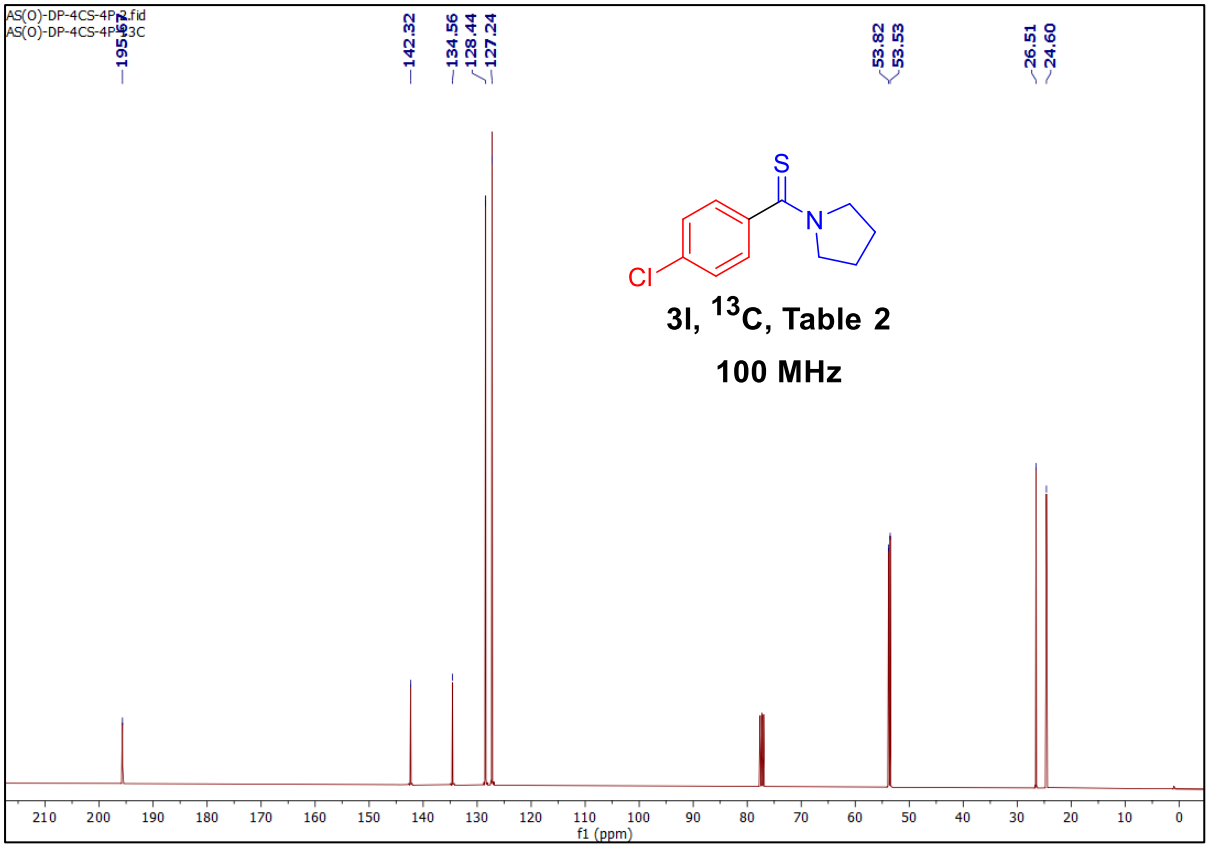
AS(O)-DP-4CS-4Pr-2.fid
AS(O)-DP-4CS-4Pr-13C
195.42
142.32
134.56
128.44
127.24
53.82
53.53
26.51
24.60
S
N
Cl
3l, 13C, Table 2
100 MHz
f1 (ppm)

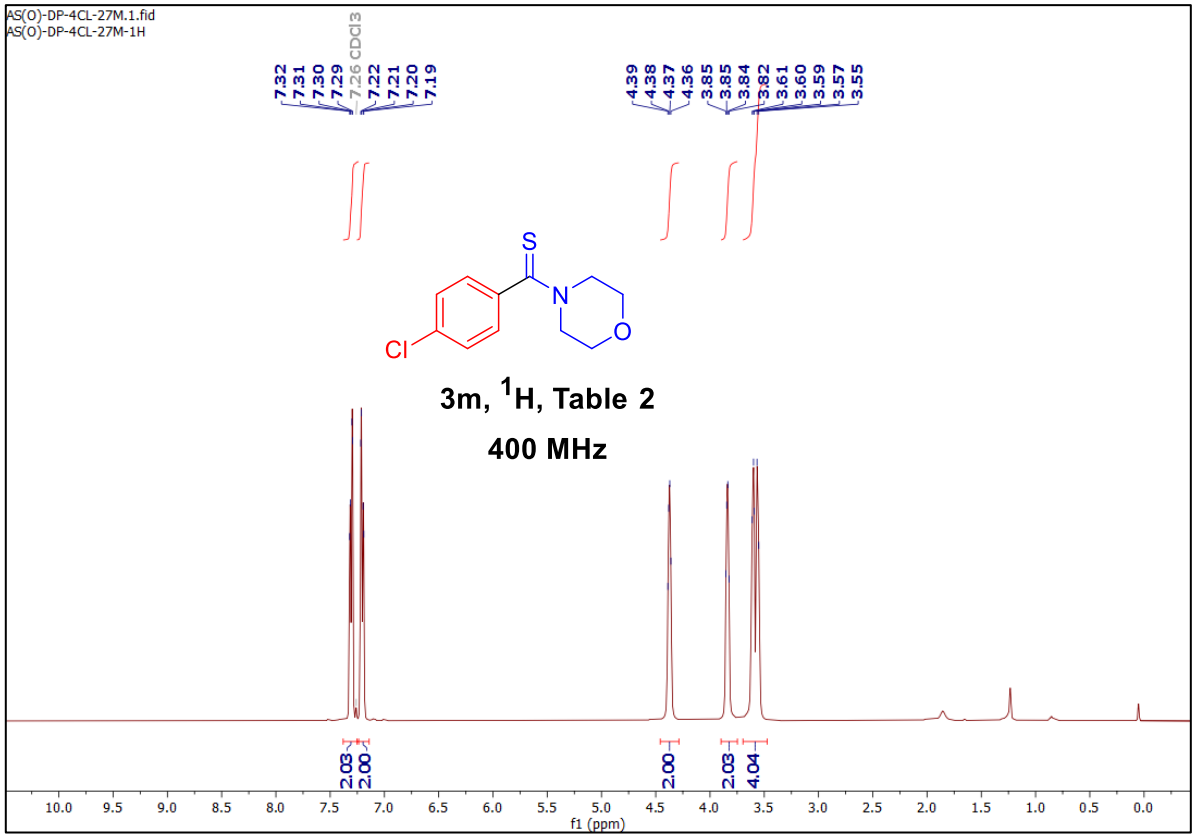
AS(O)-DP-4CL-27M.1.fid
AS(O)-DP-4CL-27M-1H
7.32
7.31
7.30
7.29
7.26 CDCl3
7.22
7.21
7.20
7.19
4.39
4.38
4.37
4.36
3.85
3.85
3.84
3.82
3.61
3.60
3.59
3.57
3.55
S
N
O
Cl
3m, 1H, Table 2
400 MHz
2.03
2.00
2.00
2.03
4.04
f1 (ppm)

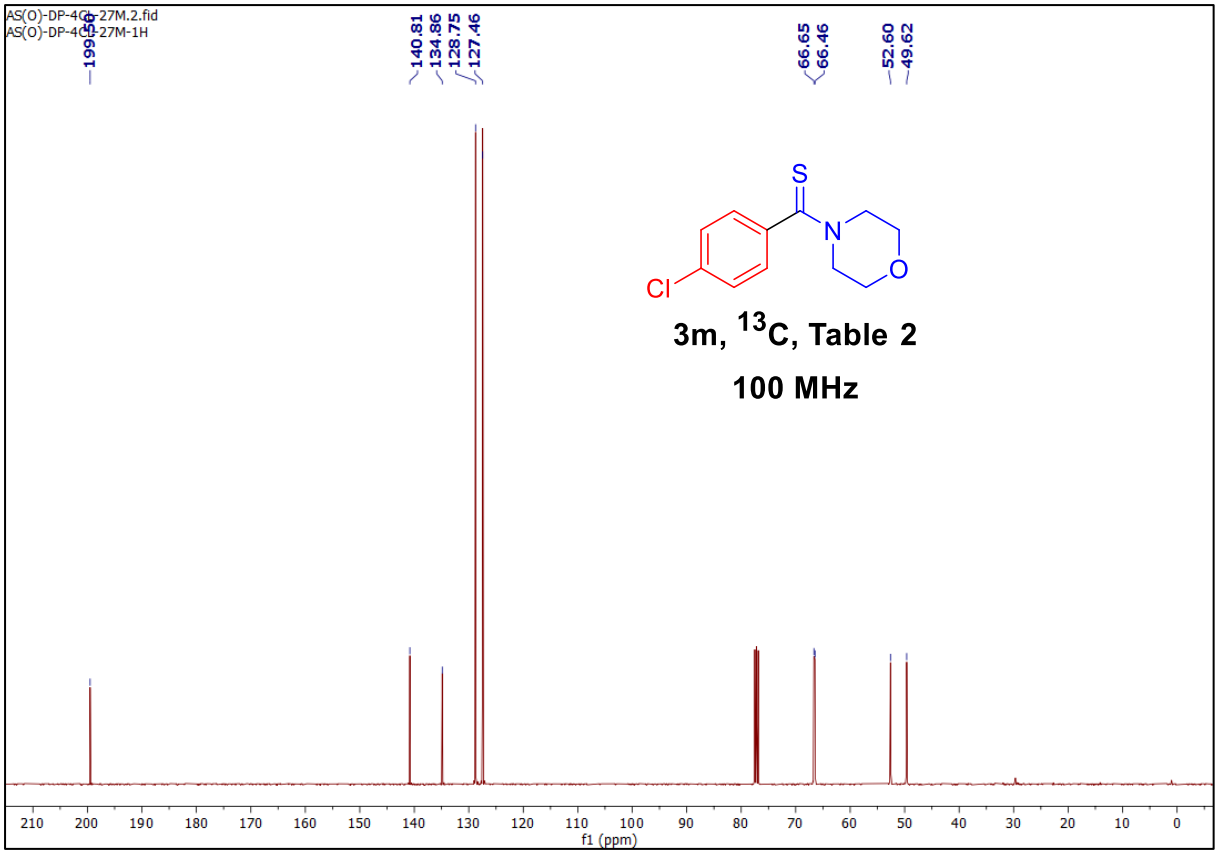

3m, ^{13}C, Table 2

100 MHz

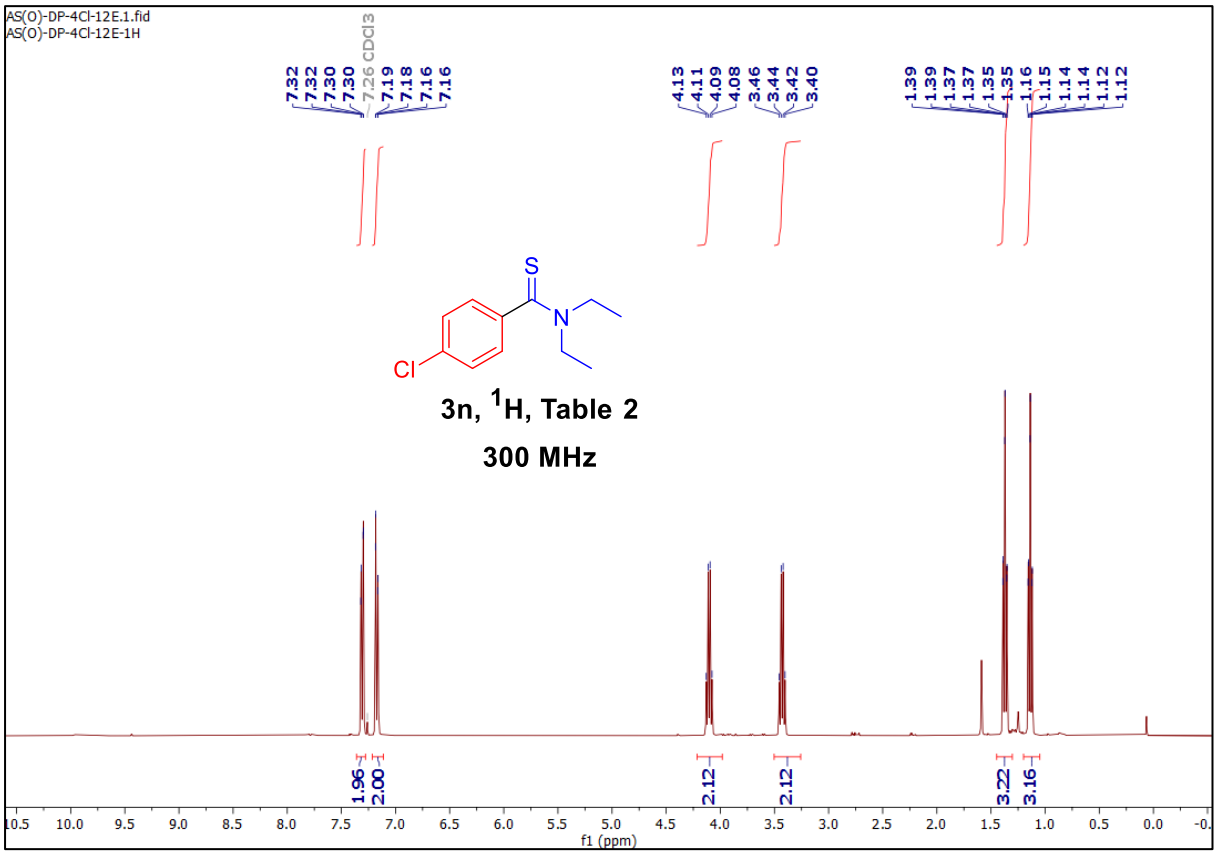

3n, ^{1}H, Table 2

300 MHz

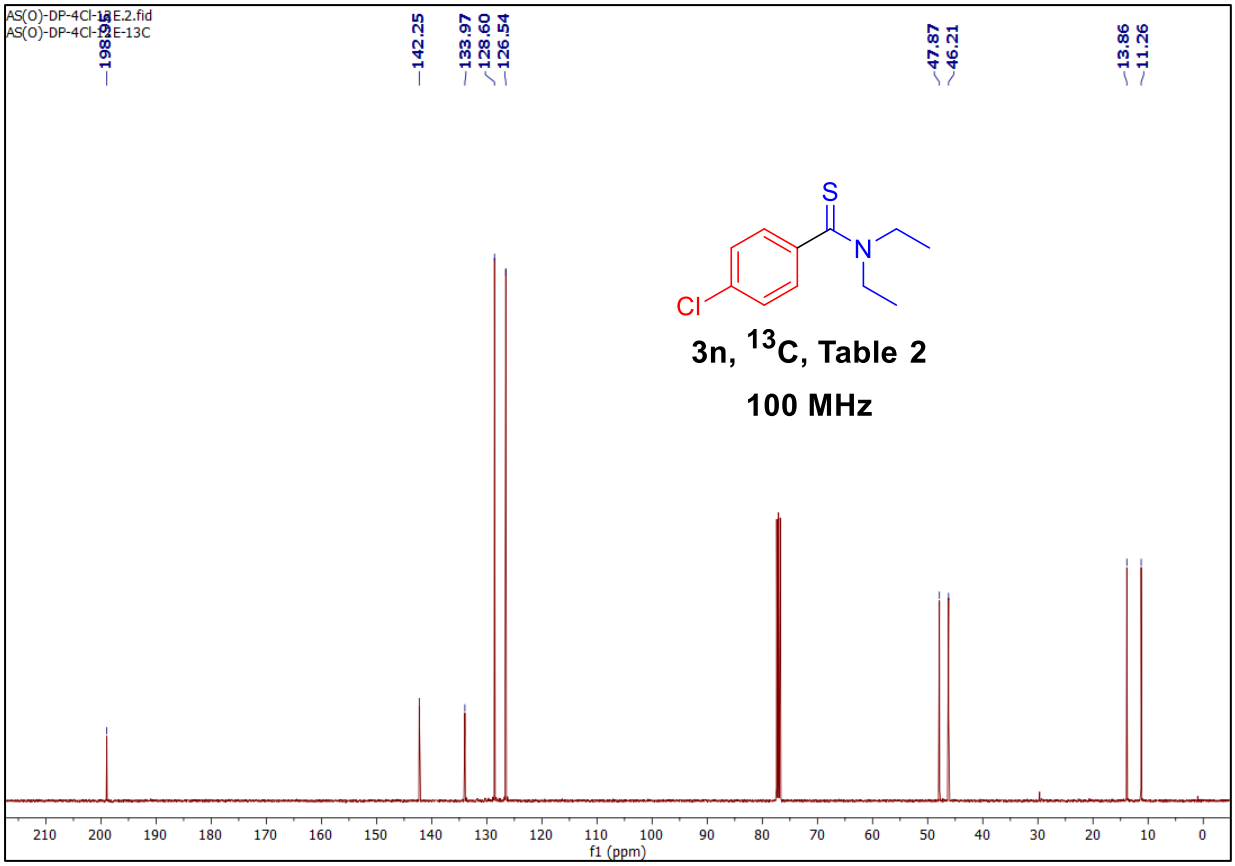
AS(O)-DP-4Cl-13E.2.fid
AS(O)-DP-4Cl-13E-13C
198.36
142.25
133.97
128.60
126.54
47.87
46.21
13.86
11.26
S
N
Cl
3n, 13C, Table 2
100 MHz
f1 (ppm)

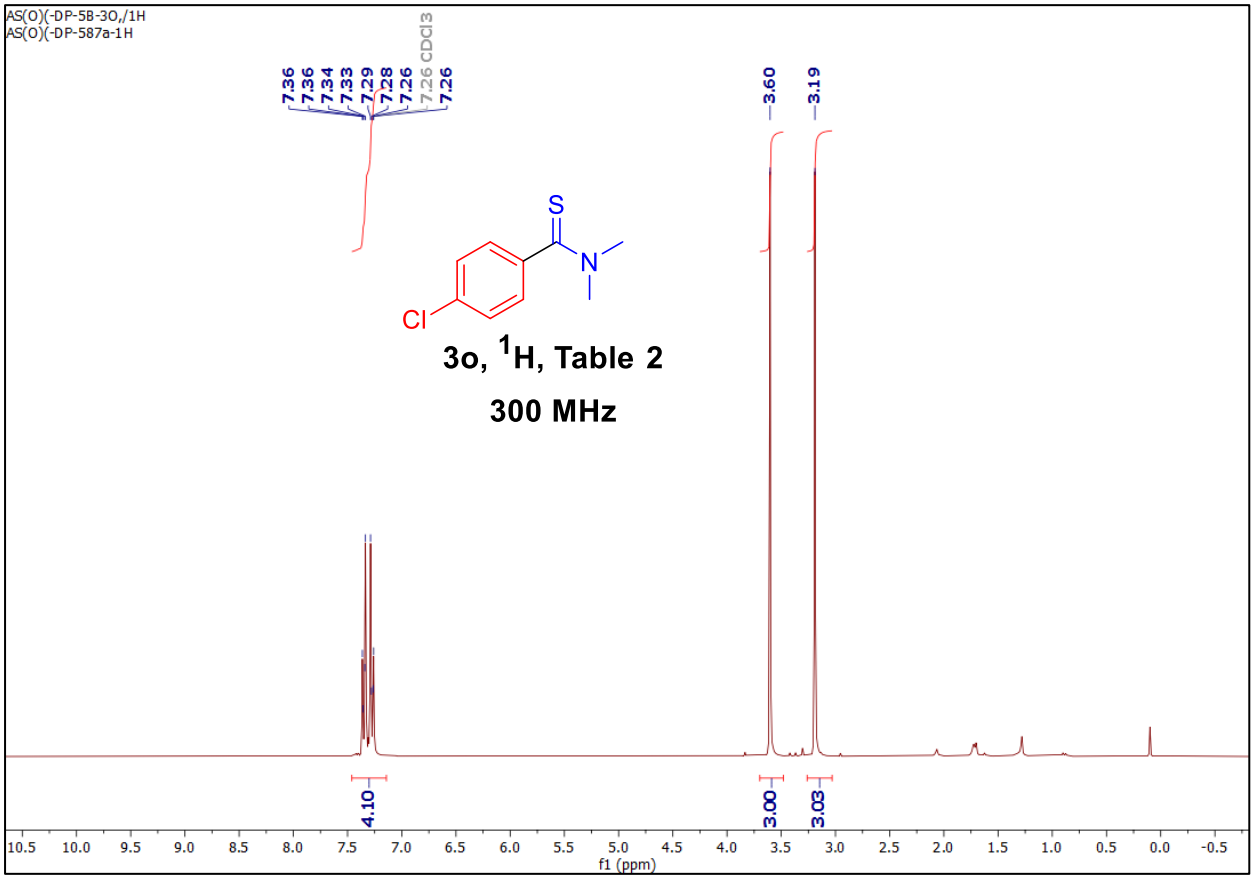
AS(O)(-DP-5B-3O,/1H
AS(O)(-DP-587a-1H
7.36
7.36
7.34
7.33
7.29
7.28
7.26
7.26 CDCl3
7.26
3.60
3.19
S
N
Cl
3o, 1H, Table 2
300 MHz
4.10
3.00
3.03
f1 (ppm)

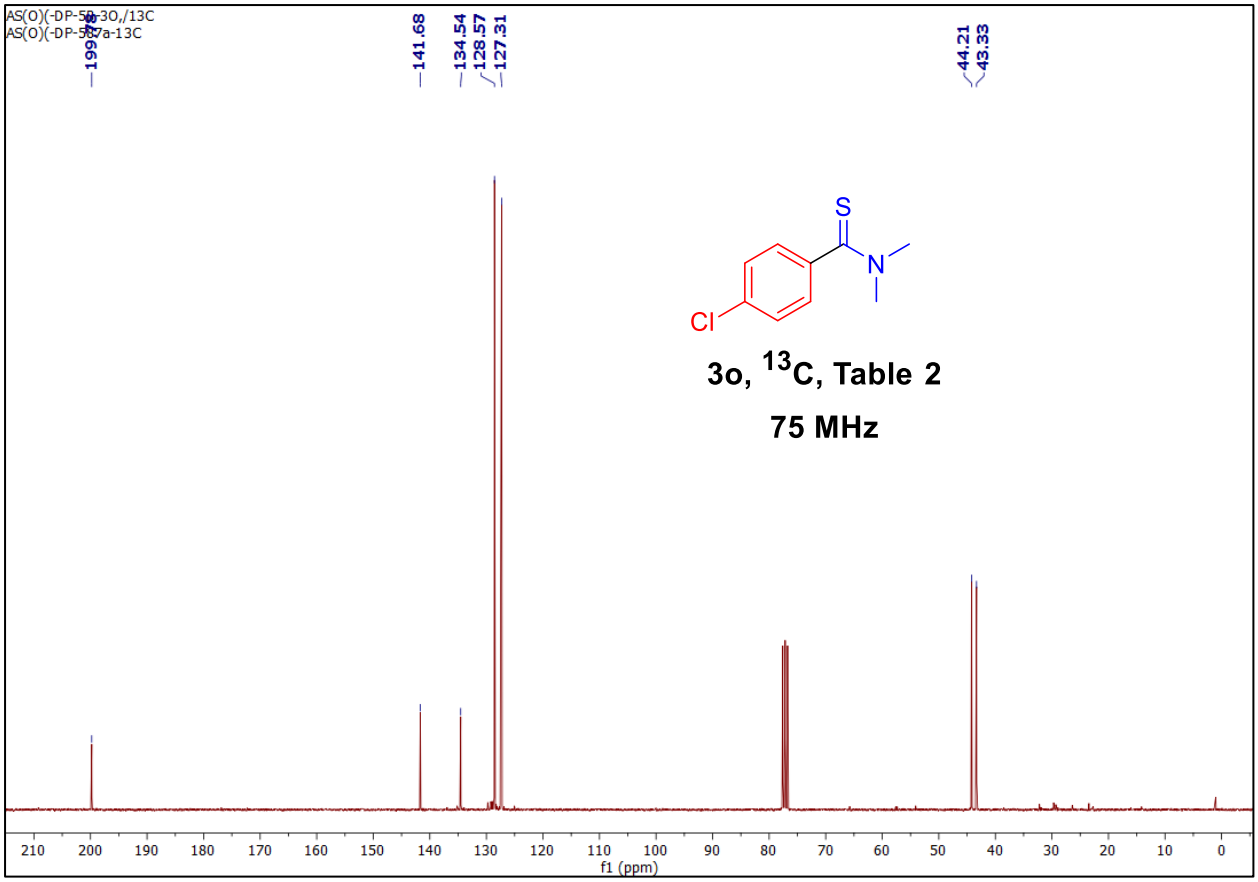
AS(O)-DP-5B-3O,/13C
AS(O)-DP-5B7a-13C
199.48
141.68
134.54
128.57
127.31
44.21
43.33
S
N
Cl
3o, 13C, Table 2
75 MHz
f1 (ppm)

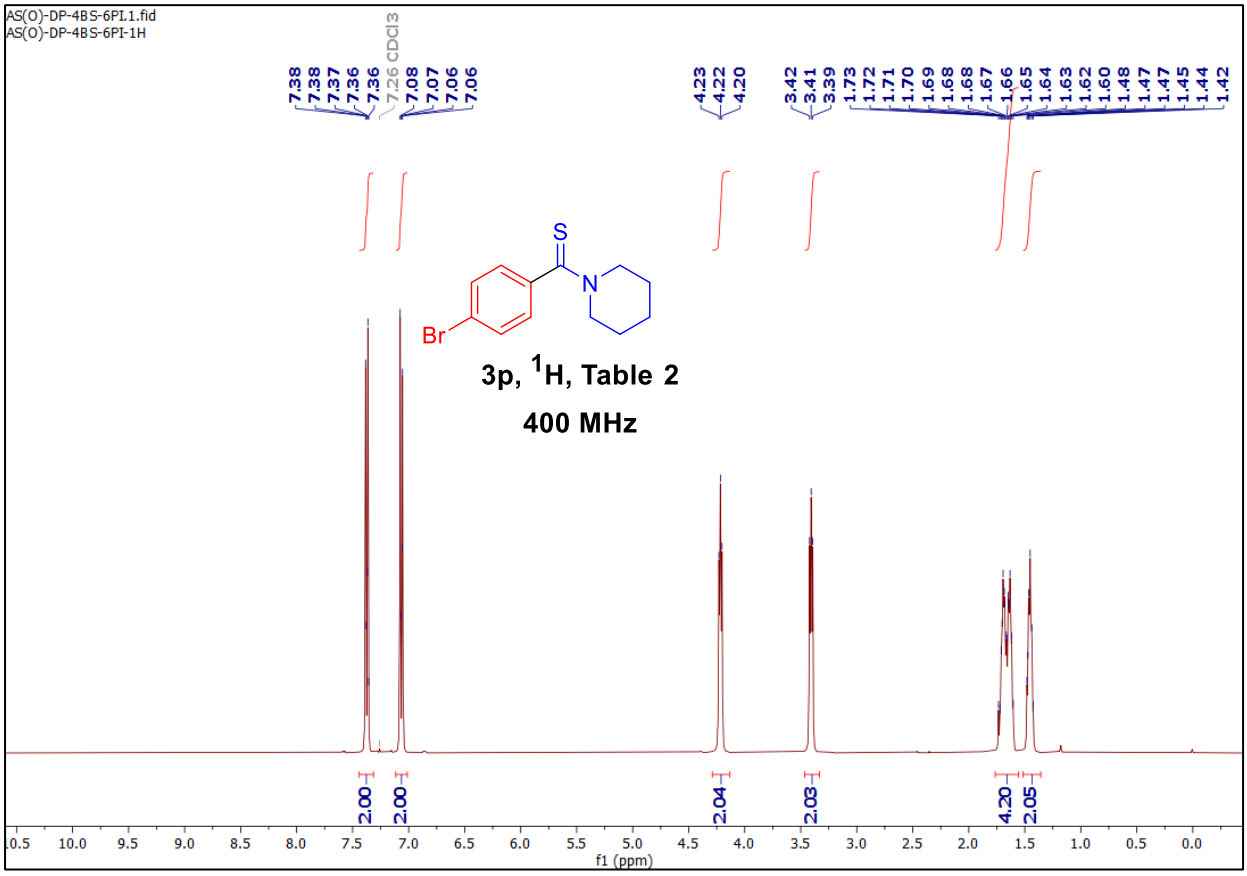
AS(O)-DP-4BS-6PI.1.fid
AS(O)-DP-4BS-6PI-1H
7.26 CDCl3
S
N
Br
3p, 1H, Table 2
400 MHz
2.00
2.00
2.04
2.03
4.20
2.05
f1 (ppm)

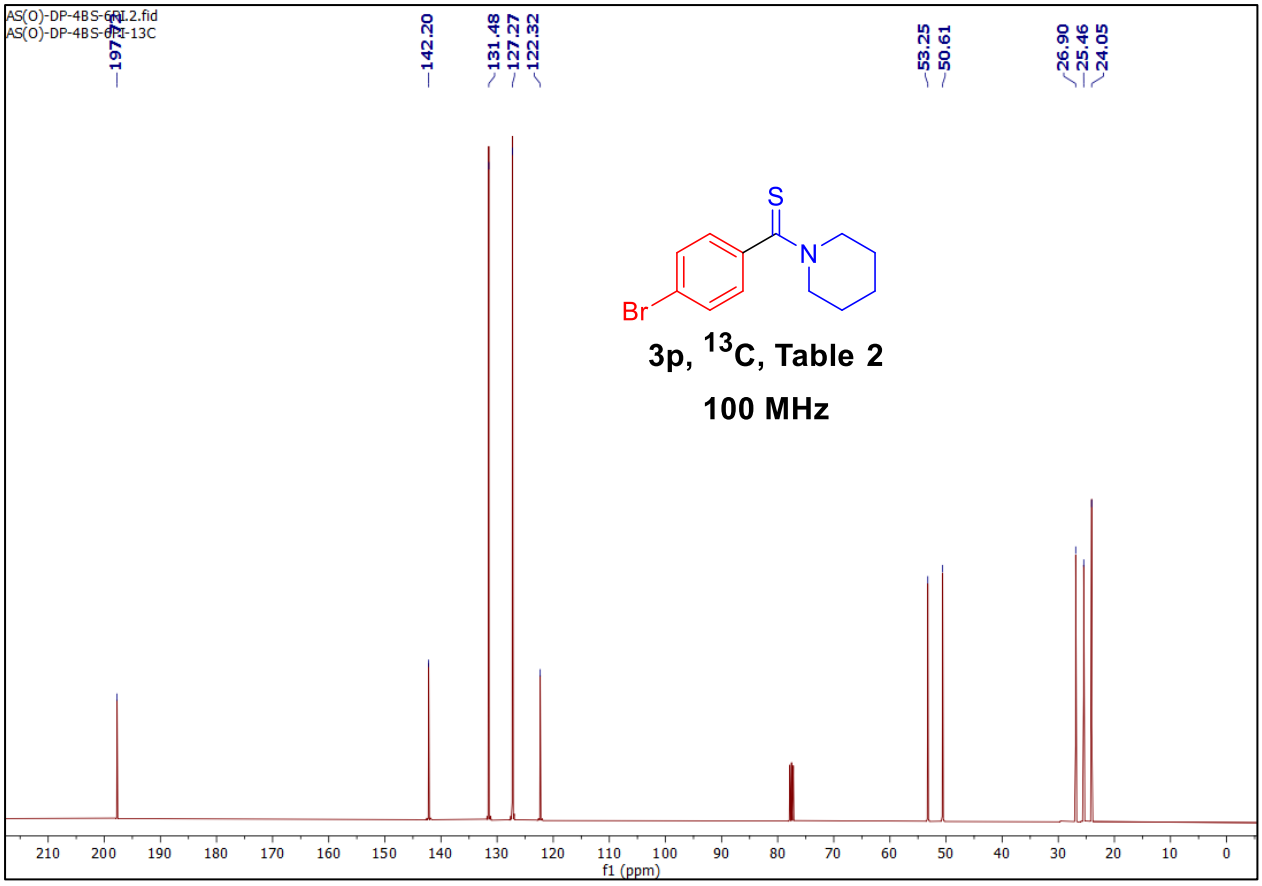
AS(O)-DP-4BS-6P1.2.fid
AS(O)-DP-4BS-6P-13C
197.
142.20
131.48
127.27
122.32
53.25
50.61
26.90
25.46
24.05
S
N
Br
3p, 13C, Table 2
100 MHz
f1 (ppm)

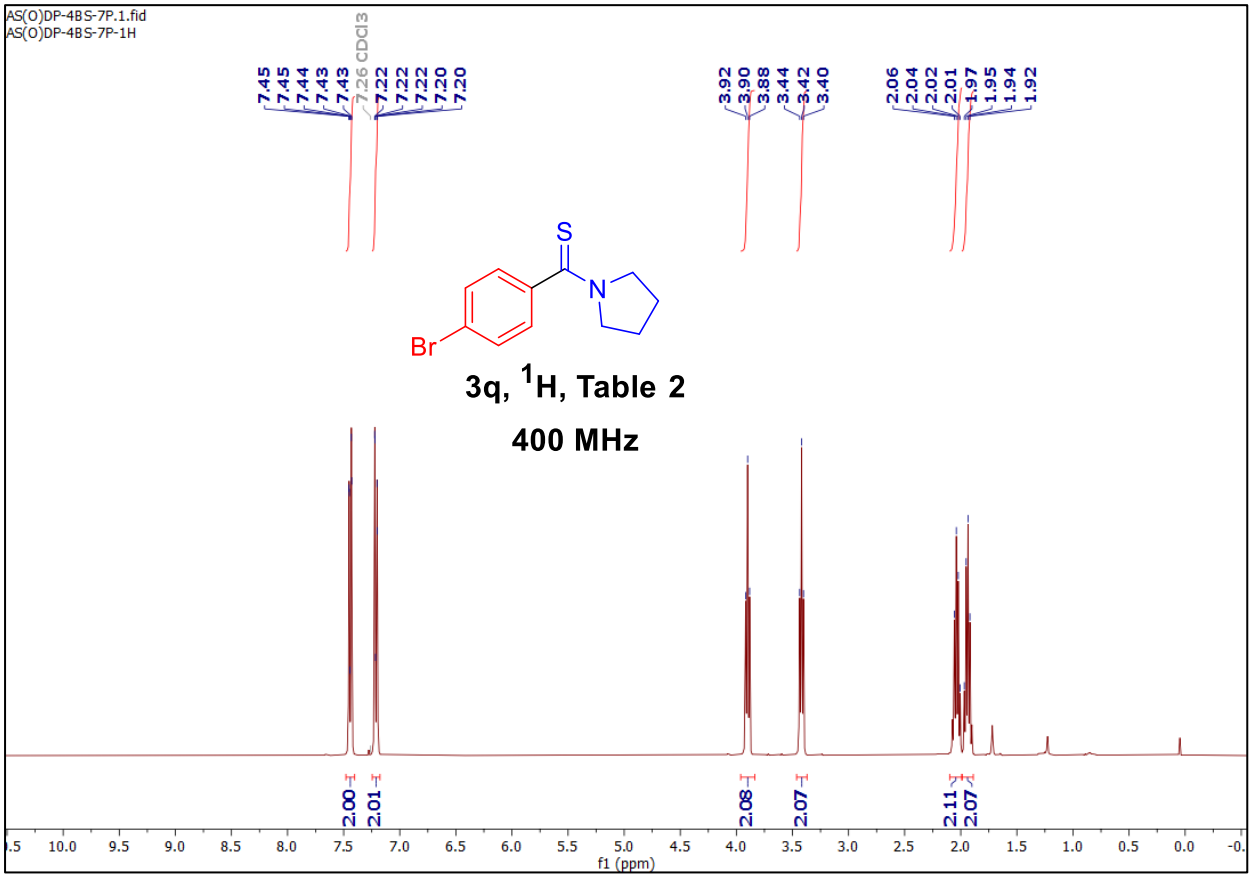
AS(O)DP-4BS-7P.1.fid
AS(O)DP-4BS-7P-1H
7.45
7.45
7.44
7.43
7.43
7.26 CDCl3
7.22
7.22
7.22
7.20
7.20
3.92
3.90
3.88
3.44
3.42
3.40
2.06
2.04
2.02
2.01
1.97
1.95
1.94
1.92
S
N
Br
3q, 1H, Table 2
400 MHz
2.00
2.01
2.08
2.07
2.11
2.07
f1 (ppm)

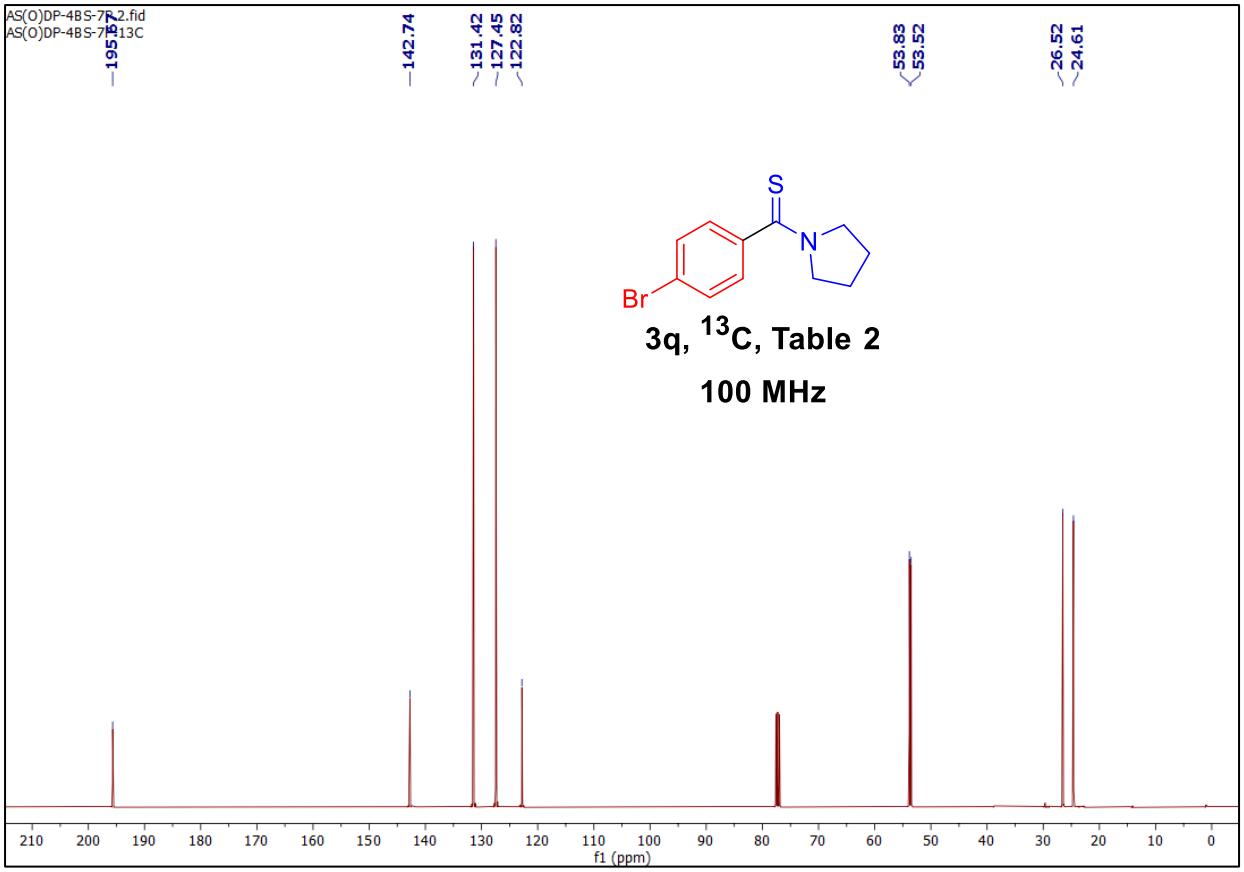
AS(O)DP-4BS-7[illegible]2.fid
AS(O)DP-4BS-7[illegible]13C
195.37
142.74
131.42
127.45
122.82
53.83
53.52
26.52
24.61
S
N
Br
3q, 13C, Table 2
100 MHz
f1 (ppm)

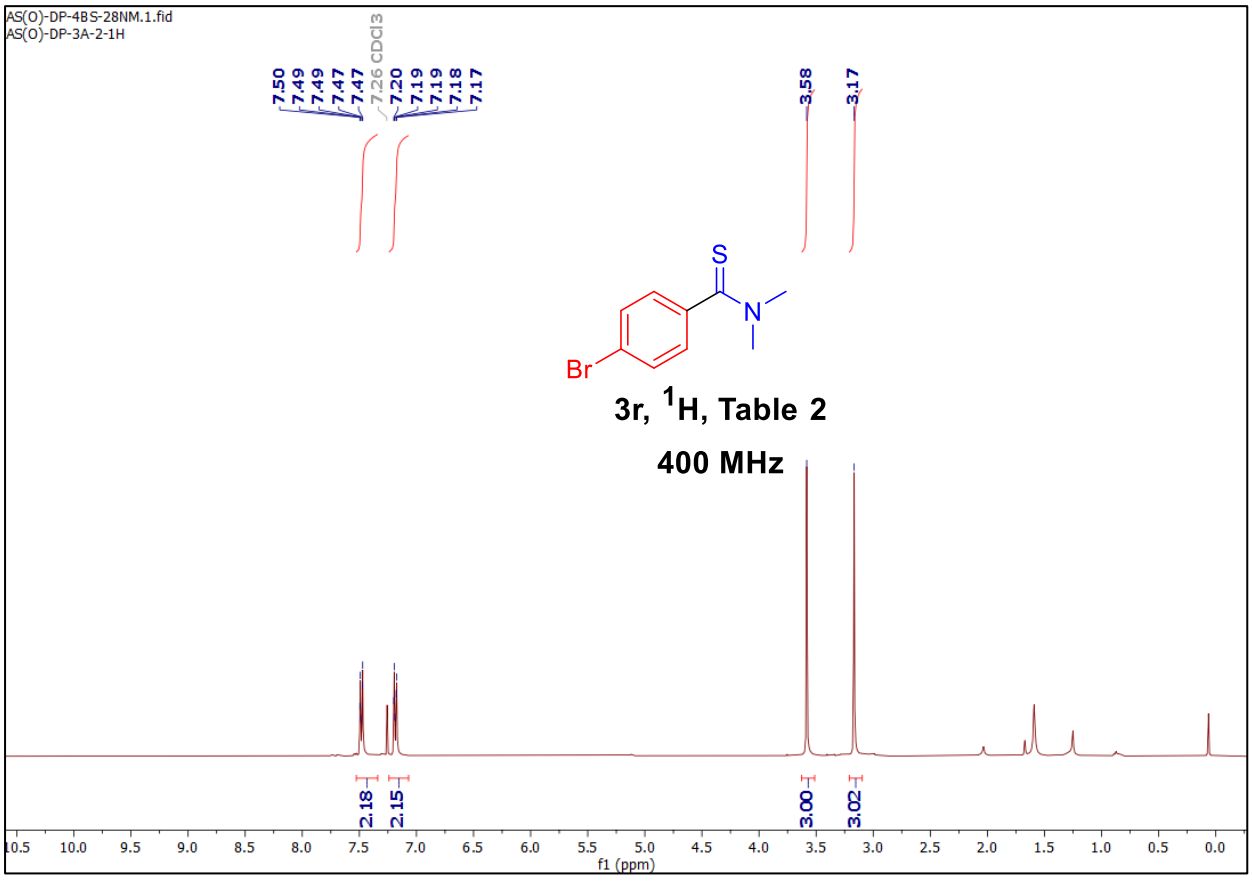
AS(O)-DP-4BS-28NM.1.fid
AS(O)-DP-3A-2-1H
7.50
7.49
7.49
7.47
7.47
7.26 CDCl3
7.20
7.19
7.19
7.18
7.17
3.58
3.17
S
N
Br
3r, 1H, Table 2
400 MHz
2.18
2.15
3.00
3.02
f1 (ppm)

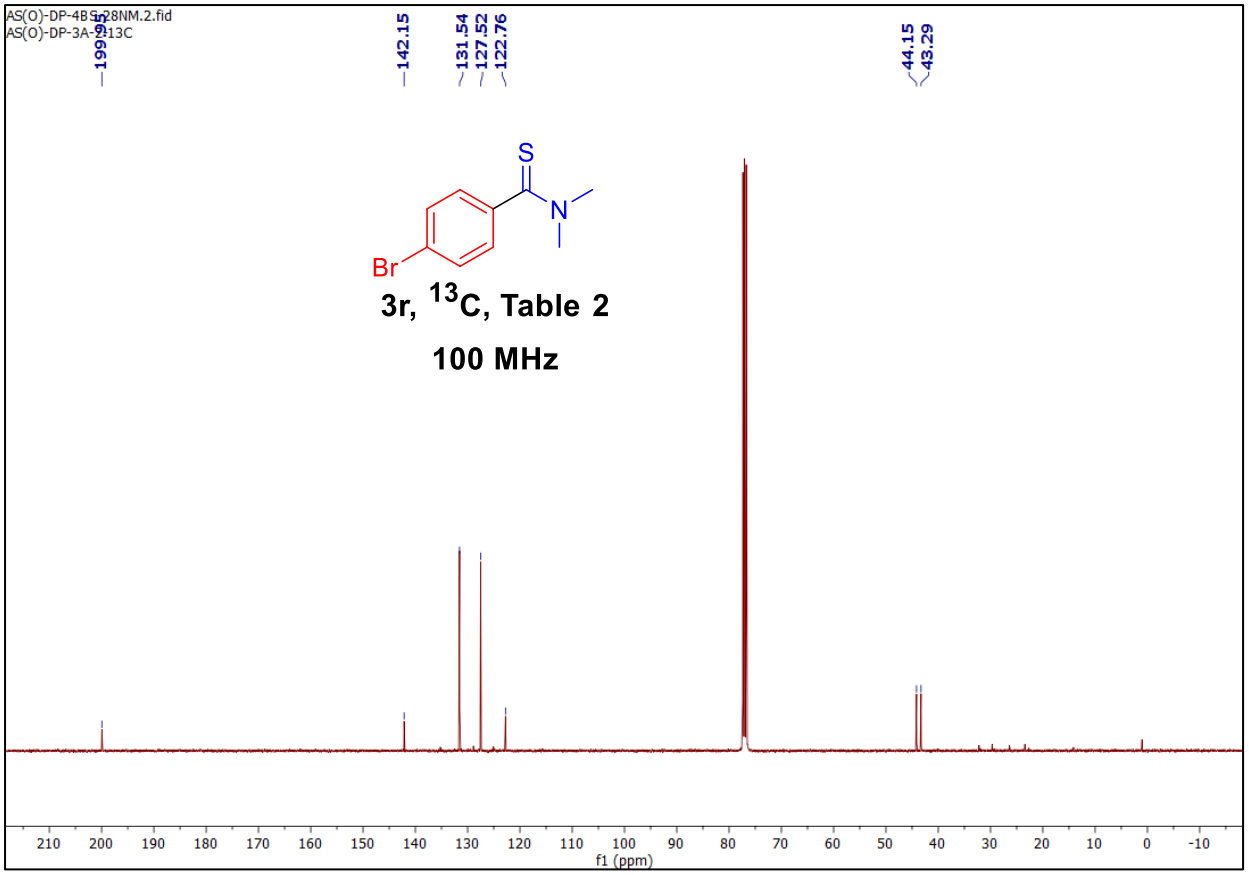
AS(O)-DP-4B-28NM.2.fid
AS(O)-DP-3A-213C
199.21
142.15
131.54
127.52
122.76
44.15
43.29
S
N
Br
3r, 13C, Table 2
100 MHz
f1 (ppm)

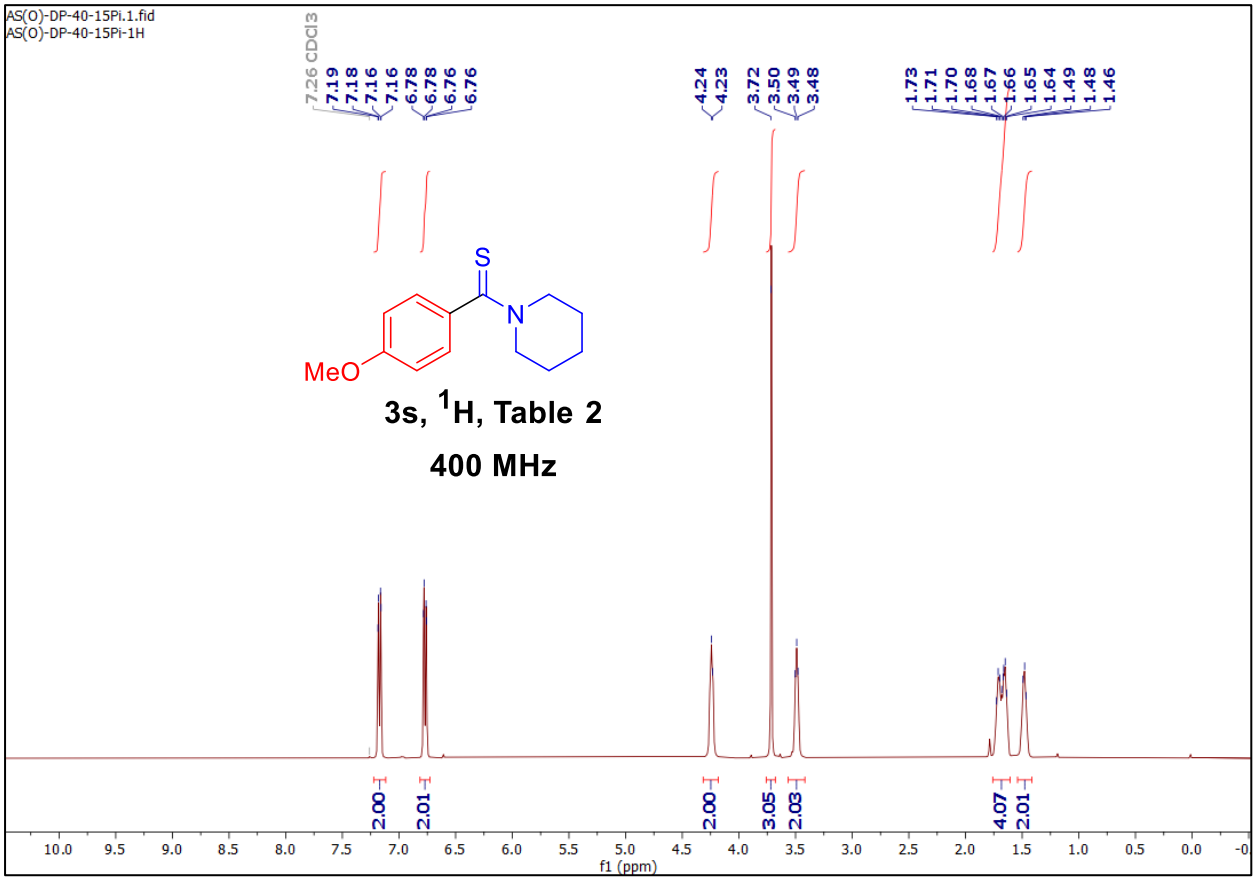
AS(O)-DP-40-15Pi.1.fid
AS(O)-DP-40-15Pi-1H
7.26 CDCl3
7.19
7.18
7.16
7.16
6.78
6.78
6.76
6.76
4.24
4.23
3.72
3.50
3.49
3.48
1.73
1.71
1.70
1.68
1.67
1.66
1.65
1.64
1.49
1.48
1.46
S
N
MeO
3s, 1H, Table 2
400 MHz
2.00
2.01
2.00
3.05
2.03
4.07
2.01
f1 (ppm)

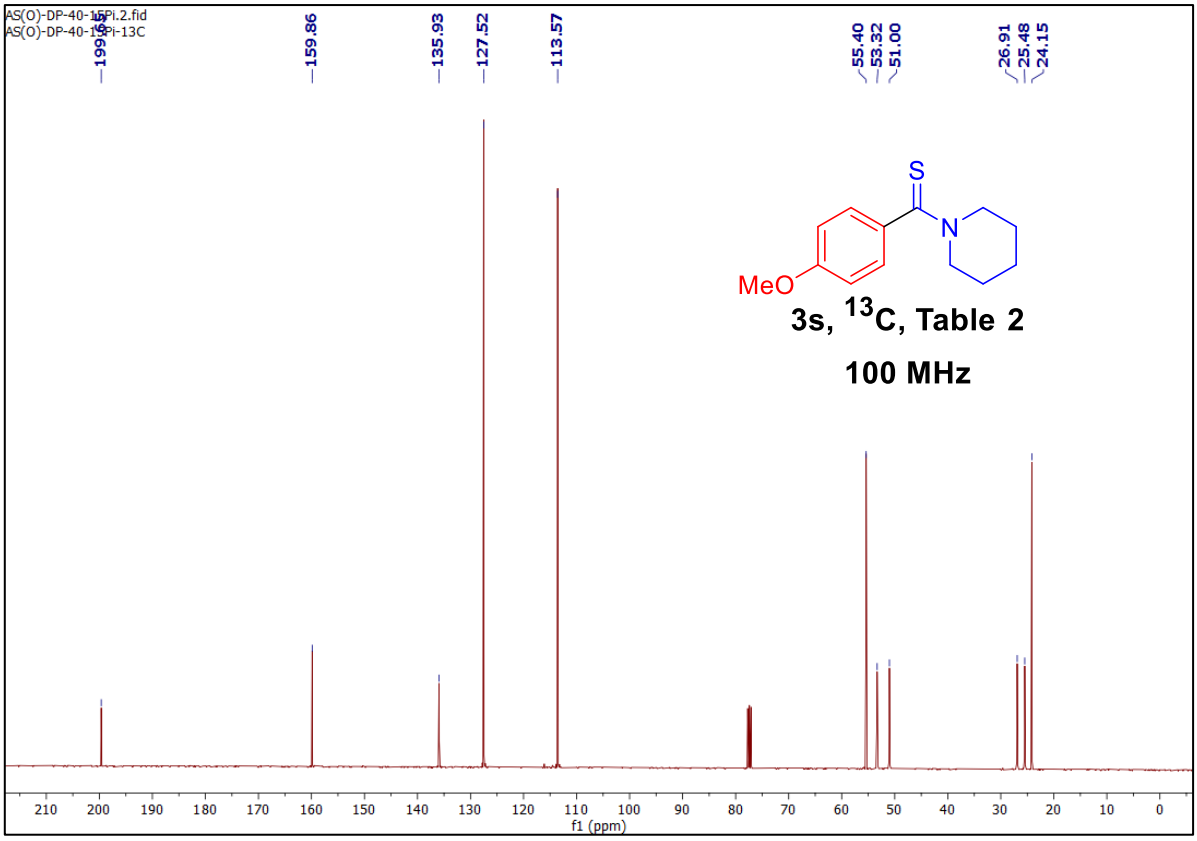
AS(O)-DP-40-15Pi.2.fid
AS(O)-DP-40-15Pi-13C
199.41
159.86
135.93
127.52
113.57
55.40
53.32
51.00
26.91
25.48
24.15
S
N
MeO
3s, 13C, Table 2
100 MHz
f1 (ppm)

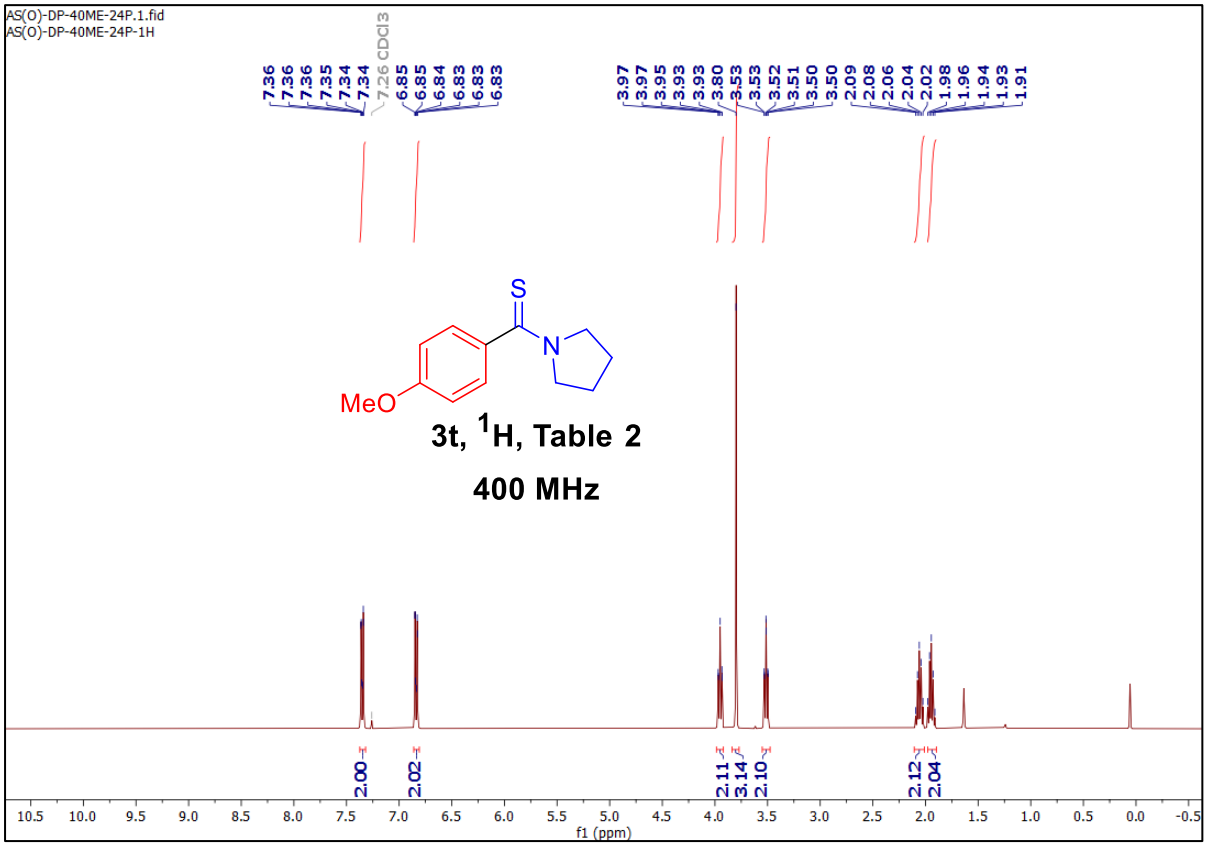
AS(O)-DP-40ME-24P.1.fid
AS(O)-DP-40ME-24P-1H
7.36
7.36
7.36
7.35
7.34
7.34
7.26 CDCl3
6.85
6.85
6.84
6.83
6.83
6.83
3.97
3.97
3.95
3.93
3.93
3.80
3.53
3.53
3.52
3.51
3.50
3.50
2.09
2.08
2.06
2.04
2.02
1.98
1.96
1.94
1.93
1.91
S
N
MeO
3t, 1H, Table 2
400 MHz
2.00
2.02
2.11
3.14
2.10
2.12
2.04
f1 (ppm)

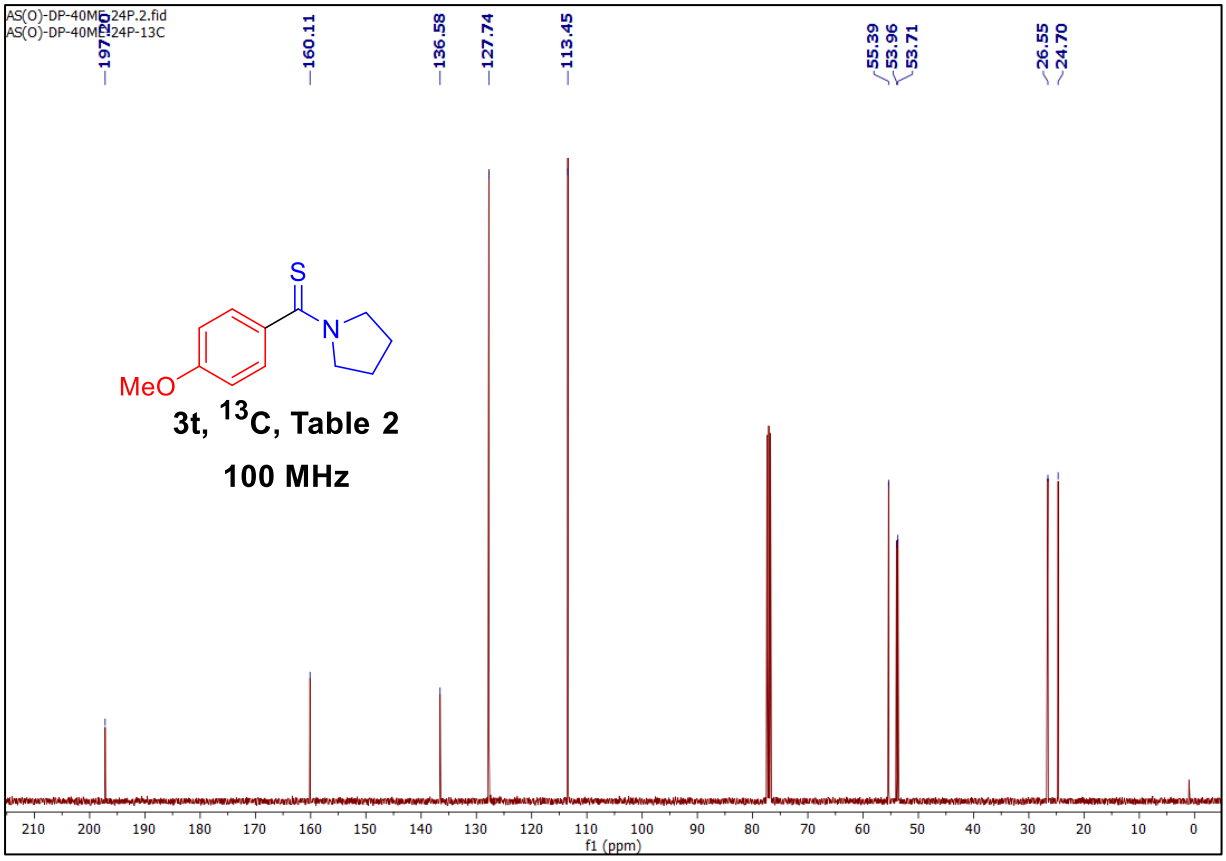
AS(O)-DP-40ME-24P.2.fid
AS(O)-DP-40ME-24P-13C
197.52
160.11
136.58
127.74
113.45
55.39
53.96
53.71
26.55
24.70
S
N
MeO
3t, 13C, Table 2
100 MHz
f1 (ppm)

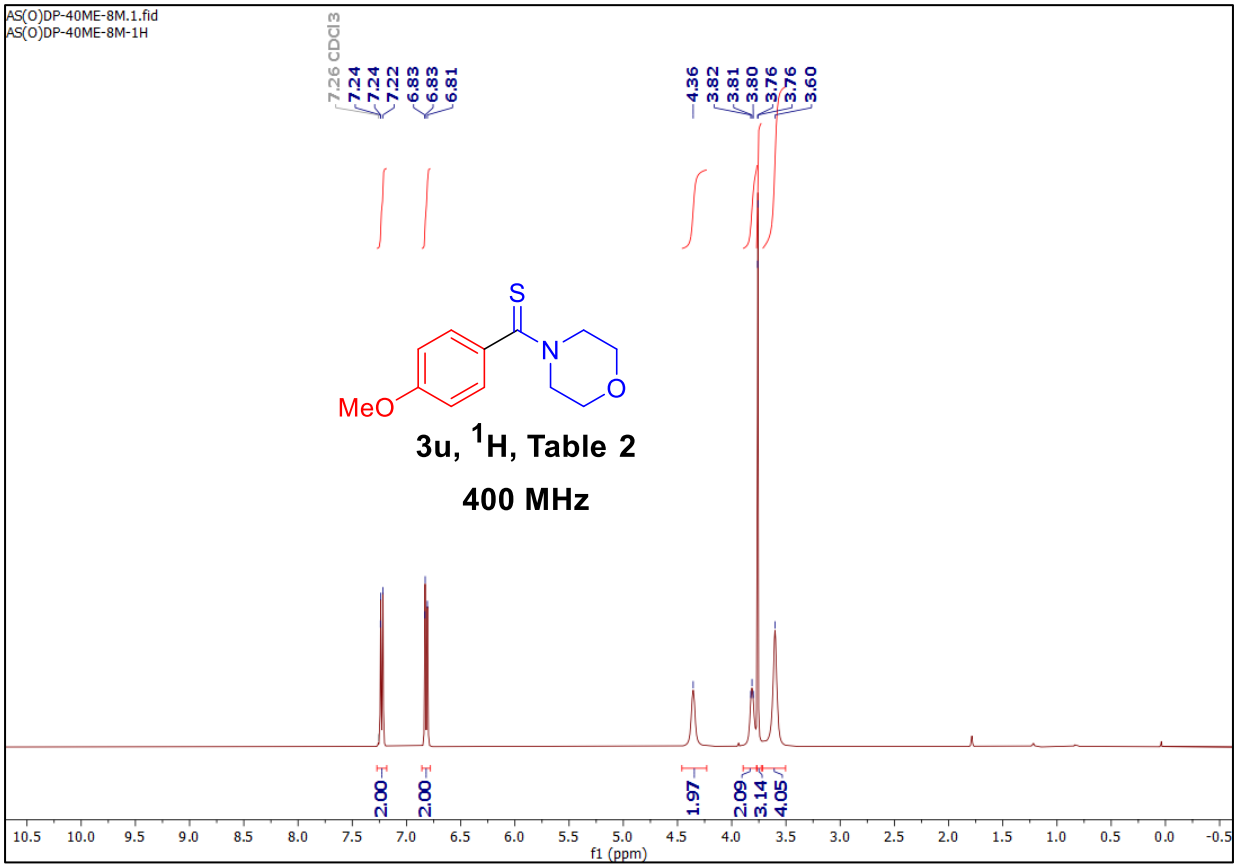
AS(O)DP-40ME-8M.1.fid
AS(O)DP-40ME-8M-1H
7.26 CDCl3
7.24
7.24
7.22
6.83
6.83
6.81
4.36
3.82
3.81
3.80
3.76
3.76
3.60
S
N
O
MeO
3u, 1H, Table 2
400 MHz
2.00
2.00
1.97
2.09
3.14
4.05
f1 (ppm)

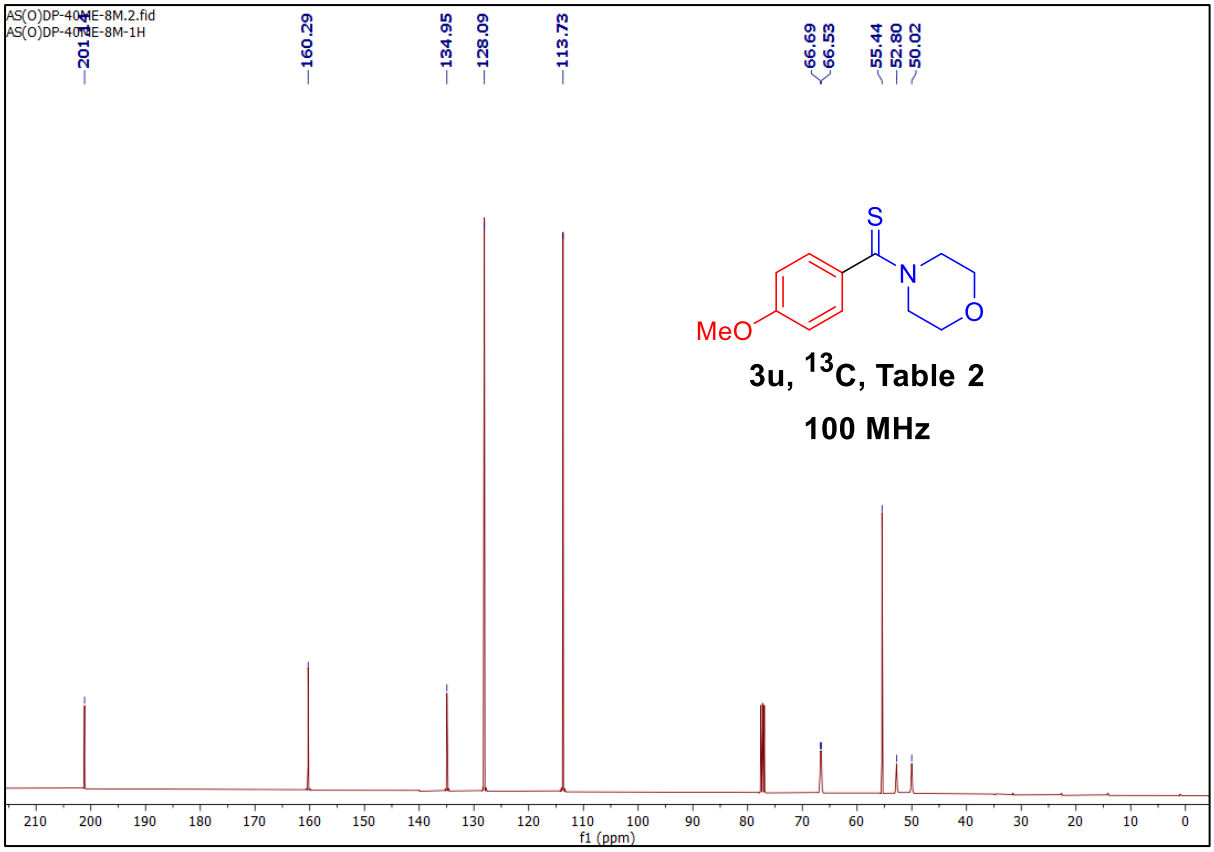
AS(O)DP-40ME-8M.2.fid
AS(O)DP-40ME-8M-1H
201.43
160.29
134.95
128.09
113.73
66.69
66.53
55.44
52.80
50.02
S
N
O
MeO
3u, 13C, Table 2
100 MHz
f1 (ppm)

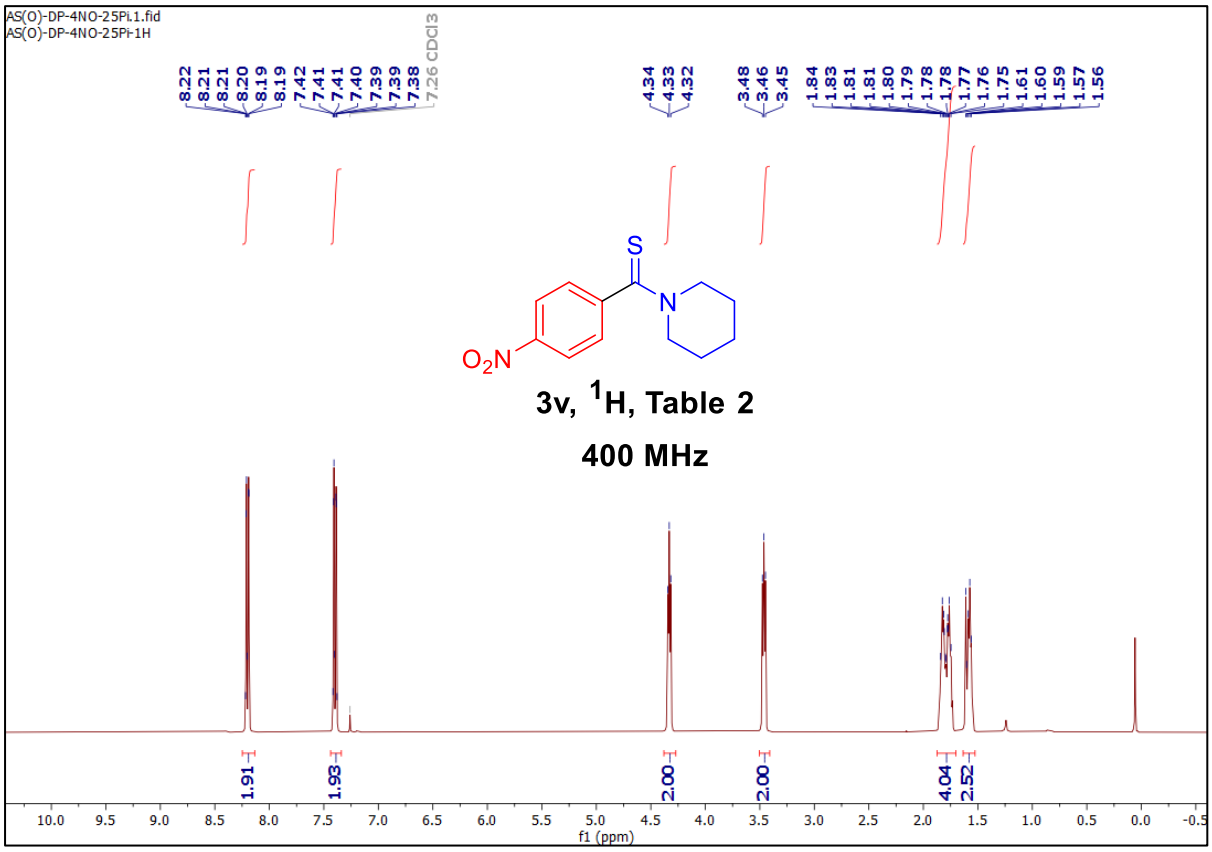
AS(O)-DP-4NO-25Pi.1.fid
AS(O)-DP-4NO-25Pi-1H
8.22
8.21
8.21
8.20
8.19
7.42
7.41
7.41
7.40
7.39
7.39
7.38
7.26 CDCl3
4.34
4.33
4.32
3.48
3.46
3.45
1.84
1.83
1.81
1.81
1.80
1.79
1.78
1.78
1.77
1.76
1.75
1.61
1.60
1.59
1.57
1.56
S
N
O2N
3v, 1H, Table 2
400 MHz
1.91
1.93
2.00
2.00
4.04
2.52
f1 (ppm)

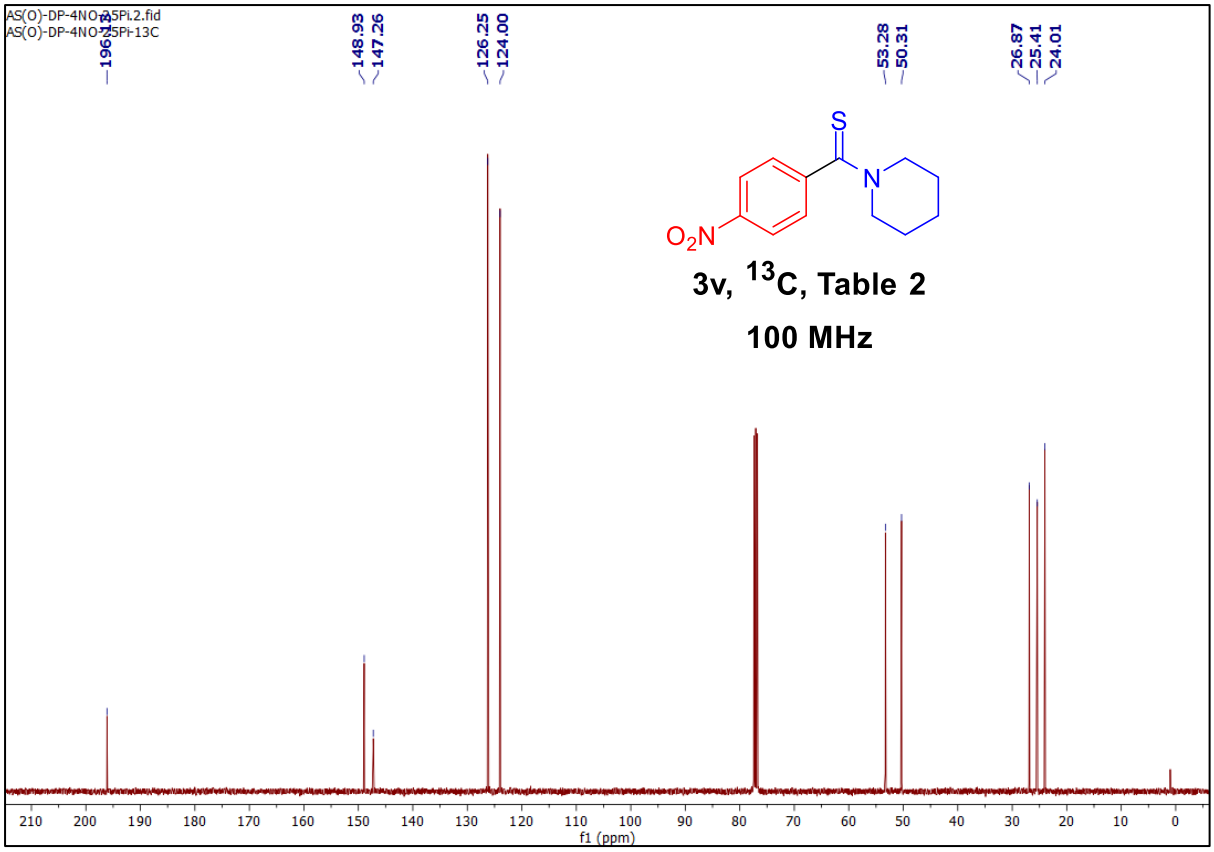
AS(O)-DP-4NO-25PI.2.fid
AS(O)-DP-4NO-25PI-13C
196.75
148.93
147.26
126.25
124.00
53.28
50.31
26.87
25.41
24.01
S
N
O2N
3v, 13C, Table 2
100 MHz
f1 (ppm)

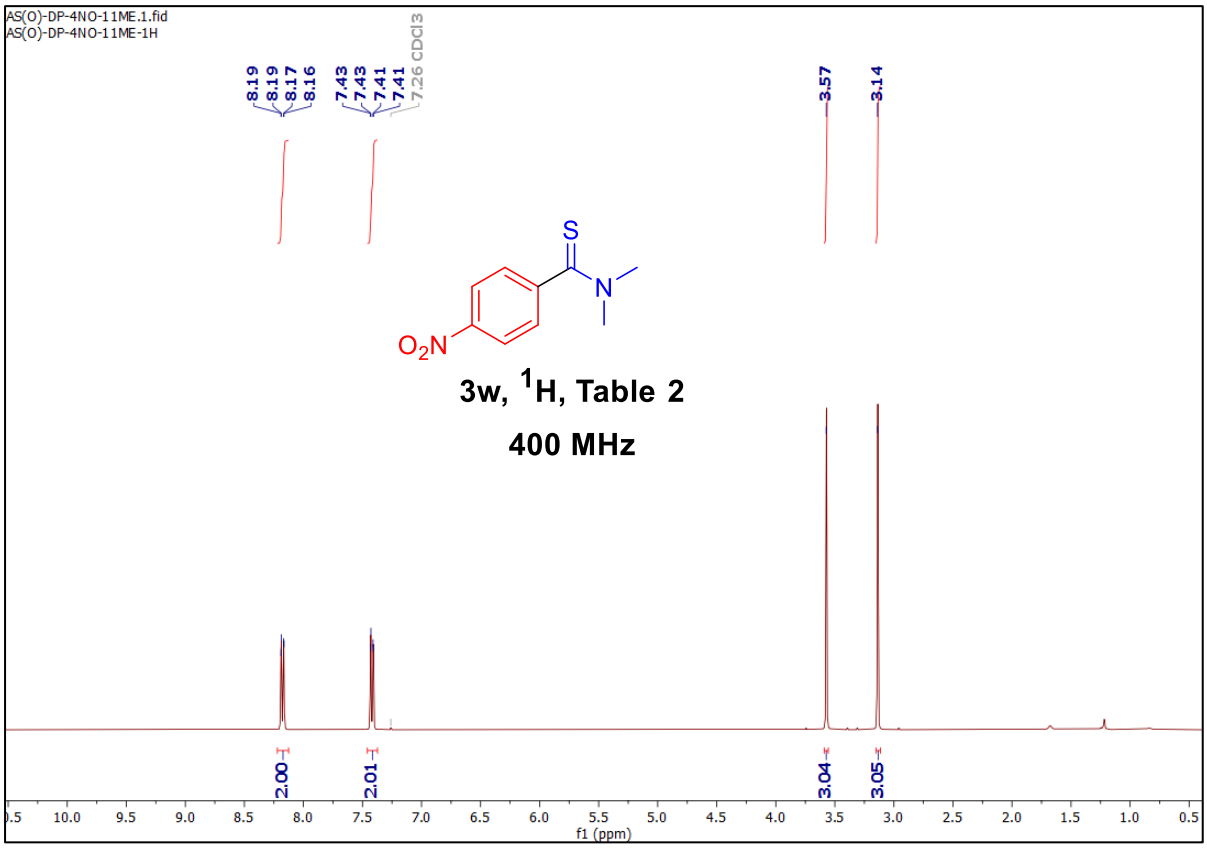
AS(O)-DP-4NO-11ME.1.fid
AS(O)-DP-4NO-11ME-1H
8.19
8.19
8.17
8.16
7.43
7.43
7.41
7.41
7.26 CDCl3
3.57
3.14
S
N
O2N
3w, 1H, Table 2
400 MHz
2.00
2.01
3.04
3.05
f1 (ppm)

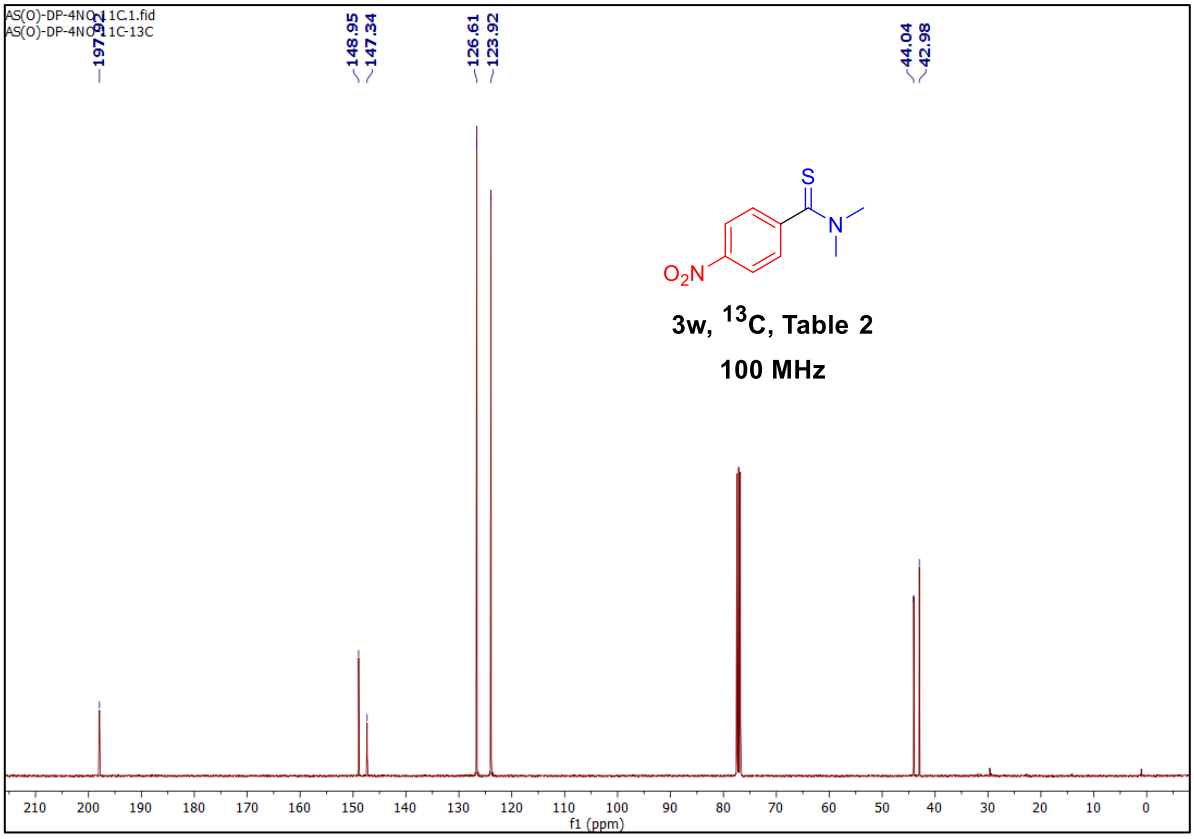
AS(O)-DP-4NO2-1C.1.fid
AS(O)-DP-4NO2-1C-13C
197.52
148.95
147.34
126.61
123.92
44.04
42.98
S
N
O2N
3w, 13C, Table 2
100 MHz
f1 (ppm)

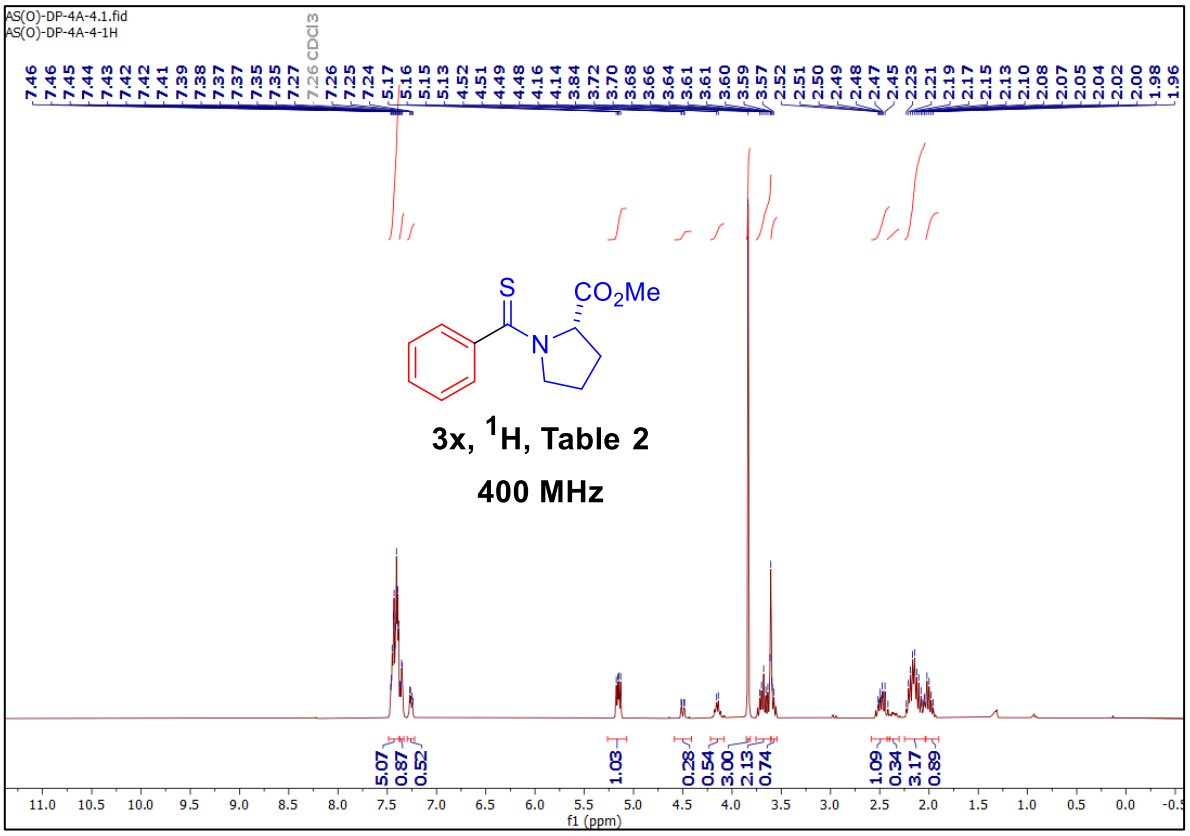
AS(O)-DP-4A-4.1.fid
AS(O)-DP-4A-4-1H
7.26 CDCl3
S
CO2Me
N
3x, 1H, Table 2
400 MHz
5.07
0.87
0.52
1.03
0.28
0.54
3.00
2.13
0.74
1.09
0.34
3.17
0.89
f1 (ppm)

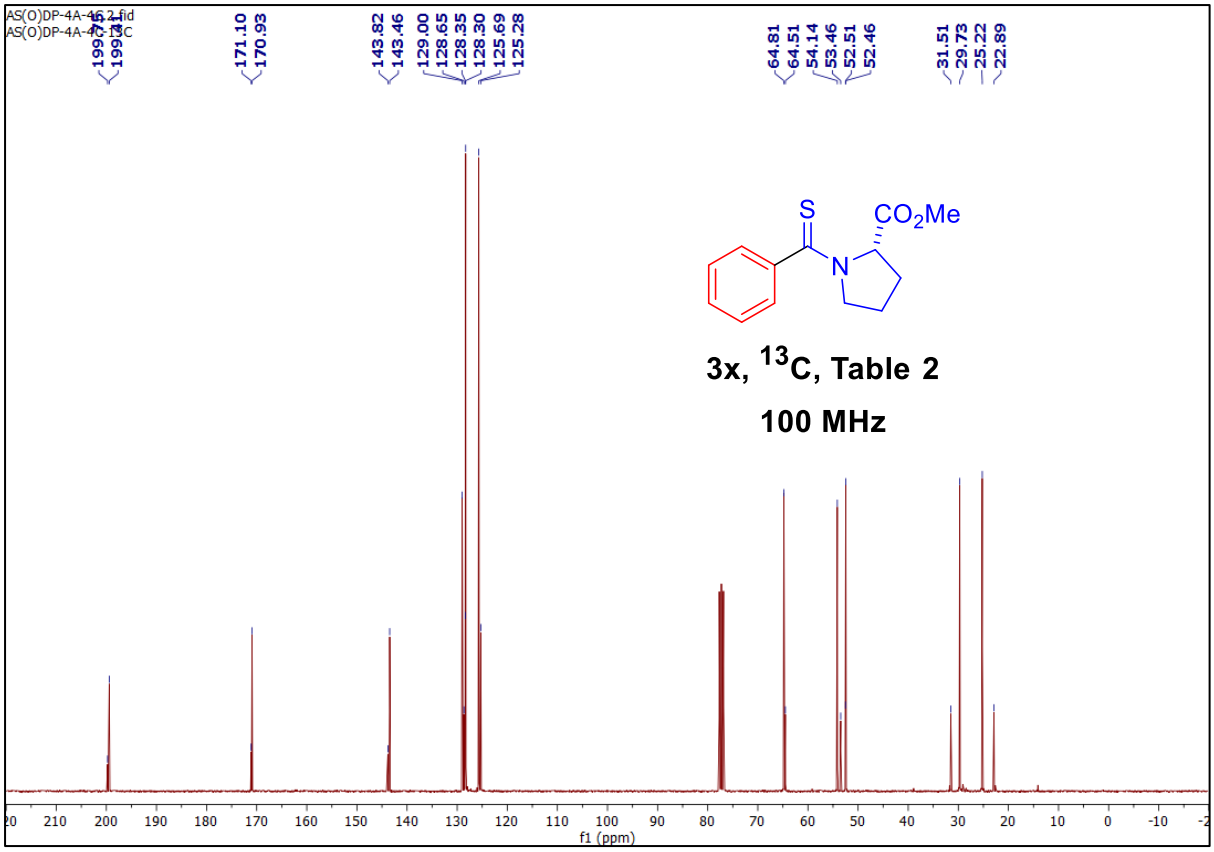
AS(O)DP-4A-46.2.fid
AS(O)DP-4A-46.13C
199.70
199.31
171.10
170.93
143.82
143.46
129.00
128.65
128.35
128.30
125.69
125.28
64.81
64.51
54.14
53.46
52.51
52.46
31.51
29.73
25.22
22.89
S
CO2Me
N
3x, 13C, Table 2
100 MHz
f1 (ppm)

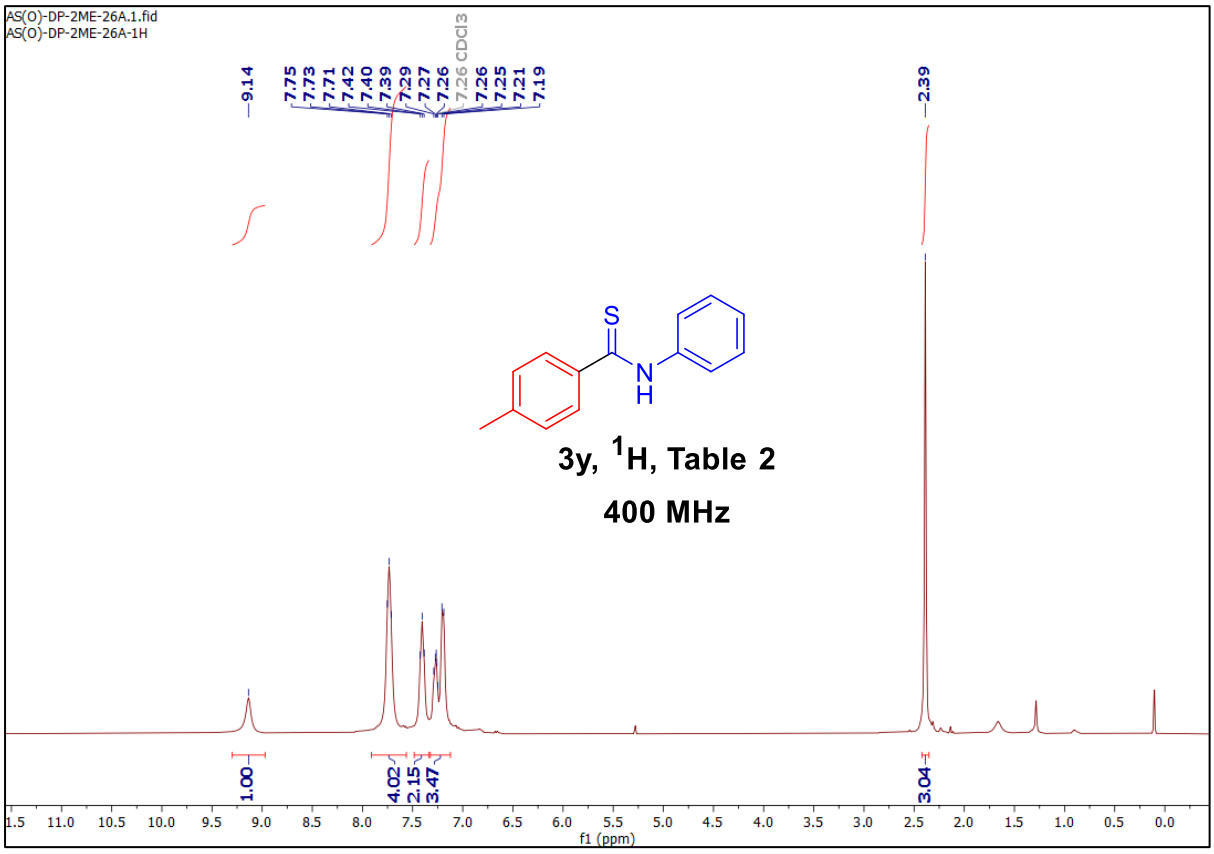
AS(O)-DP-2ME-26A.1.fid
AS(O)-DP-2ME-26A-1H
9.14
7.75
7.73
7.71
7.42
7.40
7.39
7.29
7.27
7.26
7.26 CDCl3
7.26
7.25
7.21
7.19
2.39
S
N
H
3y, 1H, Table 2
400 MHz
1.00
4.02
2.15
3.47
3.04
f1 (ppm)

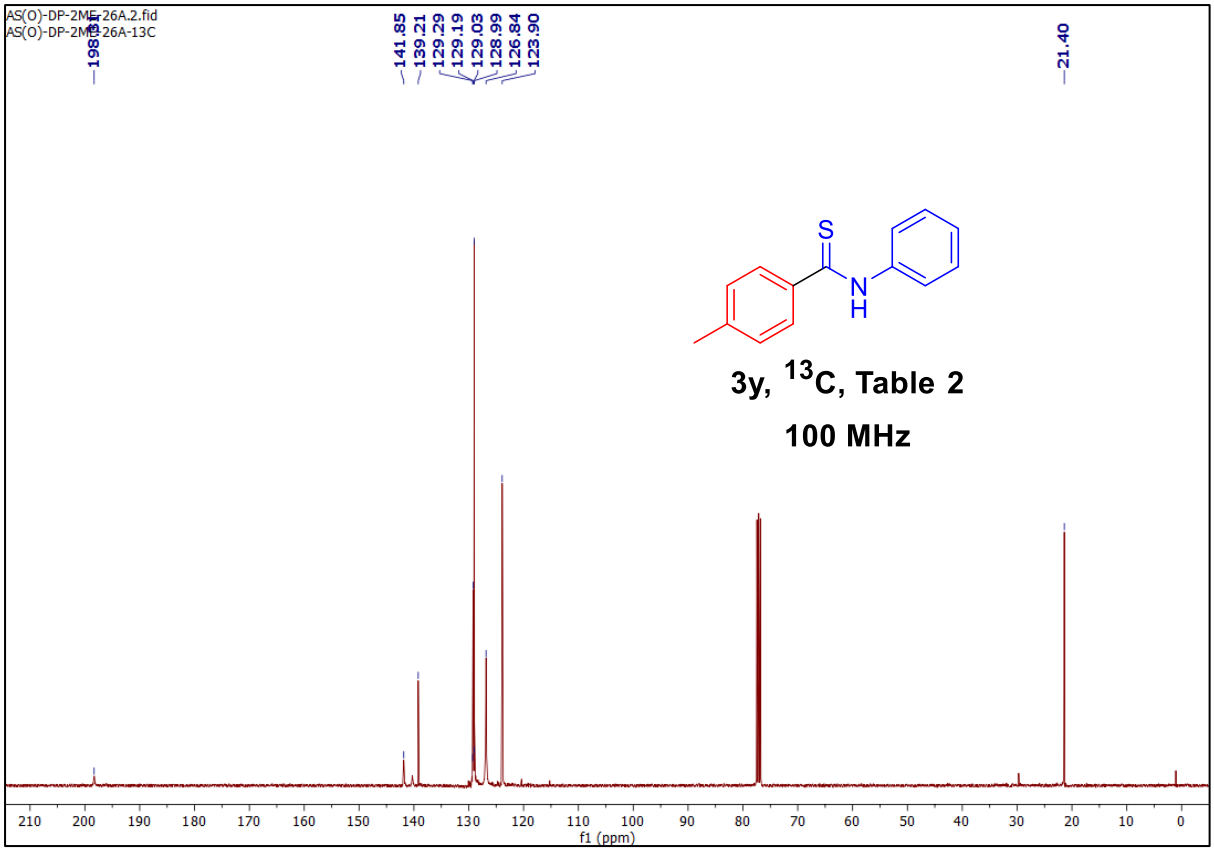
AS(O)-DP-2ME-26A.2.fid
AS(O)-DP-2ME-26A-13C
198.13
141.85
139.21
129.29
129.19
129.03
128.99
126.84
123.90
21.40
S
N
H
3y, 13C, Table 2
100 MHz
f1 (ppm)

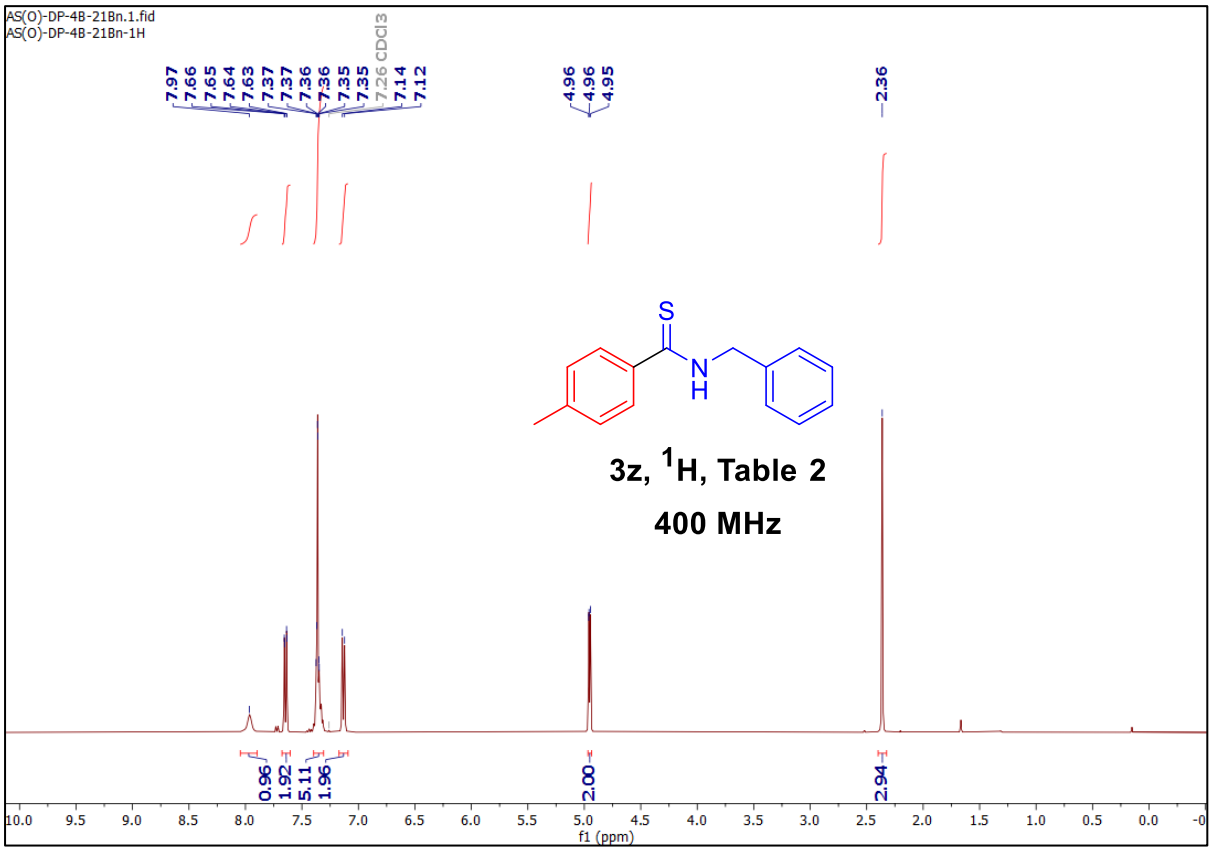
AS(O)-DP-4B-21Bn.1.fid
AS(O)-DP-4B-21Bn-1H
7.97
7.66
7.65
7.64
7.63
7.37
7.37
7.36
7.36
7.35
7.35
7.26 CDCl3
7.14
7.12
4.96
4.96
4.95
2.36
S
N
H
3z, 1H, Table 2
400 MHz
0.96
1.92
5.11
1.96
2.00
2.94
f1 (ppm)

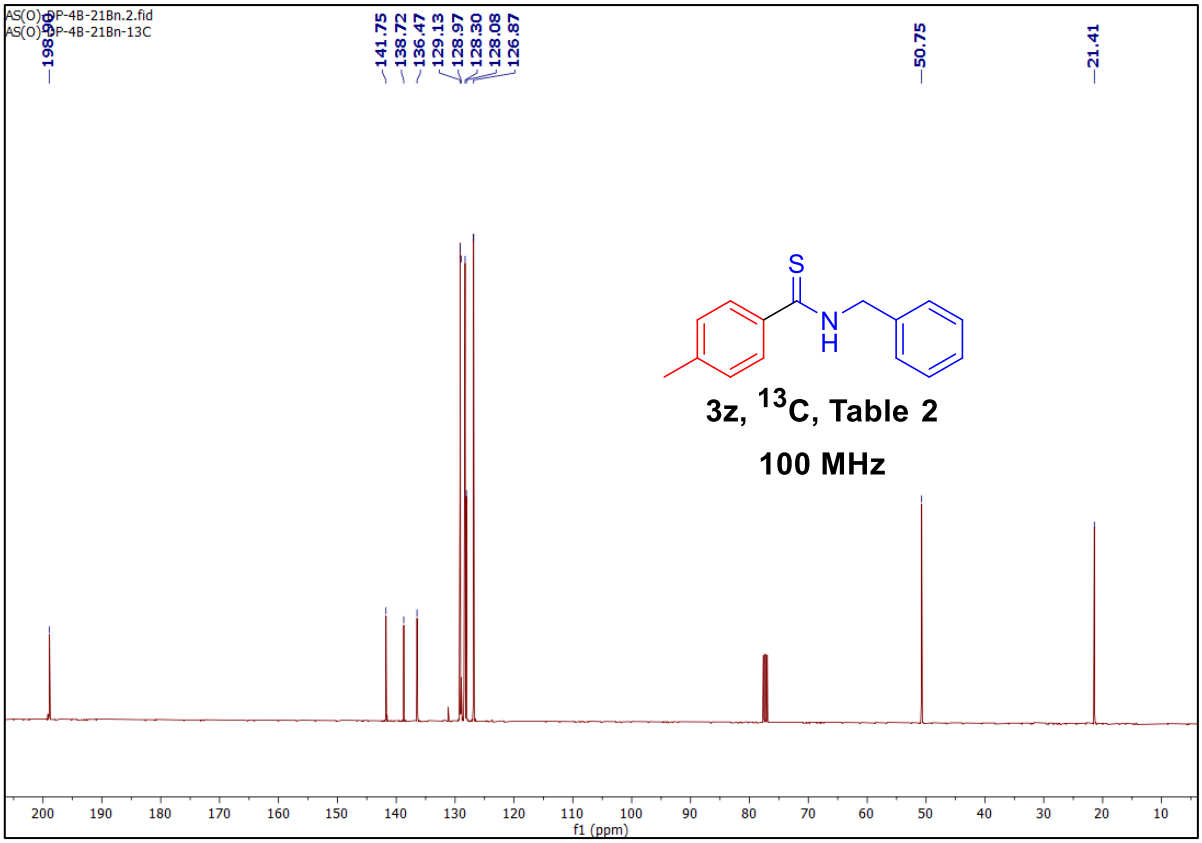
AS(O)-DP-4B-21Bn.2.fid
AS(O)-DP-4B-21Bn-13C
198.39
141.75
138.72
136.47
129.13
128.97
128.30
128.08
126.87
50.75
21.41
S
N
H
3z, 13C, Table 2
100 MHz
f1 (ppm)

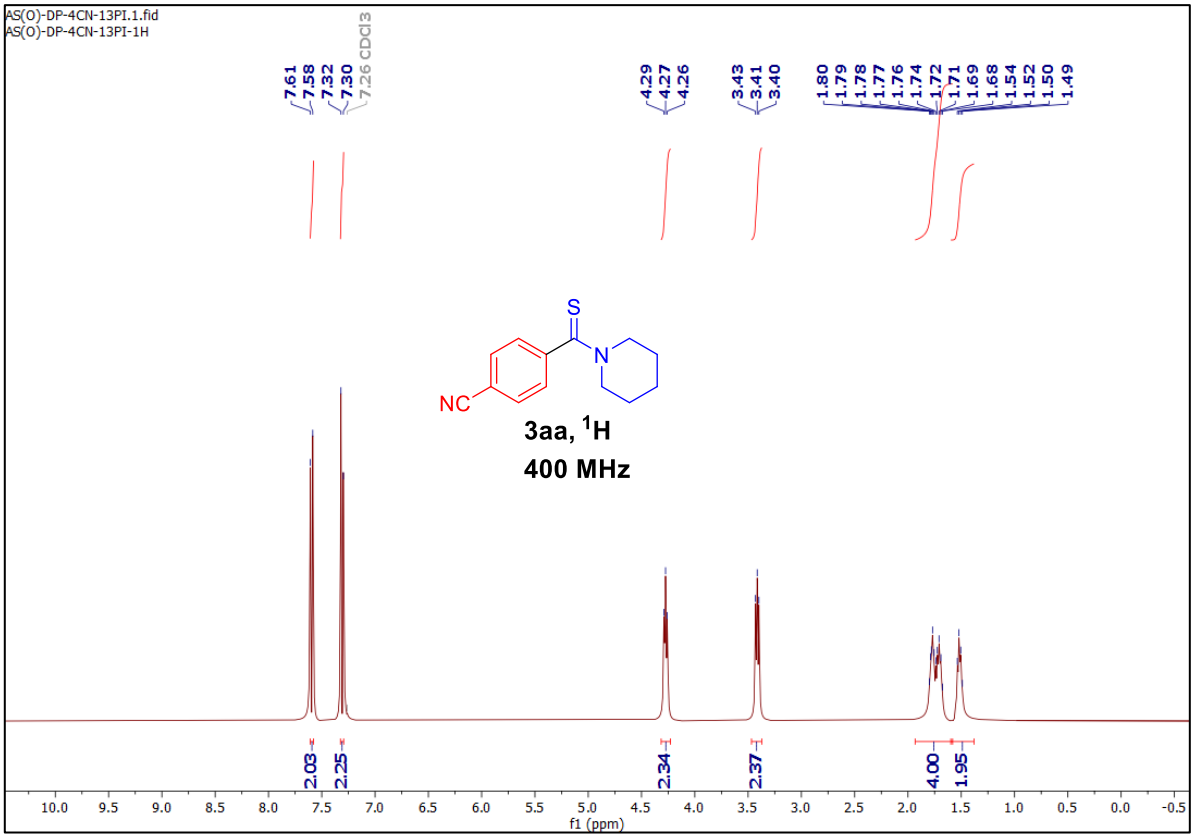
AS(O)-DP-4CN-13PI.1.fid
AS(O)-DP-4CN-13PI-1H
7.61
7.58
7.32
7.30
7.26 CDCl3
4.29
4.27
4.26
3.43
3.41
3.40
1.80
1.79
1.78
1.77
1.76
1.74
1.72
1.71
1.69
1.68
1.54
1.52
1.50
1.49
S
N
NC
3aa, 1H
400 MHz
2.03
2.25
2.34
2.37
4.00
1.95
f1 (ppm)

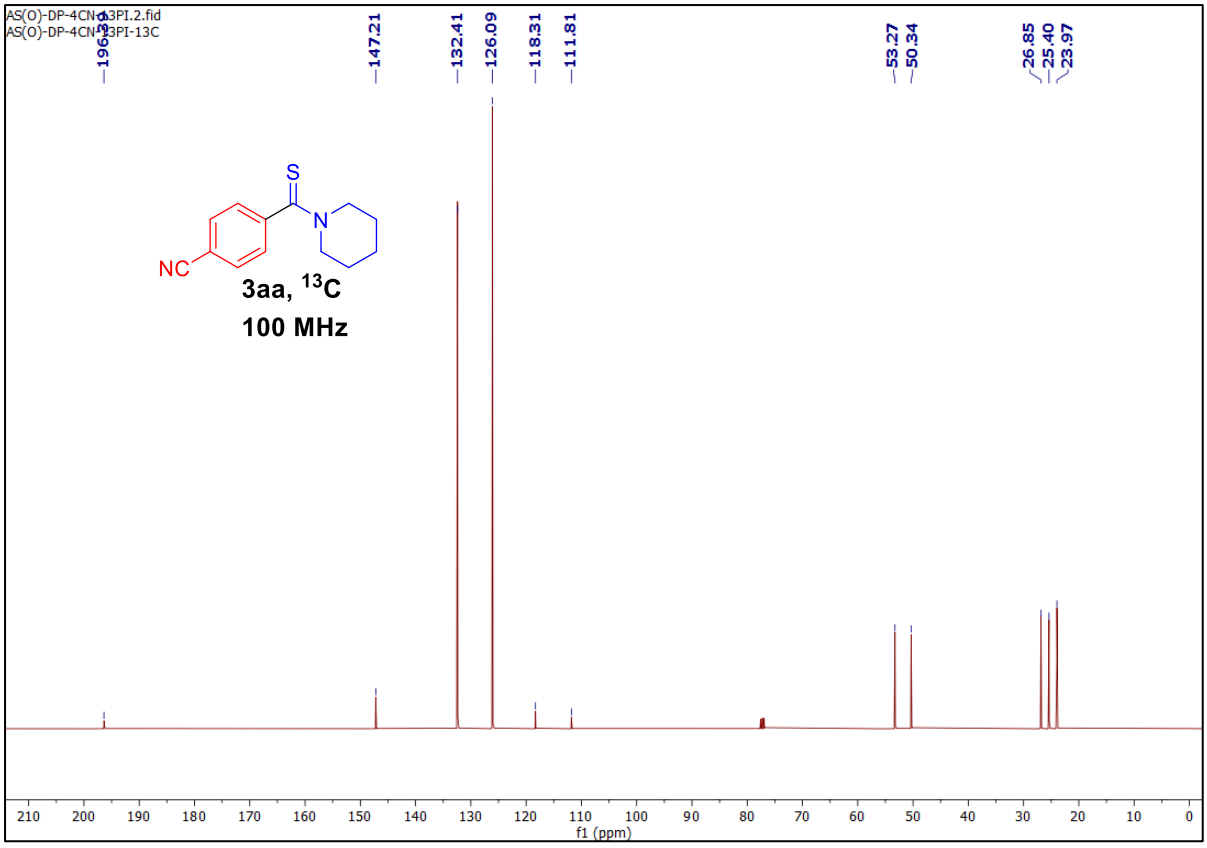
AS(O)-DP-4CN-13PI.2.fid
AS(O)-DP-4CN-13PI-13C
196.43
147.21
132.41
126.09
118.31
111.81
53.27
50.34
26.85
25.40
23.97
S
N
NC
3aa, 13C
100 MHz
f1 (ppm)

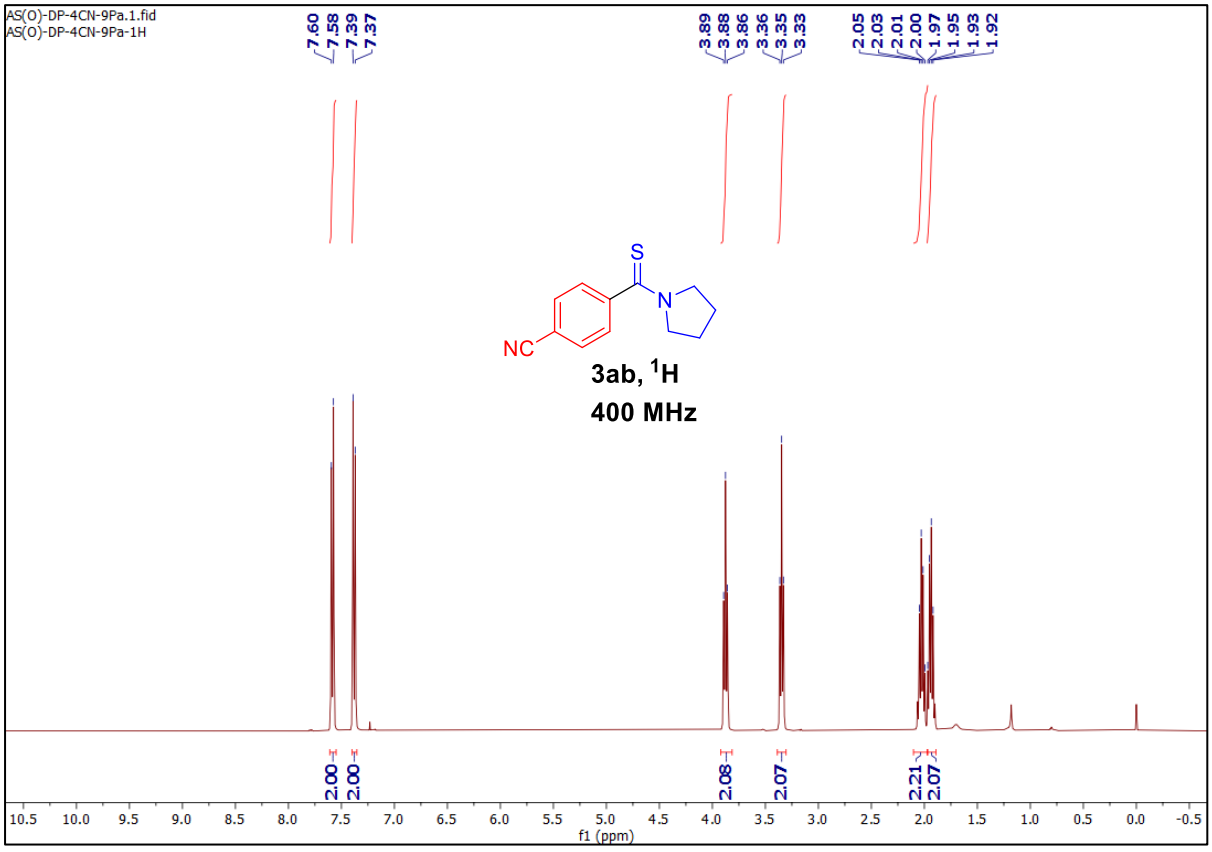
AS(O)-DP-4CN-9Pa.1.fid
AS(O)-DP-4CN-9Pa-1H
7.60
7.58
7.39
7.37
3.89
3.88
3.86
3.36
3.35
3.33
2.05
2.03
2.01
2.00
1.97
1.95
1.93
1.92
S
N
NC
3ab, 1H
400 MHz
2.00
2.00
2.08
2.07
2.21
2.07
f1 (ppm)

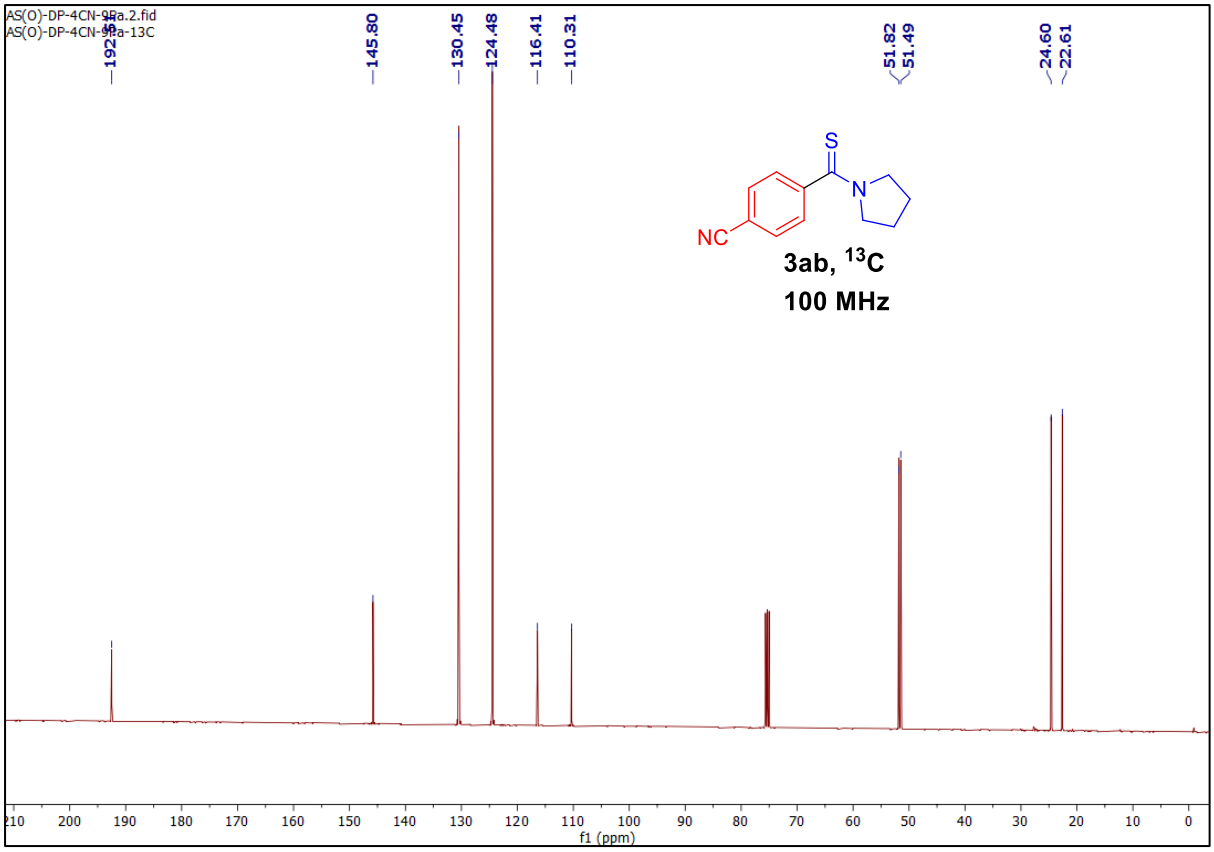
AS(O)-DP-4CN-9Ra.2.fid
AS(O)-DP-4CN-9Ra-13C
192.38
145.80
130.45
124.48
116.41
110.31
51.82
51.49
24.60
22.61
S
N
NC
3ab, 13C
100 MHz
f1 (ppm)

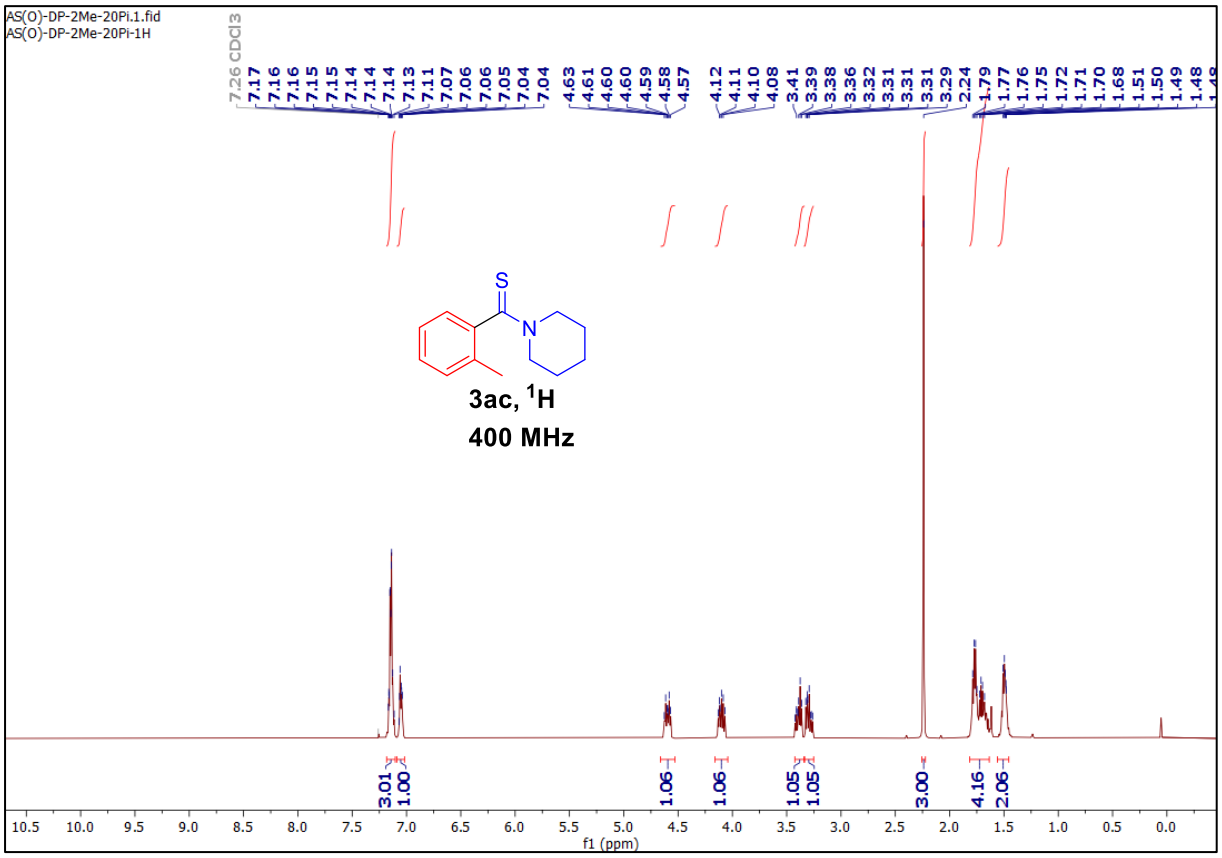
AS(O)-DP-2Me-20Pi.1.fid
AS(O)-DP-2Me-20Pi-1H
7.26 CDCl3
7.17
7.16
7.16
7.15
7.15
7.14
7.14
7.14
7.13
7.11
7.07
7.06
7.06
7.05
7.04
7.04
4.63
4.61
4.60
4.60
4.59
4.58
4.57
4.12
4.11
4.10
4.08
3.41
3.39
3.38
3.36
3.32
3.31
3.31
3.29
2.24
1.79
1.77
1.76
1.75
1.72
1.71
1.70
1.68
1.51
1.50
1.49
1.48
S
N
3ac, 1H
400 MHz
3.01
1.00
1.06
1.06
1.05
1.05
3.00
4.16
2.06
f1 (ppm)

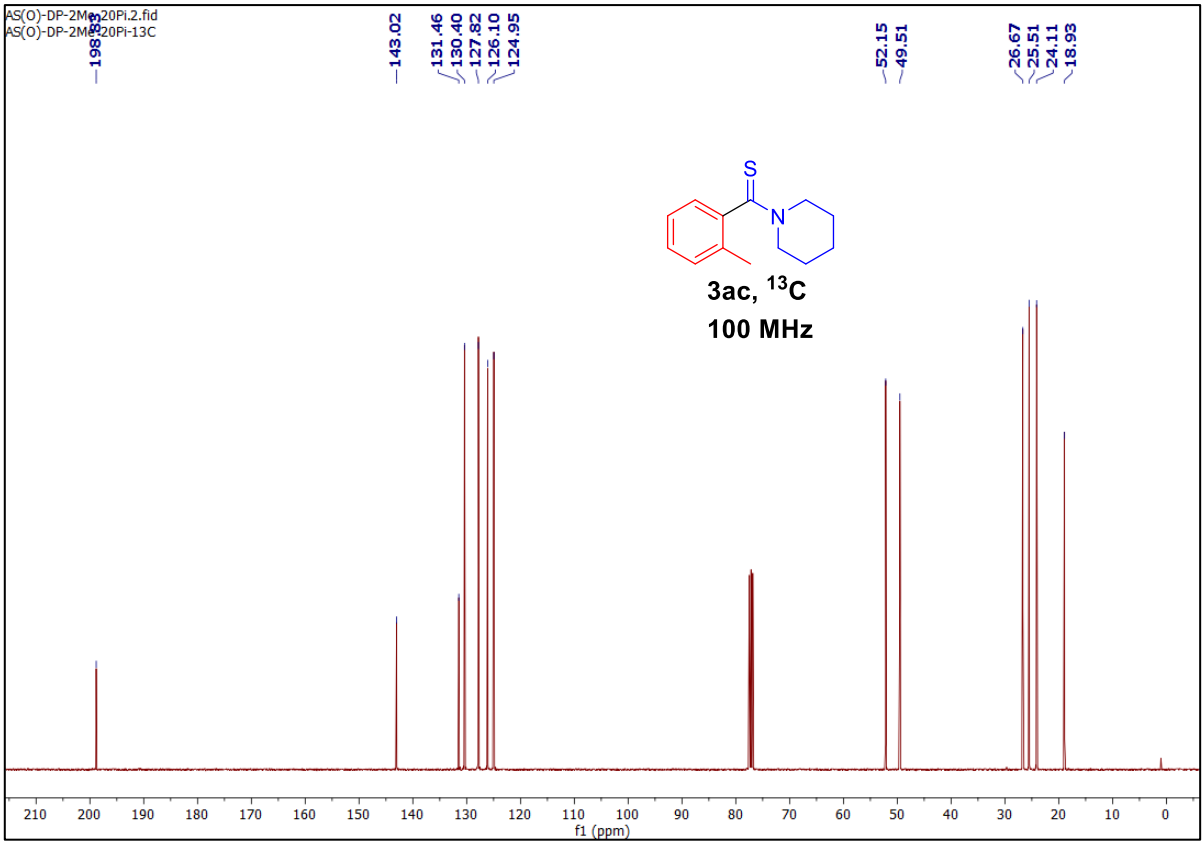
AS(O)-DP-2Me-20Pi.2.fid
AS(O)-DP-2Me-20Pi-13C
198.32
143.02
131.46
130.40
127.82
126.10
124.95
52.15
49.51
26.67
25.51
24.11
18.93
S
N
3ac, 13C
100 MHz
f1 (ppm)

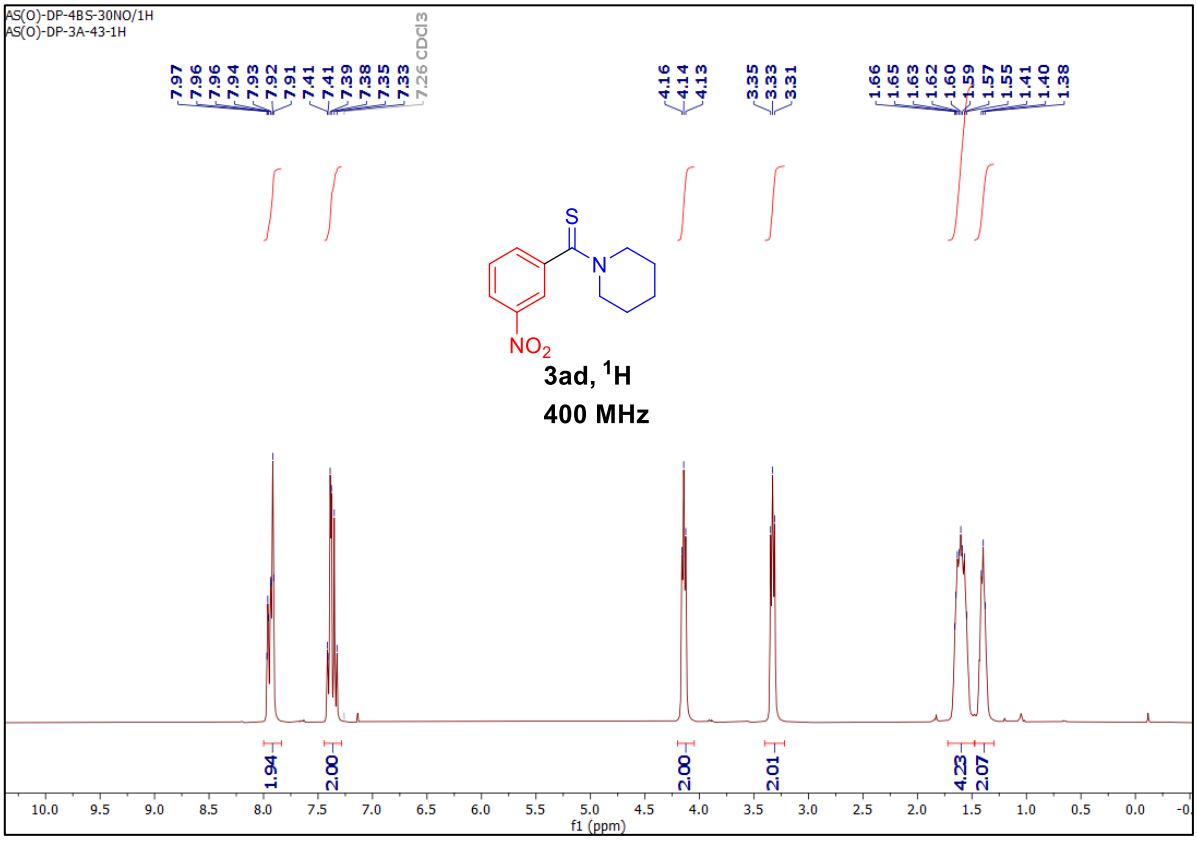
AS(O)-DP-4BS-30NO/1H
AS(O)-DP-3A-43-1H
7.97
7.96
7.96
7.94
7.93
7.92
7.91
7.41
7.41
7.39
7.38
7.35
7.33
7.26 CDCl3
4.16
4.14
4.13
3.35
3.33
3.31
1.66
1.65
1.63
1.62
1.60
1.59
1.57
1.55
1.41
1.40
1.38
S
N
NO2
3ad, 1H
400 MHz
1.94
2.00
2.00
2.01
4.23
2.07
f1 (ppm)

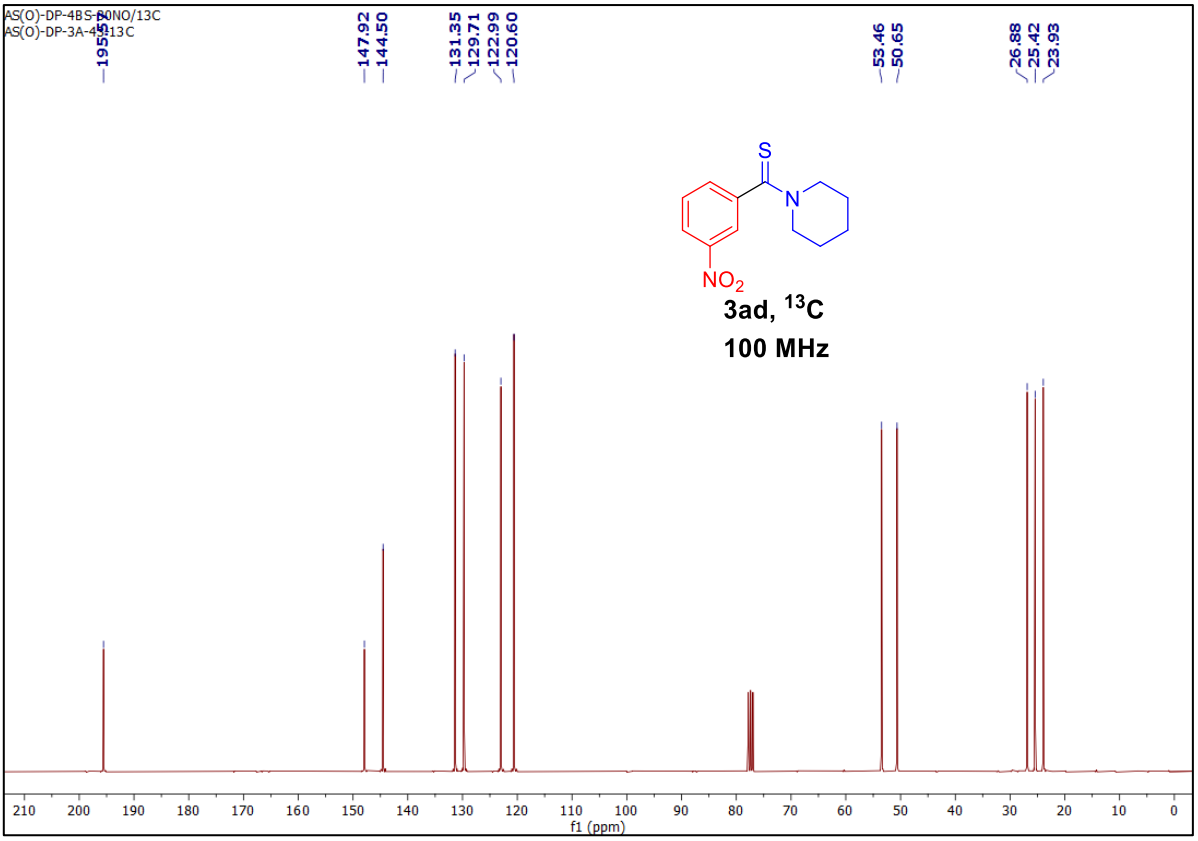
AS(O)-DP-4BS-60NO/13C
AS(O)-DP-3A-45-13C
195.45
147.92
144.50
131.35
129.71
122.99
120.60
53.46
50.65
26.88
25.42
23.93
S
N
NO2
3ad, 13C
100 MHz
f1 (ppm)

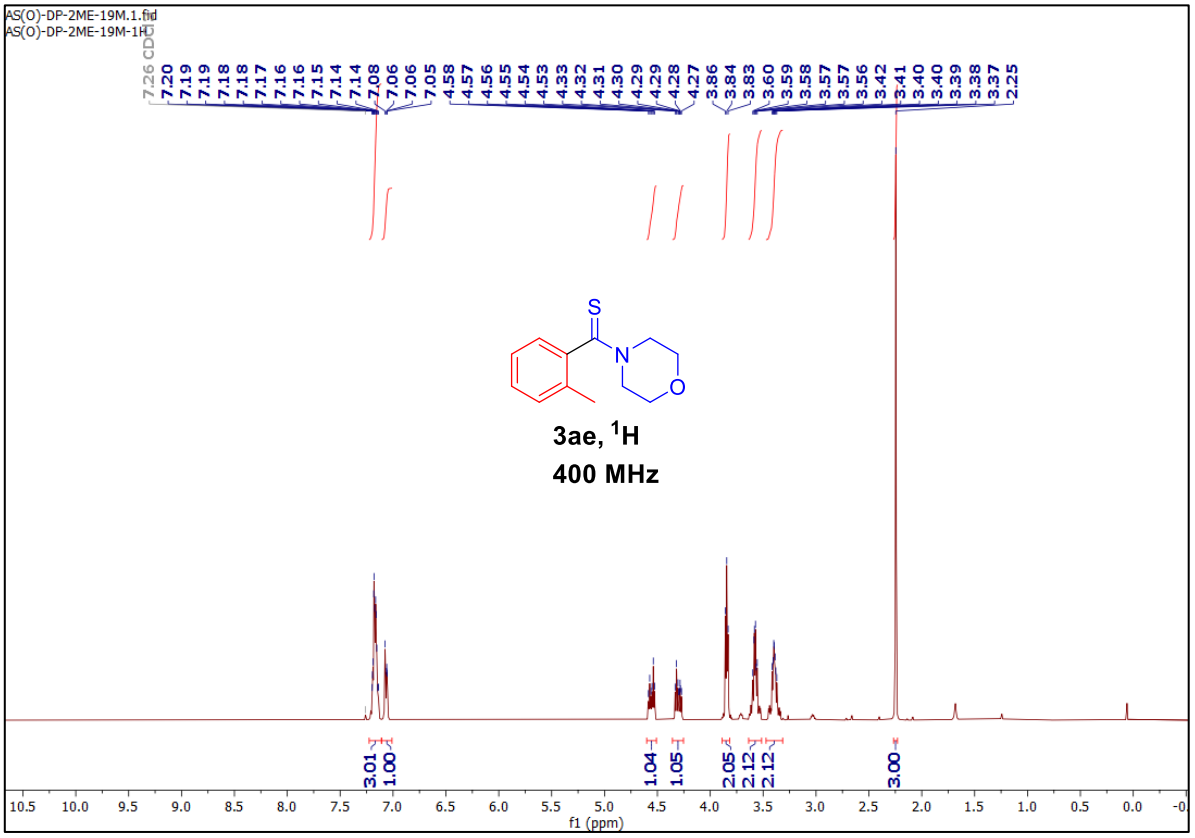
AS(O)-DP-2ME-19M.1.fid
AS(O)-DP-2ME-19M-1H
7.26 CDCl3
7.20
7.19
7.19
7.18
7.18
7.17
7.16
7.16
7.15
7.14
7.14
7.08
7.06
7.06
7.05
4.58
4.57
4.56
4.55
4.54
4.53
4.33
4.32
4.31
4.30
4.29
4.29
4.28
4.27
3.86
3.84
3.83
3.60
3.59
3.58
3.57
3.57
3.56
3.42
3.41
3.40
3.40
3.39
3.38
3.37
2.25
S
N
O
3ae, 1H
400 MHz
3.01
1.00
1.04
1.05
2.05
2.12
2.12
3.00
f1 (ppm)

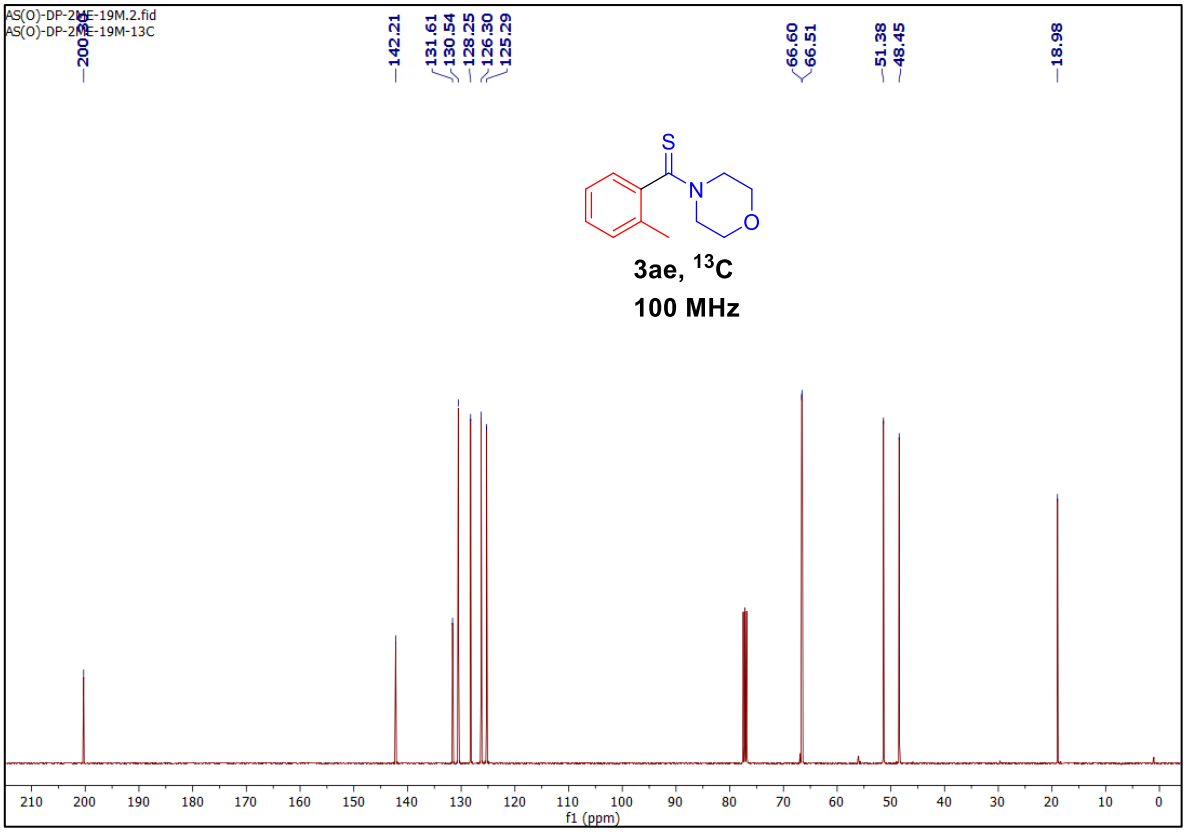
AS(O)-DP-2ME-19M.2.fid
AS(O)-DP-2ME-19M-13C
200.1
142.21
131.61
130.54
128.25
126.30
125.29
66.60
66.51
51.38
48.45
18.98
S
N
O
3ae, 13C
100 MHz
f1 (ppm)

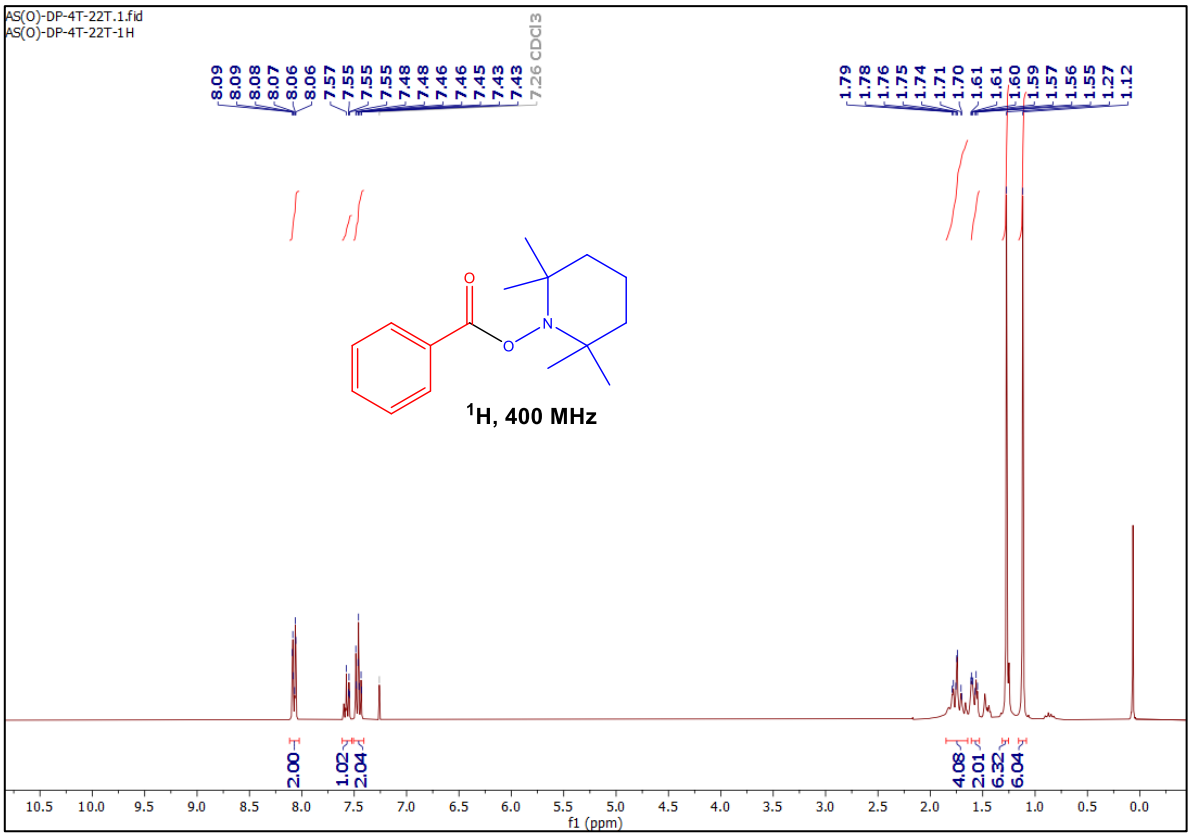
AS(O)-DP-4T-22T.1.fid
AS(O)-DP-4T-22T-1H
8.09
8.09
8.08
8.07
8.06
8.06
7.57
7.55
7.55
7.55
7.48
7.48
7.46
7.46
7.45
7.43
7.43
7.26 CDCl3
1.79
1.78
1.76
1.75
1.74
1.71
1.70
1.61
1.61
1.60
1.59
1.57
1.56
1.55
1.27
1.12
O
N
O
1H, 400 MHz
2.00
1.02
2.04
4.08
2.01
6.32
6.04
f1 (ppm)

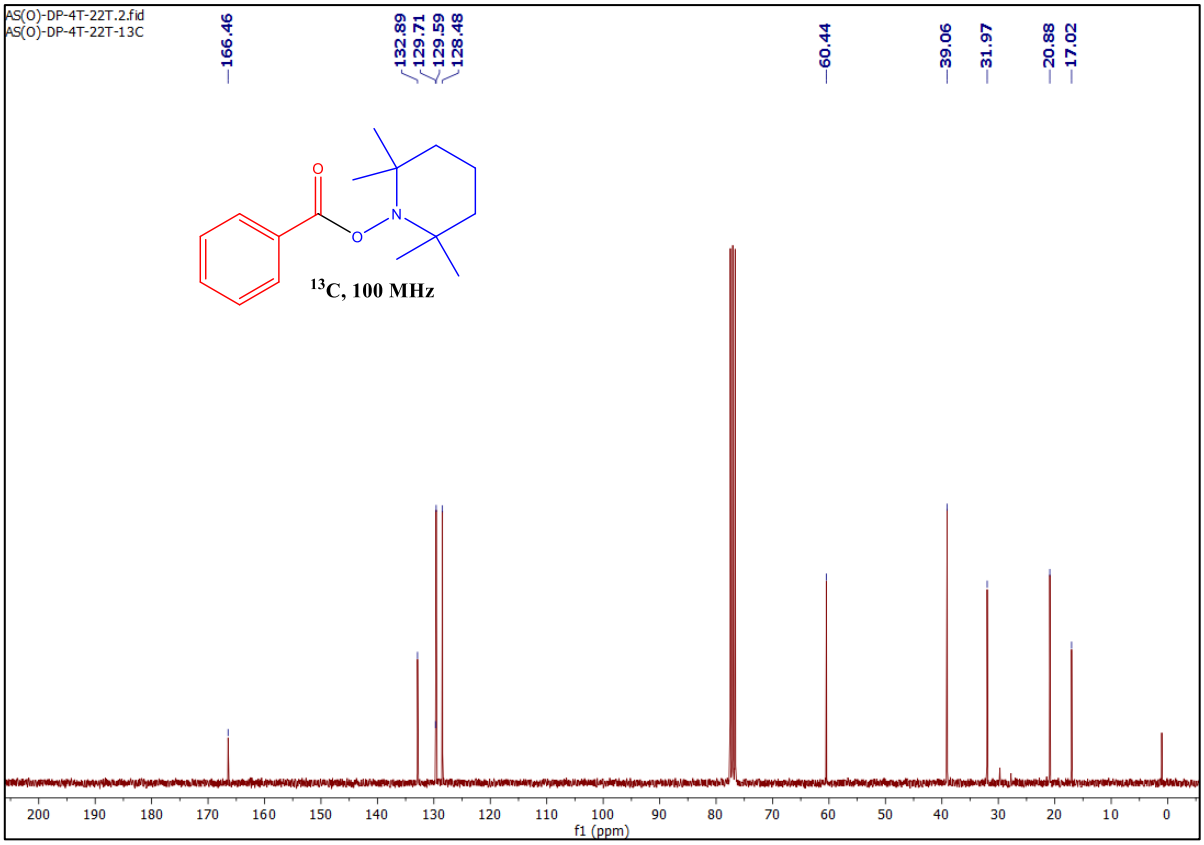
AS(O)-DP-4T-22T.2.fid
AS(O)-DP-4T-22T-13C
166.46
132.89
129.71
129.59
128.48
60.44
39.06
31.97
20.88
17.02
O
N
O
13C, 100 MHz
200 190 180 170 160 150 140 130 120 110 100 90 80 70 60 50 40 30 20 10 0
f1 (ppm)

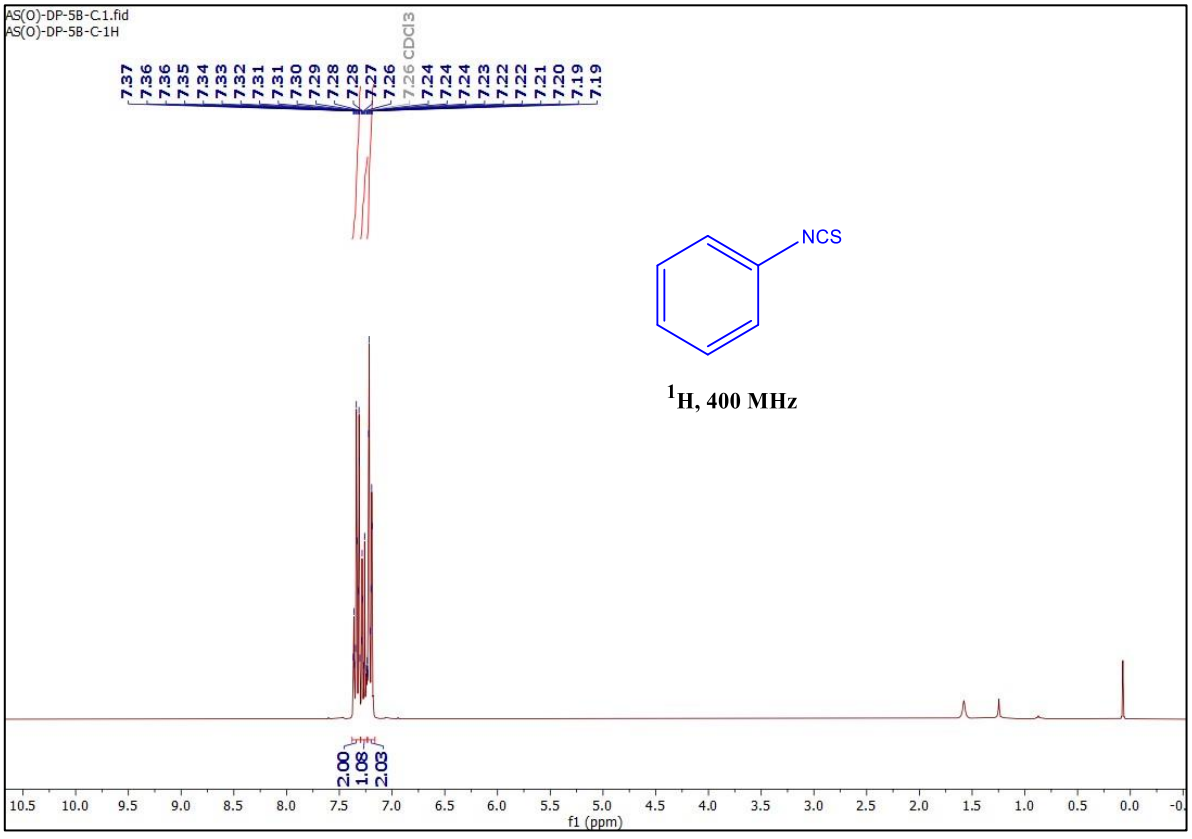
AS(O)-DP-5B-C.1.fid
AS(O)-DP-5B-C-1H
7.37 7.36 7.36 7.35 7.34 7.33 7.32 7.31 7.31 7.30 7.29 7.28 7.28 7.27 7.26 7.26 CDCl3 7.24 7.24 7.24 7.23 7.22 7.22 7.21 7.20 7.19 7.19
NCS
1H, 400 MHz
2.00 1.08 2.03
10.5 10.0 9.5 9.0 8.5 8.0 7.5 7.0 6.5 6.0 5.5 5.0 4.5 4.0 3.5 3.0 2.5 2.0 1.5 1.0 0.5 0.0
f1 (ppm)

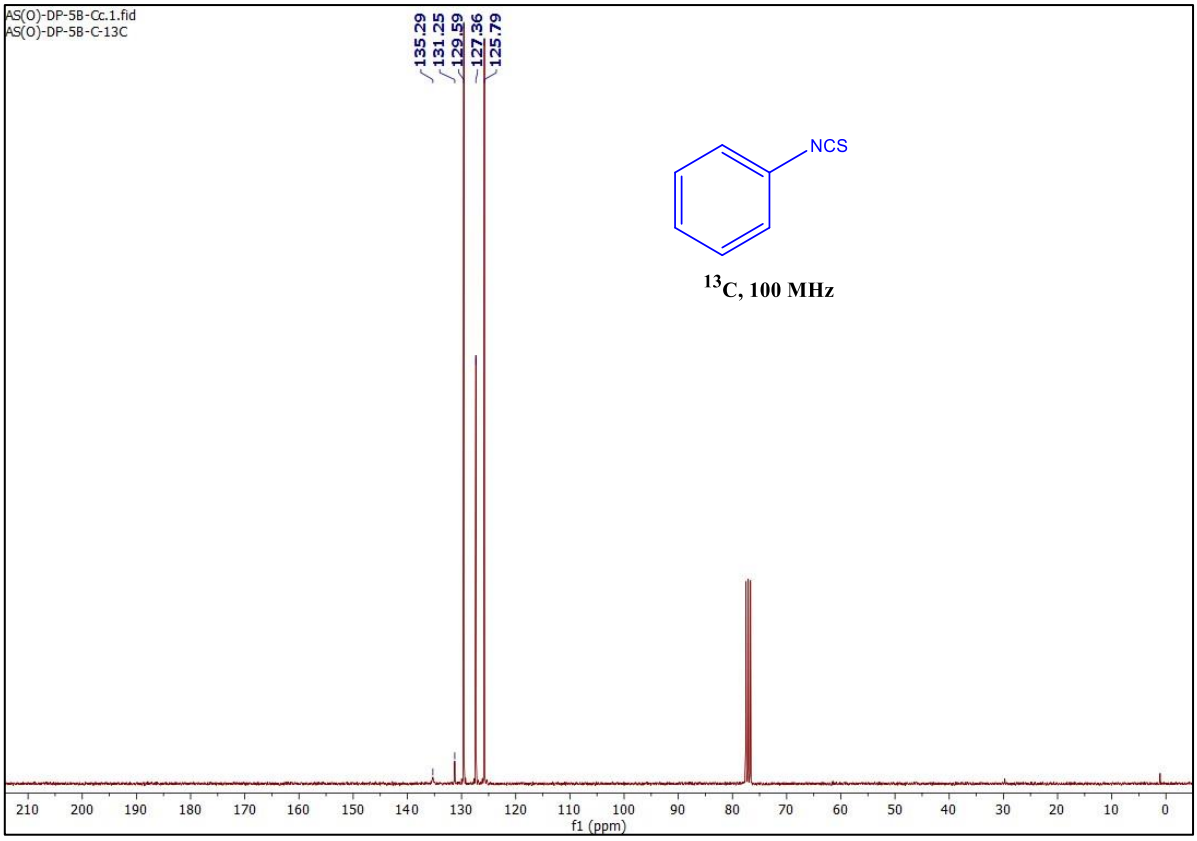

^{13}C, 100 MHz

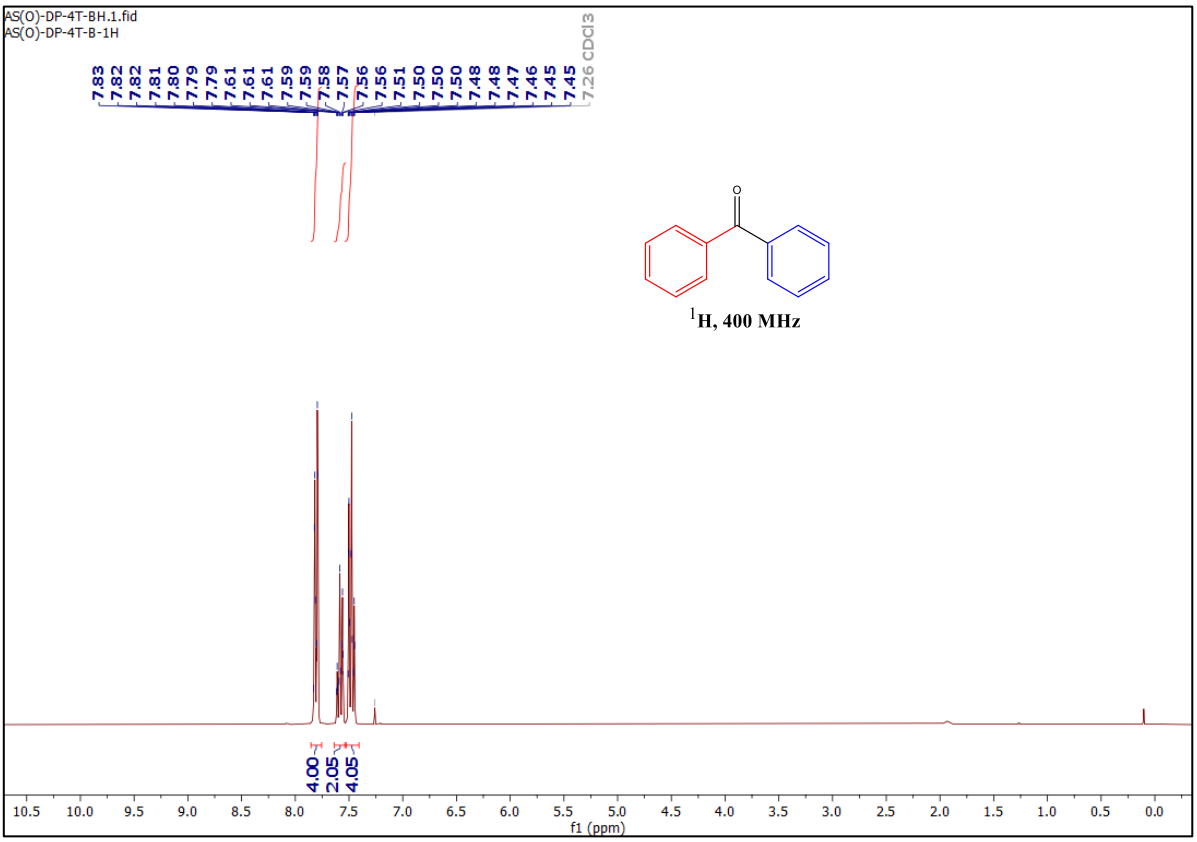

^{1}H, 400 MHz

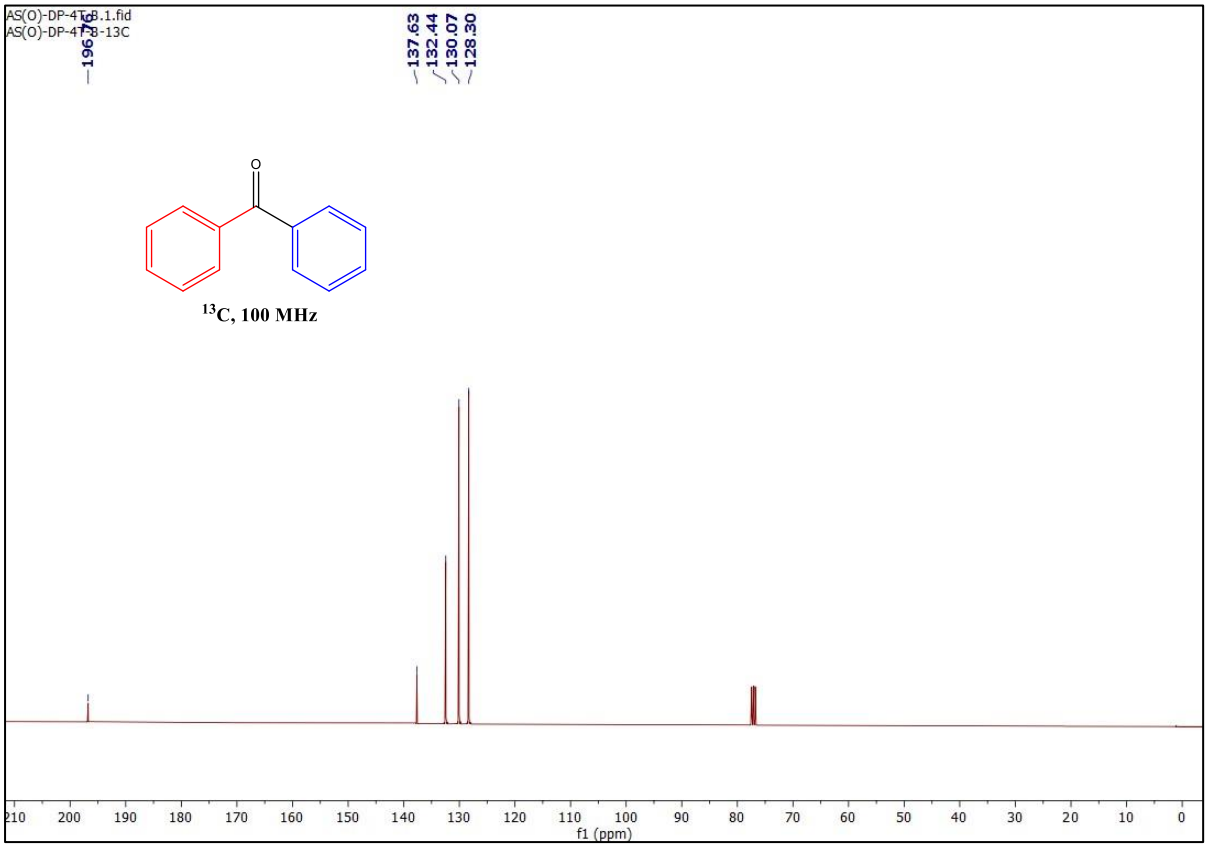
AS(O)-DP-4T
AS(O)-DP-4T
196.76
137.63
132.44
130.07
128.30
O
13C, 100 MHz
210
200
190
180
170
160
150
140
130
120
110
100
90
80
70
60
50
40
30
20
10
0
f1 (ppm)

Mass spectra of products (3x, 3ae)

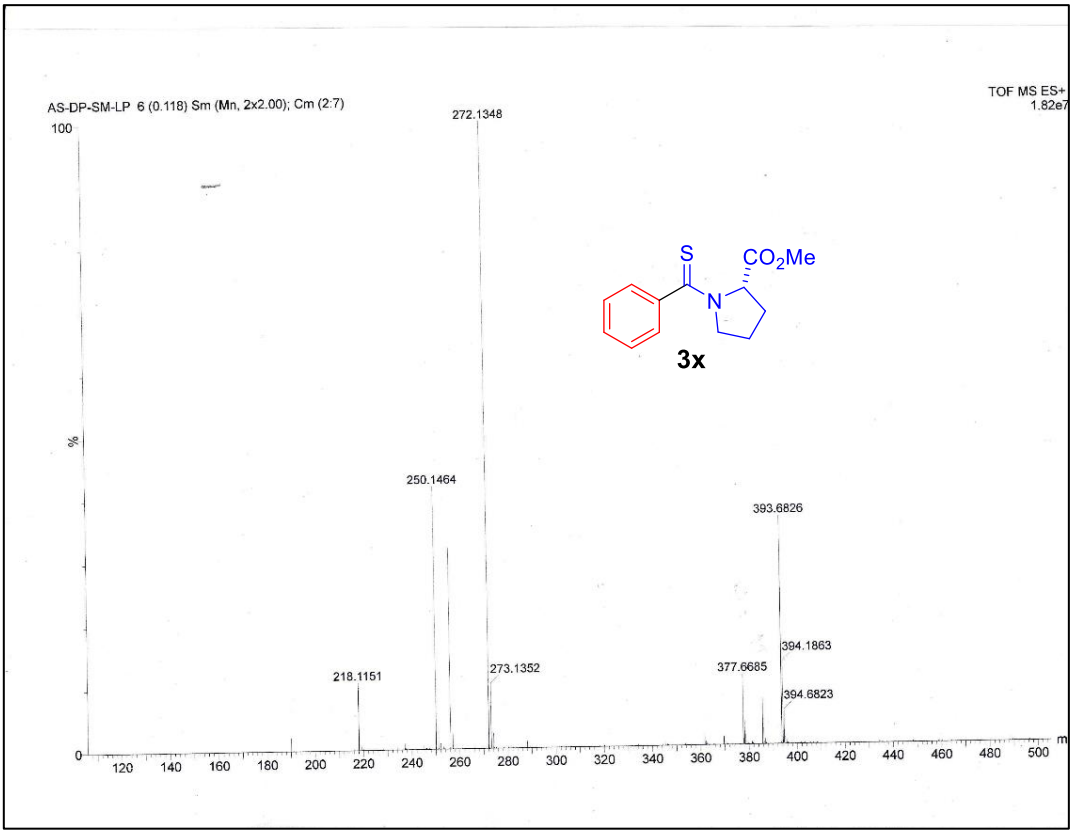

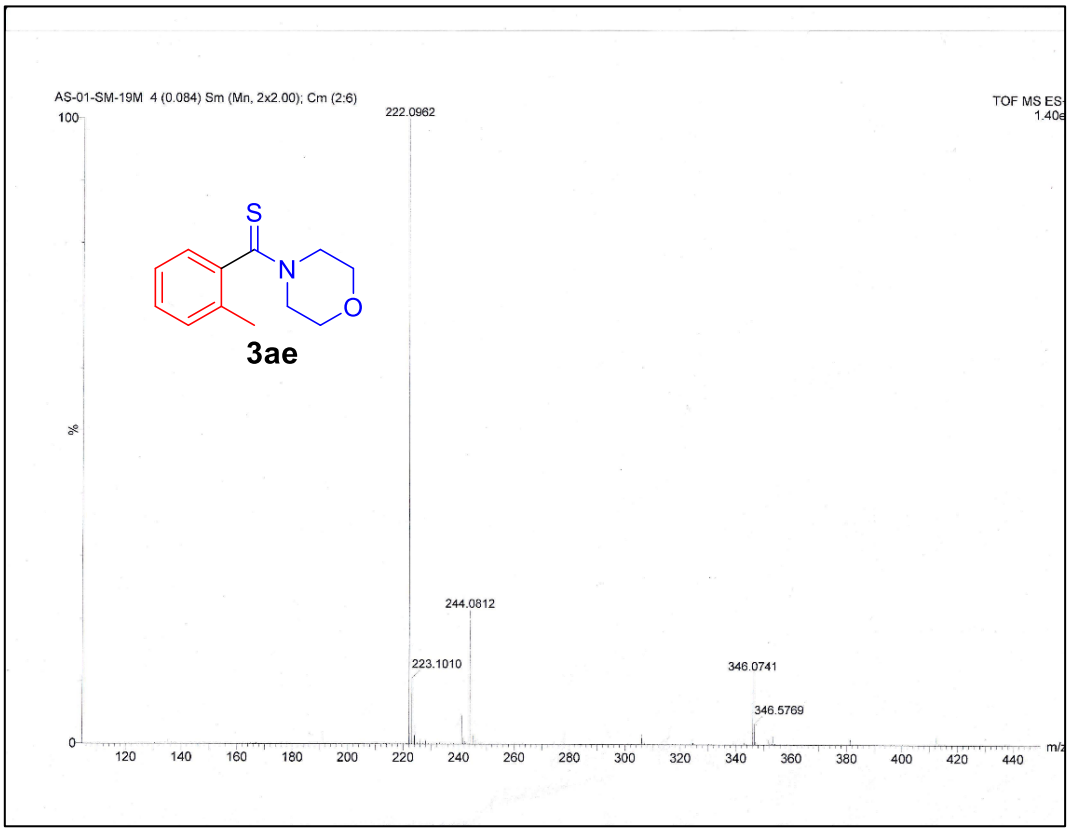

Gas chromatograms

GC-MS data were collected from PerkinElmer Clarus SQ 8 C Mass spectrometer. Column specification (COL-Elite-5mS-30).

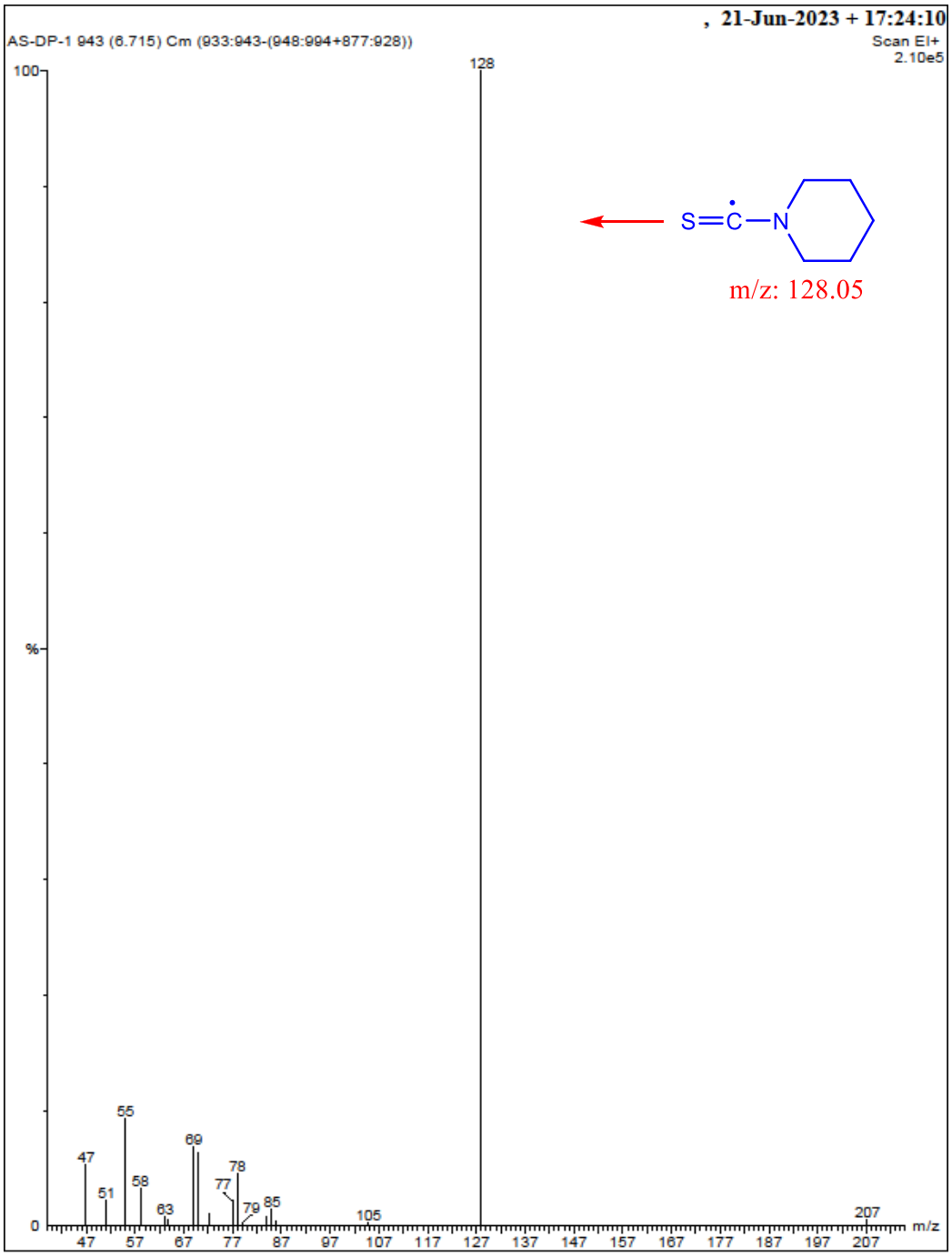

Figure 3.1 GC spectrum of the reaction mixture described in 3a product.

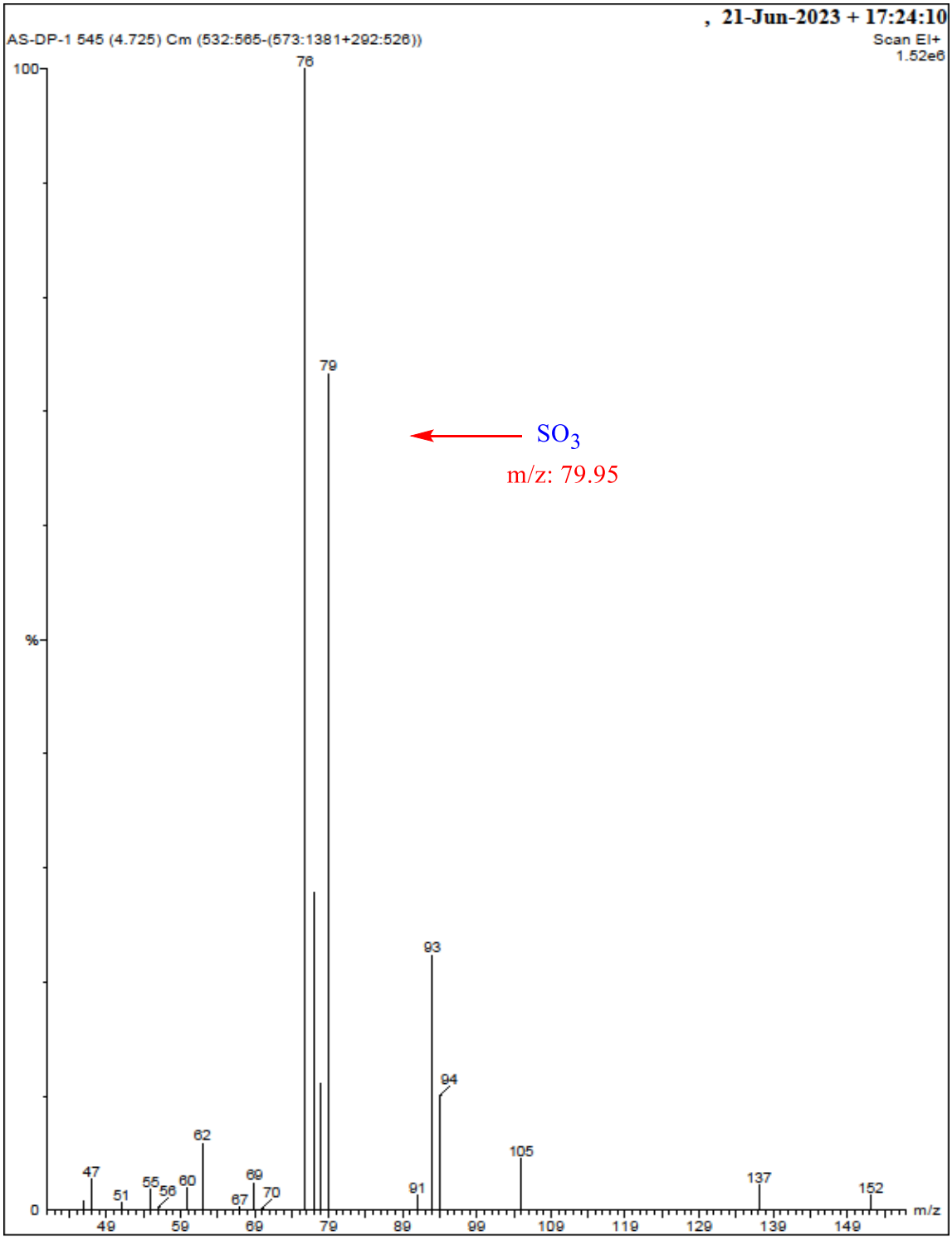

Figure 3.2 GC spectrum of the reaction mixture described in 3a product.

^{1}H NMR Spectra of crude reaction mixtures (in $CDCl_3$):

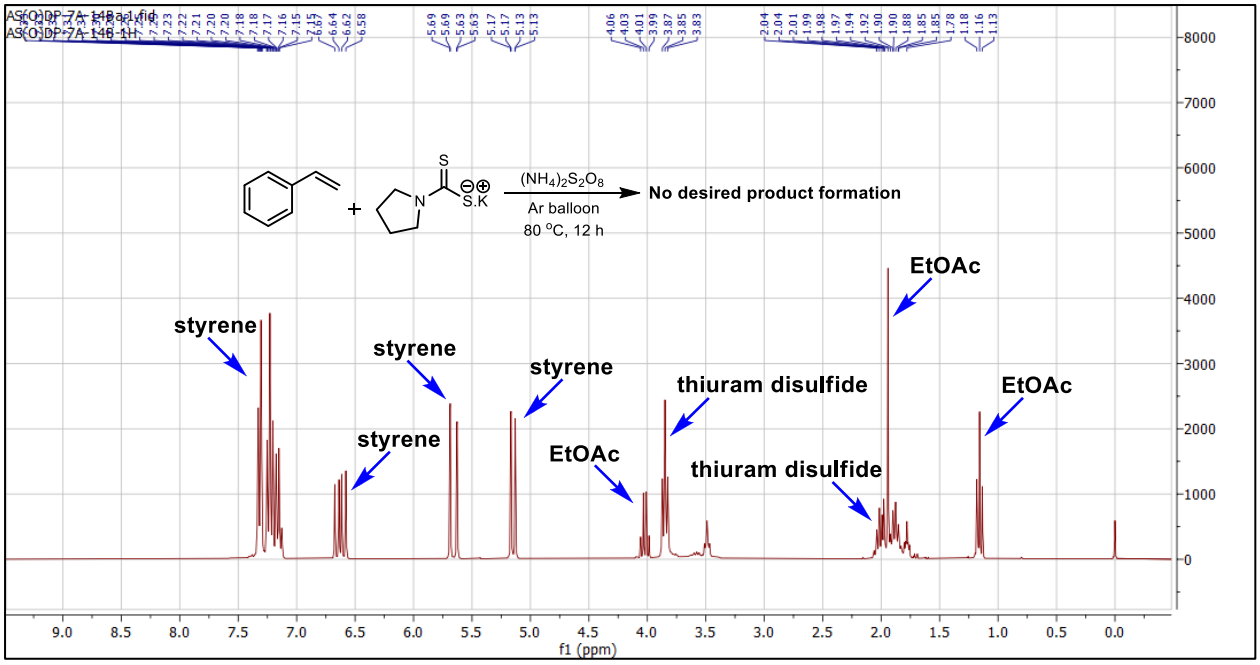

Figure 3.3 ^{1}H NMR of crude reaction mixture for the reaction between styrene and pyrrolidine-dithiocarbamate performed in argon atmosphere (Ar balloon).

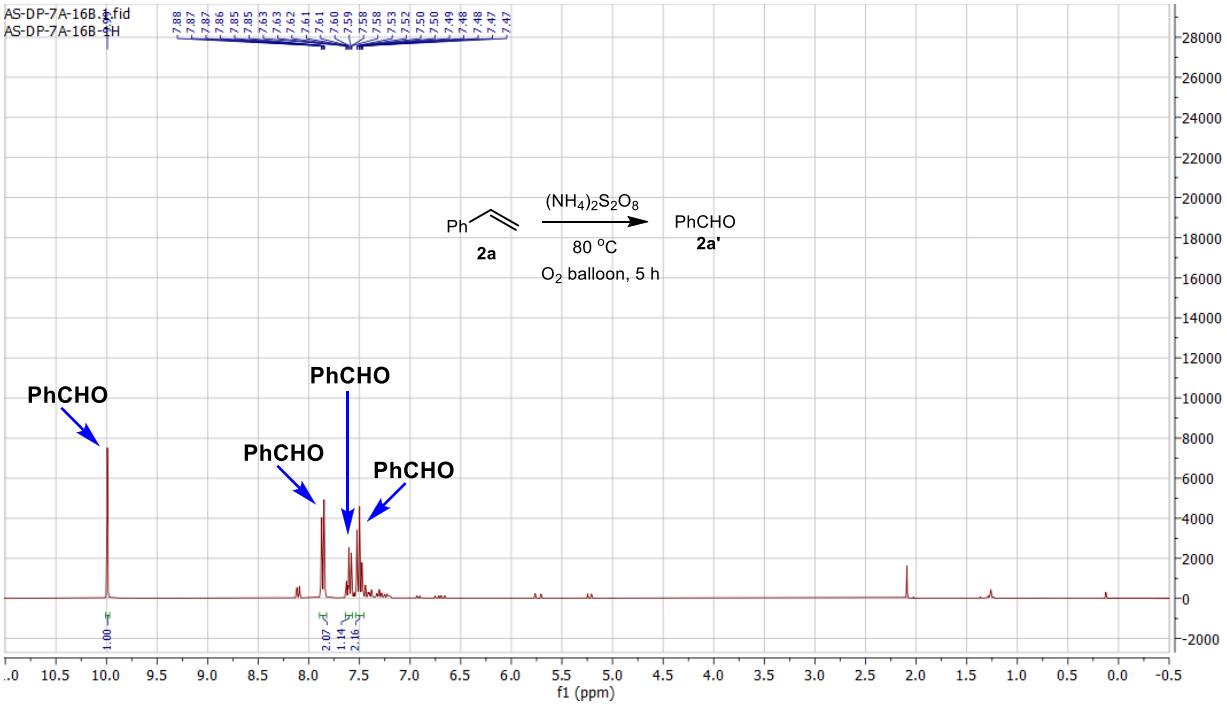

Figure 3.4. ^{1}H NMR of crude reaction mixture for the reaction between styrene and persulfate performed using O_2 balloon for 5 h of time period.

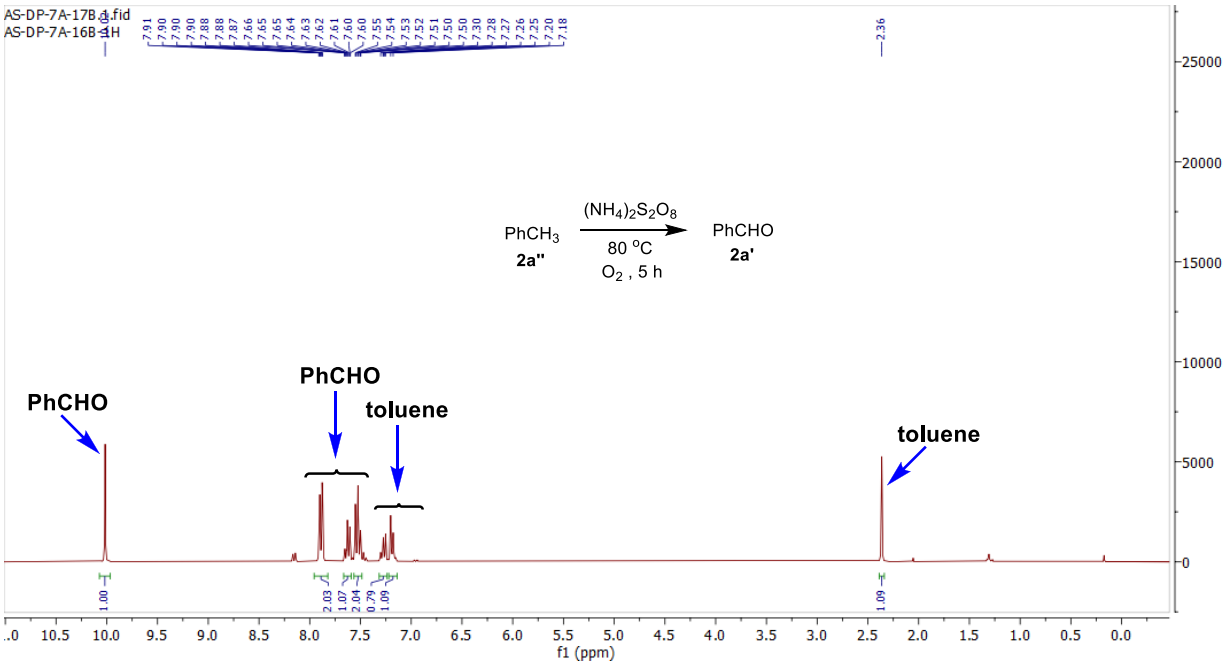

Figure 3.5. ^{1}H NMR of crude reaction mixture for the reaction between toluene and persulfate performed in O_2 for 5 h of time period.

2/f References

1. (a). 2. Rajkumar V, Gunjan G, Ashok Kumar R, Lazar M. *Ethnobotanical leaflets.* **2009**, *7*. (b) Gali-Muhtasib H, Bakkar N. *Current cancer drug targets.* **2002**, *2*, 309–336.
2. (a) Wang H, Z.hao C, Huang Y, Wang F, Li Y. medicinal journal. **2015**; *22*, 29–35. (b) Najafian Y, Hamedi SS, Farshchi MK, Feyzabadi Z. *Electronic physician.* **2018**;*10*, 6390–6399. (c) Radu N, Ghita I, Coman O, Rau I. **2010**;*523*, 273–281. (d) Radu N, Ghita I, Rau I. *molecular crystals liquid crystals.* **2010**;*523*, 236–246. (e) Dalar A, Türker M, Konczak I, *Journal of herbal medicine.* **2012**, *2*, 42–51.
3. (a) Afifi M, Salama O, Hassan M, Naeim Z, Mohammed K. *Journal of pharmaceutical sciences*. **2000**, *16*, 204–212. (b) Samuelsen AB. *Journal of ethnopharmacology.* **2000**;*71*, 1–21. (b)Rønsted N, Göbel E, Franzyk H, Jensen SR, Olsen CE. *Phytochemistry.* **2000**; *55*, 337–348. (c)Taskova R, Evstatieva L, Handjieva N, Popov S. *Zeitschrift für naturforschung C*. **2002**, *57*, 42–50.
4. (a) Janković T, Menković N, Zdunić G, Beara I, Balog K, et al. *Analytical letters.* **2010**, *43*, 2487–2495. (b) Akihisa T, Yasukawa K, Tokuda H. *Studies in natural products chemistry.* **2003**, *29*, 73–126.
5. Hertog MG, Hollman PC, Katan MB, Kromhout D. *Nutrition and cancer.* **1993**, *20*, 21–29.
6. (a) Gálvez M, Martín-Cordero C, López-Lazaro M, Cortés F, Ayuso MJ. *Journal of ethnopharmacology.* **2003**, *88*, 125–130. (b) Sugiyarto AD, Dwisetyawani A, Pitoyo A. di Gunung Lawu. *Biodiversitas.* **2006**,*7*, 143–146.
7. (a) Krishnaveni M, Dhanalakshmi R, Nandhini N. *International journal of pharmaceutical sciences review and research.* **2014**, *27*, 273–276. (b) Holetz FB, Pessini GL, Sanches NR, Cortez DAG, *Memórias do Instituto Oswaldo Cruz.* **2002**;97, 1027–1031. (c) Chiang LC, Chiang W, Chang MY, Lin CC, *American journal chinese medicine.* **2003**,*3*,225–234.
8 (a) H. Watanabe and M. Kamigaito, *J. Am. Chem. Soc*. **2023,** 145, 10948–10953. (b) F. Pourhassan and H. Eshghi, *Catalysis Letters*, **2020**, 150, 1287–1300. (c) W. Czepa, S. Witomska, P. Samorì and A. Ciesielski, *Small Sci*., **2023**, 3, 2300013.
9. C. Walpole, S. Y. KO, M. Brown, D. Beattie, E. Campbell, F. Dickenson, S. Ewan, G. A. Hughes, M. Lemaria, J. Lerpiniers, S. Patel and L. Urban, *J. Med. Chem*., **1998**, 41, 3159.
10. (a) A. Kaluszyner, R. Mechoulam and M. Breuer, Bull. Res. Council Israel, **1958**, *7A*, 135; (b) D. Duerr and V. Dittrich, ciba; Patent US 3395233, NL 6604132, 1966; Chem. Abstr., **1967**, 66, 55249; (c) R. Spaum, P. Brenneisen, A. Rochat, J. Gallay and S. A. Agripat, Patent CH 542828, **1973**; Patent DE 2143838, US3781290, 1972; Chem. Abstr., 1972, **77**, 97750; (d) D. Duerr and M. V. Orelli, Ciba, Patent US 3927087, 1975. (e) D. Derr and M. V. Orelli, Ciba, Patent US 3927087, 1975.
11. (a) J. Bernstein, H. L. Yale, K. Losee, M. Holsing, J. Martins and W. A. Lott, *J. Am. Chem. Soc*., **1951**, 73, 906; (b) B. Love, P. E. Bender, H. Bowman, A. Helt, R. McLeean and T. Jen, *J. Med. Chem*., 1972, 2024; (c) G. Vasilev and Z. Tomaleav,

Arich. *Phytopathal pflanzenshuts*, **1973**, 9, 309; (d) G. Krause, R. Franke and G. N. Vasilev, *Biochem. Physiol. Pflanz.*, **1979**, 174, 128; (e) C.S. Madabhushi, K. K. R. Mallu, V. S. Vangipuram, S. Kurva, Y. Poornachandra and C. G. Kumar, *Bioorg Med Chem Lett*., **2014**, 24, 4822.

12. (a) A. Mahajan, S. Yeh, M. Nell, C. E. J.-V. Rensburg and K. Chibale, Biorg. Med. Chem. Lett., **2007**, 17, 5683; (b) M. B. Krajacic, M. Peric, G. Landek, J. Padovan, D, Jelic, A. Ager, W. K. Milhous, W. Ellis, R. Spaventic and C. Ohrt, J. Med. Chem., 2011, 43, 381.
13. (a) J. D. Bloom, M. J. DiGrandi, R. G. Dushin, K. J. Curan, A. A. Ross, E. B. Norton, E. Terefenko, T. R. Jones, B. Feld and S. A. Lang, Bioorg. Med. Chem. Lett., **2003**, 13, 2929; (b) E. Tatar, S. G. Kucukguzel, S. Rollas and E. De Clercq, Eur. J. Med. Chem., **2008**, 43, 381.
14. A. Ranise, A. Spallarossa, O. Burno, S. Schenone, P. Fossa, G. Menozzi, F. Bondavalli, L. Mosti, A. Capuano, F. Mazzeo, G. Falcone and W. Filippeli, Farmaco, **2003**, 58, 765.
15. (a) A. M. M. E. Omar, A. M. Farghaly, A. A. B. Hazari, N. H. Eshba, F. M. Sharabi, T. T. Daabees, J. pharm. Sci., **1981**, 70, 1075; (b) A. Ulrich and J. Schlessinger, Cell, **1990**, 61, 203; (c) Y. .Dai, Y. Frey, R. R. Gauo, Z. Ji, M L. Curtin, A. A. Ahmed, D. H. Albert, L. Armold, S. S. Arries, T. Barlozzari, J. L. Bauch, J. J. Bouska; P. F. Bousquet, G. A. Cunha, K. B. Glaser, J. Guo, J. Li, P. A. Marcotte, K. C. Marsh, M. D. Moskey, L.J. Pease, K. D. Stewart, V.S. Stoll, P. Tapang, N. Wishart, S. K. Davidsen and M. R. Michaelides, J. Med. Chem., **2006**, 49, 2357; (e) S. K. Sharma, Y. Wu and Stienbergs, J. Med. Chem., **2010**, 53, 5197.
16. J. Lee, M. Kang, M. Shim, J. M. Kim, S.U, Kang, J. O. Lim, H. K. Choi, Y. G. Suh, H. G. Park, U. Oh, H. D. Kim, Y. H Park, H. J. Ha, Y. H. Kim, A. Toth, Y. Wang, R. Tran, L. V. Parce, D. J. Lundberg, and P. M, Blumberg, J. Med. Chem., **2003**, 46, 3116.
17. (a) A. K. Mallams, J. B, Morton and P. Reichert, *J. Chem. Soc.*, Perkin Trans., 1981, **1,** 2186; (b) S. Cunha, F. C. Macedo, G. A. N. Costa, M. T. Recordings, R. B. V. Verde, L. C. de Souza Neta, I. Vencato, C. Lariucci and F. P. Sa, Monatsh. Chem., 2007, **138,** 511.
18. (a) A. G. Makhsumov, A. S. Safaev and S. V. Abidova, Katal Pererab. Uglevodordn. Syrya, 1968, 101; *Chem. Abstr.*, **1969**, 71, 101668v; (b) K. Sivapriya, P. Suguna, A. Banerjee, V. Saravana, D. N. Raob and S. Chandraasekarana, Bioorg. Med. Chem. Lett., **2007**, 17**,** 6387; (c) M. Taha, N. H. Ismail, W. Jamil, K. M. Khan, U. Salar, S. M. Kashif, F. Rahim and Y. Latif, Med. Chem. Res., **2015**, 24**,** 3166; (d) D. H. Al-Amily and M. H. Mohammed, Sci.Pharm., **2019**, 87, 28; (e) S. Naz, M. Zahoor, M. N. Umar, S. Alghamdi, M.U. K. Sahibzada and W. UlBari, Open Chemistry, **2020**, 18**,** 764**.**
19. J, Chen , W, Yu, W, Zhang, C, Sun , W, Zhang, *J Clin Med.*, 2014. 13, 1397-406.
20. (a) D. L. Geffner, M. Azukizawa, J. M. Hershman, *J Clin Invest*., 1975, **55**, 224-231. (b) Schimmel M, U. RD. *Ann Intern Med*., **1977,** 87, 760-768.
21. (a) D. Forrest, J. Nunez, Encycl. of Neuroscience, **2009**, 993-1000.(b) D. Braun, U. Schweizer, *Tetrahedron Lett.*, **2018**, 106, 19-44.

22. (a) E. B. Veale, G. M. Tocci, F. M. Pfeffer, P. E. Kruger and T. Gunnlaugsson, *Org. Biomol. Chem*., **2009, 7**, 3447; (b) C. Caltagirone and P. A. Gale, *Chem. Soc. Rev*., **2009**, **7**, 3447; (c) Y. Tang, L. Deng, Y. Zhang, G. Dong, J. Chen and Z. Yang, *Org. Lett*., **2005**, **7**, 1657; (d) J. Li, L.-L. Shi, J. Chen, J. Gong and Z. Yang, Synthesis, **2014**, 46, 2007.
23. B. Mertschenk, F. beck and W. Bauer, *Encyclopedia of Industrial Chemistry*, 2002, Wiley-VCH Verlag GmbH & Co. KGaA. (b) Rajabi S, Ramazani A, Hamidi M, Naji T. Daru. **2015**;23, 204.
24. J. Zao and G. Cui, *International Journal of Electrochemical Science*, **2011**, 6, 4048.
25. P. K. Mohanta, S. Dhar, S. K. Samal, H. I1a and H. Junjappa, *Tetrahedron*, **2000**, 56, 629.
26. (a) B. G. Ateya, B. E. El-Anadouli and F. M. El-Nizamy, *Corros. Sci*., **1984,** 24, 497; (b) N. C Subramanyam, B. S. Sheshadri, S. M Mayanna, *Corros. Sci*., **1993**, 34, 563; (c) M. A. Quraishi, F. A. Ansari and D. Jamal, Mater. *Chem. Phys*., **2003**, **77**, 687. (d) M. Ozcan, I. Dehri and N.S Abd-Elshafi, Electrochim, Acta, **2006**, 51, 3296; (f) V. V. Torres, V. A. Rayol, M. Magalhaes, G. M. Viana, L. C. S. Aguiar, S. P. Machado, V. W. Faria, G. F. de Andrade, E. D' Elia, M. F. Carbal, B. A. Cotrim, G. O. Resende and F. C. deSouza, *Phosphours, Sulfer, and Silicon and the Related Elements*, **2015**, 8, 1366.
27. F. A. A. Ngh, E. I. Zakariah, N. I. Hassan, B. Yamim, S. Sapari, and S. A. Hasbullah, *Malaysian Journal of Analytical Sciences*, **2017**, 21, 1226.
28 (a) J. Smith, J. L. Liras, S. E. Scheider and E. V. Anslyn, *J. Org. Chem*., **1996**, 61, 8811; (b) Y. Tobe, S. Sasaki, K. Hirose and K. Naemura, *Tetrahedron Lett*., **1997**, 38, 4791.
29. (a) T.S. Griffin, T. S. Woods and D. L. Klayman, Thioureas in the synthesis of hetrocycles, in Advances in Heterocyclic Chemistry, ed. A. R. Katritzky and A. J. Boulton, **1975**, 18, 99 and references cited therin; (b) D. G. Patil and M. R. Chedekel, *J. Org. Chem*., **1984**, 49, 997; (c) S. Kasmi, J. Haelin and H. Benhaoua, *Tetrahedron Lett*., **1998**, 63, 196; (e) C. Boga, L. Forlain, C. Silvestroni, A. B. Corradi and P. Sgarabotto, J. Chem. Soc., Perkin Trans., **1999**, 1363; (f) M. Kidwai, R. Venkataramana and B. Dave, *Green Chem.,* **2001**, 3, 278; (g) S. Paul, M. Gupta, R. Venkataramanan and B. Dave, *Green Chem*., **2001**, 3, 278; (g) S. Paul, M. Gupta, R. Gupta and A. Loupy, *Synthesis*, **2002**, 1, 75; (h) W. Du and D. P. Curran , *Org. Lett*., **2003**, 5, 1765; (i) U. Heinelt, D. Schultheis, S. Jager, M. Lindenmarie, A. Pollex and H. S. G. Beckmann, *Tetrahedron*, 2004, **60**, 9883; (j) S. Huang, Y. Pan, Y . Zhu and A. Wu, *org. Lett*., **2005**, 7, 3797.
30. (a) N. Mahanta, D. Miklos Szantai-Kis, E. James Petersson and D. A Mitchell, *ACS Chem. Biol.,* **2019**, 14, 142–163. (b) X. Chen, E.G. Mietlicki-Baase, T. M. Barrett, L. E. McGrath, K. Koch-Laskowski, J. J. Ferrie, M. R. Hayes, E. J. Petersson, *J. Am. Chem. Soc.*, **2017**, 139, 16688–16695.
31. (a) H. T. Phan, S. G. Giannakoulias, T. M. Barrett, C. Liu and E. J. Petersson, *Chem. Sci.* **2021**, 12, 10825–10835. (b)) Y. J. Wang, D. M. Szantai-Kis and E. J. Petersson, *Org. Biomol. Chem.,* **2015**, 13, 5074-5081.

32. Rahamooz-Haghighi S, Asadi MH. *Journal of herbmed pharmacology*. **201**, *5*, 157–161.
33. Plumb JA. Cell Sensitivity Assays. In: Langdon SP, editor. *Cancer Cell Culture. Methods in Molecular Medicine™. Vol 88.* Humana Press; Retreived from: https://doi.org/10.1385/ 1-59259-406-9:165.
34. Aghajanzadeh M, Zamani M, Rashidzadeh H, Rostamizadeh K, Sharafi A, Danafar H. Amphiphilic Y shaped miktoarm star copolymer for anticancer hydrophobic and hydrophilic drugs codelivery: Synthesis, characterization, in vitro, and in vivo biocompatibility study. *Journal of biomedical materials research part a*. **2018**;*106*, 2817–2826.
35. (a) X. Chen, E. G. Mietlicki-Baase, T. M. Barrett, L. E. McGrath, K. Koch-Laskowski, J. J. Ferrie, M. R. Hayes and E. J. Petersson, *J. Am. Chem. Soc.,* **2017**, *139*, 16688–16695; (b) S. Batjargal, Y. J. Wang, J. M. Goldberg, R. F. Wissner and E. J. Petersson, *J. Am. Chem. Soc.,* **2012**, *134*, 9172–9182; (c) H. A. T. Phan, S. G. Giannakoulias, T. M. Barrett, C. Liu and E. J. Petersson, *Chem. Sci.,* **2021,** *12*, 10825-10835; (d) G. Sauve, V. S. Rao, G. Lajoie and B. Belleau, *Can. J. Chem.,* **1985**, *63*, 3089-3101; (e) Y. J Wang, D. M. Szantai-Kisa and E. J. Petersson, Semi-synthesis of thioamide containing proteins, *Org. Biomol. Chem.,* **2015**, *13*, 5074-5081.
36. (a) F. Wang, R. Langley, G. Gulten, L. G. Dover, G. S Besra, W. R. Jacobs and Jr. J. C. Sacchettini, *J. Exp. Med.,* **2007**, *204*, 73-78.; (b) J. J. Lipsky and M. O. Gallego, *Drug Interact.,* **1988**, *6*, 317-326; (c) R. V. García-Mayor and A. Larrañaga, *Med. Chem.,* **2010**, *6*, 239-246; (d) T. Cheetham, *Thyroid Research.,* **2021**, *14*, 18; (e) B. Nayak and K. Burman, *Endocrinol. Metab. Clin. North Am.,* **2006**, *35*, 663-686.
37. (a) C. R. Mason, L. Maynard-Atem, N. M. Al-Harbi, P. M. Budd, P. Bernardo, F. Bazzarelli, G. Clarizia and J. C. Jansen, *Macromolecules.,* **2011**, *44*, 6471–6479; (b) K. Bayram, B. Kiskan and Y. Yusuf, *Polym. Chem.,* **2021**, *12*, 534-544; (c) G. Tabak, T.-N. Pham, G. Levesque and R. Haraoubia, *J. Polym. Sci. A: Polym. Chem.,* **1998**, *36*, 117–127.
38. (a) N. Mahanta, D. M. Szantai-Kis, E. J. Petersson and D. A. Mitchell, *ACS Chem. Biol.,* **2019**, *14*, 142–163; (b) L. Kjaerulff, A. Sikandar, N. Zaburannyi, S. Adam, J. Herrmann, J. Koehnke and R. Muller, *ACS Chem. Biol.,* **2017**, *12*, 2837-2841; (c) S. Banala and R. D. Sussmuth, *ChemBioChem.,* **2010,** *11*, 1335–1337.
39. S. Pathania, R. K. Narang, R. K. Rawal, *Eur. J. Med. Chem.* 2019, *180*, 486-508.
40. D. S. Sitar, *Drug Metab. Rev.,* **1990**, *22*, 477-502.
41. (a) T. S. *Chem. Rev.,* **2003**, *103*, 197–228; (b) P.W. Tan and J. Seayad, *Tetrahedron Lett.,* **2019**, *60*, 151338.
42. (a) J. Wei, Y Li and X. Jiang, *Org. Lett.,* **2016**, *18*, 340−343; (b) S. P. Pathare, P. S. Chaudhari and K. G. Akamanchi, *General*, **2012**, 125, 425-426; (c) O. I. Zbruyev, N. Stiasni and C. O. Kappe, *J. Comb. Chem.,* **2003**, *5*, 145-148; (d) M. Papa, I. Chiarotto and M. Feroci, *ChemistrySelect,* **2017**, 2, 3207 – 3210; (e) Y. A. Tayade, A. D. Jangale and D. S. Dalal, *ChemistrySelect,* **2018,** 3, 8895–8900; (f) C. K. Khatri, A. S. Mali and G. U. Chaturbhuj, *Monatsh Chem.,* **2017**, *148*, 1463–1468; (g) K. Okamoto, T. Yamamoto and T. Kanbara, *Synlett , 2007, 17,* 2687–2690; (h) A. Gupta, J. K. Vankar, J. P. Jadav and G. N. Gururaja, *J. Org. Chem.,* **2022**, *87*, 2410−2420; (i) M.-

T. Zeng, M. Wang, H.-Y. Peng, Y. Cheng and Z.-B. Dong, *Synthesis,* **2018**, *50*, 644–650; (j) A. D. Kale, Y. A. Tayade, S. D. Mahale, R. D. Patil, and D. S. Dalal, *Tetrahedron,* **2019**, *75*, 130575; (k) H.-Z. Li, W.-J. Xue, G.-D. Yin and A.-X. Wu, *Tetrahedron Lett.,* **2015**, *56*, 5843–5846.

43. H. Jin, X. Ge and S. Zhou, *Eur. J. Org. Chem.,* **2021**, 6015–6021.
44. (a) X. Li, Q. Pan, R. Hu, X. Wang, Z. Yang and S. Han, *Asian J. Org. Chem.,* **2016,** *5*, 1353-1358; (b) H. Jin, X. Chen, C. Qian, X. Ge and S. Zhou, *Eur. J. Org. Chem.,* **2021**, 3403–3406.
45. X. Wang, M. Ji, S. Lim and H.-Y Jang, Thiol as a synthon for preparing thiocarbonyl: Aerobic oxidation of thiols for the synthesis of thioamides, *J. Org. Chem.* **2014,** *79*, 7256−7260.
46. (a) T. B. Nguyen, L. P. A. Nguyen and T. T. T. Nguyen, *Adv. Synth. Catal.,* **2019**, *361*, 1787– 1791; (b) S. Chen, Y. Li, J. Chen, X. Xu, L. Su, Z. Tang, C.-T. Au and R. Qiu, *Synlett,* **2016**, *27*, 2339-2344.
47. (a) B. Kurpil, B. Kumru, T. Heil, M. Antonietti and A. Savateev, *Green Chem.,* **2018**, *20*, 838–842; (b) T. B. Nguyen, L. Ermolenko, and A. Al-Mourabit, *Org. Lett.,* **2012**, *14*, 4274–4277; (c) C. J. Borths, J. Chan, B. J. Burke and R. D. Larsen, *Synlett,* **2009,** *19*, 3139–3142.
48. (a) T. B. Nguyen, M. Q. Tran, L. Ermolenko and A. Al-Mourabit, *Org. Lett.,* **2014,** *16*, 310−313; (b) K. Xu, Z. Li, F. Cheng, Z. Zuo, T. Wang, M. Wang and L. Liu, *Org. Lett.,* **2018**, *20*, 2228−2231.
49. P. Zhang, W. Chen, M. Liu and H. Wu, *J. Org. Chem.,* **2018,** *83*, 14269−14276.
50. (a) J. K. Vankar, A. Gupta, J. P. Jadav, S. H. Nanjegowdab and G. N. Gururaja, *Org. Biomol. Chem.,* **2021**, *19*, 2473–2480; (b) L. Peng, L. Maa, Y. Ran, Y. Chen and Z. Zeng, *Tetrahedron Lett.,* **2021**, *74*, 153092.
51. (a) R. N. Hurd and G. DeLaMater, *Chem. Rev.,* **1961,** *61,* 45–86; (b) M. P. Cava and M. I. Levinson, *Tetrahedron,* **1985,** *41,* 5061-5087; (c) D. L. Priebbenow and C. Bolm, *Chem. Soc. Rev.,* **2013,** 42, 7870-7880.
52. A. D. Kale, Y. A. Tayade, S. D. Mahale, R. D. Patil, D. S. Dalal, *Tetrahedron,* **2019**, *75*, 130575.
53. S. P. Pathare, P. S. Chaudhari, K. G. Akamanch, Applied Catalysis A: General, **2012**, 125–129.
54. F. M. Moghaddam and H. Zali-Boinee, *Tetrahedron Lett.* **2003**, *44*, 6253.
55. H. R. Darabi, K. Aghapoor and M. Tajbakhsh, *Tetrahedron Lett.,* **2004**, *45*, 4167.
56. F. M. Moghaddam, L. Hojabri and M. Dohendou, *Synth. Commun.,* **2003**, *33*, 4279.
57. H. R. Darabi, K. Aghapoor, Y. Balavar, E. Mobedi, H. FarhanIgian and F. Mohsenzadeh, Z. Naturforsch, *J. Chem. Sci.,* **2008**, *63*, 993.
58. H. R. Darabi, K. Aghapoor, K. Tabar-Heydar and M. Nooshabadi, *Phosphorus, Sulfur Silicon Relat. Elem.,* **2002,** *177*, 1189.
59. K. Okamoto, T. Yamamoto and T. Kanbara, *Synlett*, **2007,** 2687.
60. K. Okamoto, T. Yamamoto and T. Kanbara, *Synlett*, **2007**, 2687.
61. (a) M. Carmack, *J. Heterocycl. Chem.,* **1989,** *26,* 1319; (b) M. Carmack, M. Behforouz, G. A. Berchtold, S. M. Berkowitz, D. Wiesler and R. Barone, *J. Heterocycl. Chem.,* **1989**, *26*, 1305.

62. J. E. Valdez-Rojas, H. Rios-Guerra, A. L. Ramirez-Sanchez, G. Garcia-Gonzalez, C. Alvarez-Toledano, J. G. Lopez-Cortes, R. A. Toscano and J. G. Penieres-Carrillo, *Can. J. Chem.*, ***2012,*** *90*, 567.
63. I. S. Fedorovich, N. I. Ganushchak, V. V. Karpyak, N. D. Obushchak and A. I. Lesyuk, Russ. *J. Org. Chem.,* **2007**, *43*, 1190;
64. V. V. Kulganek and L. A. Yanovskaya, Bull. Acad. Sci. USSR, Div. *Chem. Sci.,* **1979**, *28*, 2402.
65. P. Zhang, W. Chen, M. Liu and H. Wu, *J. Org. Chem.,* **2018**, *83*, 14269−14276.
66. L. Liu, Z. Guo, K. Xu, S. Hui, Xi. Zhaoa and Y. Wu, *Org. Chem. Front.*, **2018**, *5*, 3315–3318;
67. K. Xu, Z. Li, F. Cheng, Z. Zuo, T. Wang, M. Wang and L. Liu, *Org. Lett.*, **2018**, *20*, 2228–2231.
68. C. Farina, R. Pellegata, M. Pinza and G. Pifferi, *Arch. Pharm.,* **1981**, *314*, 108.
69. D. Kadzimirsz, D. Kramer, L. Sripanom, I. M. Oppel, P. Rodziewicz, N. L. Doltsinis and G. Dyker, *J. Org. Chem.,* **2008,** *73*, 4644.
70. Y. Nomura, T. Hayama, Y. Takeuchi, S. Tomoda and Y. Kato, *Bull. Chem. Soc. Jpn.*, **1984**, *57*, 1276.
71. (a) A. Y. Solovyev, D. A. Androsov and D. C. Neckers, *J. Org. Chem.,* **2007**, *72*, 3122. (b) D. A. Androsov, A. Y. Solovyev, M. L. Petrov, R. J. Butcher and J. P. Jasinski, *Tetrahedron*, **2010**, *66*, 2474.
72. (a) Y. Imada, Y. Okada, K. Noguchi and K. Chiba, *Angew. Chem. Int. Ed.*, **2019**, *58*, 125 –129; (b) L. Legnani, G. Prina-Cerai, T. Delcaillau, *Science*, **2018**, *362*, 434–439; (c) Q. A. Ansel and J. Montgomery, *Org. Lett.*, **2020**, *22*, 8538−8543; (d) T. M. Monos, R. C. McAtee and C. R. J. Stephenson, *Science,* **2018**, *361*, 1369–1373; (e) G. Fumagalli, P. T. G. Rabet, S. Boyd and M. F. Greaney, *Angew. Chem. Int. Ed.,* **2015**, *54*, 11481–11484; (f) A. J. Musacchio, B. C. Lainhart, X. Zhang, S. G. Naguib, T. C. Sherwood and R. R. Knowles, *Science,* **2017**, 355, 727–730; (g) G. Coin, R. Patra, S. Rana, J. P. Biswas, P. Dubourdeaux, M. Clémancey, S. P. De Visser, D. Maiti, P. Maldivi and J.-M. Latour, *ACS Catalysis,* **2020**, *10*, 10010–10020; (h)N. K. Fu, G. S. Sauer, A. Saha, A. Loo and S. Lin, *Science*, **2017,** *357*, 575–579;
73. A. Zavitsas, *J. Phys. Chem. A*, 2003, 107, 897-898.
74. (a) J. Liu, J. Pan, X. Luo, X. Qiu, C. Zhang and Jiao, N, *Research*, **2020**, 7947029; (b) A. Kumar and B. A. Shah, *Org. Lett.*, **2015**, *17*, 5232−5235; (c) S. Onodera, R. Togashi, S. Ishikawa, T. Kochi and F. Kakiuchi, *J. Am. Chem. Soc.*, **2020**, *142*, 7345−7349.
75. (a) P. Zhang, W. Chen, M. Liu and H. Wu, *J. Org. Chem.,* **2018**, *83*, 14269−14276; (b) L. Liu, Z. Guo, K. Xu, S. Hui, Xi. Zhaoa and Y. Wu, *Org. Chem. Front.*, **2018**, *5*, 3315–3318; (c) K. Xu, Z. Li, F. Cheng, Z. Zuo, T. Wang, M. Wang and L. Liu, *Org. Lett.*, **2018**, *20*, 2228–2231; (d) Y. Qu, Z. Li,a, H. Xiang and X. Zhou, *Adv. Synth. Catal.,* **2013**, *355*, 3141 – 3146.
76. L. Peng, L. Ma, Y. Ran, Y. Chen and Z. Zeng, *Tetrahedron Lett.*, **2021**, *74*, 153092.
77. (a) N. Anand, Kannapu. Reddy, P. H. K. S. R. Rao and D. R. Burri, *Catal. Lett., 2011*, 141, 1355–1363;(b) M. Bonaido, F. Borin, M. Bressan and A. Morvillo, *Journal of*

Organometailic Chemistry ,**1989**, *363*, 175-179; (c) C. Mi, X.-G. Meng, X-H. Liao and X. Peng, *RSC Adv.*, **2015**, *5*, 69487-69492.

78. A. Moazzam, M. Khodadadi, F. Jafarpour and M. Ghandi, *J. Org. Chem.*, **2022**, *87*, 3630–3637.
79. (a) D. Shen, H. Wang, Y. Zheng, X. Zhu, P. Gong, B. Wang, J. You, Y. Zhao and M. Chao, *J. Org. Chem.*, **2021**, *86*, 5354−5361; (b) J. Ou, S. He, W. Wang, H. Tan and K. Liu, *Org. Chem. Front.*, **2021**, *8*, 3102-3109.
80. (a) A. Long and H. Zhang, Selective Oxidative Degradation of Toluene for the Recovery of Surfactant by an Electro/Fe2+/persulfate Process, Sci. Pollut. Res. 2015, 22, 11606–11616; (b) A. Long, Y. Lei and H. Zhang, *Ind. Eng. Chem. Res.*, **2014**, *53*, 1033−1039.
81. (a) Y. Wei, P. Hu, M Zhang and W. Su, *Chem. Rev.* **2017**, *117*, 8864–8907; (b) A. Varenikov, E. Shapiro and M. Gandelman, *Chem. Rev.*, **2021**, *121*, 412–484; (c) P. Xu, P. López-Rojas and T. Ritte, *J. Am. Chem. Soc.*, **2021,** *143*, 5349–5354; (d) X.-Q. Hu, Z.-K. Liu, Y.-X. Hou and Y. Gao, *IScience.*, **2020**, *23*, 101266; (e) L. Candish, M. Freitag, T. Gensch and F. Glorius, *Chem. Sci.* **2017**, *8*, 3618–3622; (f) N. Zrinyi and A. L.-T. Pham, *Water Res.*, **2017**, *120*, 43-51; (g) J. Lee, U. v. Gunten and J.-H. Kim, *Environ. Sci.Technol.*,**2020,** *54*, 3064−3081;
82. (a) J. Fang, D. Wang, G.-J. Deng and H. Gong, *Tetrahedron Lett.*, **2017**, *58*, 4503–4506; (b) K. Zhan and Y. Li, *Catalysts*, **2017**, *7*, 314. (c) Z. Li, K. Wang and Z.-Q. Liu, *Synlett*, **2014**, *25*, 2508–2512.

Chapter-IV

C-H activation reactions

Section-I

C-H activation reactions Using Heterogeneous metal catalysts

1/a Introduction

In past few years, direct functionalization of unreactive C–H bonds has garnered significant interest in the field of organic synthesis.[1] By eliminating the need for pre-functionalized substrates in comparison to conventional cross-coupling methods, this step-economical strategy offers a means of achieving ecologically benign and commercially appealing organic synthesis.[2] For cross-coupling reactions,[3] in fact, while well-established stoichiometric and catalytic methods[4] have provided access to important molecular structures, they also necessitate a particular pre-functionalization due to the inevitable formation of undesirable by-products, such as halides, salts, borates, etc. Consequently, C-H activation/functionalization techniques offer a more step-economically efficient substitute.[5] As a consequence, this strategy has found a growing number of applications in the preparation of pharmaceuticals,[6] naturally occurring compounds[7], agrochemicals and other practically useful products[8]. It has been possible to streamline organic synthesis with the development of powerful transition of metal catalysts for C-H activation.[9] A significant obstacle of this method is the potential to achieve site-selectivity and remarkable progress has already been made in this area. Although there have been significant advancements, most C–H activations have been accomplished using homogeneous catalysts,[10] indicating that there is still plenty of room for improvement for researchers in this field. Therefore, these catalysts, which are typically costly, have limited recyclability. Additionally, the purification of the desired products from any metal impurities often requires the use of specific reagents or chromatographic techniques, especially in the pharmaceutical industry.[11] However, in industrial settings, well-established homogeneous methods are commonly preferred for the production process.[12] Clearly, the decisions made in industries are primarily driven by economic factors, which are also greatly influenced by regulations and the cost/availability of materials. As these factors change over time, such as with the tightening of environmental regulations and the depletion of natural resources, a chemical approach that may not be economically viable currently could potentially become a viable option in the future. Heterogeneous catalytic approaches, which inherently facilitate catalyst recovery, show promise as long as the recovered catalyst can be reused without any decrease in activity. Another intriguing factor is the potential utilization of heterogeneous catalysis to attain a particular site-selectivity, or a change in selectivity in comparison to similar homogeneous processes, and potentially an enhancement in catalytic activity.[13] In the context of green chemistry, combining chemical efficiency with economic and environmental needs is of key interest. Hence, the creation of reusable heterogeneous catalysts is extremely desirable, as they not only enable easy separation through filtration and can be recycled[14], but also offer opportunities for developing innovative chemical processes. Therefore, heterogeneous catalysis surpassed homogeneous catalysis due to its portability, utility, and ability to be recycled. Heterogeneous catalyst supports that consist of metal or metal oxide nanoparticles typically exhibit higher catalytic efficiency compared to their macroscopic counterparts due to their diverse shapes, sizes, and high surface-to-volume ratios. However, challenges such as NP agglomeration, isolation of desired products, and catalyst renewability have highlighted the necessity for a safer, non-toxic, environmentally friendly, and recyclable support for

coupling reactions in heterogeneous environments.[15] Furthermore, their paramagnetic properties allow them to be easily separated from the reaction mixture and reused numerous times with the help of an external magnetic field.

1/b Review

Although there have been significant advancements and progress in metal-catalyzed C–H functionalizations, these methods are mainly relied on the use of different metal catalysts that function in a homogeneous manner. This review provides an overview of the progress made in the development of heterogeneous catalysts that are user-friendly, recyclable, and can be easily separated from the reaction mixture. This approach demonstrated high levels of selectivity for both chemo- and site-selectivities, making it suitable for the formation of C–C and C–heteroatom bonds. Hence, catalysts that can be recycled were developed for various reactions such as arylations, hydroarylations, alkenylations, acylations, nitrogenations, oxygenations, or halogenations. This short review demonstrates use of various heterogeneous metal-catalysts in C–H functionalizations.

I. Intramolecular $Pd(OH)_2/C$-catalyzed direct arylation:

Nakamura *et al.* reported the first example of heterogeneous palladium catalysed C–H arylation. This contribution introduced aryl groups into isoxazole using palladium on charcoal, resulting in few cases lower yields than the reaction facilitated by $Pd(OAc)_2$. In 2005, Fagnou *et al*[16] reported on the application of palladium hydroxide (Pearlman's catalyst) on carbon to facilitate direct C–H arylation with aryl iodides or bromides. This was seminal example of C–H arylation using a heterogeneous catalyst (Scheme 4.1). The catalytic system demonstrated high efficiency in both intramolecular arylation (resulting in benzo[c]chromenes and dihydrophenanthridine derivatives) and intermolecular processes (albeit only heteroaromatics were employed as substrates in the latter case). Two experiments were conducted to examine the characteristics of the active catalytic species.

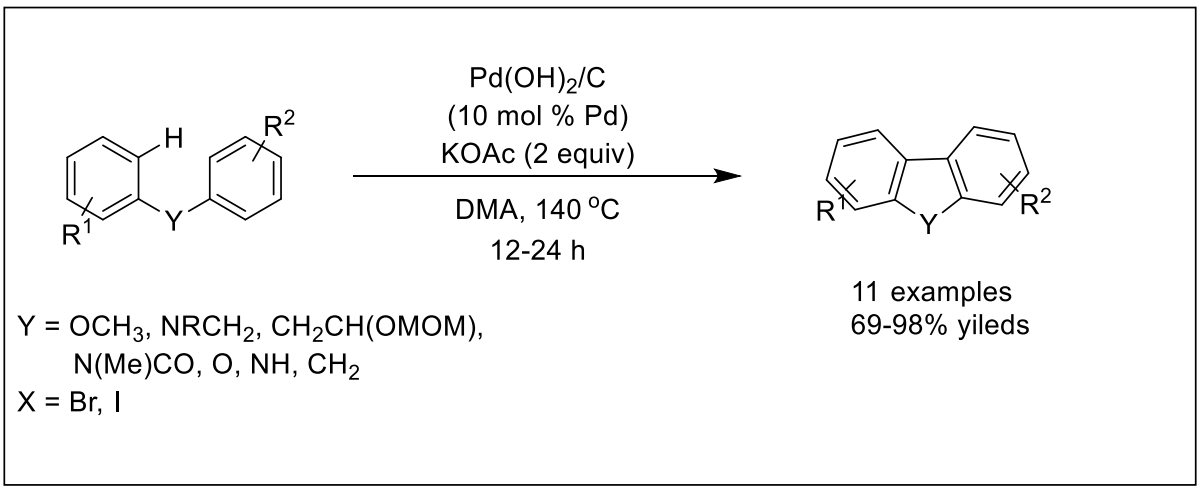

Scheme-4.1

II. Heterogeneous palladium-catalyzed approach to 2- and 2,3-substituted indoles:

Using heterogeneous palladium catalysts, Djakovitch *et al*[17] showed that 2-substituted indoles could be arylated by aryl bromides. The catalysts were either a microporous system of $[Pd(NH_3)_4]^{2+}$/NaY, obtained through ion exchange from NaY zeolite, or a mesoporous material of [Pd]/SBA-15, prepared by immobilizing a phosphine ligand on calcined SBA-15 mesoporous silica. Only two representative substrates have undergone testing, and the results have indicated extremely low reactivity. Surprisingly, the utilization of aryl iodides resulted in specific N-arylation, rather than the intended C3- arylation outcomes. This group further developed the C3-arylation process in a subsequent study, utilizing the $[Pd(NH_3)_4]^{2+}$/NaY catalyst and aryl bromides as the arylating reagent, but transitioning from NaOAc to K_2CO_3 as the base and from NMP to 1,4-dioxane as the solvent (Scheme 4.2).

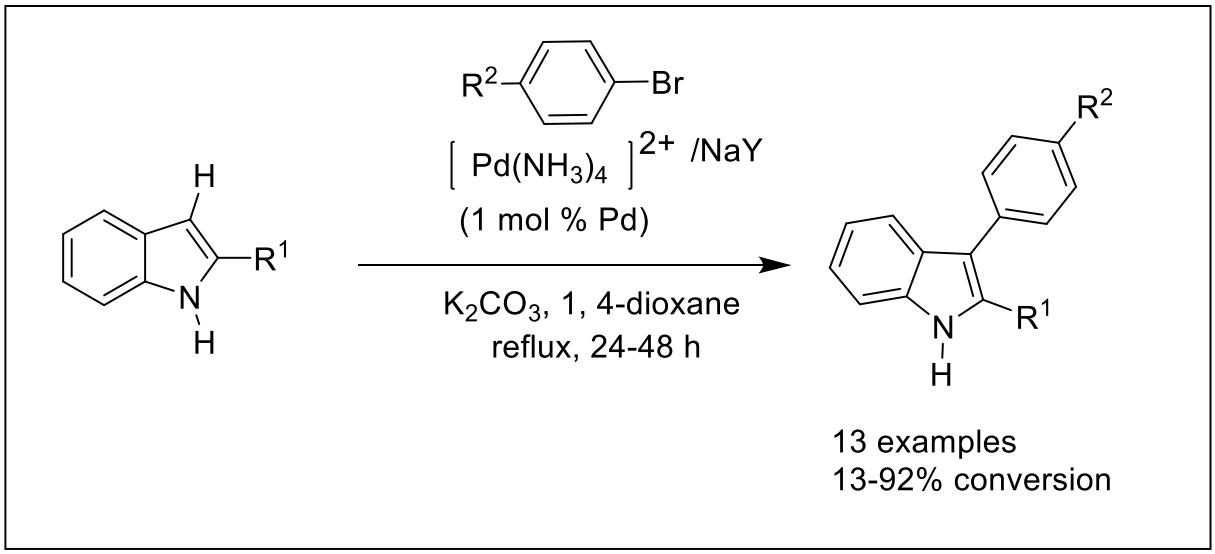

Scheme-4.2

III. Direct C–H arylation in the synthesis of pyrazolophenanthridines:

A series of pyrazolophenanthridines were synthesized by Domínguez and his co-workers[18] through the intramolecular direct arylation of diarylpyrazoles (Scheme 4.3). Utilizing a tandem amine-exchange/hetero cyclization of enaminones, the regioselective synthesis of 1,5-diarylpyrazole intermediates was successfully carried out. These intermediates exhibit a structural similarity to relevant nonsteroidal anti-inflammatory drugs like celecoxib or tepoxalin. The ultimate crucial stage involved in cyclization through intramolecular bi-aryl bond formation was achieved using two different approaches: radical coupling and catalytic direct arylation through C-H activation. In addition to other palladium sources, the reaction has the potential to be catalyzed by commercially accessible heterogeneous polymer supported palladium catalysts FibreCat 1001 and FibreCat 1000-D7. The results obtained from the utilization of heterogeneous catalysts were somehow unsatisfactory when compared to the outcomes achieved with simple $Pd(OAc)_2$. Upon recovery, the catalyst was employed in additional reaction trials, resulting in a significant decrease in conversion to only 21–25%.

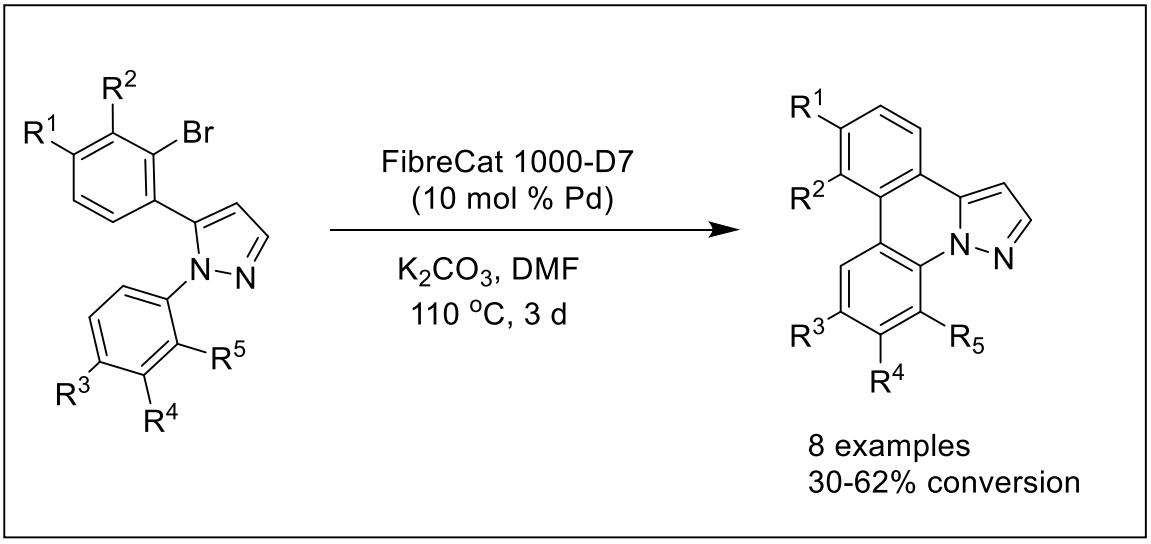

Scheme-4.3

IV. Palladium-catalyzed C2-selective arylation of NH-free pyrroles:

Pearlman's catalyst was utilized by Jafarpour and his co-workers[19] to enable the C2- site-selective C–H arylation of pyrroles with aryl iodides. This procedure provides a straightforward method to synthesize a variety of substituted 2-aryl-1H-pyrroles from readily available starting materials. The reaction protocol took place in triethylamine at a temperature of 100 °C and showed the best progress with NH-free pyrroles (R_1 = H), whereas N-methylpyrrole and N-phenylpyrrole (R = Me or Ph) produced lower yields (Scheme 4.4). Both electron-deficient and electron-rich aryl iodides are suitable for use as arylating agents. The reaction's scope is further extended to N-aryland -alkylpyrroles, albeit with reduced yields. Unfortunately, the study failed to examine both the recyclability of the catalyst and the true nature of the catalytic species.

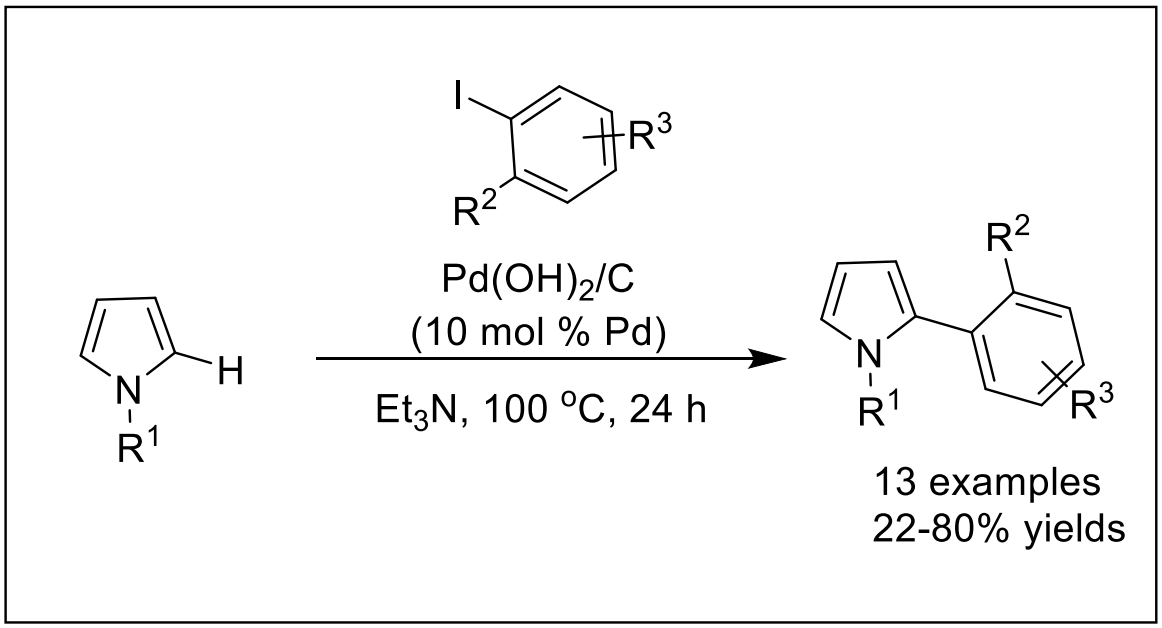

Scheme-4.4

V. Nanoparticles as reusable catalysts for indole C2-arylation:

Cai and his co-workers[20] synthesized perfluoro-tagged palladium nanoparticles supported on fluorous silica gel (Pd_{nps}/FSG) and investigated their efficacy as catalysts for the C–H arylation of indoles. The design of the catalyst depended on stabilizing metal nanoparticles with compounds containing lengthy perfluorinated alkyl chains, and on the ability to also utilize these groups to support the nanoparticles on fluorous silica gel through non-covalent fluorous interactions. The catalyst proved to be highly effective in promoting the regioselective C2-arylation of heteroarenes, even at a remarkably low catalyst loading of 0.1 mol%. The N-methyl indoles (R_2 = Me) and N-benzylindole (R_2 = Bn) proved to be the most effective, resulting in the highest yields and the NH-free substrate (R_2 = H) produces only moderate yields (Scheme 4.5). Aryl iodides (Scheme 4.5, X = I) were the preferred reagents for arylating, while the utilization of aryl bromides or chlorides (Scheme 4.5, X = Cl or Br) resulted in diminished yields. The catalyst was easily recovered through a process of centrifugation and decantation, and it was able to be reused for seven successive cycles despite a minor decrease in activity. The analysis using ICP-AAS demonstrated a low concentration of palladium in the crude reaction mixtures. The TEM analysis performed of the recovered particles exhibited a slight increase in the size of the palladium particles. The hot-filtration test provided evidence that the reaction was completely stopped after the solid catalyst was eliminated. Again ICP-AAS analysis was carried out on the filtrate, indicating a negligible amount of palladium. The results obtained strongly confirmed the occurrence of genuine heterogeneous catalysis. Cao and Co-works[15] developed the C2-selective C–H arylation of indoles by utilizing palladium nanoparticles confined within a MOF MIL-101(Cr) ($Cr_3(F, OH)(H_2O)_2O[(O_2C)–C_6H_4–(CO_2)]_3 \cdot nH_2O$; n ≈ 25) as catalysts (Scheme 4.5b). Also, in this case only 0.1 mol% of the catalyst proved sufficient, with aryl iodides emerging as the most effective arylating reagents. Conversely, aryl bromides and chlorides resulted in diminished product yields. The ICP-AES analysis identified a very low amount of palladium content in the crude mixture after the workup, measuring at 0.4 ppm. The results of the hot-filtration test indicated that the reaction was completely stopped upon the removal of the heterogeneous catalyst. In addition, the catalyst can be recovered and utilized for a minimum of five reaction sequences, demonstrating a decrease in yield of only 4% by the fifth sequence. The TEM analysis performed on the catalyst that was recovered demonstrated that the size of the palladium particles closely resembled those observed in the freshly prepared catalyst. This similarity can be attributed to the confinement of the particles within the mesoporous cages, thereby restricting their growth.

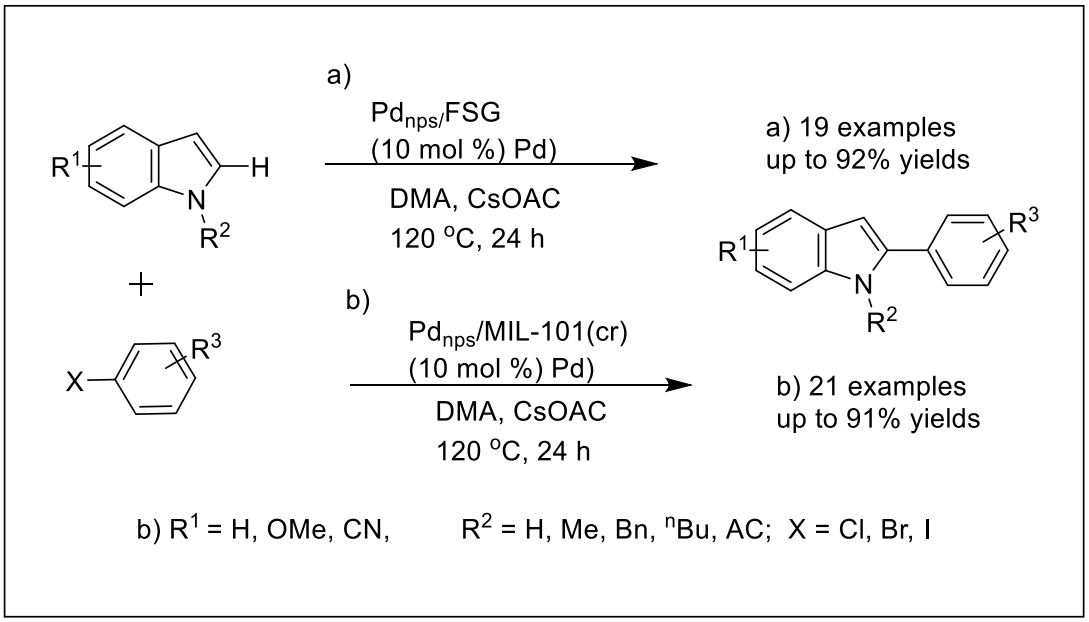

Scheme-4.5

VI. Cucurbit[6]uril-stabilized palladium nanoparticles for direct C–H functionalization of oligofluoroarenes:

Cao and Co-works[21] developed palladium nanocrystals stabilized by cucurbit[6]uril and used this system (CB[6]-PdNPs) as a heterogeneous catalyst in the direct arylation of polyfluoroarenes with aryl iodides and bromides. Several polyfluorinated arenes were found as suitable for this transformation, usually leading to the product being obtained in good yields (Scheme 4.6). When multiple potential arylation sites were available, the reaction would selectively produce monoarylation at the C–H site that was kinetically the most acidic. This method allows for the utilization of aryl halides possessing different electron-rich and electron-poor substituent. Moreover, it exhibits excellent tolerance towards a wide range of functional groups, such as esters, ketones, cyano, and trifluoromethyl substituents. The heterogeneous catalyst was recycled efficiently for five reaction cycles, without loss of catalytic activity. The yield of the desired product was 90% at the 5th cycle of reaction.

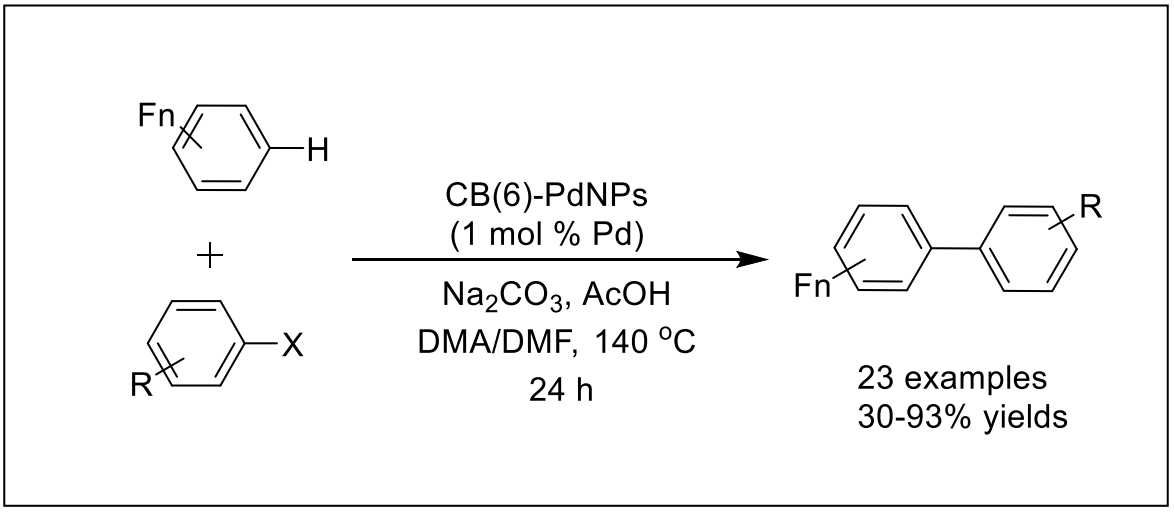

Scheme-4.6

VII. Palladium–polypyrrole nanocomposites as catalysts for the arylation of heteroaromatics:

Vorotyntsev, Hierso, and their group[22] successfully produced Pd@PPy nanocomposites through the redox polymerization of pyrrole with $[Pd(NH_3)_4Cl_2]$. These nanocomposites were subsequently tested for their catalytic efficiency in the C–H arylation of 2-butylfuran (X = O) and 2-butylthiophene (X = S) using aryl bromides (Scheme 4.7). The reaction generally occurred in selectively at the C5-position with good conversion. Catalyst recyclability was investigated but different result was obtained depending on the substrate. GC con version decreasing from 100 to 85% with a second catalytic run. According to TEM analysis, the recovered material's particle size has generally increased.

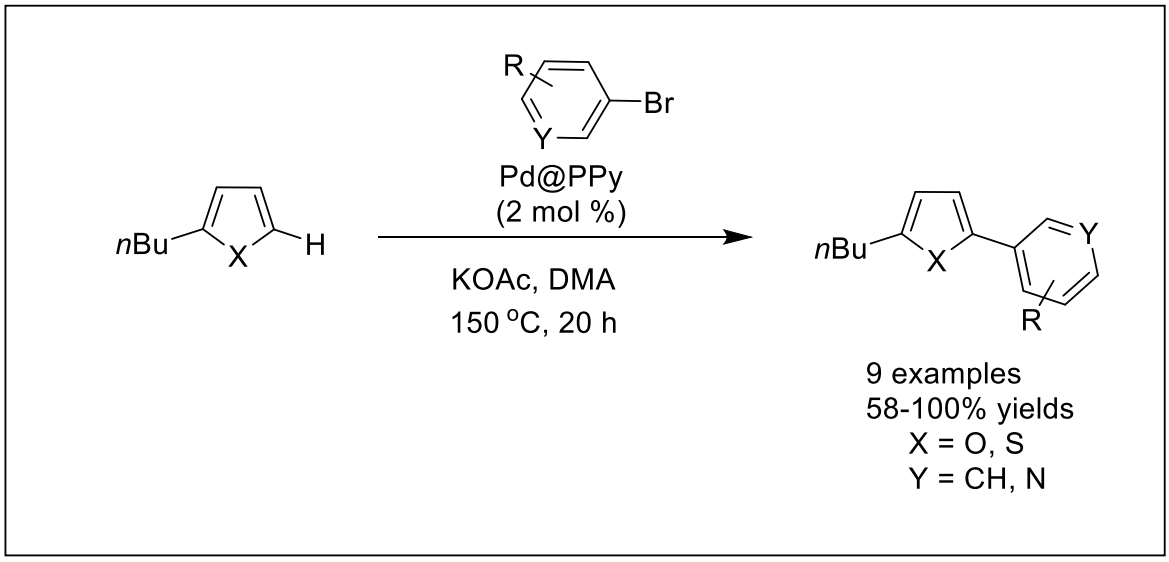

Scheme-4.7

VIII. C–H bond arylation of imidazo[1,2-a]pyridine using magnetically recyclable Pd–Fe_3O_4 nanoparticles:

Kim, Lee, and their co-workers[23] utilized nanocrystals composed of bimetallic Pd–Fe_3O_4 as a catalyst for the direct C–H arylation of imidazo[1,2-a]pyridine with various aryl bromides (Scheme 4.8). It affords the products of C3-functionalization and tolerates a wide range of functional groups including nitrile, chloride, ketone, aldehyde and ether. When considering aryl bromides, it is found that those with lower electron density generally provide better results in terms of yield, compared to their electron-rich system. After arylation, the catalyst magnetically recovered and reused for ten consecutive reaction runs without loss of catalytic activity.

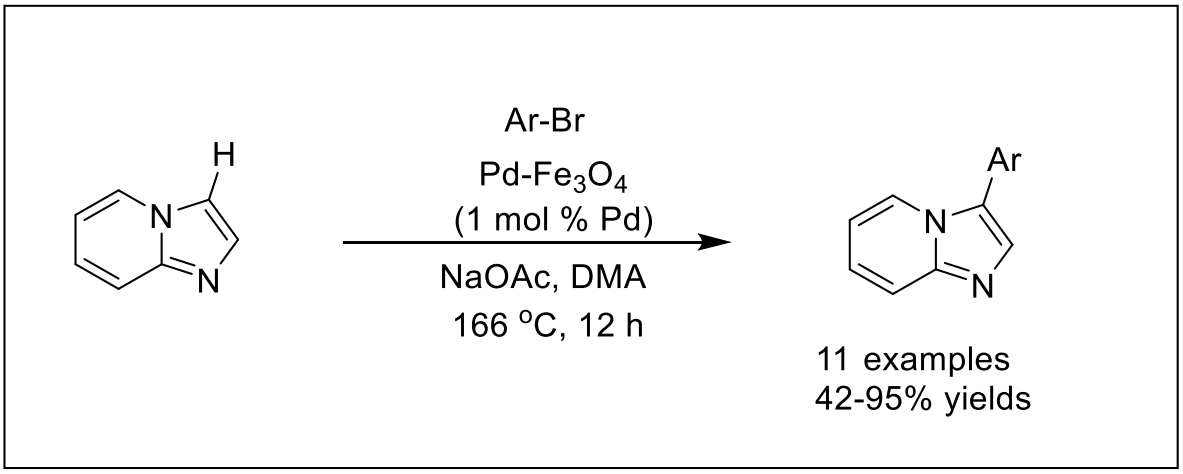

Scheme-4.8

IX.. C–H bond arylation of imidazo[1,2-a]pyridine using magnetically recyclable Pd–Fe_3O_4 nanoparticles:

Glorius and his group[24] repotted that aryl chlorides as the arylating agents could facilitate the C-3 regioselective C-H arylation of benzo[b] thiophenes when combined with commercially available Pd/C and catalytic amounts of CuCl (Scheme 4.9). The majority of methodologies reported for C–H arylations within this class of heterocycles demonstrated a notable preference for functionalization at the C-2-position. In general, electron-rich and electron-neutral aryl chlorides exhibit high product yields. However, when electron-poor arylating agents are used in the reactions, the corresponding products are obtained in lower yields. Various substituents on C5-functionalized benzo[b]thiophenes, as well as unsubstituted (R = H) ones, exhibited reactivity under the reaction conditions. The catalyst could not be efficiently recycled. The reaction was stopped by either introducing elemental mercury or by using hot filtration to eliminate the heterogeneous catalyst. Upon examination, it was observed that the addition of PPh_3, which is generally considered a poison for heterogeneous catalysts, resulted in a decrease in reactivity. The collected observations strongly indicated that the catalytic species is of a heterogeneous nature.

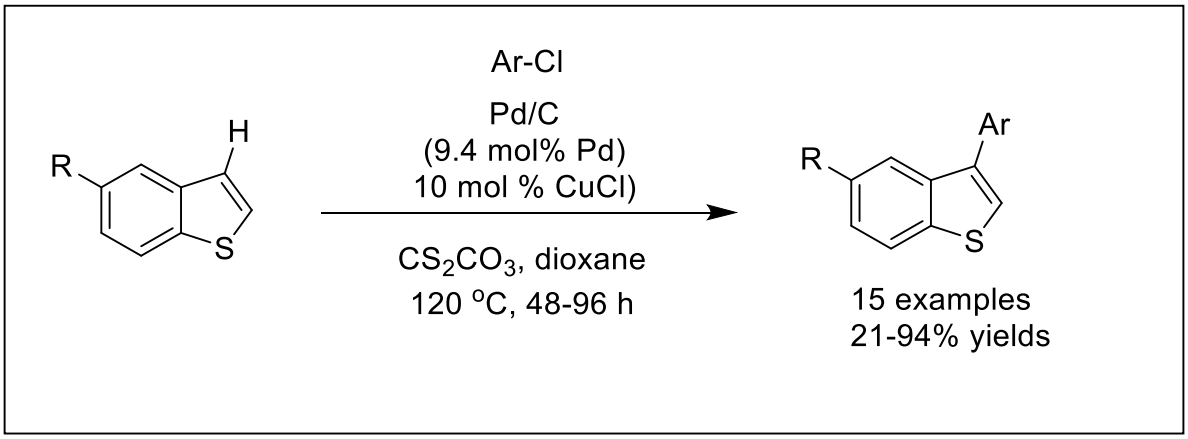

Scheme-4.9

X. Pd/C-catalyzed C–H arylation of benzo[b]thiophenes and thiophenes under mild conditions:

Consequently, Glorius and his group[25] developed an additional technique, once again utilizing Pd/C as a catalyst. However, this time they relied on iodonium salts as arylating reagents. The objective was to achieve C3-site-selective C–H arylation of benzo[b]thiophenes [R = $(CH)_4$] and thiophenes (R = H) (Scheme 4.10). The application of diphenyliodonium tetrafluoroborate $[Ph_2I]BF_4$ facilitated phenylation reactions, while the selective transfer of the less hindered aryl group was achieved by employing unsymmetrical [ArI(TRIP)]OTf (TRIP = 2,4,6-triisopropylphenyl). The C–H arylation of benzo[b]thiophenes and thiophenes can be achieved using Pd/C catalysts under mild reaction conditions with good yields (10-96%).

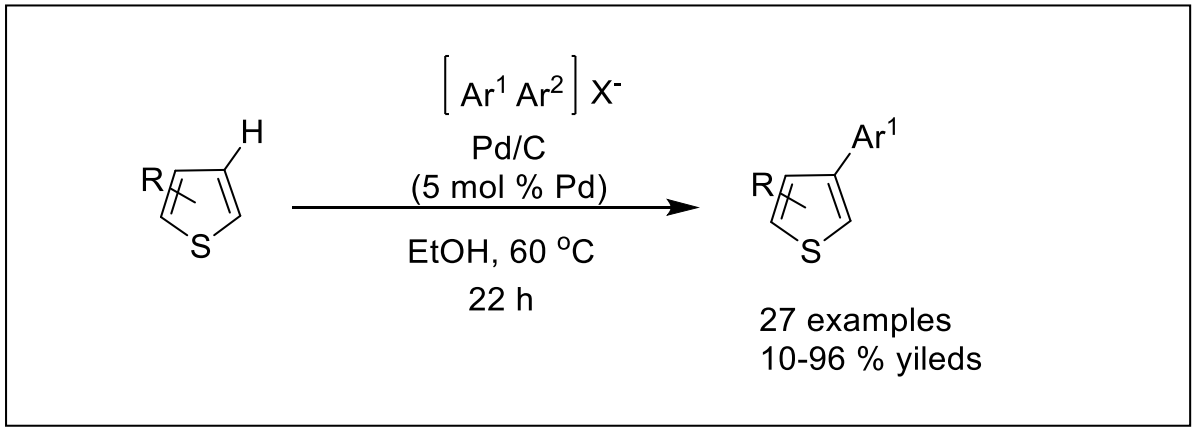

Scheme-4.10

XI. Palladium-immobilized on Fe_3O_4 magnetic nanoparticles as a catalytic system for the direct C2-arylation of indoles with arylboronic acids

Wang and co-workers[26] synthesized a magnetic Fe_3O_4 nanoparticle immobilized palladium catalyst (SiO_2@Fe_3O_4-triazolePd) and successfully utilized it for the direct C2-site-selective C–H arylation of indoles with arylboronic acids (Scheme 4.11). Preparation of the catalyst involved the application of click-chemistry on silica-coated Fe_3O_4 nanoparticles, resulting in the formation of triazoles, followed by the reaction of the particles with $Pd(OAc)_2$. The substrates for substitution included arylboronic acids which contained both electron-donating and electron-withdrawing groups. Electron-rich indoles underwent the reaction smoothly,

whereas indoles substituted with electron-withdrawing groups produced the desired product in lower yields. The heterogeneous catalyst was recycled efficiently for eight reaction cycles, without loss of catalytic activity. Further checked the ICP-AES analysis confirmed that the Pd concentration in the reaction mixture was below 0.20 ppm.

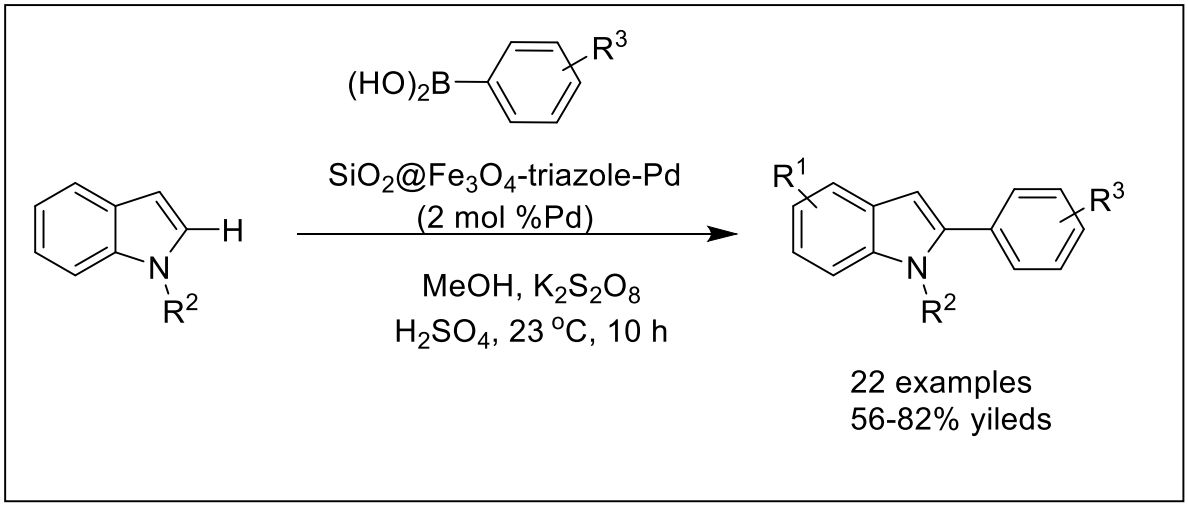

Scheme-4.11

XII. C2-selective arylation of indoles catalyzed by heterogeneous nanopalladium:

Palladium nanoparticles supported on amino-functionalized mesocellular foam (Pd0-AmP-MCF) were utilized by Bäckvall, Olofsson and their group[27] to catalyze the C2-regioselective C–H arylation of indoles with diaryliodonium salts as the arylating reagents (Scheme 4.12). The reaction occurred in water at either room temperature or 40 °C, and it could withstand a variety of functionalities on both the iodonium salt and the indole motif. Both indoles with and without protection were found to be appropriate substrates. The catalyst could be used for three consecutive reaction runs, although with a gradual decrease in activity (yield was reduced from 100 to 80 and then to 67%). The ICP-OES analysis confirmed that the filtrate contained very low amount of leached Pd at the end of the reaction, measuring at 0.6 ppm. Additionally, the authors verified in the control experiment that the leached palladium did not show any catalytic activity.

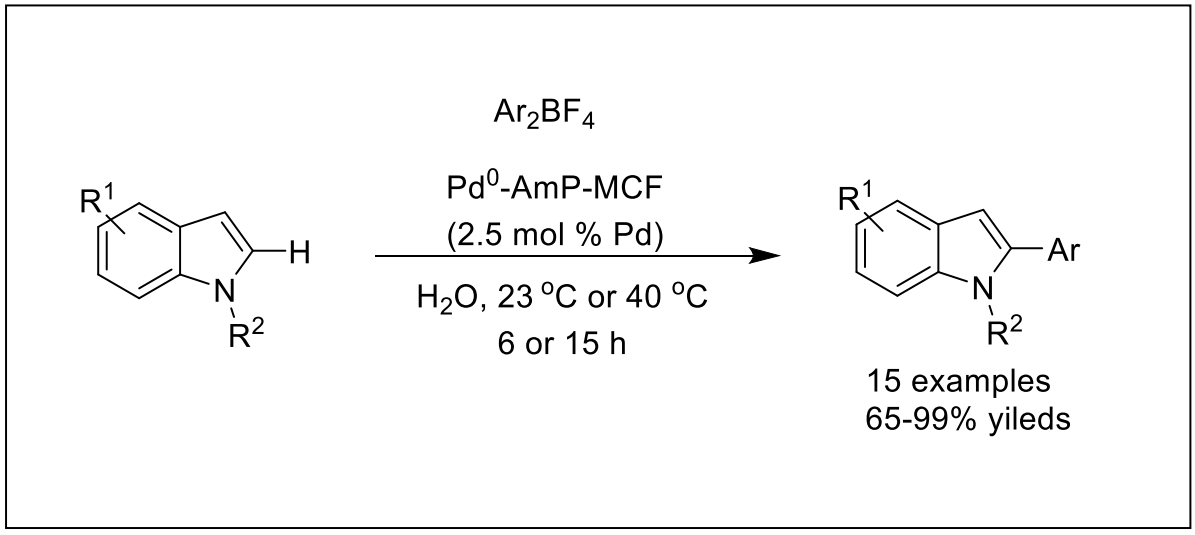

Scheme-4.12

XIII. Selective arylation of indoles catalyzed by heterogeneous nanopalladium:

Srinivasu and his group[28]synthesized a mesoporous silica material containing palladium nanoparticles (PS-3) and evaluated its efficiency in catalyzing the direct C–H arylation of benzamides with aryl iodides (Scheme 4.13). The reaction exhibited excellent site-selectivity for ortho-functionalization and proved to be tolerant towards the presence of various functional groups, including halides, ketones, and ethers. Both electron-rich and electron poor benzamides served as competent substrates for the process. The catalytic system resulted in the predominant production of monoarylated products while the formation of diarylated benzamides was restricted. Palladium was not detected in the filtrate through ICP-AES analysis upon completion of the reaction. The stability of the catalyst under the reaction conditions was confirmed by XRD, XPS (X-ray photoelectron spectroscopy), and TEM (transmission electron microscopy) analyses.

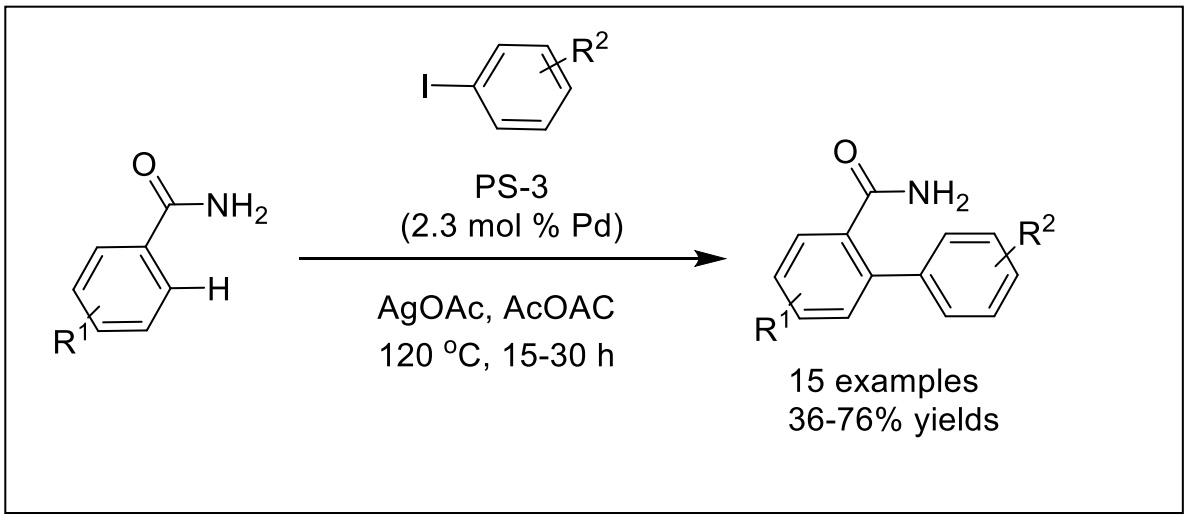

Scheme-4.13

XIV. Copper(I) and palladium nanoparticles as an efficient catalyst for the 1,3-dipolar cycloaddition/direct arylation sequence:

Keshipour and Shaabani[29] synthesized a novel heterogeneous catalyst, [Cu(I)/PdNPs@EDAC], by immobilizing Cu(I) and Pd nano particles on ethylenediamine-functionalized cellulose. This catalyst was then used in the 1,3-dipolar cycloaddition/direct arylation reaction to produce 1,4,5-trisubstituted-1,2,3-triazoles (Scheme 4.14). The initial stage involved the in situ formation of an organic azide through the reaction between benzyl bromide and sodium azide. This was followed by a 1,3-dipolar cycloaddition in the presence of copper catalyst, where the resulting organic azide reacted with phenylacetylene, yielding a 1,4-disubstituted-1,2,3-triazole product. The 1,4,5-trisubstituted-1,2,3-triazole was synthesized via palladium-catalyzed C–H arylation after addition of an aryl halide. Aryl iodides and aryl bromides were used in the reaction with satisfactory results, as well as heteroaryl bromides. It was found that the reaction was tolerant to various functional groups such as halides, ethers, esters and ketones. The heterogeneous catalyst was recycled efficiently for five consecutive cycles, with only a minor loss of catalytic activity.

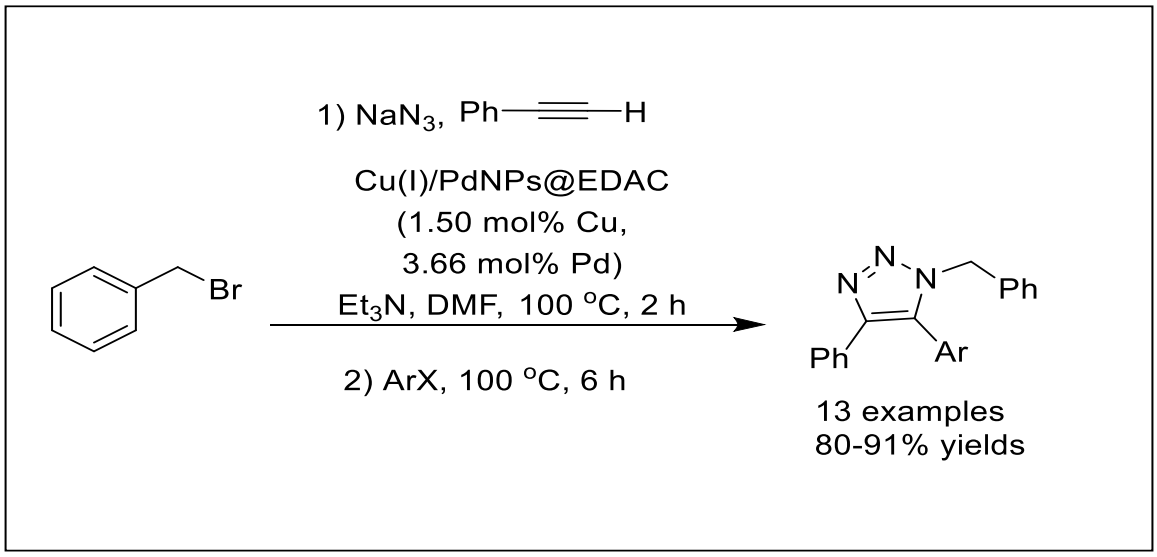

Scheme-4.14

XV. Recyclable copper catalyst for meta-selective C–H arylation:

Lee and Park[30] developed a simple general method for meta-selective C–H arylation of anilides, using a copper catalyst made up of metal nanoparticles trapped in aluminum oxyhydroxide nanofibers [Cu/AlO(OH)], along with diaryliodonium salts as arylating agents (Scheme 4.15). The pivalanilides containing electron-donating groups gave high efficiency in the reaction, whereas the arylation of 2-fluoropivalanilide (R = 2-F) led to a significantly low conversion. The ortho-phenylated derivative was the major product obtained from 3-methoxypivalanilide (R = 3-OMe) because of the para-directing effect of its methoxy-group. Ph_2IOTf is not the only iodonium salt that may be used; unsymmetrical arylmesity liodonium triflates (ArMesIOTf) also worked well to selectively transfer the less bulky aryl group, affording the meta-arylated anilide in generally good yields. The reactivity of catalyst was completely stop by a hot-filtration test, allowing the catalyst to be reused effectively for five successive reaction cycle without any loss of catalyst activity.

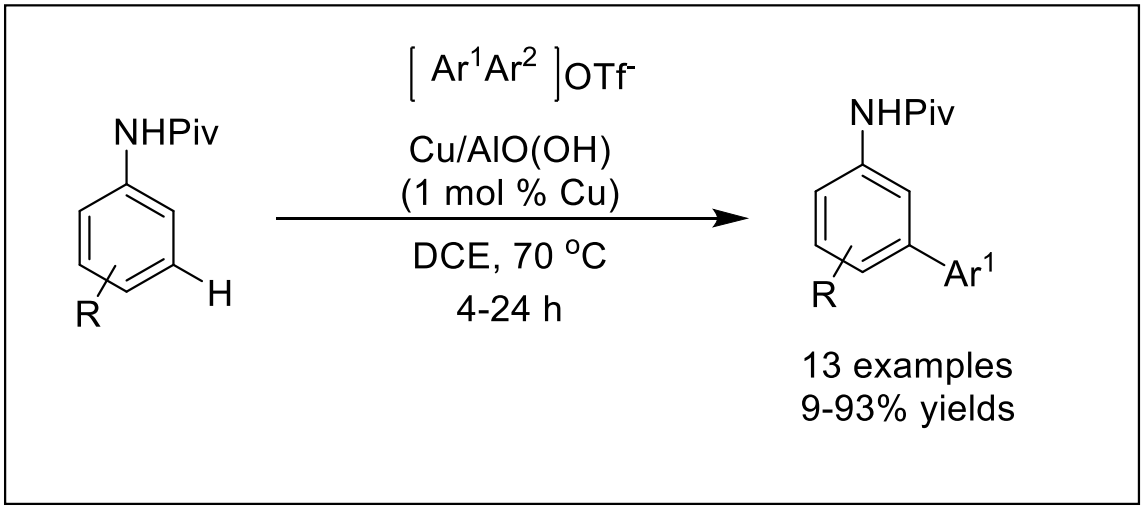

Scheme-4.15

XVI. CuO-nanospindle-catalyzed ligand-free arylation of C–H bonds in heterocycles:

Zhang, Wang and their group[31] developed a general methodology where CuO nanospindles were used as catalyst for the direct C–H arylation of heterocycles, including benzoxazole (X = O), benzothiazole (X = S), and N-methylbenzimidazole (X = NMe), in the presence of aryl iodides (Scheme 4.16). When electron-poor aryl iodides are used the reaction works efficiently and selectively resulting in higher yields. The protocol was not possible to extend in aryl bromides. The catalyst was recycled and reused effectively for three reaction cycle without loss of catalytic activity. When the catalyst was removed by centrifugation after one hour, no further conversion could be observed after 3 hours. Copper leached slightly during the reaction based on ICP-AAS analysis. The desired products were obtained in moderate to excellent yields (51-93%).

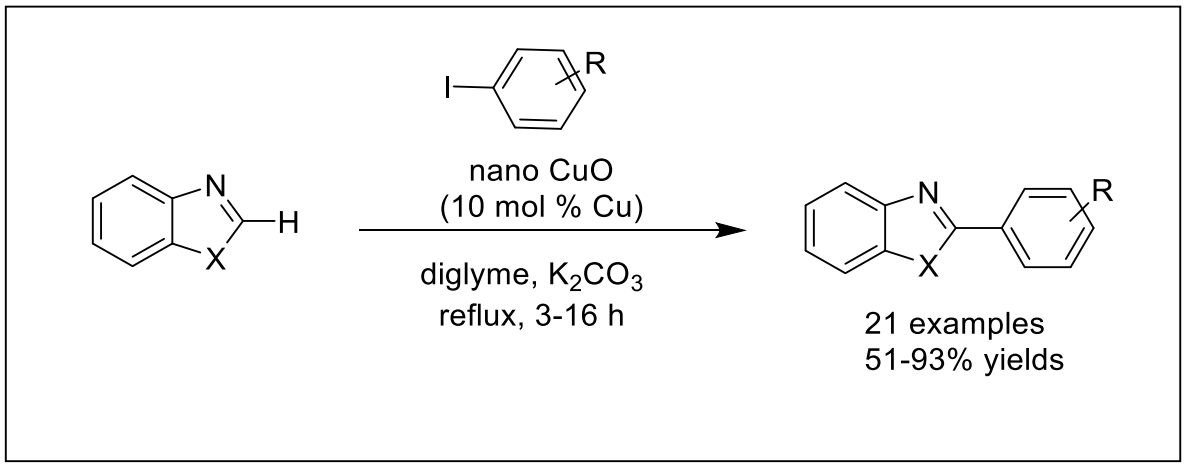

Scheme-4.16

XVII. Direct C–H arylation of heteroarenes with aryl halides over heterogeneous MOFs $Cu_2(BPDC)_2(BPY)$ and $Cu_2(OBA)_2(BPY)$:

Phan and his coworkers[32] developed a series of copper-based crystalline porous MOFs and utilized them as catalysts for the direct C–H arylation of various heterocycles with aryl halides. This reaction catalyzed by $Cu_2(BPDC)_2(BPY)$ was tested on benzoxazole, benzothiazole, 2-chloro thiophene, 4-methylthiazole, and N-methylbenzimidazole, resulting in yields that varied from moderate to excellent (Scheme 4.17a). Various aryl iodides, bromides and chlorides were performed in this reaction protocol and tolerant various functional groups such as nitrile, ketone, nitro, and ethers. The heterogeneous catalyst was recycled for six catalytic circle with limited decreases in the catalytic efficiency. The structure of the catalyst after recovery exhibited only slight changes as determined by FT-IR and XRD analysis. However, $Cu_2(OBA)_2(BPY)$ [OBA = 4,4′- oxybis(benzoate); BPY = 4,4′-bipyridine] proved to have the most superior catalytic performance compared to other Cu-MOFs in facilitating direct arylations of benzothiazole with aryl iodides 10a, utilizing *t*BuOLi as the base in dioxane at 120 °C (Scheme 4.17b).

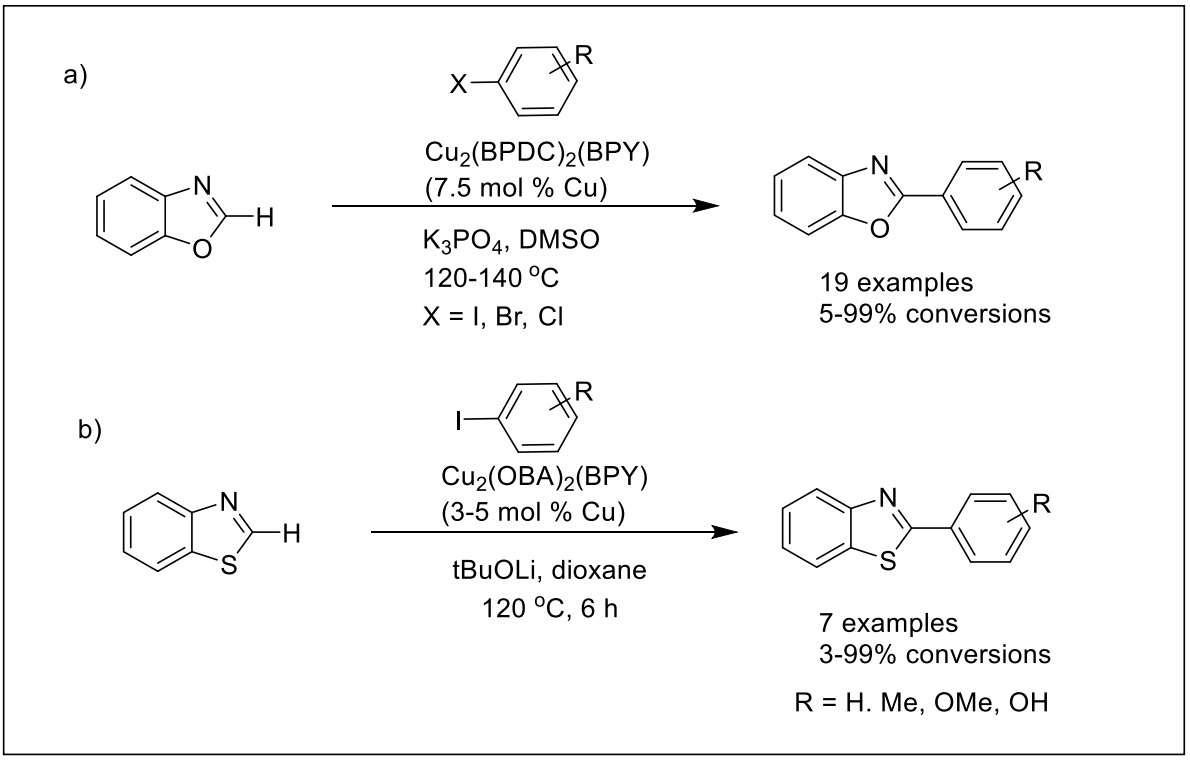

Scheme-4.17

XVIII. Solid ruthenium catalysts for the direct arylation of aromatic C–H bonds:

Wada and his group[33] developed and tested a variety of solid ruthenium catalysts for the chelation-assisted arylation of aromatic C–H bonds in substrates with aryl halides. Through the process of impregnating CeO_2 with a mixture of $[\{RuCl_2(CO)_3\}_2]$ and subsequent calcination at 400 °C, the catalytic system achieved its highest level of efficiency. Furthermore, after the solid ruthenium-system was treated with three equivalents of PPh_3 in a hydrogen atmosphere, a highly active catalyst ($3PPh_3$–Ru/CeO_2) was synthesized. The arylation products were selectively obtained in good yields when both electron-rich and electron-poor aryl chlorides (Scheme 4.18, X = Cl) reacted with benzo[h]quinoline (Scheme 4.18). Mixtures of mono- and diarylated products were obtained when the reaction was carried out on 2-phenylpyridine or on 1-phenyl-2-pyrazol 27 (Scheme 4.18, not fused aromatic ring). A sample reaction was used to assess the catalyst's recyclability. Following isolation through centrifugation, washing, calcination at 400 °C, and additional treatment with PPh_3, the catalyst was found to be reusable for at least three runs without any loss of activity.

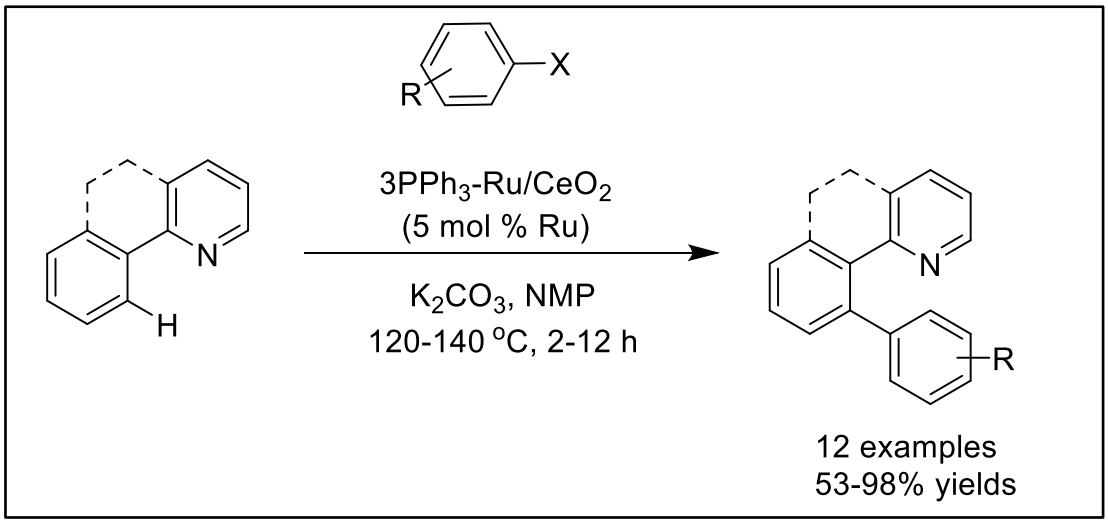

Scheme-4.18

XIX. Arylation of unactivated arenes with aryl halides over recyclable heterogeneous catalysts:

Li and his group[34] have documented a noteworthy achievement in the field of organic synthesis. They have successfully developed a transition metal-free direct C–H arylation method for aromatics, utilizing aryl iodides or bromides as reactants. This reaction is facilitated by a MOF catalyst known as MOF-253, specifically composed of Al(OH)(BPYDC) (where BPYDC refers to 2,2′-bipyridine-5,5′-dicarboxylate) (Scheme 4.19). Utilizing the arene as a reactant and solvent, the reactions were carried out at reaction temperatures ranging from 100 to 140 °C and tBuOK used as a base. When conducting the arylation of simple benzene (Scheme 4.19, R1 = H), the resulting product yields were generally very high. This was observed regardless of whether aryl iodides or bromides or heteroaryl iodides were used. More variable results were observed in terms of product yields and regioselectivity when conducting the direct arylation of substituted benzene derivatives. The catalyst exhibits the potential to be recycled for a minimum of five reaction runs without any significant decrease in yield. It was observed in the hot-filtration test that the reaction stops following the removal of the solid catalyst.

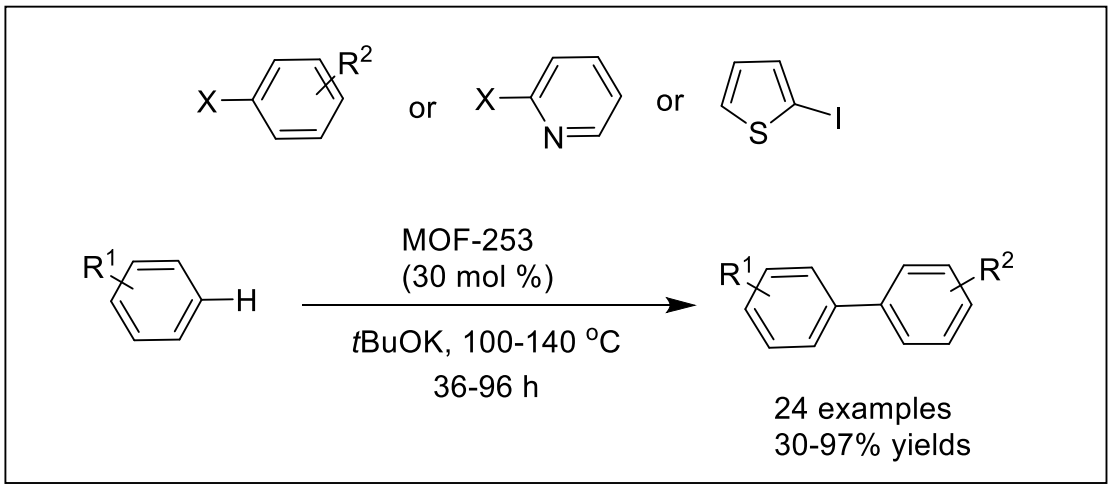

Scheme-4.19

XX. Ru/CeO_2-catalyzed hydroarylation with arenes:

Wada and his co-workers[35] have developed that the hydroarylation of vinylsilanes with various aromatic ketones can be efficiently catalyzed by ruthenium immobilized on CeO_2 (Scheme 4.20). Ethoxydimethyl(vinyl)silane has been reported as an alternative, although the main substrate employed was Triethoxy(vinyl)silane. The reaction was performed without requiring an additional reaction medium on a larger scale of 35 mmol, resulting in a significant reduction in catalyst loading to 0.06 mol%, albeit under rather drastic reaction conditions. It was observed in the hot filtration test that the reaction was fully arrested when the solid catalyst was removed. The recycling of the catalytic system proved to be unsuccessful in all attempts.

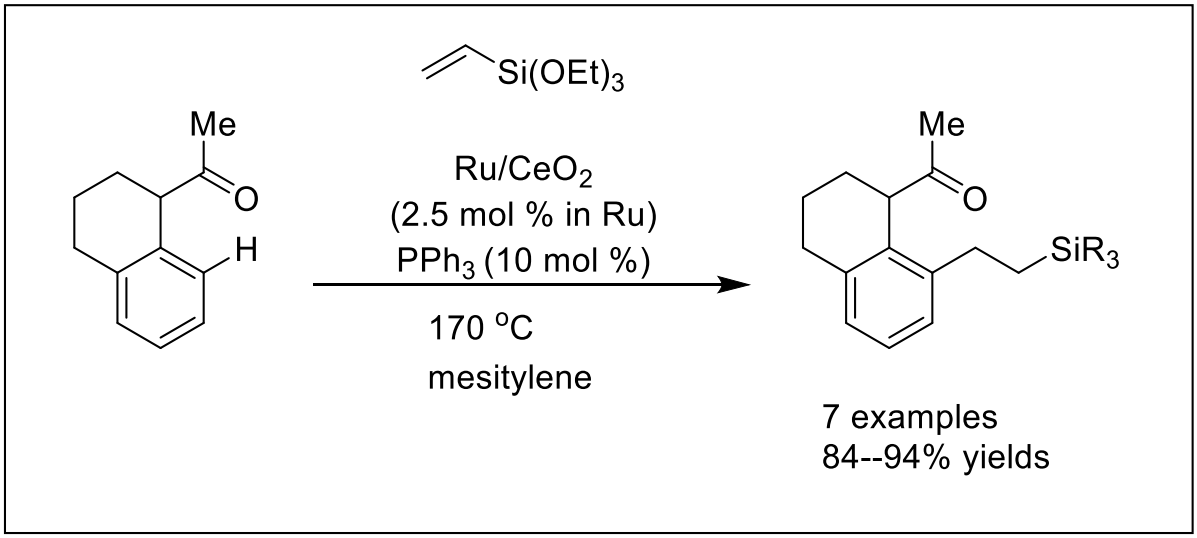

Scheme-4.20

XXI. Hydroarylations with anilidescatalyzed by heterogeneous Pd:

The oxidative Fujiwara-Moritani process has been reported to facilitate the coupling of arenes with olefins through heterogeneous catalysis. Ying and his co-workers[36] have successfully synthesized a nanomaterial called Pd-$H_6PV_3Mo_9O_{40}$/C (referred to as PdV_3Mo_9/C) by combining palladium and polyoxometalate. They conducted experiments to evaluate its effectiveness in the oxidative olefination of anilides using acrylates (where R_3 = CO_2-alkyl) as substrates. Notably, molecular oxygen was employed as the terminal oxidant in this reaction (Scheme 4.21). The reaction was found to be highly dependent on the electronic properties of the anilide, resulting in the highest yields when using unsubstituted or monomethylated substrates. The heterogeneous catalyst was recycled and without loss of catalytic activity. An ICP-MS analysis of the filtrate indicated the presence of a small quantity of leached palladium, measuring 7 ppm.

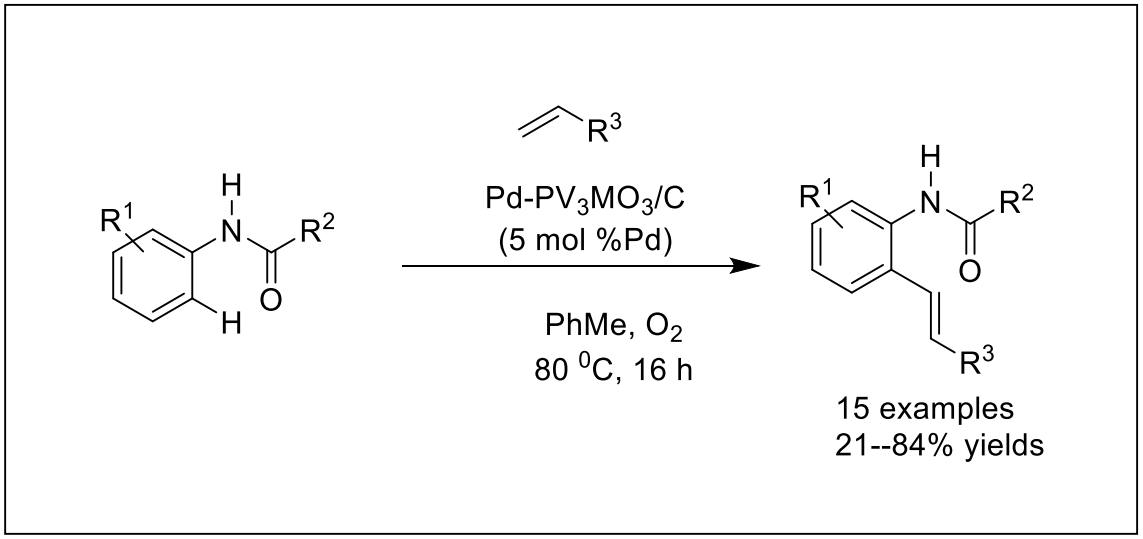

Scheme-4.21

XXII. Pd/Mg–La mixed oxide-catalyzed oxidative C(sp2)–H bond acylation using alcohols:

Kantam, Venugopal, along with their research group[37] have developed the oxidative acylation of aromatic substrates using the heterogeneous Pd(II)/Mg–La mixed oxide catalytic system. An oxidative direct acylation of 2-arylpyridines with alcohols (R_2 = aryl, alkyl) was successfully achieved by employing tert-butyl hydro peroxide (TBHP) as the oxidant in Scheme 4.22. The corresponding ketones were generally obtained in satisfactory yields by employing benzylic or aliphatic alcohols. Various functional groups, including fluoro, chloro, bromo, trifluoromethyl, and methoxy substituents were well-tolerated by the reactions. The ICP analysis revealed that the original catalyst contained 9.1% palladium (II), while the recovered catalyst had a slightly lower content of 8.9%. This indicates that there was only a minimal amount of metal leaching observed.

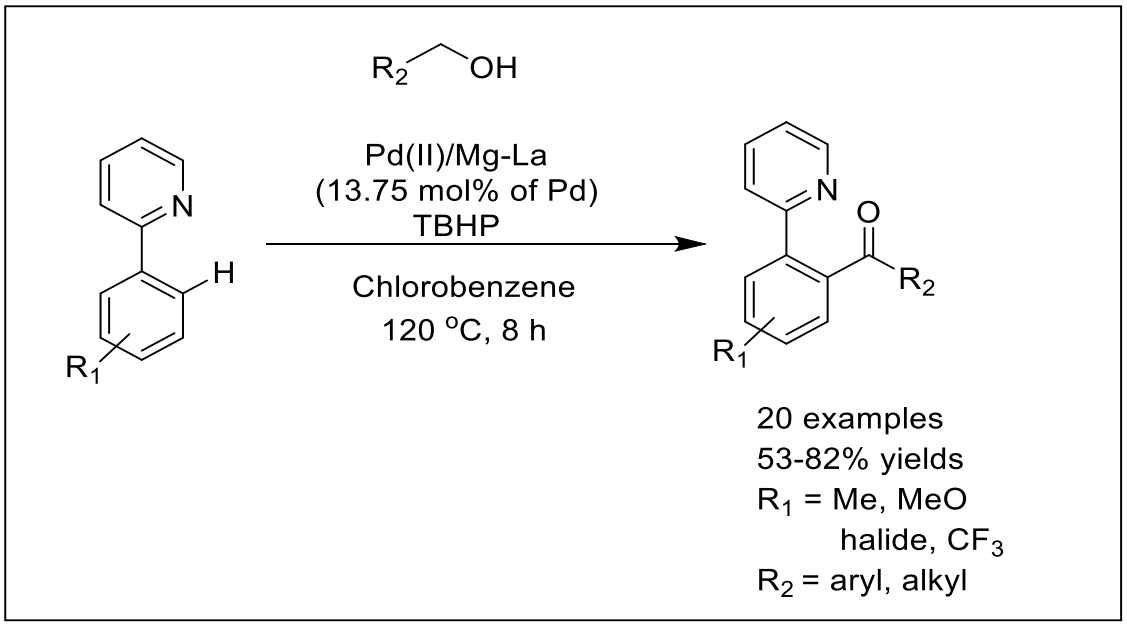

Scheme-4.22

XXIII. Pd(II)/Mg–La mixed oxide catalyst for cyanation of aromatic C–H bonds:

The C–H cyanation of 2-arylpyridine derivatives was carried out by Kantam and his coworkers[38] using their Pd(II)/Mg–La mixed oxide catalytic system. They employed NH_4HCO_3 and DMSO as a cyanating source (Scheme 4.23). The reaction was carried out effectively on various substrates containing different functional groups on the aromatic moiety. The catalyst was recyclability for four consecutive reaction runs without loss of catalytic activity.

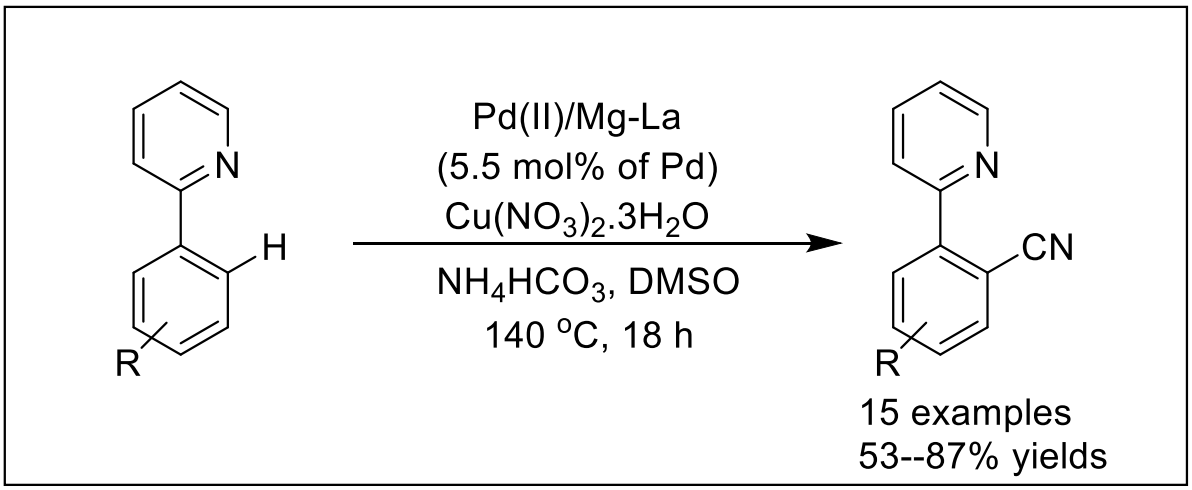

Scheme-4.23

XXIV. Regioselective α-cyanation of tertiary amines catalyzed by heterogeneous manganese oxides:

Mizuno and his coworkers[39] utilized manganese oxide-based molecular sieves (OMS-2, $KMn_8O_{16}\cdot nH_2O$) to catalyze the *α*-cyanation of tertiary amines with trimethylsilyl cyanide (TMSCN) as the cyano source and oxygen as the terminal oxidant (Scheme 4.24). On a variety of alkyl and aryl substituted amines, the reaction gave exclusively mono-cyanation usually with good selectivity in α-positions for the functionalization. ICP-AES analysis of the filtrate from the hot-filtration test indicated that leached of low amount of manganese.

The fact that the catalyst could be reused at least five times and suggests that the reaction was promoted by a heterogeneous catalyst rather than by leached homogeneous species. According to mechanistic investigations the reaction passes through an initial single-electron transfer (SET) followed by a deprotonation. The final product was obtained after a second SET and followed by attack of a cyanide ion on the iminium intermediate.

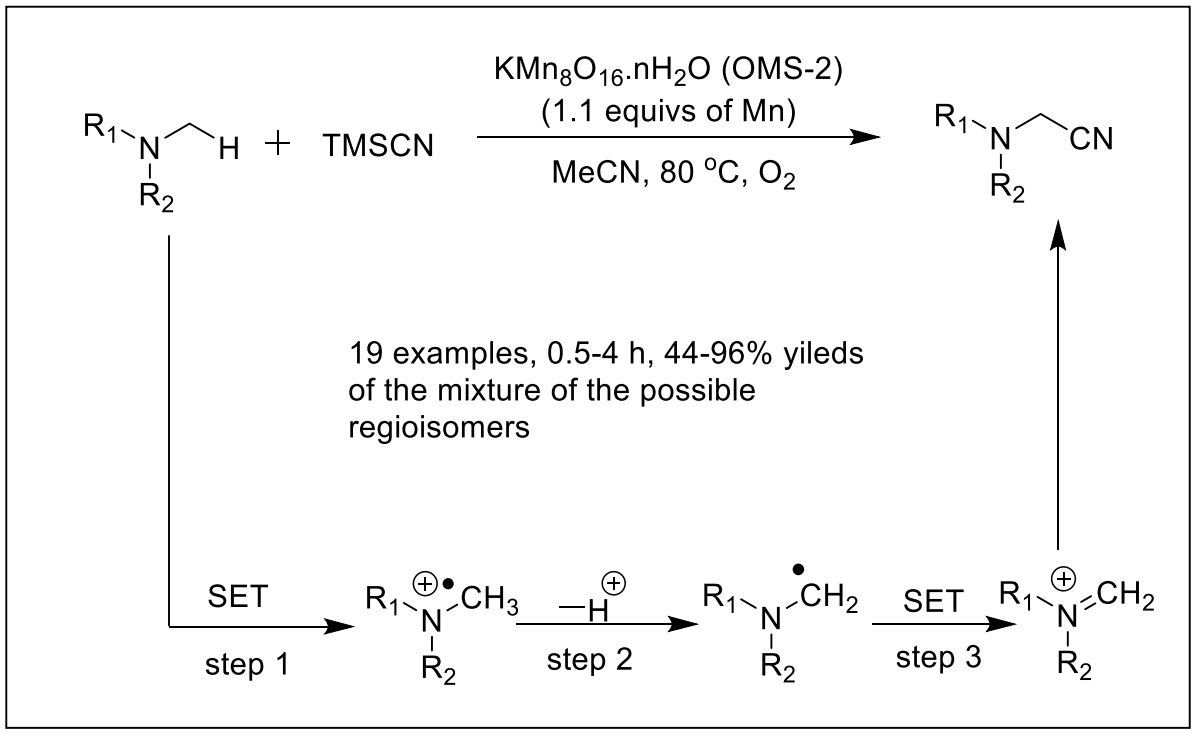

Scheme-4.24

XXV. Pd/cerium(IV) oxide-catalyzed oxidative synthesis of indoles:

Wu and his coworkers[40] have reported on a Pd/CeO_2-catalyzed oxidative synthesis of indoles from anilines and alkynes via C–H activation process (Scheme 4.25). In the reaction, copper (II) species acted as a co-catalysts and used as atmospheric oxygen for terminal oxidant. Several functional groups well tolerated under the identical reaction condition and few products were obtained in good yields. In the presence of aryl, alkyl-substituted alkynes, the reaction proceeded with high regioselectivity, positioning the alkyl group in distal to nitrogen, thus resembling the selectivity observed in homogeneous catalysis. Elemental mercury was introduced into the reaction mixture to conduct a mercury test, resulting in a 15% conversion after 15 minutes. Subsequently, after a duration of two hours, the conversion rate of the reaction reached to 20%. In contrast, the conversion rate in a control reaction without mercury was recorded at 88%. Recycling the catalyst was not possible due to a significant decrease in product yield during the second run.

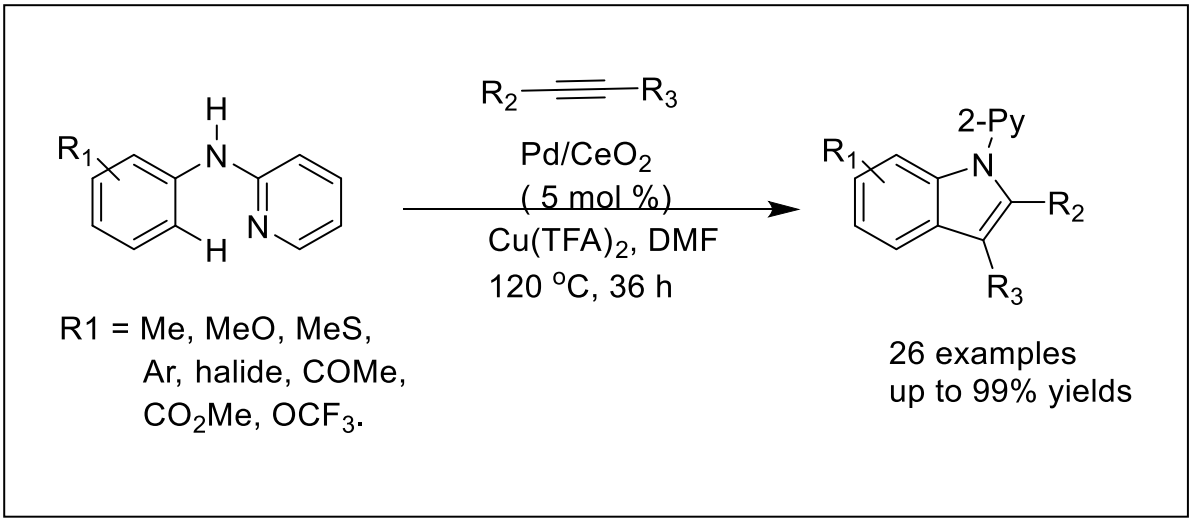

Scheme-4.25

XXVI. Metal–organic framework (MOF)-catalyzed oxidative synthesis of propargylamine:

Phan and his group[41] successfully demonstrated the catalytic potential of a copper-based metal-organic framework called MOF-199 ($Cu_3(BTC)_2$; BTC = 1,3,5-benzenetricarboxylate). This framework effectively promoted the oxidative coupling of N, N′-dimethylanilines with terminal alkynes, utilizing TBHP as a terminal oxidant. The outcome of this reaction was the synthesis of propargylamines. The substate scope of the reaction was limited. The yields of the products were obtained from moderate to good (55-81%) (Scheme 4.26). The catalyst was recycled effectively for ten catalytic cycle, without loss of catalytic activity. Further, analyses using FT-IR and XRD indicated that the catalyst remained unchanged following its recovery from the reaction mixture. A hot-filtration test was also performed indicated that the reaction was dropped after removal of the heterogeneous catalyst from reaction mixture.

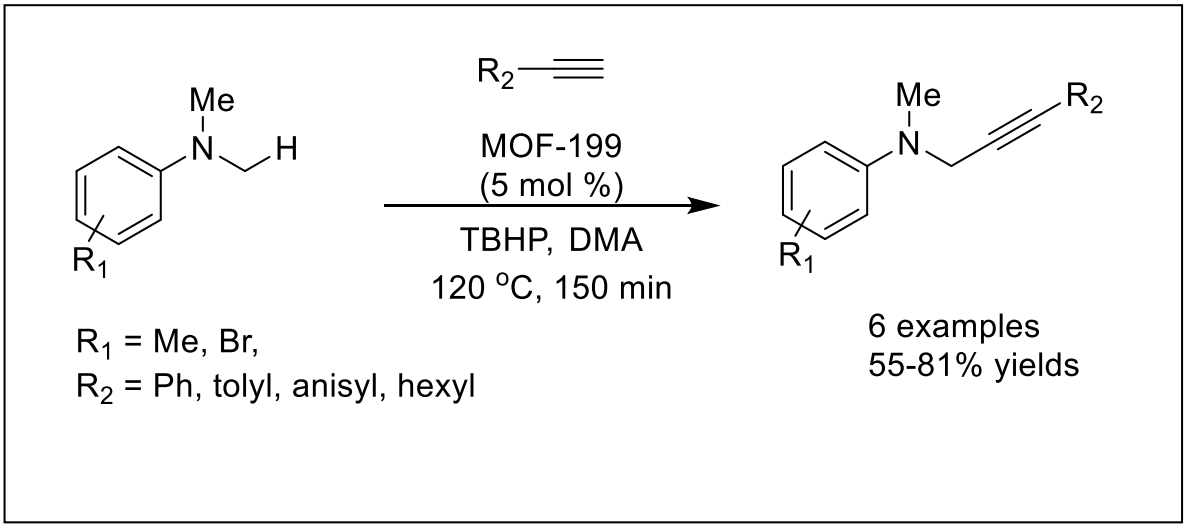

Scheme-4.26

XXVII. Palladium-polyoxometalate nanomaterials for the C–N bond formation through oxidative amination:

Ying and his group[42] employed their palladium-polyoxometalate nanomaterial Pd-$H_6PV_3Mo_9O_{40}$/C (referred to as PdV_3Mo_9/C in the text above) as a catalyst for the oxidative coupling of diaryl amines (R_1, R_2 = aryl) with acrylates (Scheme 4.27). The procedure required an oxygen atmosphere and proved to be highly responsive to the electronic properties of the substrates. In addition, the substitution of an aryl group with a butyl group, as well as the replacement of acrylate with methyl vinyl ketone, led to decreased yields. After reloading with PV_3Mo_9, the catalyst could be recycled, although with loss of activity, (1st cycle: 87; 2nd cycle: 79 and 4th cycle: 67%). According to hot-filtration result, the reaction progressed even after of the solid catalyst had been removed, demonstrating that some homogeneous Pd species can contribute to the catalysis.

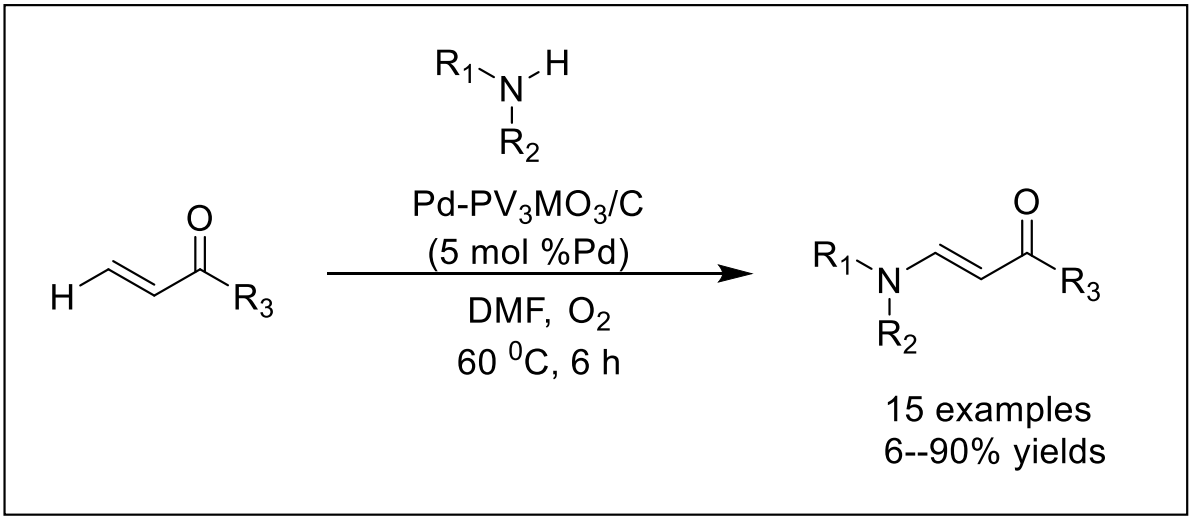

Scheme-4.27

XXVIII. Palladium on Zr(IV)-based MOF for selective C–H functionalization:

Fei and group[43] synthesized a palladium-containing metal-organic framework (MOF) by initially introducing the thiocatecholate (TCAT) ligand into a UiO-type MOF (Scheme 4.28). Subsequently, they utilized this MOF as a platform to incorporate palladium. The material UiO-66-PdTCAT exhibited its catalytic ability in the regioselective oxidative C–H alkoxylation of 7,8-benzoquinoline R_1, R_2 = –(CH)2–). The alkoxylation reaction used simple alcohols and (diacetoxyiodo)benzene as the oxidants. The conversion of the substance was nearly complete (95-99%) when using methanol, ethanol, and 2,2,2-trifluoroethanol. However, the transformation rate was significantly lower (21%) when employing 2-propanol. Additionally, homogeneous $Pd(OAc)_2$ has the ability to catalyze the methoxylation reaction with almost complete conversion and in a shorter reaction time. However, the heterogeneous catalyst exhibits a conspicuous benefit in being recyclable, allowing it to be reused for up to five reaction runs without experiencing a significant decrease in the yield. A hot-filtration test indicated that very low amount of leached Pd into the filtrate.

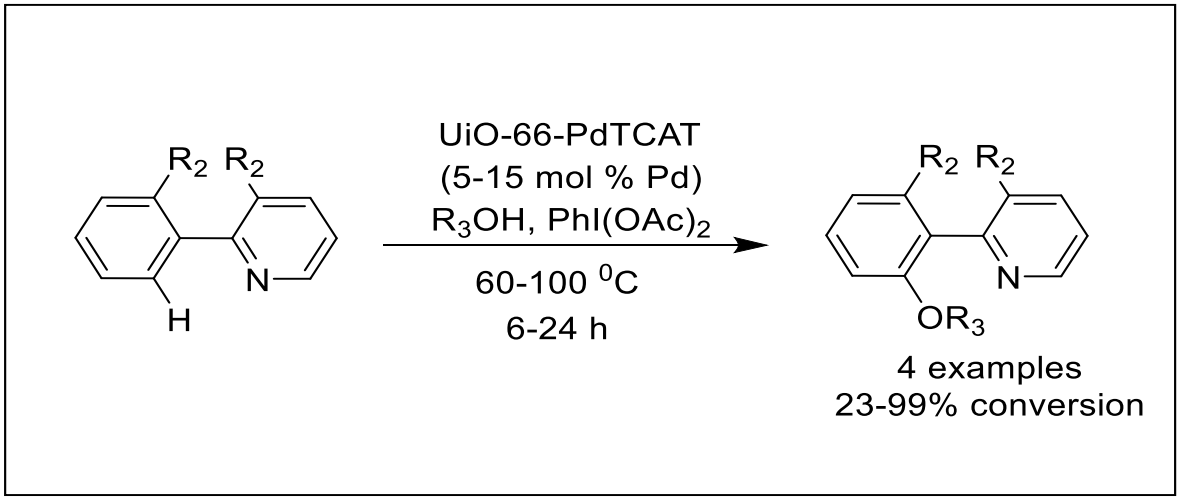

Scheme-4.28

XXIX. Oxidative C–O coupling by direct C–H activation of ethers over heterogeneous $Cu_2(BPDC)_2(BPY)$ catalyst:

Phan *et. al*.[44] prepared a crystalline porous MOF containing copper [$Cu_2(BPDC)_2(BPY)$; BPDC = 4,4′-biphenyldicarboxylate; BPY = 4,4′-bipyridine] and evaluated its efficacy in the oxidative C–O coupling of 1,4-dioxane and phenols (Scheme 4.29). Several parameters were optimized after careful screening of reaction conditions. The oxidizing agent of preference was TBHP, and the reaction could be performed by employing an excess of ether without the requirement of an additional solvent. The reaction's scope is restricted, as successful outcomes are exclusively observed with ortho-substituted phenols and 1,4-dioxane as the ether. The reactivity was halted due to the removal of the catalyst through centrifugation during the initial phases of the reaction. The catalytic activity of the catalyst remained unchanged for a minimum of eight consecutive cycles, allowing for its successful recycling.

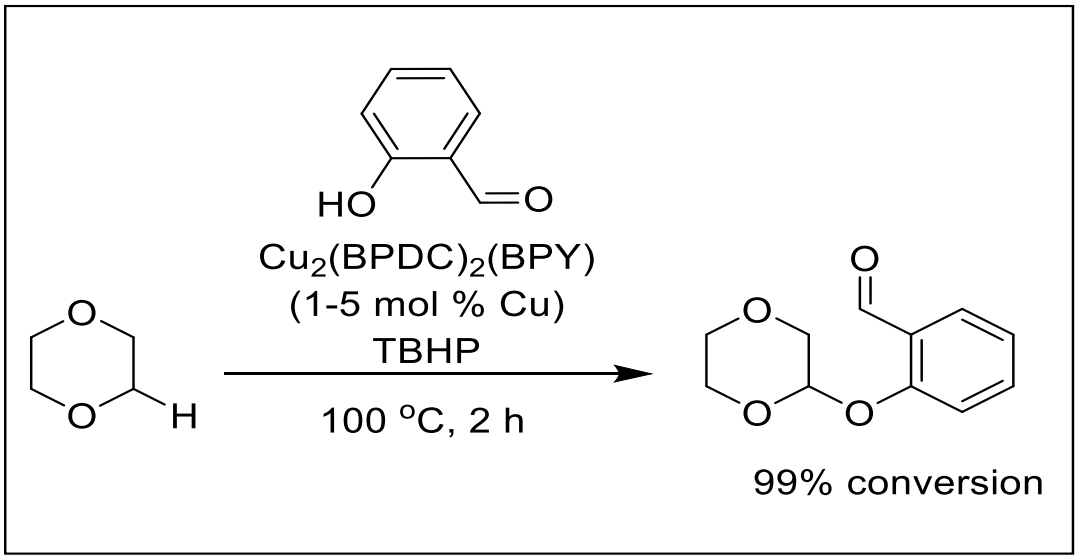

Scheme-4.29

XXX. Pd/Al_2O_3-catalyzed C–H bond thiolation of heteroarenes:

Properties of a heterogeneous catalyst were recently demonstrated in the formation of C–S bonds through a C–H activation process. Glorius and group[45] employed Pd/Al_2O_3 along with diaryldisulfides (Y = S) and $CuCl_2$ to achieve the regioselective C–H thiolation of heteroaromatics in their study (Scheme 4.30). 2-Thiophenes with substitutions were specifically functionalized at the C5 site, whereas a 2,5-disubstituted thiophene underwent reaction at C3. The reactivity of 3-substituted thiophenes was found to be lower, resulting in mixtures of C2- and C5-functionalized products. The corresponding thiolated products were obtained in good yields through the selective reaction of N-Methylindoles on the C3 carbon. In general, benzo[b]thiophenes and benzofurans exhibited lower reactivity and thus demanded more rigorous reaction conditions. In addition, the investigation also covered the range of disulfides. Both electron-rich and electron-poor disulfides exhibited reactivity, with the electron-rich substrates generally providing higher yields. The reaction proved tolerance towards various functional groups. For instance, halogens were readily accepted on both the heteroarene and the disulfide, thereby providing opportunities for additional functionalization of the products. The presence of palladium in reaction mixture was confirmed by total reflection X-ray fluorescence (TXRF). However, the outcomes of both the hot filtration test and the three-phase test indicated that these palladium species, despite being to be recycled resulted in a reduced product yield during the second reaction run. The procedure has the potential to be expanded to the selenenylation of heteroarenes through the utilization of diselenides (Y = Se) instead of disulfides. homogeneous, are unlikely to exhibit catalytic activity. Upon analysis, it was observed that the catalyst's ability.

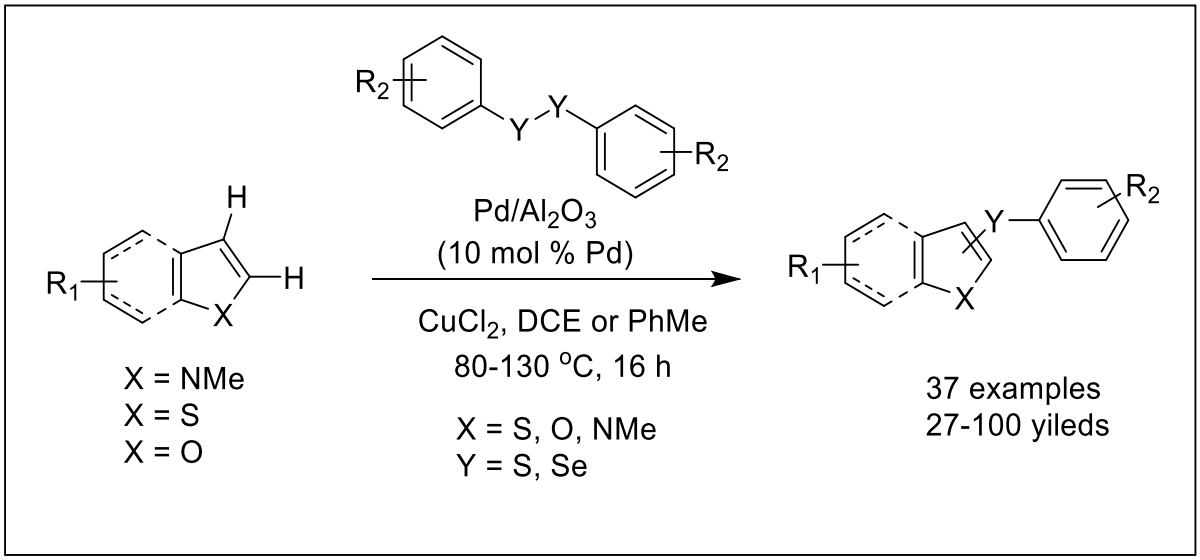

Scheme-4.30

1/c Conclusion

In conclusion, in the past few years, there has been significant advancement in metal-catalyzed C–H functionalizations. The current scenario makes it clear that a variety of generally non-benign solvents are commonly used as reaction mediums in catalytic protocols, indicating the pressing need for attention to find out environment friendly protocols. As a result, recyclable catalysts have been developed, which are highly user-friendly and can be easily separated. These materials are heterogeneous in nature and offer a broad range of substrates for reactions, displaying exceptional selectivity in both C–C and C–heteroatom formatting processes. The successful reusability of the catalytic system continues to still a major challenge. To the best of our knowledge, developed heterogeneous catalysts which are both environmentally-friendly and economically-sound, were not given enough credit until recently for their ability to directly functionalize typically unreactive C(sp3)–H and C(sp2)–H bonds. As a result, recyclable catalyst which are highly user-friendly and can be easily separated. These materials are heterogeneous in nature and offer a broad range of substrates for reactions, displaying exceptional selectivity in both C–C and C–heteroatom formatting processes. Nature's way of synthesizing organic molecules motivates scientists to find out benign reaction condition for carrying out chemical transformations. Water, the most abundant and benign solvent of the planet, has become the choice of synthetic chemists as the reaction medium. However, the water sensitivity of transition metal catalysts poses a serious limitation upon the use of water as the reaction medium in C-H activation reactions. Thus, it is very important to design air and water tolerant metal catalysts so that they can be employed in the environmentally friendly water medium reactions under aerial atmosphere. We are now intended to explore our heterogeneous Pd-catalyst in the synthetically important aqueous medium reactions. we demonstrate the C-H activation of 2-aryl-1,3-benzoxazin-4-one system in aqueous medium under open aerial atmosphere at close to room temperature (40 ^{o}C) using Pd-catalyst supported on starch coated magnetic nanoparticles. 2-Arylbenzoxazinones react with phenylglyoxylic acids via decarboxylative C-H acylation followed by cyclization reaction to produce the isoindolinone compounds. The formation of similar isoindolinones via C-H acylation of 2-aryl-1,3-benzoxazin-4-one was previously reported by B. K. Singh et. al. However, non-recyclability of the homogeneous catalyst, use of organic solvents as the reaction media and high reaction temperature restricted the protocols to be acceptable from the perspective of environmental sustainability. Herein, we report the use of recyclable magnetic Pd-catalyst in the synthesis of tetracyclic fused isoindolinone compounds in water medium via decarboxylative C-H activation reaction.

Section-II

Present Work:

Aqueous medium C-H activation of 2-arylbenzoxazinones: Synthesis of fused-isoindolinones using magnetic heterogeneous Pd-catalyst

2/a Introduction

As a continuation of our work, we are reporting here use of heterogeneous Pd-catalyst in the synthetically important aqueous medium reactions. We demonstrate the C-H activation of 2-aryl-1,3-benzoxazin-4-one system in aqueous medium in the presence of Pd-catalyst supported on starch coated magnetic nanoparticles. Aryl substituted benzoxazinone undergoes C(sp^2)-H acylation reaction with phenylglyoxylic acid in the presence of Pd(II) catalyst, $K_2S_2O_8$ and $AgNO_3$ to produce the benzoxazinone-fused isoindolinone compound efficiently in water medium under open air atmosphere at 40 ^oC (Scheme 4.31). C-H Activation provides an easy and step-economic way to functionalize the organic molecules towards complex structural frameworks and hence it is now the topic of utmost interest in the field of synthetic organic chemistry. Nature's way of synthesizing organic molecules motivates scientists to find out benign reaction condition for carrying out chemical transformations. Water, the most abundant and benign solvent of the planet, has become the choice of synthetic chemists as the reaction medium. However, the water sensitivity of transition metal catalysts poses a serious limitation upon the use of water as the reaction medium in C-H activation reactions. Thus, it is very important to design air and water tolerant metal catalysts so that they can be employed in the environmentally friendly water medium reactions under aerial atmosphere. We have immobilized Pd(II) on the surface of starch coated magnetic Fe_3O_4 nanoparticles. Magnetic heterogeneous catalysts are easy to separate from the reaction mixture with the aid of an external magnet and can be reused in the subsequent batches.[46] Isoindolinone derivatives are highly valuable in the field of pharmaceutical sciences[47] and they occur in many natural compounds.[48] Isoindolinone scaffolds show potential biological activities as anticancer,[49] antipsychotic,[50] antifungal[51] antiangiogenic[52] agents. Herein, we report the use of recyclable magnetic Pd-catalyst in the synthesis of tetracyclic fused isoindolinone compounds in water medium via decarboxylative C-H activation reaction.

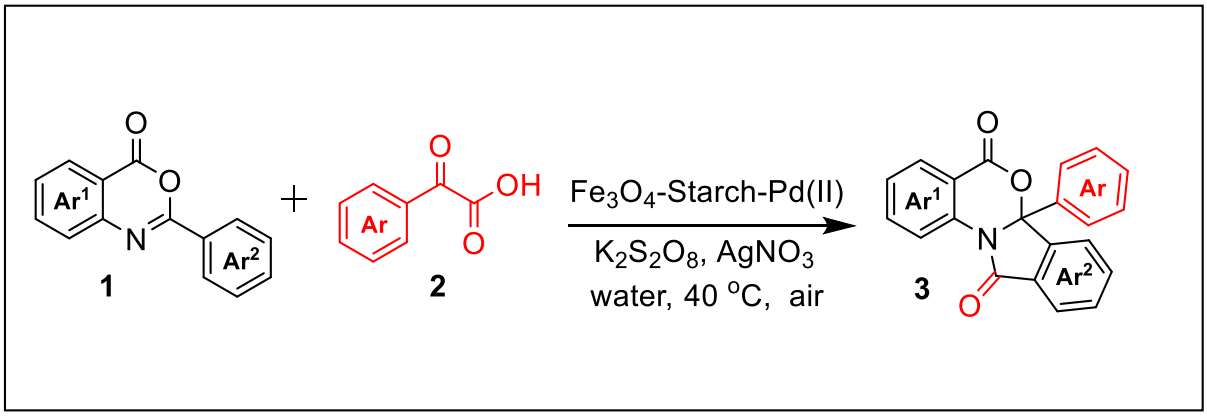

Scheme-4.31 C-H Activation of aryl substituted benzoxazinones

2/b Results and Discussion

The magnetic nanoparticles supported Pd-catalyst was prepared following the procedure as described in our earlier report.[53] Palladium has been immobilized on the surface of starch coated Fe_3O_4 nanoparticles which are prepared by addition of aqueous ammonia to the stirring reaction mixture of Fe^{3+}, Fe^{2+} and starch in water at 60 ^oC. The EcoScale percentage of the catalyst has been calculated to be 82.5%. The catalyst was characterized well by TEM (transmission electron microscopy), SEM (scanning electron microscope), EDX (Energy Dispersive X-ray), TGA analysis, BET (nitrogen adsorption isotherms) and ICP-AES analysis as reported previously. The nano-catalyst has the particle sizes 7-19 nm as revealed by TEM experiment (Figure 4.2). Pd-content of the heterogeneous magnetic catalyst was determined to be 4.95 weight% by the ICP-AES analysis. The Pd-catalyst is also characterized by XPS (X-ray photoelectron spectroscopy) analysis. The presence of Pd(II) is confirmed by the characteristic 3d binding energy signals[54] at 337.7 and 342.8 eV (Figure 4.1). We have used IR-spectroscopy in order to understand the structure of the heterogeneous Pd-catalyst. IR-spectrum of starch (Figure 4.3a) reveals the O-H stretching and bending frequencies at 3286 and 1638 cm-1 respectively. The shift of O-H signals in the IR spectra of Fe_3O_4-starch (Figure 4.3b) and Fe_3O_4-starch-PdII (Figure 4.3c) probably caused by the coordination of starch-hydroxyl groups to the metal centers. The signals at 2915 cm-1 (Figure 4.3b), 2931 cm^{-1} (Figure 4.3c) correspond to the C-H stretching absorptions and 991 cm^{-1} (Figure 4.3b), 1001 cm^{-1} (Figure 4.3c) correspond to the C-O stretching absorptions of starch in Fe_3O_4-starch and Fe_3O_4-starch-PdII respectively. The strong signal at 551 cm^{-1} attributes to the Fe-O stretching vibrations in Fe_3O_4-starch and Fe_3O_4-starch-PdII. A small hump at 624 cm^{-1} (Figure 4.3c) indicates the presence of Pd-O in the catalyst.

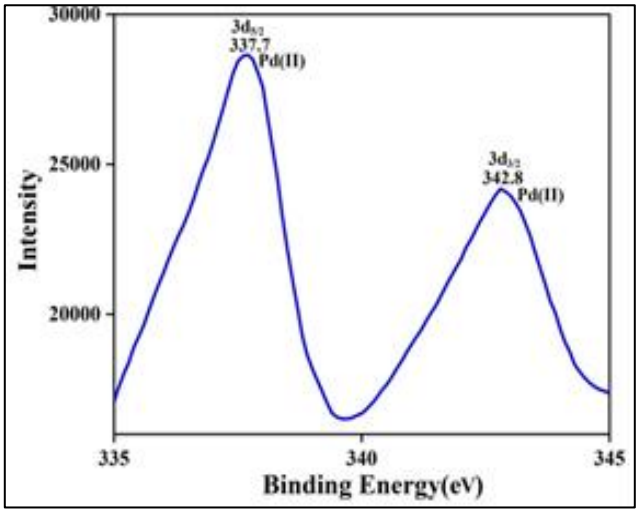

Figure 4.1 XPS spectrum of Pd(II) in the catalyst.

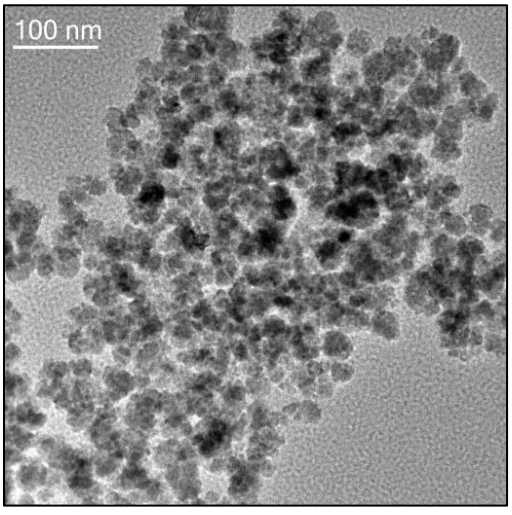

Figure 4.2 TEM image of magnetic Pd(II) catalyst.

The C-H activation reaction is very easy to perform. A mixture of 2-aryl benzoxazinone and phenylglyoxylic acid was stirred at 40 ^oC in presence of Pd-catalyst, $K_2S_2O_8$ and $AgNO_3$ in

water medium under aerial atmosphere. After completion of the reaction (checked by TLC) the Pd-catalyst was separated by an external magnet. The crude product obtained by usual work-up was purified by column chromatography.

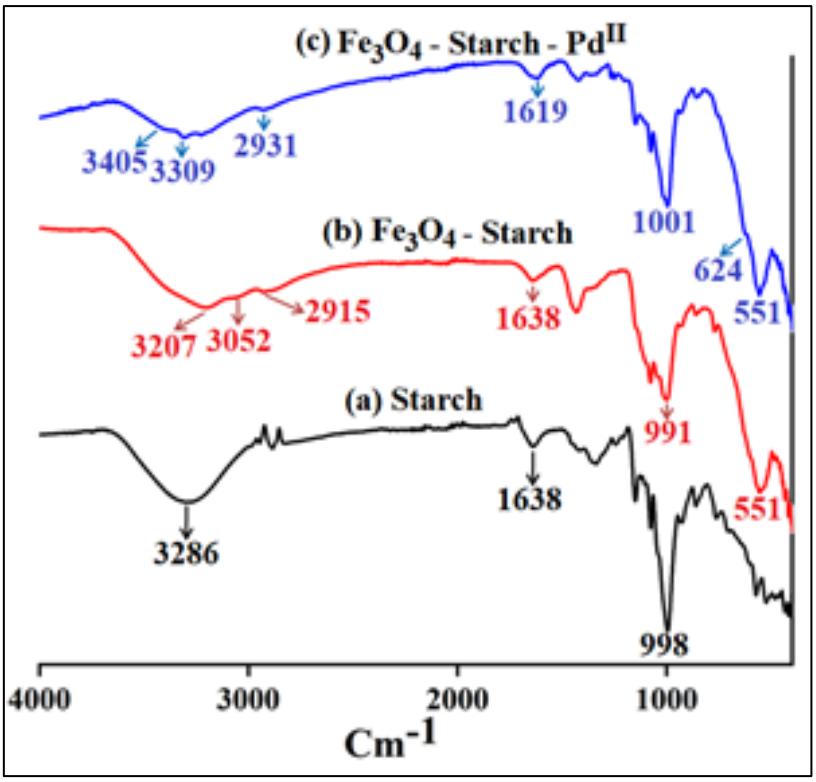

Figure 4.3 IR spectra of (a) starch, (b) Fe_3O_4-starch, (c) Fe_3O_4-starch-Pd^{II}

The C-H activation reaction is very easy to perform. A mixture of 2-aryl benzoxazinone and phenylglyoxylic acid was stirred at 40 ^oC in presence of Pd-catalyst, $K_2S_2O_8$ and $AgNO_3$ in water medium under aerial atmosphere. After completion of the reaction (checked by TLC) the Pd-catalyst was separated by an external magnet. The crude product obtained by usual work-up was purified by column chromatography. In order to optimize the reaction condition a set of experiments was performed (Table 4.1) considering 2-phenyl-1,3-benzoxazin-4-one (1a) and phenylglyoxylic acid (2a) as the model substrates. At the outset, we tried the reaction of 1a with 2a in presence of Pd-magnetic catalyst and $K_2S_2O_8$ oxidant in THF solvent medium by stirring the reaction mixture at 40 ^oC for 30 h (entry 1, Table 4.1). However, we obtained the desired isoindolinone product (3a) only in 20% of yield. Other solvent media, like dioxane, DMF, NMP, acetonitrile were not found satisfactory in the reaction (entries 2 -5, Table 4.1). The yield of the reaction was increased a bit in DCE (1,2-dichloroethane) reaction medium (yield: 48%, entry 6, Table 4.1). The Pd-catalyzed C-H acylation reaction was then tested in aqueous medium to find a marginal improvement of yield of the desired product (entry 7, Table 4.1). Surprisingly, the reaction was found to be highly effective in presence of $AgNO_3$ additive. Use of sub-stoichiometric amount of $AgNO_3$ (0.5 equiv) provides excellent reaction outcome with the desired product in 94% of yield (entry 8, Table 4.1) in aqueous reaction medium. The yield of product has found to be decreased with decreasing the amount of silver nitrate further (entry 10, Table 4.1). Other oxidant like $(NH_4)_2S_2O_8$ shows low reactivity in comparison to $K_2S_2O_8$ (entry 9, Table 4.1).

The reaction remains incomplete in shorter time period (24 h, entry 11, Table 4.1). At 25 ^{o}C the yield of the product (3a) decreased significantly (entry 12, Table 4.1). Use of other conventional heterogeneous-Pd catalysts,[55] such as Fe_3O_4-Dopamine-Pd(II), Cellulose-Pd, Pd/Al_2O_3 were not found suitable for the reaction under the present condition (entries 13 - 15, Table 4.1).

Table 4.1 Optimization of the reaction condition.

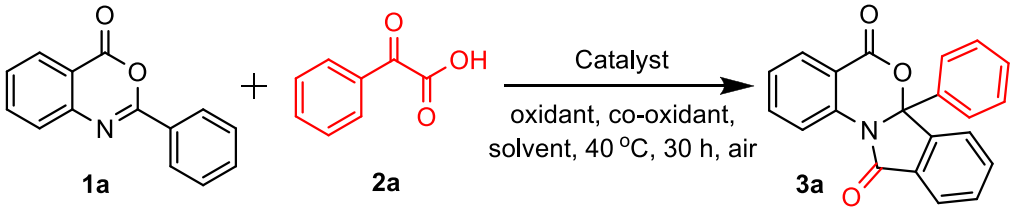

Entry	Catalyst	Oxidant	Co-oxidant	solvent	Yield [%]
1	Fe_3O_4-Starch-Pd(II)	$K_2S_2O_8$	–	THF	20
2	Fe_3O_4-Starch-Pd(II)	$K_2S_2O_8$	–	dioxane	22
3	Fe_3O_4-Starch-Pd(II)	$K_2S_2O_8$	–	DMF	15
4	Fe_3O_4-Starch-Pd(II)	$K_2S_2O_8$	–	NMP	18
5	Fe_3O_4-Starch-Pd(II)	$K_2S_2O_8$	–	CH_3CN	–
6	Fe_3O_4-Starch-Pd(II)	$K_2S_2O_8$	–	DCE	48
7	Fe_3O_4-Starch-Pd(II)	$K_2S_2O_8$	–	H_2O	51
8	Fe_3O_4-Starch-Pd(II)	$K_2S_2O_8$	$AgNO_3$	H_2O	94
9	Fe_3O_4-Starch-Pd(II)	$(NH_4)_2S_2O_8$	$AgNO_3$	H_2O	86
10[a)]	Fe_3O_4-Starch-Pd(II)	$K_2S_2O_8$	$AgNO_3$	H_2O	74
11[b)]	Fe_3O_4-Starch-Pd(II)	$K_2S_2O_8$	$AgNO_3$	H_2O	76
12[c)]	Fe_3O_4-Starch-Pd(II)	$K_2S_2O_8$	$AgNO_3$	H_2O	62
13	Fe_3O_4-Dopamine-Pd(II)	$K_2S_2O_8$	$AgNO_3$	H_2O	18
14	Cellulose-Pd	$K_2S_2O_8$	$AgNO_3$	H_2O	–
15	Pd/Al_2O_3	$K_2S_2O_8$	$AgNO_3$	H_2O	–

*Reaction condition: A mixture of **1a** (0.5 mmol), **2a** (0.75 mmol), Pd-catalyst (4 mol%), oxidant (1 mmol) and $AgNO_3$ (0.25 mmol) in 2 ml of solvent was stirred at 40 ^{o}C for 30 h under aerial atmosphere. Yields reported are the isolated yields.[a] $AgNO_3$ (0.1 mmol) has been used. [b] The reaction time period was 24 h. [c] The reaction mixture was stirred at 25 ^{o}C.*

The optimized reaction condition was then followed to carry out the reactions with a broad range of substrates (Table 4.2). Several 2-aryl benzoxazinones containing electron donating (Me, OMe) as well as electron withdrawing substituents (F, Cl, Br, I, NO_2) participated in the C-H acylation reactions to produce the desired isoindolinone compounds (**3a - 3h**, Table 4.2) in good yields. Substituted phenylglyoxylic acids containing OMe, Me, NO_2, Cl, Br functional groups responded to the reaction producing the products (**3i - 3t**, Table 4.2) satisfactorily. Isoindolinone products bearing iodo functionality (**3f**, **3q**) may be used in various post synthetic modifications *via* cross-coupling reactions involving the C(sp^2)-I moiety. The structure of the isoindolinone product, **3b** was established by single crystal XRD experiment (Figure 4.4).

Table 4.2. Synthesis of isoindolinone compounds.

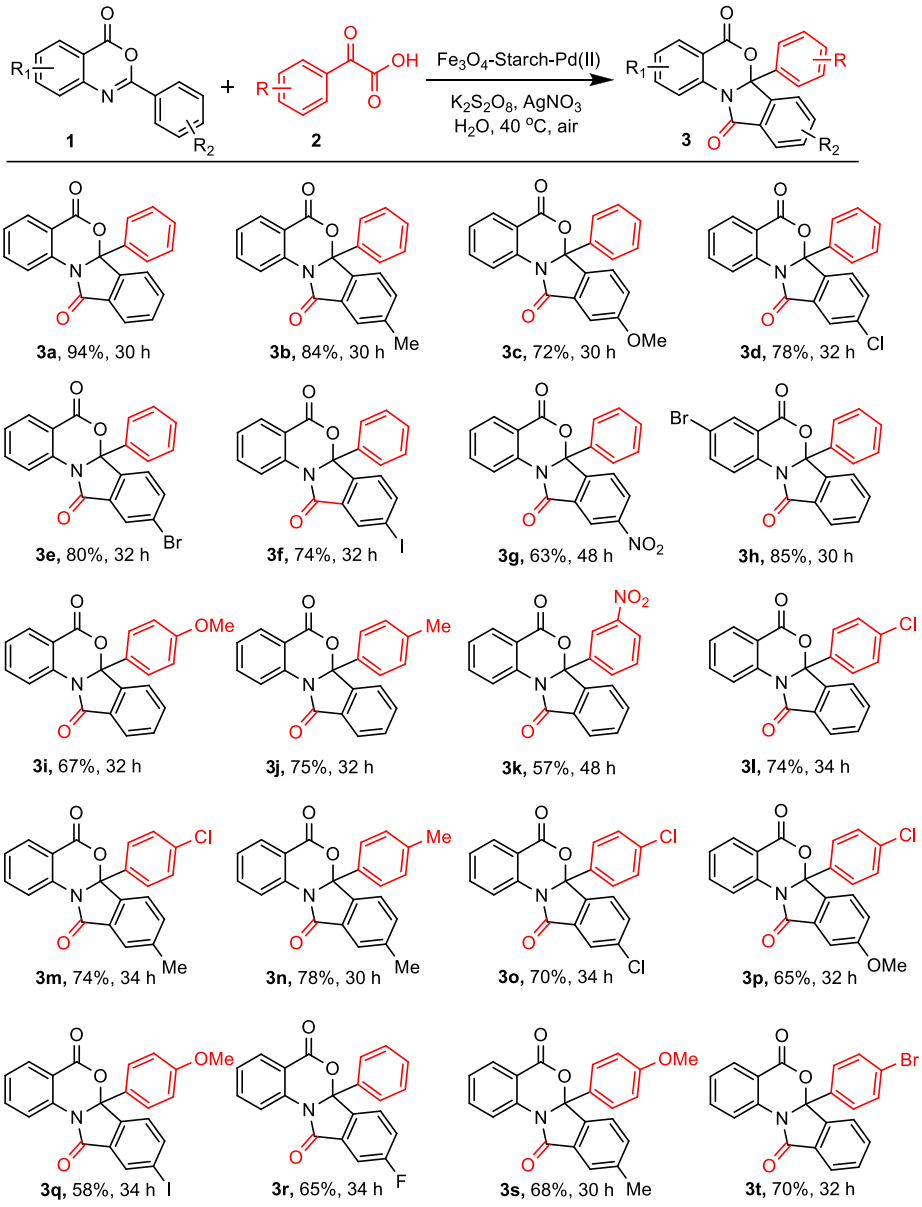

*Reaction condition: A mixture of **1** (0.5 mmol), **2** (0.75 mmol), Pd-catalyst (4 mol%), $K_2S_2O_8$ (1 mmol) and $AgNO_3$ (0.25 mmol) in 2 ml of water was stirred at 40 °C for the required time period under aerial atmosphere. Yields reported are the isolated yields.*

To test the leaching of Pd^{II} from the heterogeneous catalyst support, we separated the heterogeneous catalyst magnetically from an identical partially completed reaction mixture of **1a** and **2a** after an intermediate time period of 8 h under the hot condition. The reaction was found to be arrested completely after separating the heterogeneous magnetic catalyst from the reaction mixture. In absence of the heterogeneous catalyst, no further progress of the reaction was observed even after continuing the reaction for more 10 h under the identical reaction condition. This experiment proves that palladium does not leach out to the reaction medium during the reaction.

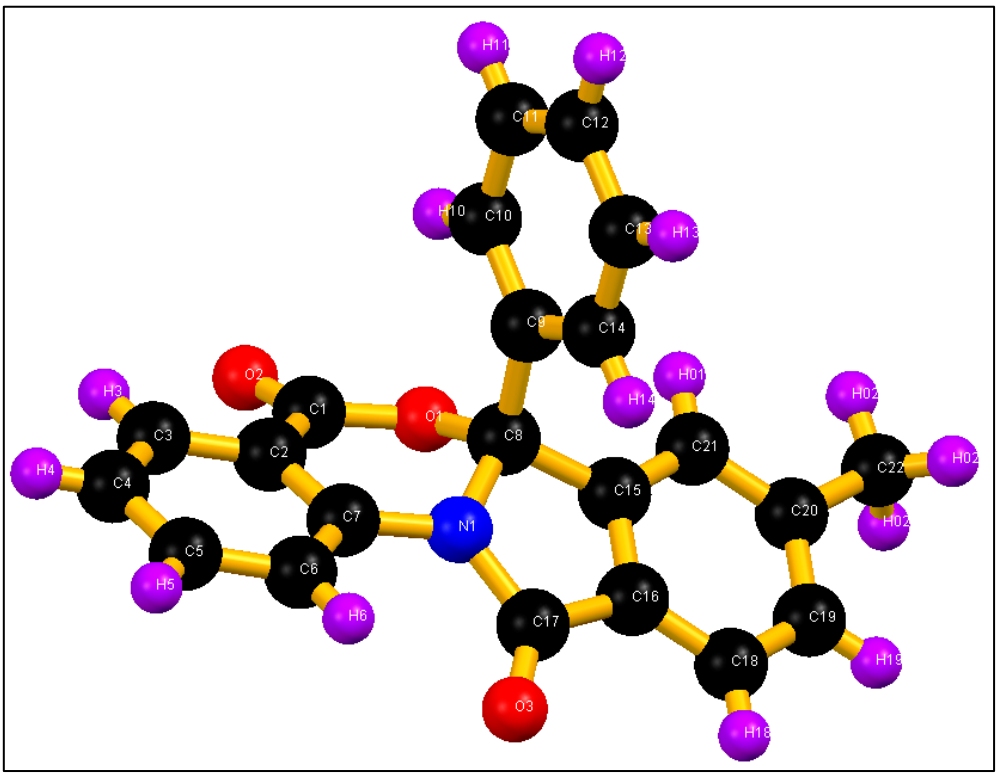

Figure 4.4 Molecular view of the isoindolinone product, **3b** (CCDC deposition no 2191787).

The heterogeneous magnetic Pd-catalyst used in this protocol shows good recyclability. The catalyst used in the reaction of 2-phenyl benzoxazinone (1a) with phenylglyoxylic acid (2a) was recovered after completion of the reaction with the help of an external magnet. The catalyst was washed with acetone, dried and was reused in the subsequent batches of the reaction for four times without much loss of reactivity (Figure 4.5). The desired product (3a) was obtained with almost identical yields (94-91%) in every batch. After fourth batch, the yield of the product was found to decrease gradually. The catalyst recovered after fourth batch was analyzed by IR spectroscopy and TGA analysis (spectra are included in the Supporting Information). In IR spectroscopy similar spectrum was obtained with the characteristic signals almost unchanged. Although TGA analysis of the recovered catalyst shows decreased thermal stability with loss of surface hydroxyl groups around 200 ^{o}C. The catalytic activity of the magnetic Pd-catalyst remains unaltered up to fourth batch of the reaction. The starch-hydroxyl groups bind the palladium on the surface of the magnetic nanoparticles firmly and make the Pd-catalyst robust and reusable.

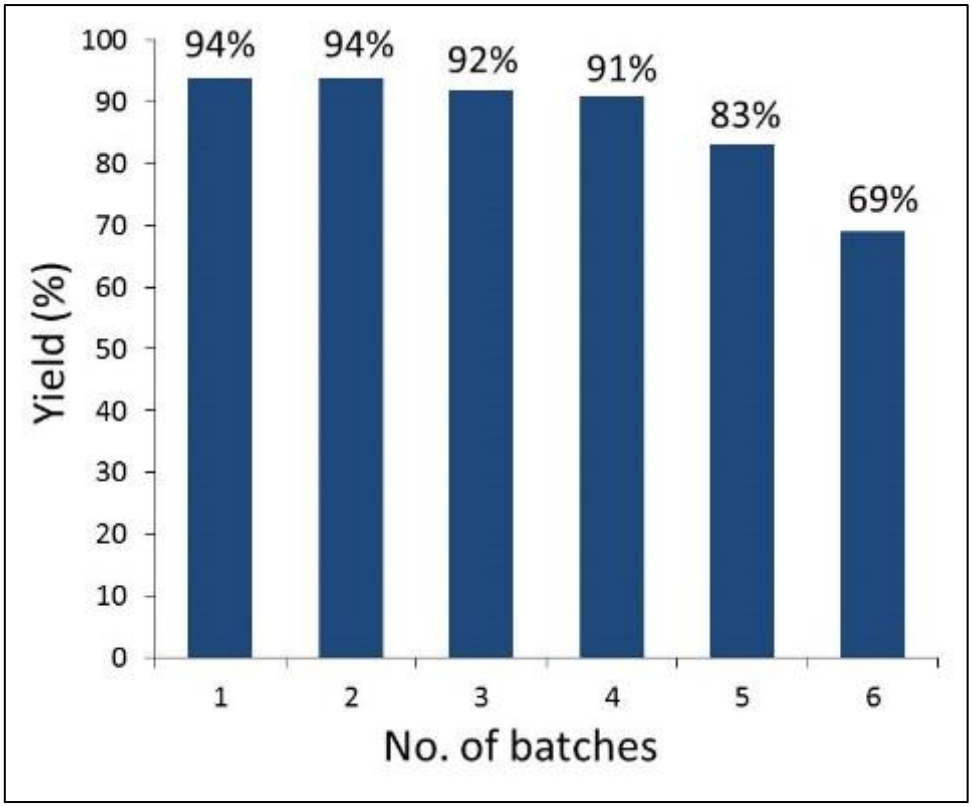

Figure 4.5 Recycling of the Pd-catalyst.

In order to find out the possible intermediate of the reaction, we conducted the C-H activation reaction for a reduced time period (5 - 6 h) at lower temperature (13 - 18 ^{o}C) (Scheme 4.32) maintaining the other reaction parameters unaltered. It has been observed that 2-arylbenzoxazinones (1) undergo ortho-C-H acylation with phenylglyoxylic acid at lower temperature in presence of Pd-catalyst, $K_2S_2O_8$ and $AgNO_3$ in water medium. The ortho-acylated products (4) were formed in good yields and the isoindolinone product (3) formation was completely arrested at this lower temperature (Scheme 4.32). The ortho-acylated compound (4) does not convert to the isoindolinone product (3) at this lower temperature even after prolonged reaction time period. Thus, we can achieve the product selectivity by controlling the reaction temperature. After formation of the ortho-acylated product (4) (checked by TLC), if the temperature of the reaction mixture is raised to 40 ^{o}C, the acylated compound (4) has been observed to undergo cyclization reaction to produce the isoindolinone compound (3). Thus, we believe the conversion of 2-arylbenzoxazinone (1) to the isoindolinone (3) compound proceeds through the intermediacy of ortho-acylated compound (4).

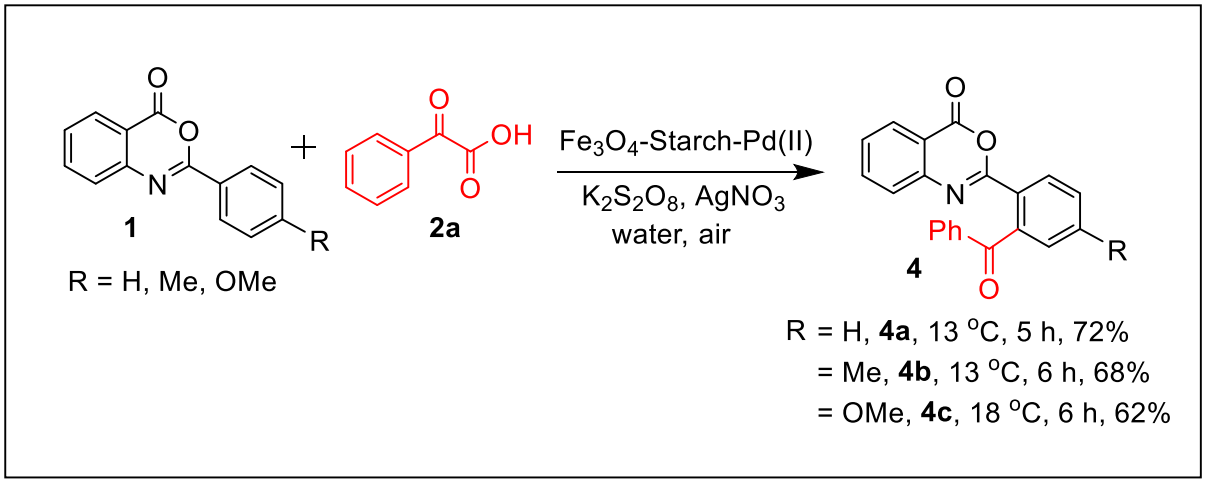

Scheme-4.32 Synthesis of ortho-acylated derivatives of 2-arylbenzoxazinones

To understand the mechanistic pathway, the reaction between 1a and 2a was carried out in presence of a radical quencher, TEMPO (2,2,6,6-tetramethylpiperidine-N-oxide) under the standardized reaction condition (Scheme 4.33). However, the benzoxazinone substrate (1a) remained totally unreacted with no desired product (3a) formation and TEMPO was found to be trapped as O-bezoylated-TEMPO (5). Therefore, we propose a radical pathway of the reaction and consider the formation of acyl radical (PhCO•) as the intermediate which gets trapped in presence of TEMPO to generate compound 5. Based on above experimental observations and previous related literatures, we assume 2-arylbenzoxazinone (1) undergoes ortho-C-H palladation[56] to produce the palladacycle complex (6) which participates in oxidative coupling with the acyl radical intermediate (7) to generate the Pd(IV) complex (8) (Scheme 4.34). In presence of $K_2S_2O_8$/$AgNO_3$, α-oxocarboxylic acid (2) produces the acyl radical species (7) via decarboxylative process.[57] Reductive elimination from intermediate-8 affords the ortho-acylated product (4) and regenerates Pd(II)-catalyst which initiates the next catalytic cycle. Ortho-acylated compound (4) undergoes cyclization reaction to produce the isoindolinone product (3). To investigate the cyclization mechanism, we separately treated the acylated-compound-4a with catalytic amount of glacial acetic acid (Scheme 4.33b) and with Fe_3O_4-Starch catalyst (Scheme 4.33c) under the similar reaction condition (at 40 ^oC in water medium for 30 h). It has been observed that compound-4a was converted to the desired isoindolinone product-3a with 57% and 23% yield in presence of acid catalyst (Scheme 4.33b) and Fe_3O_4-Starch catalyst (Scheme 4.33c) respectively.Therefore we assume the activation of ketone in compound-4 either by acid catalyst or Fe_3O_4 followed by cyclization reaction to furnish the desired product, 3.

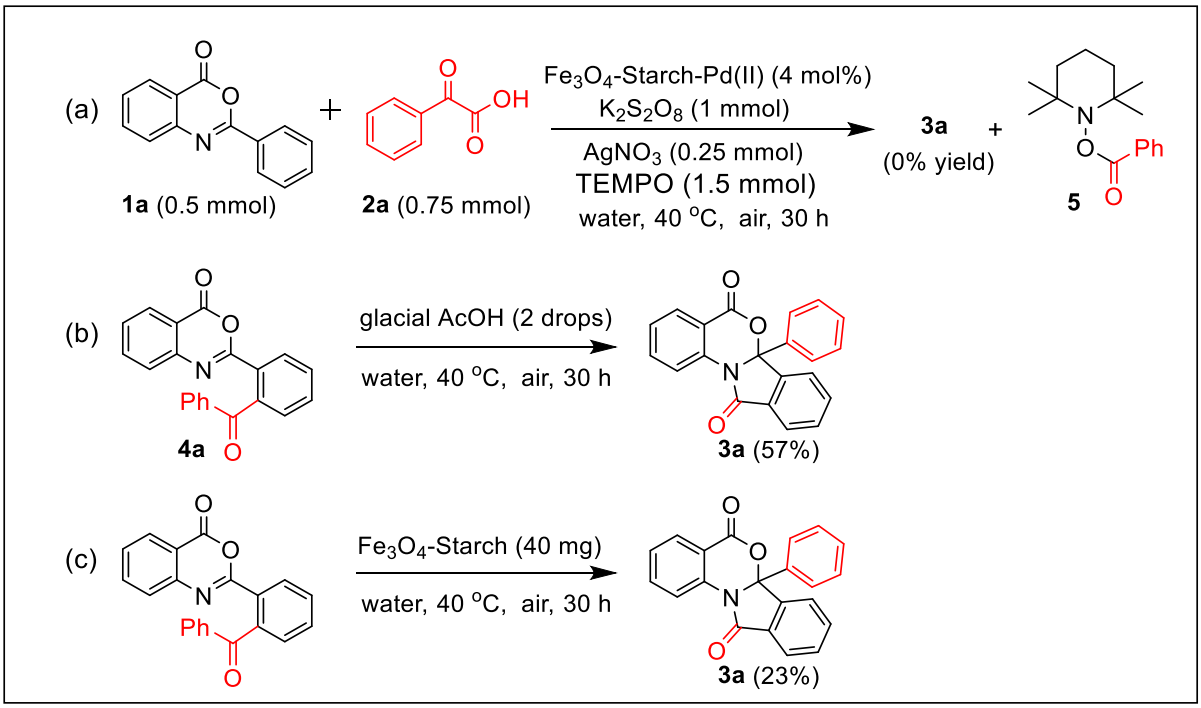

Scheme-4.33 Control experiments.

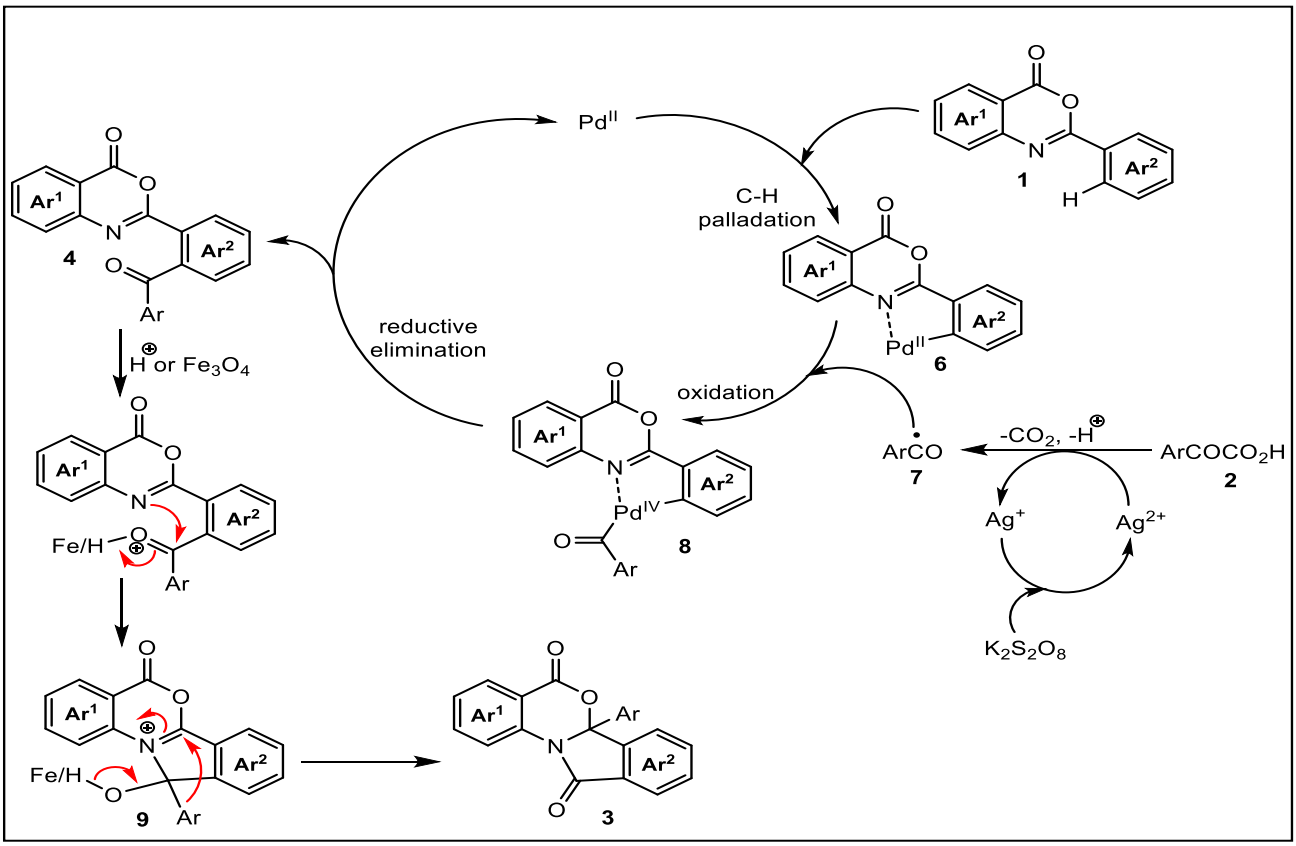

Scheme-4.34 Proposed mechanism.

The synthesized isoindolinone compounds (3) having suitable functional groups may undergo further structural modifications under the suitable reaction conditions. We have performed a C-S cross coupling reaction with the iodo-substituted isoindolinone compound (3f) using thiophenol as the coupling partner and CuI catalyst, K_2CO_3 base in DMSO solvent at 105 ^oC (Scheme 4.35).

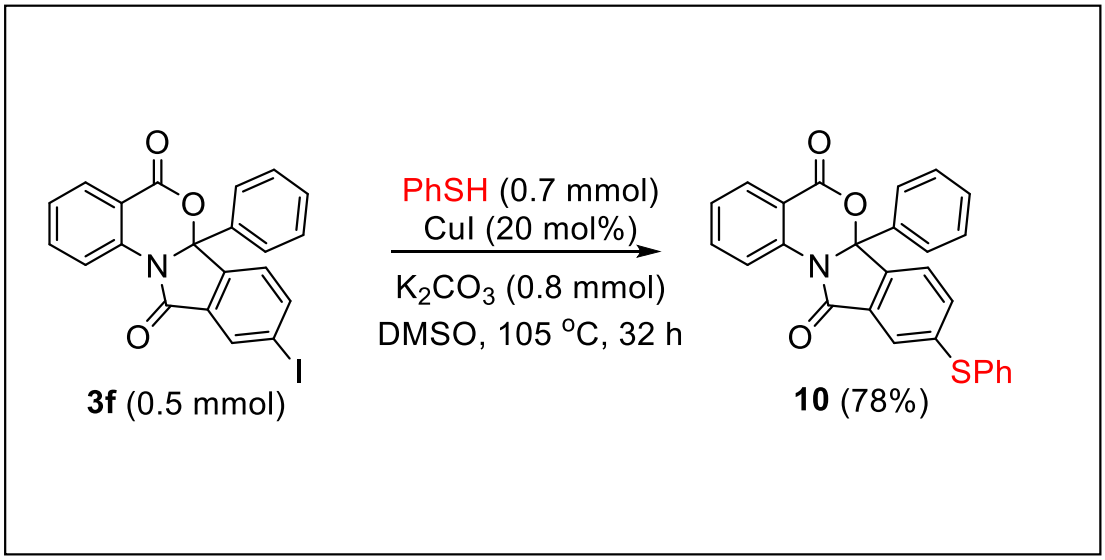

Scheme-4.35 Post-synthetic modification of synthesized isoindolinone compound, 3f

2/c Conclusion

In conclusion, we have developed an efficient environmentally friendly protocol for the synthesis of a series of isoindolinone compounds in aqueous medium. All the reactions were conducted under open aerial atmosphere at close to room temperature (40 ^oC). Thus, sophisticated inert, air and moisture free reaction set-up is avoided. Controlling the reaction temperature we can arrest the reactions at the intermediate step to obtain the ortho-acylated products (4) exclusively. The heterogeneous Pd catalyst shows good recyclability, air-moisture tolerance and easy magnetic separation which render the C-H activation protocol highly valuable from the ecology and economic points of view.

2/d Experimental Section

All the commercial starting materials and reagents were used without further purification. Silica gel (silica gel, f24) TLC plates were purchased from Merck. In column chromatographic purification process, silica gel 60-120 mesh and neutral aluminium oxide have been used. ^1H NMR spectra were recorded using Brucker Spectrometer at 300 MHz, 400 MHz and 500 MHz. ^{13}C NMR spectra were recorded at 75 MHz, 100 MHz and 125 MHz. In all NMR experiments, DMSO-d_6, $CDCl_3$ were used as solvent and TMS as internal

standard. The chemical shifts are reported in ppm scale considering standard signal of TMS at 0.00 ppm. The coupling constants *(J* values) are measured in Hz. HRMS were measured in methanol solvent on a Waters Micromass Q-tofMicromass spectrometer.

Representative experimental procedure for the synthesis of isoindolinone compound 3a.

A mixture of 2-phenyl-4H-benzo[d] [1, 3] oxazin-4-one (0.5 mmol, 112 mg), with phenylglyoxylic acid (0.75 mmol, 112 mg), Pd-catalyst (4 mol%, 35 mg), $K_2S_2O_8$ (1 mmol, 270 mg), and $AgNO_3$ (0.25 mmol, 42 mg) in H_2O (2 ml), was stirred at 40 ^oC for 30 h under aerial atmosphere. The progress of the reaction was monitored by TLC. After completion of the reaction the Pd-catalyst was separated by an external magnet and the crude product was obtained by usual work-up using EtOAc. The crude product was purified by column chromatography over neutral aluminium oxide using petroleum ether-ethyl acetate (96: 4) solvent mixture.

Experimental procedure for ortho-acylation reaction: Representative experimental procedure for the synthesis of ortho-acylated compound 4a.

A mixture of 2-phenyl-4H-benzo[d] [1, 3] oxazin-4-one (0.5 mmol, 112 mg), with phenylglyoxylic acid (0.75 mmol, 112 mg), Pd-catalyst (4 mol%, 35 mg), $K_2S_2O_8$ (1 mmol, 270 mg), and $AgNO_3$ (0.25 mmol, 42 mg) in H_2O (2 ml), was stirred at 14 **^{o}C** for 6 h under aerial atmosphere. The progress of the reaction was monitored by TLC. After completion of the reaction the Pd-catalyst was separated by an external magnet and the crude product was obtained by usual work- up using EtOAc. The crude product was purified by column chromatography over silica gel using petroleum ether-ethyl acetate (92: 8) solvent mixture.

Preparation of Pd-catalyst:

Preparation of starch coated Fe_3O_4 nanoparticles:

2 g of starch was added to 50 mL of distilled water and the mixture was stirred at 60 ^oC for 1 h. $FeSO_4.7H_2O$ (1.4 g) and $Fe_2(SO_4)_3$ (2 g) were added to the starch solution at 60 ^oC and stirred for further 1 h at 60 ^oC. Now NH_4OH solution (25%) was added dropwise to the solution to make the mixture sufficiently alkaline (pH around 10), black colored Fe_3O_4 nanoparticles appeared to come and the mixture was stirred for more 2 h at 60 ^oC. The nanoparticles were centrifuged and washed with acetone for 3 times. The nanoparticles were dried under vacuum.

Immobilization of Pd(II) on the surface of starch coated Fe_3O_4 nanoparticles:

200 mg of $PdCl_2$ was added to a methanolic (15 mL MeOH) suspension of starch coated Fe_3O_4 nanoparticles (1 g of nanoparticles) and the mixture was stirred for 15 h at room temperature. The Pd(II)-nano catalyst was separated by centrifugation and dried under vacuum.

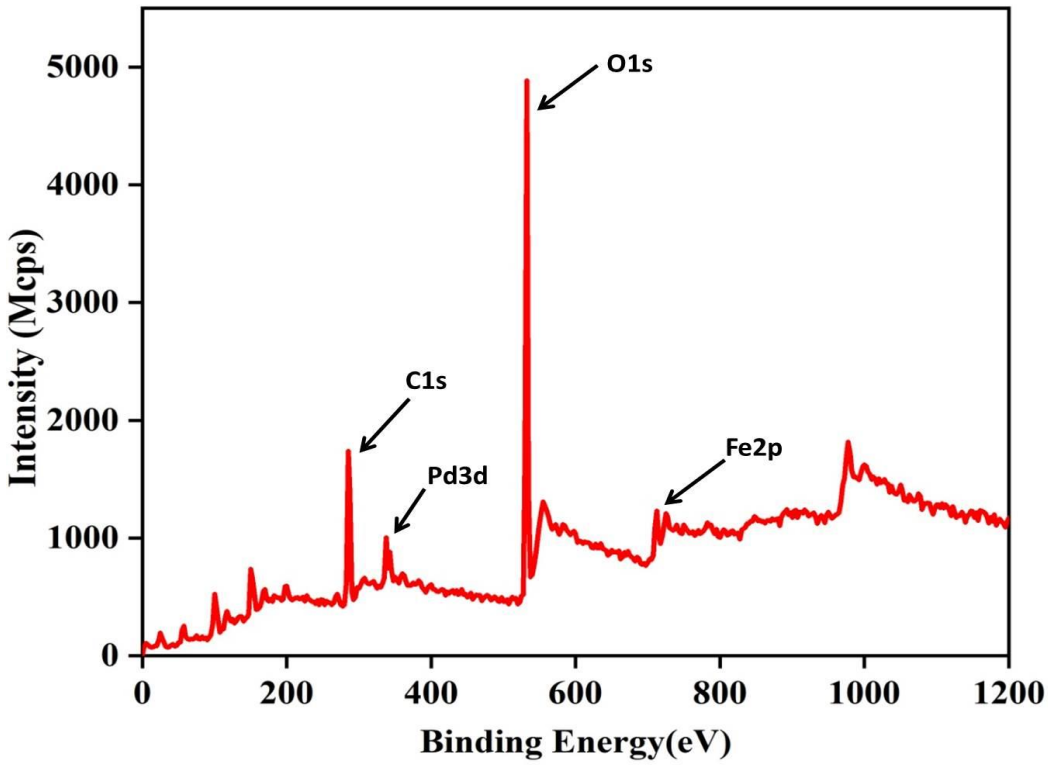

Figure 4.4 Characterization of the catalyst: XPS data of Pd-catalyst.

Characterization data of all synthesized products

6a-Phenyl-5H-benzo[4,5][1,3]oxazino[2,3-a]isoindole-5,11(6aH)-dione (3a, Table 2) white solid: ^{1}H NMR (300 MHz, $CDCl_3$): δ 8.16 (1H, d, *J*=6 Hz), 8.01–7.98 (2H, m), 7.72– 7.69 (1H, m), 7.66–7.58 (2H, m), 7.53–7.51 (3H, m), 7.32–7.21 (4H, m). ^{13}C NMR (75 MHz, $CDCl_3$): δ 165.73, 162.42, 144.95, 137.41, 136.58, 135.83, 134.12, 130.73, 130.70, 129.57, 129.29, 125.63, 125.54, 124.80, 123.58, 121.15, 116.21, 94.46.

9-Methyl-6a-phenyl-5H-benzo[4,5][1,3]oxazino[2,3-a]isoindole-5,11(6aH)-dione (3b,Table 2) White solid: ^{1}H NMR (300 MHz, d_6-DMSO): δ 8.10 (1H, d, *J*=9 Hz), 7.91-7.80 (3H, m), 7.55-7.52 (4H, m), 7.51-7.31(4H, m), 2.41 (3H, s). ^{13}C NMR (75 MHz, d_6-DMSO): δ 165.21, 162.11, 146.16, 145.13, 137.68, 136.72, 132.49, 130.50, 130.13, 129.89, 126.56, 126.21, 126.00, 124.92, 124.31, 121.67, 116.10, 94.27, 21.91.

9-methoxy-6a-phenyl-5H-benzo[4,5][1,3]oxazino[2,3-a]isoindole-5,11(6aH)-dione (3c, Table 2) White solid : ^{1} H NMR (300 MHz, d_6-DMSO): δ 8.09 (1H, d, *J*=6 .0 Hz), 7.92-7.79 (3H, m), 7.55 (2H, d *J*= 7.8 Hz), 7.40-7.29(4H, m), 7.24-7.16 (2H, m), 3.83 (3H, s). ^{13}C NMR (75 MHz, d_6-DMSO): δ 164.93, 162.17, 147.28, 137.58, 136.82, 136.77, 130.50, 130.20, 129.89, 126.90, 126.08, 126.01, 121.49, 121.08, 118.10, 115.93, 108.85, 93.92, 56.69.

9-Chloro-6a-phenyl-5H-benzo[4,5][1,3]oxazino[2,3-a]isoindole-5,11(6aH)-dione (3d, Table 2) White solid: ^{1}H NMR (400 MHz, $CDCl_3$): δ 7.99 (1H, d, *J*=6.8 Hz),7.98- 7.95 (1H, m),7.92-7.69(1H, m), 7.67-7.56 (1H, m), 7.51–7.48 (3H, m), 7.36-7.23 (5H, m), ^{13}C NMR

(100 MHz, $CDCl_3$): δ 164.64, 161.90, 146.40, 140.59, 136.74, 136.33, 135.92, 131.35, 130.78, 129.87, 129.48, 127.68, 126.01, 125.75, 125.58, 124.14, 121.10, 116.13, 93.83.

9-bromo-6a-phenyl-5H-benzo[4,5][1,3]oxazino[2,3-a]isoindole-5,11(6aH)-dione (**3e, Table** 2) **White solid:** ^{1}H NMR (500 MHz, $CDCl_3$): δ 8.15 (1H, d, *J*=8 Hz), 8.01 (1H, d, *J*=8 Hz), 7.86 (1H, d, J=8Hz), 7.75-7.71(2H, m)7.70-7.66(1H, m), 7.53-7.51 (2H, m), 7.37-7.27 (4H, m),^{13}C NMR (125 MHz, $CDCl_3$): δ 164.90, 162.00, 146.62, 136.90, 136.46, 136.03, 134.38, 130.92, 130.01, 129.62, 129.07, 128.33, 127.22, 126.27, 125.89, 125.74, 121.26, 116.30, 93.96. HRMS (ESI) m/z calcd for $C_{21}H_{12}BrNO_3$ $[M + H]^+$, 406.00, found 408.02.

9-iodo-6a-phenyl-5H-benzo[4,5][1,3]oxazino[2,3-a]isoindole-5,11(6aH)-dione (**3f, Table 2**) **White solid:** ^{1} H NMR (300 MHz, d_6-DMSO): δ 8.10-8.07 (3H, m), 7.90-7.81 (2H, m), 7.75 (1H, d, J=9 Hz), 7.58-7.55 (2H, m), 7.41-7.32 (4H, m), ^{13}C NMR (75 MHz, d_6-DMSO): δ 164.67, 161.80, 146.03, 140.82, 137.01, 136.80, 136.35, 132.61, 130.56, 130.38, 129.96, 128.74, 126.74, 126.51, 126.15, 121.73, 116.12, 103.11, 93.74. HRMS (ESI) m/z calcd for $C_{21}H_{12}INO_3$ $[M + H]^+$, 453.99, found 454.014.

9-Nitro-6a-phenyl-5H-benzo[4,5][1,3]oxazino[2,3-a]isoindole-5,11(6aH)-dione (3g, **Table 2**) **Yellow solid**: ^{1}H NMR (400 MHz, $CDCl_3$): δ 8.48-8.46 (1H, m), 8.34-8.32 (1H, m), 8.18-8.15(2H, m), 8.03-8.01 (1H, m), 7.76-7.71 (1H, m), 7.55-7.39 (2H, m), 7.37-7.29 (4H, m) ^{13}C NMR (100 MHz, $CDCl_3$): δ 163.33, 161.34, 151.50, 146.00, 136.11, 135.89, 135.88, 134.39, 130.98, 130.28, 129.75, 126.36, 126.30, 126.07, 125.60, 125.57, 121.10, 119.30, 116.18, 93.82,

3-bromo-6a-phenyl-5H-benzo[4,5][1,3]oxazino[2,3-a]isoindole-5,11(6aH)-dione (3h, Table 2) White solid: ^{1}H NMR (400 MHz, $CDCl_3$): δ 8.18 (1H, S), 7.91-7.82 (4H, m), 7.78-7.71 (2H, m), 7.59-7.46 (4H, m), 7.38-7.33 (1H ,m) ^{13}C NMR (100 MHz, d_6-DMSO): δ 165.08, 160.94, 144.53, 139.37, 137.31, 135.89, 135.29, 132.56, 131.88, 130.33, 129.97, 129.00, 126.04, 125.19, 124.16, 123.85, 118.19, 118.00, 94.49.

6a-(4-Methoxyphenyl)-5H-benzo[4,5][1,3]oxazino[2,3-a]iso-indole-5,11(6aH)-dione (3i, Table 2) White solid: ^{1}H NMR (300 MHz, $CDCl_3$): δ 8.16-8.13 (1H, m), 8.02-7.97(2H, m), 7.96-7.50 (3H, m), 7.43 (2H, d, J=9 Hz), 7.27-7.22 (2H, m), 6.82 (2H, d, J=9 Hz), 3.73 (3H, s). ^{13}C NMR (75 MHz, $CDCl_3$): δ 165.73, 162.56, 160.41, 145.24, 136.55, 135.77, 134.09, 130.65, 130.61, 129.19, 129.13, 127.06, 125.49, 124.74, 123.46, 121.15, 116.33, 114.62, 94.50, 55.29.

6a-(p-Tolyl)-5H-benzo[4,5][1,3]oxazino[2,3-a]isoindole-5,11(6aH)-dione (3j, Table 2) white solid: ^{1}H NMR (300 MHz, d_6-DMSO): δ 8.11-8.08 (1H, m), 8.01-7.98(1H, m), 7.92–7.66 (4H, m), 7.42 (2H, d, J=9 Hz), 7.37-7.31 (1H, m,), 7.17-7.7.16 (2H, m), 2.20 (3H, s). ^{13}C NMR (75 MHz, d_6-DMSO): δ 165.17, 162.13, 144.84, 139.88. 136.68, 136.60, 135.09, 134.59, 131.69, 130.50, 130.43, 129.12, 126.30, 125.92, 125.05, 124.04, 121.69, 116.22, 94.46, 21.01.

6a-(3-nitrophenyl)-5H-benzo[4,5][1,3]oxazino[2,3-a]isoindole-5,11(6aH)-dione (3k, Table 2) **white solid:** ^{1}H NMR (300 MHz, $CDCl_3$): δ 8.32-8.31 (1H,m), 8.9-8.15 (2H, m), 8.06-7.97 (3H, m), 7.77-7.71 (1H, m), 7.68-7.64 (2H, m), 7.60-7.50 (2H, m), 7.30 (1H, d J=6 Hz) ^{13}C NMR (75 MHz, $CDCl_3$): δ 165.48, 161.55, 148.91, 143.87, 140.16, 136.35, 134.50,

131.66, 131.35, 130.93, 130.70, 129.20, δ 126.04, 125.29, 124.69, 123.46, 121.42, 120.72, 115.75, 93.49.

6a-(4-Chlorophenyl)-5H-benzo[4,5][1,3]oxazino[2,3-a]isoindole-5,11(6aH)-dione (3l, Table 2) white solid :^{1}H NMR (300 MHz, d_6-DMSO): δ 8.12-8.09 (1H, m), 8.03–8.00 (1H, m), 7.94-7.71(5H,m), 7.63–7.58(2H, m), 7.47-7.40 (2H, m), 7.38-7.35 (1H, m). ^{13}C NMR (75 MHz, d_6-DMSO): δ 165.11, 161.85, 144.28, 136.83, 136.62, 136.47, 135.22, 135.06, 131.91, 130.58, 129.97, 129.18, 128.10, 126.47, 125.18, 124.10, 121.83, 116.05, 93.99.

6a-(4-chlorophenyl)-9-methyl-5H-benzo[4,5][1,3]oxazino[2,3-a]isoindole-5,11(6aH)-dione (3m, Table 2) white solid: ^{1}H NMR (300 MHz, d_6-DMSO): δ 8.10-8.06(1H, m), 7.92-7.80 (3H, m,), 7.58-7.50 (4H, m), 7.44 (2H, d, J=9 Hz), 7.36-7.31 (1H, m), 2.41 (3H, S), ^{13}C NMR (75 MHz, d_6-DMSO): δ 165.13., 161.90, 146.26, 144.70, 136.79, 136.71, 136.58, 135.01, 132.60, 130.55, 129.95, 128.08, 126.54, 126.32, 124.98, 124.32, 121.77, 115.98, 93.86, 21.90. HRMS (ESI) m/z calcd for $C_{22}H_{14}ClNO_3$ $[M + H]^+$, 376.07, found 376.12.

9-methyl-6a-(p-tolyl)-5H-benzo[4,5][1,3]oxazino[2,3-a]isoindole-5,11(6aH)-dione (3n, Table 2) white solid : ^{1}H NMR (300 MHz, d_6-DMSO): δ 8.10-8.07(1H, m), 7.91-7.80 (3H, m), 7.40 (2H, d, J=6 Hz), 7.42-7.30 (3H, m), 7.19-7.16(2H, m), 2.41 (3H,S), 2.21 (3H, S) ^{13}C NMR (75 MHz, d_6-DMSO): δ 165.11, 162.12, 146.10, 145.27, 139.83, 136.73, 136.65, 134.70, 132.41, 130.46, 126.52, 126.15, 125.93, 124.87, 124.28, 121.64, 116.16, 94.33 21.90, 21.02.

9-chloro-6a-(4-chlorophenyl)-5H-benzo[4,5][1,3]oxazino[2,3-a]isoindole-5,11(6aH)-dione (3o, Table 2) white solid : ^{1}H NMR (300 MHz, d_6-DMSO): δ 8.10-8.07(1H, m), 8.02 (1H, d, J= 9 Hz), 7.94-7.77 (4H, m), 7.64 (2H, d, J=9.4 Hz), 7.45 (2H, d, J=9 Hz), 7.40-7.35 (1H, m), ^{13}C NMR (75 MHz, d_6-DMSO): δ 164.06, 161.52, 145.09, 139.94, 136.89, 136.29, 135.99, 135.30, 132.20, 130.62, 129.98, 128.33, 128.11, 127.00, 126.62, 124.38, 121.79, 116.03, 93.40.

6a-(4-chlorophenyl)-9-methoxy-5H-benzo[4,5][1,3]oxazino[2,3-a]isoindole-5,11(6aH)-dione (3p, Table 2) white solid: ^{1}H NMR (300 MHz, d_6-DMSO): δ 8.10-8.07 (1H, m), 7.92-7.79 (3H, m), 7.60(2H, d, J=9 Hz), 7.44 (2H, d, *J*=9 Hz), 7.35-7.28 (1H, m), 7.25-7.23 (2H, m), 3.85 (3H, S), ^{13}C NMR (75 MHz, d_6-DMSO): δ 165.01, 164.79, 161.91, 146.92, 136.82, 136.72, 136.69, 135.03, 130.55, 129.92, 128.17, 126.89, 126.14, 121.58, 121.10, 118.36, 115.84, 108.82, 93.51, 56.74. HRMS (ESI) m/z calcd for $C_{22}H_{14}ClNO_4$ $[M + H]^+$, 392.06, found 392.06.

9-iodo-6a-(4-methoxyphenyl)-5H-benzo[4,5][1,3]oxazino[2,3-a]isoindole-5,11(6aH)-dione (3q, Table 2), white solid: ^{1}H NMR (300 MHz, $CDCl_3$): δ 8.12 (1H, d, *J*=9 Hz), 8.01-7.98 (1H, m), 7.94-7.91 (1H, m), 7.85-7.70 (1H, m), 7.71-7.65 (2H, m), 7.41(2H, d, *J*=9 Hz), 7.28-7.23 (1H,m), 6.83 (2H,d, *J*=9 Hz), 3.74 (3H, S), ^{13}C NMR (75 MHz, $CDCl_3$): δ 165.02, 162.05, 160.63, 146.53, 139.98, 136.22, 135.84, 132.80, 130.72, 128.67, 128.39, 127.06, 125.99, 125.71, 121.16, 116.26, 114.82, 101.18, 93.76, 55.33.

9-fluoro-6a-phenyl-5H-benzo[4,5][1,3]oxazino[2,3-a]isoindole-5,11(6aH)-dione (3r, Table 2) white solid : H NMR (300 MHz, d_6-DMSO): δ 8.11-8.03 (2H, m), 7.91-7.80 (2H, m),

7.69-7.65 (1H, m), 7.59-7.51 (3H, m), 7.38-7.33 (4H, m), ^{13}C NMR (75 MHz, d_6-DMSO): δ 167.21, 164.08, 161.78, 147.28, 137.06, 136.76, 136.53, 130.55, 130.35, 129.89, 127.88, 126,36, 126.12, 125.50, 121.57, 119.44, 116.07, 111.79, 93.66. HRMS (ESI) m/z calcd for $C_{21}H_{12}FNO_3$ [M + Na] $^+$, 368.08, found 368.06.

6a-(4-methoxyphenyl)-9-methyl-5H-benzo[4,5][1,3]oxazino[2,3-a]isoindole-5,11(6aH)-dione (3s, Table 2) white solid : ^{1}H NMR (300 MHz, d_6-DMSO): δ 8.10-8..07(1H, m), 7.91-7.79 (3H, m), 7.50-7.42 (4H, m), 7.35-7.29 (1H, m), 6.91-6.88 (2H, m), 3.67 (3H,S), 2.41 (3H, S), ^{13}C NMR (75 MHz, d_6-DMSO): δ 165.18, 162.22, 160.46, 146.05, 145.46, 136.71, 136.60, 132.31, 130.45, 129.27, 127.49, 126.44, 126.11, 124.82, 124.21, 121.67, 116.23, 115.16, 94.31, 55.63, 21.91.

6a-(4-Bromophenyl)-5H-benzo[4,5][1,3]oxazino[2,3-a]isoindole-5,11(6aH)-dione (3t, Table 2) White solid: ^{1}H NMR (300 MHz, d_6-DMSO): δ 8.11-8.08(1H, m), 8.02-8.01(1H, m), 7.93-7.69 (5H, m), 7.59–7.50 (4H, m),7.39-7.33 (1H, m) ^{13}C NMR (75 MHz, d_6-DMSO): δ 165.11, 161.84, 144.22, 137.05, 136.82, 136.46, 135.21, 132.89, 131.90, 130.59, 129.17, 128.32, 126.47, 125.18, 124.09, 123.75, 121.81, 116.04, 94.03.

2-(2-benzoylphenyl)-4H-benzo[d][1,3]oxazin-4-one (4a, Scheme 2) White solid: ^{1}H NMR (400 MHz, $CDCl_3$): δ 8.29-8.24 (1H, m), 8.11-8.07 (1H, m), 7.81-7.78 (2H, m), 7.71-7.63 (3H, m), 7.54-7.49 (1H, m), 7.47-7.32 (4H, m), 7.25-7.23 (1H, m), ^{13}C NMR (100 MHz, $CDCl_3$): δ 196.97, 158.93, 155.45, 145.93, 141.18, 137.84, 136.47, 132.82, 132.14, 129.99, 129.06, 129.01, 128.86, 128.59, 128.45, 128.39, 126.84, 126.81, 116.48.

2-(2-benzoyl-4-methylphenyl)-4H-benzo[d][1,3]oxazin-4-one (4b, Scheme 2) White solid: **^{1}H** NMR (300 MHz, $CDCl_3$): δ 8.15 (1H,d, *J*=9 Hz), 8.08 (1H, d, *J*=9 Hz), 7.81-7.78 (2H, m), 7.70-7.62 (1H, m), 7.50-7.43 (2H, m), 7.42-7.30 (4H, m), 7.21 (1H, d, *J*=9 Hz), 2.49 (3H, S), ^{13}C NMR (75 MHz, $CDCl_3$): δ 197.20 159.08, 155.46, 146.08, 143.22, 141.31, 137.95, 136.40, 132.73, 130.60, 129.15, 129.01, 128.96, 128.91, 128.41, 128.33, 126.68, 125.92, 116.43, 21.63.

2-(2-benzoyl-4-methoxyphenyl)-4H-benzo[d][1,3]oxazin-4-one (4c, Scheme 2) White solid: ^{1}H NMR (300 MHz, d_6-DMSO): δ 8.13 (1H, d, *J*=9.6Hz), 7.99 (1H, d, J=6.8Hz), 7.76-7.72 (1H, m), 7.71 (2H, d, J=7.5Hz), 7.53-7.39 (4H, m), 7.33-7.28 (1H, m), 7.17 (1H, d, *J*= 7.8Hz), 7.11 (1H, d, J=2.4Hz), 3.91 (3H, S), ^{13}C NMR (75 MHz, d_6-DMSO): δ 195.89, 162.82, 158.80, 155.44, 146.03, 143.14, 137.80, 137.31, 133.36, 131.39, 129.72, 129.06, 129.01, 128.96, 128.45, 126.42, 120.67, 116.39, 115.93, 114.56, 56.44.

6a-phenyl-9-(phenylthio)-5H-benzo[4,5][1,3]oxazino[2,3-a]isoindole-5,11(6aH)-dione (10) Yellow solid: **^{1}H** NMR (300 MHz, $CDCl_3$): δ 8.13 (1H,d J=8.1Hz), 7.96 (1H, d, *J*=7.5Hz), 7.78 (1H, d, *J*=8.7Hz), 7.72-7.63 (1H, m), 7.50-7.30 (6H, m), 7.31-7.18 (8H, m), ^{13}C NMR (75 MHz, $CDCl_3$): δ 165.25, 162.27, 147.33, 145.64, 137.18, 136.63, 135.85, 134.32, 130.95, 130.71, 129.94, 129.61, 129.39,129.29, 129.11, 126.27, 125.56, 125.45, 125.06, 121.74, 121.07, 116.11, 94.03. HRMS (ESI) m/z calcd for $C_{27}H_{17}NO_3S$ [M + H] $^+$, 436.09, found 436.04.

2/e

^{1}H and ^{13}C NMR spectra of all synthesized products described in Section -2

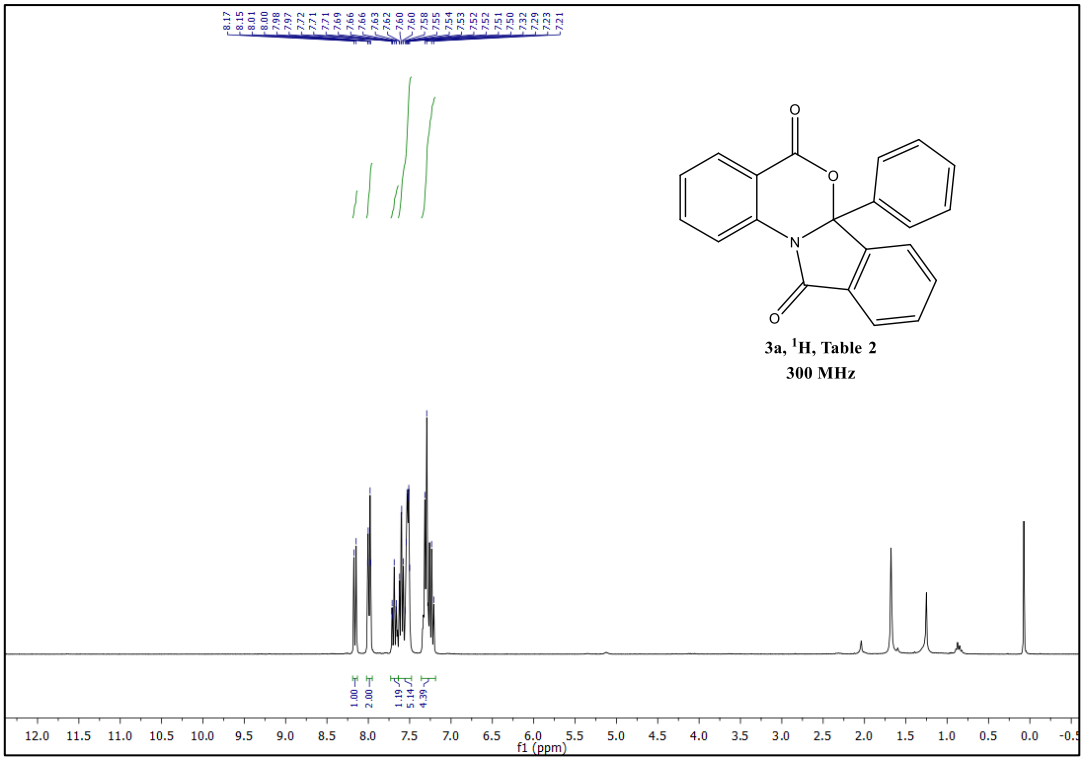

3a, ^{1}H, Table 2
300 MHz

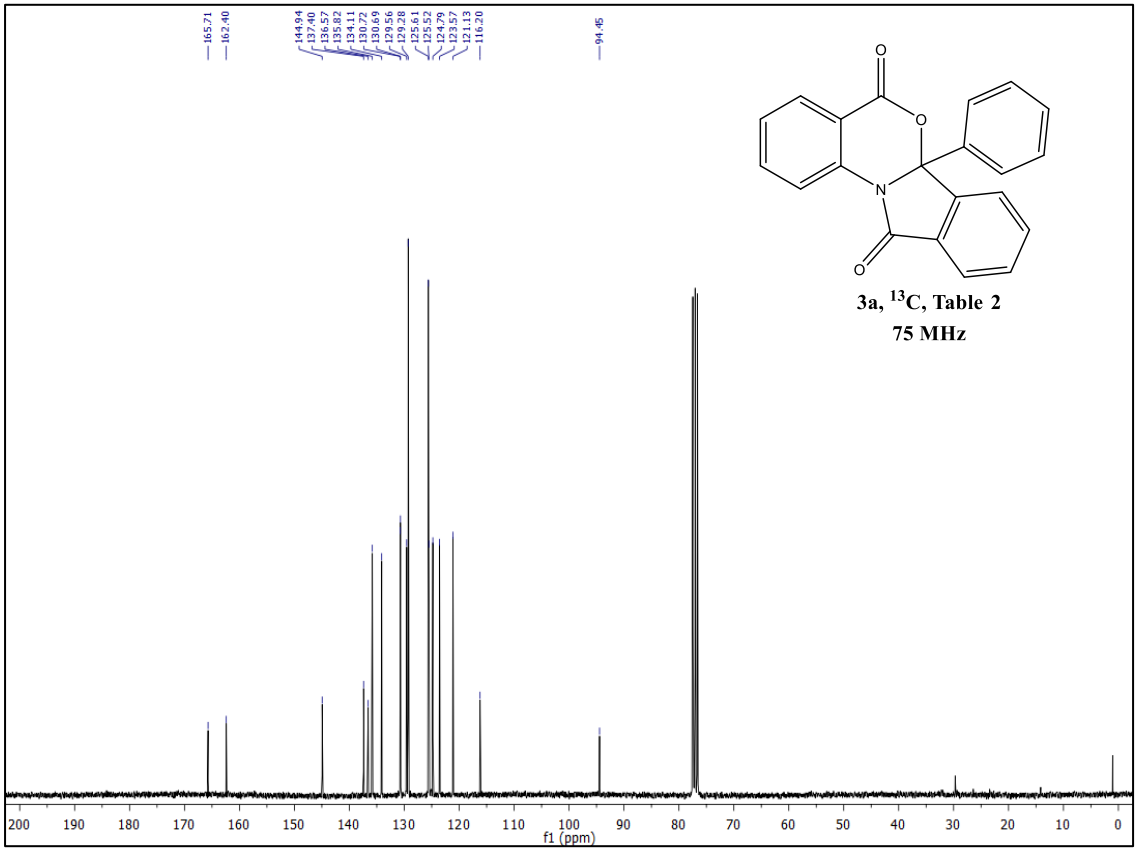

3a, ^{13}C, Table 2
75 MHz

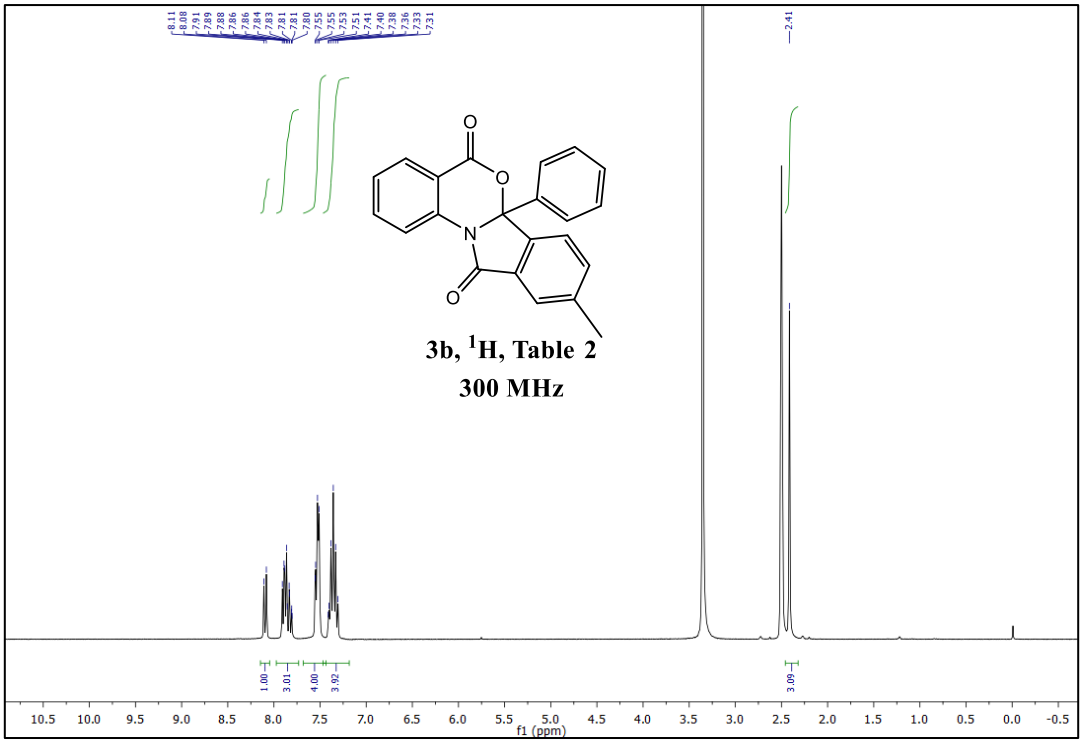
3b, ^{1}H, Table 2
300 MHz
f1 (ppm)

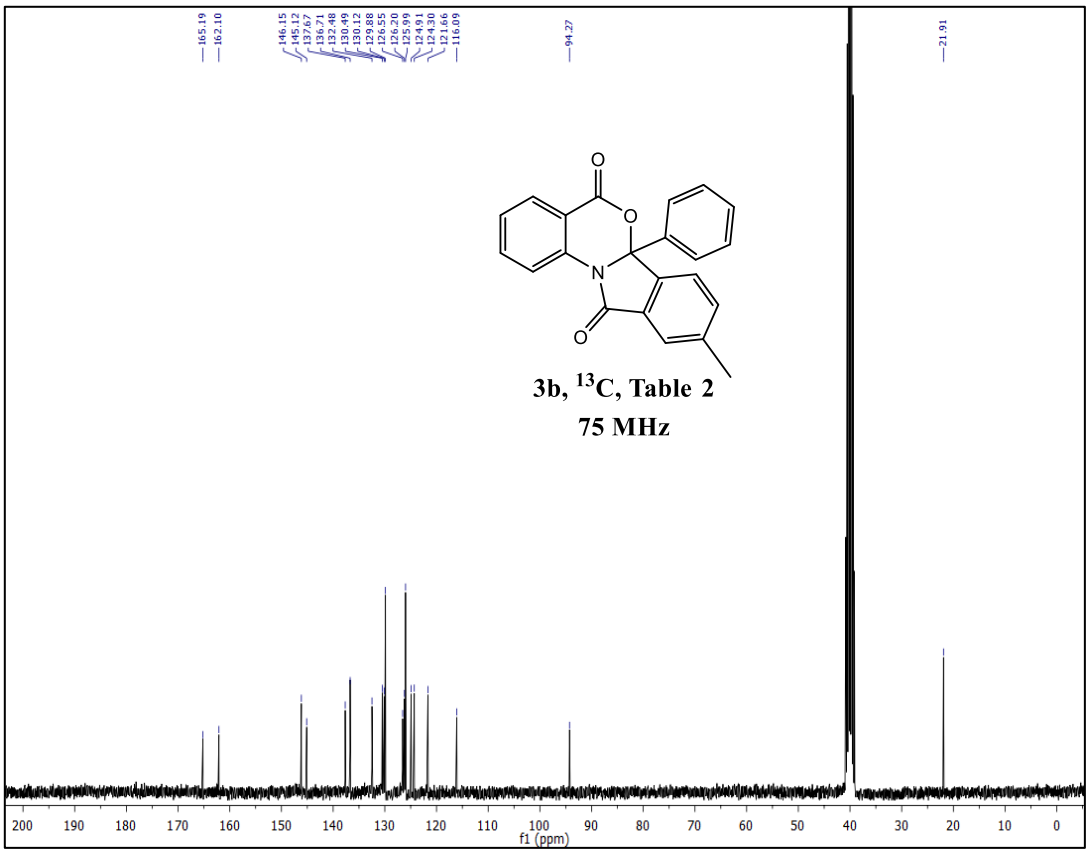
3b, ^{13}C, Table 2
75 MHz
f1 (ppm)

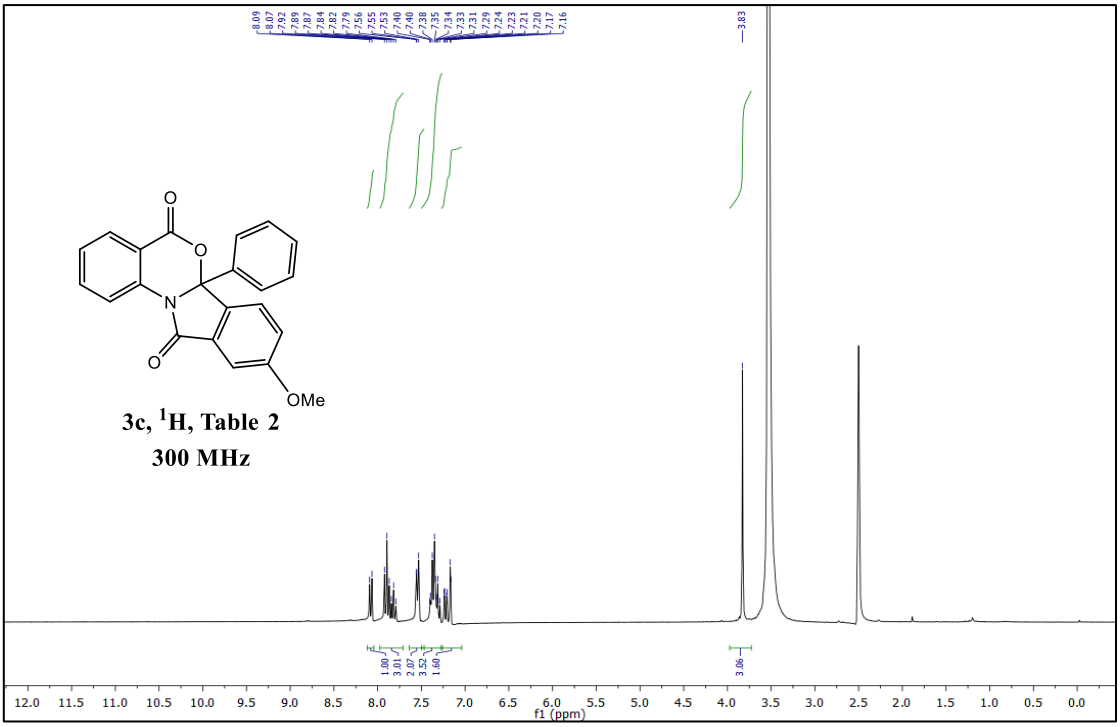

3c, ^{1}H, Table 2

300 MHz

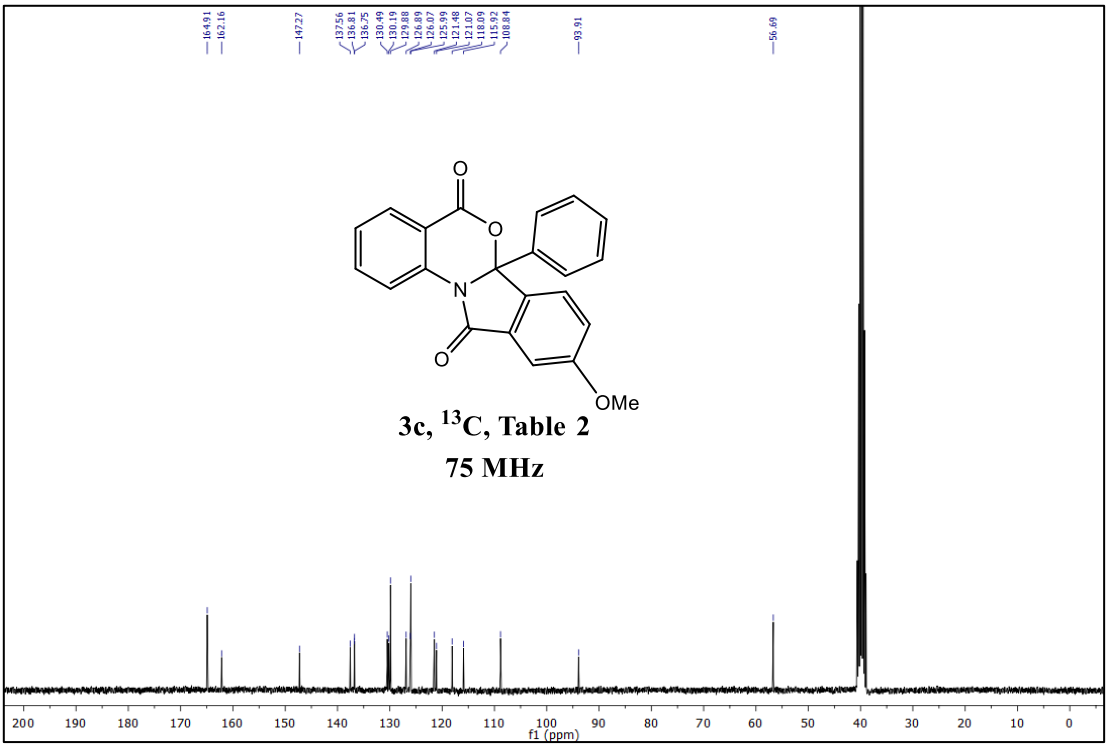

3c, ^{13}C, Table 2

75 MHz

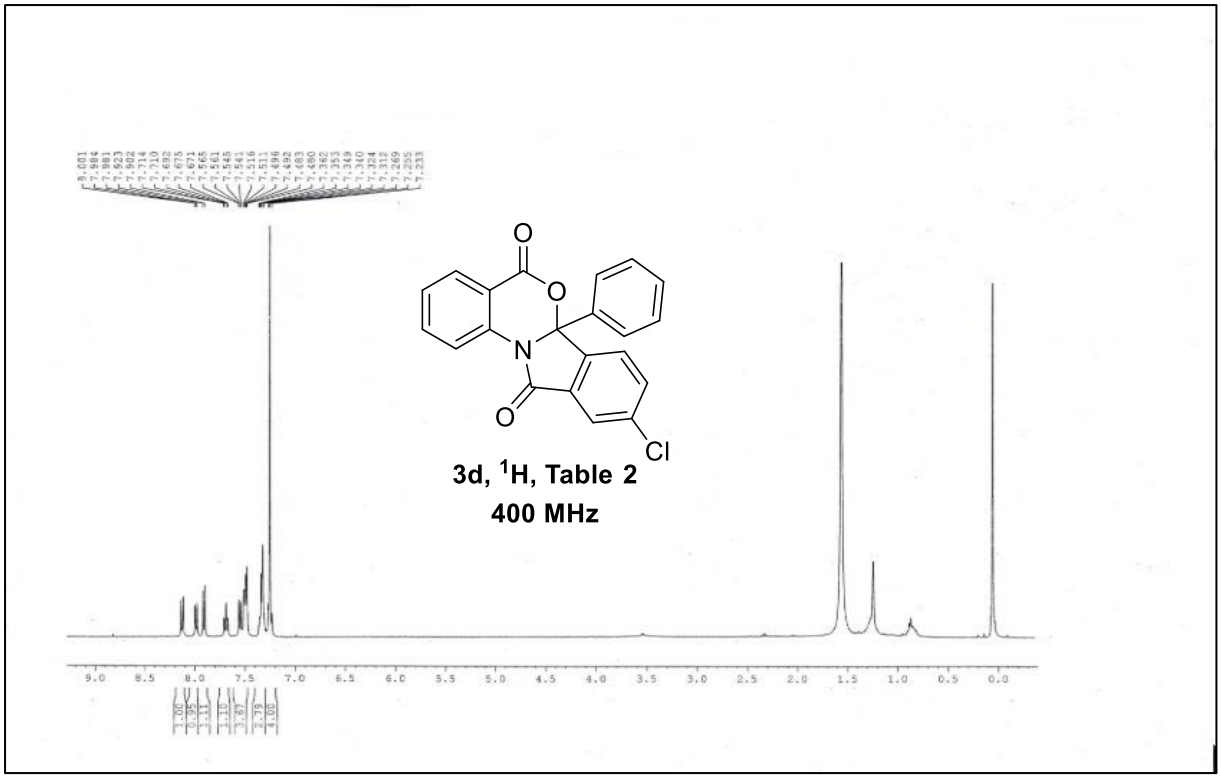
3d, ^{1}H, Table 2
400 MHz

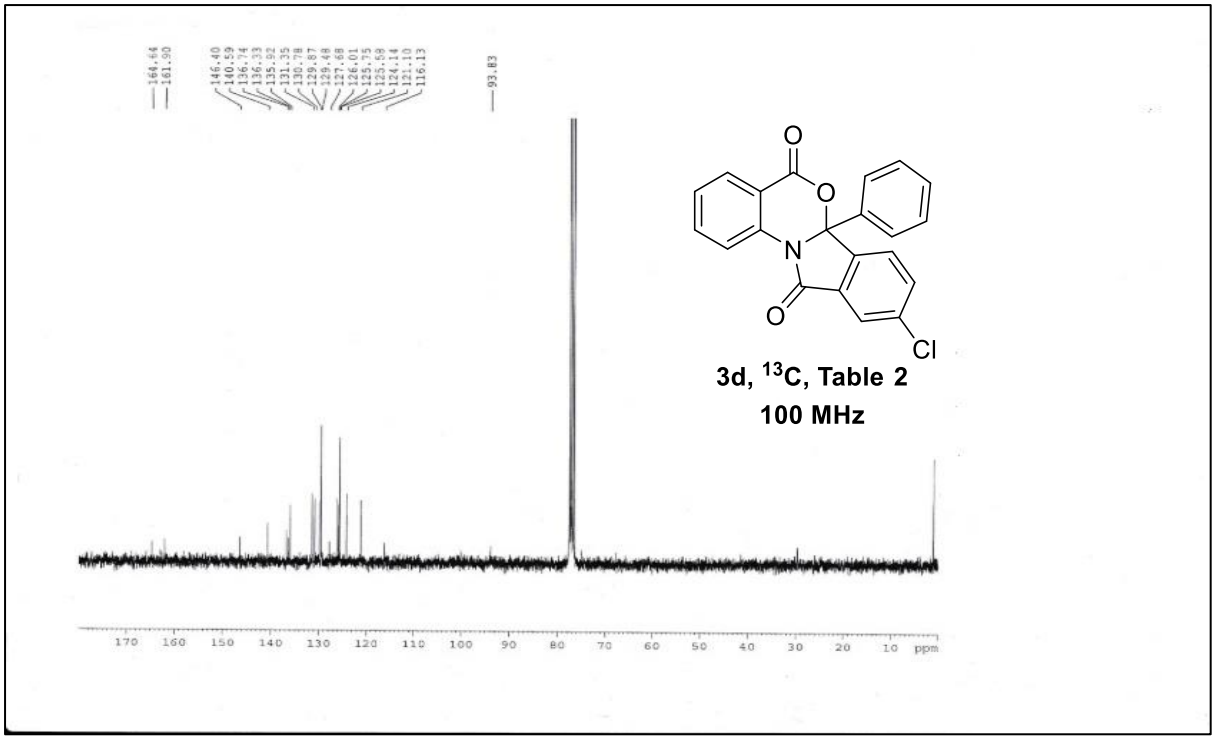
3d, ^{13}C, Table 2
100 MHz

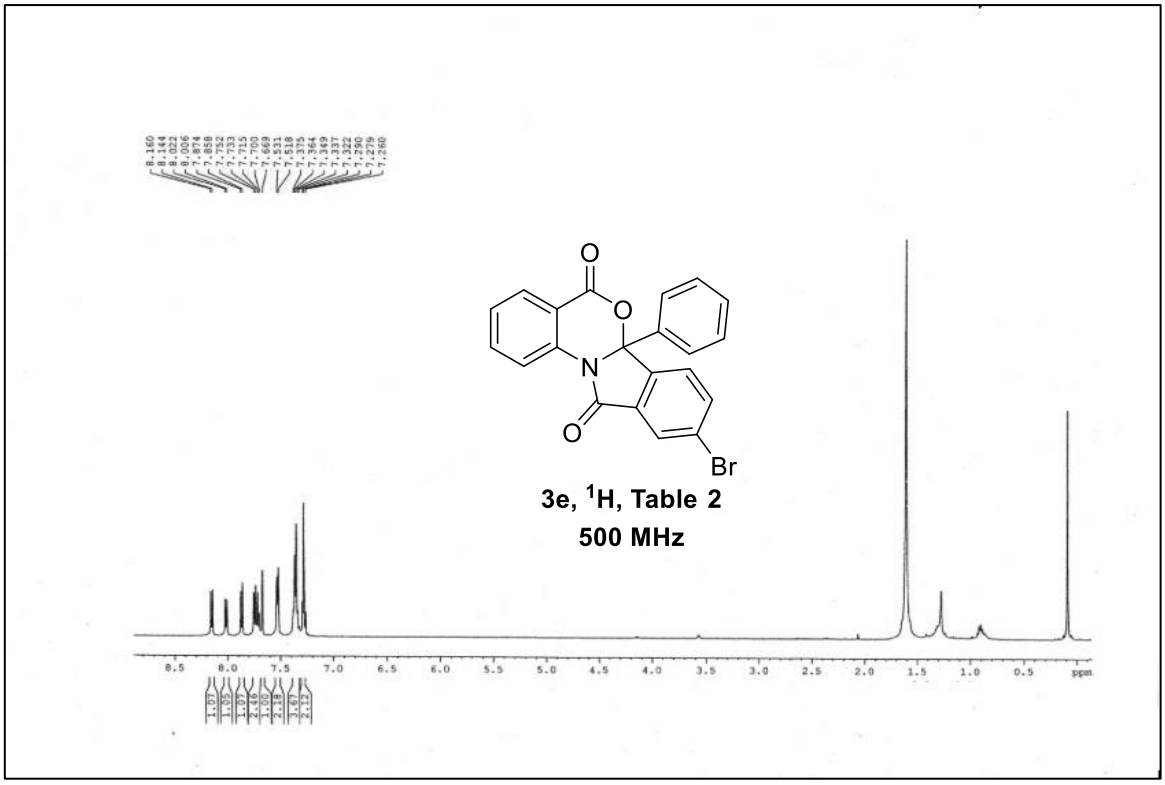
O
O
N
O
Br
3e, 1H, Table 2
500 MHz

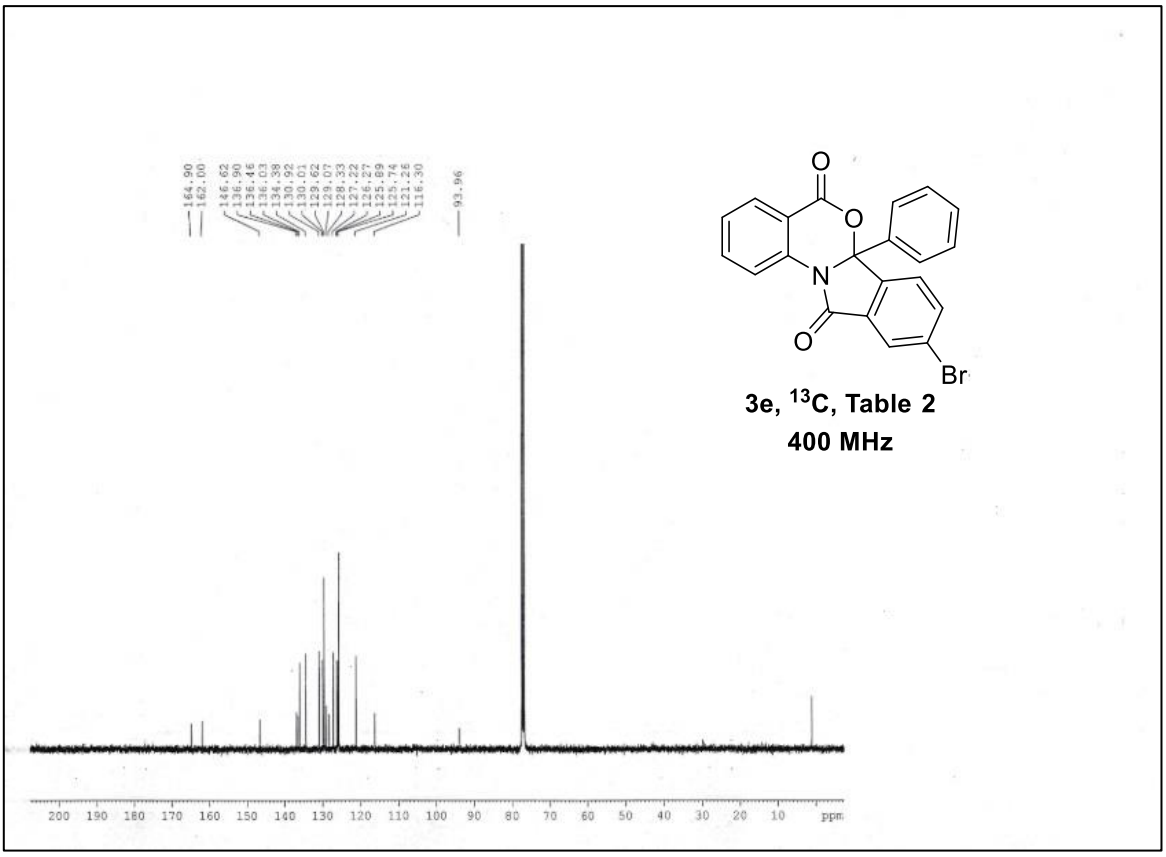
O
O
N
O
Br
3e, 13C, Table 2
400 MHz

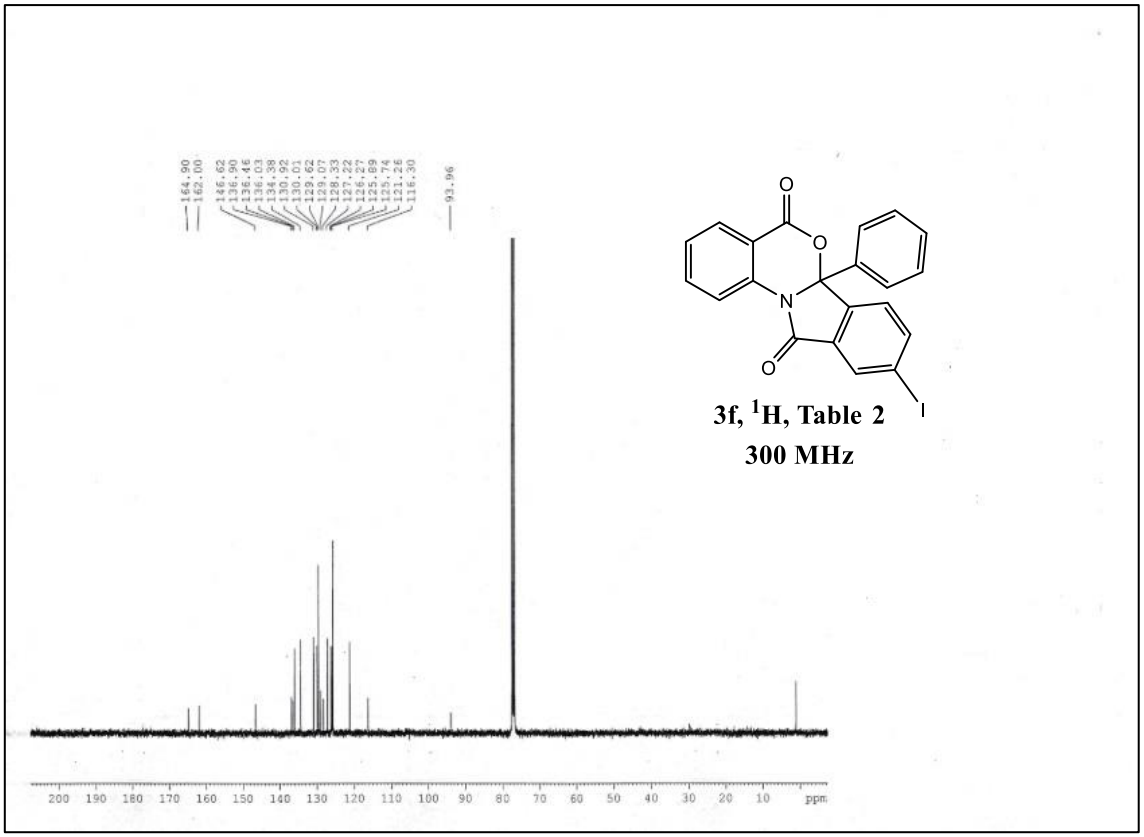

3f, ^{1}H, Table 2
300 MHz

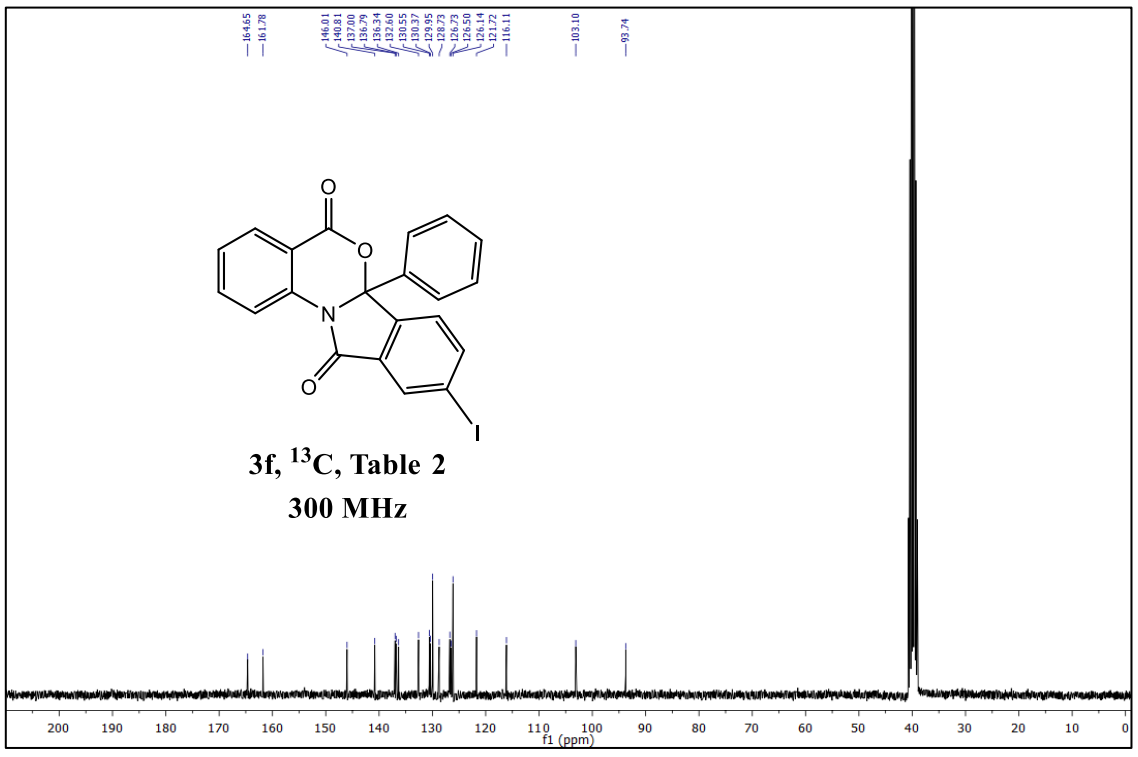

3f, ^{13}C, Table 2
300 MHz

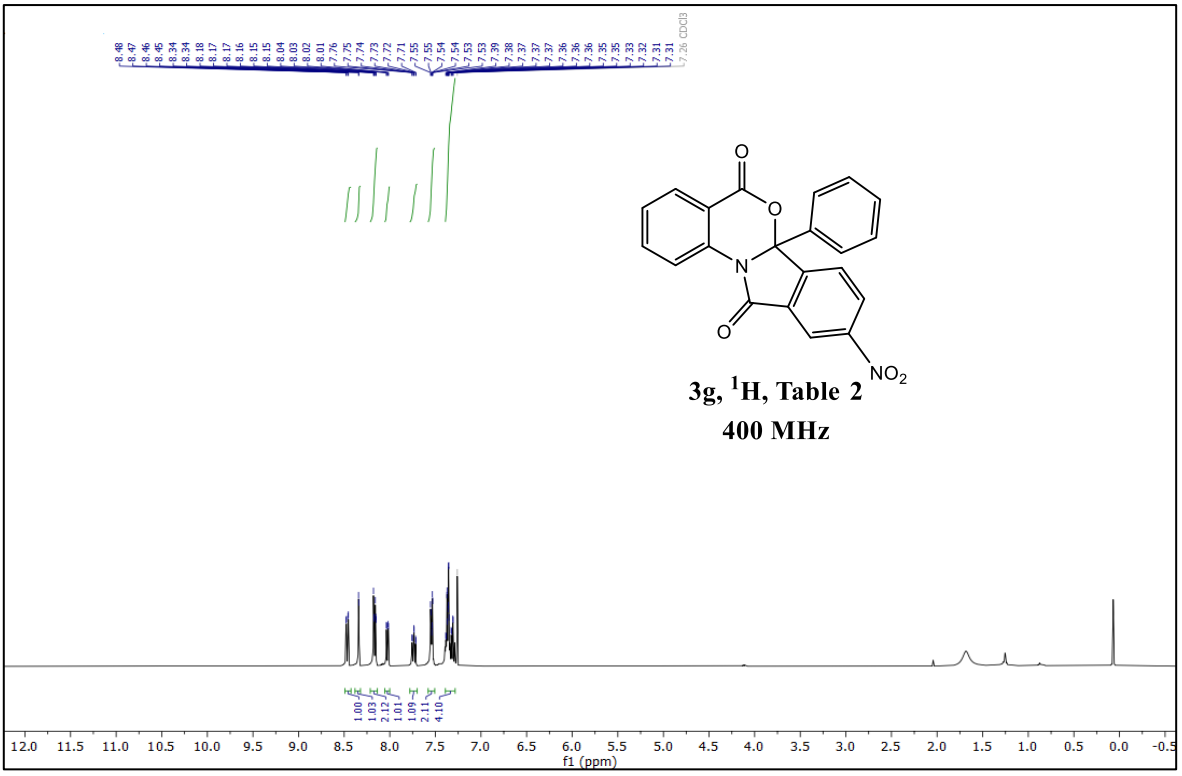
3g, ^{1}H, Table 2
400 MHz
f1 (ppm)

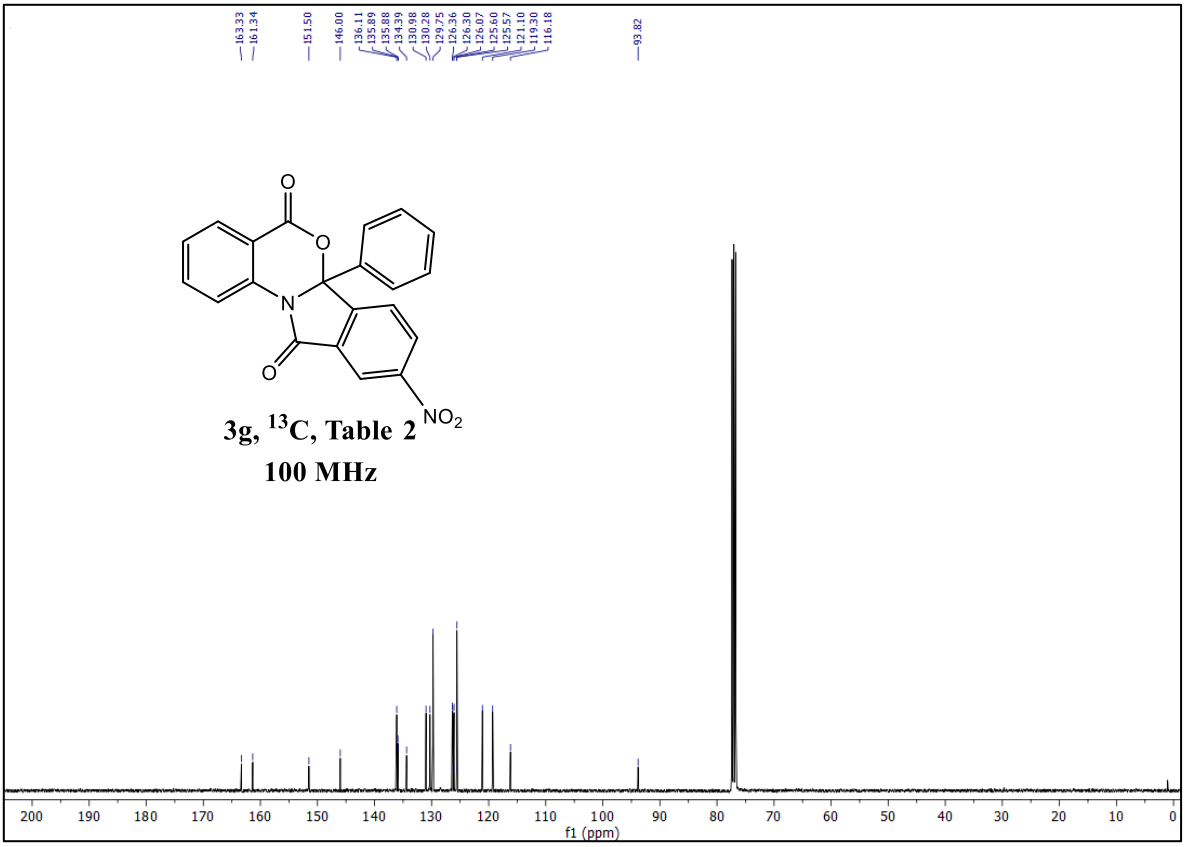
3g, ^{13}C, Table 2
100 MHz
f1 (ppm)

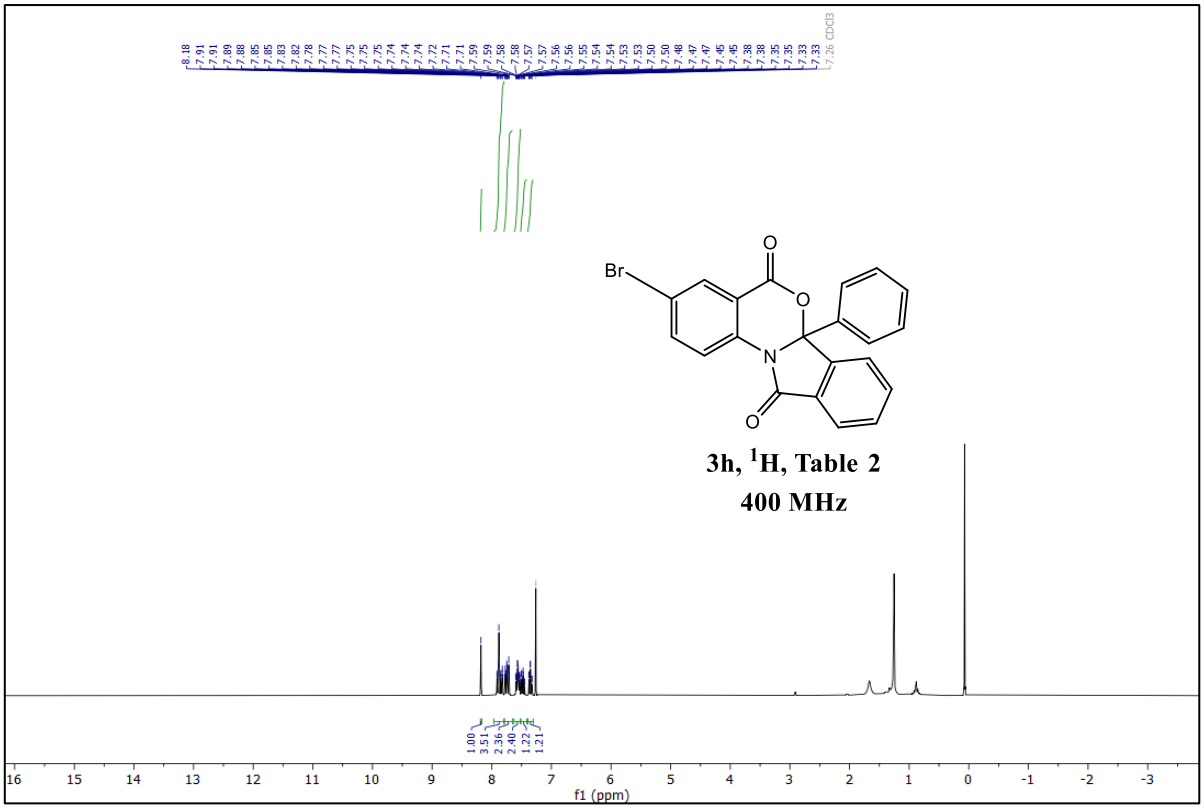

3h, ^{1}H, Table 2
400 MHz

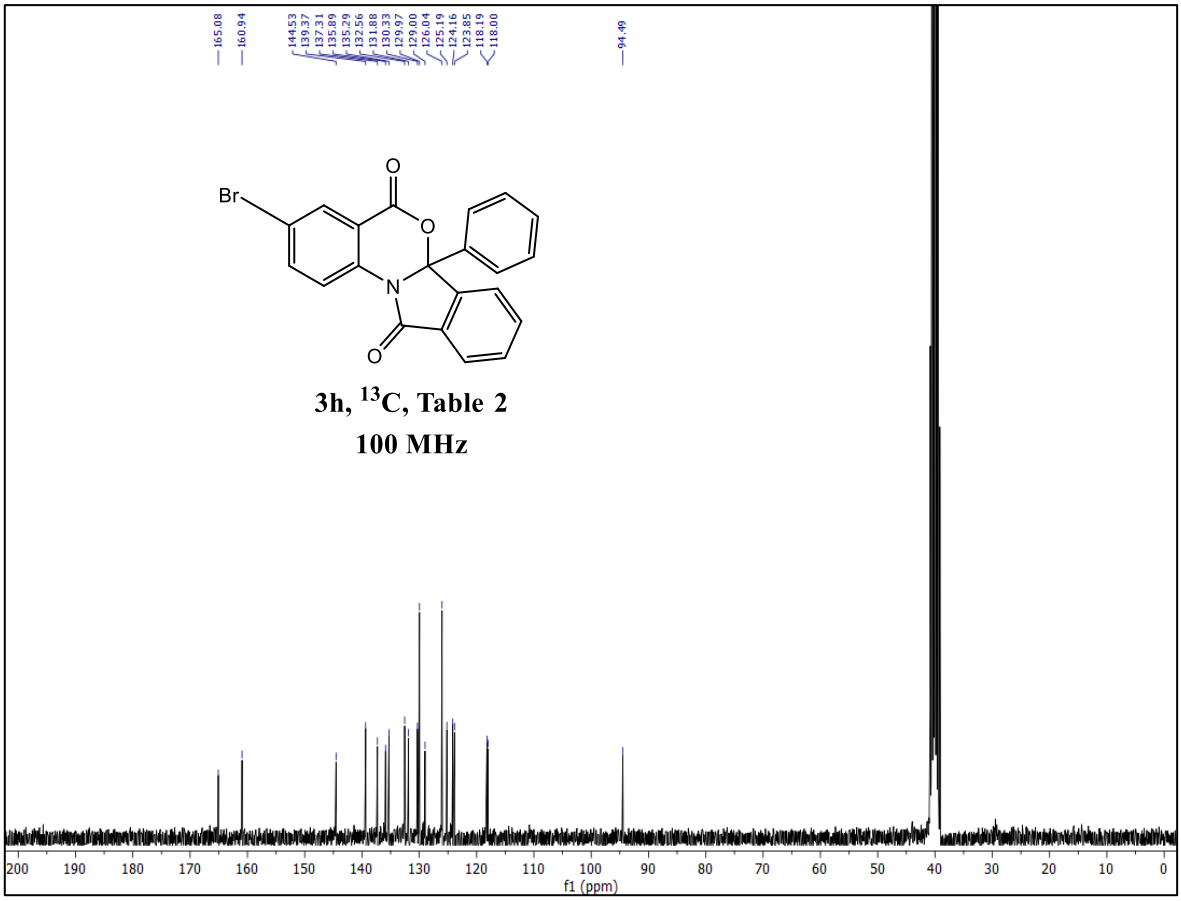

3h, ^{13}C, Table 2
100 MHz

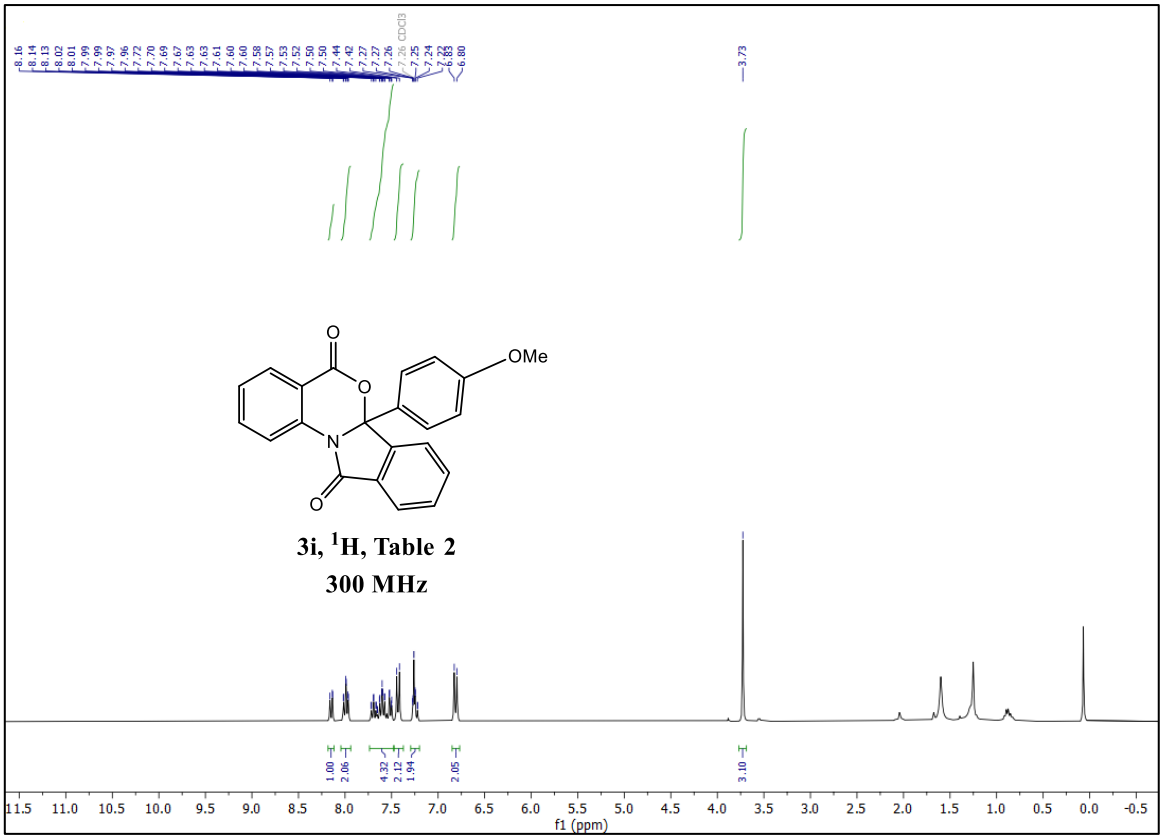

3i, ^{1}H, Table 2
300 MHz

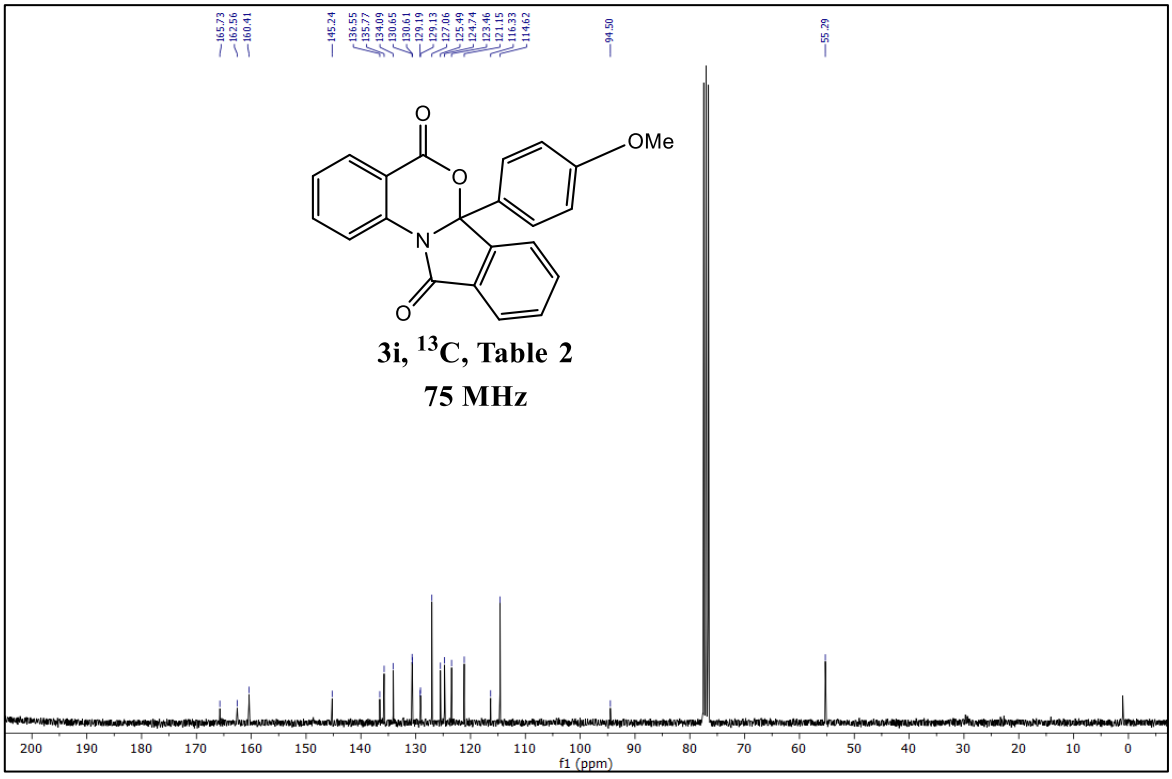

3i, ^{13}C, Table 2
75 MHz

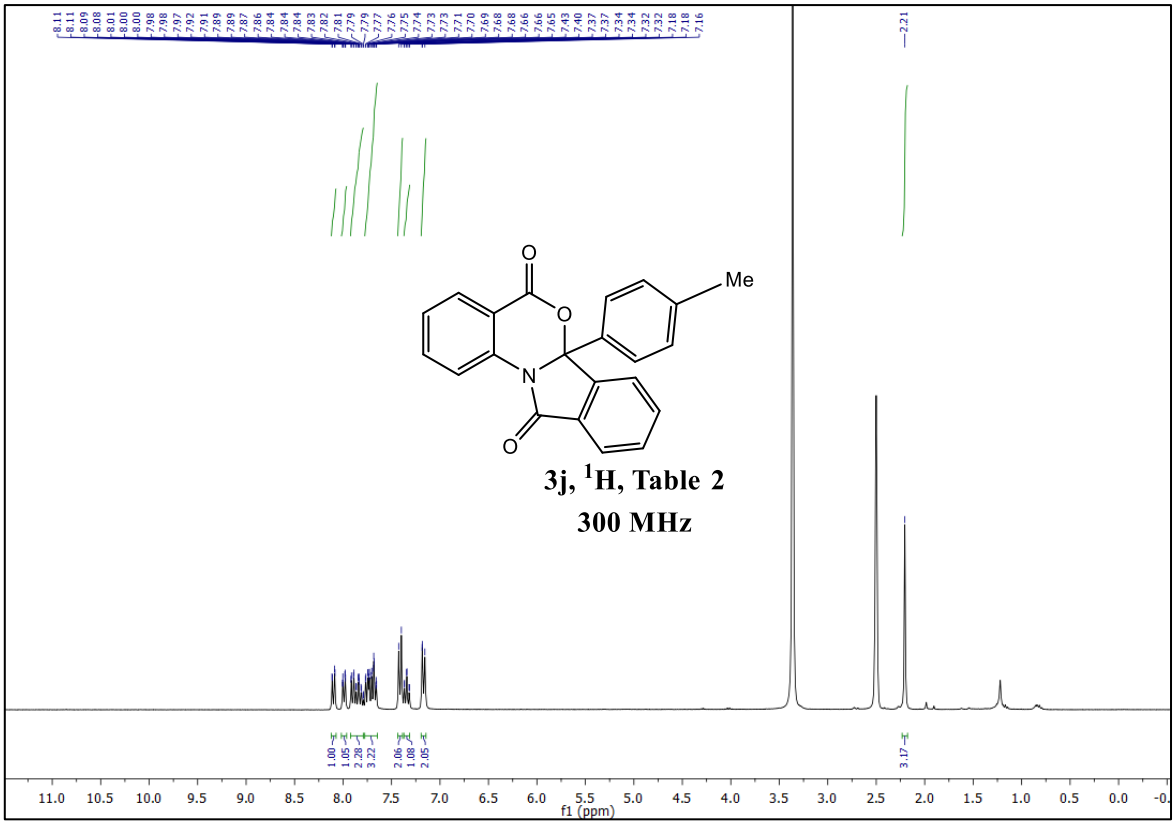

3j, ^{1}H, Table 2
300 MHz

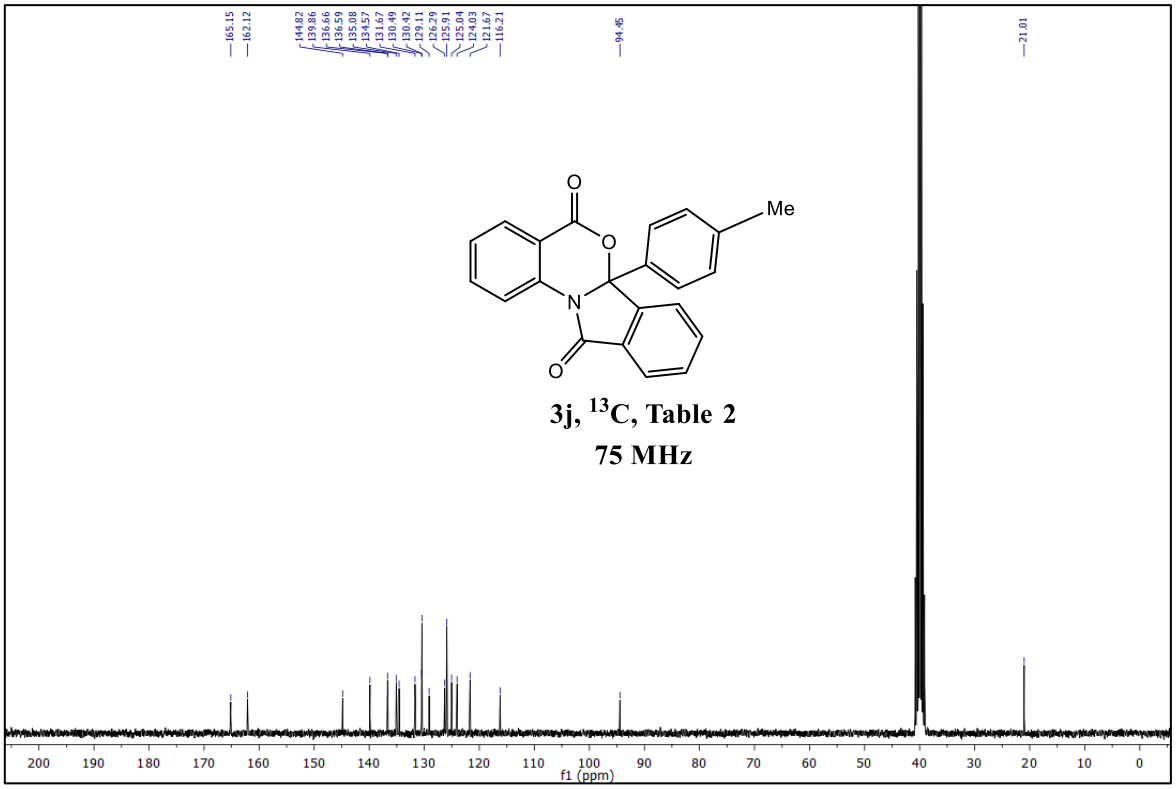

3j, ^{13}C, Table 2
75 MHz

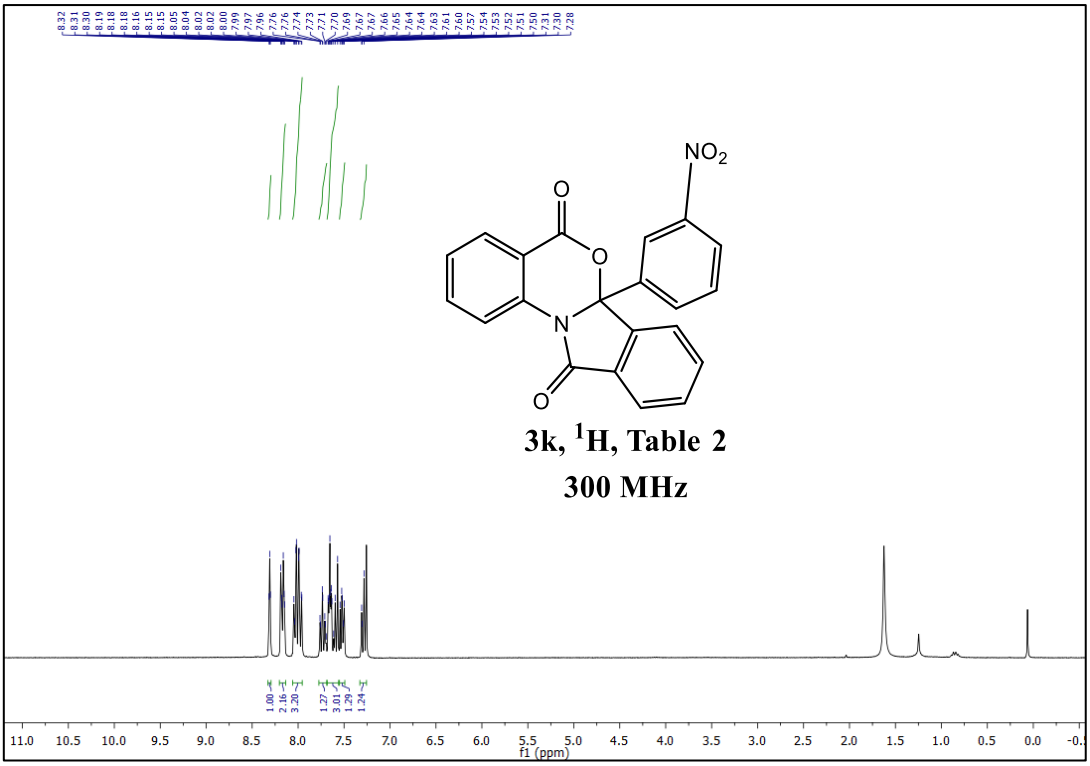

3k, ^{1}H, Table 2

300 MHz

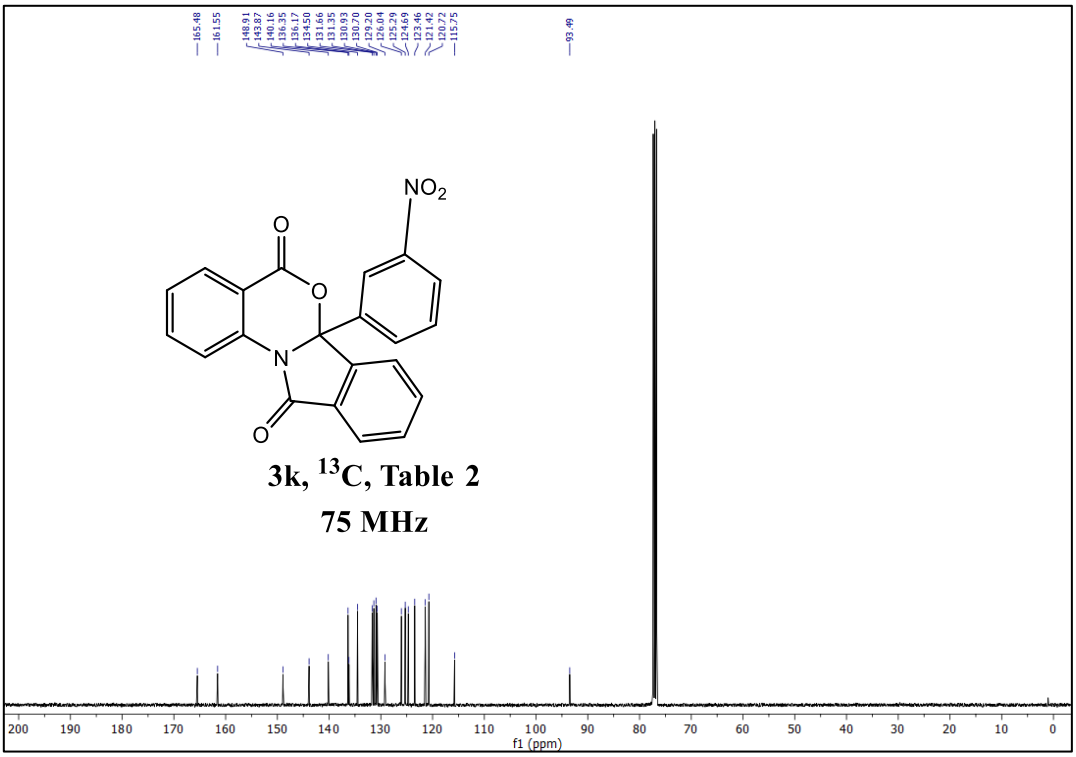

3k, ^{13}C, Table 2

75 MHz

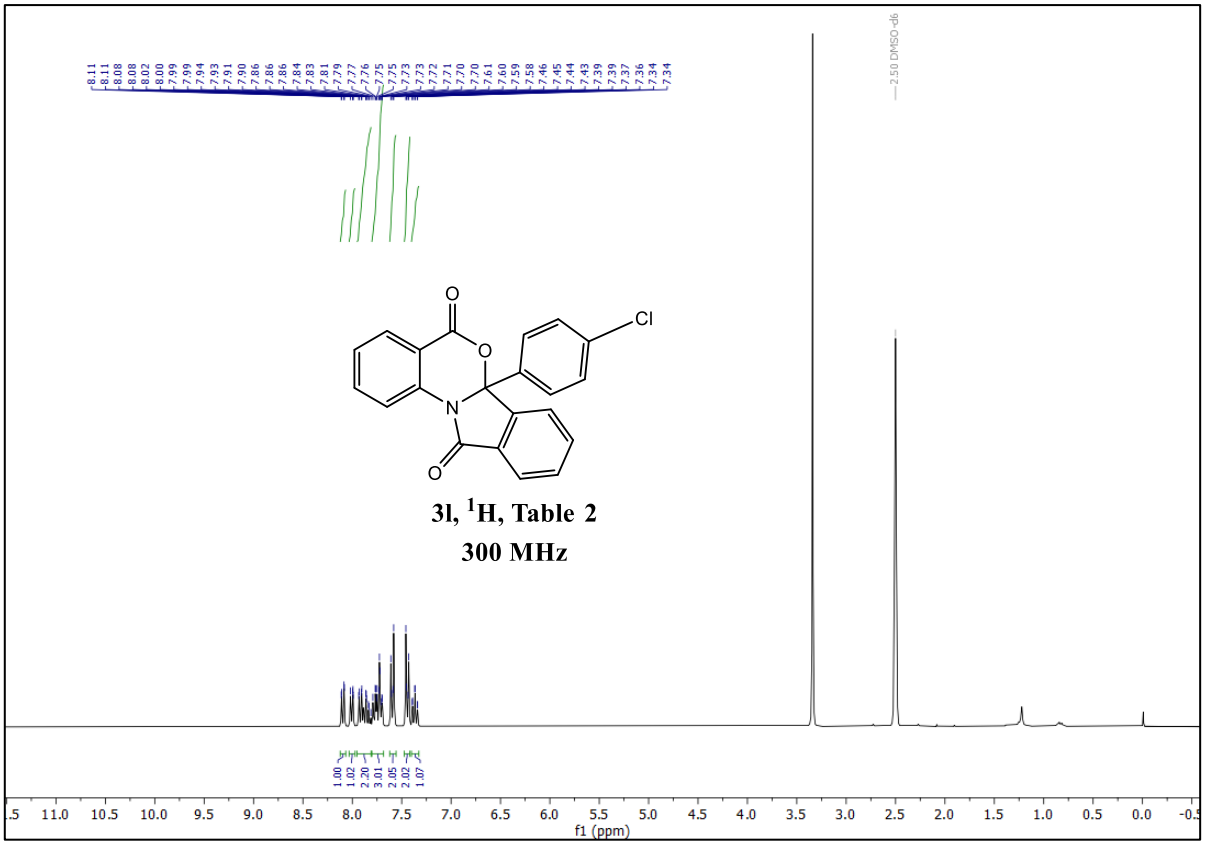

3l, ^{1}H, Table 2

300 MHz

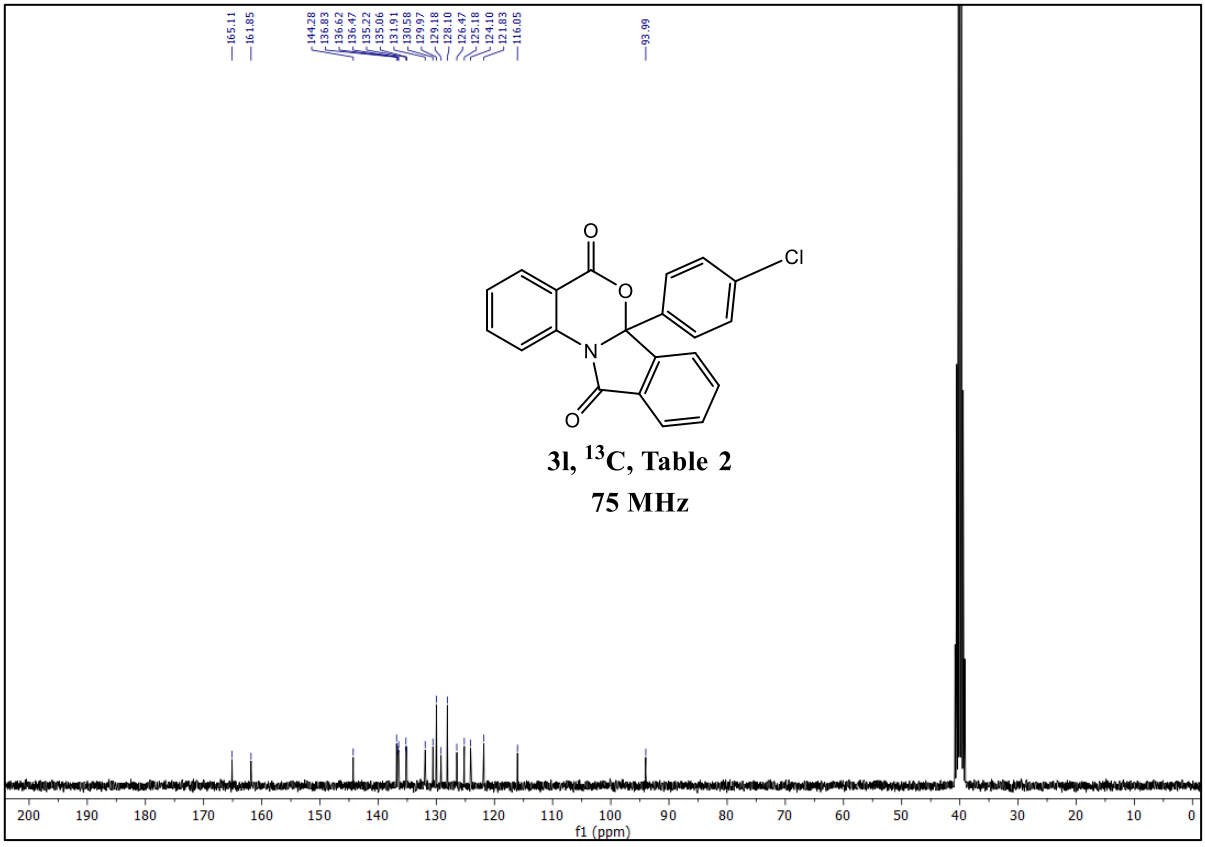

3l, ^{13}C, Table 2

75 MHz

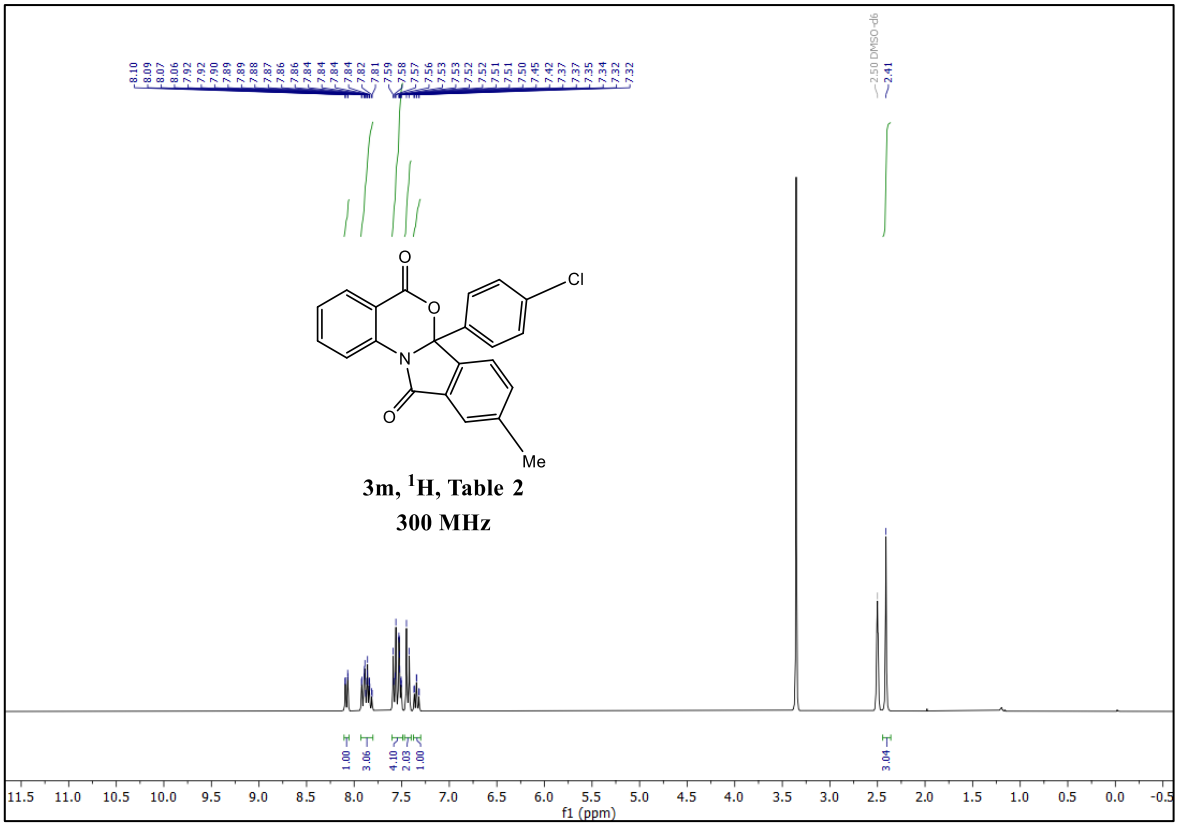

3m, ^{1}H, Table 2

300 MHz

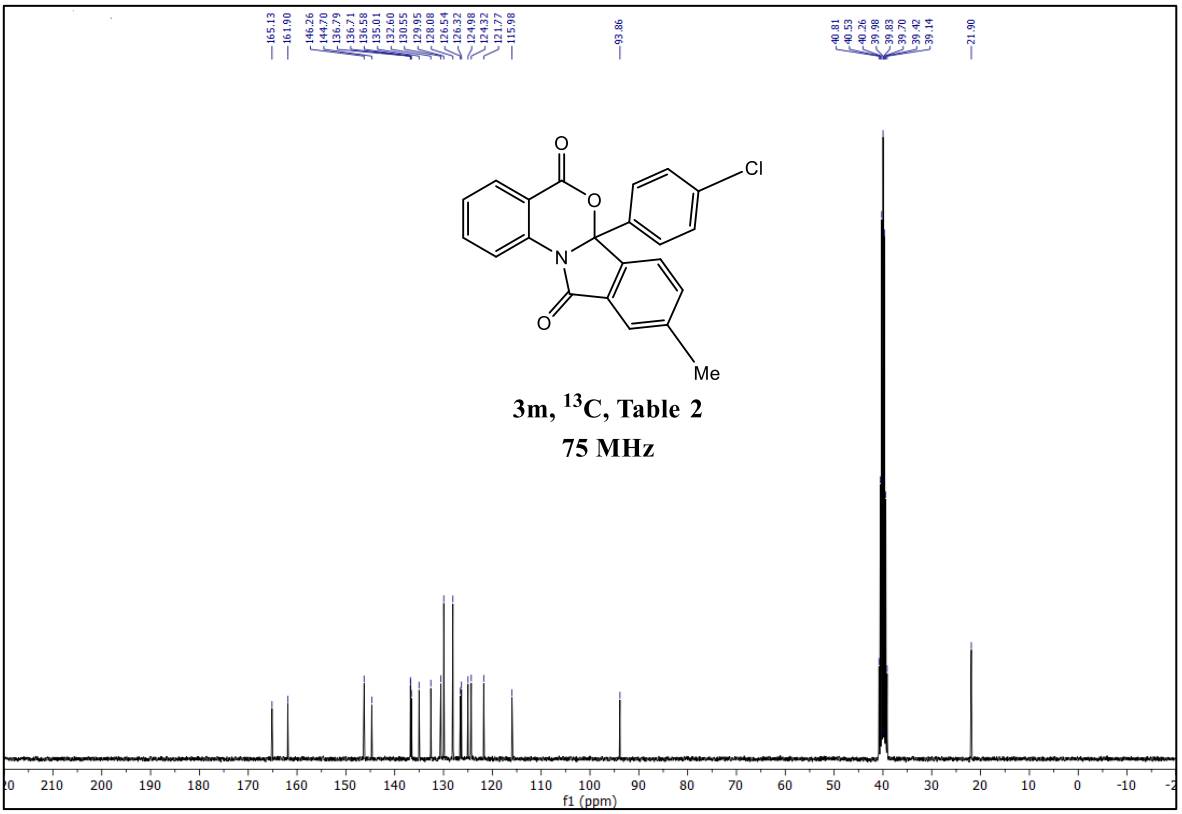

3m, ^{13}C, Table 2

75 MHz

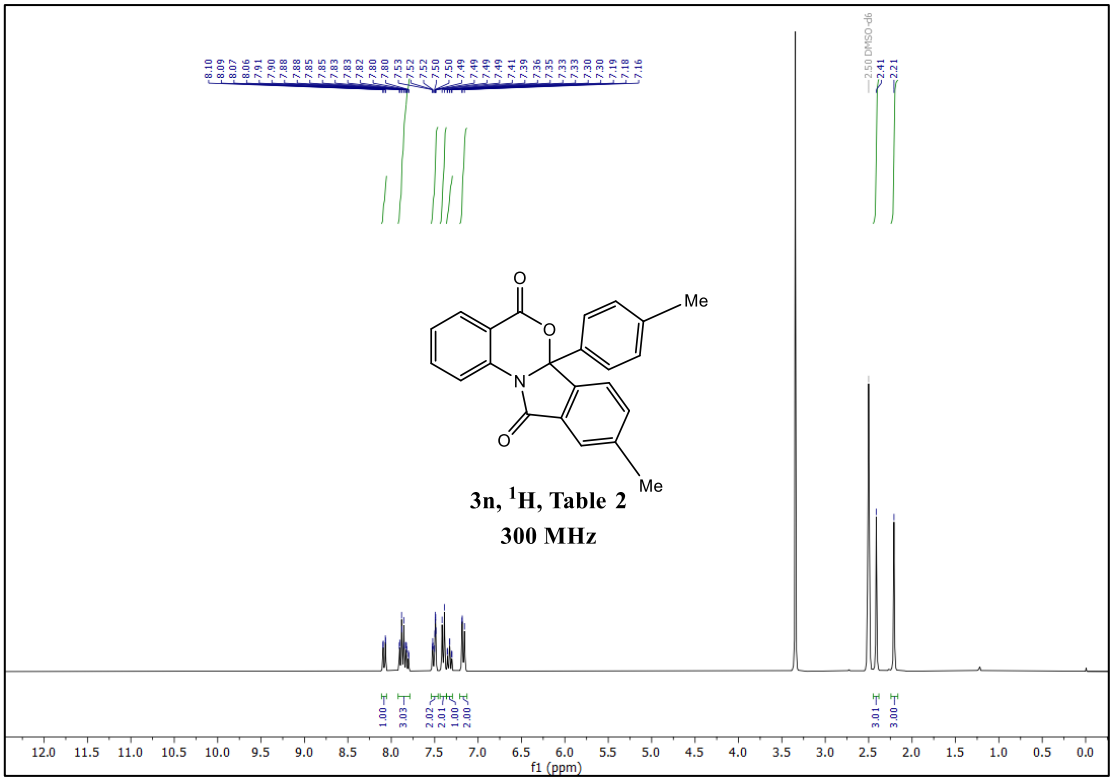

3n, ^{1}H, Table 2

300 MHz

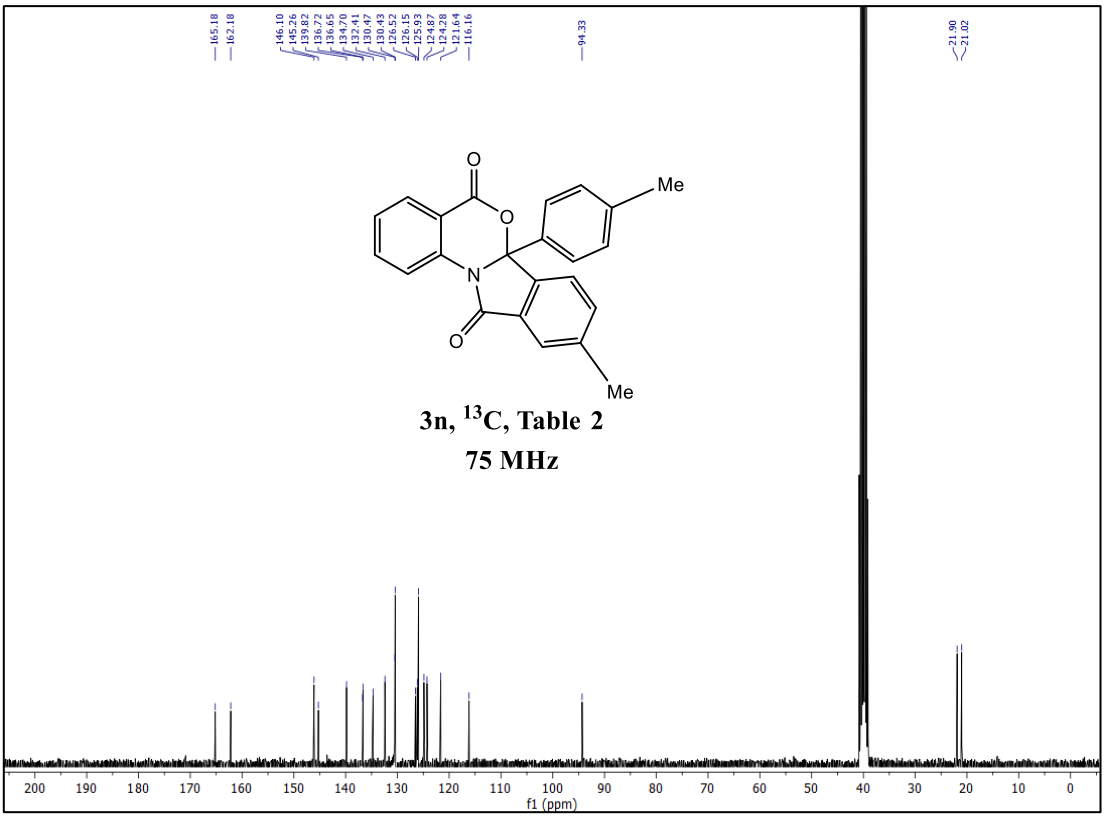

3n, ^{13}C, Table 2

75 MHz

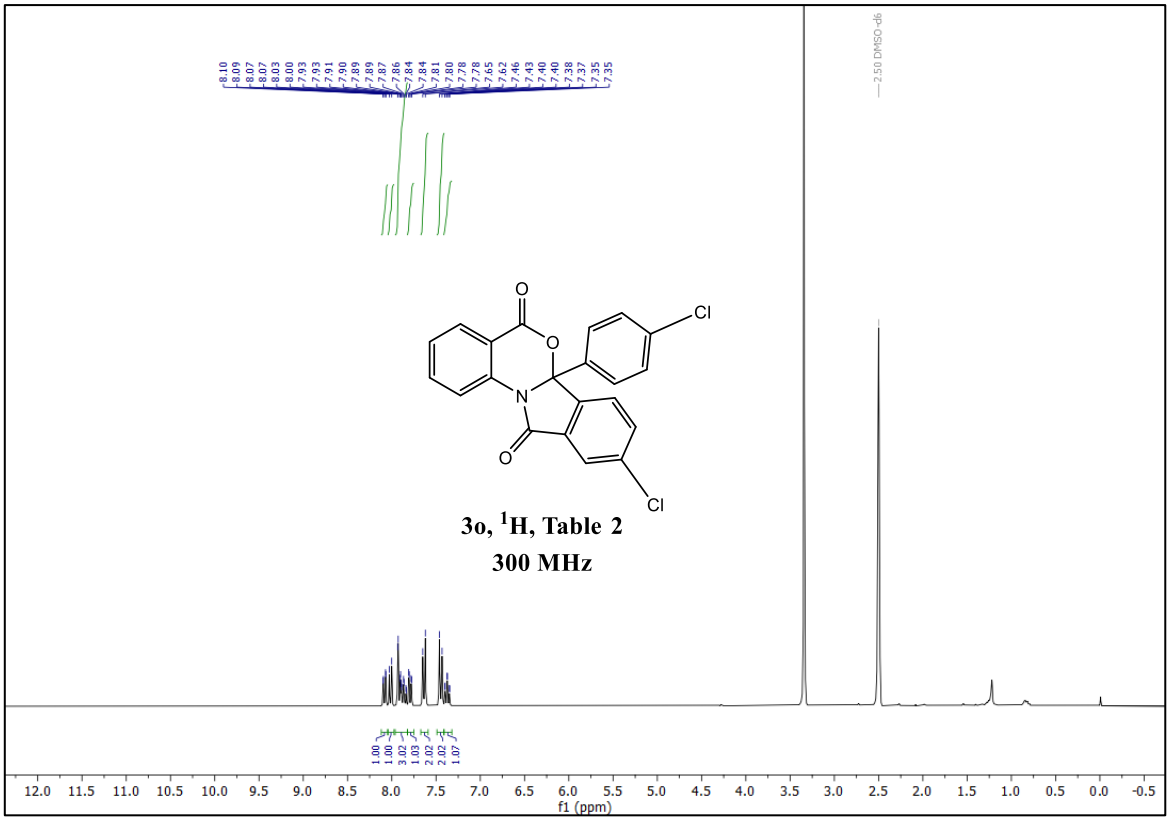

3o, ^{1}H, Table 2
300 MHz

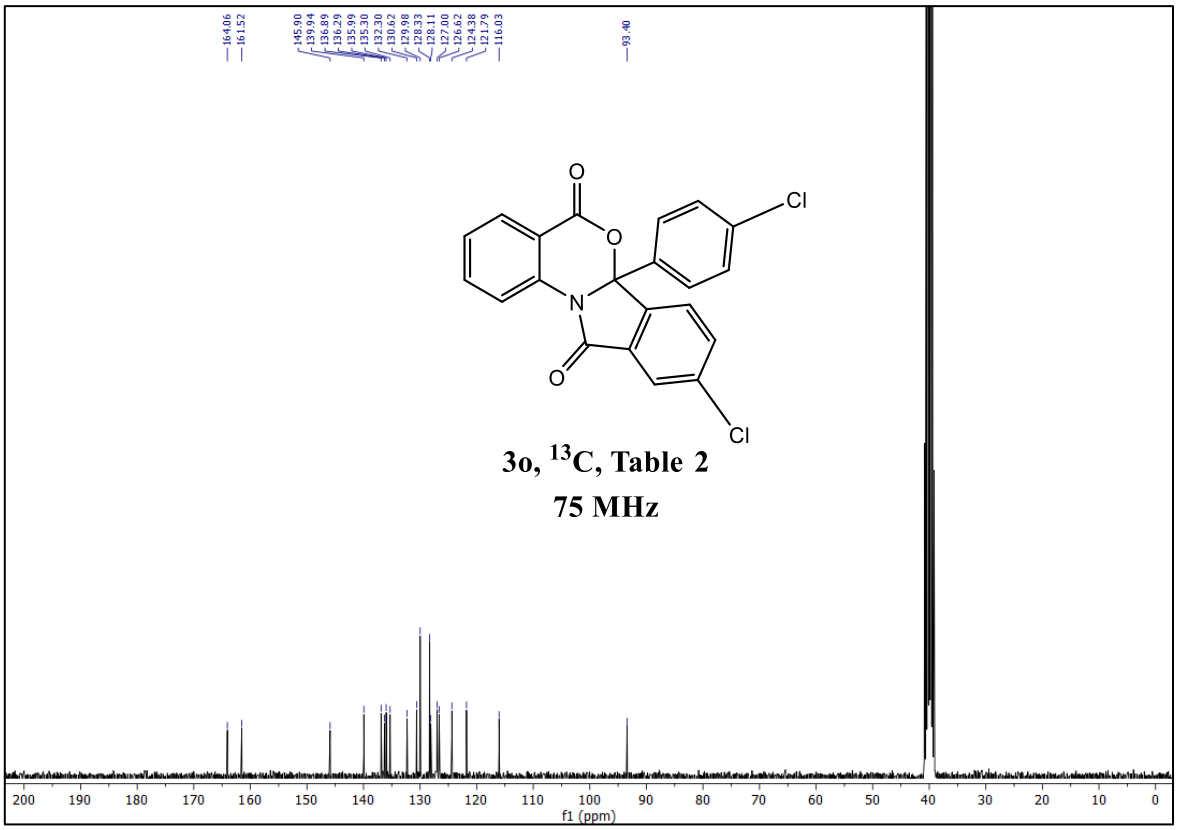

3o, ^{13}C, Table 2
75 MHz

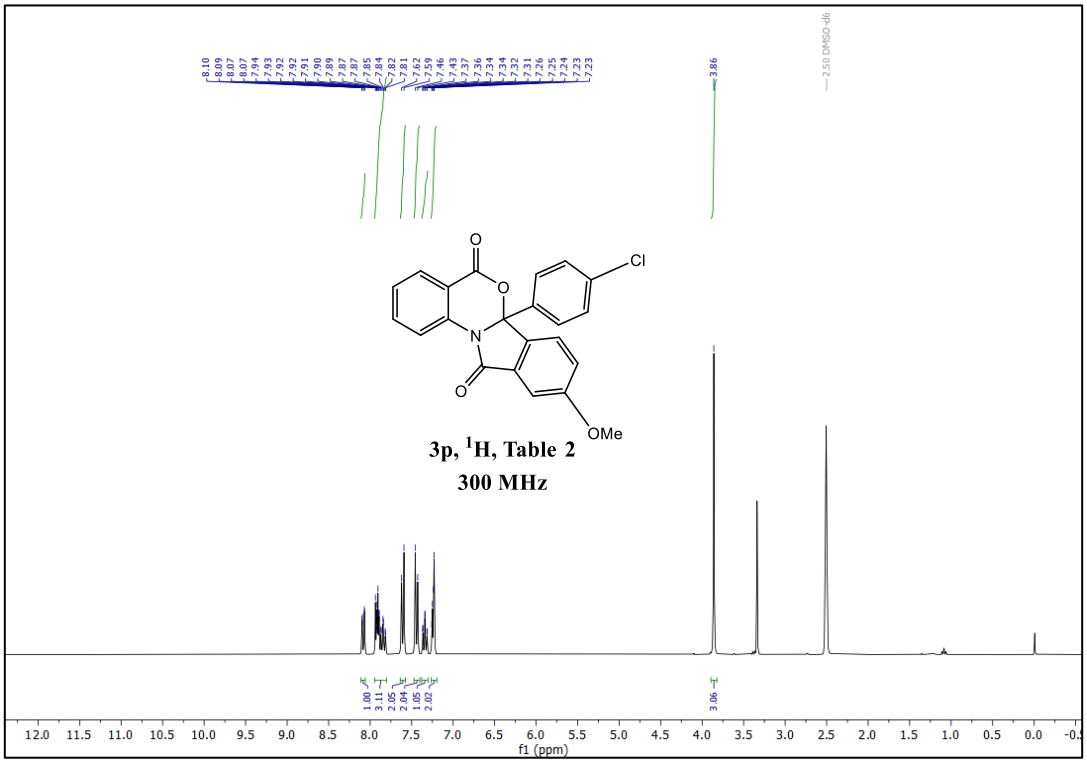

3p, ^{1}H, Table 2

300 MHz

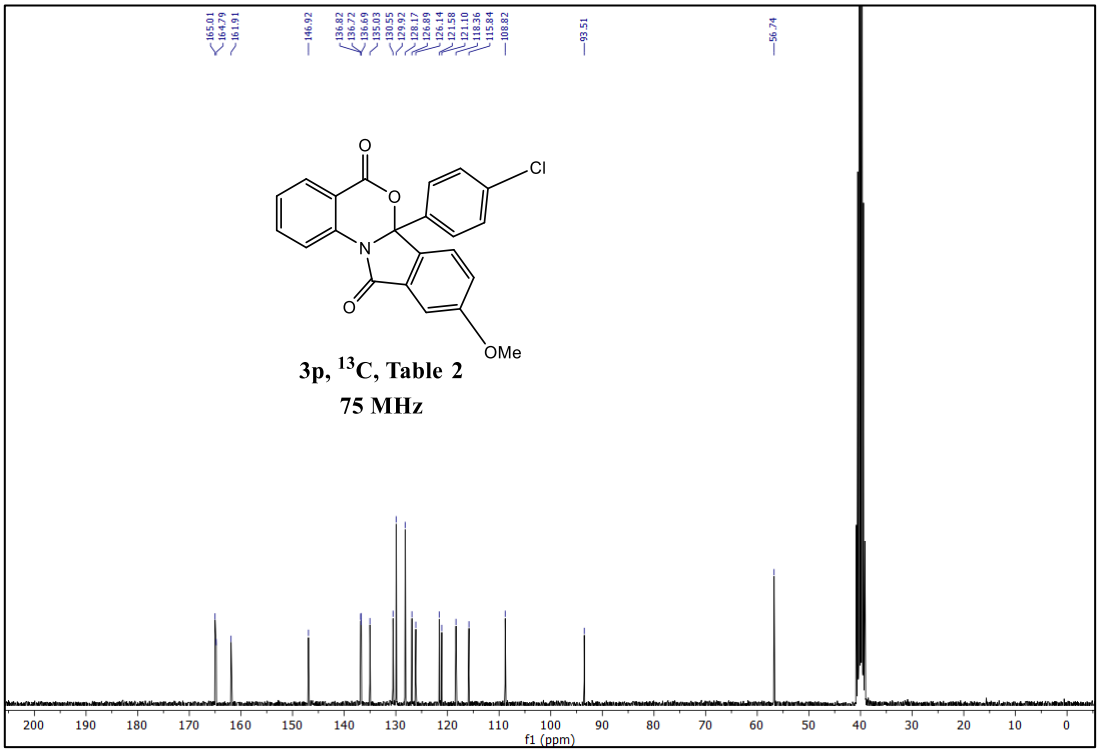

3p, ^{13}C, Table 2

75 MHz

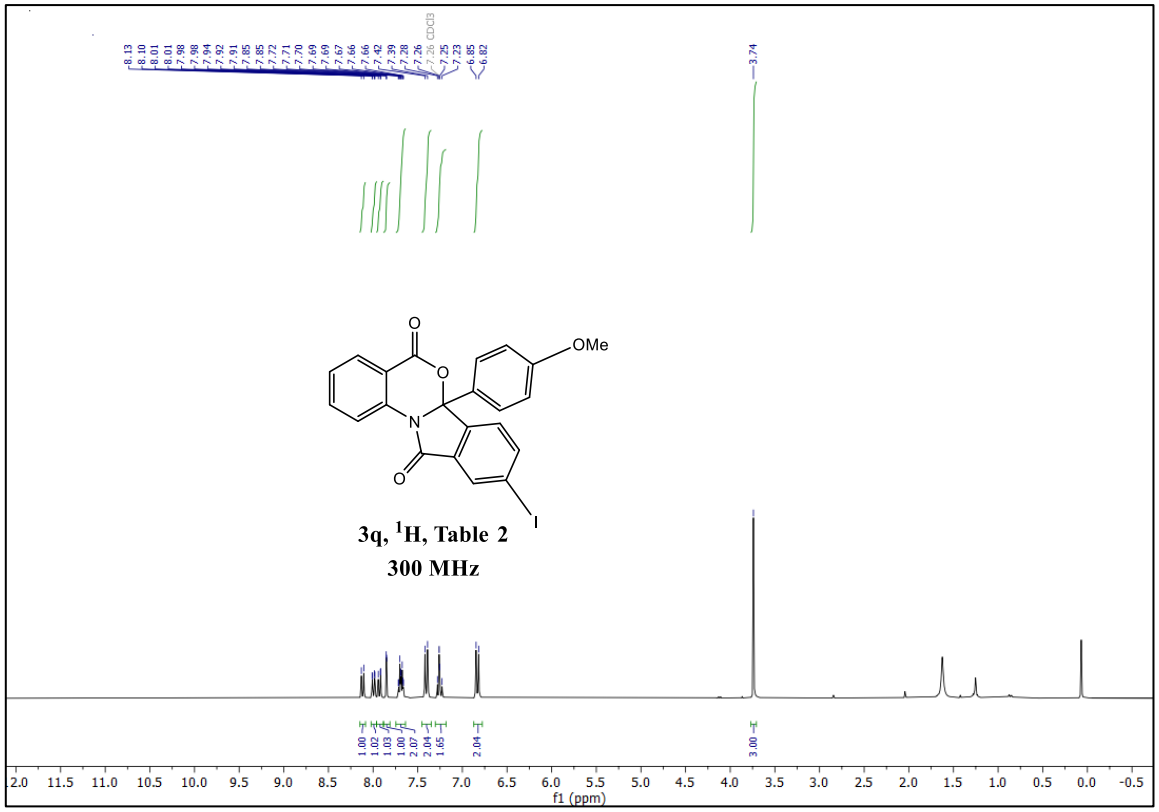
OMe
I
3q, ^{1}H, Table 2
300 MHz
f1 (ppm)

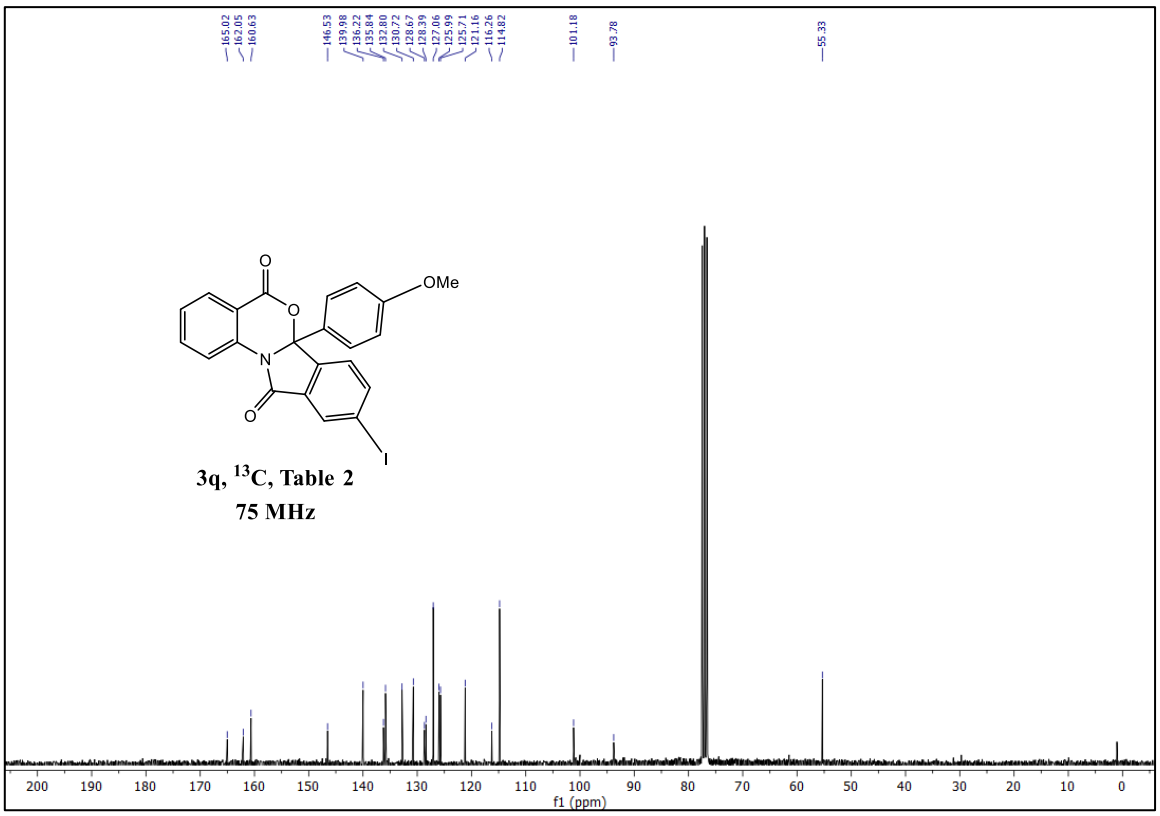
OMe
I
3q, ^{13}C, Table 2
75 MHz
f1 (ppm)

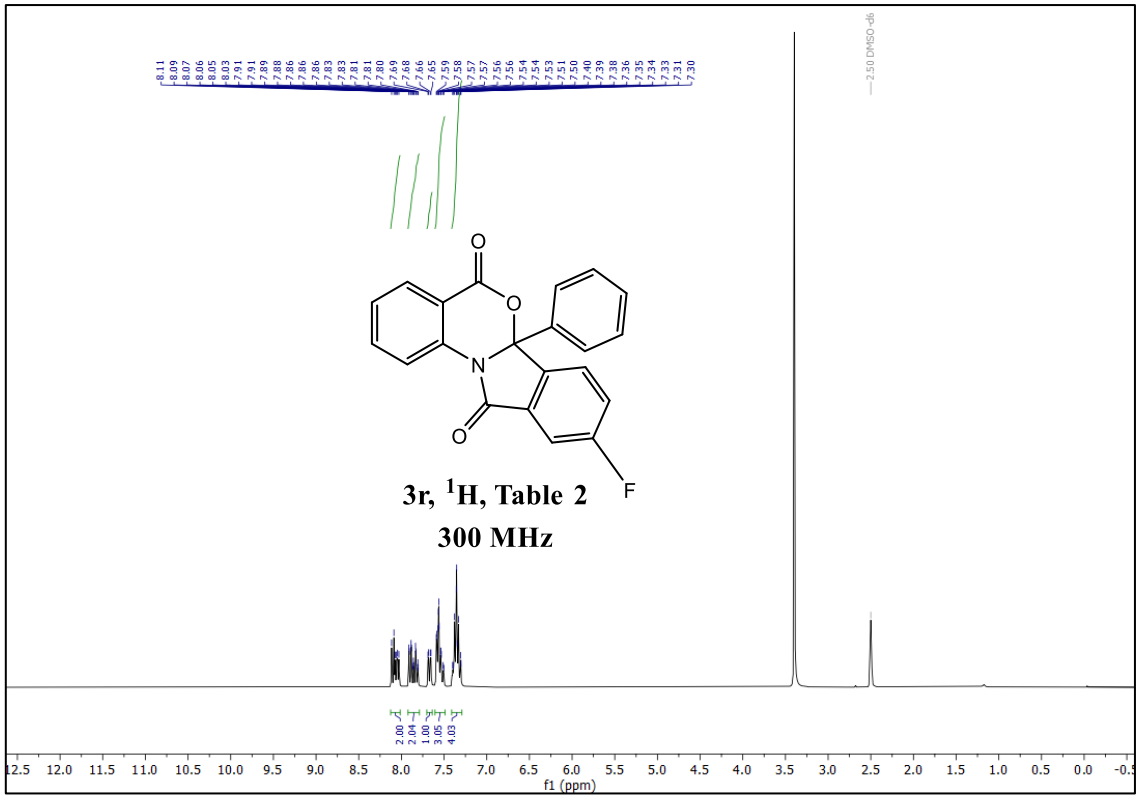
3r, ^{1}H, Table 2
300 MHz
f1 (ppm)

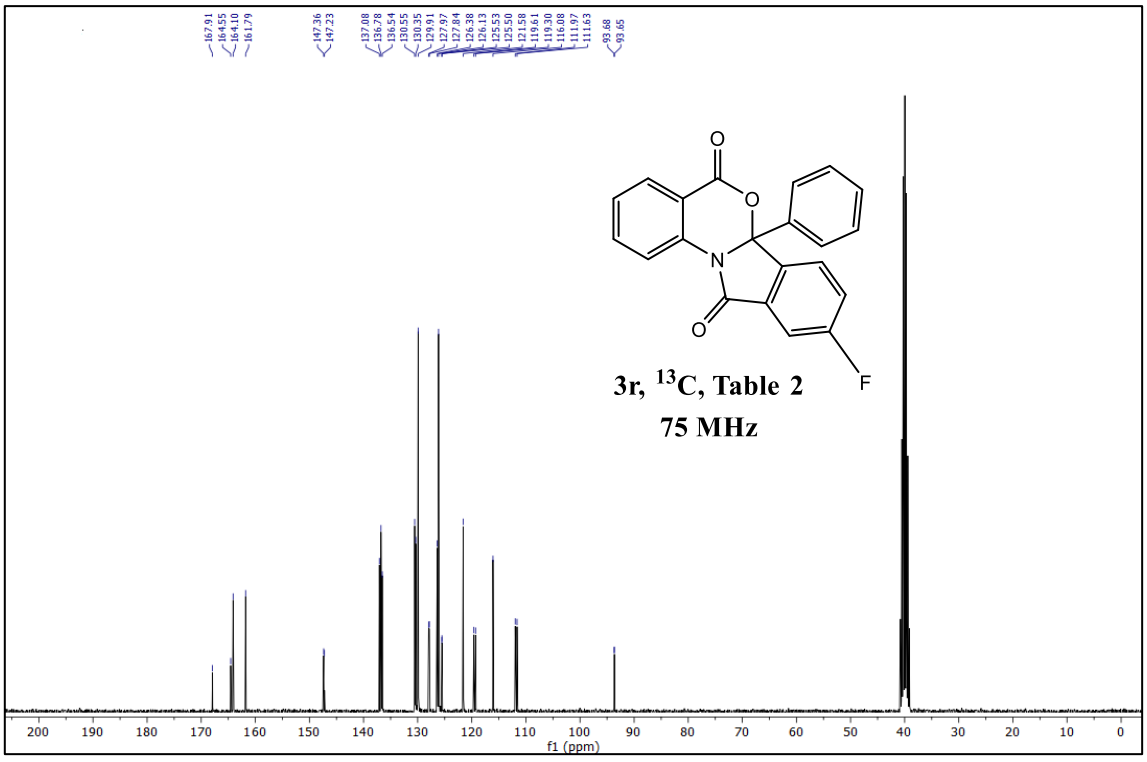
3r, ^{13}C, Table 2
75 MHz
f1 (ppm)

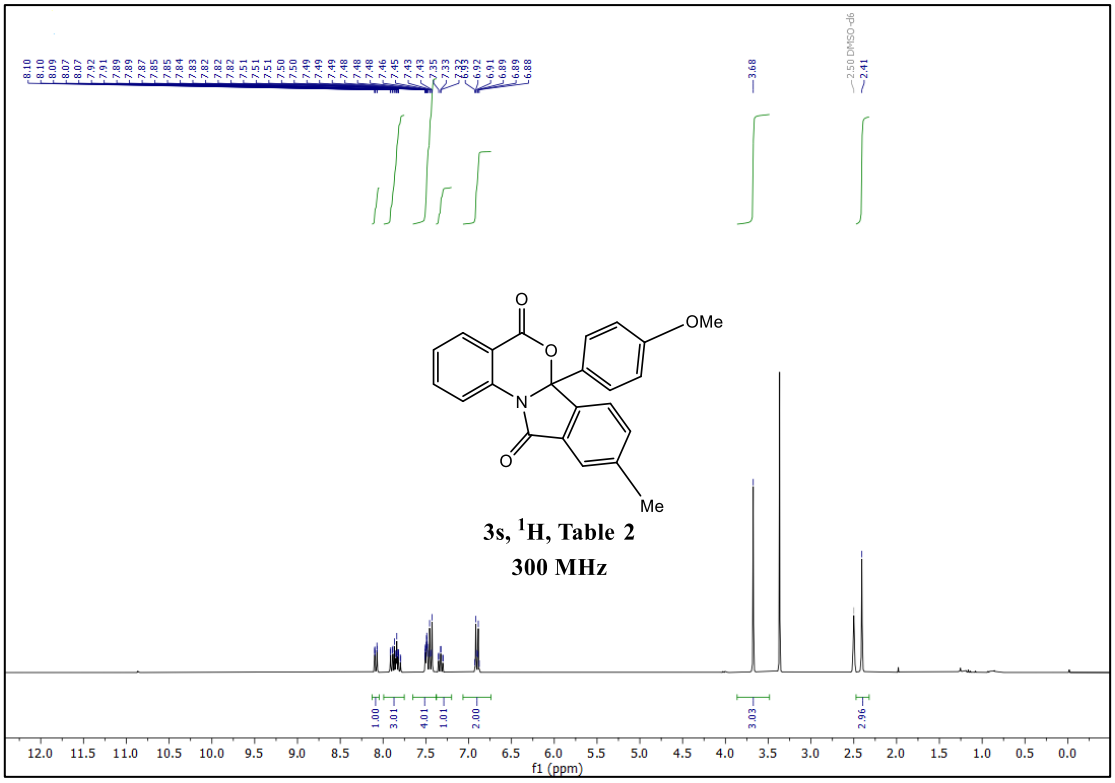

3s, ^{1}H, Table 2
300 MHz

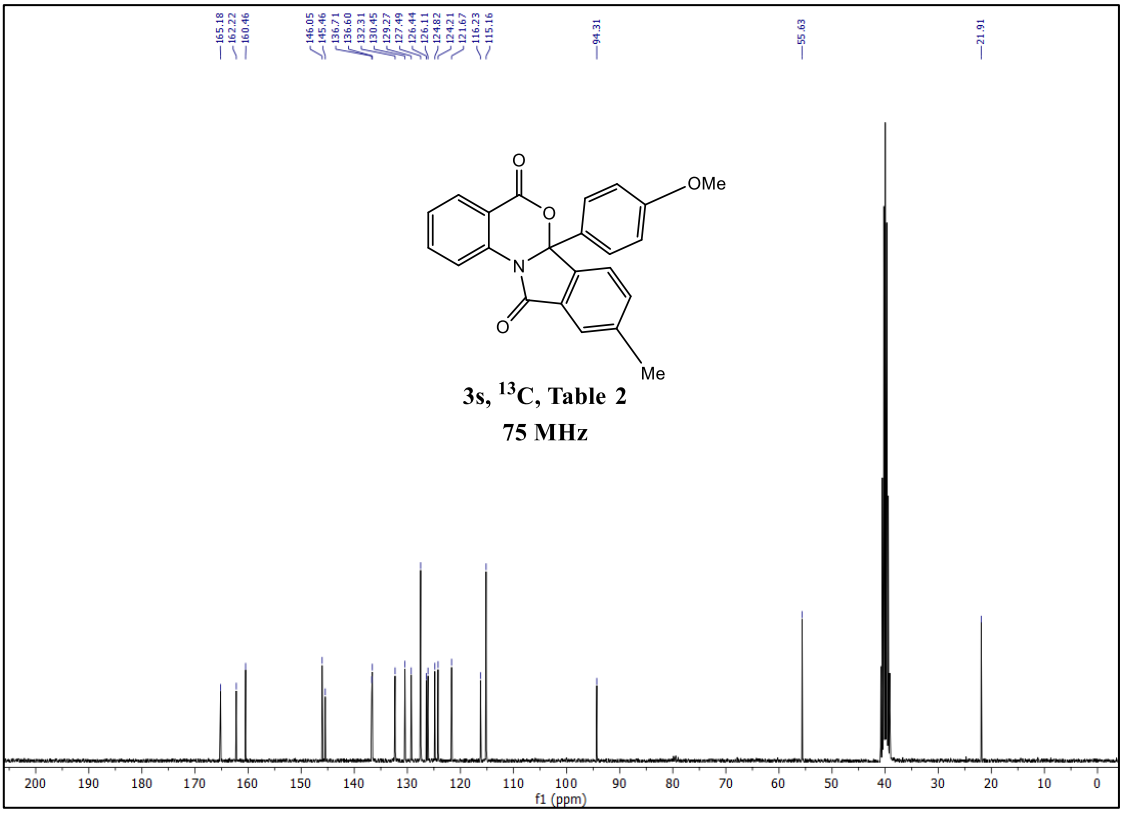

3s, ^{13}C, Table 2
75 MHz

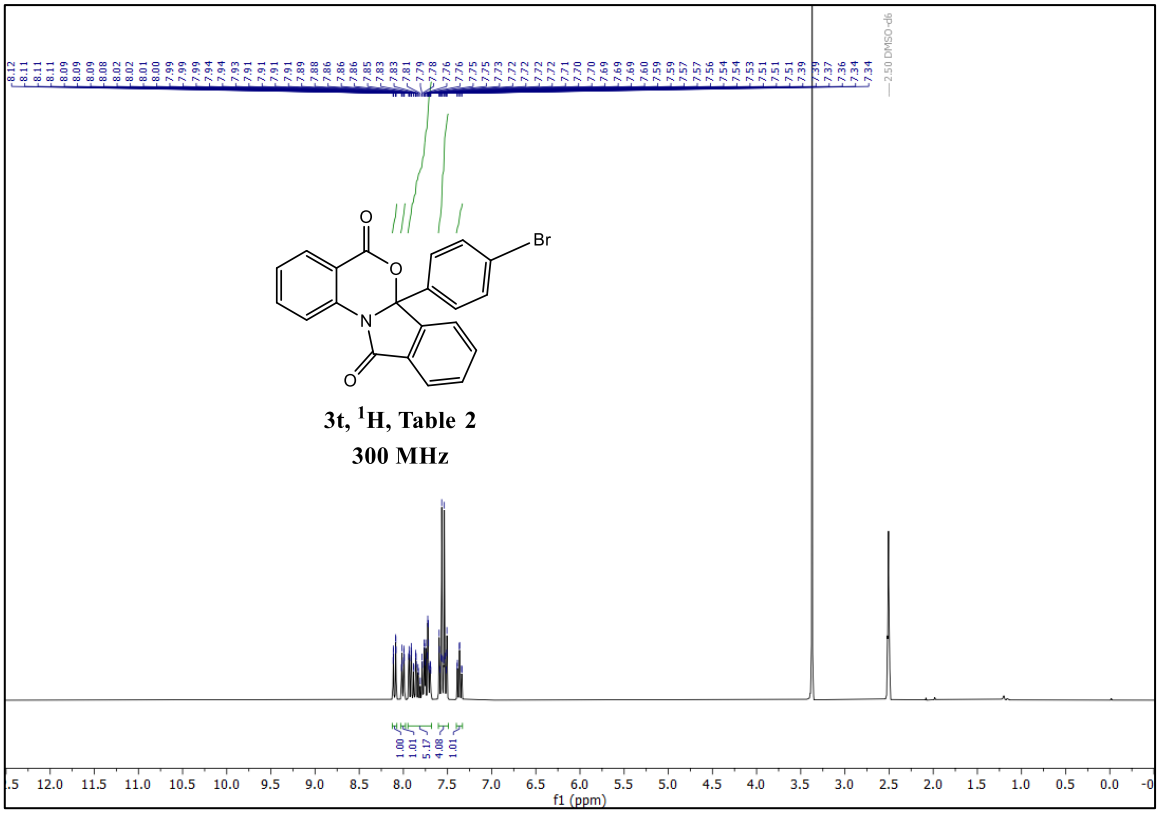

3t, ^{1}H, Table 2
300 MHz

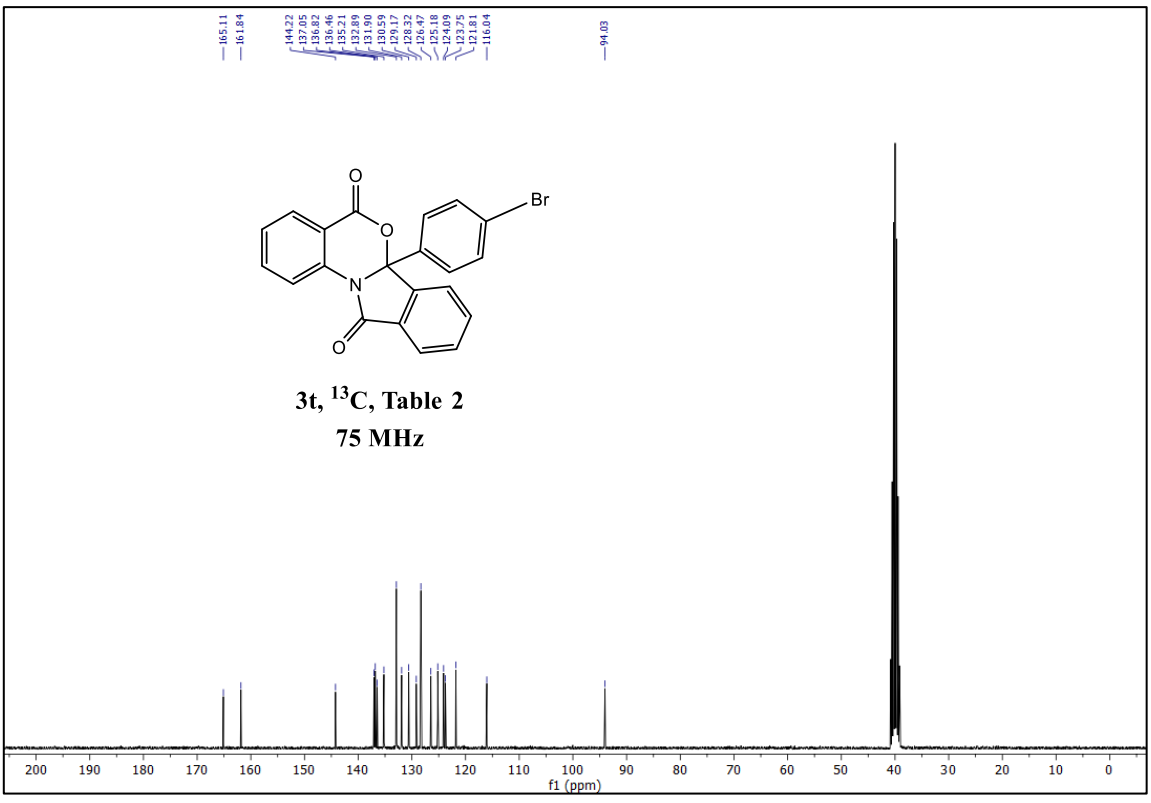

3t, ^{13}C, Table 2
75 MHz

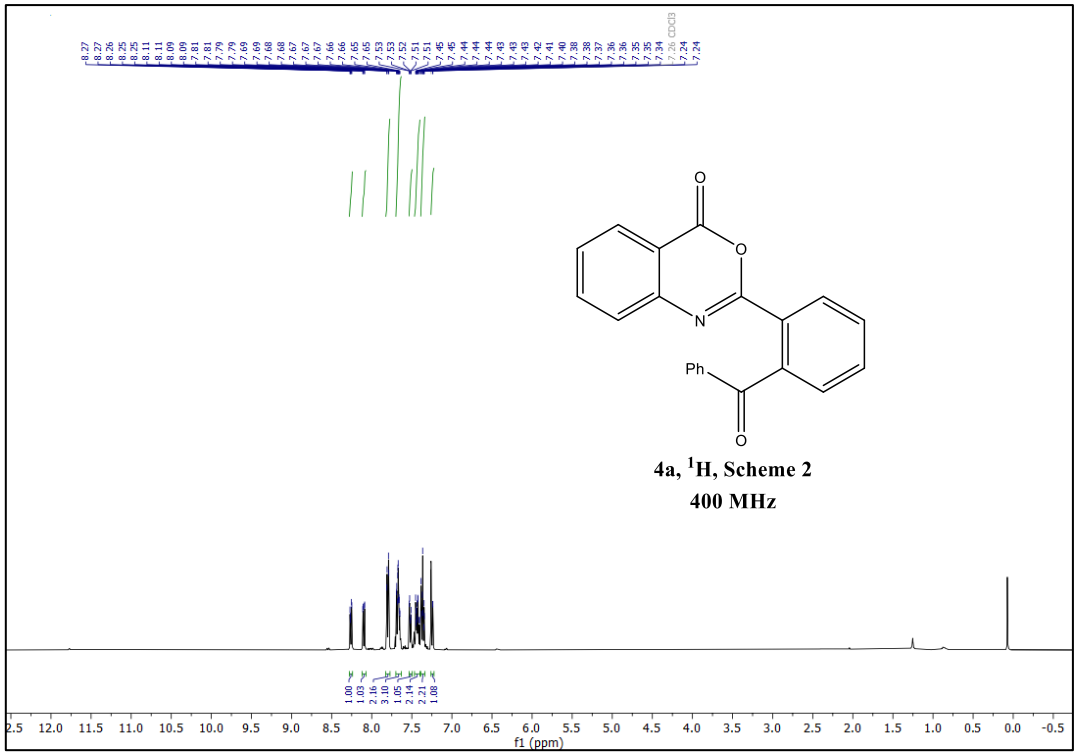

4a, ^{1}H, Scheme 2
400 MHz

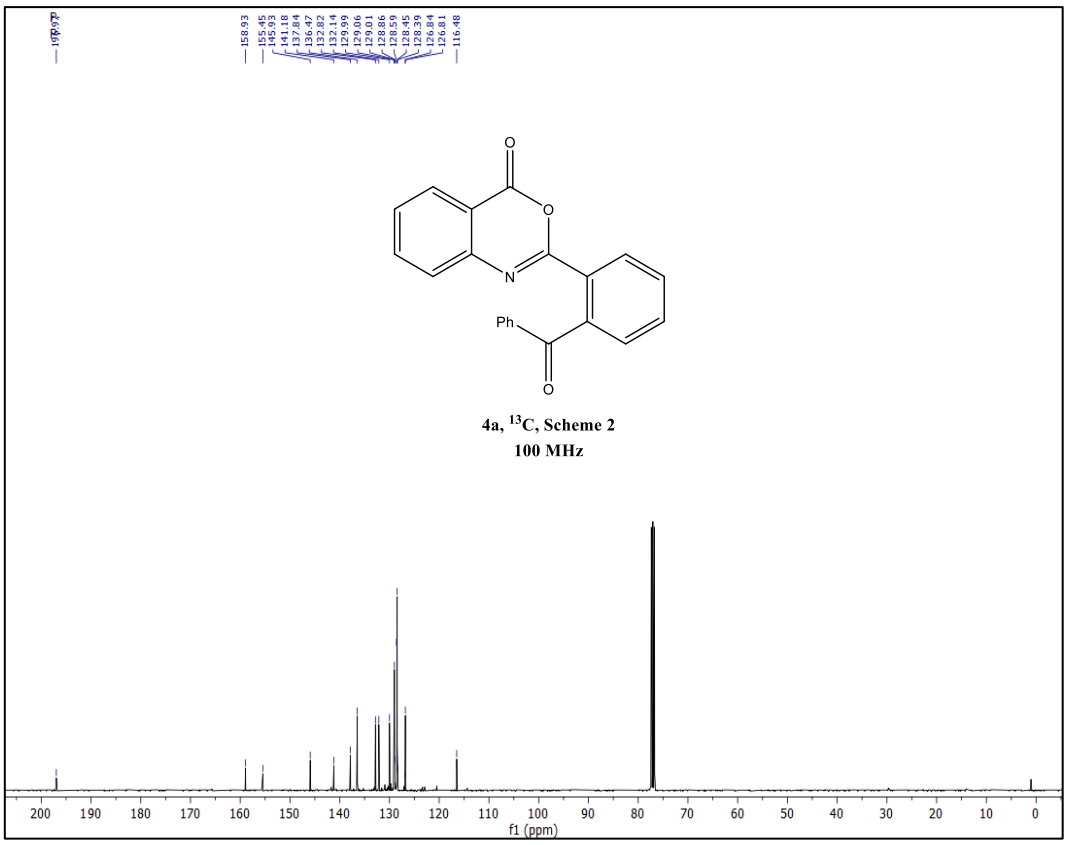

4a, ^{13}C, Scheme 2
100 MHz

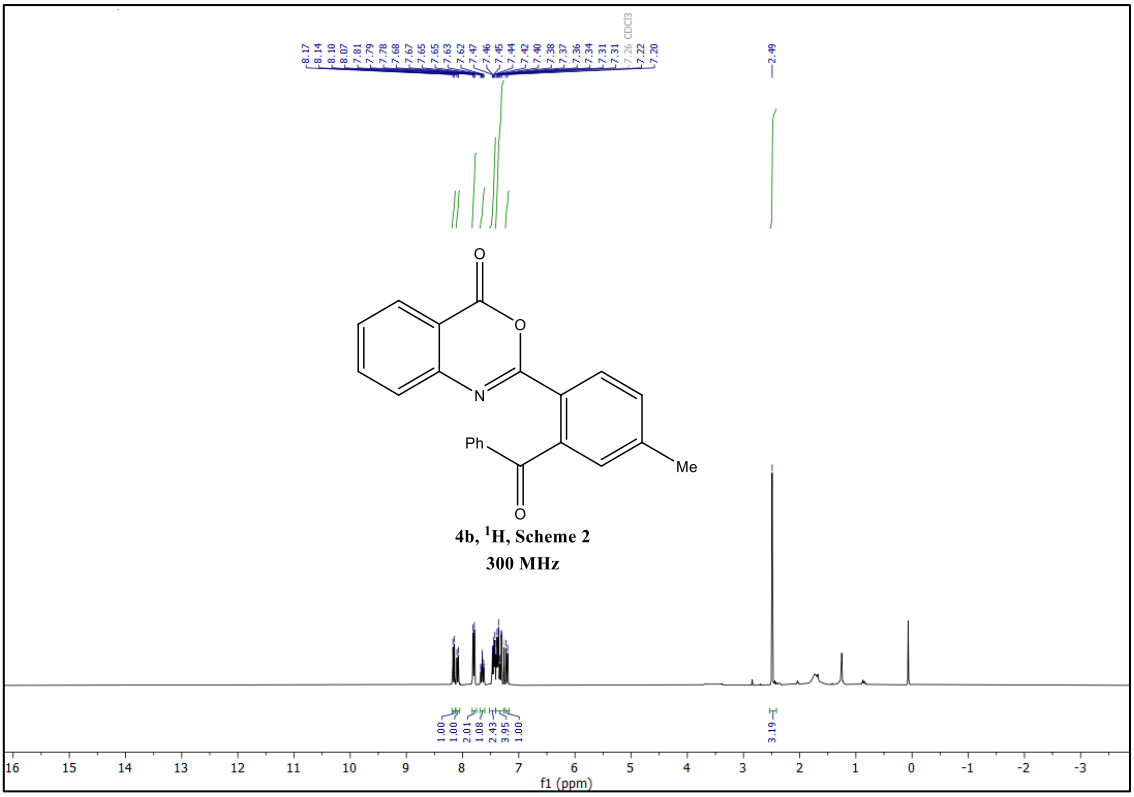
8.17
8.14
8.10
8.07
7.81
7.79
7.78
7.68
7.67
7.65
7.65
7.63
7.62
7.47
7.46
7.46
7.44
7.42
7.40
7.38
7.37
7.36
7.34
7.31
7.31
7.25 CDCl3
7.22
7.20
2.49
O
O
N
Ph
Me
O
4b, 1H, Scheme 2
300 MHz
1.00
1.00
2.01
1.08
2.43
3.95
1.00
3.19
16 15 14 13 12 11 10 9 8 7 6 5 4 3 2 1 0 -1 -2 -3
f1 (ppm)

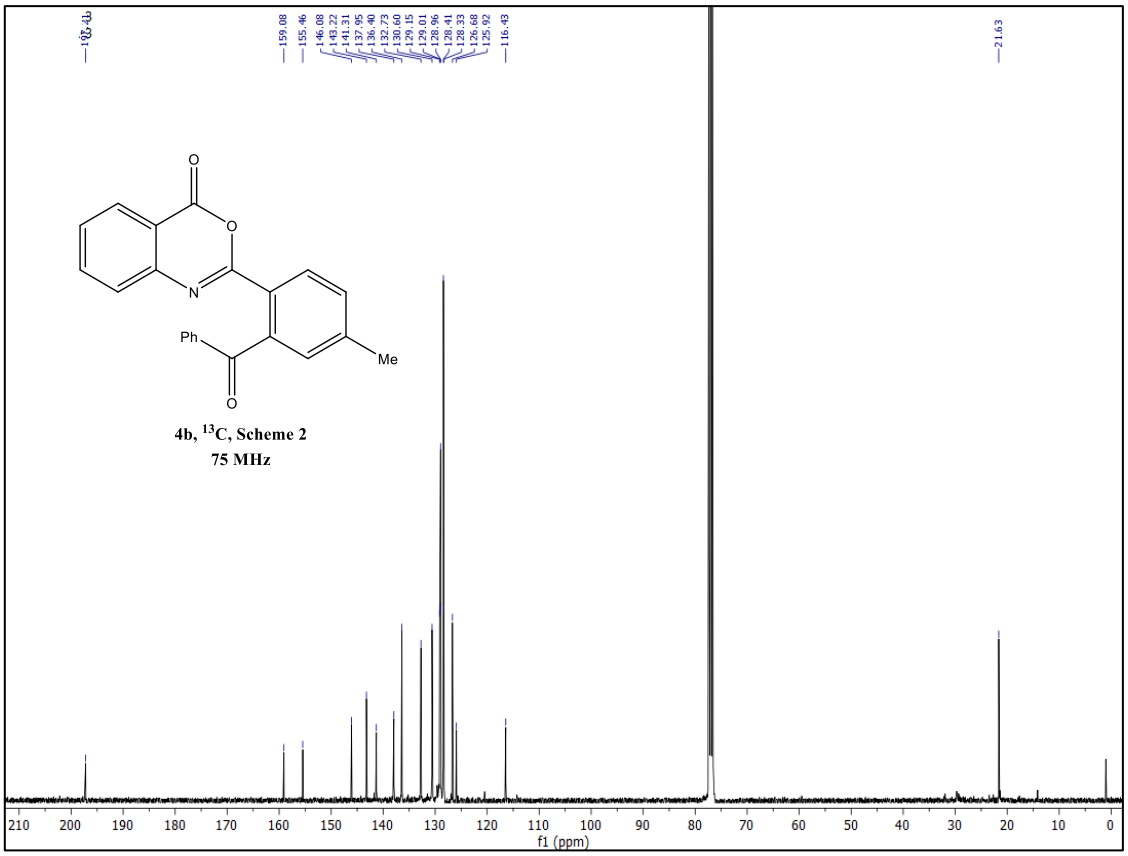
159.08
155.46
146.08
143.22
141.31
137.95
136.40
132.73
130.60
129.15
129.01
128.96
128.41
128.33
126.68
125.92
116.43
21.63
O
O
N
Ph
Me
O
4b, 13C, Scheme 2
75 MHz
210 200 190 180 170 160 150 140 130 120 110 100 90 80 70 60 50 40 30 20 10 0
f1 (ppm)

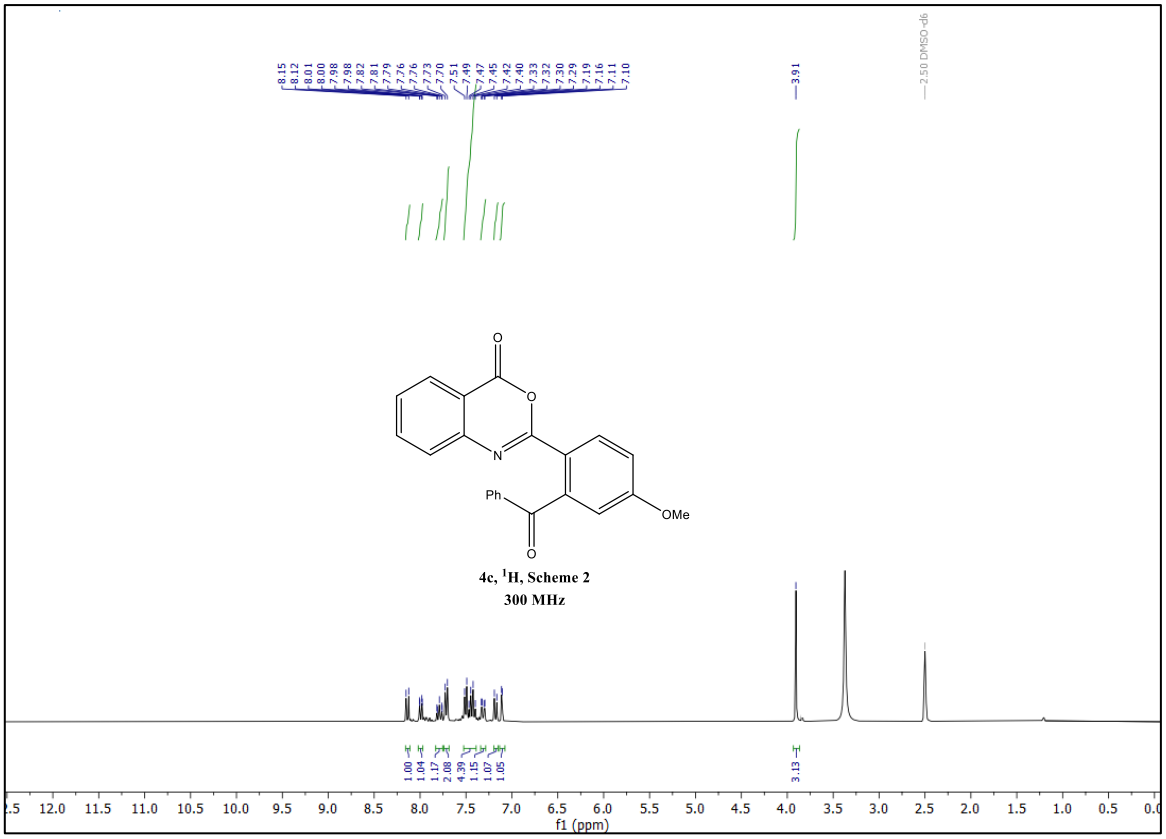

4c, ^{1}H, Scheme 2
300 MHz

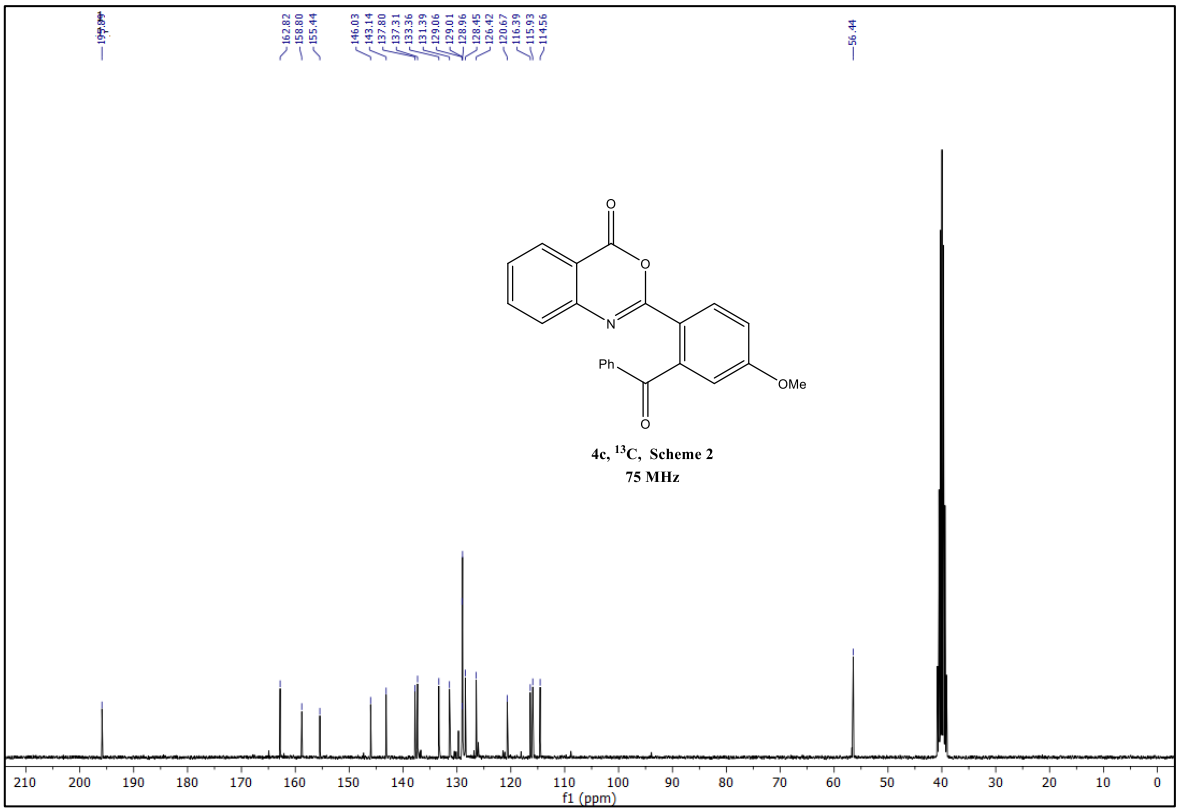

4c, ^{13}C, Scheme 2
75 MHz

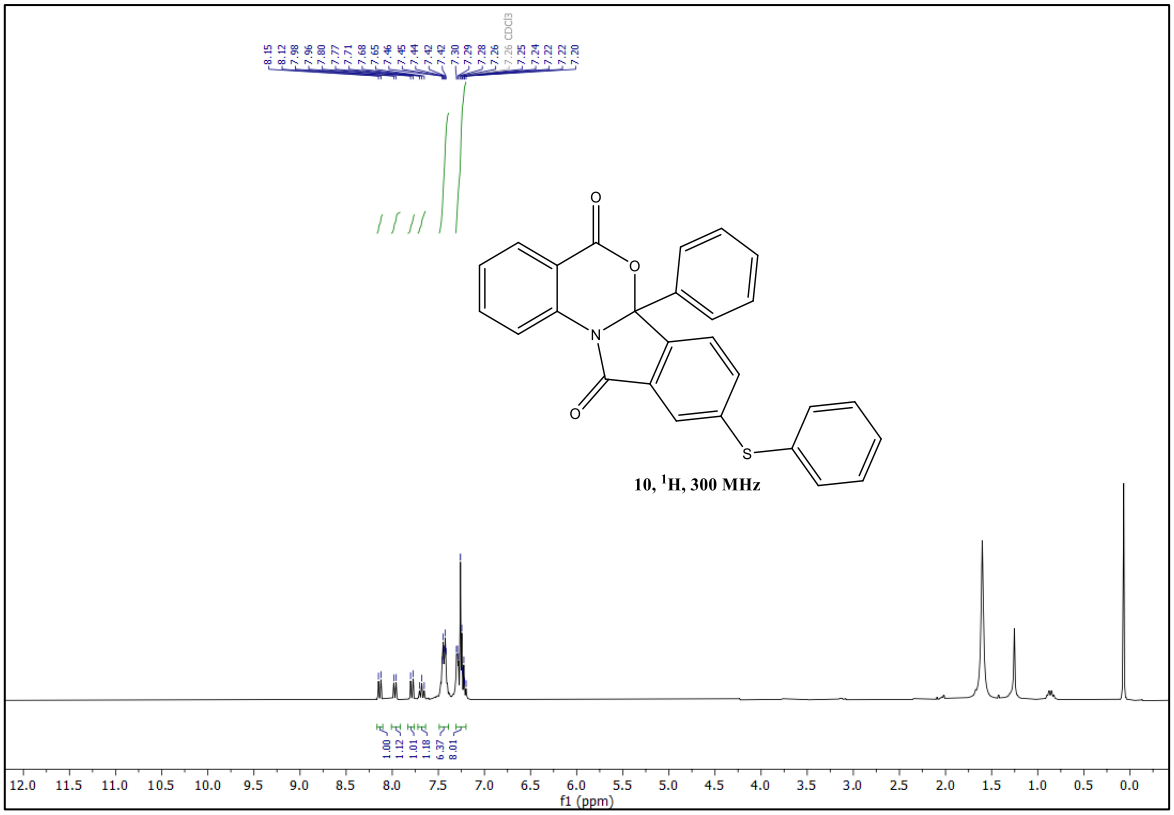

10, ^{1}H, 300 MHz

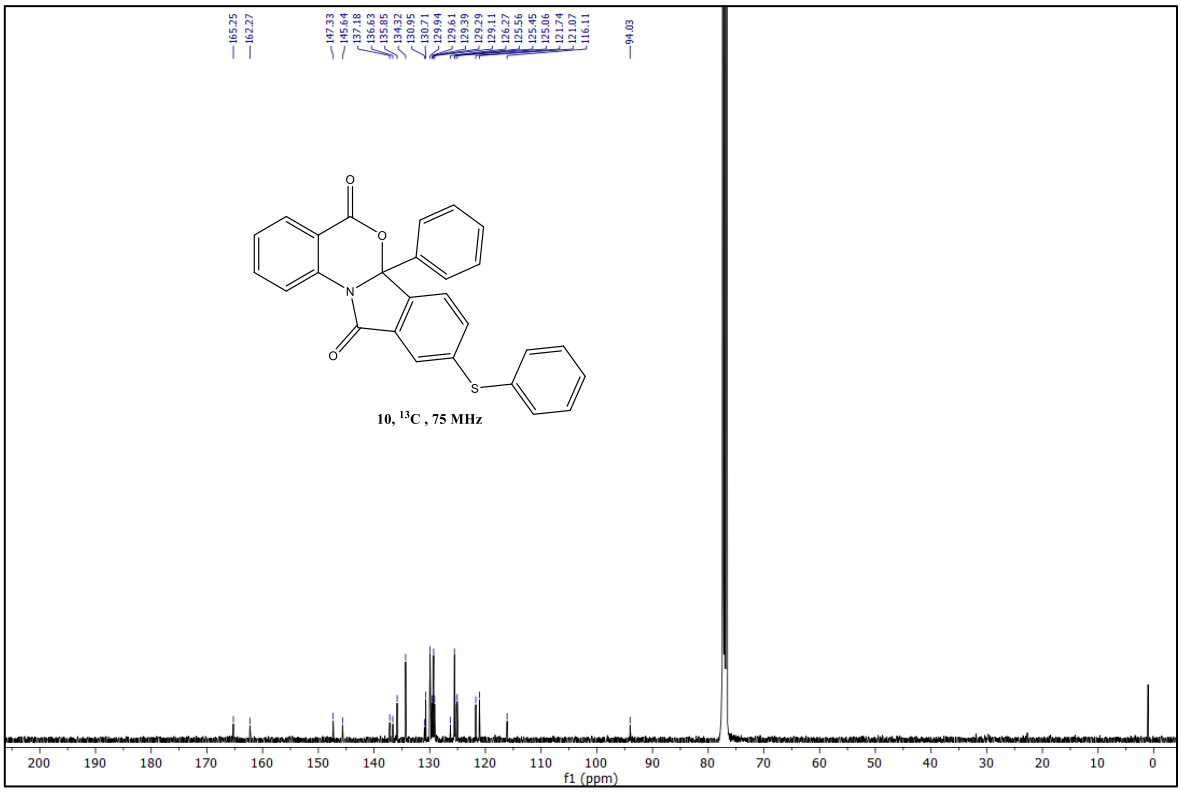

10, ^{13}C , 75 MHz

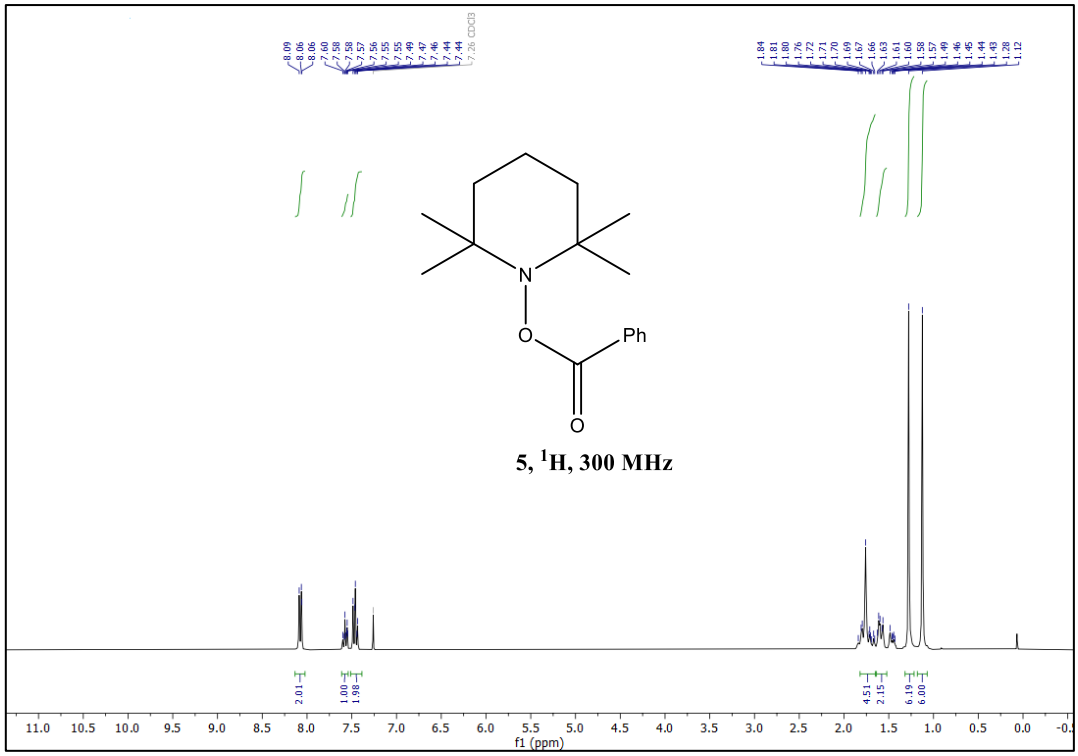

5, ^{1}H, 300 MHz

Mass spectra of products (3e, 3f, 3m, 3p, 3r, 10)

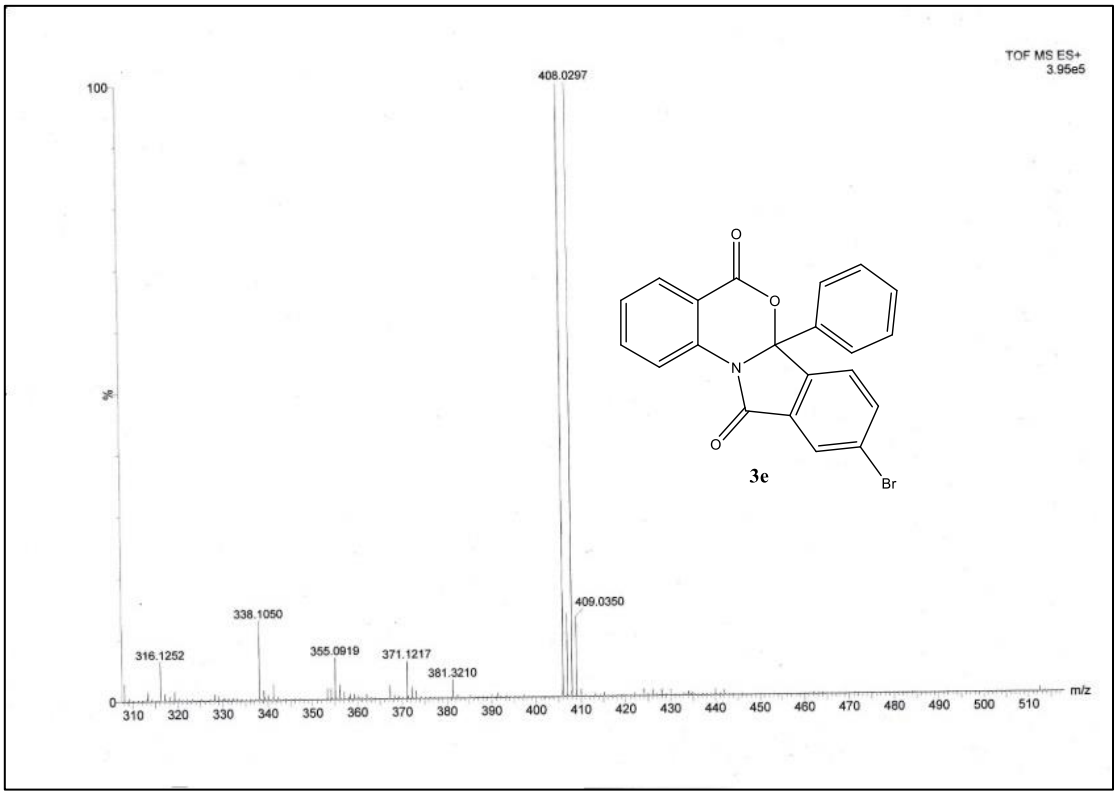

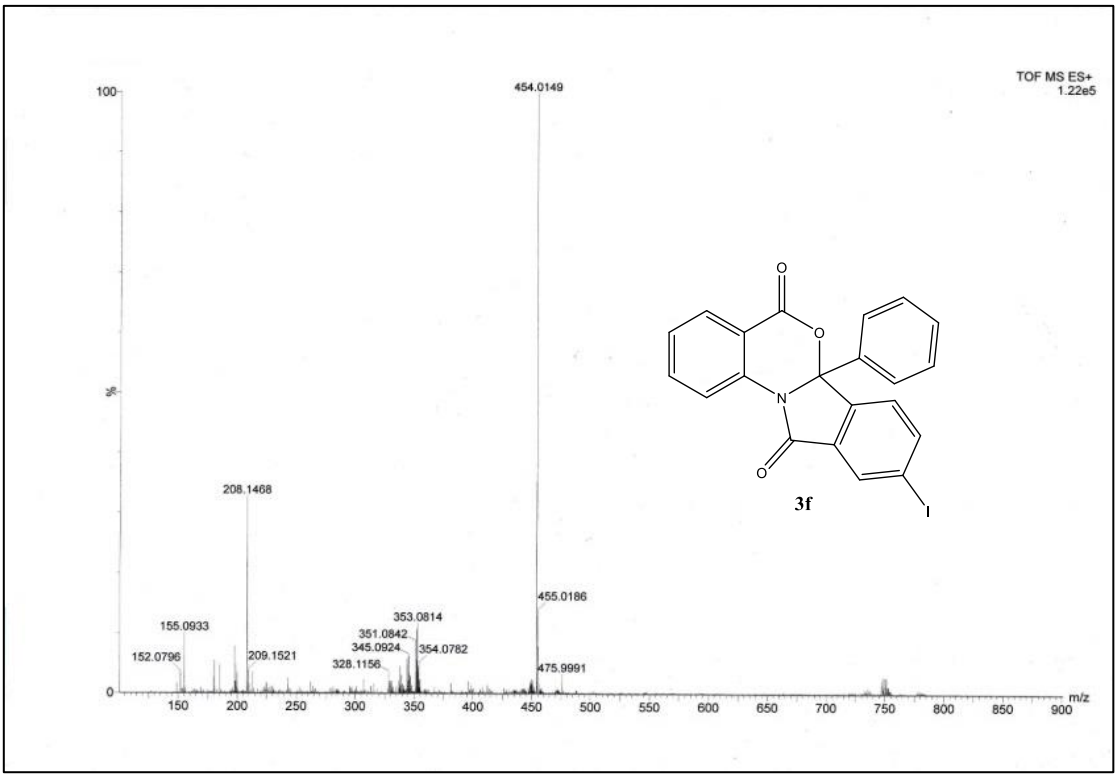

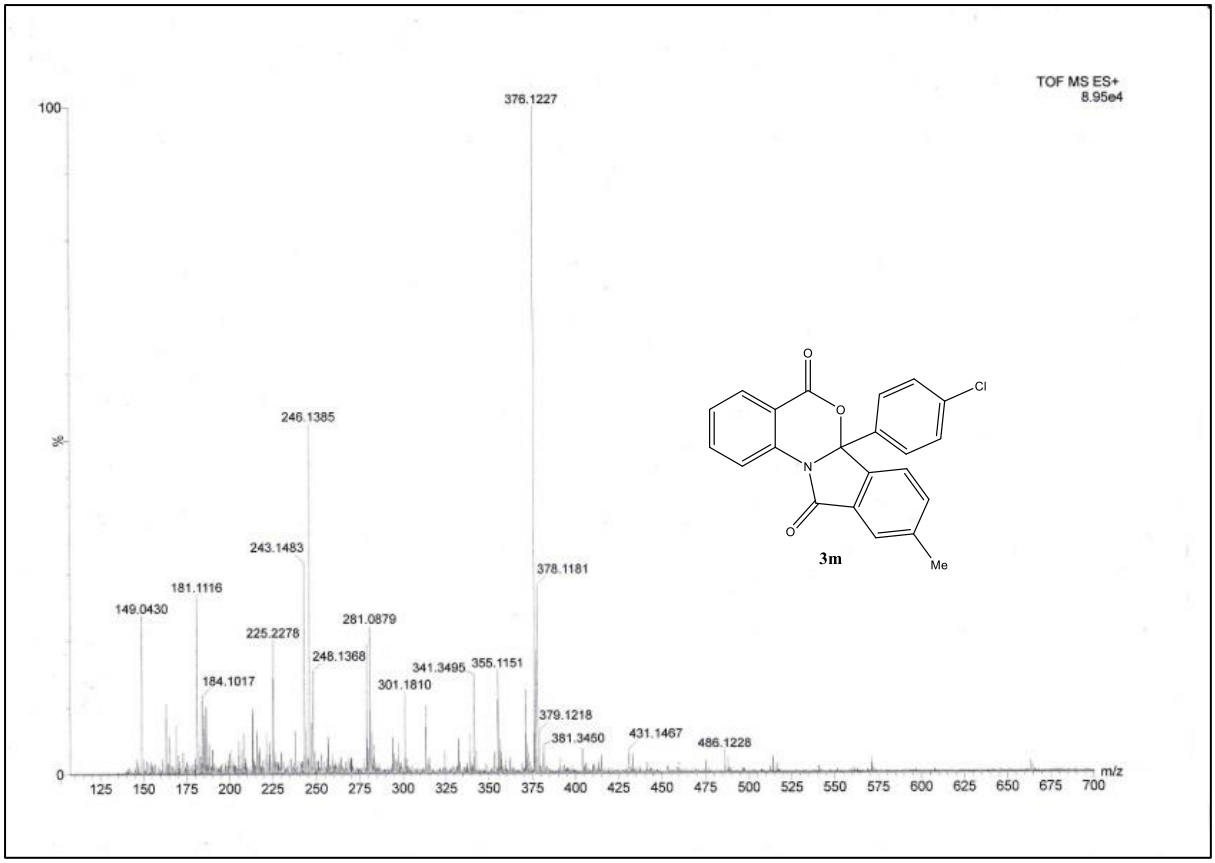
TOF MS ES+
8.95e4
376.1227
246.1385
243.1483
181.1116
149.0430
378.1181
281.0879
225.2278
248.1368
341.3495
355.1151
184.1017
301.1810
379.1218
381.3450
431.1467
486.1228
m/z
O
Cl
N
Me

3m

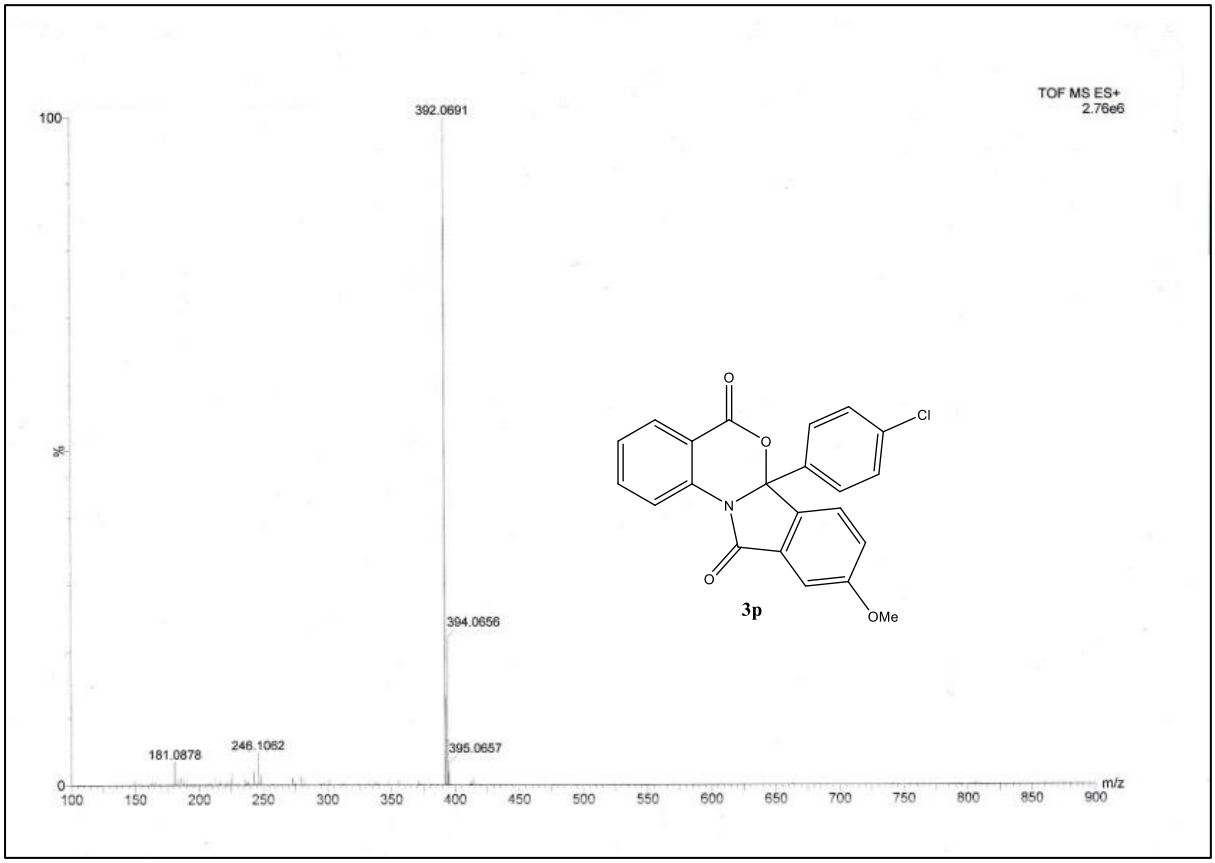
TOF MS ES+
2.76e6
392.0691
394.0656
395.0657
246.1062
181.0878
m/z
O
Cl
N
OMe

3p

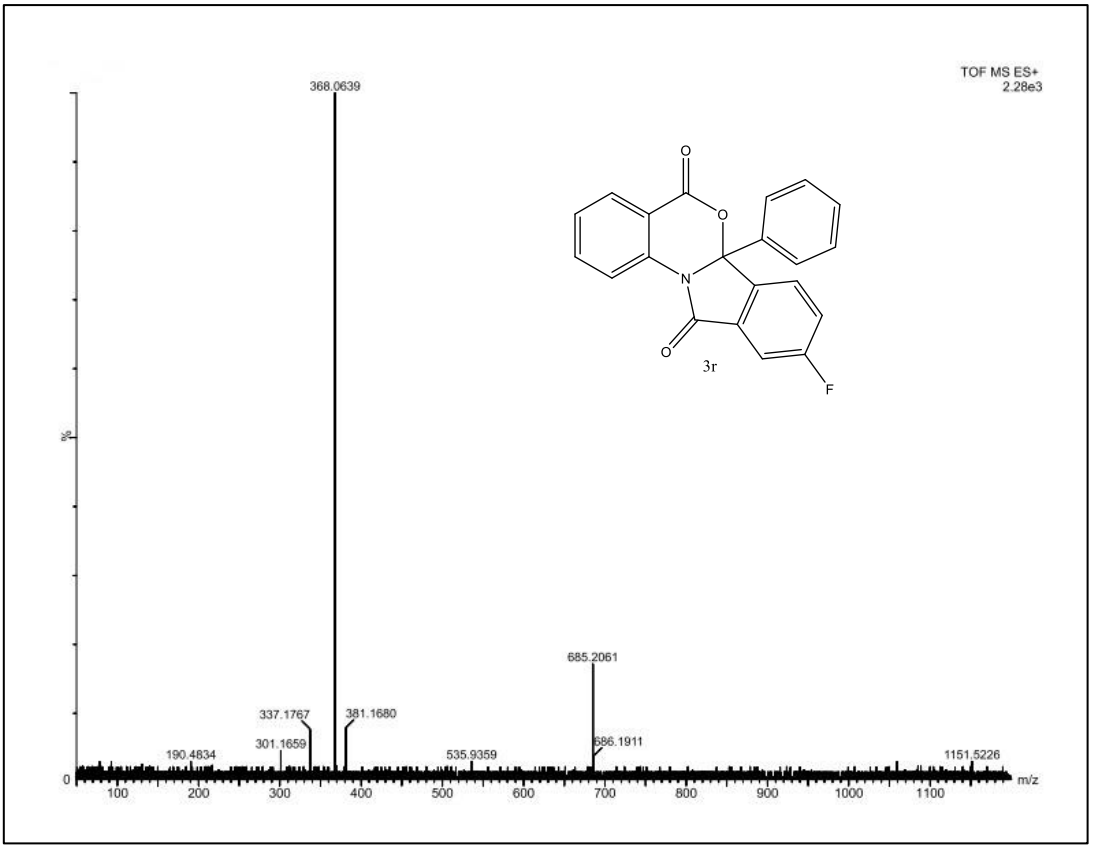
TOF MS ES+
2.28e3
368.0639
685.2061
337.1767
381.1680
301.1659
686.1911
190.4834
535.9359
1151.5226
%
0
100
200
300
400
500
600
700
800
900
1000
1100
m/z
O
O
N
O
F
3r

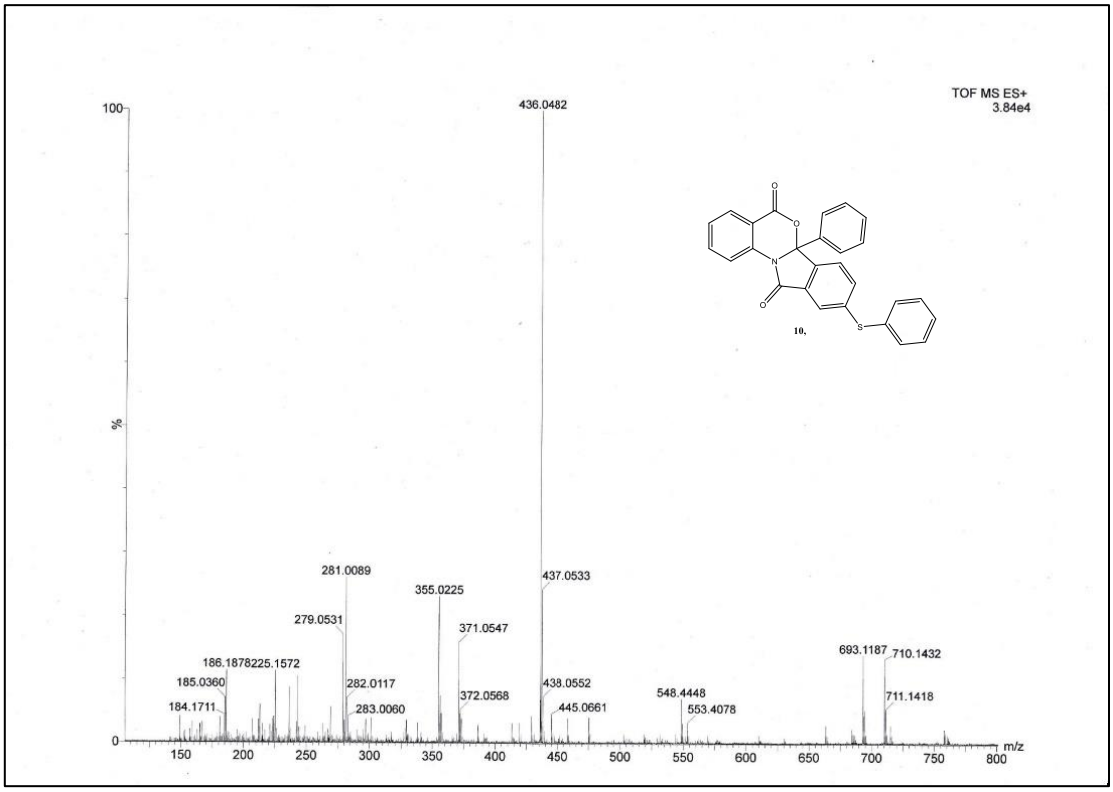
TOF MS ES+
3.84e4
100
436.0482
281.0089
355.0225
437.0533
279.0531
371.0547
693.1187
710.1432
186.1878225.1572
185.0360
282.0117
438.0552
548.4448
372.0568
711.1418
184.1711
283.0060
445.0661
553.4078
%
0
150
200
250
300
350
400
450
500
550
600
650
700
750
800
m/z
O
O
N
O
S
10.

X-ray Crystallography Data:

Figure 1, ORTEP diagram of the crystal structure of 3b at 50% probability level

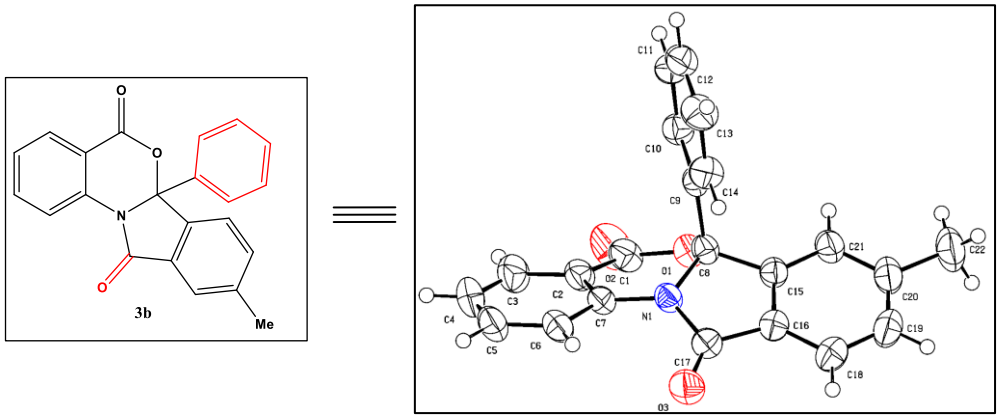

Details of the crystal structure investigation can be obtained from the Cambridge crystallographic data centre, 12 Union Road, Cambridge, CB2 1EZ, UK. (3b: CCDC deposition no 2191787)

Crystallographic data and structural refinement parameters for 3b

Bond precision: C-C = 0.0021 A Wavelength=0.71073

Cell: a=8.9803(7) b=9.0768(7) c=12.128(1)

Alpha =98.810(2) beta=108.023(2) gamma=110.028(2)

Temperature: 293 K

	Calculated	Reported
Volume	845.26(12)	845.26(12)
Space group	P -1	P -1
Hall group	-P 1	-P 1
Moiety formula	C22 H15 N O3	?
Sum formula	C22 H15 N O3	C44 H30 N2 O6
Mr	341.35	682.70
Dx,g cm-3	1.341	1.341
Z	2	1
Mu (mm-1)	0.090	0.090
F000	356.0	356.0
F000’	356.17	
h,k,lmax	11,11,15	11,11,15
Nref	3911	3865
Tmin,Tmax	0.984,0.991	0.810,0.884
Tmin’	0.984	

Correction method= # Reported T Limits: Tmin=0.810 Tmax=0.884
AbsCorr = MULTI-SCAN

Data completeness= 0.988 Theta (max) = 27.562

R (reflections) = 0.0436(3445) wR2 (reflections) = 0.1293(3865)

S = 1.018 Npar= 235

2/f References

1. (a) Z. Huang, H. N. Lim, F. Mo, M. C. Young and G. Dong, *Chem. Soc. Rev.,* **2015**, *44*, 7764– 7786; (b) J. Yang, *Org. Biomol. Chem.,* **2015**, *13*, 1930–1941; (c) B. Ye and N. Cramer, *Acc. Chem. Res.,* **2015**, *48*, 1308– 1318; (d) K. Shin, H. Kim and S. Chang, *Acc. Chem. Res.,* **2015**, *48*, 1040–1052; (e) O. Daugulis, J. Roane and L. D. Tran, *Acc. Chem. Res.,* **2015**, *48*, 1053–1064; (f) B. Liu, F. Hu and B.-F. Shi, *ACS Catal.,* **2015**, *5*, 1863–1881; (g) Y. Segawa, T. Maekawa and K. Itami, *Angew. Chem., Int. Ed.,* **2015**, *54*, 66–81; (h) M. Zhang, Y. Zhang, X. Jie, H. Zhao, G. Li and W. Su, *Org. Chem. Front.,* **2014**, *1*, 843– 895; (i) L. Ackermann, *J. Org. Chem.,* **2014**, *79*, 8948–8954; (j) T. Mesganaw and J. A. Ellman, *Org. Process Res. Dev.*, **2014**, *18*, 1097–1104; (k) S. Tani, T. N. Uehara, J. Yamaguchi and K. Itami, *Chem. Sci.,* **2014**, *5,* 123–135; (l) S. A. Girard, T. Knauber and C.-J. Li, *Angew. Chem., Int. Ed.,* **2014**, *53,* 74–100; (m) G. Rouquet and N. Chatani, *Angew. Chem., Int. Ed.,* **2013**, *52,* 11726–11743; (n) J. Wencel-Delord and F. Glorius, *Nat. Chem.,* **2013**, *5,* 369–375; (o) J. Schipper and K. Fagnou, *Chem. Mater.,* **2011**, *23,* 1594–1600; (p) C. S. Yeung and V. M. Dong, *Chem. Rev.,* **2011**, *111*, 1215–1292; (q) T. Satoh and M. Miura, *Chem. – Eur. J.,* **2010**, *16,* 11212–11222; (r) O. Daugulis, *Top. Curr. Chem.,* **2010**, *292,* 57–84; (s) P. Sehnal, R. J. K. Taylor and I. J. S. Fairlamb, *Chem. Rev.,* **2010**, *110,* 824–889; (t) R. Giri, B.-F. Shi, K. M. Engle, N. Maugel and J.-Q. Yu, *Chem. Soc. Rev.,* **2009**, *38*, 3242–3272; (u) L. Ackermann, R. Vicente and A. Kapdi, *Angew. Chem., Int. Ed.,* **2009**, *48*, 9792–9826; (v) X. Chen, K. M. Engle, D.-H. Wang and J.-Q. Yu, *Angew. Chem., Int. Ed.,* **2009**, *48*, 5094–5115; (w) D. Alberico, M. E. Scott and M. Lautens, *Chem. Rev.,* **2007**, *107*, 174– 238.
2. (a) Y. Kuninobu and S. Sueki, *Synthesis,* **2015**, 3823–3845; (b) F. J. Lombard and M. J. Coster, *Org. Biomol. Chem.,* **2015**, *13,* 6419–6431; (c) L. Ackermann, Org. Process *Res. Dev.,* **2015**, *18,* 260–269; (d) J. Hong, *Chem. – Eur. J.,* **2014**, *20*, 10204–10212; (e) J. Yamaguchi, A. D. Yamaguchi and K. Itami, *Angew. Chem., Int. Ed.,* **2012**, *51*, 8960–9009; (f) Y.-K. Chen and S. W. Youn, *Chem. – Eur. J.,* **2012**, *18,* 9452–9474; (g) L. McMurray, F. O'Hara and M. J. Gaunt, *Chem. Soc. Rev.,* **2011**, *40,* 1885–1898; (h) W. R. Gutekunst and P. S. Baran, *Chem. Soc. Rev.,* **2011**, *40*, 1976–1991.
3. (a) J. Li, S. D. Sarkar and L. Ackermann, Top. *Organomet. Chem.,* **2016,** *55,* 217–257. (b) J. Schranck, A. Tlili and M. Beller, *Angew. Chem., Int. Ed.,* **2014**, *53*, 9426–9428; (c) F. Juliá-Hernández, M. Simonetti and I. Larrosa, *Angew. Chem., Int. Ed.,* **2013**, *52*, 11458–11460. (d) Y. Kuninobu, H. Ida, M. Nishi and M. Kanai, *Nat. Chem.,* **2015**, *7*, 712–717; (e) A. J. Paterson, S. St John-Campbell, M. F. Mahon, N. J. Press and C. G. Frost, *Chem. Commun.,* **2015**, *51*, 12807–12810; (f) J. Li, S. Warratz, D. Zell, S. D. Sarkar, E. E. Ishikawa and L. Ackermann, *J. Am. Chem. Soc.,* **2015**, *137*, 13894–13901; (g) R. Y. Tang, G. Li and J.-Q. Yu, *Nature,* **2014**, *507*, 215–220; (h) S. Lee, H. Lee and K. L. Tan, *J. Am. Chem. Soc.,* **2013**, *135*, 18778– 18781; (i) N. Hofmann and L. Ackermann, *J. Am. Chem. Soc.,* **2013**, *135*, 5877–5884; (j) D. Leow, G. Li, T. S. Mei and J.-Q. Yu, *Nature,* **2012**, *486,* 518–522; (k) O. Saidi, J. Marafie, A. E. Ledger, P. M. Liu, M. F. Mahon, G. Kociok-Kohn, M. K. Whittlesey and C. G. Frost, *J. Am.*

Chem. Soc., **2011***, 133*, 19298–19301; (l) L. Ackermann, N. Hofmann and R. Vicente, *Org. Lett.,* **2011**, *13*, 1875–1877.

4. S. Hübner, J. G. de Vries and V. Farina, *Adv. Synth. Catal.,* **2016**, *358*, 3–25.
5. (a)J. Lee, J. Chung, S. M. Byun, B. M. Kim and C. Lee, *Tetrahedron,* **2013**, *69,* 5660–5664: (b) A. J. Reay and I. J. S. Fairlamb, *Chem. Commun.,* **2015**, *51*, 16289–16307; (c) R. Cano, A. F. Schmidt and G. P. McGlacken*, Chem. Sci.,* **2015**, *6,* 5338–5346; (d) L. Djakovitch and F.-X. Felpin, *ChemCatChem*, **2014**, *6,* 2175–2187. (e)Tajima and K. Sakai, *Heterocycles,* **1982**, *17,* 235–245. (f) M. Parisien, D. Valette and K. Fagnou, *J. Org. Chem.,* **2005**, *70,* 7578–7584.
6. N. Nakamura, Y. Tajima and K. Sakai, *Heterocycles,* **1982**, *17,* 235–245.
7. M. Parisien, D. Valette and K. Fagnou, *J. Org. Chem.,* **2005**, *70,* 7578–7584.
8. (a) L. Djakovitch, V. Dufaud and R. Zaidi, *Adv. Synth. Catal.,* **2006**, *348*, 715–724.: (b) L. Joucla and L. Djakovitch, *Adv. Synth. Catal.,* **2009**, *351*, 673–714.
9. G. Cusati and L. Djakovitch, *Tetrahedron Lett.,* **2008**, *49,* 2499–2502.
10. (a) S. Sahnoun, S. Messaoudi, J.-F. Peyrat, J.-D. Brion and M. Alami, *Tetrahedron Lett.,* **2008**, *49,* 7279–7283; (b) S. Sahnoun, S. Messaoudi, J.-D. Brion and M. Alami, *Org. Biomol. Chem.,* **2009**, *7,* 4271–4278. 11. S. Hernández, I. Moreno, R. SanMartin, G. Gómez, M. T. Herrero and E. Domínguez, *J. Org. Chem.,* **2010**, *75*, 434–441.
12. (a)S. Hübner, J. G. de Vries and V. Farina, *Adv. Synth. Catal.,* **2016**, *358,* 3–25. (b)F. Jafarpour, S. Rahiminejadan and H. Hazrati, *J. Org. Chem.,* **2010**, *75,* 3109–3112.
13 D. Saha, L. Adak and B. C. Ranu, *Tetrahedron Lett.,* **2010**, *51,* 5624–5627.
14. (a) L. Wang, W.-B. Yi and C. Cai, *Chem. Commun.,* **2011**, *47*, 806–808.: (b) A. J. Reay, L. K. Neumann and I. J. S. Fairlamb, *Synlett,* **2016**, 27, 1211–1216.
15. (a) A. J. Reay and I. J. S. Fairlamb, *Chem. Commun.,* **2015**, *51*, 16289–16307; (b) R. Cano, A. F. Schmidt and G. P. McGlacken, *Chem. Sci.,* **2015**, *6,* 5338–5346; (c) L. Djakovitch and F.-X. Felpin, *ChemCatChem,* **2014**, *6,* 2175–2187. (d) G. Bianchini, M. Crucianelli, C. Crestini and R. Saladino, *Top. Catal.,* **2006**, *40,* 221–227; (e) G. Bianchini, M. Crucianelli, F. De Angelis, V. Neri and R. Saladino, *Tetrahedron Lett.*, **2005**, *46,* 2427–2432; (f) H. Sajiki, F. Aoki, H. Esaki, T. Maegawa and K. Hirota, *Org. Lett.,* **2004**, *6,* 1485–1487; (g) R. Burch, D. J. Crittle and M. J. Hayes, *Catal. Today,* **1999**, *47*, 229– 234; (h) T. H. Ballinger and J. T. Yates, Jr., *J. Phys. Chem.,* **1992**, *24,* 9979–9983; (i) W. F. Maier, *Angew. Chem., Int. Ed. Engl.,* **1989**, *28,* 135–145.
16. M. Parisien, D. Valette and K. Fagnou, *J. Org. Chem.,* **2005,** *70,* 7578–7584.
17. (a) L. Djakovitch, V. Dufaud and R. Zaidi, *Adv. Synth. Catal.,* **2006,** *348,* 715–724. (b) L. Joucla and L. Djakovitch*, Adv. Synth. Catal.,* **2009,** *351*, 673–714.
18. S. Hernández, I. Moreno, R. SanMartin, G. Gómez, M. T. Herrero and E. Domínguez, *J. Org. Chem.,* **2010,** *75,* 434–441.
19. F. Jafarpour, S. Rahiminejadan and H. Hazrati, *J. Org. Chem.,* **2010,** *75,* 3109–3112.
20. (a) L. Wang, W.-B. Yi and C. Cai, *Chem. Commun.,* **2011,** *47,* 806–808. (b) A. J. Reay, L. K. Neumann and I. J. S. Fairlamb, *Synlett,* **2016,** *27*, 1211–1216.
21. (a) M. Cao, D. Wu, W. Su and R. Cao, *J. Catal.,* **2015,** *321,* 62–69 (b) M. Lafrance, C. N. Rowley, T. K. Woo and K. Fagnou, *J. Am. Chem. Soc.,* **2006,** *128,* 8754–8756; (c) L. Ackermann and S. Fenner, *Chem. Commun.,* **2011**, *47*, 430–432.

22. V. A. Zinovyeva, M. A. Vorotyntsev, I. Bezverkhyy, D. Chaumont and J.-C. Hierso, *Adv. Funct. Mater.,* **2011,** *21,* 1064–1075.
23. J. Lee, J. Chung, S. M. Byun, B. M. Kim and C. Lee, *Tetrahedron,* **2013,** *69,* 5660–5664.
24. (a) D.-T. D. Tang, K. D. Collins and F. Glorius, *J. Am. Chem. Soc.,* **2013,** *135*, 7450–7453 (b) K. Ueda, S. Yanagisawa, J. Yamaguchi and K. Itami, *Angew. Chem., Int. Ed.,* **2010,** *49,* 8946–8949.
25. (a) D.-T. D. Tang, K. D. Collins, J. B. Ernst and F. Glorius, *Angew. Chem., Int. Ed.,* **2014,** *53,* 1809–1813. (b) E. A. Merritt and B. Olofsson, *Angew. Chem., Int. Ed.,* **2009,** *121,* 9052–9070. (d) R. Narayan, S. Manna and A. P. Antonchick, *Synlett,* **2015,** 1785–1803; (e) T. W. Lyons and M. S. Sanford, *Chem. Rev.,* **2010,** *110,* 1147–1169; (f) N. R. Deprez, D. Kalyani, A. Krause and M. S. Sanford, *J. Am. Chem. Soc.,* **2006,** *128,* 4972–4973; (g) Y. Zhu, M. Bauer, J. Ploog and L. Ackermann, *Chem. – Eur. J.,* **2014,** *20,* 13099–13102.
26. L. Zhang, P. Li, C. Liu, J. Yang, M. Wang and L. Wang, *Catal. Sci. Technol.,* **2014,** *4,* 1979–1988.
27. J. Malmgren, A. Nagendiran, C.-W. Tai, J.-E. Bäckvall and B. Olofsson, *Chem. – Eur. J.,* **2014,** *20*, 13531–13535.
28. T. Parsharamulu, D. Venkanna, M. L. Kantam, S. K. Bhargava and P. Srinivasu, *Ind. Eng. Chem. Res.,* **2014,** *53,* 20075–20084.
29. (a) S. Keshipour and A. Shaabani, *Appl. Organomet. Chem.,* **2014,** *28,* 116–119.: (b) L. Ackermann, H. K. Potukuchi, D. Landsberg and R. Vicente, *Org. Lett.,* **2008,** *10*, 3081–3084; (c) R. Jeyachandran, H. K. Potukuchi and L. Ackermann, Beilstein *J. Org. Chem.,* **2012**, *8,* 1771– 1777.
30. (a) E. Y. Lee and J. Park, *ChemCatChem*, 2011, *3*, 1127– 1129. (b) R. J. Phipps and M. J. Gaunt, *Science,* **2009,** *323,* 1593– 1597.
31. W. Zhang, Q. Zeng, X. Zhang, Y. Tian, Y. Yue, Y. Guo and Z. Wang, *J. Org. Chem.,* **2011,** *76,* 4741–4745.
32. (a) H. T. N. Le, T. T. Nguyen, P. H. L. Vu, T. Truong and N. T. S. Phan, *J. Mol. Catal. A: Chem.,* **2014,** *391*, 74–82; (b) T. Truong, V. T. Nguyen, H. T. X. Le and N. T. S. Phan, *RSC Adv.,* **2014,** *4,* 52307–523154. (c) A. Kulkarni and O. Daugulis, *Synthesis,* **2009**, 4087– 4109; (d) H.-Q. Do and O. Daugulis, *J. Am. Chem. Soc.,* **2007,** *129,* 12404–12405.
33. (a) H. Miura, K. Wada, S. Hosokawa and M. Inoue, *Chem. – Eur. J*., **2010,** *16,* 4186–4189; (b) H. Miura, K. Wada, S. Hosokawa and M. Inoue, *Patent application* JP 002010184881 A, 2010. (c) L. Ackermann and R. Vicente, *Top. Curr. Chem.,* **2010,** *292,* 211–229; (d) S. Oi, H. Sato, S. Sugawara and Y. Inoue, *Org. Lett.,* **2008**, *10*, 1823–1826; (e) L. Ackermann, A. Althammer and R. Born, *Angew. Chem., Int. Ed.,* **2006**, *45,* 2619–2622; (f) L. Ackermann, R. Vicente and A. Althammer, *Org. Lett.,* **2008,** *10,* 2299– 2302.
34. H. Liu, B. Yin, Z. Gao, Y. Li and H. Jiang, *Chem. Commun.,* **2012,** *48,* 2033–2035.
35. (a) H. Miura, K. Wada, S. Hosokawa and M. Inoue, *ChemCatChem,* **2010,** *2,* 1223–1225. (b) S. Murai, F. Kakiuchi, S. Sekine, Y. Tanaka, A. Kamatani, M. Sonoda and N. Chatani, *Nature,* **1993,** *366,* 529–531; (c) L. N. Lewis and J. F. Smith, *J. Am. Chem.*

Soc., **1986,** *108,* 2728–2735; (d) F. Kakiuchi and S. Murai, *Acc. Chem. Res.,* **2002,** *35,* 826–834; (e) M. Schinkel, I. Marek and L. Ackermann, *Angew. Chem., Int. Ed.,* **2013,** *52,* 3977–3980.

36. (a) I. Moritani and I. Y. Fujiwara, *Tetrahedron Lett.,* **1967**, *8*, 1119–1122; (b) T. Kitamura and Y. Fujiwara, *RSC Publishing, Cambridge,* **2014.** 33–54; (c) S. I. Kozhushkov and L. Ackermann, *Chem. Sci.,* **2013,** *4,* 886–896.: (d) L. Zhou and W. Lu, Chem. – Eur. J., 2014, 20, 634–642; (e) J. Le Bras and J. Muzart, *Chem. Rev.,* **2011,** *111,* 1170–1214; (f) C. S. Yeung and V. M. Dong, *Chem. Rev.,* **2011,** *111,* 1215–1292; (g) T. Satoh and M. Miura, *Synthesis,* **2010,** 3395–3409.
37. R. Kishore, M. L. Kantam, J. Yadav, M. Sudhakar, S. Laha and A. Venugopal, *J. Mol. Catal. A: Chem.,* **2013,** *379,* 213– 218.
38. (a) R. Kishore, J. Yadav, B. Venu, A. Venugopal and M. L. Kantam, *New J. Chem.,* **2015**, *39,* 5259–5264. (b) A. B. Pawar and S. Chang, *Org. Lett.,* **2015,** *17,* 660–663; (c) J. Li and L. Ackermann, *Angew. Chem., Int. Ed.,* **2015,** *54*, 3635–3638; (d) D.-G. Yu, T. Gensch, F. de Azambuja, S. Vásquez-Céspedes and F. Glorius, *J. Am. Chem. Soc.,* **2014,** *136,* 17722–17725; (e) W. Liu and L. Ackermann, *Chem. Commun.,* **2014,** *50,* 1878–1881.
39. K. Yamaguchi, Y. Wang and N. Mizuno, *ChemCatChem,* **2013,** *5,* 2835–2838.
40. (a) J. Chen, L. He, K. Natte, H. Neumann, M. Beller and X.-F. Wu, *Adv. Synth. Catal.,* **2014,** *356,* 2955–2959; b) L. Ackermann, *Acc. Chem. Res.,* **2014,** *47*, 281–295; (c) T. Satoh and M. Miura, *Chem. – Eur. J.,* ***2010,*** *16,* 11212–11222; (d) G. Song, F. Wang and X. Li, *Chem. Soc. Rev.,* **2012,** *41,* 3651–3678; (e) W. Song and L. Ackermann, *Chem. Commun.,* **2013***, 49,* 6638–6640; (f) L. Ackermann and A. V. Lygin, *Org. Lett.,* **2012,** *14,* 764–767.
41. G. H. Dang, D. T. Nguyen, D. T. Le, T. Truong and N. T. S. Phan, *J. Mol. Catal. A: Chem.,* **2014,** *395,* 300– 306.
42. L. L. Chng, J. Zhang, J. Yang, M. Amoura and J. Y. Ying, *Adv. Synth. Catal.,* **2011,** *353,* 2988–2998.
43. (a) H. Fei and S. M. Cohen, *J. Am. Chem. Soc.,* **2015**, *137,* 2191–2194. (b) L. Wang and L. Ackermann, *Chem. Commun.,* **2014,** *50,* 1083–1085.
44. N. T. S. Phan, P. H. L. Vu and T. T. Nguyen, *J. Catal.,* **2013**, *306*, 38–46.
45. S. Vásquez-Céspedes, A. Ferry, L. Candish and F. Glorius, *Angew. Chem., Int. Ed.,* **2015,** *54,* 5772–5776.
46. (a) Q. Zhang, X. Yang, J. Guan, *ACS Appl. Nano Mater.* **2019**, *2*, 4681−4697; (b) L. M. Rossi, N. J. S. Costa, F. P. Silva, R. Wojcieszak, *Green Chem.* **2014**, *16*, 2906–2933; (c) A. Hu, G. T. Yee, W. Lin, *J. Am. Chem. Soc.* **2005**, *127*, 12486-12487;(d) A. S. Perera, *Sustainable Magnetic Nanocatalysts in Heterogeneous Catalysis, Smart Materials No. 26, Magnetic Nanomaterials: Applications in Catalysis and Life Sciences*, Edited by: S. H. Bossmann and H. Wang, The Royal Society of Chemistry **2017**; (e) A. Saha, J. Leazer, R. S. Varma, *Green Chem.* **2012**, *14*, 67–71; (f) B. R. Vaddula, A. Saha, J. Leazer, R. S. Varma, *Green Chem.* **2012**, *14*, 2133-2136; g) M. K. Abbasabadi, H. Shirkhanloo, *J. Pharm. Biomed. Anal.* **2020**, *189*, 113455; (h) S. Khodabakhshi, M. K. Abbasabadi, S. Heydarian, S. G. Shirazi, F. Marahel, *Lett. Org. Chem.* **2015**, *12*, 465-470;(i) M. K. Abbasabadi, D. Azarifar, H. R. E. Zand, *Appl.*

Organomet. Chem. **2020**, *34*, e6004; j) M. K. Abbasabadi, D. Azarifar, *Appl. Organomet. Chem.* **2020**, *34*, e5872; (k) S. M.-G. Yek, D. Azarifar, M. K. Abbasabadi, H. Keypour, M. Mahmoudabadi, *Appl. Organomet. Chem.* **2020**, *34*, e5989;(l) D. Azarifar, M. K. Abbasabadi, *Res. Chem. Intermed.* **2019**, *45*, 199-222.

47. (a) S.-H. Zhang, C.-Y. Wang, Z.-Z. Jiang, P.-Z. Ni, J.-P. Zhou, B.-M. Xi, W.-H. Chen, *Chem. Pharm. Bull.* **2011**, *59*, 96 – 99; b) Y. Kato, H. Ebiike, K. Achiwa, N. Ashizawa, T. Kurihara, F. Kobayashi, *Chem. Pharm. Bull.* **1990**, *38*, 2060 - 2062.
48. (a) K. Speck, T. Magauer, *Beilstein J. Org. Chem.* **2013**, *9*, 2048–2078; b) S. P. Upadhyay, P. Thapa, R. Sharma, M. Sharma, *Fitoterapia*, **2020**, *146*, 104722; c) Y. Sadahiro, H. Kato, R. M. Williams, S. Tsukamoto, *J. Nat. Prod.* **2020**, *83*, 1368-1373; d) H. Kamauchi, Y. Shiraishi, A. Kojima, N. Kawazoe, K. Kinoshita, K. Koyama, *J. Nat. Prod.* **2018**, *81*, 1290–1294.
49. (a) K. H. Kim, H. J. Noh, S. U. Choi, K. R. Lee, *J. Antibiot.* **2012**, *65*, 575–577; b) R. K. Bhatia, *Current Topics in Medicinal Chemistry*. **2017**, *17*, 189-207; c) E. C. Taylor, P. Zhou, L. D. Jenning, Z. Mao, B. Hu, J. -G. Jun, *Tetrahedron Lett.* **1997**, *38*, 521–524; d) S. K. Nayak, G. L Khatik, R. Narang, V. Monga, H. K. Chopra, *Curr. Cancer Drug Targets*, **2018**, *18*, 749-772; e) X. Armoiry, G. Aulagner, T. Facon, *J. Clin. Pharm. Ther.* **2008**, *33*, 219–226.
50. S. Ito, Y. Hirata, Y. Nagatomi, A. Satoh, G. Suzuki, T. Kimura, A. Satow, S. Maehara, H. Hikichi, M. Hata, H. Ohta, H. Kawamoto, *Bioorg. Med. Chem. Lett.* **2009**, *19*, 5310–5313.
51. M. V. Tejesvi, A. M. Pirttilä in *Endophytes of Forest Trees: Biology and Applications. Forestry Sciences* (Eds.: A. M. Pirttilä, A. C. Frank), Springer, Berlin. **2011**, *80*, pp.302.
52. F. A. Luzzio, A. V. Mayorov, S. S. W. Ng, E. A. Kruger, W. D. Figg, *J. Med. Chem.* **2003**, *46*, 3793–3799.
53 D. Patra, S. Panja, A. Saha, *Eur. J. Org. Chem.* **2020**, 878–883.
54. a) R. S. K. Lalji, P. Kumar, M. Gupta, V. S. Parmar, B. K. Singh, *Adv. Synth. Catal.* **2020**, *362*, 552 – 560; b) P. Kumar, M. Gupta, V. Bahadur, V. S. Parmar, B. K. Singh, *Eur. J. Org. Chem.* **2018**, 1552–1558.
55. J. P. Mathew, M. Srinivasan, *Eur. Polym. J.* **1995**, *31*, 835-839.
56. (a) B. R. Vaddula, A. Saha, R. S. Varma, J. Leazer, *Eur. J. Org. Chem.* **2012**, 6707–6709; b) N. S. Babu, N. Lingaiah, R. Gopinath, P. S. S. Reddy, P. S. S. Prasad, *J. Phys. Chem. C*. **2007**, *111*, 6447–6453.
57. (a) J. M. Anderson, J. K. Kochi, *J. Am. Chem. Soc.* **1970**, *92*, 1651 – 1659; (b) W. E. Fristad, M. A. Fry, J. A. Klang, *J. Org. Chem.* **1983**, *48*, 3575–3577; (c) S. Chang, J. F. Wang, L. L. Dong, D. Wang, B. Feng, Y. T. Shi, *RSC Adv.* **2017**, *7*, 51928–51934; (d) W.-C. Yang, P. Dai, K. Luo, Y.-G. Ji, L. Wu, *Adv. Synth. Catal.* **2017**, *359*, 2390–2395; (e) J. Kan, S. Huang, J. Lin, M. Zhang, W. Su, *Angew. Chem. Int. Ed.* **2015**, *54*, 2199 –2203.

List of Publications

Papers

1) C–C Cross-Coupling Reactions of Organosilanes with Terminal Alkenes and Allylic Acetates Using PdII Catalyst Supported on Starch Coated Magnetic Nanoparticles, **Debabrata Patra**, Subir Panja and Amit Saha, *Eur. J. Org. Chem.* **2020**, 7, 878–883.

2) C-H Activation of 2-Arylbenzoxazinones in Aqueous Medium: Synthesis of Fused Isoindolinones Using a Heterogeneous Magnetic Pd-Catalyst, **Debabrata Patra** and Amit Saha, *Eur. J. Org. Chem.* **2022**, e202201042.

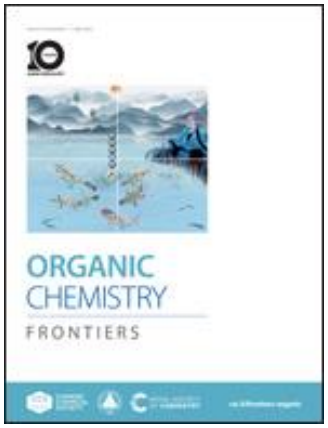

3) Dithiocarbamate-mediated thioamidation of arylglyoxylic acids by decarboxylative decarbonylative C–C bond formation reactions, **Debabrata Patra** and Amit Saha, *Org. Chem. Front.,* **2023**, 10, 1686–1693.

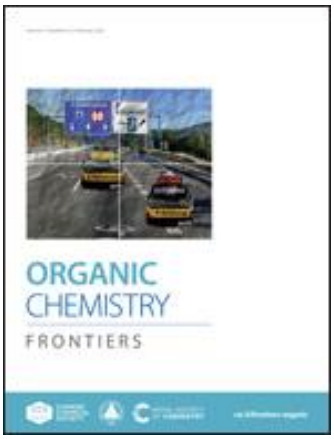

4) Dithiocarbamate mediated thioamidation via C–C single bond cleavage of styrene: study of the protocol in decarbonylative and decarboxylative thioamidations, **Debabrata Patra** and Amit Saha, Org. Chem. Front., **2024**,11,1150–1156.

5) Disulfide mediated ruthenium catalyzed direct C-H thiolation in benzoxazinone systems: selective synthesis of *ortho*-thiolated 2-arylbenzoxazinones, **Debabrata Patra** and Amit Saha, (*Manuscript Communicated*).

6) Thiuram disulfide mediated Cu-catalyzed C-S cross-coupling: synthesis of S-thiocarbamate compounds, Sourav Mandol**, Debabrata Patra** and Amit Saha, (*Manuscript Communicated*).